

# UC Irvine

## UC Irvine Electronic Theses and Dissertations

### Title

The Total Synthesis of The Indano[2,1-c]chromans ( $\pm$ )-Brazilin, ( $\pm$ )-Pestalachloride C, and ( $\pm$ )-Pestalachloride D and Enantioselective Palladium-Catalyzed Carbene Insertion into the N-H Bonds of Aromatic Heterocycles

### Permalink

<https://escholarship.org/uc/item/1xt858qr>

### Author

Arredondo, Vanessa

### Publication Date

2019

Peer reviewed|Thesis/dissertation

UNIVERSITY OF CALIFORNIA,  
IRVINE

The Total Synthesis of The Indano[2,1-*c*]chromans  
(±)-Brazilin, (±)-Pestalachloride C, and (±)-Pestalachloride D

and

Enantioselective Palladium-Catalyzed Carbene Insertion  
into the N–H Bonds of Aromatic Heterocycles

DISSERTATION

submitted in partial satisfaction of the requirements  
for the degree of

DOCTOR OF PHILOSOPHY

in Chemistry

by

Vanessa Arredondo

Dissertation Committee:  
Professor David L. Van Vranken, Chair  
Professor Suzanne A. Blum  
Professor Sergey V. Pronin

2019

Portion of Chapter 1 © 2014 American Chemical Society  
Portion of Chapter 3 © 2019 American Chemical Society  
Chapter 4 © 2017 John Wiley and Sons  
All other materials © 2019 Vanessa Arredondo

## **DEDICATION**

To

Pennie, Charlie, Mickie, Joey, Hachi, and Benji – my children

for rescuing me  
and  
for giving me a reason and purpose to live

and

to my Paul, forever always.

Your journey, and mine;  
Singular, like no other –  
Stronger in the end.

## TABLE OF CONTENTS

LIST OF FIGURES .....	vi
LIST OF SCHEMES.....	viii
LIST OF TABLES.....	xiii
ACKNOWLEDGMENTS .....	xiv
CURRICULUM VITAE.....	xxiv
ABSTRACT OF THE DISSERTATION.....	xxviii

### CHAPTER 1

Palladium-Catalyzed Three-Component Carbenylative Cross-Coupling Reactions Involving $\eta^3$ Benzylpalladium(II) Intermediates .....	1
Introduction: Comparison of Palladium(0) and Palladium(II) Carbene Intermediates in Cross-Coupling Reactions .....	1
Utility of Accessing $\eta^3$ -Allyl and $\eta^3$ -Benzylpalladium(II) Complexes in Carbenylative Insertion Reactions.....	3
Accessing $\eta^3$ -Benzylpalladium Complexes from Carbenylative Insertion.....	7
Accessing $\eta^3$ -Benzylpalladium Complexes from Carbenylative Insertion to Construct the 1-Arylindane and 1-Aryltetralin Structural Framework .....	7
Intramolecular Carbenylative Cross-Coupling: New [4+1] and [5+1] Carbenylative Processes.....	9
References.....	16

### CHAPTER 2

Total Synthesis of the Indano[2,1- <i>c</i> ]chroman, ( $\pm$ )-Brazilin, via Palladium-Carbenylative Cross-Coupling Reaction .....	21
Homioisoflavonoids of the indano[2,1- <i>c</i> ]chroman Structural Type from the Fabaceae Family of Plants .....	21

Proposed Biosynthetic Pathway of Homoisoflavonoids of the Indano[2,1- <i>c</i> ]chroman Structure .....	24
History of Brazilin – Isolation and Structural Elucidation .....	29
History of Brazilin – Synthesis of Indano[2,1- <i>c</i> ]chroman Core and Brazilin .....	32
Some Pharmacological Properties of Brazilin .....	37
Friedel–Crafts Cyclization as a Synthetic Approach to Brazilin .....	38
Cyclization of $\eta^3$ -Benzyl Palladium Intermediates Derived from Carbene Insertions as an Approach to the Synthesis of ( $\pm$ )-Brazilin .....	39
Results (unpublished).....	40
Conclusion .....	46
References.....	47
Supporting Information .....	53
Experimental Procedures .....	55
References.....	92
 <b>CHAPTER 3</b>	
Total Synthesis of the Indano[2,1- <i>c</i> ]chromans, ( $\pm$ )-Pestalachloride C and ( $\pm$ )-Pestalachloride D via a Knoevenagel-Hetero-Diels–Alder Cyclization .....	93
Plant-Derived Indano[2,1- <i>c</i> ]chromans.....	93
Fungus-Derived Indano[2,1- <i>c</i> ]chromans .....	94
Palladium-Carbenylative Insertion Result .....	95
Proposed Biosynthesis of the Pestalachlorides .....	97
Proposed Biosynthesis Relation to Knoevenagel/hetero-Diels–Alder Tietze Cascade Reactions.....	99
Initial Results of KHDA to Construct the Indano[2,1- <i>c</i> ]chroman Core .....	101
Total Synthesis Results and Discussion.....	102
Conclusion .....	107
References.....	109
Supporting Information.....	113
Experimental Procedures .....	115

References.....	143
<b>CHAPTER 4</b>	
Early History of Metal-Catalyzed Carbene Insertions of Diazo Compounds into	
Heteroatom–H Bonds (X–H) .....	144
General Mechanistic Model of Metal-Catalyzed Insertion of Diazo Compounds into	
X–H bonds .....	148
Asymmetric Metal-Catalyzed Insertions of Diazo Compounds into X–H Bonds .....	150
Asymmetric Palladium-Catalyzed X–H Insertions with Diazo Compounds.....	152
<i>N</i> -Substituted Aromatic Nitrogen Heterocycles via Transition Metal Catalysis .....	159
Results and Discussion .....	164
Conclusion .....	175
References.....	176
Supporting Information.....	184
Experimental Procedures .....	188
References.....	225
Appendix A: Chapter 2 – NMR.....	227
Appendix B: Chapter 2 – X-Ray Data for Compound S2.62b .....	311
Appendix C: Chapter 3 – NMR .....	328
Appendix D: Chapter 4 – NMR.....	381

## LIST OF FIGURES

	Page	
<b>CHAPTER 1</b>		
Figure 1-1	Examples of brazilin and related compounds sporting the 1-arylindane structural framework	13
Figure 1-2	Synthesized 1-arylindanes from aryl iodide <b>1.44</b>	14
<b>CHAPTER 2</b>		
Figure 2-1	Homoisoflavonoid term coined to describe eucomin and eucomol structures	22
Figure 2-2	Structural classification of homoisoflavonoids isolated from <i>Caesalpinia</i> and <i>Haematoxylum</i> spp. of Fabaceae plant family	23
Figure 2-3	Indano[2,1- <i>c</i> ]chroman term used to describe brazilin-type structural framework	23
Figure 2-4	Plant-based indano[2,1- <i>c</i> ]chromans isolated from <i>Caesalpinia</i> and <i>Haematoxylum</i> spp	24
Figure 2-5	Revised structures <b>2.20</b> and <b>2.21</b> by Gilbody, Perkin, and Yates to account for isolation of acids from oxidation studies	30
Figure 2-6	Crabtree and Robinson synthesize the first compounds containing a brazilin skeleton – the brazylum salts	34
Figure 2-7	Palladium-catalyzed insertion of oxygenated aryl iodides <b>2.52</b> and <i>N</i> -tosylhydrazones <b>2.53</b>	41
<b>CHAPTER 3</b>		
Figure 3-1	Indano[2,1- <i>c</i> ]chromans from plants	93
Figure 3-2	New racemic indano[2,1- <i>c</i> ]chromans from marine fungi	94
Figure 3-3	Depiction of transition states leading to pestalachloride C and D	99



Figure 3-4	Characteristic proton shifts and coupling constants of pestalachloride C and D	101
------------	--	-----

## CHAPTER 4

Figure 4-1	General mechanism of X–H insertion of diazo compound catalyzed by palladium(0), rhodium(II), copper(I) and other metals	149
Figure 4-2	Depictions of possible ylide intermediates in metal catalyzed X–H insertion	149
Figure 4-3	Examples of <i>N</i> -substituted aromatic nitrogen heterocycles in pharmaceutical drugs	160
Figure 4-4	Biologically active <i>N</i> -alkyl indoles with stereocenters adjacent to nitrogen	161
Figure 4-5	Scope of diazo compounds in N–H insertion with carbazole	168
Figure 4-6	Reaction scope with various carbazoles	170
Figure 4-7	Indole substrate scope	172
Figure 4-8	X-ray crystal structure of indole <b>4.6db</b>	173
Figure 4-9	Examples of other N–H heterocycles investigated for this reaction	174
Figure 4-10	Synthesis of the core of 5-HT6 receptor antagonist <b>4.0b</b>	175

## LIST OF SCHEMES

	Page	
<b>CHAPTER 1</b>		
Scheme 1-1	Reactivity for palladium(0) carbene complexes	1
Scheme 1-2	Reactivity for palladium(II) carbene complexes	2
Scheme 1-3	Mechanistic comparison of a carbenylative cross-coupling reaction (a) with a carbonylative cross-coupling reaction (b) highlighting the key migratory insertion step of the corresponding palladium(II) intermediate	2
Scheme 1-4	(a) Mechanism of double carbonylation. (b) Mechanism of iterative carbene over-insertions in carbenylative process	3
Scheme 1-5	$\eta^3$ - Coordination of $\pi$ -allylpalladium(II) intermediates disfavors over-insertion of carbenes	4
Scheme 1-6	Reaction pathways of $\eta^3$ -coordinated allyl/benzyl palladium(II) intermediates following a migratory insertion event	4
Scheme 1-7	First three-component carbenylative cross-coupling of aryl iodides, TMSD, and aryl stannane by Van Vranken and co-workers and unwanted reaction pathways	5
Scheme 1-8	General mechanism for carbenylative amination accessing $\eta^3$ -allylpalladium(II) species	6
Scheme 1-9	Examples of attack on palladium vs on allyl in carbenylative insertion cross-coupling reaction	8
Scheme 1-10	Access to bicyclic compounds with $sp^3$ centers	9
Scheme 1-11	General reaction explored by colleague Eugene Gutman	9
Scheme 1-12	General published carbenylative reaction to construct 1-arylindanes and 1-aryltetralins	10
Scheme 1-13	Insertion of a highly hindered benzylidene group necessitated different reaction conditions	11
Scheme 1-14	Proposed mechanism for carbenylative cyclization and formation of side products	12

Scheme 1-15	Evidence against alternative $\eta^3$ -benzylpalladium intermediates	13
Scheme 1-16	Synthesis of oxygenated aryl halides to test in the carbenylative insertion reaction	14
<b>CHAPTER 2</b>		
Scheme 2-1	Biosynthesis of chalcones provides access to various homoisoflavonoids	25
Scheme 2-2	2'-Methoxychalcones are the proposed biosynthetic precursors to homoisoflavonoids of the sappanin-type structure such as eucomin and eucomol	26
Scheme 2-3	Proposed biosynthetic pathway to indano[2,1- <i>c</i> ]chroman brazilin from sappanchalcone	27
Scheme 2-4	Proposed biosynthetic pathway that connects sappanchalcone, brazilin, brazilein, and protosappanin A homoisoflavonoids	28
Scheme 2-5	Robinson's analysis of expected oxidation products between previously proposed structure <b>2.21</b> of brazilin by Gilbody, Perkin, and Yates, and his alternative structure, <b>2.24</b>	31
Scheme 2-6	Synthesis of veratrylidene-7-chromanone <b>2.29</b> reported by Perkin and Robinson, and the structure of <i>O</i> -trimethylbrazilin for comparison	32
Scheme 2-7	Synthesis of 3,4'-dimethoxy-benzyl-chromanone <b>2.32</b> reported by Pfeiffer and Grimmer, and the structure of <i>O</i> -trimethylbrazilin for comparison	33
Scheme 2-8	Robinson and Crabtree's primary strategy to access indano[2,1- <i>c</i> ]chroman core <b>2.34</b> through dehydration of chroman-4-one <b>2.33</b>	34
Scheme 2-9	Synthesis of deoxytrimethylbrazilone, <b>2.34</b> , the indano[2,1- <i>c</i> ]chroman resulting from Friedel-Crafts dehydrative cyclization of chroman-4-one <b>2.33</b>	35
Scheme 2-10	A plausible mechanism showing the key Friedel-Crafts cyclization/dehydration step to construct the indano[2,1- <i>c</i> ]chroman core <b>2.34</b>	36

Scheme 2-11	Synthetic route to (±)-brazilin <b>2.40</b> by Robinson and co-workers	37
Scheme 2-12	Selected examples of racemic and asymmetric synthesis invoking FCC in the synthesis of brazilin	39
Scheme 2-13	Formal synthesis of (±)-picropodophyllone using a [5+1] palladium-catalyzed carbene insertion	40
Scheme 2-14	Initial synthetic strategy to brazilin involving late-stage formation of dihydropyran ring	42
Scheme 2-15	Dihydroxylation proceeds on same face as aryl substituent	43
Scheme 2-16	Synthetic strategy to access indano[2,1- <i>c</i> ]chroman core lactone <b>2.71</b>	44
Scheme 2-17	Total synthesis of (±)-brazilin from bis-mesylate <b>2.77</b>	45
<b>CHAPTER 3</b>		
Scheme 3-1	Coupling partners necessary for carbenylative insertion reaction	96
Scheme 3-2	Synthesis of <i>N</i> -tosylhydrazone <b>3.2</b>	96
Scheme 3-3	Palladium-catalyzed carbenylative insertion model reaction with chlorinated <i>N</i> -tosylhydrazone <b>3.2</b>	97
Scheme 3-4	Shao, Wang and co-workers' proposed biosynthesis of pestalachlorides and pestalone	98
Scheme 3-5	Knoevenagel/hetero-Diels–Alder products depend on structure of starting materials	100
Scheme 3-6	Initial approach towards pestalachlorides C and D involved late-stage introduction of formyl group	102
Scheme 3-7	Premature intramolecular carbonyl-ene process competes with the Knoevenagel-hetero-Diels–Alder cascade reaction	103
Scheme 3-8	Synthesis of less crowded benzaldehyde <b>3.15</b> for Knoevenagel-hetero-Diels–Alder reaction	104
Scheme 3-9	Knoevenagel/hetero-Diels–Alder reaction. (a) Initial results. (b) Optimized results	105
Scheme 3-10	Basic conditions lead to complex mixtures of side products and byproducts	106

Scheme 3-11	Total synthesis of pestalachlorides C and D through a Knoevenagel/hetero-Diels–Alder cascade reaction of benzaldehyde <b>3.15</b> and resorcinol <b>3.10</b> .	106
-------------	--	-----

#### CHAPTER 4

Scheme 4-1	First synthetic transformation involving transition-metal-catalyzed insertion of diazo compounds into O–H bond	145
Scheme 4-2	Copper-bronze-catalyzed investigation of diazo decomposition by Yates leads to products resulting from O–H insertion	146
Scheme 4-3	Copper-catalyzed insertion of $\alpha$ -diazoacetophenone into the X–H bonds of aromatic heterocycles and piperidine. Mechanistic consideration proposed	147
Scheme 4-4	Practical application of N–H insertion catalyzed by rhodium(II) acetate	148
Scheme 4-5	Some early examples of asymmetric X–H insertion	150
Scheme 4-6	First reports of highly efficient O–H and N–H catalytic insertions of diazo compounds catalyzed by copper catalysts	151
Scheme 4-7	First example of enantioselective palladium-catalyzed carbene insertion via zwitterionic intermediate trapping with imine	153
Scheme 4-8	First asymmetric palladium-catalyzed insertion of diazo compounds into N–H bonds	154
Scheme 4-9	Side by side comparisons of previously published work in asymmetric palladium-catalyzed carbene insertion into X–H bonds utilizing chiral ligands	159
Scheme 4-10	Selected examples of typical asymmetric alkylations of indole catalyzed by metals	163
Scheme 4-11	Intrinsic regioselectivity of unsubstituted indole	164
Scheme 4-12	Decomposition of methyl $\alpha$ -diazobutanoate	169
Scheme 4-13	(a) Absolute stereochemistry assigned by X-ray analysis of alcohol <b>4.5</b> . (b) View of crystals through microscope lens (left) X-ray crystal structure (right)	169



## LIST OF TABLES

	Page	
<b>CHAPTER 4</b>		
Table 4-1	Selected entries of Zhou, Zhu and co-workers' screening conditions for optimization of insertion into phenol	155
Table 4-2	Selected entries of Feng, Liu and co-workers' screening conditions for optimization of insertion into anilines	157
Table 4-3	Zhou and co-workers selected screening conditions for C–H insertion into <i>N</i> -substituted indole	158
Table 4-4	Reaction optimization for carbazole <b>4.1a</b>	165
Table 4-5	Effects of different ligands on N–H insertion with ethyl-3-indoleacetate <b>4.6c</b>	173

## ACKNOWLEDGMENTS

Chapter 1 has been reprinted (adapted) with permission from Gutman, E. S.; Arredondo, V.; Van Vranken, D. L. *Org. Lett.* **2014**, *16*, 5498–5501. Copyright 2014 American Chemical Society. The text of this thesis/dissertation is a reprint of the material as it appears in *Org. Lett.* **2014**, *16*, 5498–5501. The co-author listed in this publication directed and supervised research which forms the basis for the thesis/dissertation. Chapter 3 has been reprinted (adapted) with permission from Arredondo, V.; Roa, D. S.; Yan, S.; Liu-Smith, F.; Van Vranken, D. L. *Org. Lett.* **2019**, *21*, 1755–1759. Copyright 2019 American Chemical Society. Chapter 4 has been reprinted (adapted) with permission from Arredondo, V.; Hiew, S. C.; Gutman, E. S.; Premachandra, I. D. U. A.; Van Vranken, D. L. *Angew. Chem. Int. Ed.* **2017**, *56*, 4156. Copyright 2017 John Wiley & Sons.

None of this work would be possible without the support of multiple philanthropic agencies. I would like to acknowledge the National Science Foundation for their financial support through an NSF Graduate Research Fellowship; the University of California Irvine and the Department of Chemistry for their financial support through a Regents' Dissertation Fellowship and through teaching assistantship stipends; and the University of California Irvine for their continued support in my success academically, and personally. I would also like to thank the various research facilities and their corresponding staff for exceptional and unparalleled assistance with my project needs – Mass Spectrometry (Dr. John Greaves, Beniam Berhane, Dr. Felix Grun) Nuclear Magnetic Resonance Spectrometry (NMR) (Dr. Phil Dennison), X-Ray Crystallography (Dr. Joe Ziller), and the Physical Sciences Glass Shop (Jorg C. Meyer) – in the chemistry department at University of California Irvine.



A special thanks to the following organizations for their continued emotional, personal, professional, academic, and financial support throughout my time at University of California, Irvine.

I would like to thank Great Minds in STEM and my scholarship donors, Ray and Carmella Mellado for all the support and encouragement you gave me. Meeting the staff, the many talented individuals that attended the HENAAC Conference, your organization, and all the wonderful leaders in the STEM fields have left me forever inspired.

I would also like to thank South Central Scholars Organization for the financial and emotional support provided by all the board of directors and staff, especially Dr. London, Trish, and Stuart and Stephanie Liner. Dr. London and Trish – thank you so much for believing in me and for showing me that there are wonderful people in the world genuinely passionate in helping people like me succeed. The help I received during my college and graduate career has been motivational and encouraging. Stephanie and Stuart Liner, thank you not only for sponsoring my scholarships through South Central Scholars, but also for taking care of me throughout my undergraduate and graduate career. Your altruistic kindness has kept me faithful in humanity throughout tough times. Mr. Rubalcava, thank you for pointing me in the right direction – towards developing a career that gives me endless opportunities. I would also like to thank the South Central Scholars staff. Mr. Winston, thank you for your continued support and for keeping me in your heart and prayers. Meredith Curry and Amparo Diaz, thank you for all the crazy and productive times in the office, but, most importantly, for all the opportunities you gave me to help the organization that has given me so much. To all of you, your generosity and thoughtfulness towards a me has left a positive imprint on my soul. Thank you.

I would also like to thank the University of California Irvine Student Affairs and the Wellness, Health, and Counseling Services offices for their invaluable resources. In particular, I want to thank Brenda Lapinid. Brenda, this past year you have been an immense force in helping me push through the program. Thank you from the bottom of my heart. I am not sure where I would be without your advocacy. Additionally, Kerri Sherwood, Palo Verde Housing Associate Director of Residential Life, I would like to thank for all the support you gave me, for hearing my story, and for guiding me to resources I needed. Thank you for caring and for keeping me in consideration. I would also like to thank Dr. Lindsay Palmer, who helped me overcome my fears and stresses and was also there to help see me through to the end of the program.

Dave, if there was ever an Olympic gold medal for invaluable advisor and professor, it would be yours. There are no words, nor gestures that could describe my gratitude and appreciation for all that you have done for me. Thank you for your patience and most importantly, thank you for believing in me, for your confidence in me, and for helping me through this enlightening, yet, tempestuous program. I have learned so much from you and because of you I feel I have grown academically, professionally, and personally. Thank you for motivating me and for teaching me that stumbling blocks are nothing but bumps in the road that make the journey a little bit more interesting. Lastly, I am grateful for the knowledge that you have shared with me and the group. Understanding the world at the level of atoms of bonds and understanding reactivity and how things work mechanistically has helped me improve as a teacher and has given me a different appreciation for the small things in life.

Professor Vanderwal and Professor Overman, thank you for your continued support and for guiding me throughout my graduate career. Your invaluable advice, experience, and guidance helped me navigate the trials and tribulations of my projects and helped motivate me. Thank you

for also treating me as a person and genuinely caring for my success as an individual in a sea of ever-growing graduate students. Professor Suzanne A. Blum and Professor Sergey V. Pronin, thank you very much for your time and effort in helping me whenever I needed help. Thank you for seeing me to the end of my graduate career.

Thank you to all the graduate students in the Vanderwal, Overman, Rychnovsky, Pronin and Blum labs over the past few years for all their help and expertise imparted to me. Whenever I needed help from anyone from these labs, they were always ready to help. They would put aside what they were doing to help their fellow graduate student. The comradery between all the students in the chemistry department is truly one that I will always cherish.

Additionally, I want to thank all previous and current group members of the Van Vranken lab, in particular Udara, Eugene, Thi, and Stan. Thank you for all the mentorship, friendship, and support I received. Stan – thank you for all your support and unconditional friendship throughout these tough times in our journey. Thank you for being a reliable friend and for caring for me. I appreciate it.

I would also like to thank the wonderful young talent I had the privilege to mentor – Daniel Roa. You worked extremely hard – as hard as one of us – and now you are one of us. Thank you for all the effort and independent work you did as part of our projects. Songyuan, thank you for all the hard work and energy you brought into the lab and our projects – it was a delight. I would also like to all the undergraduate student members of the Van Vranken lab who made the lab an exciting and interesting place to work.

Prior to UCI, I had an immense amount of support and would like to acknowledge them. Thank you to many amazing advisors, friends, and professors from Vanderbilt University who were with me every step of the way towards a bachelor's degree in chemistry and who supported

and encouraged me towards following my passion into graduate school. Dr. Carmelo J. Rizzo, Dr. Timothy Hanusa, Dr. Gerald Stubbs, Dr. Prasad Polavarapu – thank you so much for all the help and guidance you gave me during my time at Vanderbilt University. It was a pleasure being in all of your classes and I learned so much. All of you were extremely patient with me and never gave up on me. Thank you for all the additional hours beyond office hours spent in helping me understand the very same concepts I apply daily. Dr. Rizzo, thank you for your kindness and for being an amazing professor. I still remember how I would send you long emails with many questions and you would write back answering every single one. I just wanted to say that I appreciate that very much. Dr. Hanusa, thank you so much for your kindness and friendship during my time at Vanderbilt. I learned so much from you and your enthusiasm for science has certainly left a lasting impression. I still remember all the nifty gadgets you had in your office that you would show me to teach me inorganic concepts. Dr. Stubbs, biochemistry is the bomb and I appreciate how you taught it – with a fundamental understanding for the chemical concepts. Your class made me appreciate life and understand how chemistry is not just in the lab. It was the best biology class I have ever taken. Dr. Polavarapu, I want to thank you for your unwavering patience. Thank you for all the time you spent re-iterating the same concept in different languages so I could understand. I still remember the time in your office when you spent more than thirty minutes trying to explain charge transfer until it finally clicked. I can assure you those thirty minutes were not in vain. You made physical chemistry fun!

I also want to acknowledge Dr. Joel B. Tellinghuisen and Pat. Dynamic duo! Dr. Tellinghuisen, thank you as well for your unwavering patience in guiding me through the perils of physical chemistry lab. It was a really fun class and I would take it again! A heartfelt thanks to and appreciation for Pat Tellinghuisen who was my mentor and friend throughout my volunteering

experience at Vanderbilt Student Volunteers for Science. Pat, you have done an amazing job with VSVS. Participating in the program was as much fun as educational and a personally rewarding experience. I think you have one of the best jobs in the world. VSVS is certainly making a difference and I want to thank you for letting me be a part of it. I still have the VSVS bear and long-sleeve t-shirt, which is still my favorite long-sleeve tee. Thank you both for inviting me to your home and for filling my heart with the joys of science.

I want to thank my undergraduate research advisor, Dr. Jeffrey N. Johnston for all the help and guidance you gave me during my time in your lab. It was a pleasure meeting all the lab members and taking your classes. Thank you for all your help with applying to the fellowships and for talking with me about potential career paths. I learned so many things in your lab and I appreciate every lesson. I remember when you took time out of your day to teach me how to run a column. Thank you for caring about me and my professional improvement.

I am truly grateful for Sandra E. Ford. Sandra, without you I would not have traveled to the beautiful state of Virginia for an ACS regional meeting and without your help I would not have learned and obtained the opportunity to do an NSF REU program. Thank you for all the help and guidance and mentorship you gave me. It was and is always a delight seeing you at meetings at the Vanderbilt booth. I can't express my thanks enough.

Dr. Sofia Papatheodorou, I love saying your name. Thank you for all your mentorship and guidance and for all the opportunities you gave me while in your care. Thank you for taking in that short, peppy, high-schooler and making her a part of Science Society at CSUDH. My years with Science Society were definitely the key experiences that kept me fascinated in pursuing a career in science. Thank you for all that you did for me, Dr. Sofia, from the bottom of my heart. You introduced me to the American Chemical Society and gave me the opportunity to go to at least one

ACS conference. Working with you, I met many individuals pursuing careers in chemistry, showing me that there was more than one path I could take in life. Thank you for allowing me to be a part of Science Society and be a part of the outstanding National Chemistry Week event “Having a Ball with the Chemistry of Sports” in the nation back when I was in college. And thank you for allowing me to stay a part of Science Society even after I transferred out of CSUDH. Those years with Science Society are a treasure to me.

A special heart-felt thanks to all my teachers who noticed my proclivity for science and fostered it and encouraged my passion: Ms. O’Neill, Dr. Fiedler, Ms. Lewis, Mr. Delaby, Ms. Brakel, and Mr. Jett from California Academy of Mathematics and Science, and Ms. Gaeta, my middle-school science teacher, who devoted time and effort outside of teaching to help me succeed in life. Ms. Gaeta, you were the push that led me to California Academy of Mathematics and Science, and from there all of this stemmed. Thank you all!

Thank you to all my friends who have stuck with me from beginning to end. Miranda Pearl Diebel, Camille Isobel Maginas, Kyra Nicole Young, and Monica Quezada. Thank you for your continued support, love and care. Miranda and Camille, a special thanks to both of you for caring for me and for always thinking of me and including me in outings you guys plan. Thanks for dragging me out of my shell.

I am grateful for the new friendships I have made during my time at UCI. Thank you to Dr. Natasha Alohilani Emmerson and Dr. Andrew Clarke Schneider for their friendship, care, and crazy movie nights. Thank you also for Kai Mako – such a wonderful and delightful child who makes me throw him across the slip n’ slide so he can have fun and I can get some exercise. Tasha, thanks for the emotional support through these past two years in the program. And thanks for always being chill. Thank you both for all the support and trust you have given me. I also want to

thank Dr. Ben and Michelle Lourie for their care and concern, and for their friendship and hospitality, and for making game night super fun! (And for dealing with my crazy personality with such grace!)

I want to thank my extended family – my tias and tios Gloria, Javier, Lupito, Leva, Lupe, Aide, and my cousins Mayra, Javier, Adrian (Zot! Zot! Zot!), Samantha, and everyone in my family tree – for always welcoming me with open arms and treating me as a friend from yesterday even though I have gone months and years without seeing them as I pursued my doctoral degree. Thank you to my other family – Leti, Mauricio, Abuel[it]a (shhh! do–not tell her), and Jolie, who have never hesitated to help me when I needed it, and for being patient with me and the way I express myself. Thank you for all the emotional help and support you have given us. Thank you for everything! And also, thank you for Paul, and for letting him go so we can start a new life together.

I also want to thank my children – Pennie, Charlie, Mickie, Hachi, Joey, Benji – and my adopted child, Coco. Their unconditional, genuine love has more than once saved me from myself and the deep pits I was prone to falling into. Their wagging tails and butts brought so much joy and light into my life reminding me that there are reasons to be happy even when the reaction you have been working on has failed for six months straight. You all live in the moment, and I strive to as well, to enjoy every moment, and enjoy what I have instead of worrying about what I lack. Caring for you the way you care for me has been therapeutic, in a sense, and purposeful to me. I hope to use my talents in a way that is beneficial for you, and everyone’s canine children. You are all dear to me. Pennie, you have taught me to understand my feelings and emotions, and that its okay to be alone once in a while. Charlie, you have taught me that there is nothing better than being and feeling loved. Mickie, you have taught me to be a better person, and are still challenging

me to become a better leader. Hachi, you have taught me to have fun no matter what your size, and to love and to trust those who care for you. Joey, you have taught me that playtime is all the time and I need to teach you there is a place and time for everything. Coco, you have taught me that not everything is as it seems, and giving someone a chance might be the best thing you could do for someone else. Benji, my first child. You have taught me the most – how to be a mom, how to be organized, how to care for someone who cannot speak, and more. You have taught me that no matter what crazy stuff happens in life there is always a reason to live. You are still with us and will always be.

If anyone really knows or loves me dearly, they know that I always save the best for last. The four people who have had an everlasting impact in my life – mom, dad, brother, and Paul. Hmm, let me clarify, Paul Fernando Koppenhaver, born 1988. (Just in case your name is Paul, but are not my Paul). This is probably the most difficult paragraph to write because nothing compares to the love and support you have all given me. Babe, I have no idea where to start, because there are just no words to the wonderful experiences we have shared together – some sad, some hilarious, others amazing, and even some, well, flat-out embarrassing ones...but that is what makes our journey rich and great. I am grateful for all the things you did for me while I was working. You deserve a PhD just for the amount of work and turmoil I gave you. Thank you for all the food deliveries, for all the emotional support, and for all that you do for me. I can't wait to see what our next chapter will be.

Mom and Dad, I don't know of any other parents who would do the crazy insane things that you both have done for me to help me through the program. Mom, I love you very much and there is no one in the world like you. Dad, I love you very much too and want to thank you for all that you do for me. Thank you also for always being there for me without fault. I can always count



on you to help me out. Bro, you and I are so different, but that isn't a bad thing. Keeps things interesting in the family, no? Thanks for always having my back and for always being proud of me. I am proud of you too and love you too. Can't wait to do more Six Flags runs!!! This family has had its ups and downs but I would never trade it for anything in the world. Mom, you always felt like you never could give enough to your children. I am letting you know that you have given us more than enough – more than anyone in the world could hope for. In all heartfelt sincerity, I dedicate all my hard work in this dissertation to you. Everything that you have done for me is embodied in this work. Thank you for always being there for me without question – for leaving work and driving out to me when I needed you. Thank you.

Hopefully, my love and actions for you all expresses more than what I can write on these pages.

# CURRICULUM VITAE

## VANESSA ARREDONDO

---

### Education

---

2013–2019      **Ph.D. in Organic Chemistry**, University of California Irvine  
Irvine, CA      Advisor: David Van Vranken

#### Awards

Latino Excellence and Achievement Award  
President's Dissertation Fellowship  
HENAAC Scholarship Graduate Student Award  
Michael E. Gebel Award  
Chemistry Department Teaching Program Award

2009 – 2012      **B.A., summa cum laude, in Chemistry** (with Honors), Vanderbilt  
Nashville, TN      University

#### Awards

NSF Graduate Student Fellowship  
Phi Beta Kappa Award  
D. Stanley and Ann T. Tarbell Prize in Organic Chemistry

### Research

---

- **Total Synthesis of Indano[2,1-*c*]chroman Natural Products**
- **Development of New C–C and C–N Reactions Catalyzed by Palladium**

### Research Experience

---

2013 – 2019      University of California, Irvine  
Irvine, CA      Advisor: David L. Van Vranken

2012 – 2013      University of California, Irvine  
Irvine, CA      Advisor: Zhibin Guan and Vy Dong

2011 – 2012      Vanderbilt University  
Nashville, TN      Advisor: Jeffrey N. Johnston

2011              Georgia Institute of Technology (NSF REU)  
Atlanta, GA      Advisor: Stefan France

## Publications

---

6. “Total Synthesis of (±)-Brazilin Using a [4+1] Palladium-Catalyzed Carbenylative Annulation.” **Arredondo, V.**; Roa, D. E.; Gutman, E. S.; Huynh, N. O; Van Vranken, D. L. submitted for publication, **2019**.
5. “Total Synthesis of (±)-Pestalachloride C and (±)-Pestalachloride D through a Biomimetic Knoevenagel/Hetero-Diels–Alder Cascade.” **Arredondo, V.**; Roa, D. E.; Yan, S.; Liu-Smith, F.; Van Vranken, D. L. *Org. Lett.* **2019**, 21, 1755.
4. “Enantioselective Palladium-Catalyzed Carbene Insertion into the N–H Bonds of Aromatic Heterocycles.” **Arredondo, V.**; Hiew, S. C.; Gutman, E. S.; Premachandra, I. D. U. A.; Van Vranken, D. L. *Angew. Chem. Int. Ed.* **2017**, 56, 4156.
3. **Arredondo, V.**; Van Vranken, D. L. (2017) “80. ¿Es posible una vida basada en el silicio?” in Ciencia, y además lo entiendo!!! Ed. Guerrero, Q. <http://divulgacioncientificadecientificos.blogspot.com.es/p/libro-book.html>
2. “Cyclization of  $\eta^3$ -Benzylpalladium Intermediates Derived from Carbene Insertion.” Gutman, E. S.; **Arredondo, V.**; Van Vranken, D. L. *Org. Lett.* **2014**, 16, 5498.
1. “Organocatalytic, Diastereo- and Enantioselective Synthesis of Nonsymmetric *cis*-Stilbene Diamines: A Platform for the Preparation of Single-Enantiomer *cis*-Imidazolines for Protein–Protein Inhibition.” Vara, B. A.; Mayasundari, A.; Tellis, J. C.; Danneman, M. W.; **Arredondo, V.**; *et al.*, Johnston, J. N. *J. Org. Chem.* **2014**, 79, 6913.

## Networking Poster Presentations

---

- |             |  |
|-------------|--|
| 2017        | <b>UCI NSF-GRFP “Training for Tomorrow” Symposium, Irvine, CA</b><br>“Enantioselective Palladium Catalyzed Carbene Insertion into the N–H bonds of Aromatic Heterocycles.”   |
| 2014 – 2019 | <b>UCI Chemistry Department Recruitment Sessions, Irvine, CA</b><br>“Van Vranken Group Research Projects.”<br>“Enantioselective Palladium Catalyzed Carbene Insertion into the N–H bonds of Aromatic Heterocycles.”<br>“Palladium Carbenes – It’s more than just rings.”<br>“Harnessing Palladium-Carbenoid Reactivity.” |
| 2012        | <b>ACS 244<sup>th</sup> National Meeting, Philadelphia, PA</b><br><i>Successful Student Chapters</i><br>“Science Society honored ...for the outstanding student event in the nation.” Araujo, J.; Osorio, J.; <b>Arredondo, V.</b> ; Papatheodorou, S.   |
| 2011        | <b>ACS Southeastern 63<sup>rd</sup> Regional Meeting, Richmond, VA</b><br><i>Organic Chemistry Poster</i><br>“C–H Functionalization Studies with Perylene Bisimide and Indole Derivatives.” <b>Arredondo, V.</b> ; France, S. F.   |

## Presentations

---

- 2016 **Vertex Day, UCI Chemistry Department**  
“Enantioselective N–H Insertion Reactions of Palladium Carbenes.”
- 2015 **Graduate Colloquium, UCI Chemistry Department**  
“Palladium-Catalyzed Carbenylative Migratory Insertions: Application Towards a Total Synthesis of Brazilin.”

## Professional Development

---

- 2015 – 2019 **GPS-BIOMED** *Graduate Professional Success for PhD students*
- 2016 – 2019 **Cheeky Scientist Association** *Industry Training for PhD students*
- 2016 **Science Communication Skills Course** *with Sandra Tsing Loh*
- 2015 **Scientist to CSO Leadership Program** *SciPhD.com Certificate Program*
- 2009 – 2013 **ACS Student Member**

## Leadership and Outreach

---

- 2015 – 2019 **Mentor to UCI Undergraduate Researchers**, Van Vranken Lab
- 2015 – 2017 **Science Olympiad at UCI**, Regional Event Coordinator and Event Writer
- 2012 – 2013 **Chemistry Outreach Program at UCI**, Volunteer
- 2012 **STEM Career Panelist**, South Central Scholars Business Conference
- 2009 – 2012 **Chemistry Outreach**, Vanderbilt Student Volunteers for Science
- 2009 **ACS 237<sup>th</sup> National Meeting**, ChemDemo Exchange Event Volunteer
- 2007 – 2009 **CSUDH Chemistry Outreach**, Science Society Event Coordinator

## Teaching and Work Experience

---

- 2019 **Staff Research Associate III, UCI Mass Spectrometry Facility**
- 2018 – 2019 **Teaching Assistant at UCI**  
Organic Chemistry Lecture Series  
Majors and non-majors Organic Chemistry Lab  
Upper Division Chemical Biology Lab
- 2018 **Teaching Assistant for UCI COSMOS Chemical Biology Cluster**  
CA State Summer School for Math & Science at UCI  
Theme: “Can you make the next billion-dollar antibiotic?”
- 2017 **Teaching Assistant for UCI COSMOS Chemical Biology Cluster**  
CA State Summer School for Math & Science at UCI  
Theme: “Extracting and Analyzing Molecules from Nature.”
- 2016 – 2017 **Teaching Assistant at UCI**  
Organic Chemistry Lecture Series  
Organic Chemistry Lab Series  
General Chemistry Lecture  
Upper Division Chemical Biology Lab
- 2013 – 2018 **Laboratory Inventory and Purchasing Lead**, Van Vranken Lab
- 2012 **Intern**, South Central Scholars Organization
- 2011 – 2012 **Laboratory Assistant**, Vanderbilt Student Volunteers for Science

This page is intentionally left blank.

# ABSTRACT OF THE DISSERTATION

The Total Synthesis of The Indano[2,1-*c*]chromans  
(±)-Brazilin, (±)-Pestalachloride C, and (±)-Pestalachloride D

and

Enantioselective Palladium-Catalyzed Carbene Insertion  
into the N–H Bonds of Aromatic Heterocycles

By

Vanessa Arredondo

Doctor of Philosophy in Chemistry

University of California, Irvine, 2019

Professor David L. Van Vranken, Chair

This body of work revolves around two themes: palladium-catalyzed construction of new carbon–nitrogen (C–N) bonds in an enantioselective fashion, and the total synthesis of naturally occurring indano[2,1-*c*] chromans of biological interest.

The development of new methods to synthesize complex molecules in an efficient and stereocontrolled manner is an essential goal. Transition metal catalysis has broadened the types of disconnections and connections available to synthetic chemists. Palladium carbene intermediates provide a new point of disconnection that has gained popularity. Not only do palladium carbene intermediates generate new carbon–carbon and carbon–heteroatom bonds, but they do so while providing an avenue for chiral control. Many biologically active compounds, such as RYDAPT®, contain aromatic heterocycles attached to chiral centers through a C–N bond. Methods to generate

these types of linkages from achiral fragments with control of stereochemistry are invaluable. This work describes a method to access chiral C–N bonds between achiral  $\alpha$ -aryl- $\alpha$ -diazocarbonyl compounds and achiral aromatic heterocycles containing N–H bonds.

Naturally occurring indano[2,1-*c*]chromans, such as ( $\pm$ )-brazilin, ( $\pm$ )-pestalachloride C, and ( $\pm$ )-pestalachloride D, are of analytical or biological importance. The second part of this work describes the synthesis of these three biologically active indano[2,1-*c*]chromans. ( $\pm$ )-Brazilin, a highly oxygen sensitive species, has been studied for its pharmacological activity since the discovery of its structural framework. Prior syntheses of ( $\pm$ )-brazilin that have utilized a common strategy: a Friedel–Crafts-type alkylation of an aromatic ring. The total synthesis described in this work takes advantage of a palladium-catalyzed carbene insertion reaction to provide the core structure of ( $\pm$ )-brazilin through a non-obvious bond disconnection.

The carbene insertion approach was less efficient when applied to the synthesis of the highly functionalized indano[2,1-*c*]chroman core of ( $\pm$ )-pestalachloride C and ( $\pm$ )-pestalachloride D which occur in nature as racemates. These compounds exhibit interesting, dramatically different biological activity. For example, pestalachloride C exhibits teratogenic activity, whereas pestalachloride D does not. A biomimetic synthesis of these two compounds was developed which seems to support the Knoevenagel/hetero-Diels–Alder cascade reaction proposed for their biosynthesis. This concise synthesis facilitates construction of chemical analogues with potentially higher potency.

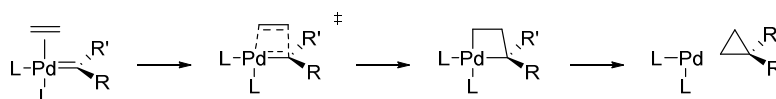
## Chapter 1

### Palladium-Catalyzed Three-Component Carbenylative Cross-Coupling

#### Reactions Involving $\eta^3$ -Benzylpalladium(II) Intermediates

##### Introduction: Comparison of Palladium(0) and Palladium(II) Carbene Intermediates in Cross-Coupling Reactions

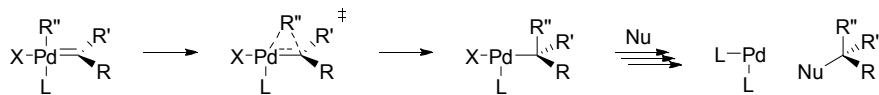
Palladium(0) carbene intermediates exhibit distinct reactivity from palladium(II) carbene intermediates. Palladium(0) carbene intermediates are most familiar in cyclopropanation reactions where they undergo [2+2] type reactions with alkenes to generate palladacyclobutanes that undergo reductive elimination to form cyclopropanes (Scheme 1-1).<sup>1</sup> Palladium(II) precatalysts tend to be more effective than palladium(0) precatalysts in cyclopropanation reactions, but the experimental evidence and theoretical studies are most consistent with active palladium(0) catalyst species.<sup>2</sup>



**Scheme 1-1.** Reactivity for palladium(0) carbene complexes.

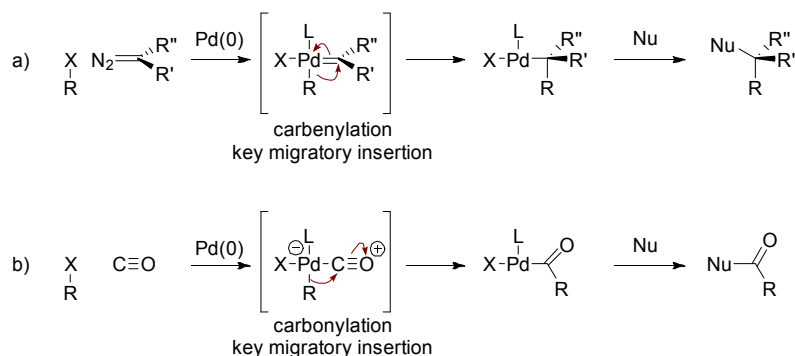
Palladium(II) carbene intermediates have two features that distinguish them from palladium(0) carbenes. Anionic donor ligands on arylpalladium(II) intermediates, generated from oxidative addition, are more nucleophilic than those of palladium(0) carbene complexes. In addition, the palladium(II) carbene carbon is more electrophilic than that of the palladium(0) carbene intermediate due to the higher oxidation state of the metal. These two key differences favor migration of the anionic ligand to the electrophilic carbene carbon (Scheme 1-2).





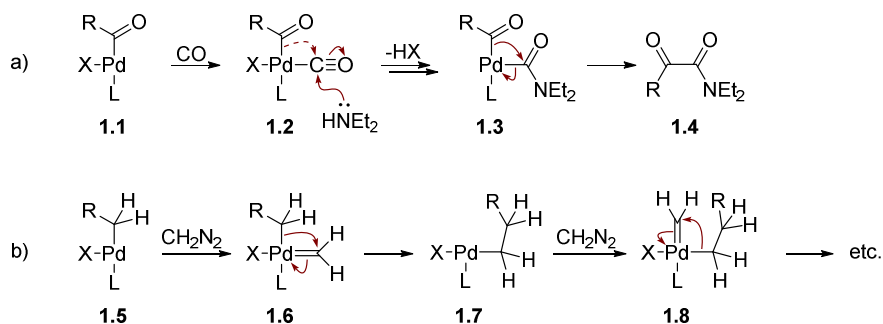
**Scheme 1-2.** Reactivity for palladium(II) carbene complexes.

This *carbenylative* migratory insertion process (Scheme 1-3a) is analogous to the palladium-catalyzed carbonylative migratory insertion process with carbon monoxide (CO) ligand (Scheme 1-3b).



**Scheme 1-3.** Mechanistic comparison of a carbenylative cross-coupling reaction (a) with a carbonylative cross-coupling reaction (b) highlighting the key migratory insertion step of the corresponding palladium(II) intermediate.

The migration of an anionic group to the carbon monoxide ligand in a carbonylative process is limited to one insertion event (Scheme 1-4a). The resulting acylpalladium(II) intermediate **1.1** can coordinate another CO ligand to generate acylpalladium **1.2**, but due to the low migratory aptitude of acyl ligands to CO ligands, complex **1.2** will not insert CO into the palladium-acyl bond to afford a 1,2-dicarbonyl product.<sup>3</sup> However, it is possible to generate 1,2-dicarbonyl products. The mechanism for double insertion does not involve successive insertion due to the low migratory aptitude of acyl ligand, but rather a nucleophilic addition to a second CO ligand of acylpalladium(II) intermediate **1.2** to generate a bis(acyl)palladium(II) complex **1.3** that reductively eliminates to afford the 1,2-dicarbonyl product **1.4** (Scheme 1-4a).<sup>4</sup>



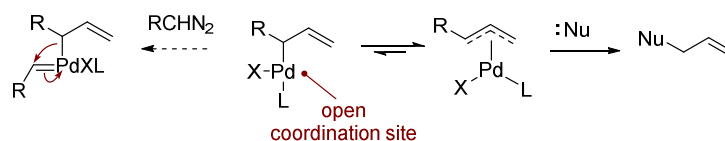
**Scheme 1-4.** (a) Mechanism of double carbonylation. (b) Mechanism of iterative carbene over-insertions in carbenylative process.

In contrast, mono-insertion of carbenes is difficult to achieve because alkyl groups migrate readily to carbene ligands (Scheme 1.4b). After the first migratory insertion, the newly formed alkylpalladium(II) intermediate **1.5** can coordinate another diazo compound to generate the new alkylpalladium(II) carbene intermediate **1.6**. With an anionic, alkyl ligand perfectly poised to migrate, another insertion occurs to generate **1.7**, which can further undergo more migratory insertion events resulting in higher molecular weight over-insertion products. For example, palladium dichloride is a highly effective catalyst for polymerization of ethyl diazoacetate.<sup>5</sup> The over-insertion reactivity of palladium(II) carbene complexes in the presence of carbene precursors, provides an unwanted pathway to inefficient catalytic transformations.

### Utility of Accessing $\eta^3$ -Allyl and $\eta^3$ -Benzylpalladium(II) Complexes in Carbenylative Insertion Reactions

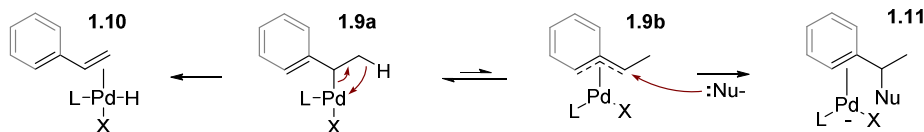
Over-insertion of carbenes can be circumvented in the case of allylic or benzylic ligands on palladium capable of generating  $\eta^3$ -allyl or  $\eta^3$ -benzylpalladium(II) intermediates after the initial migratory insertion step (Scheme 1-5). An  $\eta^1$ -allylpalladium complex is susceptible to insertion of another carbene group at the open coordination site, but isomerization to an  $\eta^3$ -allylpalladium

complex prevents additional insertions and facilitates attack of nucleophiles on the electrophilic allyl ligand.



**Scheme 1-5.**  $\eta^3$ -Coordination of  $\pi$ -allylpalladium(II) intermediates disfavors over-insertion of carbenes.

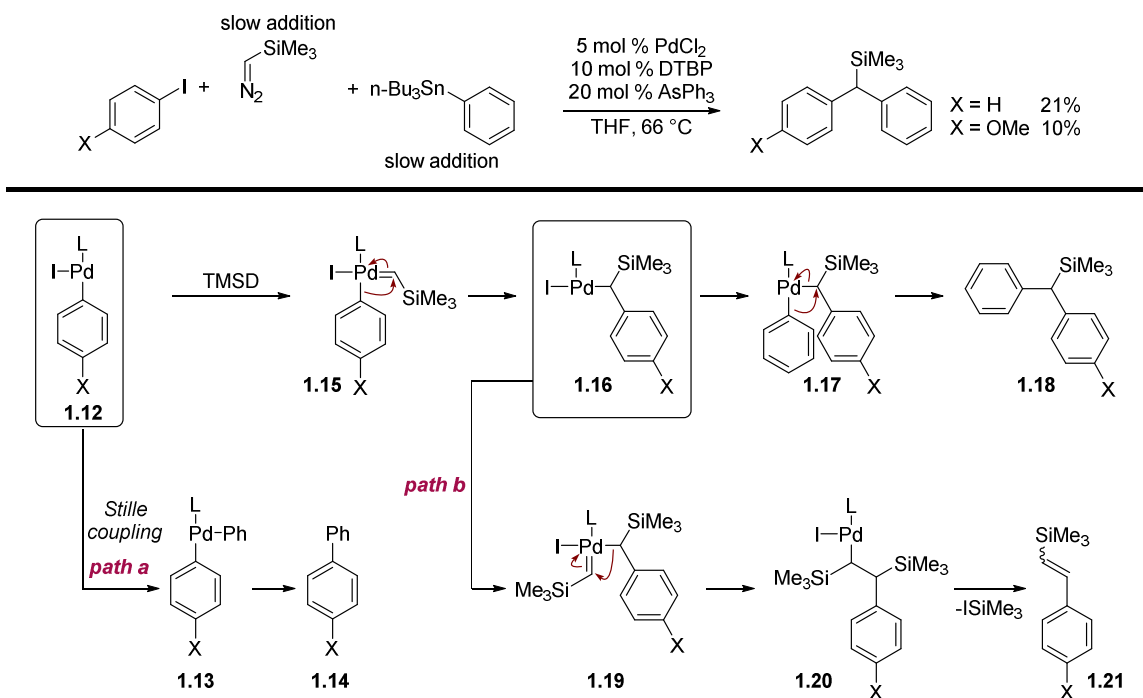
When there are beta hydrogens adjacent to the allyl or benzyl ligand, there is a competition between nucleophilic attack on the ligand and  $\beta$ -hydride elimination (Scheme 1-6). When the  $\eta^1$ -complex is favored, as in the case of  $\eta^1$ -benzylpalladium(II) complex **1.9a**, it is susceptible to  $\beta$ -hydride elimination. However, nucleophilic attack can be favored by high concentrations of nucleophile or by tethered nucleophiles that are poised to attack the  $\eta^3$ -benzylpalladium(II) complex **1.9b**. Three-component carbenylative cross-couplings are most successful when carbene insertion is followed by  $\eta^1$  to  $\eta^3$  isomerization followed by rapid nucleophilic attack by an intramolecular nucleophile.



**Scheme 1-6.** Reaction pathways of  $\eta^3$ -coordinated allyl/benzyl palladium(II) intermediates following a migratory insertion event.

Van Vranken and co-workers were first to report a three-component carbenylative cross-coupling reaction of trimethylsilyldiazomethane (TMSD), aryl iodide and aryl tributylphenylstannane (Scheme 1-7).<sup>6</sup> Since this seminal report, the area of transition-metal

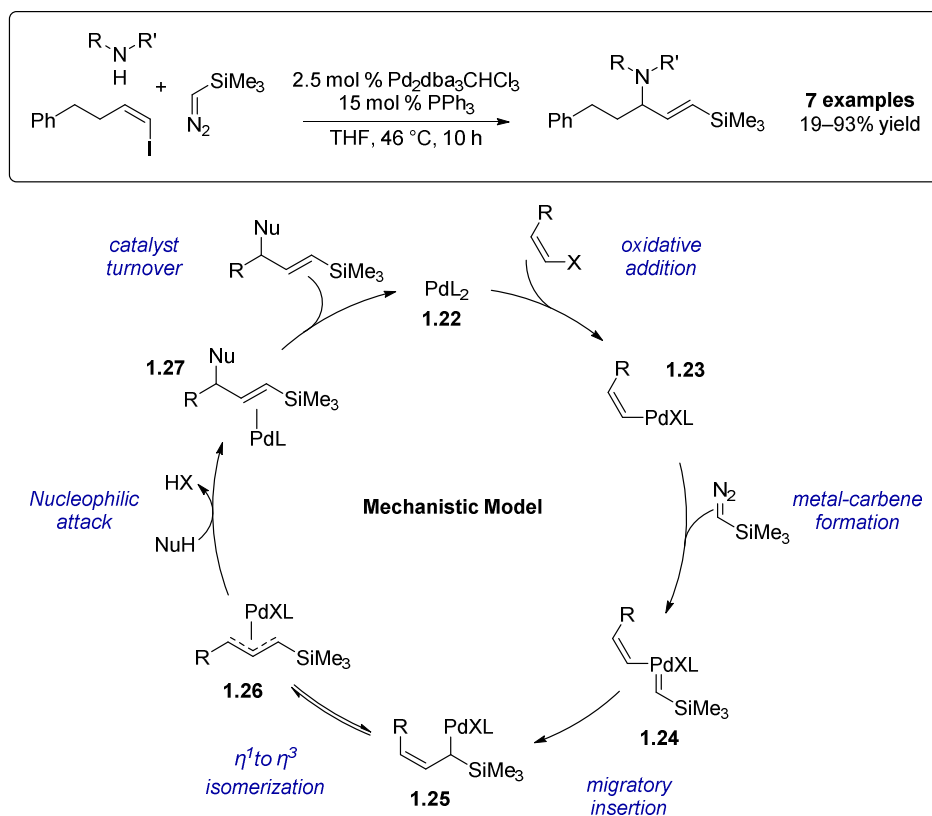
catalyzed carbenylative insertions, as well as palladium-catalyzed carbenylative insertion reactions have been exploited and reviewed.<sup>7</sup> Unfortunately, the utility of the new carbenylative cross-coupling process reported by Van Vranken and co-workers was limited by two competing side reactions: Stille coupling (path **a**) and over-insertion of the diazo compound (path **b**).



**Scheme 1-7.** First three-component carbenylative cross-coupling of aryl iodides, TMSD, and aryl stannane by Van Vranken and co-workers and unwanted reaction pathways.

The Van Vranken group showed that vinyl halides generate  $\eta^3$ -allylpalladium(II) species, after the key migratory insertion, which are then trapped by soft nucleophiles (Scheme 1-8).<sup>8</sup>  $\eta^1$ -Allylpalladium(II) species have typically been accessed through oxidative addition of allyl carbonates and allyl acetates, which can be subsequently trapped by nucleophiles to afford more complex allyl derivatives.<sup>9</sup> Carbenylative insertion provides an alternative way to access these useful intermediates without the need for specialized allyl carbonates or acetates. After oxidative addition of the vinyl halide and addition of the diazo compound to generate palladium(II) carbene

**1.24**, the vinyl anionic ligand migrates to afford  $\eta^1$ -allylpalladium(II) **1.25** which isomerizes to  $\eta^3$ -allylpalladium(II) **1.26**. An external nucleophile then attacks the electrophilic  $\eta^3$ -coordinated allyl ligand to generate, in this example, vinyl silane **1.27**.



**Scheme 1-8.** General mechanism for carbonylative amination accessing  $\eta^3$ -allylpalladium(II) species.

This carbonylative amination was later extended to the use of stabilized carbon nucleophiles (carbonylative alkylation) to afford new derivatives of vinyl silanes<sup>10</sup> and to the use of ethyl diazoacetate (EDA) to access the  $\alpha,\beta$ -unsaturated  $\gamma$ -amino esters.<sup>11</sup> In 2012, the Van Vranken group also demonstrated the versatility of these carbonylative cross-coupling reactions as applied in an intramolecular setting with *N*-tosylhydrazone, a safer diazo precursor.<sup>12</sup> In this

transformation, the resulting  $\eta^3$ -allylpalladium species is trapped by cyclization of a pendant amino group, leading to pyrrolidine and piperidine ring systems.

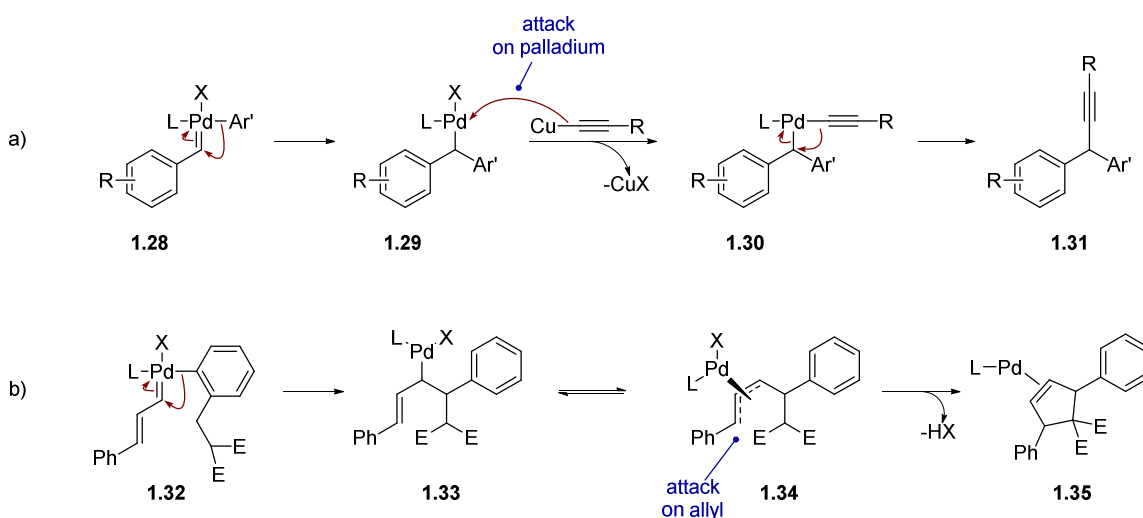
### **Accessing $\eta^3$ -Benzylpalladium Complexes from Carbenylative Insertion**

Analogous cross-coupling processes could be envisioned for  $\pi$ -benzylpalladium(II) complexes. Traditionally,  $\eta^1$ -benzylpalladium intermediates have been accessed similarly to  $\eta^1$ -allyl species – through oxidative addition of palladium to benzyl carbonates, benzyl acetates, or benzyl halides.<sup>13</sup> The isomerization of  $\eta^1$ -benzylpalladium to  $\eta^3$ -benzylpalladium leads to loss of aromaticity, costing up to 36 kcal/mol,<sup>14</sup> but increases the *d* electron count and coordination number of palladium, a thermodynamically favored process when the metal is coordinately unsaturated, as would be the case after a migratory insertion event.<sup>15</sup> This de-aromatization makes  $\eta^3$ -benzylpalladium a powerful electrophile and highly susceptible to nucleophilic attack, as it has a huge driving force to regain aromaticity. Despite the energetic cost of accessing  $\eta^3$ -benzylpalladium, these intermediates have been accessed by oxidative addition and have been intercepted previously with various oxygen, carbon, sulfur, and nitrogen nucleophiles.<sup>16</sup> In 2002, Albéniz and co-workers showed that  $\eta^3$ -benzylpalladium(II) intermediates could be accessed through migratory insertion of carbenes, but not in a catalytic process.<sup>17</sup>

### **Accessing $\eta^3$ -Benzylpalladium Complexes from Carbenylative Insertion to Construct the 1-Arylindane and 1-Aryltetralin Structural Framework**

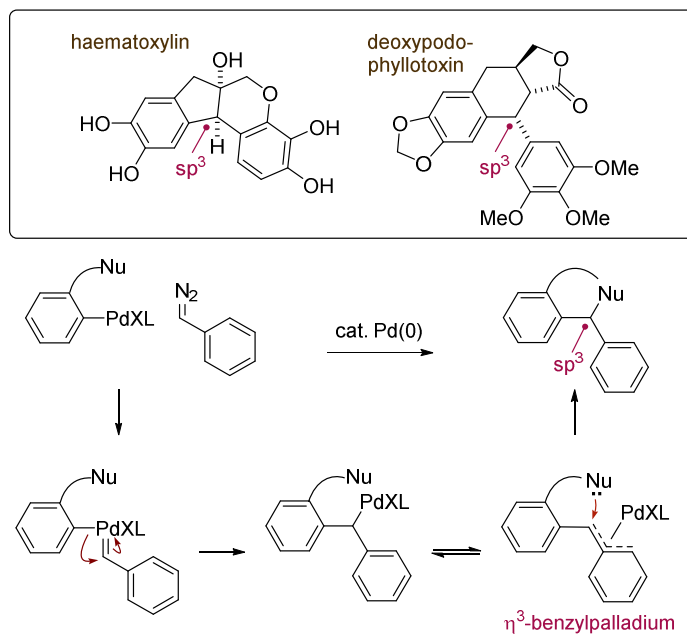
There is growing interest in  $\eta^3$ -benzylpalladium complexes as intermediates in catalytic reactions.<sup>15, 18</sup> Migratory insertion of carbenes have been previously been reported to access  $\eta^1$ -benzylpalladium intermediates that undergo nucleophilic attack on palladium.<sup>6, 19</sup> For example, Wang and co-workers have intercepted  $\eta^1$ -benzylpalladium intermediates without  $\beta$ -hydrogens

through carbene insertion, which then undergo transmetalation with copper acetylides and reductively eliminate (Scheme 1-9a).<sup>20</sup> Alternatively, migratory insertion of carbenes has been used to access  $\eta^3$ -allyl- and  $\eta^3$ -oxaallylpalladium intermediates that are trapped by nucleophilic attack on the ligand.<sup>10, 21</sup> For example, Liang and co-workers have intercepted  $\eta^3$ -allylpalladium intermediates derived from carbene insertion with stabilized enolates that attack the  $\pi$ -allyl ligand to form 5- and 6-membered rings (Scheme 1-9b).<sup>22</sup>



**Scheme 1-9.** Examples of attack on palladium vs on allyl in carbonylative insertion cross-coupling reaction.

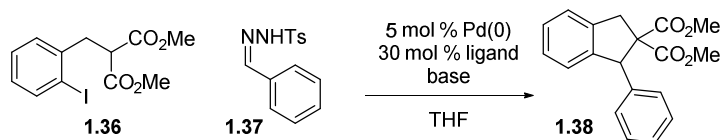
We envisioned that  $\eta^1$ -benzylpalladium intermediates derived from benzylidene insertion could isomerize to  $\eta^3$ -benzylpalladium intermediates that would then be attacked by pendant enolates at the benzylic position to generate highly desirable 1-arylidanes and 1-aryltetralins – common elements of biologically active products.<sup>23</sup> We rationalized that an analogous carbonylative<sup>7d, 24</sup> cyclization would provide the central  $\text{sp}^3$  carbon of 1-arylidanes and 1-aryltetralins through  $\eta^1$ -benzylpalladium that could isomerize to  $\eta^3$ -benzylpalladium intermediates (Scheme 1-10).



**Scheme 1-10.** Access to bicyclic compounds with sp<sup>3</sup> centers

### Intramolecular Carbenylative Cross-Coupling: New [4+1] and [5+1] Carbenylative Processes

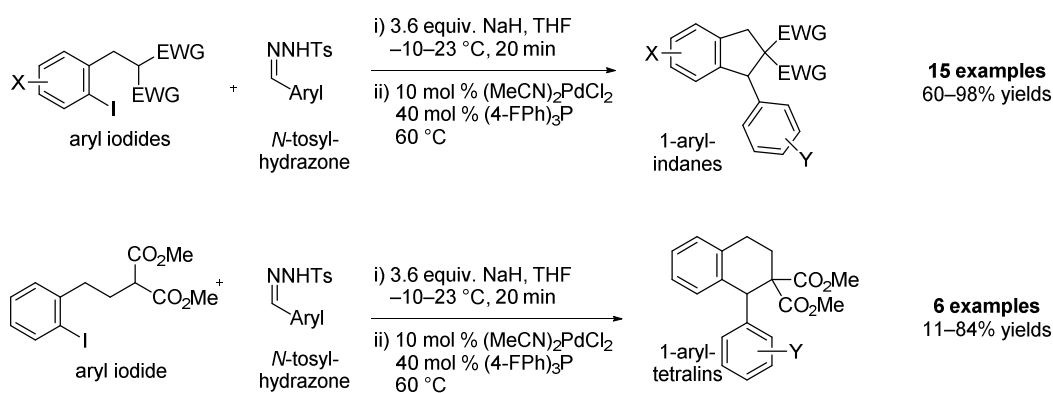
At the time I joined the Van Vranken lab, my colleague Eugene Gutman had explored and optimized the carbenylative cyclization reaction of dimethyl (2-iodobenzyl) malonate **1.36** using the *N*-tosylhydrazone **1.37**, derived from benzaldehyde, as a precursor to phenyldiazomethane (Scheme 1-11).<sup>25</sup>



**Scheme 1-11.** General reaction explored by colleague Eugene Gutman.

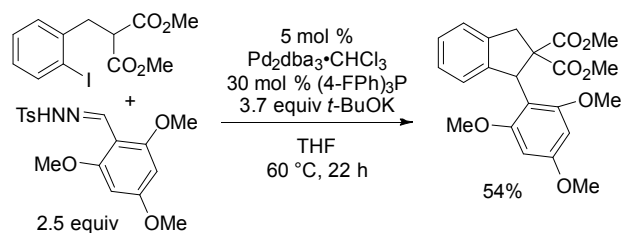


Eugene Gutman found that the best results were obtained with 2 equivalents of the *N*-tosylhydrazone, 3.6 equivalents of 60% NaH, 40 mol% tris-(4-fluorophenyl)phosphine, and a palladium(II) precatalyst at 60 °C in THF. Additionally, the yield was further increased by pre-forming the sodium enolate and sodium *N*-tosylhydrazone salt with sodium hydride. Under the optimized conditions, 1-arylidane **1.38** was formed in 86% yield in 1.5 h. The electronics on the *N*-tosylhydrazone and aryl iodide were explored and led to 15 published examples of 1-arylidanes in 60 to 98% yields (Scheme 1-12).<sup>26</sup> Eugene Gutman also applied the reaction conditions to generate 1-aryltetralins in up to 84% yields (Scheme 1-12); a low yield of 11% resulted from an inefficient crystallization procedure.



**Scheme 1-12.** General published carbonylative reaction to construct 1-arylidanes and 1-aryltetralins.

Extremely hindered benzylidene groups were poorly tolerated under optimized conditions, but under different optimized conditions using potassium *tert*-butoxide, useful yields of 1-arylidane were obtained (Scheme 1-13).

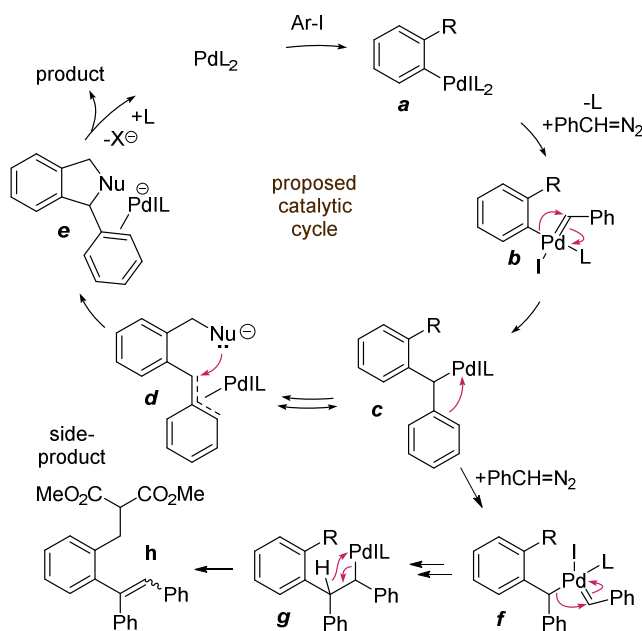


**Scheme 1-13.** Insertion of a highly hindered benzylidene group necessitated different reaction conditions.

The solubility of the *N*-tosylhydrazone anion and the reaction temperature are important factors that determine the rate at which diazo compound is generated in the reaction. *N*-Tosylhydrazones generate diazo compound in situ through a base-catalyzed Bamford-Stevens decomposition.<sup>27</sup> The rate at which the diazo compound is formed differs on the electronic nature of the *N*-tosylhydrazone. *N*-Tosylhydrazones with an electron rich arene generate aryldiazomethanes at a slower rate than when the arene is electron poor.<sup>28</sup> The partial solubility of the *N*-tosylhydrazone anion is a critical factor for the success of the reaction and may lead to some of the observed differences in yields and rates.

Our mechanistic rationale for the reaction involves addition of the diazo compound to arylpalladium iodide **a** to form an arylpalladium carbene intermediate **b** (Scheme 1-14). Migratory insertion of the aryl ligand generates  $\eta^1$ -benzylpalladium iodide intermediate **c**. Direct cross-coupling of the pendant enolate with the  $\eta^1$ -benzylpalladium moiety in intermediate **c** would require a highly unfavorable reductive elimination that is not likely to be facile under our reaction conditions.<sup>29</sup> The  $\eta^1$ -benzylpalladium iodide **c** has two choices. Kuwano has shown that benzhydrylpalladium intermediates couple with malonates through an outer sphere attack on the  $\eta^3$ -benzylhydryl ligand,<sup>13b</sup> so it is expected that the structurally analogous  $\eta^3$ -benzhydrylpalladium

intermediate **d** can undergo 5-*exo*-trig cyclization through an outer sphere mechanism to generate product.

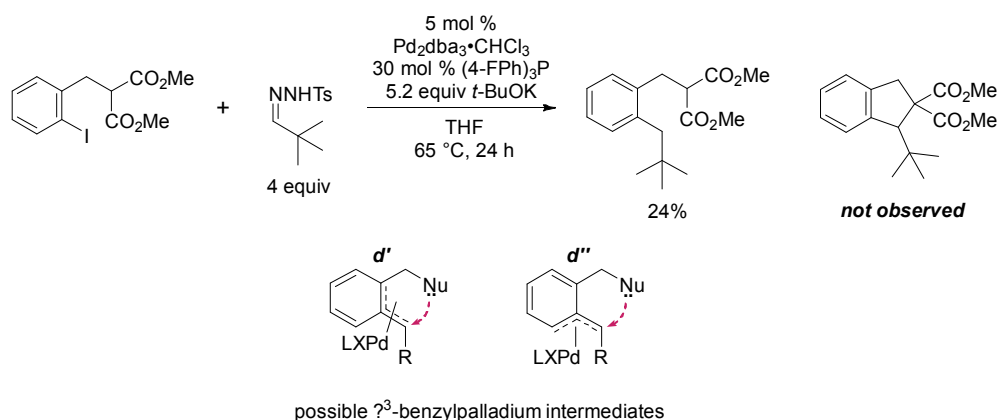


**Scheme 1-14.** Proposed mechanism for carbonylative cyclization and formation of side products.

Other types of  $\eta^3$ -benzylpalladium complexes are possible, but 5-*endo*-trig ring closures onto analogous  $\eta^3$ -allylpalladium intermediates are strongly disfavored.<sup>30</sup> Alternatively,  $\eta^1$ -benzylpalladium intermediate **c** can insert another carbene<sup>31</sup> followed by rapid  $\beta$ -hydride elimination<sup>32</sup> to afford a stilbene side product **h**. However, no tetralin from the  $\eta^3$ -benzylpalladium complex derived from the cyclization of **g** was observed. In some cases, over 10% of stilbene **h** was observed, but through optimization we reduced the formation of stilbene to just a few percent, implying that the desired pathway was at least an order of magnitude faster than the second insertion of the diazo compound.

To probe the intermediacy of  $\eta^3$ -benzylpalladium intermediates other than **d** we attempted to carry out the reaction with the *tert*-butyl-*N*-tosylhydrazone, derived from pivalaldehyde (Scheme 1-15). Insertion product was isolated in low yield, but none of the desired 1-aryllindane

was observed, suggesting that  $\eta^3$ -benzylpalladium intermediates *d'* and *d''* are not viable intermediates.



**Scheme 1-15.** Evidence against alternative  $\eta^3$ -benzylpalladium intermediates.

The 1-aryllindane core is found in the indano[2,1-*c*]chroman class of natural products such as brazilin (Figure 1-1). A high degree of oxygenation is a key feature of this class of compounds. Brazilin is extracted from the heartwood of *Caesalpinia sappan*,<sup>33</sup> and is historically important (Chapter 2). The brazilin rich extracts have long been used in traditional Asian medicine to treat many ailments such as inflammation and blood pressure.<sup>34</sup> Brazilin is now known to exhibit cytotoxicity towards HepG2 and Hep3B cancer cell lines, to act as a micromolar telomerase inhibitor, and to produce nicks in DNA.<sup>35</sup>

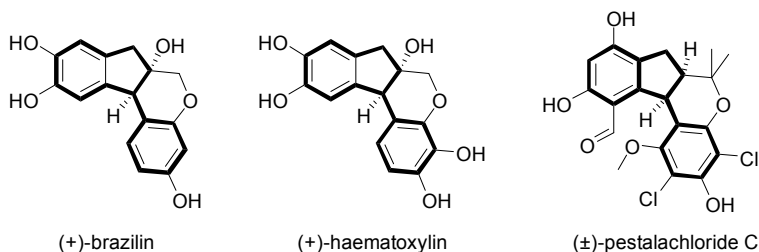
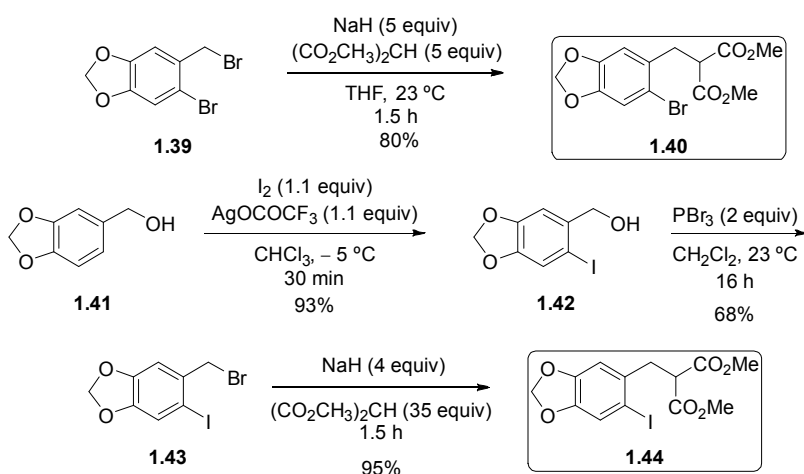


**Figure 1-1.** Examples of brazilin and related compounds sporting the 1-aryllindane structural framework.

The natural product targets accessible using our carbenylative [4+1] and [5+1] insertion processes have high levels of oxygenation on the aromatic rings. Therefore, I synthesized the aryl bromide **1.40** in order to test whether oxygenation on the aryl halide was tolerated under the optimized reaction conditions (Scheme 1-16). Under the reaction conditions, the aryl bromide **1.40** was less efficient (< 20% yields determined by <sup>1</sup>H NMR of desired 1-arylidane) which led us to conclude that the low reactivity was due to sluggish oxidative addition of palladium to aryl bromide.<sup>36</sup> To determine if this was the case, I synthesized aryl iodide **1.44** (Scheme 1-16).



**Scheme 1-16.** Synthesis of oxygenated aryl halides to test in the carbenylative insertion reaction.

Dramatically improved results were obtained by using aryl iodide **1.44** in the carbenylative insertion process. I obtained 1-arylidanes **1.45–1.47** in great yields and reasonable reaction times (Figure 1-2).

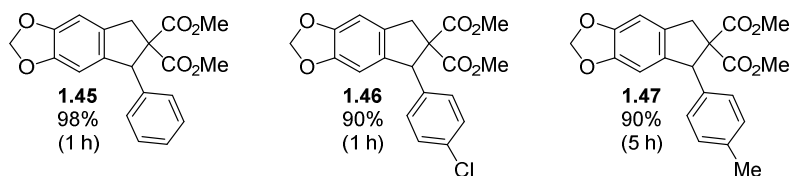


**Figure 1-2.** Synthesized 1-arylidanes from aryl iodide **1.44**.

In summary, we developed a palladium-catalyzed carbenylative cyclization reaction that generates 1-arylindanes and 1-aryltetralins in good yields. The reaction generates  $sp^3$  centers through a mechanism involving the alkylation of an  $\eta^3$ -benzylpalladium complex. Having shown that oxygenated 1-arylindanes are accessible with this carbenylative insertion reaction I was now ready to apply this powerful reaction to the total synthesis of indano[2,1-*c*]chroman natural products.

## References

1. (a) Armstrong, R. K. Decomposition of Ethyl Diazoacetate by a  $\pi$ -Allylic Palladium Chloride Complex. *J. Org. Chem.* **1966**, *31*, 618–620; (b) Martin, C.; Molina, F.; Alvarez, E.; Belderrain, T. R. Stable *N*-heterocyclic carbene (NHC)-palladium(0) complexes as active catalysts for olefin cyclopropanation reactions with ethyl diazoacetate. *Chemistry* **2011**, *17*, 14885–14895; (c) Anciaux, A. J.; Hubert, A. J.; Noels, A. F.; Petiniot, N.; Teyssie, P. Transition-metal-catalyzed reactions of diazo compounds. 1. Cyclopropanation of double bonds. *J. Org. Chem.* **1980**, *45*, 695–702; (d) Shishilov, O. N.; Stromnova, T. A.; Campora, J.; Palma, P.; Cartes, M. A.; Martinez-Prieto, L. M. Palladium(II) carboxylates and palladium(I) carbonyl carboxylate complexes as catalysts for olefin cyclopropanation with ethyl diazoacetate. *Dalton Trans* **2009**, 6626–6633; (e) Yang, F.; Zhang, Y.-M.; Qiu, W.-W.; Tang, J.; He, M.-Y. Immobilization of Pd(II) Catalysts for Cyclopropanation in Ionic Liquid. *Chin. J. Chem.* **2002**, *20*, 114–116; (f) Lakshmi Kantam, M.; Haritha, Y.; Mahender Reddy, N.; Choudary, B. M.; Figueras, F. Cyclopropanation of Olefins Using a Silica Gel Anchored Palladium Phosphine Complex. *Catal. Lett.* **2002**, *83*, 187–190; (g) Majchrzak, M. W.; Kotełko, A.; Lambert, J. B. Palladium(II) Acetate, an Efficient Catalyst for Cyclopropanation Reactions with Ethyl Diazoacetate. *Synthesis* **1983**, *1983*, 469–470; (h) Doyle, M. P.; Dorow, R. L.; Buhro, W. E.; Griffin, J. H.; Tamblyn, W. H.; Trudell, M. L. Stereoselectivity of catalytic cyclopropanation reactions. Catalyst dependence in reactions of ethyl diazoacetate with alkenes. *Organometallics* **1984**, *3*, 44–52; (i) Doyle, M. P.; Van Leusen, D.; Tamblyn, W. H. Efficient Alternative Catalysts and Methods for the Synthesis of Cyclopropanes from Olefins and Diazo Compounds. *Synthesis* **1981**, *1981*, 787–789; (j) Taber, D. F.; Amedio, J. C.; Sherrill, R. G. Palladium-mediated diazo insertions: preparation of 3-alkyl-2-carbomethoxycyclopetenones. *J. Org. Chem.* **1986**, *51*, 3382–3384; (k) Maas, G., Transition-metal catalyzed decomposition of aliphatic diazo compounds — New results and applications in organic synthesis. In *Organic Synthesis, Reactions and Mechanisms. Topics in Current Chemistry, vol 137.*, Springer: Berlin, Heidelberg, 1987; pp 75–253; (l) Tomilov, Y. V.; Dokichev, V. A.; Dzhemilev, U. M.; Nefedov, O. M. Catalytic decomposition of diazomethane as a general method for the methylenation of chemical compounds. *Russ. Chem. Rev.* **1993**, *62*, 799–838; (m) Tomilov, Y. V.; Bordakov, V. G.; Dolgii, I. E.; Nefedov, O. M. Reaction of diazoalkanes with unsaturated compounds. Communication 2. Cyclopropanation of olefins by diazomethane in the presence of palladium compounds. *Russ. Chem. Bull.* **1984**, *33*, 533–538; (n) Dzhemilev, U. M.; Dokichev, V. A.; Mайданова, I. O.; Nefedov, O. M.; Tomilov, Y. V. Interaction of diazoalkanes with unsaturated compounds. 12. Stereochemistry of cyclopropanation of norbornenes with diazomethane in the presence of transition metal complexes. *Russ. Chem. Bull.* **1993**, *42*, 697–700; (o) Dzhemilev, U. M.; Dokichev, V. A.; Sultanov, S. Z.; Khusnutdinov, R. I.; Tomilov, Y. V.; Nefedov, O. M.; Tolstikov, G. A. Reactions of diazoalkanes with unsaturated compounds. 6. Catalytic cyclopropanation of unsaturated hydrocarbons and their derivatives with diazomethane. *Russ. Chem. Bull.* **1989**, *38*, 1707–1714; (p) Denmark, S. E.; Stavenger, R. A.; Faucher, A. M.; Edwards, J. P. Cyclopropanation with Diazomethane and Bis(oxazoline)palladium(II) Complexes. *J. Org. Chem.* **1997**, *62*, 3375–3389.

2. (a) Nakamura, A.; Koyama, T.; Otsuka, S. Some Aspects on the Mechanism of Palladium-complex-catalyzed Decomposition of and Cyclopropanation with Ethyl Diazoacetate. *Bull. Chem. Soc. Jpn.* **1978**, *51*, 593–595; (b) Bernardi, F.; Bottoni, A.; Miscione, G. P. DFT Study of the Palladium-Catalyzed Cyclopropanation Reaction. *Organometallics* **2001**, *20*, 2751–2758; (c) Rodríguez-García, C.; Oliva, A.; Ortuño, R. M.; Branchadell, V. Mechanism of olefin cyclopropanation by diazomethane catalyzed by palladium dicarboxylates: a density functional study. *J. Am. Chem. Soc.* **2001**, *123*, 6157–6163; (d) Rodríguez-García, C.; González-Blanco, Ò.; Oliva, A.; Ortuño, R. M.; Branchadell, V. Density Functional Study of Possible Intermediates in the Mechanism of Olefin Cyclopropanation Catalyzed by Metal Carboxylates. *Eur. J. Inorg. Chem.* **2000**, *2000*, 1073–1078; (e) Illa, O.; Rodríguez-García, C.; Acosta-Silva, C.; Favier, I.; Picurelli, D.; Oliva, A.; Gómez, M.; Branchadell, V.; Ortuño, R. M. Cyclopropanation of Cyclohexenone by Diazomethane Catalyzed by Palladium Diacetate: Evidence for the Formation of Palladium(0) Nanoparticles. *Organometallics* **2007**, *26*, 3306–3314; (f) Berthon-Gelloz, G.; Marchant, M.; Straub, B. F.; Marko, I. E. Palladium-catalyzed cyclopropanation of alkenyl silanes by diazoalkanes: evidence for a Pd(0) mechanism. *Chemistry* **2009**, *15*, 2923–2931; (g) Straub, B. F. Pd(0) mechanism of palladium-catalyzed cyclopropanation of alkenes by CH<sub>2</sub>N<sub>2</sub>: a DFT study. *J. Am. Chem. Soc.* **2002**, *124*, 14195–14201.
3. Hegedus, L. S., *Transition Metals in the Synthesis of Complex Organic Molecules*. 2<sup>nd</sup> ed.; University of Science Books: Sausalito, 1999.
4. (a) Yamamoto, A.; Ozawa, F.; Osakada, K.; Huang, L.; Son, T.; Kawasaki, N.; Doh, M. K. Mechanisms of double and single carbonylation reactions catalyzed by palladium complexes. *Pure Appl. Chem.* **1991**, *63*, 687–696; (b) Chen, J. T.; Sen, A. Mechanism of transition-metal-catalyzed double carbonylation reactions. Synthesis and reactivity of benzoylformyl complexes of palladium(II) and platinum(II). *J. Am. Chem. Soc.* **1984**, *106*, 1506–1507.
5. (a) Ihara, E.; Kida, M.; Fujioka, M.; Haida, N.; Itoh, T.; Inoue, K. Palladium-mediated copolymerization of diazocarbonyl compounds with phenyldiazomethane. *J. Polym. Sci., Part A: Polym. Chem.* **2007**, *45*, 1536–1545; (b) Ihara, E.; Haida, N.; Iio, M.; Inoue, K. Palladium-Mediated Polymerization of Alkyl Diazoacetates To Afford Poly(alkoxycarbonylmethylene)s. First Synthesis of Polymethylenes Bearing Polar Substituents. *Macromolecules* **2003**, *36*, 36–41.
6. Greenman, K. L.; Carter, D. S.; Van Vranken, D. L. Palladium-catalyzed insertion reactions of trimethylsilyldiazomethane. *Tetrahedron* **2001**, *57*, 5219–5225.
7. (a) Franssen, N. M. G.; Walters, A. J. C.; Reek, J. N. H.; de Bruin, B. Carbene insertion into transition metal–carbon bonds: a new tool for catalytic C–C bond formation. *Catal. Sci. Technol.* **2011**, *1*, 153–165; (b) Zhang, Y.; Wang, J. Recent Developments in Pd-Catalyzed Reactions of Diazo Compounds. *Eur. J. Org. Chem.* **2011**, *2011*, 1015–1026; (c) Xia, Y.; Qiu, D.; Wang, J. Transition-Metal-Catalyzed Cross-Couplings through Carbene Migratory Insertion. *Chem. Rev.* **2017**, *117*, 13810–13889; (d) Xia, Y.; Zhang, Y.; Wang, J. Catalytic Cascade Reactions Involving Metal Carbene Migratory Insertion. *ACS Catal.* **2013**, *3*, 2586–2598; (e) Albéniz, A. C. Reactive Palladium Carbenes: Migratory Insertion and Other Carbene-Hydrocarbyl Coupling Reactions on Well-Defined Systems. *Eur. J. Inorg. Chem.* **2018**, *2018*, 3693–3705; (f) Wang, J.; Wang, K. Transition-Metal-Catalyzed Cross-Coupling with Non-Diazo Carbene Precursors. *Synlett* **2018**, *30*, 542–



- 551; (g) Biemolt, J.; Ruijter, E. Advances in Palladium-Catalyzed Cascade Cyclizations. *Adv. Synth. Catal.* **2018**, *360*, 3821–3871; (h) Shao, Z.; Zhang, H. *N*-tosylhydrazones: versatile reagents for metal-catalyzed and metal-free cross-coupling reactions. *Chem. Soc. Rev.* **2012**, *41*, 560–572; (i) Xiao, Q.; Zhang, Y.; Wang, J. Diazo compounds and *N*-tosylhydrazones: novel cross-coupling partners in transition-metal-catalyzed reactions. *Acc. Chem. Res.* **2013**, *46*, 236–247.
8. Devine, S. K.; Van Vranken, D. L. Palladium-catalyzed carbene insertion into vinyl halides and trapping with amines. *Org. Lett.* **2007**, *9*, 2047–2049.
  9. Negishi, E.-i., *Handbook of Organopalladium Chemistry for Organic Synthesis*. John Wiley & Sons, Inc.: New York, USA, 2002; Vol. 1 and 2.
  10. Devine, S. K.; Van Vranken, D. L. Palladium-catalyzed carbene insertion and trapping with carbon nucleophiles. *Org. Lett.* **2008**, *10*, 1909–1911.
  11. Kudirka, R.; Devine, S. K.; Adams, C. S.; Van Vranken, D. L. Palladium-catalyzed insertion of  $\alpha$ -diazoesters into vinyl halides to generate  $\alpha,\beta$ -unsaturated  $\gamma$ -amino esters. *Angew. Chem. Int. Ed.* **2009**, *48*, 3677–3680.
  12. Khanna, A.; Maung, C.; Johnson, K. R.; Luong, T. T.; Van Vranken, D. L. Carbenylative amination with *N*-tosylhydrazones. *Org. Lett.* **2012**, *14*, 3233–3235.
  13. (a) Legros, J. Y.; Toffano, M.; Fiaud, J. C. Palladium-Catalyzed Substitution of Esters of Naphthylmethanols, 1-Naphthylethanols, and Analogs by Sodium Dimethyl Malonate - Stereoselective Synthesis from Enantiomerically Pure Substrates. *Tetrahedron* **1995**, *51*, 3235–3246; (b) Kuwano, R.; Kusano, H. Palladium-catalyzed nucleophilic substitution of diarylmethyl carbonates with malonate carbanions. *Chem. Lett.* **2007**, *36*, 528–529; (c) McLaughlin, M. Suzuki-Miyaura cross-coupling of benzylic phosphates with arylboronic acids. *Org. Lett.* **2005**, *7*, 4875–4878.
  14. Wheland, G. W., *Resonance in Organic Chemistry*. Wiley: New York, 1955.
  15. Kuwano, R. Catalytic Transformations of Benzylic Carboxylates and Carbonates. *Synthesis* **2009**, *2009*, 1049–1061.
  16. (a) Kuwano, R.; Kusano, H. Benzyl protection of phenols under neutral conditions: Palladium-catalyzed benzylations of phenols. *Org. Lett.* **2008**, *10*, 1979–1982; (b) Kuwano, R.; Kondo, Y.; Matsuyama, Y. Palladium-catalyzed nucleophilic benzylic substitutions of benzylic esters. *J. Am. Chem. Soc.* **2003**, *125*, 12104–12105; (c) Kuwano, R.; Kondo, Y.; Shirahama, T. Transformation of carbonates into sulfones at the benzylic position via palladium-catalyzed benzylic substitution. *Org. Lett.* **2005**, *7*, 2973–2975; (d) Legros, J.-Y.; Fiaud, J.-C. Palladium-catalyzed nucleophilic substitution of naphthylmethyl and 1-naphthylethyl esters. *Tetrahedron Lett.* **1992**, *33*, 2509–2510.
  17. Albéniz, A. C.; Espinet, P.; Manrique, R.; Pérez-Mateo, A. Observation of the Direct Products of Migratory Insertion in Aryl Palladium Carbene Complexes and Their Subsequent Hydrolysis. *Angew. Chem. Int. Ed.* **2002**, *41*, 2363–2366.
  18. (a) Trost, B. M.; Czabaniuk, L. C. Structure and reactivity of late transition metal  $\eta^3$ -benzyl complexes. *Angew. Chem. Int. Ed.* **2014**, *53*, 2826–2851; (b) Liegault, B.; Renaud, J. L.; Bruneau, C. Activation and functionalization of benzylic derivatives by palladium catalysts. *Chem. Soc. Rev.* **2008**, *37*, 290–299.
  19. Chen, Z. S.; Duan, X. H.; Zhou, P. X.; Ali, S.; Luo, J. Y.; Liang, Y. M. Palladium-catalyzed divergent reactions of  $\alpha$ -diazocarbonyl compounds with allylic esters: construction of quaternary carbon centers. *Angew. Chem. Int. Ed.* **2012**, *51*, 1370–1374.

20. (a) Zhou, L.; Ye, F.; Zhang, Y.; Wang, J. Pd-catalyzed three-component coupling of *N*-tosylhydrazone, terminal alkyne, and aryl halide. *J. Am. Chem. Soc.* **2010**, *132*, 13590–13591; (b) Xia, Y.; Hu, F.; Liu, Z.; Qu, P.; Ge, R.; Ma, C.; Zhang, Y.; Wang, J. Palladium-catalyzed diarylmethyl C(sp<sup>3</sup>)-C(sp<sup>2</sup>) bond formation: a new coupling approach toward triarylmethanes. *Org. Lett.* **2013**, *15*, 1784–1787.
21. Zhou, P. X.; Luo, J. Y.; Zhao, L. B.; Ye, Y. Y.; Liang, Y. M. Palladium-catalyzed insertion of *N*-tosylhydrazones for the synthesis of isoindolines. *Chem. Commun.* **2013**, *49*, 3254–3256.
22. Ye, Y. Y.; Zhou, P. X.; Luo, J. Y.; Zhong, M. J.; Liang, Y. M. Palladium-catalyzed insertion of  $\alpha,\beta$ -unsaturated *N*-tosylhydrazones and trapping with carbon nucleophiles. *Chem. Commun.* **2013**, *49*, 10190–10192.
23. (a) Prat, L.; Mojovic, L.; Levacher, V.; Dupas, G.; Quéguiner, G.; Bourguignon, J. Deracemization of diarylmethanes via lateral lithiation–protonation sequences by means of sparteine. *Tetrahedron: Asymmetry* **1998**, *9*, 2509–2516; (b) Acheson, R. M.; MacPhee, K. E.; Philpott, P. G.; Barltrop, J. A. 140. Compounds of potential pharmacological interest. Part II. Some heterocyclic and carbocyclic systems related to 1-phenylindane. *J. Chem. Soc.* **1956**, 698–705; (c) Saxena, D. B. Phenyl indane from acorus calamus. *Phytochemistry* **1986**, *25*, 553–555; (d) Barltrop, J. A.; Dodsworth, R. F. 141. Compounds of potential pharmacological interest. Part III. 2-Substituted 1-phenylindanes. *J. Chem. Soc.* **1956**, 706–708; (e) Ishii, H.; Koyama, H.; Hagiwara, K.; Miura, T.; Xue, G.; Hashimoto, Y.; Kitahara, G.; Aida, Y.; Suzuki, M. Synthesis and biological evaluation of deoxy-hematoxylin derivatives as a novel class of anti-HIV-1 agents. *Bioorg. Med. Chem. Lett.* **2012**, *22*, 1469–1474; (f) Vitale, M.; Prestat, G.; Lopes, D.; Madec, D.; Kammerer, C.; Poli, G.; Girnita, L. New picropodophyllin analogs via palladium-catalyzed allylic alkylation-Hiyama cross-coupling sequences. *J. Org. Chem.* **2008**, *73*, 5795–5805.
24. Liu, Z.; Wang, J. Cross-coupling reactions involving metal carbene: from C=C/C–C bond formation to C–H bond functionalization. *J. Org. Chem.* **2013**, *78*, 10024–10030.
25. (a) Aggarwal, V. K.; Alonso, E.; Hynd, G.; Lydon, K. M.; Palmer, M. J.; Porcelloni, M.; Studley, J. R. Catalytic Asymmetric Synthesis of Epoxides from Aldehydes Using Sulfur Ylides with In Situ Generation of Diazocompounds. *Angew. Chem. Int. Ed.* **2001**, *40*, 1430–1433; (b) Barluenga, J.; Valdes, C. Tosylhydrazones: new uses for classic reagents in palladium-catalyzed cross-coupling and metal-free reactions. *Angew. Chem. Int. Ed.* **2011**, *50*, 7486–7500.
26. Gutman, E. S.; Arredondo, V.; Van Vranken, D. L. Cyclization of  $\eta^3$ -Benzylpalladium Intermediates Derived from Carbene Insertion. *Org. Lett.* **2014**, *16*, 5498–5501.
27. Bamford, W. R.; Stevens, T. S. 924. The Decomposition of Toluene-*p*-sulphonylhydrazones by Alkali. *J. Chem. Soc.* **1952**, 4735–4740.
28. Davies, H. W.; Schwarz, M. The Effects of Hydrogen Bonding on the Absorption Spectra of Some Substituted Benzaldehyde Tosylhydrazone Anions. *J. Org. Chem.* **1965**, *30*, 1242–1244.
29. (a) Beare, N. A.; Hartwig, J. F. Palladium-catalyzed arylation of malonates and cyanoesters using sterically hindered trialkyl- and ferrocenyldialkylphosphine ligands. *J. Org. Chem.* **2002**, *67*, 541–555; (b) Wolkowski, J. P.; Hartwig, J. F. Generation of Reactivity from Typically Stable Ligands: C–C Bond-Forming Reductive Elimination from Aryl Palladium(II) Complexes of Malonate Anions. *Angew. Chem. Int. Ed.* **2002**, *41*, 4289–4291.

30. (a) Hashimoto, S.; Shinoda, T.; Ikegami, S. A Novel Lithium Iodide-Promoted Vinylcyclopropane-Cyclopentene Rearrangement: Efficient Synthesis of Bicyclo[3.3.0]oct-6-en-2-one, Versatile Building Block for Polycyclopentanoid Natural Products. *Tetrahedron Lett.* **1986**, *27*, 2885–2888; (b) Thorimbert, S.; Malacria, M. Silicon Effect Favoring the Formation of a Cyclopentene via Palladium-Catalyzed 5-*Endo-trig* Cyclisation. *Tetrahedron Lett.* **1998**, *39*, 9659–9660.
31. (a) Greenman, K. L.; Van Vranken, D. L. Palladium-catalyzed carbene insertion into benzyl bromides. *Tetrahedron* **2005**, *61*, 6438–6441; (b) Yu, W. Y.; Tsoi, Y. T.; Zhou, Z.; Chan, A. S. Palladium-catalyzed cross coupling reaction of benzyl bromides with diazoesters for stereoselective synthesis of (*E*)- $\alpha,\beta$ -diarylacrylates. *Org. Lett.* **2009**, *11*, 469–472; (c) Kudirka, R.; Van Vranken, D. L. Cyclization reactions involving palladium-catalyzed carbene insertion into aryl halides. *J. Org. Chem.* **2008**, *73*, 3585–3588.
32. (a) Barluenga, J.; Moriel, P.; Valdes, C.; Aznar, F. *N*-tosylhydrazones as reagents for cross-coupling reactions: a route to polysubstituted olefins. *Angew. Chem. Int. Ed.* **2007**, *46*, 5587–5590; (b) Barluenga, J.; Tomas-Gamasa, M.; Aznar, F.; Valdes, C. Synthesis of Dienes by Palladium-Catalyzed Couplings of Tosylhydrazones with Aryl and Alkenyl Halides. *Adv. Synth. Catal.* **2010**, *352*, 3235–3240.
33. Wang, X.; Zhang, H.; Yang, X.; Zhao, J.; Pan, C. Enantioselective total synthesis of (+)-brazilin, (-)-brazilein and (+)-brazilide A. *Chem. Commun.* **2013**, *49*, 5405–5407.
34. Min, B. S.; Cuong, T. D.; Hung, T. M.; Min, B. K.; Shin, B. S.; Woo, M. H. Compounds from the Heartwood of *Caesalpinia sappan* and their Anti-inflammatory Activity. *Bioorg. Med. Chem. Lett.* **2012**, *22*, 7436–7439.
35. (a) Yen, C. T.; Nakagawa-Goto, K.; Hwang, T. L.; Wu, P. C.; Morris-Natschke, S. L.; Lai, W. C.; Bastow, K. F.; Chang, F. R.; Wu, Y. C.; Lee, K. H. Antitumor agents. 271: Total synthesis and evaluation of brazilein and analogs as anti-inflammatory and cytotoxic agents. *Bioorg. Med. Chem. Lett.* **2010**, *20*, 1037–1039; (b) Woongchon, M.; Hyun-Tai, L.; Kang-Hoon, J.; Hye-Young, C.; Eun-Kyoung, S. A DNA Strand-Nicking Principle of a Higher Plant, *Caesalpinia sappan*. *Arch. Pharm. Res.* **2003**, *26*, 147–150.
36. Jutand, A.; Mosleh, A. Rate and Mechanism of Oxidative Addition of Aryl Triflates to Zerovalent Palladium Complexes - Evidence for the Formation of Cationic ( $\sigma$ -Aryl)Palladium Complexes. *Organometallics* **1995**, *14*, 1810–1817.

## Chapter 2

### Total Synthesis of the Indano[2,1-*c*]chroman, (±)-Brazilin, via Palladium-Carbenylative Cross-Coupling Reaction

#### Homoisoflavonoids of the Indano[2,1-*c*]chroman Structural Type from the Fabaceae

##### Family of Plants

Indano[2,1-*c*]chromans of the *Caesalpinia* and *Haematoxylum* spp. of the *Fabaceae* family of plants, are deeply rooted in the history of dyes and traditional oriental medicine. As early as the 2<sup>nd</sup> century BC, indano[2,1-*c*]chromans, present in the extracts of the heartwood of sappanwood (*Caesalpinia sappan*) from Asia and the Pacific Islands, of brazilwood (*Caesalpinia echinata*) from Brazil, and of logwood (*Haematoxylum campechianum*) from South America, have been sought after for their rich red color or medicinal properties.<sup>1</sup>

The extracts of these plants are rich in homoisoflavonoids, which are phenolic compounds found in nature and whose isolation have been restricted to a small number of plant families – Hyacinthaceae, Liliaceae, Asparagaceae, Agavaceae, Polygonaceae, and Fabaceae.<sup>2</sup>

The term homoisoflavonoid was first used by Böhler and Tamm in 1967 to describe the structure of eucomin and eucomol (Figure 2-1).<sup>3</sup> These two new natural products isolated from *Eucomis bicolor* Bak. (Asparagaceae) differed from the general isoflavonoid structure by an additional carbon unit. The term, homoisoflavonoid, however, has been scrutinized. Dewick, in 1973, conducted labeling experiments suggesting that the biosynthesis of eucomin involved addition of an extra carbon unit into a C<sub>15</sub> skeleton like that of a chalcone, which stems from a general flavonoid structure.<sup>4</sup> Dewick states, “The formation of isoflavonoid compounds in Nature

involves a characteristic 1,2-aryl migration step, but no such rearrangement occurs during the biosynthesis of eucomin. The ‘homoisoflavonoids’ seem to represent a further modification of the unrearranged flavonoid skeleton.”

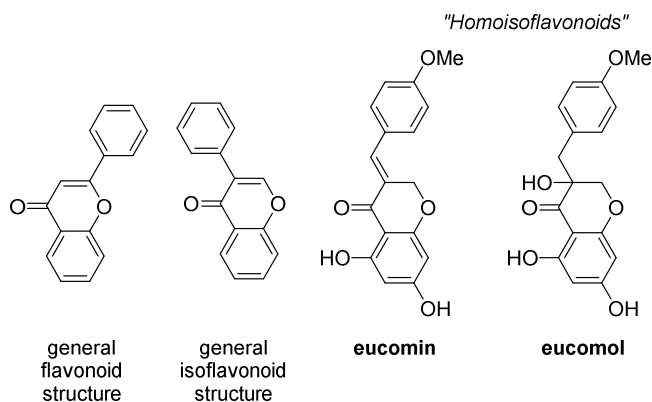


**Figure 2-1.** Homoisoflavonoid term coined to describe eucomin and eucomol structures.

This biosynthetic association between eucomin and chalcones proposed by Dewick’s feeding experiments in 1975, prompted efforts to devise a naming system that would clearly classify all homoisoflavonoids as stemming from flavonoid or chalcone skeletons.<sup>2, 5</sup>

In 2014, Lin and co-workers provided a more complete classification of homoisoflavonoids that has been adopted recently. These new “homoisoflavonoid” phenolic compounds were further classified into five different molecular scaffolds – sappanin-type (I), scillascillin-type (II), brazilin-type (III), caesalpin-type (IV), and protosappanin-type (V) (Figure 2-2).<sup>2, 6</sup> Under this new classification, eucomin and eucomol would fall under the category of sappanin-type homoisoflavonoid.

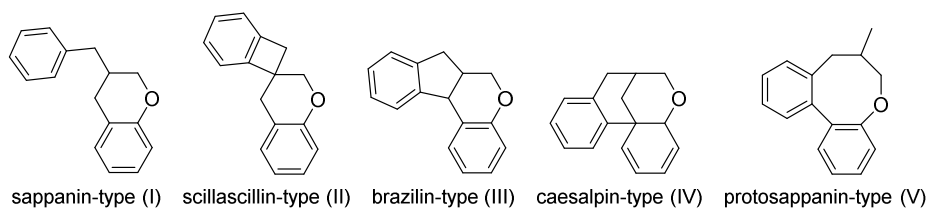


**Figure 2-2.** Structural classification of homoisoflavonoids isolated from *Caesalpinia* and *Haematoxylum* spp. of Fabaceae plant family.

In this text, the brazilin-type (III) structural class of the homoisoflavonoids isolated from the *Caesalpinia* and *Haematoxylum* spp. of the Fabaceae plant family will be described as indano[2,1-*c*]chromans (Figure 2-3).

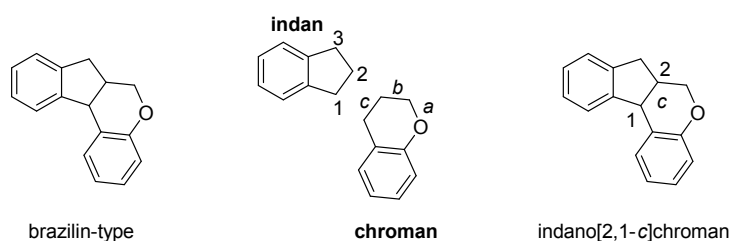


**Figure 2-3.** Indano[2,1-*c*]chroman term used to describe brazilin-type structural framework.

The plant-based indano[2,1-*c*]chromans, (+)-brazilin,<sup>7a</sup> (+)-3'-*O*-methylbrazilin,<sup>7</sup> (±)-4'-*O*-methylbrazilin,<sup>7</sup> (+)-brazilane,<sup>7b</sup> caesalpiniafenol E,<sup>7b</sup> and neoprotosappanin<sup>8</sup> have mainly been isolated from the heartwood of *Caesalpinia sappan*, while (-)-isohaematoxylin,<sup>9</sup> and (+)-haematoxylin – still used as a common cell stain – have mainly been isolated from the heartwood of *Haematoxylum campechianum* (Figure 2-4). Others, like the protosappanins<sup>8a, 10</sup> have been isolated from both species of plants.

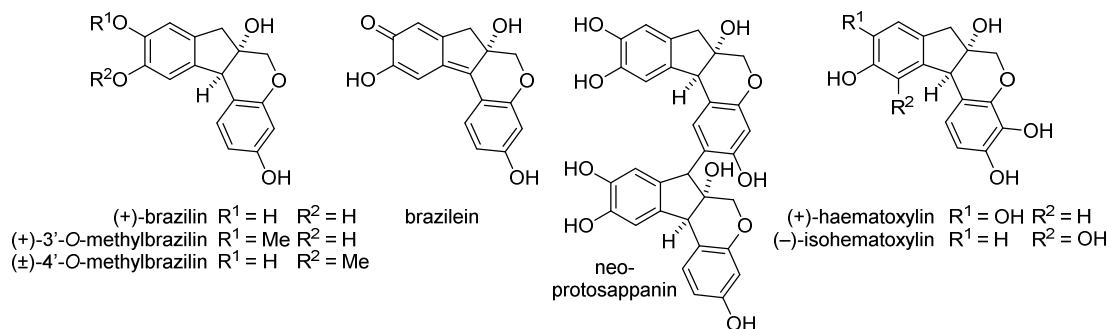
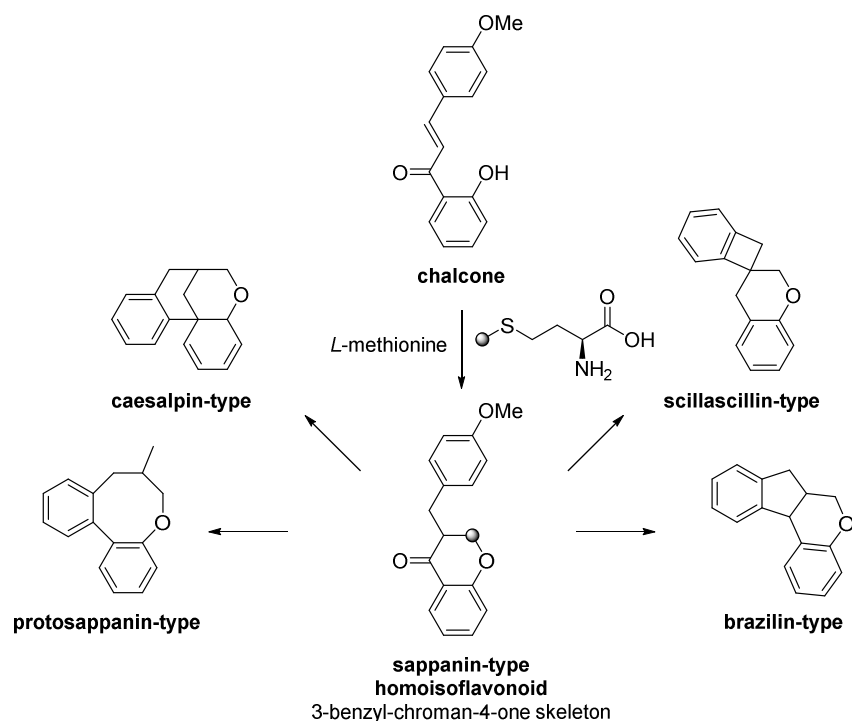


**Figure 2-4.** Plant-based indano[2,1-*c*]chromans isolated from *Caesalpinia* and *Haematoxylum* spp.

### Proposed Biosynthetic Pathway of Homoisflavonoids of the Indano[2,1-*c*]chroman

#### Structure<sup>2, 4-6, 9, 11</sup>

The biosynthetic pathway for formation of these indano[2,1-*c*]chromans are widely believed to arise from the C<sub>15</sub> chalcone biosynthetic pathway and a central sappanin-type homoisflavonoid key unit, 3-benzylchroman-4-one (Scheme 2-1).<sup>5-6</sup> The additional carbon unit distinguishing chalcones from the sappanin-type homoisflavonoid nucleus is believed to originate from the methyl group of methionine – a belief that has been supported by feeding experiments performed by Dewick.<sup>4-5, 11a, 12</sup> In the presence of methionine, chalcones can generate the sappanin-type homoisflavonoid nucleus.

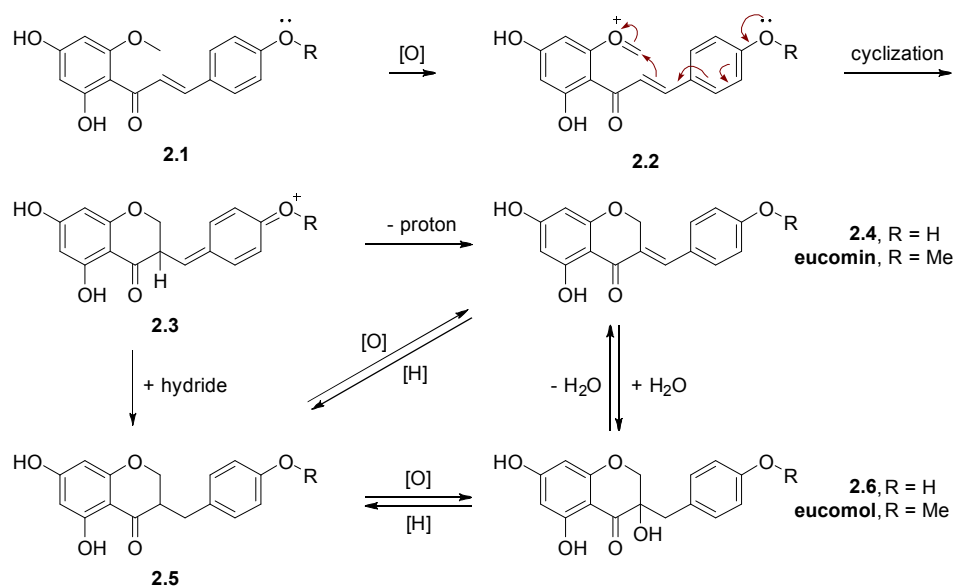


**Scheme 2-1.** Biosynthesis of chalcones provides access to various homoisoflavonoids.

The other homoisoflavonoid structural types – scillascillin, caesalpin, protosappanin, and in particular, indano[2,1-*c*]chromans, can all be derived from the key 3-benzylchroman-4-one sappanin structural unit.<sup>6b</sup> Indano[2,1-*c*]chromans are proposed to originate from the corresponding sappanin-type skeleton containing the correct oxygenation substitution pattern.

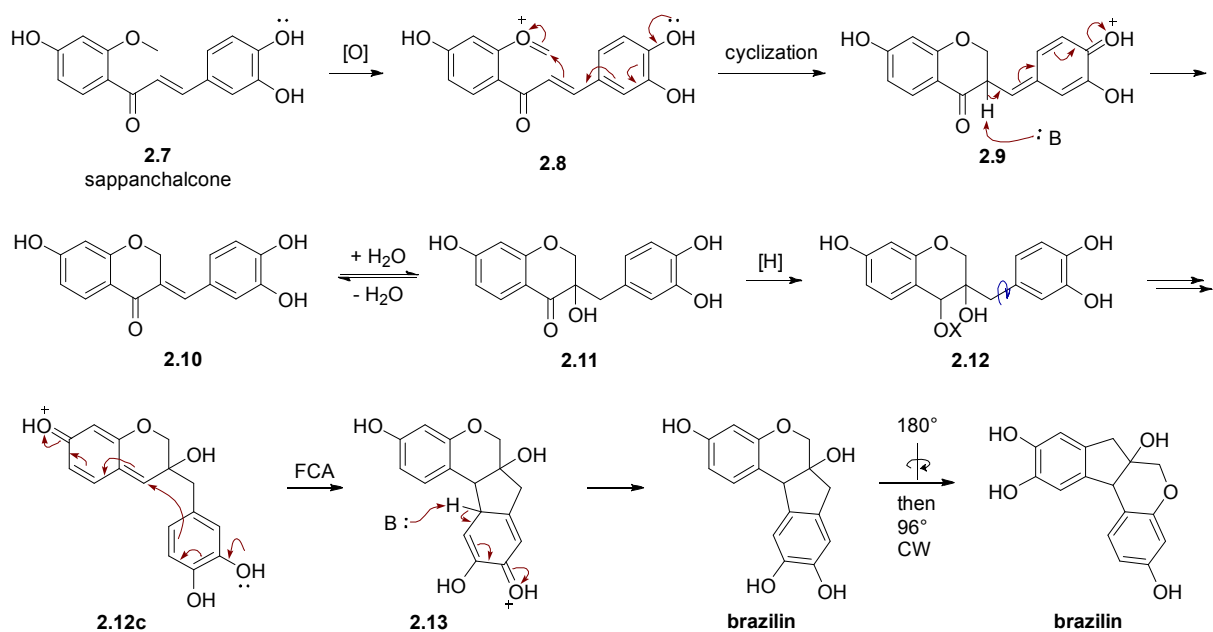
The biosynthetic pathway for the indano[2,1-*c*]chromans is derived from the feeding and labelling experiments conducted by Dewick to determine the biosynthetic pathway for eucomin and eucomol (Scheme 2-2).<sup>5, 11a</sup> The biosynthetic pathway proposed by Dewick for eucomin and eucomol begins with oxidation of chalcone **2.1** to generate oxocarbenium **2.2**. This oxocarbenium intermediate is poised perfectly to undergo a Prins cyclization to construct the 3-benzylchroman-4-one **2.3**. Loss of proton generates the 3-benzylidene-chroman-4-one, **2.4**, or eucomin (R = Me). Hydration of eucomin, or oxidation of 3-benzyl-chroman-4-one **2.5**, could then afford eucomol.





**Scheme 2-2.** 2'-Methoxychalcones are the proposed biosynthetic precursors to homoisoflavonoids of the sappanin-type structure such as eucomin and eucomol. (Modified from Dewick, ref 5).

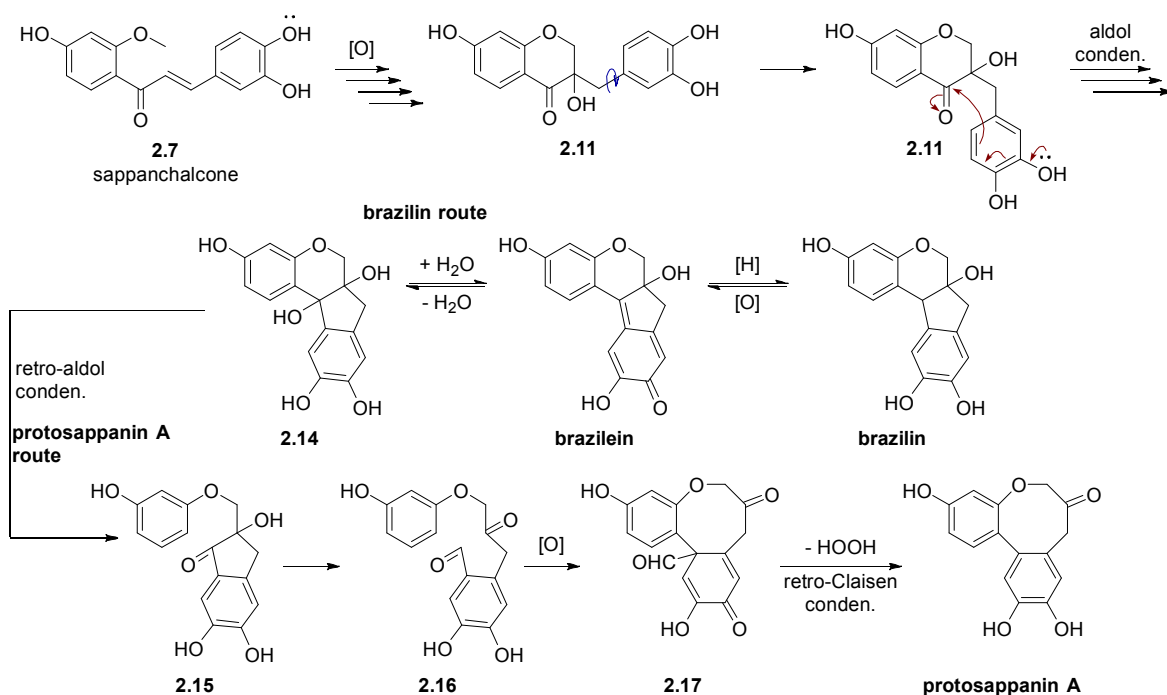
Homoisoflavonoids of the scillascillin-type and the indano[2,1-*c*]chroman structure have been proposed to originate from modifications of the sappanin-type homoisoflavonoid, **2.6**. In 1984, a new phenolic homoisoflavonoid, termed sappanchalcone, was isolated from the heartwood of *Caesalpinia sappan* L. and implicated as the biosynthetic precursor of the indano[2,1-*c*]chroman brazilin.<sup>11b</sup> Through a similar sequence of modifications shown in Scheme 2-2, brazilin, and by analogy, indano[2,1-*c*]chromans, were proposed to have originated from the newly isolated sappanchalcone, **2.7** (Scheme 2-3).



**Scheme 2-3.** Proposed biosynthetic pathway to indano[2,1-*c*]chroman brazilin from sappanchalcone. (Modified from Nagai, M. et al., ref 10) FCA = Friedel–Crafts alkylation.

The key modification in the eucomol biosynthetic pathway towards brazilin is reduction of 3-benzylchroman-4-one, **2.11**, to generate diol **2.12**. Subsequent elimination affords a reactive *para*-quinone methide intermediate **2.12c** that can undergo a Friedel–Crafts alkylation/cyclization to produce brazilin. Further support for this biogenetic pathway was provided by Saitoh and co-workers in 1986. The concurrent isolation of sappanchalcone, 1,2-diol **2.12a** (X = H), and 1,2-diol **2.12b** (X = Me) along with 17 other aromatic compounds from *Caesalpinia sappan* L. link all of these intermediates in the biosynthetic pathway towards brazilin from sappanchalcone.<sup>11d</sup>

A slightly modified biogenesis of brazilin was proposed by Nagai and co-workers in 1986 to explain how the synthesis of brazilin, sappanchalcone, and newly isolated protosappanin A from *Caesalpinia sappan* L. were interconnected (Scheme 2-4).<sup>11c</sup>



**Scheme 2-4.** Proposed biosynthetic pathway that connects sappanchalcone, brazilin, brazilein, and protosappanin A homoisoflavonoids. (Modified from Nagai, M. *Chem. Pharm. Bull.* **1986**, *34*, 1–6.)

The biogenetic pathway proposed begins with formation of 3-benzyl-4-chroman-4-one, **2.11**, as shown in Scheme 2-3. Instead of reduction, the authors propose an intramolecular aldol condensation of 3-benzylchroman-4-one **2.11** resulting in diol **2.14** which can undergo two potential fates. Diol **2.14** can undergo dehydration to afford brazilein, and then brazilin following a reduction reaction (the authors suggest a hydrogenation reaction). Alternatively, diol **2.14** could undergo a retro-aldol condensation followed by an overall bond splitting to generate keto-aldehyde **2.15**, the precursor to protosappanin A.

The synthetic routes used to access these indano[2,1-*c*]chromans parallel nicely with the biogenetic proposals involving an intramolecular aryl cyclization leading to the highly sought after indano[2,1-*c*]chromans from the extracts of sappanwood, brazilwood, and logwood. In particular,

the main constituent of these extracts, brazilin, has held the interest of generations of synthetic chemists and has been the subject of continual interest for over 70 years since its discovery.

### History of Brazilin – Isolation and Structural Elucidation

The key constituent of the sappanwood and brazilwood extracts, brazilin, was reported as crystals in 1808 by Chevreul, but the structure was not inferred until 1901 by Gilbody, Perkin and Yates<sup>13</sup> and correctly deduced in 1908.<sup>14</sup> The empirical formula of brazilin was disclosed by Bolley in 1864 as C<sub>22</sub>H<sub>20</sub>O<sub>7</sub> following several analysis but it was only ten years afterwards that the formula was correctly deduced as C<sub>16</sub>H<sub>14</sub>O<sub>5</sub> by Liebermann and Burg.<sup>13a, 15</sup> Additionally, it was determined that brazilin was a derivative of resorcinol, and was composed of three aromatic/phenolic hydroxyls and one alkyl hydroxyl.

Gilbody, Perkin and Yates added to the structural elucidation of brazilin by carefully studying the oxidation products of trimethylbrazilin. Under varied and structured conditions, brazilin was confirmed to contain a catechol nucleus<sup>16</sup> and that brazilin's constitution incorporated *m*-hemipinic acid, 2-carboxy-5-methoxyphenoxyacetic acid, and brazilic acid (Figure 2-5).<sup>17</sup> A fourth acid – named brazilinic acid – was also obtained, but investigations into its structure were reported the following year.<sup>18</sup> The identity of the former three acids prompted a revision of previously proposed structures by Gilbody and Perkin (structure **2.18**),<sup>17a</sup> and by Feuerstein and Kostanecki (structure **2.19**)<sup>19</sup> to structures **2.20** and **2.21** which account for the formation of the isolated acids from the oxidation of brazilin (Figure 2-5).

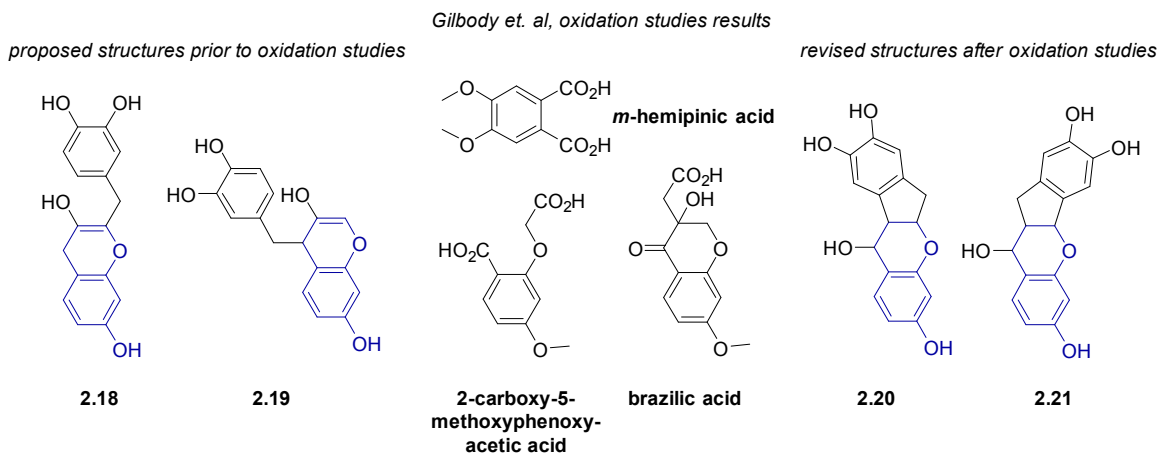
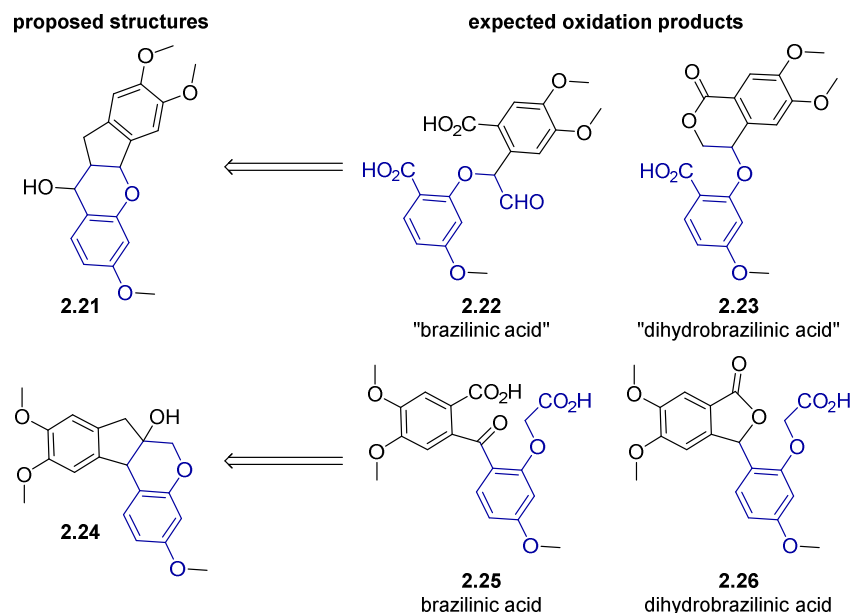


**Figure 2-5.** Revised structures **2.20** and **2.21** by Gilbody, Perkin, and Yates to account for isolation of acids from oxidation studies.

In this revised structure, Gilbody, Perkin, and Yates recognized that brazilin was composed of an indane and chroman ring system, but unfortunately, proposed the incorrect ring fusion and mis-assigned the alcohols as secondary instead of tertiary. The oxidation products of brazilinic acid, formed in considerable amounts in the oxidation of trimethylbrazilin, were further studied by Perkin, but the studies offered no conclusive evidence as to their identity.<sup>18</sup> Still, Perkin proposed a constitution for brazilinic acid whose correct constitution was obtained by Perkin and his post-graduate pupil R. Robinson.<sup>14</sup> An alternative structure to those suggested by Gilbody, Perkin, and Yates was proposed by Robinson, which unknown to him at the time, was the correct structure of brazilin. By elucidating the structure of brazilinic acid, Robinson obtained the necessary results to support his alternative structure.

Robinson reasoned that if the true structure of brazilin was that proposed of indano[1,2-*b*]chroman **2.21**, then the corresponding oxidation products of proposed trimethylbrazilin **2.21**, brazilinic acid and dihydrobrazilinic acid, would have the structures **2.22** and **2.23**, respectively (Scheme 2-5). On the other hand, if the true structure of brazilin was the indano[2,1-*c*]chroman

**2.24**, which he proposed, then the corresponding oxidation products, brazilinic acid and dihydrobrazilinic acid, would have the corresponding structures **2.25** and **2.26**, respectively (Scheme 2-5).

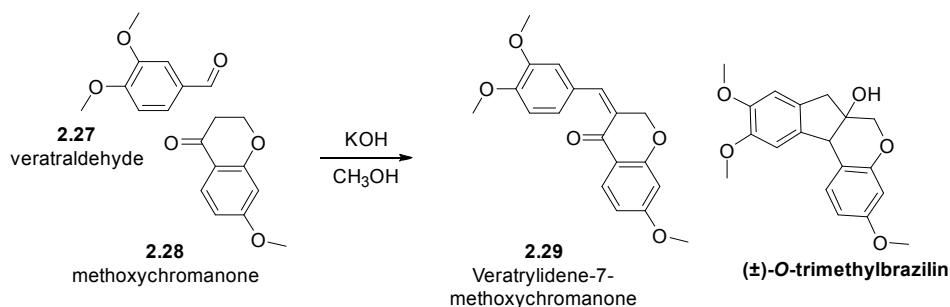


**Scheme 2-5.** Robinson's analysis of expected oxidation products between previously proposed structure **2.21** of brazilin by Gilbody, Perkin, and Yates, and his alternative structure, **2.24**.

Robinson embarked on a synthetic plan to conclusively establish the structure of brazilin and was successful, under Perkin's tutelage. Both of the degradation products **2.25** and **2.26** were successfully synthesized and found to be identical to the oxidation products brazilinic acid and dihydrobrazilinic acid, respectively. The chemical evidence generated by Robinson supported his proposed structure.<sup>20</sup> Further investigations into this chemistry were concerned with understanding the chemistry of *O*-trimethylbrazilone, brazilein, and other derivatives of haematoxylin and brazilin.<sup>13b,21</sup> The work by Robinson and Perkin during the years 1901–1908 has been summarized by Engels, et al.,<sup>21b</sup> and a more digestible account has been summarized by Perkin's son, Arthur George Perkin, and Arthur Ernest Everest.<sup>21c</sup>

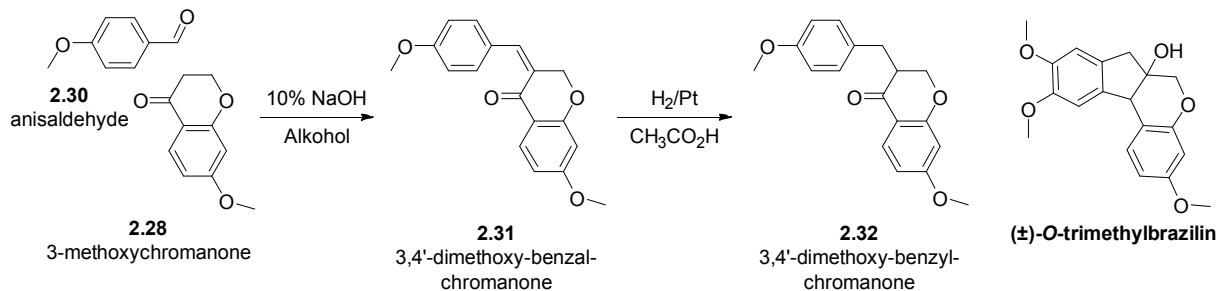
## History of Brazilin – Synthesis of the Indano[2,1-*c*]chroman Core and Brazilin

After the chemical structure of brazilin was advocated by Perkin and Robinson, the race to synthesize the indano[2,1-*c*]chroman core of brazilin began. In a 1912 preliminary note, Perkin and Robinson comment on the similar constitution of veratrylidene-7-methoxychromanone **2.29** and *O*-trimethylbrazilin (Scheme 2-6).<sup>22</sup> In this note, they report two important items: 1) The synthesis of veratrylidene-7-methoxychromanone **2.29** by the reaction of methoxychromanone **2.28** and veratraldehyde **2.27**, and 2) they indicate that veratrylidene-7-chromanone **2.29** could be converted into a derivative of brazilin.



**Scheme 2-6.** Synthesis of veratrylidene-7-chromanone **2.29** reported by Perkin and Robinson, and the structure of *O*-trimethylbrazilin for comparison. The compound names in this scheme are taken directly from the author's report. The IUPAC names are as follows: 7-methoxychroman-4-one (**2.28**), and 3-(3,4-dimethoxybenzylidene)-7-methoxychroman-4-one (**2.29**).

In 1917, Pfeiffer and Grimmer, who had previously suggested the correct constitution of brazilin without any chemical evidence,<sup>23</sup> announced their intention of conclusively settling the matter on the correct constitution of brazilin by way of 3,4'-dimethoxy-benzyl-chromanone, utilizing the method indicated in Perkin and Robinson's preliminary note (Scheme 2-7).<sup>24</sup>



**Scheme 2-7.** Synthesis of 3,4'-dimethoxy-benzyl-chromanone **2.32** reported by Pfeiffer and Grimmer, and the structure of *O*-trimethylbrazilin for comparison. The compound names in this scheme are taken directly from the author's report. The IUPAC names are as follows: 7-methoxychroman-4-one (**2.28**), 7-methoxy-3-(4-methoxybenzylidene)chroman-4-one (**2.31**), and 7-methoxy-3-(4-methoxybenzyl)chroman-4-one (**2.32**).

That same year, Robinson notes that the strategy suggested by them, of utilizing dimethoxybenzaldehyde **2.27**, results in a compound nearer in constitution to brazilin, **2.29**, and have indicated at the probability of converting it into a derivative of brazilin; whereas, Pfeiffer and Grimmer's strategy results in a compound further away from brazilin's constitution and offer no report on its possibility of being converted into a derivative of brazilin.<sup>24b</sup> Still, Pfeiffer continued their studies with the compound **2.31** derived from condensation of anisaldehyde **2.30**.<sup>25</sup> Robinson and Crabtree proceeded to synthesize isobrazilein salts which confirmed the validity of the proposed ring system of the brazilin structure (Figure 2-6).<sup>24b, 26</sup>



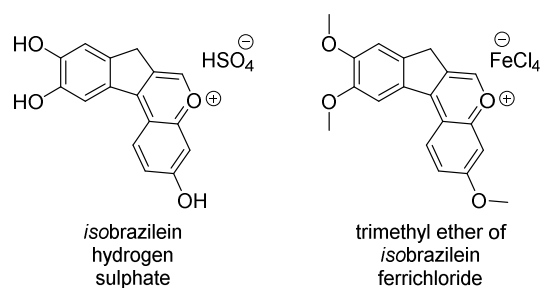
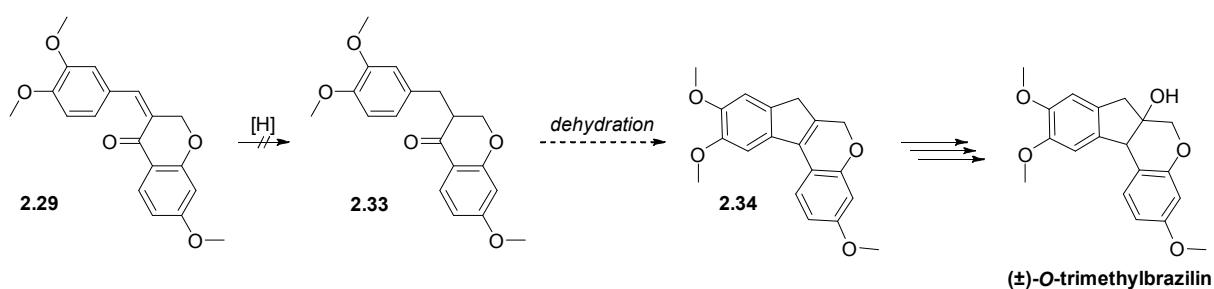


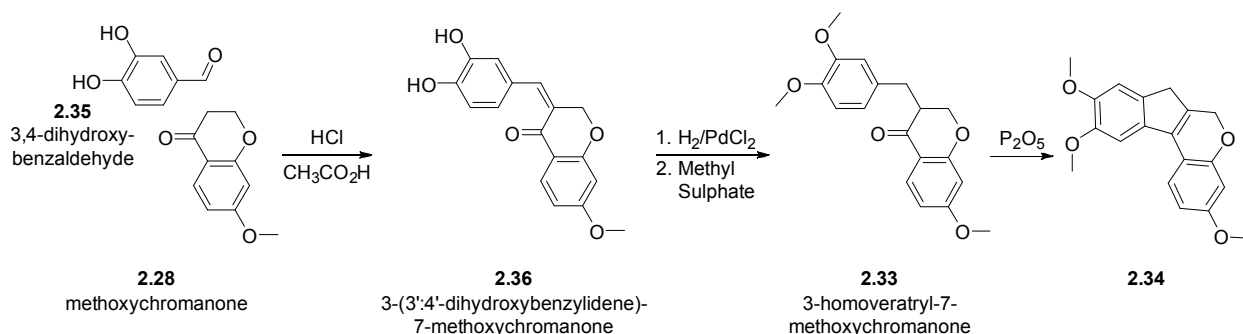
**Figure 2-6.** Crabtree and Robinson synthesize the first compounds containing a brazilin skeleton – the brazylium salts.

Afterwards Robinson and Crabtree attempted the synthesis of the brazilin core utilizing veratrylidene-7-methoxychromanone **2.29** as described in their 1912 preliminary note. Their approach focused on the reduction of veratrylidene-7-methoxychromanone **2.29** to chroman-4-one **2.33** which they thought it feasible to dehydrate into the indano[2,1-*c*]chroman core **2.34** (Scheme 2-8).<sup>27</sup>



**Scheme 2-8.** Robinson and Crabtree's primary strategy to access indano[2,1-*c*]chroman core **2.34** through dehydration of chroman-4-one **2.33**.

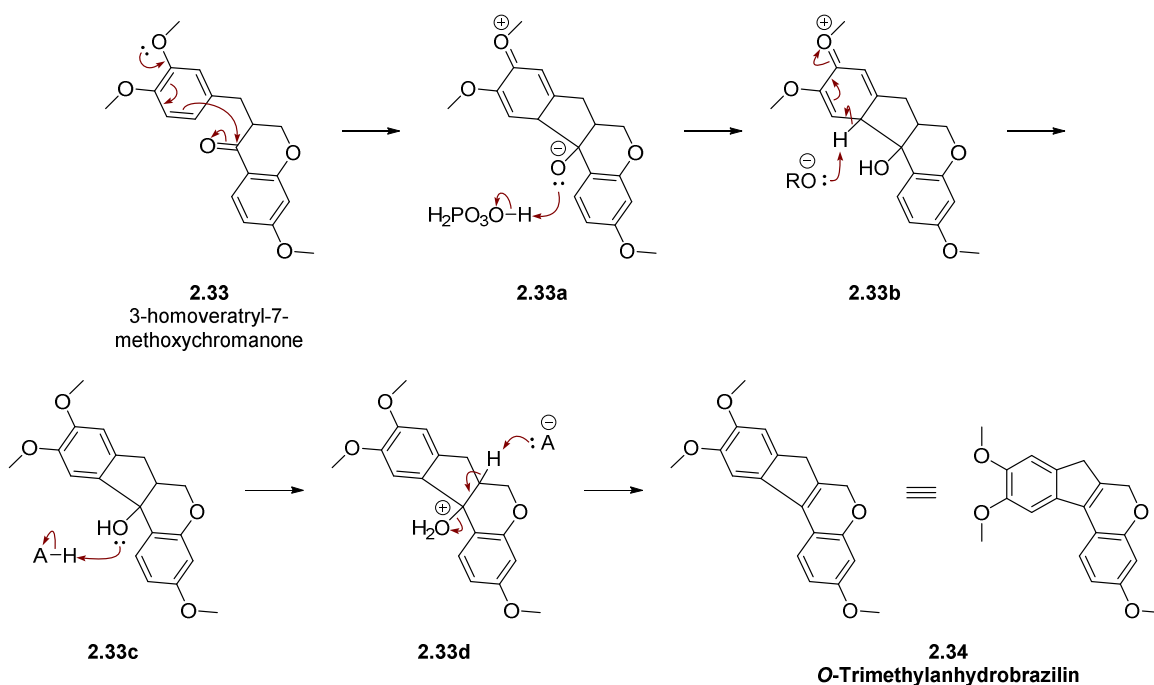
The method used for the reduction, H<sub>2</sub>/PdCl<sub>2</sub>, led to concomitant reduction of the chroman-4-one carbonyl moiety to yield a chromane unsuited for a dehydrative cyclization. The authors avoided over-reduction of **2.29** by synthesizing the catechol derivative **2.36** from the condensation of 3,4-dihydroxybenzaldehyde **2.35** and chromanone **2.28** (Scheme 2-9).



**Scheme 2-9.** Synthesis of deoxytrimethylbrazilone, **2.34**, the indano[2,1-*c*]chroman resulting from Friedel–Crafts dehydrative cyclization of chroman-4-one **2.33**.

Condensation of the aldehyde and ketone went smoothly, and the resulting benzylidene was successfully reduced with palladium(II) chloride and subsequently methylated to afford the desired 3-homoveratryl-7-methoxychromanone **2.33**.<sup>28</sup> Upon treatment with phosphorous pentoxide, chromanone **2.33** underwent an intramolecular Friedel–Crafts cyclization (FCC) to afford deoxytrimethylbrazilone (*O*-trimethylanhydrobrazilin) **2.34**, to conclusively settle the constitution of brazilin. All subsequent syntheses of brazilin have exploited this biomimetic Friedel–Crafts cyclization. The remaining text will refer to compound **2.34** as *O*-trimethylanhydrobrazilin, which more accurately conveys its relation to its parent compound, brazilin.

The dehydrative FCC process is the initial key step in the formation of the indano[2,1-*c*]chroman core **2.34** from chroman-4-one **2.33**. Nearly at the same time, Pfeiffer and Oberlin reported a synthesis of *O*-trimethylanhydrobrazilin **2.34** by virtually the same method.<sup>29</sup>

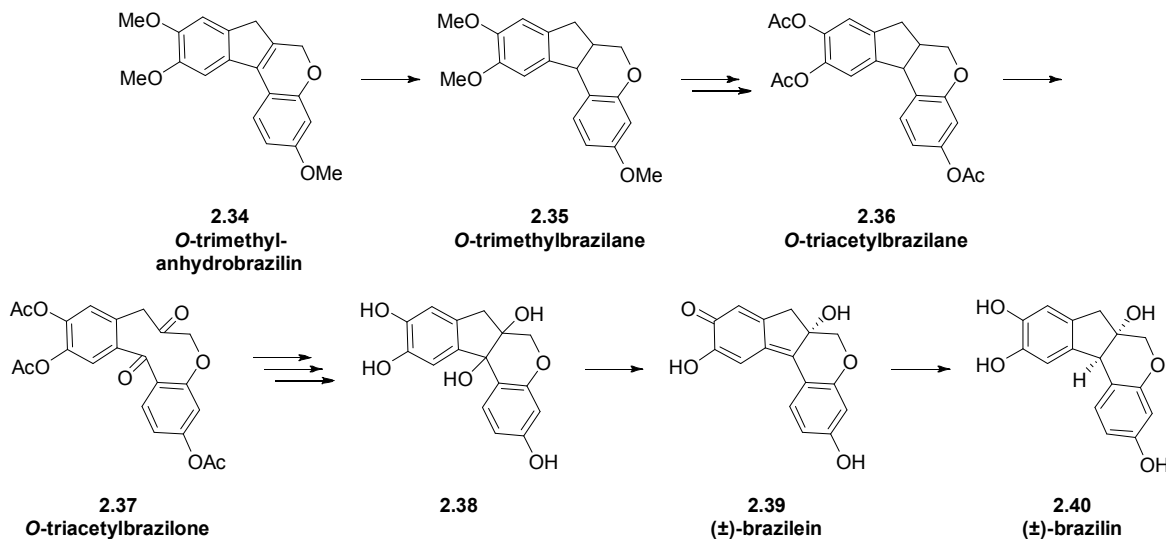


**Scheme 2-10.** A plausible mechanism showing the key Friedel–Crafts cyclization/dehydration step to construct the indano[2,1-*c*]chroman core **2.34**.

Robinson and co-workers then engaged in synthesizing *O*-trimethylbrazilin from *O*-trimethylanhydrobrazilin **2.34**. The most direct way to achieve the goal was through hydration of compound **2.34**, but the simple task proved unwieldy – anhydrobrazilin **2.34** was prone to oxidation leading to various product mixtures, such as *isobrazilein* salts, and prone to disproportionation.<sup>30</sup>

The issues presented by what seemed a straightforward transformation prompted an alternate route which proved successful (Scheme 2-11).<sup>31</sup> Catalytic hydrogenation of anhydrobrazilin **2.34** yielded *O*-trimethylbrazilane **2.35**, which upon demethylation and acetylation afforded *O*-triacetylbrazilane **2.36**. Oxidation with chromic anhydride generated *O*-triacetylbrazilone **2.37**. Following reduction by zinc/acetic acid, basic hydrolysis, and acidification of diketone **2.37** afforded the phenolic pinacol **2.38** which readily dehydrated under acidic

conditions to form (±)-brazilein **2.39**. Finally, stereoselective reduction of (±)-brazilein **2.39** with potassium borohydride afforded (±)-*cis*-brazilin **2.40**.



**Scheme 2-11.** Synthetic route to (±)-brazilin **2.40** by Robinson and co-workers.

The synthesis of brazilin from the Friedel–Crafts cyclization-dehydration of chroman-4-one **2.33** provided a template for alternative synthetic strategies for brazilin, a versatile bioactive compound.

### Some Pharmacological Properties of Brazilin

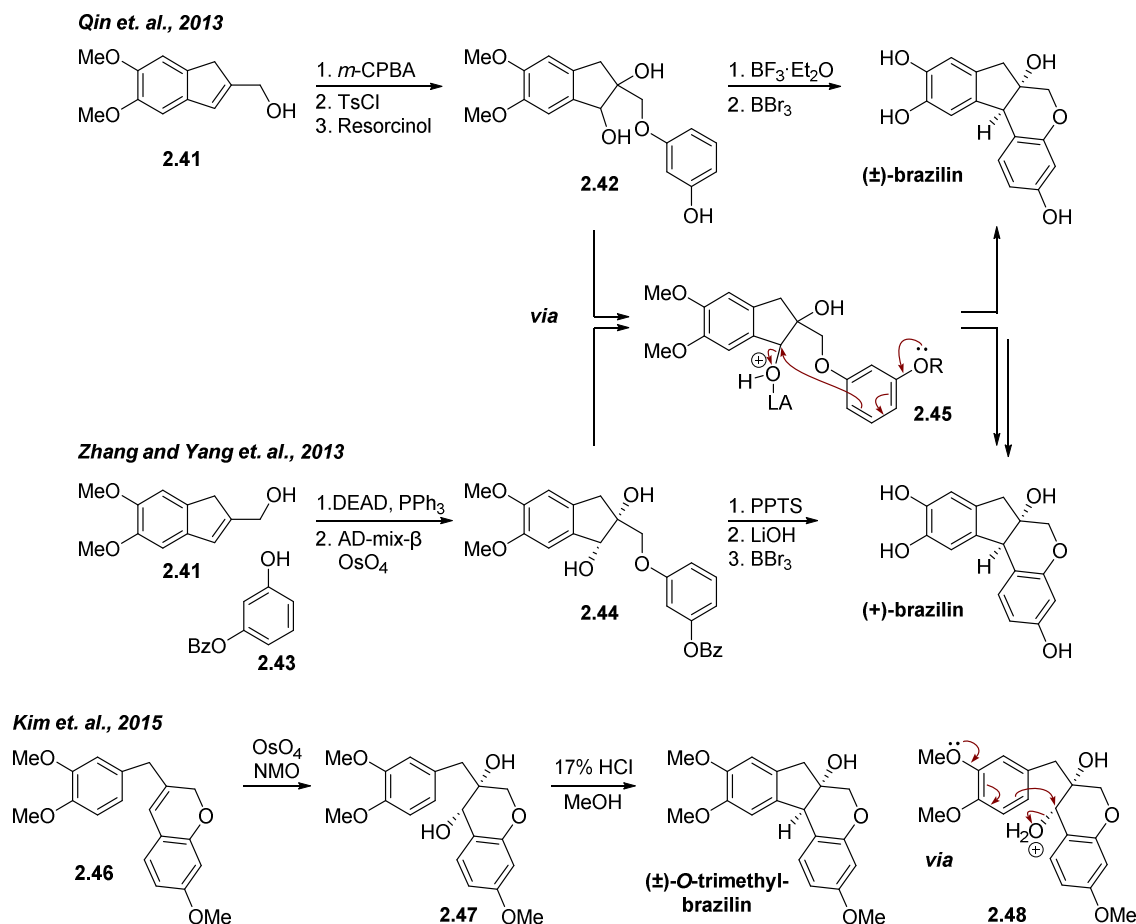
Even before the elucidation of its structure, the brazilin-rich extracts of *Caesalpinia sappan* have been used for centuries in Thai folk medicine to treat ailments such as “tuberculosis, diarrhea, dysentery, skin infections and anemia,” as well as in traditional Chinese medicine for improving blood circulation, and as an analgesic and anti-inflammatory agent.<sup>32</sup> More detailed accounts regarding other uses of sappanwood extracts<sup>33</sup> in traditional medicine have been well documented.<sup>1, 6a, 11e, 32-33</sup>

Dapson et al., nicely summarize scientific research conducted with pure brazilin.<sup>1</sup> For example, brazilin is a potent antibiotic that kills methicillin-resistant *Staphylococcus aureus* and vancomycin-resistant enterococci, without inducing bacterial resistance up to 20 cycles of culturing.<sup>34</sup> It also acts indirectly as an anti-oxidant by increasing the activity of heme oxygenase-1 (HO-1), an enzyme responsible for protecting cells against certain oxidative stresses.<sup>35</sup>

In general, scientific studies into the pharmacological properties of pure brazilin began in the late 1970s, following the reported synthesis by Robinson and co-workers. However, since the elucidation of its structure and its synthesis,<sup>30, 31b</sup> the brazilin-rich extracts, and pure brazilin, have been the subject of continuous and extensive study against targets that include diabetes,<sup>36</sup> arthritis,<sup>37</sup> and various cancer types.<sup>38</sup>

### **Friedel–Crafts Cyclization as a Synthetic Approach to Brazilin**

Brazilin's therapeutic potential has made it an attractive target for synthesis. Perkin and Robinson first reported the synthesis of the brazilin indano[2,1-*c*]chroman ring system using a biomimetic<sup>5-6, 11a, 11b, 11d</sup> Friedel–Crafts cyclization<sup>22, 28-29</sup> to form the five-membered ring (Scheme 2-9 – Scheme 2-11). Friedel–Crafts cyclizations have been adopted in nearly all subsequent syntheses<sup>21a, 39</sup> to form the five-membered indane (in racemic,<sup>40</sup> asymmetric,<sup>7a, 41</sup> and analogue<sup>42</sup> syntheses), or the six-membered dihydropyran ring (in racemic,<sup>43</sup> asymmetric,<sup>44</sup> and analogue<sup>45</sup> syntheses) (Scheme 2-12). Yadav and co-workers add the aryl ring to an indane core using an *intermolecular* Friedel–Crafts followed by cyclization to form the six-membered dihydropyran.<sup>46</sup>



**Scheme 2-12.** Selected examples of racemic and asymmetric synthesis invoking FCC in the synthesis of brazilin.

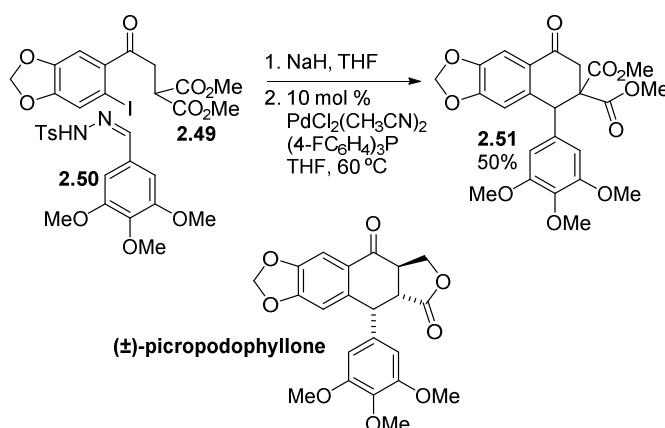
In 2013, Qin and others,<sup>43b</sup> and Zhang and others,<sup>44</sup> both published synthesis to (±)-brazilin and (+)-brazilin, respectively, via a similar diol intermediate (**2.42** and **2.44**) that underwent a FCC to construct the core of brazilin. A similar FCC was invoked by Kim and Jung on diol intermediate **2.47**. The Friedel-Crafts cyclization has also been used to prepare chemical analogues.<sup>39, 42, 45, 47</sup>

### Cyclization of $\eta^3$ -Benzyl Palladium Intermediates Derived from Carbene Insertions as an Approach to the Synthesis of (±)-Brazilin

Alternative synthetic strategies broaden access to derivatives with improved activity so we were prompted to investigate an alternative synthesis of brazilin through a non-obvious

disconnection. In 2014, we developed palladium-catalyzed [5+1] and [4+1] carbene insertions of aryl iodides and *N*-tosyl hydrazones which gave access to the 1-aryltetralin and 1-arylindane cores present in natural products such as podophyllotoxin and brazilin, respectively.<sup>48</sup>

When the [5+1] palladium-catalyzed carbene insertion was applied to aryl iodide **2.49** and *N*-tosylhydrazone **2.50**, it generated 1-aryltetralin derivative **2.51** which was a key intermediate in the Kende syntheses of (±)-picropodophyllone and (±)-podophyllotoxin (Scheme 2-13).<sup>49</sup> Given the modest yield for the [5+1] annulation reaction and the difficulty removing an azine side product, we set out to explore the applicability of the [4+1] palladium-catalyzed carbene insertion to a total synthesis of (±)-brazilin.



**Scheme 2-13.** Formal synthesis of (±)-picropodophyllone using a [5+1] palladium-catalyzed carbene insertion.

### Results (unpublished work submitted for publication)

During our initial development of the palladium-catalyzed [4+1] carbene insertion process my colleague, Eugene Gutman, and I found that *ortho*-oxygenation on *N*-tosylhydrazone **2.53** was slightly detrimental whereas oxygenation on the aryl iodide **2.52** was slightly beneficial as exemplified by previously published yields for arylindanes **2.54** and **2.55**, respectively (Figure 2-

7).<sup>50</sup> These substituent effects appear to counter each other leading to useful yields of highly oxygenated 1-arylidanes **2.56–2.58** (Figure 2-7).

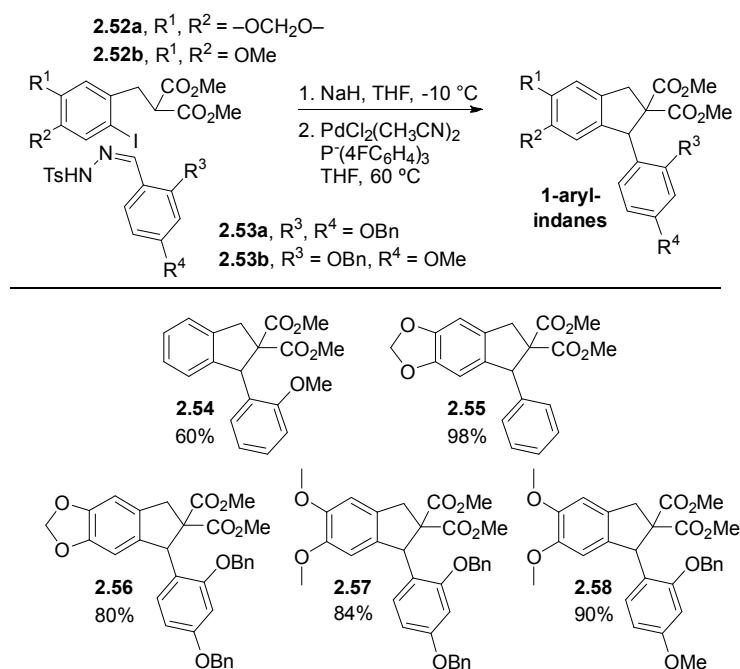


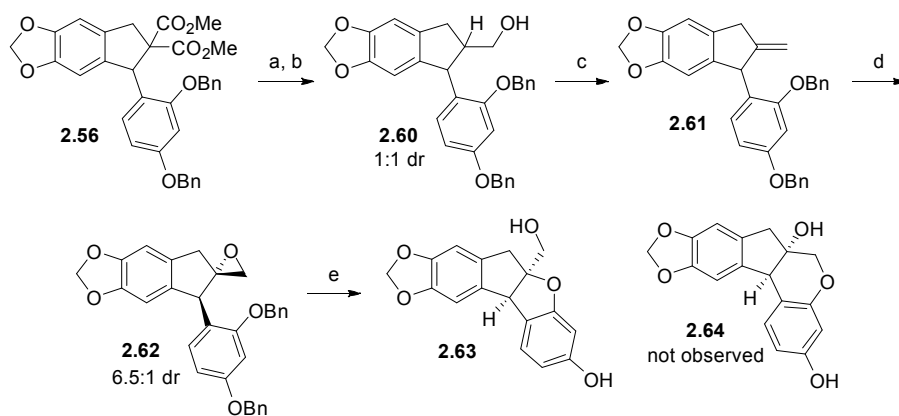
**Figure 2-7.** Palladium-catalyzed insertion of oxygenated aryl iodides **2.52** and *N*-tosylhydrazones **2.53**.

Broadened peaks and a minor impurity were particularly apparent in the <sup>1</sup>H NMR spectra of 1-arylidanes **2.57** and **2.58** in spite of chromatographic homogeneity under all conditions tested. Counter to the expectations of A<sub>1,3</sub> strain, these hindered compounds, and some of the 1-arylidanes described later, appear to exist as two conformers based on the presence of two sets of broadened peaks in the <sup>1</sup>H NMR spectra in a *ca* 5:1 ratio. For 1-arylidane **2.58**, the peaks converge at 110–120 °C and sharpen into well-resolved signals at 0 °C in DMF-*d*<sub>7</sub>. In a 1D gradient NOE experiment, irradiation of the benzylic methine proton at 5.10 ppm in the major conformer of 1-arylidane **2.58** at 0 °C in CDCl<sub>3</sub>, led to a reduction in signal of the benzylic methine proton at 4.64 ppm in the minor conformer, consistent with conformational interconversion.<sup>51</sup>



With access to a number of *O*-protected 1-arylidane intermediates we set out to remove the vestigial carboxymethyl group and close the dihydropyran ring (Scheme 2-14). Intramolecular cyclization under either neutral or basic conditions should favor 6-endo-*tet* cyclization<sup>52</sup> on the less substituted position of a 1,1-disubstituted epoxide. Krapcho decarboxylation of geminal diester **2.56** generated a 1:1 mixture of carboxymethyl epimers (**2.59**) that were reduced to primary alcohol **2.60** as a mixture of isomers. Initial attempts to eliminate the alcohol via the mesylate failed, but exocyclic alkene **2.61** was obtained through a selenoxide elimination.

Treatment of alkene **2.61** with *m*-CPBA gave epoxide **2.62** as an inseparable 6.5:1 mixture of diastereomers, presumably from the face opposite the allylic arene substituent. Debenzylation was accompanied by spontaneous 5-*exo-tet* cyclization, producing exclusively the indano[2,1-*b*]benzofuran **2.63** containing the core of the kaempferiaosides A and B,<sup>53</sup> but not the desired indano[2,1-*c*]chroman ring system of brazilin, **2.64**. 5-*Exo-tet* cyclization on the more substituted position of the epoxide was favored even when the debenzylation was carried out in the presence of base.

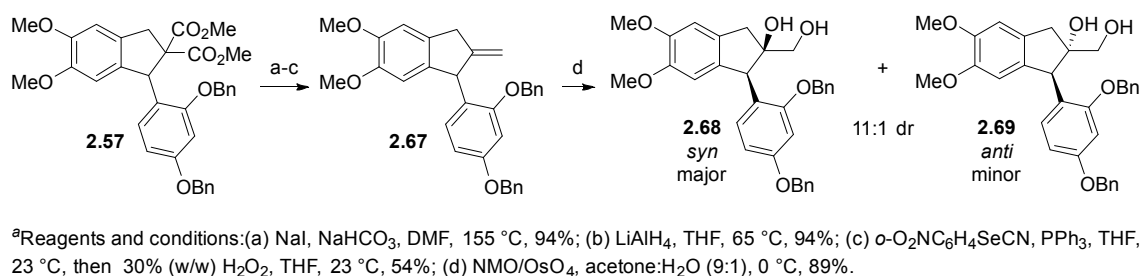


<sup>a</sup>Reagents and conditions: (a) NaI, NaHCO<sub>3</sub>, DMF, 155 °C, 86%; (b) LiAlH<sub>4</sub>, THF, 65 °C, 94%; (c) *o*-O<sub>2</sub>NC<sub>6</sub>H<sub>4</sub>SeCN, PPh<sub>3</sub>, THF, 23 °C, then 30% (w/w) H<sub>2</sub>O<sub>2</sub>, THF, 23 °C, 38%; (d) *m*-CPBA, NaHCO<sub>3</sub>, DCM, 23 °C, 40%; (e) 49 mol % Pd(OH)<sub>2</sub>/C, H<sub>2</sub>, MeOH:THF (1:1), 23 °C, 49%.

**Scheme 2-14.** Initial synthetic strategy to brazilin involving late-stage formation of dihydropyran ring.<sup>a</sup>

We recognized the possibility of intercepting an exocyclic alkene **2.67** previously reported by both Zhang<sup>47</sup> and Yadav<sup>46</sup> and used by Yadav in a synthesis of ( $\pm$ )-brazilin. Bis-methoxy alkene **2.67** was prepared using the same sequence employed for synthesis of methylenedioxy alkene **2.61** in 48% overall yield from arylindane **2.57** (Scheme 2-15). Epoxidation of alkene **2.67** also generated a *ca* 7:1 mixture of diastereomeric epoxides corresponding to **2.61**, but the major isomer could be crystallized by vapor diffusion ( $\text{CH}_2\text{Cl}_2$ /hexane) and the epoxide oxygen was confirmed to be *anti* to the axial aryl substituent on the five-membered ring (see supporting information for **2.62b**).

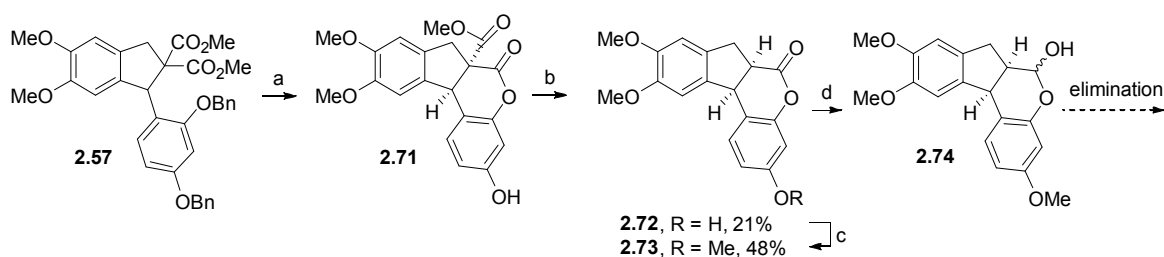
Following the dihydroxylation procedure of Zhang and co-workers, we obtained an 11:1 ratio of diastereomers **2.68** and **2.69** (Scheme 2-15). Surprisingly, the minor diastereomer **2.69** from dihydroxylation, and not the major diastereomer **2.68**, was found to match the diol prepared by Yadav through a different route, suggesting that the dihydroxylation proceeds from the same face as the hindered aryl substituent and that the other dihydroxylation product had been previously mis-assigned. That structural mis-assignment would explain the fact that the Yadav diol **2.69** was convertible to brazilin, whereas the Zhang diol **2.68** was not.



**Scheme 2-15.** Dihydroxylation proceeds on same face as aryl substituent.<sup>a</sup>

Given the challenges associated with stereoselective functionalization of the exocyclic alkene **2.67** and subsequent 5-*exo-tet* cyclization, we returned to the cyclic malonate **2.57**

generated from the palladium-catalyzed [4+1] (Scheme 2-16), hoping to form the lactone with one of the ester groups.



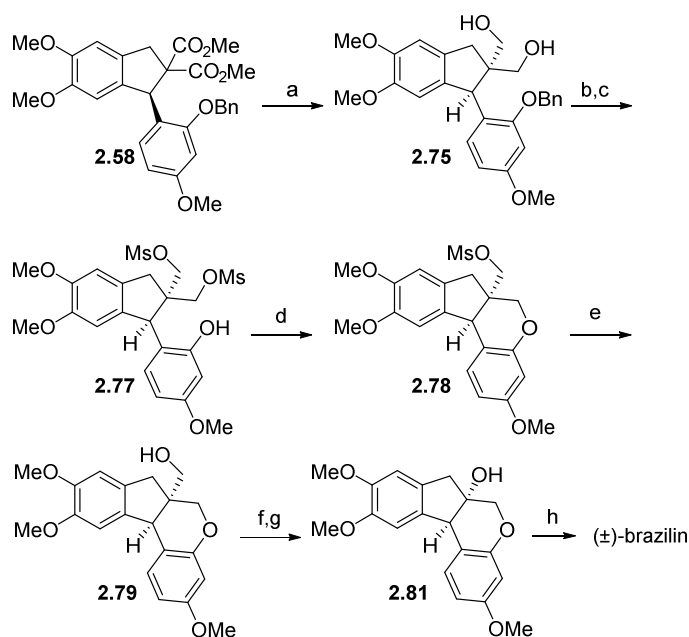
<sup>a</sup>Reagents and conditions: a) 24 mol % Pd(OH)<sub>2</sub>/C, H<sub>2</sub>, MeOH:THF (1:1), 23 °C; then 30 mol % *p*-TsOH·H<sub>2</sub>O, toluene, 110 °C, 93%; (b) KCl, DMSO, 160 °C; (c) Me<sub>2</sub>SO<sub>4</sub>, K<sub>2</sub>CO<sub>3</sub>, acetone, 56 °C, 90%; (d) DIBAL-H, DCM, -78 °C, 48%.

**Scheme 2-16.** Synthetic strategy to access indano[2,1-*c*]chroman core lactone **2.71**.<sup>a</sup>

Hydrogenolysis of dibenzyl ether **2.57** gave the free resorcinol **2.70** and the desired lactone product **2.71** containing the tetracyclic ring system of brazilin. The remaining resorcinol **2.70** was driven to chromanone **2.71** by heating with *p*-toluenesulfonic acid. Krapcho decarboxylation of the methyl ester of **2.71** was accompanied by a competing methylation of the free phenolic group by the chloromethane byproduct to afford *O*-methyl ether **2.73** as the major product. Attempts to prevent the unwanted methylation were unsuccessful, so the remaining phenol **2.72** was alkylated with dimethyl sulfate to afford the *O*-methyl ether **2.73** in 90% for an overall yield of 67% for the decarboxylation/methylation process.

With chromanone **2.73** in hand, I proceeded to investigate a reduction,<sup>54</sup> dehydration,<sup>55</sup> and hydroboration oxidation<sup>56</sup> reaction sequence to access *O*-trimethylbrazilin. The lactone **2.73** was reduced to lactol **2.74** in 48% yield (5.8:1 mixture of lactol isomers). Attempts to dehydrate the lactol were unsuccessful under E<sub>1</sub>, E<sub>2</sub> and *syn*-elimination conditions possibly attributable to the incompatibility between oxocarbenium intermediates and electron-rich arenes, or the sensitivity of the enol ether.

The great facility of lactonizing one of the two geminal carboxymethyl groups of malonate **2.57**, inspired a similar approach involving cyclization onto one of two geminal mesylates by one of the four phenolic groups protected as an *O*-benzyl ether (Scheme 2-17).



<sup>a</sup>Reagents and conditions: (a) LiAlH<sub>4</sub>, THF, 0 °C, 71%; (b) MsCl, NEt<sub>3</sub>, 0 to 5 °C, 95%; (c) 24 mol % Pd(OH)<sub>2</sub>/C, H<sub>2</sub>, MeOH:THF (1:1), 23 °C, 99%; (d) NaH, THF, 0 °C, 81%; (e) LiAlH<sub>4</sub>, THF, 65 °C, 90% (f) DMP, DCM, 0 to 5 °C, 86%; (g) NaOH, 30% (w/w) H<sub>2</sub>O<sub>2</sub>, MeOH, 65 °C, 42%; (h) BBr<sub>3</sub>, DCM, 0 to 23 °C, 68%.

**Scheme 2-17.** Total synthesis of (±)-brazilin from bis-mesylate **2.77**.

This was easily accomplished by reducing the carboxymethyl groups of geminal ester **2.58** to afford the corresponding diol **2.75** in 71% yield. Mesylation of the hydroxyl groups and hydrogenolysis of the benzylic protecting group generated the phenolic mesylate **2.77** in high yield. As described for 1-arylidane **2.58**, diol **2.75**, bis-mesylate **2.76**, and even bis-mesylate **2.77** (lacking an *O*-benzyl group) exhibited a second minor conformer evident in the <sup>1</sup>H NMR spectrum. Deprotonation of the phenolic group was followed by facile cyclization onto the *syn* mesylate to form the desired dihydropyran ring of the indanochroman **2.78** in 81% yield. The extraneous

mesylate was removed with lithium aluminum hydride to afford the neopentyl alcohol **2.79** which was oxidized to aldehyde **2.80** in 88% yield using Dess-Martin periodinane.

The aldehyde was subjected to Bayer-Villiger oxidation under nucleophilic conditions in order to minimize collateral oxidation of the electron-rich aromatic ring to afford *O*-trimethylbrazilin, **2.81**, in 42% (>95% purity) yield upon treating aldehyde **2.80** with NaOH and 30% (w/w) H<sub>2</sub>O<sub>2</sub>. The methyl groups were removed with BBr<sub>3</sub>, as previously reported, to afford (±)-brazilin in 68% (>95% purity by HNMR); as noted by others,<sup>57</sup> the catechol brazilin is highly sensitive to oxidation.

## Conclusion

Palladium-catalyzed [5+1] and [4+1] carbenylative annulation reactions with electron-rich aromatic rings have led to a formal synthesis of (±)-podophyllotoxin and a total synthesis of (±)-brazilin. The [4+1] annulation reaction approach to brazilin varies dramatically from the Perkin-Robinson strategy first proposed over a century ago. The powerful palladium reaction brings in nearly all of the necessary functionality, but strategies to access the dihydropyran ring via epoxide ring opening or lactonization proved unworkable. Ultimately, a strategy involving construction of the dihydropyran ring through diastereotopic displacement of a mesylate paved the way for the synthesis of (±)-brazilin in 8 steps and 12% yield from the corresponding aryl iodide, and 11% overall yield in the longest linear sequence from commercial 3,4-dimethoxybenzyl alcohol (11 steps total).

## References

1. Dapson, R. W.; Bain, C. L. Brazilwood, sappanwood, brazilin and the red dye brazilin: from textile dyeing and folk medicine to biological staining and musical instruments. *Biotech. Histochem.* **2015**, *90*, 401–423.
2. Castelli, M. V.; López, S. N., Homoisoflavonoids: Occurrence, Biosynthesis, and Biological Activity. In *Stud. Nat. Prod. Chem.*, Atta-ur-Rahman, Ed. Elsevier B.V.: 2017; Vol. 54, pp 315–354.
3. Böhler, P.; Tamm, C. The homo-isoflavones, a new class of natural product. Isolation and structure of eucomin and eucomol. *Tetrahedron Lett.* **1967**, *8*, 3479–3483.
4. Dewick, P. M. Biosynthesis of the 3-benzylchroman-4-one eucomin. *J. Chem. Soc., Chem. Commun.* **1973**, *0*, 438–439.
5. Dewick, P. M. Biosynthesis of the 3-benzylchroman-4-one eucomin in *Eucomis bicolor*. *Phytochemistry* **1975**, *14*, 983–988.
6. (a) Lin, L. G.; Liu, Q. Y.; Ye, Y. Naturally Occurring Homoisoflavonoids and Their Pharmacological Activities. *Planta Med.* **2014**, *80*, 1053–1066 and references therein; (b) Baldim, J. L.; Rosa, W.; Santos, M. F. C.; Chagas□Paula, D. A.; Lago, J. H. G.; Soares, M. G., Homoisoflavonoids from *Caesalpinia spp.*: A Closer Look at Chemical and Biological Aspects. In *Flavonoids - From Biosynthesis to Human Health*, 2017; pp 97–111.
7. (a) Namikoshi, M.; Nakata, H.; Yamada, H.; Nagai, M.; Saitoh, T. Homoisoflavonoids and related compounds. II. Isolation and absolute configurations of 3,4-dihydroxylated homoisoflavans and brazilins from *Caesalpinia sappan* L. *Chem. Pharm. Bull.* **1987**, *35*, 2761–2773; (b) Min, B. S.; Cuong, T. D.; Hung, T. M.; Min, B. K.; Shin, B. S.; Woo, M. H. Compounds from the Heartwood of *Caesalpinia sappan* and their Anti-inflammatory Activity. *Bioorg. Med. Chem. Lett.* **2012**, *22*, 7436–7439.
8. (a) Nguyen, M. T.; Awale, S.; Tezuka, Y.; Tran, Q. L.; Kadota, S. Xanthine oxidase inhibitors from the heartwood of Vietnamese *Caesalpinia sappan*. *Chem. Pharm. Bull.* **2005**, *53*, 984–988; (b) Chen, F.-Z.; Zhao, Q.; Yan, J.; Guo, X.-Q.; Song, Q.; Yao, Q.; Gou, X.-J. Antioxidant Activity and Antioxidant Mechanism of Brazilin and Neoprotosappanin from *Caesalpinia sappan* Lignum. *Asian J. Chem.* **2014**, *26*, 4979–4981.
9. Lin, L. G.; Xie, H.; Li, H. L.; Tong, L. J.; Tang, C. P.; Ke, C. Q.; Liu, Q. F.; Lin, L. P.; Geng, M. Y.; Jiang, H.; Zhao, W. M.; Ding, J.; Ye, Y. Naturally occurring homoisoflavonoids function as potent protein tyrosine kinase inhibitors by c-Src-based high-throughput screening. *J. Med. Chem.* **2008**, *51*, 4419–4429.
10. Nagai, M.; Nagumo, S. Protosappanins E-1 and E-2, Stereoisomeric Dibenzoxocins Combined with Brazilin from Sappan Lignum. *Chem. Pharm. Bull.* **1990**, *38*, 1490–1494.
11. (a) Heller, W.; Tamm, C., Homoisoflavanones and Biogenetically Related Compounds. In *Progress in the Chemistry of Organic Natural Products*, Herz W; Grisebach H; Kirby G. W, Eds. Springer-Verlag: New York, 1981; Vol. 40, pp 105–152; (b) Nagai, M.; Nagumo, S.; Eguchi, I.; Lee, S. M.; Suzuki, T. Sappanchalcone from *Caesalpinia sappan* L., the proposed biosynthetic precursor of brazilin. *Yakugaku Zasshi* **1984**, *104*, 935–938; (c) Nagai, M.; Nagumo, S.; Lee, S.-M.; Eguchi, I.; Kawai, K.-I. Protosappanin A, a novel biphenyl compound from Sappan Lignum. *Chem. Pharm. Bull.* **1986**, *34*, 1–6; (d) Saitoh, T.; Sakashita, S.; Nakata, H.; Shimokawa, T.; Kinjo, J.-E.; Yamahara, J.; Yamasaki, M.; Nohara, T. 3-Benzylchroman derivatives related to brazilin from Sappan Lignum. *Chem.*

- Pharm. Bull.* **1986**, *34*, 2506–2511; (e) Abegaz, B. M.; Mutanyatta-Comar, J.; Nindi, M. Naturally occurring homoisoflavonoids: Phytochemistry, biological activities and synthesis. *Nat. Prod. Commun.* **2007**, *2*, 475–498.
12. Dewick, P. M., *Medicinal natural products: a biosynthetic approach*. 3rd ed.; John Wiley & Sons Ltd: Chichester, UK, 2009.
  13. (a) Gilbody, A. W.; Perkin, W. H.; Yates, J. CXLVI.—Brazilin and haematoxylin. Part I. *J. Chem. Soc., Trans.* **1901**, *79*, 1396–1411; (b) Robinson, R. Chemistry of Brazilin and Haematoxylin. *Bull. Soc. Chim. Fr.* **1958**, 125–134.
  14. Perkin, W. H.; Robinson, R. XLVI.—Brazilin and haematoxylin. Part VIII. Synthesis of brazilinic acid, the lactones of dihydrobrazilinic and dihydrohaematoxylinic acids anhydrobrazilic acid, etc. The constitution of brazilin, haematoxylin, and their derivatives. *J. Chem. Soc., Trans.* **1908**, *93*, 489–517.
  15. Liebermann, C.; Burg, O. Ueber das Brasilin. *Ber. Dtsch. Chem. Ges.* **1876**, *9*, 1883–1888.
  16. The authors comment that Herzig (Monatsh., 1898, 19, 738) "was actually the first to discover that brazilin is a derivative of catechol."
  17. (a) Perkin, W. H.; Gilbody, A. W. 46. "On Brasilin and Haematoxylin. II.". *Proc. Chem. Soc., London* **1899**, *15*, 69–76 (see pp 75–76); (b) Perkin, W. H.; Gilbody, A. W. 25. "On brasilin and haematoxylin.". *Proc. Chem. Soc., London* **1899**, *15*, 11–44 (see pp 27–29); (c) Perkin, W. H.; Gilbody, A. W. 168. "On brasilin and haematoxylin. Part III.". *Proc. Chem. Soc., London* **1899**, *15*, 235–246 (see p 241); (d) Perkin, W. H.; Gilbody, A. W.; Yates, J. 64. "On brazilin. IV.". *Proc. Chem. Soc., London* **1900**, *16*, 105; (e) Perkin, W. H.; Yates, J. 65. "On haematoxylin. V.". *Proc. Chem. Soc., London* **1900**, *16*, 107.
  18. Perkin, W. H. CV.—Brazilin and haematoxylin. Part IV. On dimethoxycarboxybenzoylformic acid, brazilinic acid, etc. *J. Chem. Soc., Trans.* **1902**, *81*, 1008–1040.
  19. Feuerstein, W.; Kostanecki, S. V. Zur Kenntniss des Brasilins. *Ber. Dtsch. Chem. Ges.* **1899**, *32*, 1024–1030.
  20. The structure had previously been suggested by Wener and Pfeiffer ( *Chem. Zeitsch.* 1904, *3*, 421), but it was suggested with no chemical evidence.
  21. (a) Livingstone, R. Anthocyanins, Brazilin, and Related Compounds. *Nat. Prod. Rep.* **1987**, *4*, 25–33; (b) Engels, P.; Perkin, W. H.; Robinson, R. Brazilin haematoxylin, and their derivatives. Part IX. On Brazilein, haematein, and their derivatives. *J. Chem. Soc.* **1908**, *93*, 1115–1162; (c) Perkin, A. G.; Everest, A. E., Brazilwood. In *The Natural Organic Colouring Matters*, Longmans, Green & Co. London, 1918; pp 345–363; (d) Perkin, W. H.; Robinson, R.; Turner, M. R. The synthesis and constitution of certain pyranol salts related to brazilein and haematein. *J. Chem. Soc.* **1908**, *93*, 1085–1115; (e) Perkin, W. H.; Robinson, R. Brazilin, haematoxylin, and their derivatives. Part X. The constitution of trimethylbrazilone, of  $\alpha$ - and  $\beta$ -anhydrotrimethylbrazilone, and of the corresponding haematoxylin derivatives. *J. Chem. Soc.* **1909**, *95*, 381–407.
  22. Perkin, W. H.; Robinson, R. 12. "Experiments on the synthesis of brazilin and haematoxylin and their derivatives." (Preliminary note.). *Proc. Chem. Soc., London* **1912**, *28*, 1–11.
  23. Werner, A.; Pfeiffer, P. *Chem. Zeitschr.* **1904**, *3*, 421.
  24. (a) Pfeiffer, P.; Grimmer, J. Zur Kenntnis der Chromanone. (I. Mitteilung zur Brasilin-Frage.). *Ber. Dtsch. Chem. Ges.* **1917**, *50*, 911–927; (b) Crabtree, H. G.; Robinson, R.

- LXXVIII.—A synthesis of isobrazilein and certain related anhydropyranol salts. Part I. *J. Chem. Soc., Trans.* **1918**, 113, 859–880.
25. (a) Pfeiffer, P.; Emmer, H. J. Zur Kenntnis der Chromanone, II. (II. Mitteilung zur Brasilin- und Hämatoxylin-Frage). *Ber. dtsh. Chem. Ges. A/B* **1920**, 53, 945–953; (b) Pfeiffer, P.; Oberlin, J. Das Schall-Drallesche Abbauprodukt des Brasilins. (III Mitteilung zur Brasilin- und Hämatoxylin-Frage.). *Ber. dtsh. Chem. Ges. A/B* **1924**, 57, 208–213; (c) Pfeiffer, P.; Oberlin, H.; Konermann, E. Über Methoxychromonole und das Schall-Drallesche Abbauprodukt des Brasilins. (IV. Mitteilung zur Brasilin- und Hämatoxylin-Frage). *Ber. dtsh. Chem. Ges. A/B* **1925**, 58, 1947–1958.
  26. Crabtree, H. G.; Robinson, R. A synthesis of isobrazilein and certain related anhydropyranol salts. Part II. Synthesis of isohaematein. *J. Chem. Soc.* **1922**, 121, 1033–1041.
  27. Perkin, W. H.; Rây, J. N.; Robinson, R. CXXXIII.—Experiments on the synthesis of brazilin and haematoxylin and their derivatives. Part I. Veratrylidene-7-methoxychromanone and an account of a new synthesis of some benzopyrylium salts. *J. Chem. Soc.* **1926**, 941–953.
  28. Perkin, W. H.; Rây, J. N.; Robinson, R. CCLXXVII.—Experiments on the synthesis of brazilin and haematoxylin and their derivatives. Part II. A synthesis of deoxytrimethylbrazilone and of isobrazilein ferrichloride trimethyl ether. *J. Chem. Soc.* **1927**, 2094–2100.
  29. Pfeiffer, P.; Oberlin, H. Über die Synthese eines Trimethyl-anhydro-brasilins. (V. Mitteilung zur Brasilin- und Hämatoxylin-Frage). *Chem. Ber.* **1927**, 60, 2142–2148.
  30. Perkin, W. H.; Rây, J. N.; Robinson, R. CXC VIII.—Experiments on the synthesis of Brazilin and haematoxylin and their derivatives. Part III. *J. Chem. Soc.* **1928**, 1504–1513.
  31. (a) Morsingh, F.; Robinson, R., In *14th International Congress of Pure and Applied Chemistry*, Zurich, 1955; p 260; (b) Morsingh, F.; Robinson, R. The syntheses of brazilin and haematoxylin. *Tetrahedron* **1970**, 26, 281–289.
  32. Nirmal, N. P.; Rajput, M. S.; Prasad, R. G.; Ahmad, M. Brazilin from *Caesalpinia sappan* heartwood and its pharmacological activities: A review. *Asian Pac. J. Trop. Med.* **2015**, 8, 421–430.
  33. (a) Zanin, J. L.; de Carvalho, B. A.; Martineli, P. S.; dos Santos, M. H.; Lago, J. H.; Sartorelli, P.; Viegas, C., Jr.; Soares, M. G. The genus *Caesalpinia* L. (Caesalpinaceae): phytochemical and pharmacological characteristics. *Molecules* **2012**, 17, 7887–7902; (b) Badami, S.; Moorkoth, S.; Suresh, B. *Caesalpinia sappan*, a medicinal and dye yielding plant. *Nat. Prod. Rad.* **2004**, 3, 75–82.
  34. Xu, H. X.; Lee, S. F. The antibacterial principle of *Caesalpinia sappan*. *Phytother. Res.* **2004**, 18, 647–651.
  35. (a) Choi, B. M.; Kim, B. R. Upregulation of heme oxygenase-1 by brazilin via the phosphatidylinositol 3-kinase/Akt and ERK pathways and its protective effect against oxidative injury. *Eur. J. Pharmacol.* **2008**, 580, 12–18; (b) Choi, B.-M.; Lee, J.-A.; Gao, S. S.; Eun, S. Y.; Kim, Y.-S.; Ryu, S.-Y.; Choi, Y.-H.; Park, R.; Kwon, D. Y.; Kim, B.-R. Brazilin and the extract from *Caesalpinia sappan* L. protect oxidative injury through the expression of heme oxygenase-1. *BioFactors* **2007**, 30, 149–157.
  36. (a) You, E. J.; Khil, L. Y.; Kwak, W. J.; Won, H. S.; Chae, S. H.; Lee, B. H.; Moon, C. K. Effects of brazilin on the production of fructose-2,6-bisphosphate in rat hepatocytes. *J. Ethnopharmacol.* **2005**, 102, 53–57; (b) Li, Z. Y.; Zheng, Y.; Chen, Y.; Pan, M.; Zheng, S.



- B.; Huang, W.; Zhou, Z. H.; Ye, H. Y. Brazilin Ameliorates Diabetic Nephropathy and Inflammation in db/db Mice. *Inflammation* **2017**, *40*, 1365–1374.
37. (a) Cuong, T. D.; Hung, T. M.; Kim, J. C.; Kim, E. H.; Woo, M. H.; Choi, J. S.; Lee, J. H.; Min, B. S. Phenolic Compounds from *Caesalpinia sappan* Heartwood and Their Anti-inflammatory Activity. *J. Nat. Prod.* **2012**, *75*, 2069–2075; (b) Jayakumar, T.; Chang, C. C.; Lin, S. L.; Huang, Y. K.; Hu, C. M.; Elizebeth, A. R.; Lin, S. C.; Choy, C. S. Brazilin Ameliorates High Glucose-Induced Vascular Inflammation via Inhibiting ROS and CAMs Production in Human Umbilical Vein Endothelial Cells. *Biomed. Res. Int.* **2014**, 1–10; (c) Jung, E. G.; Han, K. I.; Hwang, S. G.; Kwon, H. J.; Patnaik, B. B.; Kim, Y. H.; Han, M. D. Brazilin isolated from *Caesalpinia sappan* L. inhibits rheumatoid arthritis activity in a type-II collagen induced arthritis mouse model. *BMC Complement. Altern. Med.* **2015**, *15*, 1–11; (d) Lee, H. J.; Kang, S. W.; Byun, H. S.; Jeon, J.; Park, K. A.; Kang, K. D.; Seo, W. Y.; Won, M. H.; Seok, J. H.; Han, M. D.; Shen, H. M.; Hur, G. M. Brazilin Limits Inflammatory Responses through Induction of Prosurvival Autophagy in Rheumatoid Fibroblast-Like Synoviocytes. *Plos One* **2015**, *10*, 15; (e) Weinmann, D.; Mueller, M.; Walzer, S. M.; Hobusch, G. M.; Lass, R.; Gahleitner, C.; Viernstein, H.; Windhager, R.; Toegel, S. Brazilin blocks catabolic processes in human osteoarthritic chondrocytes via inhibition of NFKB1/p50. *Journal of Orthopaedic Research* **2018**, *36*, 2431–2438.
38. (a) Sang-Gu, H.; Jin-Seon, L.; Seung-Hwa, B.; Byung-Hun, J.; Won-Hong, W.; Hyun-Ja, C. Inhibitory Effects of Butyl Alcohol Extract from *Caesalpinia sappan* L. on Melanogenesis in Melan-a Cells. *Korean Journal of Pharmacognosy* **2002**, *33*, 130–136; (b) Woongchon, M.; Hyun-Tai, L.; Kang-Hoon, J.; Hye-Young, C.; Eun-Kyoung, S. A DNA Strand-Nicking Principle of a Higher Plant, *Caesalpinia sappan*. *Arch. Pharm. Res.* **2003**, *26*, 147–150; (c) Bae, I. K.; Min, H. Y.; Han, A. R.; Seo, E. K.; Lee, S. K. Suppression of lipopolysaccharide-induced expression of inducible nitric oxide synthase by brazilin in RAW 264.7 macrophage cells. *Eur. J. Pharmacol.* **2005**, *513*, 237–242; (d) Sasaki, Y.; Hosokawa, T.; Nagai, M.; Nagumo, S. *In vitro* study for inhibition of NO production about constituents of Sappan Lignum. *Biol. Pharm. Bull.* **2007**, *30*, 193–196; (e) Saenjum, C.; Chaiyasut, C.; Kadchumsang, S.; Chansakaow, S.; Suttajit, M. Antioxidant activity and protective effects on DNA damage of *Caesalpinia sappan* L. extract. *J. Med. Plants Res.* **2010**, *4*, 1594–1600; (f) Kim, B.; Kim, S. H.; Jeong, S. J.; Sohn, E. J.; Jung, J. H.; Lee, M. H.; Kim, S. H. Brazilin induces apoptosis and G2/M arrest via inactivation of histone deacetylase in multiple myeloma U266 cells. *J. Agric. Food. Chem.* **2012**, *60*, 9882–9889; (g) Lee, D. Y.; Lee, M. K.; Kim, G. S.; Noh, H. J.; Lee, M. H. Brazilin inhibits growth and induces apoptosis in human glioblastoma cells. *Molecules* **2013**, *18*, 2449–2457; (h) Nirmal, N. P.; Panichayupakaranant, P. Antioxidant, antibacterial, and anti-inflammatory activities of standardized brazilin-rich *Caesalpinia sappan* extract. *Pharm. Biol.* **2015**, *53*, 1339–1343; (i) Handayani, S.; Susidarti, R. A.; Jenie, R. I.; Meiyanto, E. Two Active Compounds From *Caesalpinia sappan* L. In Combination With Cisplatin Synergistically Induce Apoptosis And Cell Cycle Arrest On WiDr Cells. *Adv. Pharm. Bull.* **2017**, *7*, 375–380; (j) He, Z. J.; Zhu, F. Y.; Li, S. S.; Zhong, L.; Tan, H. Y.; Wang, K. Inhibiting ROS-NF- $\kappa$ B-dependent autophagy enhanced brazilin-induced apoptosis in head and neck squamous cell carcinoma. *Food Chem. Toxicol.* **2017**, *101*, 55–66; (k) Meiyanto, E.; Jenie, R. I.; Handayani, S.; Susidarti, R. A.; Udin, Z.; Ilmawati, G. P. N.; Amalina, N. D. Cytotoxic and Antimetastatic Effect of Brazilin in Combination with Doxorubicin on MCF-7/HER2 Cells. *Cancer Science* **2018**, *109*, 364–

- 364; (l) Kang, Y.; He, P. H.; Wang, H.; Ye, Y. B.; Li, X.; Xie, P. G.; Wu, B. W. Brazilin induces FOXO3A-dependent autophagic cell death by disturbing calcium homeostasis in osteosarcoma cells. *Cancer Chemotherapy and Pharmacology* **2018**, *82*, 479–491; (m) Zhang, T.; He, J.; Zhang, S.; Wang, G.; Ma, E.; Wang, J.; Yang, X.; Zheng, Y.; Zhang, J. Brazilin induces T24 cell death through c-Fos and GADD45 $\beta$  independently regulated genes and pathways. *IUBMB Life* **2018**, *70*, 1101–1110; (n) Meiyanto, E.; Lestari, B.; Sugiyanto, R. N.; Jenie, R. I.; Utomo, R. Y.; Sasmito, E.; Murwanti, R. *Caesalpinia sappan* L. heartwood ethanolic extract exerts genotoxic inhibitory and cytotoxic effects. *Oriental Pharmacy and Experimental Medicine* **2019**, *19*, 27–36; (o) Wan, Y. J.; Xu, L.; Song, W. T.; Liu, Y. Q.; Wang, L. C.; Zhao, M. B.; Jiang, Y.; Liu, L. Y.; Zeng, K. W.; Tu, P. F. The Ethanolic Extract of *Caesalpinia sappan* Heartwood Inhibits Cerebral Ischemia/Reperfusion Injury in a Rat Model Through a Multi-Targeted Pharmacological Mechanism. *Frontiers in Pharmacology* **2019**, *10*, 15.
39. Wang, X. Q.; Liu, W.; Duan, S. Y.; Yang, X. D.; Zhang, H. B. Research Progress on the Synthesis of Brazilin-Type Natural Products. *Chin. J. Org. Chem.* **2015**, *35*, 1585–1597.
40. (a) Dann, O.; Hofmann, H. Chromane, XV. Synthese von ( $\pm$ )-Brasilin. *Liebigs Annalen* **1963**, *667*, 116–125; (b) Kirkiacharian, B. S.; Billet, D.; Durgeat, M.; Heitz, S.; Adjangba, M. K. New Synthesis of ( $\pm$ )-Trimethylbrazilin. *Bull. Soc. Chim. Fr.* **1975**, 1770–1772.
41. (a) Davis, F. A.; Chen, B. C. Enantioselective synthesis of (+)-*O*-trimethylsappanone B and (+)-*O*-trimethylbrazilin. *J. Org. Chem.* **1993**, *58*, 1751–1753; (b) Javed, U.; Karim, M.; Jahng, K. C.; Park, J. G.; Jahng, Y. Enantioselective syntheses of (+)- and (-)-brazilin. *Tetrahedron: Asymmetry* **2014**, *25*, 1270–1274; (c) Jung, Y.; Kim, I. Total Synthesis of Brazilin. *J. Org. Chem.* **2015**, *80*, 2001–2005; (d) Jung, Y.; Kim, I. A concise synthetic approach to brazilin via Pd-catalyzed allylic arylation. *Org. Biomol. Chem.* **2015**, *13*, 4331–4335.
42. Yen, C. T.; Nakagawa-Goto, K.; Hwang, T. L.; Wu, P. C.; Morris-Natschke, S. L.; Lai, W. C.; Bastow, K. F.; Chang, F. R.; Wu, Y. C.; Lee, K. H. Antitumor agents. 271: Total synthesis and evaluation of brazilein and analogs as anti-inflammatory and cytotoxic agents. *Bioorg. Med. Chem. Lett.* **2010**, *20*, 1037–1039.
43. (a) Huang, Y. D.; Zhang, J. S.; Pettus, T. R. R. Synthesis of ( $\pm$ )-Brazilin using IBX. *Org. Lett.* **2005**, *7*, 5841–5844; (b) Li, L. Q.; Li, M. M.; Wang, K.; Qin, H. B. Total synthesis of ( $\pm$ )-brazilin and formal synthesis of ( $\pm$ )-brazilein, ( $\pm$ )-brazilide A using *m*-CPBA. *Tetrahedron Lett.* **2013**, *54*, 6029–6031.
44. Wang, X.; Zhang, H.; Yang, X.; Zhao, J.; Pan, C. Enantioselective total synthesis of (+)-brazilin, (-)-brazilein and (+)-brazilide A. *Chem. Commun.* **2013**, *49*, 5405–5407.
45. (a) Pan, C. X.; Zeng, X. H.; Guan, Y. F.; Jiang, X. L.; Li, L. A.; Zhang, H. B. Design and Synthesis of Brazilin-Like Compounds. *Synlett* **2011**, 425–429; (b) Pan, C. X.; Guan, Y. F.; Zhang, H. B. Synthesis of Aza-brazilin/diarylindan-Based Hybrid. *Chin. J. Org. Chem.* **2012**, *32*, 1116–1120; (c) Wang, X. Q.; Li, Y.; Yang, X. D.; Zhang, H. B. Design, Synthesis and Cytotoxic Activity of Novel Hybrid Compounds between Aza-brazilin and Imidazolium. *Chin. J. Org. Chem.* **2015**, *35*, 1276–1285.
46. Yadav, J. S.; Mishra, A. K.; Das, S. Formal synthesis of ( $\pm$ )-brazilin and total synthesis of ( $\pm$ )-brazilane. *Tetrahedron* **2014**, *70*, 7560–7566.
47. Pan, C. X.; Guan, Y. F.; Zhang, H. B. Synthesis of a Brazilin Analog. *Acta Chim. Sinica* **2012**, *70*, 183–189.

48. (a) Gutman, E. S.; Arredondo, V.; Van Vranken, D. L. Cyclization of  $\eta^3$ -Benzylpalladium Intermediates Derived from Carbene Insertion. *Org. Lett.* **2014**, *16*, 5498–5501; (b) Ishii, H.; Koyama, H.; Hagiwara, K.; Miura, T.; Xue, G.; Hashimoto, Y.; Kitahara, G.; Aida, Y.; Suzuki, M. Synthesis and biological evaluation of deoxy-hematoxylin derivatives as a novel class of anti-HIV-1 agents. *Bioorg. Med. Chem. Lett.* **2012**, *22*, 1469–1474.
49. Kende, A. S.; King, M. L.; Curran, D. P. Total synthesis of ( $\pm$ )-4'-demethyl-4-epipodophyllotoxin by insertion-cyclization. *J. Org. Chem.* **1981**, *46*, 2826–2828.
50. Arredondo, V.; Roa, D. E.; Yan, S.; Liu-Smith, F.; Van Vranken, D. L. Total Synthesis of ( $\pm$ )-Pestalachloride C and ( $\pm$ )-Pestalachloride D through a Biomimetic Knoevenagel/Hetero-Diels–Alder Cascade. *Org. Lett.* **2019**, *21*, 1755–1759.
51. Hu, D. X.; Grice, P.; Ley, S. V. Rotamers or diastereomers? An overlooked NMR solution. *J. Org. Chem.* **2012**, *77*, 5198–5202.
52. (a) Baldwin, J. E. Rules for Ring-Closure. *J. Chem. Soc., Chem. Commun.* **1976**, 734–736; (b) Krohn, K.; Baltus, W. Synthesis of Rac-Fridamycin-E and Ent-Fridamycin-E. *Tetrahedron* **1988**, *44*, 49–54; (c) Chen, H.-H.; May, J. A.; Severns, B. S. Pyranoindazoles and their use for the treatment of glaucoma. US 6,696,476 B2, Feb. 24, 2004; (d) Kawamura, K.; Ohta, T.; Otani, G. A New Method for the Synthesis of 3-Chromanol Derivatives by Sodium Iodide-Catalyzed Cyclization of Epoxide. *Chem. Pharm. Bull.* **1990**, *38*, 2088–2091; (e) Ganguly, N. C.; Nayek, S.; Chandra, S. An efficient regioselective bromination protocol of activated coumarins using 2,4,4,6-tetrabromo-2,5-cyclohexadienone. *Can. J. Chem.* **2013**, *91*, 1155–1159; (f) Doherty, E. M.; Retz, D.; Gavva, N. R.; Tamir, R.; Treanor, J. J.; Norman, M. H. 4-Aminopyrimidine tetrahydronaphthols: a series of novel vanilloid receptor-1 antagonists with improved solubility properties. *Bioorg. Med. Chem. Lett.* **2008**, *18*, 1830–1834; (g) Perner, R. J.; Koenig, J. R.; DiDomenico, S.; Bayburt, E. K.; Daanen, J. F.; Gomtsyan, A.; Kort, M. E.; Kym, P. R.; Schmidt, R. G.; Vasudevan, A.; Voight, E. TRPV1 antagonists. US 7,998,993 B2, Aug. 16, 2011; (h) Barrero, A. F.; Alvarez-Manzaneda, E. J.; Chahboun, R.; Cortés, M.; Armstrong, V. Synthesis and antitumor activity of puupehedione and related compounds. *Tetrahedron* **1999**, *55*, 15181–15208.
53. Chaipech, S.; Morikawa, T.; Ninomiya, K.; Yoshikawa, M.; Pongpiriyadacha, Y.; Hayakawa, T.; Muraoka, O. Structures of Two New Phenolic Glycosides, Kaempferiaosides A and B, and Hepatoprotective Constituents from the Rhizomes of *Kaempferia parviflora*. *Chem. Pharm. Bull.* **2012**, *60*, 62–69.
54. Srikrishna, A.; Vasantha Lakshmi, B. Construction of vicinal quaternary carbon atoms by Ireland ester Claisen rearrangement: total synthesis of ( $\pm$ )-herbertenolide, ( $\pm$ )-herberteneacetal, ( $\pm$ )-herbertene-1,14-diol and ( $\pm$ )-herbertene-1,15-diol. *Tetrahedron Lett.* **2005**, *46*, 4879–4881.
55. Findlay, J. A.; Mebe, P.; Stern, M. D.; Givner, M. L. Total synthesis of 3,17 $\beta$ -dihydroxy-6-oxaestra-1,3,5(10),7-tetraen and related miroestrol analogues. *Can. J. Chem.* **1980**, *58*, 1427–1434.
56. Clark-Lewis, J. W.; McGarry, E. J. Hydroboration of chromenes, flav-2-enes, flavylum salts, and flavones. *Aust. J. Chem.* **1973**, *26*, 819–826.
57. Rondão, R.; Seixas de Melo, J. S.; Pina, J.; Melo, M. J.; Vitorino, T.; Parola, A. J. Brazilwood reds: the (photo)chemistry of brazilin and brazilin. *J. Phys. Chem. A* **2013**, *117*, 10650–10660.

## Supporting Information

### General Information and Reagents

**Reactions and materials:** Unless otherwise specified, all reactions were performed under an atmosphere of dry N<sub>2</sub> gas. Anhydrous solvents and reagents, where applicable, were transferred using Schlenk technique. Toluene, tetrahydrofuran (THF), diethyl ether (Et<sub>2</sub>O), and dichloromethane (CH<sub>2</sub>Cl<sub>2</sub>) were dried by passage through alumina according to the procedure of Grubbs and co-workers.<sup>1</sup> All other solvents were purified according to reported procedures.<sup>2</sup> Unless otherwise noted, all reagents were commercially obtained and used without prior purification. Where applicable, acetone Optima™ (Fisher), and 30% (w/w) H<sub>2</sub>O<sub>2</sub> (Fisher) was used.

**Analysis and Purification:** All reactions were monitored by thin-layer chromatography (TLC) and visualized by UV (254 nm) illumination and by KMnO<sub>4</sub> and *p*-anisaldehyde (*p*-anis) dip stains. The *p*-anis stain was prepared by adding 25 mL of concentrated sulfuric acid to a chilled solution of 95% ethanol (676 mL, made from 200 proof ethanol and de-ionized water). Glacial acetic acid (7.5 mL) and *p*-anisaldehyde (99%, 18.4 mL) were then added to afford a colorless solution. The stain was stored at 0 °C. Analytical TLC was performed using EMD Millipore 0.25 mm Silica gel 60 F<sub>254</sub> 20 × 20 cm plates (EM1.05715.0001). “Flash” chromatography on silica gel was performed using Agela Technologies Flash Silica sorbent (40-63 μm) silica gel of 230-400 mesh (CS605025-P).

**Identity:** Unless otherwise noted, <sup>1</sup>H and <sup>13</sup>C NMR spectral data were recorded at 23 °C using a Bruker Avance 500 or 600 MHz spectrometer equipped with a cryoprobe. All spectra were calibrated to tetramethylsilane (0.00 ppm) unless otherwise specified, in which case the reference

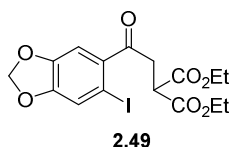
peak will be reported as Shift (reference). In general, NMR spectra taken in Chloroform-*d* were calibrated to tetramethylsilane (0.00 ppm). <sup>1</sup>H and <sup>13</sup>C NMR spectra taken in Methanol-*d*<sub>4</sub> were calibrated to 3.31 ppm and 49.15 ppm, respectively. <sup>1</sup>H and <sup>13</sup>C NMR spectra taken in *N,N*-Dimethyl-formamide-*d*<sub>7</sub> were calibrated to 2.75 ppm, and 163.15 ppm, respectively. Variable temperature <sup>1</sup>H NMR stacked spectra taken in *N,N*-Dimethyl-formamide-*d*<sub>7</sub> were calibrated to 8.03 ppm. <sup>1</sup>H and <sup>13</sup>C NMR spectra taken in Toluene-*d*<sub>8</sub> were calibrated to 2.09 ppm and 20.4 ppm, respectively.

The NMR data are reported as follows: chemical shift in ppm ( $\delta$ ), multiplicity (br = broad, app = apparent, s = singlet, d = doublet, t = triplet, q = quartet and m = multiplet), coupling constants (Hz), and integration. NMR data was processed using Mestrelab Research MestReNova 11.0.2 software, using automatic baseline correction, automatic phasing, and the multiplet analysis function. Infrared spectroscopy data was acquired using a PerkinElmer Spectrum Two IR Spectrometer or a Thermo Scientific iD5 ATR (Nicolet iS5) Spectrometer. Mass spectra were obtained using a Waters (Micromass) LCT premier with a TOF analyzer using the ionization method indicated. Melting points were taken on a Thermo Scientific Electrothermal Mel-Temp<sup>®</sup> apparatus (Model No. 1001D) using a mercury thermometer. The reported melting point values are uncorrected. Chemical names found in the supporting information were generated using PerkinElmer ChemBioDraw Ultra 13.0 software.

## Experimental Procedures

### Synthesis of Malonate 2.49

#### Diethyl 2-(2-(6-iodobenzo[*d*][1,3]dioxol-5-yl)-2-oxoethyl)malonate, 2.49



Malonate **2.49** was synthesized following a modified procedure from Ziegler and co-workers.<sup>3</sup> Briefly, a 25 mL 2-neck round-bottom flask was equipped with a stir bar, flame-dried, and charged with aryl iodide 1-(6-iodobenzo[*d*][1,3]dioxol-5-yl)ethan-1-one<sup>4</sup> (0.300 g, 1.03 mmol). The round-bottom flask was evacuated and backfilled with N<sub>2</sub> (× 3) before being charged with DCM (6.1 mL) and TFA (0.04 mL, 0.52 mmol). To the yellow solution was added pyridinium tribromide (0.363 g, 1.14 mmol) in four portions over four hours. The flask was wrapped in aluminum foil during the reaction to exclude light. After 10 h, starting material was no longer detectable by TLC (100% toluene). The crude reaction mixture was quenched with saturated aqueous NaHCO<sub>3</sub> (6.0 mL) and stirred until gas ceased evolving. The crude reaction mixture was transferred to a separatory funnel and washed once with 6 mL of aqueous 1 N HCl. The aqueous layer was extracted with DCM (1 × 12 mL) and the combined organic phases were washed with brine (1 × 20 mL), dried (Na<sub>2</sub>SO<sub>4</sub>), and concentrated *in vacuo*. The resulting yellow oil was immediately purified by flash chromatography (10:90 hexanes:toluene) to afford  $\alpha$ -bromoketone as a clear oil (0.203 g, 0.55 mmol). *R*<sub>f</sub> = 0.55 (100% toluene). <sup>1</sup>H NMR (500 MHz, CDCl<sub>3</sub>)  $\delta$  7.36 (s, 1H), 7.02 (s, 1H), 6.07 (s, 2H), 4.40 (s, 2H). <sup>13</sup>C NMR (126 MHz, CDCl<sub>3</sub>)  $\delta$  193.5, 150.9, 148.3, 134.1, 120.5, 109.5, 102.6, 82.4, 32.7.

A flame-dried 25 mL, 2-necked round-bottom flask equipped with a short-stem vacuum adapter and rubber septum was charged with NaH (0.066 g, 1.65 mmol, 60% dispersion in mineral oil), and a stir bar. The flask cooled was to -10 °C in a brine-ice bath, and charged with THF (4.5 mL). Diethyl malonate (0.272 g, 1.65 mmol) was added dropwise via syringe over 5 min resulting

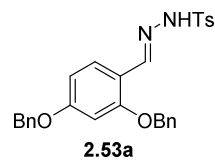
in a white slurry. After 25 min, a solution of  $\alpha$ -bromoketone from the previous step (0.203 g, 0.55 mmol) in THF (1.0 mL) was added dropwise via syringe over 1 min. The reaction was removed from the brine-ice bath and warmed to 23 °C while stirring. After 4.5 h,  $\alpha$ -bromoketone was no longer detectable by TLC (25:75 EtOAc:hexanes).

The reaction mixture was quenched with 15 mL of saturated aqueous  $\text{NH}_4\text{Cl}$  and transferred to a separatory funnel. The mixture was extracted with  $\text{Et}_2\text{O}$  ( $3 \times 20$  mL) and the combined organic phases were dried ( $\text{Na}_2\text{SO}_4$ ) and concentrated *in vacuo* to afford a clear oil. The oil was purified by flash chromatography (10:90 EtOAc:hexanes) to yield diethyl 2-(2-(6-iodobenzo[*d*][1,3]dioxol-5-yl)-2-oxoethyl)malonate **2.49** as a clear oil (0.153 g, 62%).

$R_f = 0.51$  (20:80 EtOAc:hexanes).  $^1\text{H}$  NMR (500 MHz, Chloroform-*d*)  $\delta$  7.36 (s, 1H), 7.15 (s, 1H), 6.05 (s, 2H), 4.23 (qd,  $J = 7.1, 3.2$  Hz, 4H), 4.06 (t,  $J = 7.2$  Hz, 1H), 3.45 (d,  $J = 7.2$  Hz, 2H), 1.29 (t,  $J = 7.1$  Hz, 6H);  $^{13}\text{C}$  NMR (126 MHz, Chloroform-*d*)  $\delta$  198.5, 168.8, 150.6, 148.3, 135.6, 120.7, 109.2, 102.4, 81.5, 61.9, 47.5, 40.2, 14.1; HRMS (ESI):  $m/z$  calcd for  $\text{C}_{16}\text{H}_{17}\text{O}_7\text{INa}$   $[\text{M} + \text{Na}]^+$  470.9917, found 470.9906.

## Synthesis of *N*-tosylhydrazones

### *N'*-(2,4-bis(benzyloxy)benzylidene)-4-methylbenzenesulfonohydrazide, **2.53a**

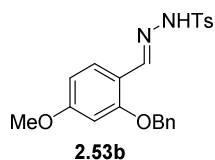


3,5-Dibenzoyloxy-*N*-tosylhydrazone **2.53a** was synthesized as published by Aggarwal and co-workers with slight modification.<sup>5</sup> To a solution of *p*-toluenesulfonyl hydrazide (1.8 g, 9.5 mmol) in 5 mL of MeOH was added 2,4-dibenzoyloxybenzaldehyde (3.0 g, 9.4 mmol) in three portions over 15 min. A thick yellow precipitate formed during the course of the reaction. Additional MeOH (25 mL) was added to ensure proper stirring. Upon complete consumption of the starting benzaldehyde, the reaction was cooled (0 °C) for 15 min. The yellow precipitate was filtered, washed with cold MeOH, and then

purified by flash chromatography (0:100 – 20:80 EtOAc:hexanes) to yield product **2.53a** as a pale yellow solid (3.8 g, 83%).

$R_f$  = 0.37 (30:70 EtOAc:hexanes). mp = 154–155 °C;  $^1\text{H}$  NMR (500 MHz, Chloroform-*d*)  $\delta$  8.07 (s, 1H), 7.84 (dd,  $J$  = 8.4, 2.2 Hz, 2H), 7.78 (d,  $J$  = 8.8 Hz, 1H), 7.61 (s, 1H), 7.45 – 7.30 (m, 10H), 7.26 (d,  $J$  = 8.4 Hz, 2H), 6.57 (dd,  $J$  = 8.7, 2.3 Hz, 1H), 6.52 (d,  $J$  = 2.3 Hz, 1H), 5.04 (s, 2H), 4.97 (s, 2H), 2.38 (s, 3H);  $^{13}\text{C}$  (125 MHz, Chloroform-*d*)  $\delta$  161.9, 158.3, 144.06, 144.04, 136.3, 136.1, 135.4, 129.6, 128.77, 128.75, 128.3, 128.2, 127.9, 127.8, 127.5, 115.2, 106.9, 100.1, 70.4, 70.2, 21.6; IR (ATR) 3201, 1601, 1164  $\text{cm}^{-1}$ . HRMS (ESI):  $m/z$  calcd for  $\text{C}_{28}\text{H}_{26}\text{N}_2\text{O}_4\text{SNa}$   $[\text{M} + \text{Na}]^+$  509.1511, found 509.1499.

#### ***N'*-(2-(benzyloxy)-4-methoxybenzylidene)-4-methylbenzenesulfonylhydrazide, 2.53b**



To a stirring solution of commercially available 2-hydroxy-4-methoxybenzaldehyde (8.05 g, 52.6 mmol) and anhydrous  $\text{K}_2\text{CO}_3$  (7.99 g, 57.8 mmol) in DMF (60.0 mL) was added benzyl bromide (17.5 mL, 63.1 mmol) in one portion. The reaction was stirred at 23 °C until no starting material was detected by TLC. The reaction mixture was poured into 300 mL of 0.1 M HCl, and the aqueous layer extracted with EtOAc (3  $\times$  100 mL). The combined organic layers were washed with  $\text{H}_2\text{O}$  (3  $\times$  300 mL) and brine (1  $\times$  300 mL). The organic layer was dried ( $\text{MgSO}_4$ ) and concentrated *in vacuo* to afford a yellow solid. The yellow solid was purified by flash chromatography (5:95 EtOAc:hexanes) to yield 2-benzyloxy-4-hydroxybenzaldehyde<sup>6</sup> as a white solid (11.9 g, 93%) which was carried on to the next step without further purification.

To a cooled (0 °C) solution of *p*-toluenesulfonyl hydrazide (11.7 g, 62.7 mmol) in THF (105 mL) was added 2-benzyloxy-4-methoxybenzaldehyde (11.9 g, 52.3 mmol). After stirring for 30 min, the reaction mixture was warmed to 23 °C. A thick yellow precipitate formed during the

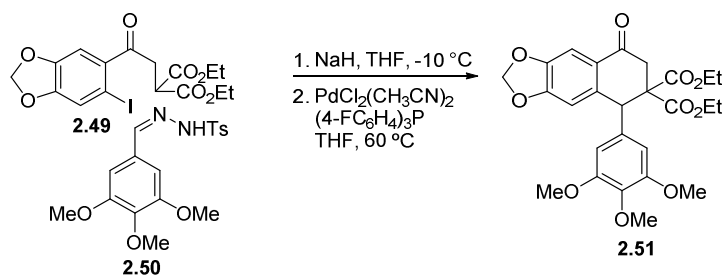


course of the reaction. Upon consumption of the aldehyde, the reaction was concentrated *in vacuo* and recrystallized from MeOH to afford product **2.53b** as an off-white solid (15.6 g, 73%). The filtrate was further recrystallized to afford additional *N*-tosylhydrazone **2.53b** as an off-white solid (2.78 g, 13%). The identical samples were combined to afford *N*-tosylhydrazone **2.53b** in 86% yield.

$R_f = 0.44$  (40:60 EtOAc:hexanes, stains orange by *p*-anis dip stain). mp = 162–163 °C.  $^1\text{H}$  NMR (600 MHz, Chloroform-*d*)  $\delta$  8.09 (s, 1H), 7.84 (d,  $J = 8.3$  Hz, 2H), 7.79 (d,  $J = 8.6$  Hz, 1H), 7.40 – 7.31 (m, 5H), 7.28 – 7.26 (m, 2H), 6.50 (dd,  $J = 8.7, 2.3$  Hz, 1H), 6.44 (d,  $J = 2.3$  Hz, 1H), 5.00 (s, 2H), 3.79 (s, 3H), 2.38 (s, 3H); 5.00 (s, 2H), 3.79 (s, 3H), 2.38 (s, 3H).  $^{13}\text{C}$  NMR (151 MHz, Chloroform-*d*)  $\delta$  162.8, 158.4, 144.1, 144.0, 136.2, 135.5, 129.6, 128.7, 128.3, 128.0, 127.9, 127.5, 115.1, 106.1, 99.2, 70.5, 55.5, 21.6; IR (ATR) 3193, 3066, 3035, 2862, 2840, 1606, 1506, 1442, 1279, 1155, 1022, 822  $\text{cm}^{-1}$ . HRMS (ESI)  $m/z$  calcd for  $\text{C}_{22}\text{H}_{22}\text{O}_4\text{SH}$   $[\text{M} + \text{H}]^+$  411.1378, found 411.1378.

### Synthesis of 1-Aryltetralin, 2.51, and 1-Arylindanes 2.56–2.58

#### Diethyl 8-oxo-5-(3,4,5-trimethoxyphenyl)-7,8-dihydronaphtho[2,3-*d*][1,3]dioxole-6,6(5*H*)-dicarboxylate, 2.51.



A flame-dried 5 mL, pear-shaped flask was charged with PdCl<sub>2</sub>(MeCN)<sub>2</sub> (2.6 mg, 0.01 mmol), tris(4-fluorophenyl)phosphine (12.6 mg, 0.04 mmol), and a stir bar. The flask was purged

and backfilled with nitrogen three times and then fitted with a rubber septum. THF (0.3 mL) was then added and the mixture was stirred for 10 min, resulting in a clear yellow solution.

A separate flame-dried 5 mL, pear-shaped flask containing malonate **2.49** (44.5 mg, 0.10 mmol), *N*-tosylhydrazone **2.50** (72.9 mg, 0.20 mmol), and a stir bar was purged and backfilled with nitrogen three times and fitted with a rubber septum. THF (0.3 mL) was added and the mixture was stirred for 10 min resulting in a clear solution.

A separate flame-dried 15 mL, round-bottom flask was equipped with a short-stem vacuum adapter and charged with un-rinsed 60% NaH/mineral oil (14.4 mg, 0.36 mmol) and a stir bar. The flask was purged and backfilled with nitrogen three times and fitted with a rubber septum. THF (0.8 mL) was added and the suspension was cooled to  $-10\text{ }^{\circ}\text{C}$  in a brine-ice bath. The solution of malonate **2.49** and *N*-tosylhydrazone **2.50** in THF was then added dropwise via syringe over 5 min to the 15 mL flask containing a stirring NaH suspension. During the course of addition, a white solid precipitated out of solution. The flask containing malonate **2.49** and *N*-tosylhydrazone **2.50** was washed with THF ( $2 \times 0.3\text{ mL}$ ) and the washes were added to the 15 mL flask.

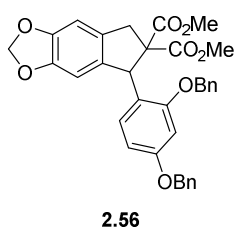
The flask was then warmed to  $23\text{ }^{\circ}\text{C}$  and stirred for 20 min. Under a stream of nitrogen, the yellow catalyst solution was added to the reaction. The flask containing catalyst solution was washed with THF ( $2 \times 0.3\text{ mL}$ ) and the washes were added to the reaction. The reaction mixture was heated at  $60\text{ }^{\circ}\text{C}$ . After 1.5 h, malonate **2.49** was no longer detectable by TLC.

The reaction mixture was cooled to  $23\text{ }^{\circ}\text{C}$ , diluted with 15 mL of  $\text{Et}_2\text{O}$ , and passed through a plug of silica. The plug of silica was washed with  $\text{Et}_2\text{O}$  ( $3 \times 100\text{ mL}$ ) and the filtrate was concentrated *in vacuo*. The product was purified by flash chromatography on silica gel (25:75

EtOAc:hexanes) to afford a mixture of tetralone **2.51** and azine (9:1 tetralone **2.51**:azine) as a yellow solid. (24.5 mg, 50%).

$R_f = 0.20$  (10:90 EtOAc:toluene).  $^1\text{H NMR}$  (500 MHz,  $\text{CDCl}_3$ )  $\delta$  7.47 (s, 1H), 6.64 (s, 1H), 6.23 (s, 2H), 6.02 (s, 2H), 5.05 (s, 1H), 4.19 – 3.98 (m, 4H), 3.80 (s, 3H), 3.73 (s, 6H), 3.28 (d,  $J = 18.1$  Hz, 1H), 3.21 (d,  $J = 18.0$  Hz, 1H), 1.18 (t,  $J = 7.2$  Hz, 3H), 1.14 (t,  $J = 7.1$  Hz, 3H);  $^{13}\text{C NMR}$  (126 MHz,  $\text{CDCl}_3$ )  $\delta$  193.1, 169.4, 168.0, 153.4, 153.1, 147.9, 140.5, 137.6, 132.9, 129.5, 128.8, 126.3, 108.8, 107.9, 106.7, 105.4, 103.4, 102.0, 62.4, 62.0, 60.8, 59.9, 56.1, 49.8, 38.4, 13.9, 13.8. HRMS (ESI)  $m/z$  calcd for  $\text{C}_{26}\text{H}_{28}\text{O}_{10}\text{Na}$   $[\text{M} + \text{Na}]^+$  523.1580, found 523.1570.

### Dimethyl 5-(2,4-bis(benzyloxy)phenyl)-5,7-dihydro-6H-indeno[5,6-d][1,3]dioxole-6,6-dicarboxylate, **2.56**



1-Arylindane **2.56** was synthesized using the same carbonylative annulation procedure for tetralone **2.51** above. To a stirring, chilled ( $-10$  °C) solution of un-rinsed 60% NaH/mineral oil (184 mg, 4.59 mmol) in THF (21.3 mL) was added a pre-stirred solution of malonate **2.52a** (0.500 g, 1.28 mmol) and *N*-tosylhydrazine **2.53a** (1.24 g, 2.55 mmol), in THF (7.1 mL). Additional THF ( $2 \times 7.1$  mL) was used to transfer any remaining reagent solution. After 15 min, the stirring, cooled, heterogeneous solution was warmed to 23 °C, and stirred an additional 20 min. A pre-stirred solution of  $\text{PdCl}_2(\text{CH}_3\text{CN})_2$  (33.1 mg, 0.128 mmol) and  $\text{P}(4\text{-FC}_6\text{H}_5)_3$  (161 mg, 0.510 mmol) in THF (7.1 mL) was then added. Additional THF ( $2 \times 7.1$  mL) was used to transfer any remaining catalyst solution. The reaction was heated (60 °C) and monitored for the consumption of malonate **2.52a** and *N*-tosylhydrazine **2.53a** starting material. After 2 h, neither was detectable by TLC. The mixture was cooled to 23 °C, diluted with  $\text{Et}_2\text{O}$  (25 mL), and then passed through a pad of silica gel. The pad was rinsed with  $\text{Et}_2\text{O}$  ( $3 \times 15$  mL) and the filtrate concentrated *in vacuo* to afford a crude red-

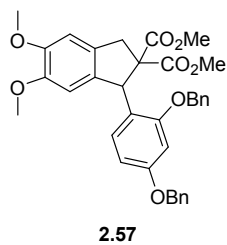
brown oil. The oil was purified by two rounds of flash chromatography (0:100 – 10:90 EtOAc:hexanes; then 1:99 EtOAc:toluene) to yield arylindane **2.56** as a yellow solid (574 mg, 80%).

$R_f$  = 0.30 (20:80 EtOAc:hexanes, stains mahogany by *p*-anis dip stain). mp = 48–58 °C.  $^1\text{H}$  NMR (500 MHz,  $\text{CDCl}_3$ , 298.0 K)  $\delta$  7.54 (s, 2H), 7.43 – 7.29 (m, 6H), 6.68 (s, 0.7H), 6.57 (s, 0.6H), 6.50 (s, 0.3H), 6.41 (s, 1H), 5.89 (s, 4H), 5.08 (s, 2H), 5.03 – 4.92 (m, 2H), 3.97 (d,  $J$  = 16.7 Hz, 0.6H), 3.71 (s, 3H), 3.30 (d,  $J$  = 16.1 Hz, 0.4H), 3.20 (s, 3H);  $^{13}\text{C}$  NMR (126 MHz,  $\text{CDCl}_3$ , 298.0 K)  $\delta$  172.3, 170.0, 158.8, 157.0, 147.4, 137.2, 136.8, 132.5, 130.4, 128.6, 128.5, 128.0, 127.7, 127.6, 127.0, 122.1, 105.5, 104.3, 101.0, 100.3, 70.2, 70.0, 66.3, 52.9, 52.0, 47.9, 39.9; IR (ATR) 2950, 1732, 1233, 1166, 1036  $\text{cm}^{-1}$ ; HRMS (ESI)  $m/z$  calcd for  $\text{C}_{34}\text{H}_{30}\text{O}_8\text{Na}$  [ $\text{M} + \text{Na}$ ] $^+$  589.1838, found 589.1836.

Broadened peaks are apparent in the  $^1\text{H}$  NMR, suggesting rotamers. Additional  $^1\text{H}$  NMR data is reported below. The corresponding  $^1\text{H}$  NMR spectra can be found in Appendix A.

$^1\text{H}$  NMR (500 MHz,  $\text{CDCl}_3$ , 253.0 K)  $\delta$  7.60 – 7.52 (m, 2H), 7.49 – 7.33 (m, 8H), 6.73 (s, 1H), 6.60 (d,  $J$  = 2.3 Hz, 1H), 6.52 – 6.49 (m, 1H), 6.46 (s, 1H), 6.43 (dd,  $J$  = 8.5, 2.3 Hz, 1H), 5.95 – 5.93 (m, 2H), 5.91 (s, 1H), 5.17 – 5.04 (m, 2H), 5.05 – 4.90 (m, 2H), 4.00 (d,  $J$  = 16.8 Hz, 1H), 3.76 (d,  $J$  = 1.1 Hz, 3H), 3.34 (d,  $J$  = 16.8 Hz, 1H), 3.25 (s, 3H);  $^1\text{H}$  NMR (600 MHz,  $\text{CDCl}_3$ , 328.0 K)  $\delta$  7.75 – 7.25 (m, 9H), 6.88 – 6.20 (m, 4H), 5.98 – 5.74 (m, 2H), 5.19 – 4.87 (m, 4H), 3.94 (d,  $J$  = 16.6 Hz, 1H), 3.69 (s, 3H), 3.39 – 3.02 (m, 5H);  $^1\text{H}$  NMR (600 MHz,  $\text{C}_6\text{D}_5\text{CD}_3$ , 372.5 K)  $\delta$  7.33 (s, 2H), 7.26 – 7.13 (m, 4H), 7.11 – 7.02 (m, 4H), 6.99 – 6.96 (m, 1H), 6.78 (s, 1H), 6.55 (d,  $J$  = 2.4 Hz, 1H), 6.44 (s, 1H), 6.38 (d,  $J$  = 5.1 Hz, 1H), 6.33 (dd,  $J$  = 8.4, 2.4 Hz, 1H), 6.02 (s, 1H), 5.38 (d,  $J$  = 7.4 Hz, 1H), 4.78 (s, 2H), 4.75 (s, 2H), 4.10 (d,  $J$  = 16.5 Hz, 1H), 3.39 (d,  $J$  = 1.3 Hz, 3H), 3.27 (d,  $J$  = 16.5 Hz, 1H), 3.03 (d,  $J$  = 1.3 Hz, 3H).

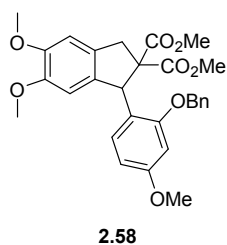
**Dimethyl 1-(2,4-bis(benzyloxy)phenyl)-5,6-dimethoxy-1,3-dihydro-2*H*-indene-2,2-dicarboxylate, **2.57****



1-Arylindane **2.57** was synthesized using the same carbenylative annulation procedure for tetralone **2.51**. Reaction of malonate **2.52b** (2.00 g, 4.89 mmol), *N*-tosylhydrazone **2.53a** (3.75 g, 7.34 mmol), un-rinsed 60% NaH/mineral oil (607 mg, 15.2 mmol), PdCl<sub>2</sub>(CH<sub>3</sub>CN)<sub>2</sub> (127 mg, 0.489 mmol), and P(4-FC<sub>6</sub>H<sub>5</sub>)<sub>3</sub> (620 mg, 1.95 mmol) in THF (245 mL) for 2 hr at 60 °C afforded a crude golden-brown solid that was subjected to three rounds of flash chromatography (25:75 – 30:70 EtOAc:hexanes (× 2); then 1:99 EtOAc:toluene) to afford a solid mixture of arylindane **2.57** and *N*-tosylhydrazone **2.53a**. Upon diluting the mixture with Et<sub>2</sub>O, a white solid remained insoluble. The mixture was cooled (–78 °C) for 20 min and then filtered. The white solid was washed with cold Et<sub>2</sub>O to yield arylindane **2.57** (2.38 g, 84%).

$R_f = 0.28$  (30:70 EtOAc:hexanes, stains red by *p*-anis dip stain). mp = 124–126 °C. <sup>1</sup>H NMR (500 MHz, CDCl<sub>3</sub>) δ 7.57 (d,  $J = 7.5$  Hz, 2H), 7.45 – 7.28 (m, 8H), 6.75 (s, 1H), 6.60 (s, 1H), 6.49 (s, 1H), 6.48 – 6.37 (m, 2H), 5.96 (s, 1H), 5.09 (s, 2H), 5.04 – 4.93 (m, 2H), 4.03 (d,  $J = 16.6$  Hz, 1H), 3.87 (s, 3H), 3.73 (s, 3H), 3.71 (s, 3H), 3.35 (d,  $J = 16.6$  Hz, 1H), 3.20 (s, 3H); <sup>13</sup>C NMR (126 MHz, CDCl<sub>3</sub>) δ 172.4, 170.1, 158.8, 157.1, 148.9, 148.8, 137.1, 136.8, 135.9, 131.5, 130.5, 128.6, 128.5, 128.0, 127.7, 127.6, 127.1, 122.2, 107.7, 106.7, 105.5, 100.2, 70.2, 70.0, 66.4, 55.9, 52.9, 52.0, 48.3, 40.1; IR (ATR) 2948, 1731, 1502, 1215, 1170, 1151, 1097 cm<sup>-1</sup>; HRMS (ESI)  $m/z$  calcd for C<sub>35</sub>H<sub>34</sub>O<sub>8</sub>Na [M + Na]<sup>+</sup> 605.2151, found 605.2137.

**Dimethyl 1-(2-(benzyloxy)-4-methoxyphenyl)-5,6-dimethoxy-1,3-dihydro-2H-indene-2,2-dicarboxylate, 2.58**



1-Arylindane **2.58** was synthesized using the same carbenylative annulation procedure for tetralone **2.51**. To a stirring solution of 60% NaH/mineral oil (705 mg, 17.6 mmol) in THF (27.0 mL) at  $-10\text{ }^{\circ}\text{C}$  was added a pre-stirred solution of malonate **2.52b** (2.0 g, 4.89 mmol) and *N*-tosylhydrazone **2.53b** (4.00 g, 9.79 mmol) in THF (27.0 mL). Additional THF ( $2 \times 27.0\text{ mL}$ ) was used to transfer the remaining reagent solution. After 15 min, the stirring, cooled, heterogeneous solution was warmed to  $23\text{ }^{\circ}\text{C}$ , and stirred an additional 20 min. A pre-stirred solution of  $\text{PdCl}_2(\text{CH}_3\text{CN})_2$  (127 mg, 0.489 mmol) and  $(4\text{-FC}_6\text{H}_4)_3\text{P}$  (620 mg, 1.95 mmol) in THF (27.0 mL) was then added. Additional THF ( $2 \times 27.0\text{ mL}$ ) was used to transfer any remaining catalyst solution. The reaction was then heated ( $60\text{ }^{\circ}\text{C}$ ) and monitored by TLC for the consumption of malonate **2.52b** and *N*-tosylhydrazone **2.53b**. After 1.5 h, neither was detectable by TLC. The mixture was cooled to  $23\text{ }^{\circ}\text{C}$ , diluted with  $\text{Et}_2\text{O}$  (25 mL), and then passed through a pad of silica gel. The pad was rinsed with  $\text{Et}_2\text{O}$  ( $3 \times 60\text{ mL}$ ), and the filtrate concentrated *in vacuo* to afford a crude green fluff. The solid was purified by flash chromatography to afford mixed fractions of product and co-eluting impurities. Successive purifications yielded product **2.58** as a yellow fluff that was crushed into a solid (2.23 g, 90%). Column eluent conditions: four column volumes of 15:85 EtOAc:hexanes, followed by two column volumes of 20:80 DCM:toluene, followed by 25:85 – 30:70 EtOAc:hexanes. Mixed fractions were then subjected to 5:95 – 8:92 EtOAc:toluene, followed by 5:95 – 15:85 EtOAc hexanes.

$R_f = 0.08$  (25:75 EtOAc:hexanes, stains pink by *p*-anis dip stain).  $R_f = 0.08$  (20:80 acetone:hexanes). mp =  $144\text{--}146\text{ }^{\circ}\text{C}$ .  $^1\text{H NMR}$  (600 MHz,  $\text{CDCl}_3$ , 298.0 K)  $\delta$  7.64 – 7.51 (broad

m, 2H), 7.46 – 7.36 (broad m, 2H), 7.36 – 7.26 (broad m, 1H), 6.93 (s, 0.4H), 6.75 (broad s, 1H), 6.52 (broad s, 1H), 6.48 (s, 1H), 6.32 (broad d,  $J = 8.6$  Hz, 1H), 5.96 (broad s, 1H), 5.33 – 4.90 (broad m, 2H), 4.69 (s, 0.2H), 4.59 (s, 0.2H), 4.03 (broad d,  $J = 16.6$  Hz, 1H), 3.87 (broad s, 3H), 3.74 (s, 3H and s, 1H), 3.73 (s, 3H), 3.71 (s, 3H), 3.35 (d,  $J = 16.7$  Hz, 1H), 3.23 (s, 3H).  $^{13}\text{C}$  NMR (151 MHz,  $\text{CDCl}_3$ , 298.0 K)  $\delta$  172.4, 170.1, 159.7, 157.1, 149.0, 148.8, 137.2, 136.0, 131.5, 130.6, 128.5, 127.7, 127.1, 122.0, 107.8, 106.7, 104.4, 99.4, 70.2, 66.4, 55.93, 55.91, 55.2, 52.9, 52.0, 48.3, 40.1; IR (ATR) 1731, 1504, 1218, 1158, 1098  $\text{cm}^{-1}$ ; HRMS (ESI)  $m/z$  calcd for  $\text{C}_{29}\text{H}_{30}\text{O}_8\text{Na}$   $[\text{M} + \text{Na}]^+$  529.1838, found 529.1812.

Broadened peaks are apparent in the  $^1\text{H}$ NMR. Using the method of Ley and co-workers, the broadened peaks are determined to be of rotamers.<sup>7</sup> The difference spectrum for the 1D gradient NOE is provided in Appendix A. Peaks sharpen into well-resolved signals at temperature below 23 °C.

$^1\text{H}$  NMR (600 MHz,  $\text{CDCl}_3$ , 274.2 K)  $\delta$  7.60 (d,  $J = 7.5$  Hz, 2H), 7.43 (t,  $J = 7.6$  Hz, 2H), 7.35 (t,  $J = 7.4$  Hz, 1H), 6.93 (d,  $J = 7.1$  Hz, 0.4H), 6.77 (s, 1H), 6.52 (d,  $J = 2.4$  Hz, 1H), 6.50 (s, 1H), 6.48 (d,  $J = 8.6$  Hz, 1H), 6.37 (s, 0.2H), 6.32 (dd,  $J = 8.5, 2.4$  Hz, 1H), 6.30 (s, 0.2H), 5.96 (s, 1H), 5.19 (s, 0.2H), 5.16 – 5.05 (m, 2H), 4.69 (d,  $J = 10.9$  Hz, 0.2H), 4.59 (d,  $J = 11.0$  Hz, 0.2H), 4.05 (d,  $J = 16.6$  Hz, 1H), 3.89 (s, 3H), 3.81 (s, 0.5H), 3.78 (s, 0.3H), 3.75 (s, 4H), 3.74 (s, 7H), 3.73 (s, 3H), 3.71 (s, 0.6H), 3.36 (d,  $J = 16.6$  Hz, 1H), 3.24 (s, 4H), 3.01 (d,  $J = 16.2$  Hz, 0.2H).  $^{13}\text{C}$  NMR (151 MHz,  $\text{CDCl}_3$ , 274.2 K)  $\delta$  172.4, 170.2, 159.5, 156.8, 148.6, 148.5, 137.0, 135.7, 131.2, 130.5, 128.5, 127.7, 126.9, 121.6, 107.3, 106.3, 104.0, 99.2, 69.9, 66.2, 55.82, 55.76, 55.2, 53.0, 52.1, 48.0, 39.9.

$^1\text{H}$  NMR (600 MHz,  $\text{DMF-}d_7$ , 298 K)  $\delta$  7.68 (d,  $J = 7.6$  Hz, 2H), 7.47 (t,  $J = 7.8$  Hz, 2H), 7.38 (t,  $J = 7.4$  Hz, 1H), 6.98 (s, 1H), 6.75 (s, 1H), 6.59 (s, 1H), 6.42 (s, 2H), 5.95 (s, 1H), 5.30 (d,

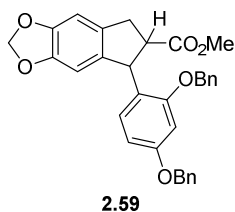
$J = 12.2$  Hz, 1H), 5.21 (d,  $J = 12.2$  Hz, 1H), 4.02 (d,  $J = 16.7$  Hz, 1H), 3.83 (s, 3H), 3.78 (s, 3H), 3.75 (s, 3H), 3.67 (s, 3H), 3.34 (d,  $J = 16.7$  Hz, 1H), 3.26 (s, 3H).  $^{13}\text{C}$  NMR (151 MHz, DMF- $d_7$ , 298 K)  $\delta$  172.6, 170.0, 160.2, 157.5, 149.8, 149.6, 138.1, 136.7, 131.8, 130.5, 128.7, 128.0, 127.6, 121.9, 108.2, 107.9, 105.3, 99.7, 70.3, 66.5, 55.8, 55.7, 55.2, 52.9, 51.9, 48.2, 40.0.

$^1\text{H}$  NMR (600 MHz, DMF- $d_7$ , 274.2 K)  $\delta$  7.69 (d,  $J = 7.5$  Hz, 2H), 7.49 (t,  $J = 7.5$  Hz, 2H), 7.39 (t,  $J = 7.4$  Hz, 1H), 7.33 – 7.24 (m, 0.1H), 7.00 (s, 1H), 6.93 (s, 0.1H), 6.76 (d,  $J = 2.1$  Hz, 1H), 6.61 (s, 1H), 6.45 – 6.39 (m, 2H), 5.95 (s, 1H), 5.31 (d,  $J = 12.2$  Hz, 1H), 5.21 (d,  $J = 12.3$  Hz, 1H), 4.86 (d,  $J = 11.8$  Hz, 0.1H), 4.79 (d,  $J = 12.0$  Hz, 0.1H), 4.03 (d,  $J = 16.6$  Hz, 1H), 3.83 (s, 3H), 3.78 (s, 3H), 3.77 (s, 3H), 3.68 (s, 3H), 3.35 (d,  $J = 16.7$  Hz, 1H), 3.27 (s, 3H).  $^{13}\text{C}$  NMR (151 MHz, DMF- $d_7$ , 274.2 K)  $\delta$  172.7, 170.0, 160.2, 157.4, 149.6, 149.5, 138.2, 136.5, 131.6, 130.6, 128.8, 128.1, 127.6, 121.7, 107.8, 107.6, 105.2, 99.5, 70.2, 66.5, 55.6, 55.57, 55.2, 53.0, 52.1, 48.2, 40.0.

Additional overlays of  $^1\text{H}$  NMR in DMF- $d_7$  of **2.58** from 405.0 to 274.2 K has been provided in the spectra section. Those spectra have been referenced to 8.03 ppm.

## Synthesis of Compounds **2.59**–( $\pm$ )-Brazilin

### Methyl 5-(2,4-bis(benzyloxy)phenyl)-6,7-dihydro-5*H*-indeno[5,6-*d*][1,3]dioxole-6-carboxylate, **2.59** (1:1 *syn/anti*).



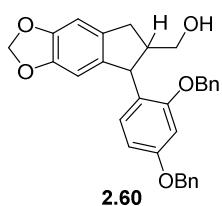
A round-bottom flask containing 1-arylidane **2.56** (0.559 g, 0.988 mmol), anhydrous NaI (0.454 g, 3.06 mmol), and NaHCO<sub>3</sub> (0.339 g, 4.04 mmol), was evacuated and backfilled with N<sub>2</sub> ( $\times$  3). Anhydrous DMF (8.0 mL) was then added. The flask was connected to a water jacketed condenser, and then submerged in an oil bath (160 °C). The reaction was stirred and monitored for the consumption of aryidane (6 h). The mixture was cooled to 23 °C. Then, H<sub>2</sub>O (80 mL) was added while stirring, and the resulting



solution extracted with Et<sub>2</sub>O (4 × 50 mL). The combined organic layers were washed with H<sub>2</sub>O (× 3) and with brine (× 1). The organic solution was then dried (MgSO<sub>4</sub>), and concentrated *in vacuo*. The resulting crude yellow oil was purified by flash chromatography (10:90 EtOAc:hexanes) to afford methyl ester **2.59** as an inseparable 1:1 mixture of diastereomers as a white foam (0.433 g, 86%).

$R_f = 0.43$  (20:80 EtOAc:hexanes). mp = 40–58 °C. <sup>1</sup>H NMR (500 MHz, CDCl<sub>3</sub>) δ 7.50 – 7.27 (m, 16.1H), 7.20 (d,  $J = 7.3$  Hz, 2.1H), 6.94 (d,  $J = 8.4$  Hz, 1.1H), 6.77 – 6.68 (m, 1.7H), 6.66 (s, 1.1H), 6.63 (d,  $J = 2.4$  Hz, 1.2H), 6.59 (d,  $J = 2.4$  Hz, 0.9H), 6.51 (dd,  $J = 8.4, 2.4$  Hz, 1.2H), 6.47 (s, 0.9H), 6.44 (dd,  $J = 8.5, 2.4$  Hz, 1H), 6.38 (s, 1H), 5.92 – 5.89 (m, 2.9H), 5.89 – 5.87 (m, 1.1H), 5.18 (d,  $J = 10.0$  Hz, 0.9H), 5.09 – 4.93 (m, 7.3H), 4.89 (d,  $J = 7.6$  Hz, 1H), 3.75 (td,  $J = 8.9, 6.4$  Hz, 0.9H), 3.54 (s, 3.1H), 3.48 – 3.36 (m, 1.5H), 3.35 (d,  $J = 6.5$  Hz, 0.5H), 3.19 (s, 2.7H), 3.12 (d,  $J = 8.4$  Hz, 2.1H), 2.99 (dd,  $J = 15.9, 8.6$  Hz, 0.9H); <sup>13</sup>C NMR (126 MHz, CDCl<sub>3</sub>) δ 175.5, 173.9, 159.0, 158.7, 157.4, 157.3, 147.0, 146.9, 146.8, 137.8, 137.1, 136.9, 136.79, 136.77, 135.5, 134.1, 130.0, 129.7, 128.6, 128.57, 128.5, 128.4, 128.04, 127.98, 127.87, 127.7, 127.6, 127.3, 127.1, 124.3, 122.5, 105.44, 105.40, 105.3, 105.1, 104.7, 104.6, 101.0, 100.9, 100.7, 100.2, 70.2, 70.16, 70.0, 69.9, 52.1, 51.7, 51.1, 49.4, 35.5, 34.3; IR (ATR) 2916, 1732, 1609, 1584, 1502, 1474, 1248, 1167, 1036, 735 cm<sup>-1</sup>; HRMS (ESI)  $m/z$  calcd for C<sub>32</sub>H<sub>28</sub>O<sub>6</sub>Na [M + Na]<sup>+</sup> 531.1783, found 531.1788.

**(5-(2,4-Bis(benzyloxy)phenyl)-6,7-dihydro-5H-indeno[5,6-*d*][1,3]dioxol-6-yl)methanol, 2.60**  
(1:1 *syn/anti*)

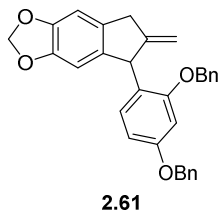


To a cooled (0 °C) solution of methyl ester **2.59** (1:1 *syn/anti*, 0.420 g, 0.826 mmol) in THF (69.0 mL) was added LiAlH<sub>4</sub> (62.7 mg, 1.65 mmol) portion wise over 5 minutes, with vigorous stirring. The reaction mixture was warmed

to 23 °C and then heated at reflux. Upon consumption of the methyl ester (1 h), the mixture was cooled to 23 °C. After, aqueous 0.4 M NaOH (25 mL) was added and the mixture stirred for 5 min. H<sub>2</sub>O (50 mL) was added to help solubilize the aluminum salts. The resulting mixture was then filtered through tightly packed Celite, and the pad was rinsed with EtOAc (3 × 50 mL). The biphasic mixture was poured into a separatory funnel and the organic layer removed. The aqueous layer was extracted with EtOAc (3 × 50 mL). The combined organic layers were dried (MgSO<sub>4</sub>), and concentrated *in vacuo*. The resulting crude peach solid was purified by flash chromatography (20:80 EtOAc:hexanes) to afford alcohol **2.60** as an inseparable 1:1 mixture of diastereomers as a white solid (0.375 g, 94%).

R<sub>f</sub> = 0.19 (20:80 EtOAc:hexanes, stains purple by *p*-anis dip stain). mp = 118–120 °C. <sup>1</sup>H NMR (500 MHz, CDCl<sub>3</sub>) δ 7.49 – 7.29 (m, 17H), 6.85 (d, *J* = 8.4 Hz, 1H), 6.73 (s, 1H), 6.70 (s, 2H), 6.69 (s, 1H), 6.68 (d, *J* = 2.4 Hz, 1H), 6.52 (dd, *J* = 8.4, 2.4 Hz, 1H), 6.49 (s, 1H), 6.46 (d, *J* = 8.0 Hz, 1H), 6.43 (s, 1H), 6.40 (d, *J* = 8.4 Hz, 0.5H), 5.93 – 5.90 (m, 3H), 5.89 (d, *J* = 1.4 Hz, 1H), 5.19 – 5.06 (m, 1H), 5.05 (s, 2H), 5.03 (s, 2H), 5.00 (s, 2H), 4.81 (d, *J* = 7.9 Hz, 1H), 4.45 (d, *J* = 7.1 Hz, 1H), 3.69 – 3.56 (m, 1H), 3.37 (s, 1H), 3.23 (t, *J* = 10.1 Hz, 1H), 3.03 – 2.98 (m, 0.4H), 2.95 (dd, *J* = 15.6, 8.1 Hz, 2H), 2.79 (dd, *J* = 15.4, 7.8 Hz, 1H), 2.66 (dd, *J* = 15.5, 7.3 Hz, 1H), 2.58 (dd, *J* = 15.4, 9.6 Hz, 1H), 2.51 (h, *J* = 7.0 Hz, 1H), 2.26 (d, *J* = 9.1 Hz, 1H), 1.68 (t, *J* = 6.2 Hz, 1H); <sup>13</sup>C NMR (126 MHz, CDCl<sub>3</sub>) δ 158.5, 157.1, 156.5, 146.8, 146.72, 146.66, 146.55, 138.8, 138.2, 136.9, 136.8, 136.3, 136.13, 136.12, 135.9, 130.3, 129.3, 128.8, 128.7, 128.6, 128.4, 128.3, 128.1, 128.0, 127.78, 127.75, 127.58, 127.57, 125.6, 122.2, 106.4, 106.0, 105.8, 105.6, 104.9, 104.8, 100.93, 100.90, 100.8, 100.5, 71.0, 70.6, 70.20, 70.18, 65.2, 63.9, 52.6, 48.2, 46.1, 44.0, 34.4, 33.7; IR (ATR) 3390, 2922, 1607, 1583, 1500, 1472, 1166, 1035 cm<sup>-1</sup>; HRMS (ESI) *m/z* calcd for C<sub>31</sub>H<sub>28</sub>O<sub>5</sub>Na [M + Na]<sup>+</sup> 503.1834, found 503.1830.

### 5-(2,4-Bis(benzyloxy)phenyl)-6-methylene-6,7-dihydro-5H-indeno[5,6-d][1,3]dioxole, **2.61**

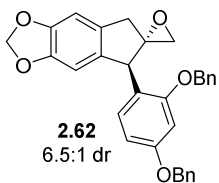


A flame-dried flask was charged with alcohol **2.60** (0.302 g, 0.625 mmol), 2-nitrophenyl selenocyanate (0.865 g, 3.12 mmol.) and THF (2.0 mL). The heterogeneous solution was stirred briefly prior to adding P(*n*-Bu)<sub>3</sub> (0.77 mL, 3.12 mmol) dropwise over 30 min via syringe pump. Upon addition, the heterogeneous solution turned red in color. At 30 min, additional THF (1.0 mL) was added to ensure proper stirring of the slurry. The mixture was stirred at 23 °C and monitored by TLC. At 1 h 15 min, the mixture was concentrated *in vacuo* and subjected to flash chromatography (30:70 – 40:60 ether:hexanes) to afford a yellow oil that was carried on to the next step without further purification. The yellow oil was dissolved in THF (2.0 mL) and then cooled (0 °C) and stirred. Then, degassed 30% (w/w) H<sub>2</sub>O<sub>2</sub> (146 μL, 6.25 mmol) was added dropwise. Upon completion (3.5 h), the cooled mixture was quenched with saturated aqueous Na<sub>2</sub>S<sub>2</sub>O<sub>3</sub> (0.15 mL) and stirred vigorously for 5 min. The mixture was partitioned between H<sub>2</sub>O (30 mL) and EtOAc (15 mL). The layers were separated and the aqueous extracted with EtOAc (2 × 15 mL), ether (1 × 15 mL), and EtOAc (1 × 15 mL) in sequence. The combined organic layers were washed with saturated NaHCO<sub>3</sub> (1 × 50 mL), brine (1 × 50 mL), dried (Na<sub>2</sub>SO<sub>4</sub>), and concentrated *in vacuo*. The crude oil was purified by flash chromatography (2.5:0:97.5 – 2.5:8:89.5 NEt<sub>3</sub>:EtOAc:hexanes) to afford alkene **2.61** as a yellow oil (0.109 g, 38%).

$R_f = 0.65$  (20:80 EtOAc:hexanes, stains blue by *p*-anis dip stain). <sup>1</sup>H NMR (500 MHz, CDCl<sub>3</sub>) δ 7.47 – 7.24 (m, 10H), 6.88 (d, *J* = 8.3 Hz, 1H), 6.64 (s, 2H), 6.49 (d, *J* = 8.5 Hz, 1H), 6.45 (s, 1H), 5.86 (s, 2H), 5.24 (s, 1H), 5.12 – 4.90 (m, 4H and s, 1H), 4.87 (s, 1H), 3.62 (s, 2H). <sup>13</sup>C NMR (126 MHz, CDCl<sub>3</sub>) δ 158.6, 157.2, 154.1, 146.7, 139.0, 137.0, 136.9, 134.3, 130.1, 128.6, 128.4, 128.0, 127.8, 127.6, 127.3, 126.4, 108.3, 105.7, 105.3, 104.6, 100.74, 100.70, 70.19,

70.15, 49.5, 38.8. IR (ATR) 3064, 3032, 1721, 1608, 1036, 939, 735, 696 cm<sup>-1</sup>; HRMS (ESI)  $m/z$  calcd for C<sub>31</sub>H<sub>26</sub>O<sub>4</sub>Na [M + Na]<sup>+</sup> 485.1729, found 485.1752.

**5-(2,4-Bis(benzyloxy)phenyl)-5,7-dihydrospiro[indeno[5,6-*d*][1,3]dioxole-6,2'-oxirane], **2.62****



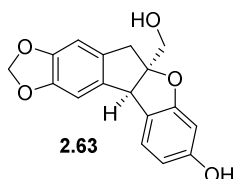
To a flame-dried flask was added a solution of alkene **2.61** (0.205 g, 0.443 mmol) in DCM (1.1 mL). The solution was stirred briefly before adding NaHCO<sub>3</sub> (49.4 mg, 0.589 mmol) and *m*-CPBA (112 mg, 0.456 mmol, 70%).

The reaction was monitored by TLC for the consumption of alkene **2.61**. The reaction was forced to completion by adding *m*-CPBA (0.443 mmol) and DCM (0.3 mL) within 1 h, and adding *m*-CPBA (0.310 mmol), NaHCO<sub>3</sub> (0.443 mmol) and DCM (1.0 mL) at 2 h. At 3 h, the reaction was quenched with aqueous 10% (w/w) Na<sub>2</sub>SO<sub>3</sub> (5 mL) and stirred vigorously for 10 min. The layers were separated and the aqueous layer was extracted with DCM (3 × 10 mL). The combined organic layers were washed with aqueous 5% (w/w) NaHCO<sub>3</sub> (1 × 30 mL), dried (MgSO<sub>4</sub>), and concentrated *in vacuo*. The crude oil was purified by flash chromatography (15:85 EtOAc:hexanes) to yield epoxide **2.62** as an inseparable 6.5:1 mixture of diastereomers as a yellow oil (87.7 mg) containing a small amount (18 mol %, 4 wt.% by <sup>1</sup>H NMR) of EtOAc (40% yield of **2.62**). The major diastereomer is reported below.

$R_f$  = 0.36 (20:80 EtOAc:hexanes, stains purple by *p*-anis dip stain). <sup>1</sup>H NMR (500 MHz, CDCl<sub>3</sub>) δ 7.45 – 7.28 (m, 10H), 7.23 – 7.17 (m, 2H), 6.85 (d,  $J$  = 8.4 Hz, 1H), 6.63 (s, 1H), 6.60 (d,  $J$  = 2.4 Hz, 1H), 6.48 (dd,  $J$  = 8.5, 2.5 Hz, 1H), 6.45 (s, 1H), 5.90 (q,  $J$  = 1.5 Hz, 2H), 5.01 (s, 2H), 4.92 (d,  $J$  = 3.3 Hz, 2H), 4.54 (s, 1H), 3.19 (d,  $J$  = 17.2 Hz, 1H), 2.91 (d,  $J$  = 17.2 Hz, 1H), 2.73 (d,  $J$  = 4.7 Hz, 1H), 2.69 (d,  $J$  = 4.8 Hz, 1H); <sup>13</sup>C NMR (126 MHz, CDCl<sub>3</sub>) δ 159.2, 157.3, 147.04, 146.99, 137.5, 137.0, 136.7, 133.1, 130.6, 128.8, 128.6, 128.2, 128.0, 127.7, 127.5, 122.9,

105.5, 105.3, 104.8, 101.0, 100.9, 70.3, 70.2, 68.6, 52.1, 51.2, 38.9; HRMS (ESI)  $m/z$  calcd for  $C_{31}H_{26}O_5Na$   $[M + Na]^+$  501.1678, found 501.1678.

**5a-(Hydroxymethyl)-5a,10b-dihydro-5H-[1,3]dioxolo[4',5':5,6]-indeno[2,1-*b*]benzofuran-8-ol, **2.63****



A portion of the above isolated epoxide **2.62** (28.2 mg, 0.0589 mmol) was dissolved in 1:1 MeOH/THF (1.0 mL) and stirred at 23 °C prior to adding Pearlman's catalyst, 20 wt. % Pd(OH)<sub>2</sub>/C (20.6 mg, 0.0294 mmol). The contents of the flask were evacuated and backfilled with H<sub>2</sub> (× 3). Upon consumption of epoxide **2.62** (30 min), the flask was evacuated and backfilled with N<sub>2</sub>. The mixture was then diluted with EtOAc (3 mL) and filtered through tightly packed Celite pad. The pad was rinsed with EtOAc (3 × 10 mL), and the organic fraction purged with N<sub>2</sub>, and concentrated *in vacuo* to afford a pink oil. The oil was purified by flash chromatography with degassed solvents (40:60 EtOAc:hexanes) to yield indano[2,1-*b*]benzofuran **2.63** as an off-white oil (9.0 mg) containing a small amount (5 mol %, 1.7 wt. % and 6 mol %, 1.6 wt. % by <sup>1</sup>H NMR) of EtOAc and benzene, respectively (49% yield of **2.63**). Benzofuran **2.63** was isolated as an inseparable 10:1 mixture with a structurally similar compound not matching the desired indano[2,1-*c*]chroman. This sample was stored in benzene at -20 °C.

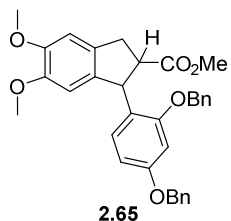
$R_f = 0.47$  (50:50 EtOAc:hexanes, stains pink by *p*-anis dip stain). <sup>1</sup>H NMR (600 MHz, CD<sub>3</sub>OD) δ 7.15 (d,  $J = 8.0$  Hz, 1H), 6.83 (s, 1H), 6.64 (s, 1H), 6.29 (dd,  $J = 8.1, 2.2$  Hz, 1H), 6.18 (d,  $J = 2.2$  Hz, 1H), 5.88 (d,  $J = 1.4$  Hz, 1H), 5.85 (d,  $J = 1.5$  Hz, 1H), 4.51 (s, 1H), 3.76 (d,  $J = 11.8$  Hz, 1H), 3.70 (d,  $J = 11.7$  Hz, 1H), 3.25 (d,  $J = 17.2$  Hz, 1H), 3.13 (d,  $J = 17.3$  Hz, 1H). <sup>13</sup>C NMR (151 MHz, CD<sub>3</sub>OD) δ 161.6 (C), 159.2 (C), 148.9 (C), 148.7 (C), 137.7 (C), 133.9 (C), 125.3 (CH), 122.0 (C), 108.5 (CH), 106.0 (CH), 105.3 (CH), 102.3 (CH<sub>2</sub>), 101.4 (C), 98.4 (CH),

66.3 (CH<sub>2</sub>), 54.8 (CH), 42.5 (CH<sub>2</sub>). IR (ATR) 3321, 1620, 1473, 1144, 1035, 963, 734 cm<sup>-1</sup>.

HRMS (ESI) *m/z* calcd for C<sub>17</sub>H<sub>14</sub>O<sub>5</sub>Na [M + Na]<sup>+</sup> 321.0739, found 321.0739.

### Methyl 1-(2,4-bis(benzyloxy)phenyl)-5,6-dimethoxy-2,3-dihydro-1*H*-indene-2-carboxylate,

#### 2.65

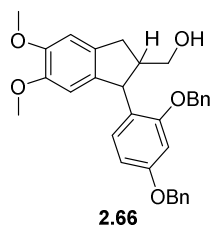


A round-bottom flask containing 1-arylidane **2.57** (0.357 g, 0.608 mmol), anhydrous NaI (0.274 g, 1.83 mmol), and NaHCO<sub>3</sub> (0.205 g, 2.43 mmol) was evacuated and backfilled with N<sub>2</sub> (× 3). Anhydrous DMF (4.9 mL) was then added. The flask was connected to a water jacketed condenser, and then submerged in an oil bath (160 °C). The reaction was stirred and monitored for the consumption of arylidane (6 h). The mixture was cooled to 23 °C. Then, H<sub>2</sub>O (50 mL) was added and stirred vigorously. The resulting solution was extracted with Et<sub>2</sub>O (4 × 50 mL). The combined organic layers were washed with H<sub>2</sub>O (× 3) and with brine (× 1). The organic solution was then dried (MgSO<sub>4</sub>), and concentrated *in vacuo*. The crude peach solid was purified by flash chromatography (15:85 EtOAc:hexanes) to afford methyl ester **2.65** as an inseparable 1.1:1 mixture of diastereomers as a white solid (0.299 g, 94%).

*R<sub>f</sub>* = 0.25 (20:80 EtOAc:hexanes, stains violet by *p*-anis dip stain). mp = 39–46 °C. <sup>1</sup>H NMR (600 MHz, CDCl<sub>3</sub>) δ 7.48 (s, 2H), 7.45 – 7.26 (m, 18H), 7.22 (d, *J* = 7.4 Hz, 2H), 6.92 (d, *J* = 8.3 Hz, 1H), 6.79 (s, 1H), 6.74 (s, 1H), 6.73 – 6.69 (m, 1H), 6.64 (d, *J* = 2.4 Hz, 1H), 6.60 (d, *J* = 2.4 Hz, 1H), 6.54 (s, 1H), 6.51 (dd, *J* = 8.4, 2.4 Hz, 1H), 6.47 (s, 1H), 6.44 (dd, *J* = 8.5, 2.4 Hz, 1H), 5.25 (s, 1H), 5.07 (s, 2H), 5.03 (s, 2H), 5.02 – 4.93 (m, 5H), 3.88 (s, 4H), 3.88 (s, 3H), 3.76 (dd, *J* = 8.9, 6.5 Hz, 1H), 3.74 (s, 3H), 3.73 (s, 3H), 3.53 (s, 3H), 3.42 (dd, *J* = 15.8, 6.5 Hz, 1H), 3.35 (q, *J* = 7.8 Hz, 1H), 3.19 (s, 3H), 3.17 (d, *J* = 8.1 Hz, 2H), 3.04 (dd, *J* = 15.8, 8.5 Hz, 1H); <sup>13</sup>C NMR (151 MHz, CDCl<sub>3</sub>) δ 175.7, 174.0, 158.9, 158.7, 157.5, 157.4, 148.6, 148.5, 148.46,

148.4, 137.1, 136.9, 136.8, 136.4, 135.6, 134.4, 133.2, 129.9, 129.85, 128.6, 128.57, 128.5, 128.4, 128.05, 127.99, 127.9, 127.7, 127.6, 127.3, 127.1, 124.7, 122.7, 108.0, 107.7, 107.22, 107.17, 105.4, 105.3, 100.6, 100.2, 70.2, 70.17, 70.05, 69.95, 56.1, 56.03, 56.02, 56.0, 52.2, 51.7, 51.1, 49.3, 35.6, 34.4; IR (ATR) 2946, 1730, 1606, 1583, 1502, 1164, 1092, 1025, 735  $\text{cm}^{-1}$ ; HRMS (ESI)  $m/z$  calcd for  $\text{C}_{33}\text{H}_{32}\text{O}_6\text{Na}$   $[\text{M} + \text{Na}]^+$  547.2097, found 547.2084.

**(1-(2,4-Bis(benzyloxy)phenyl)-5,6-dimethoxy-2,3-dihydro-1H-inden-2-yl)methanol, 2.66**

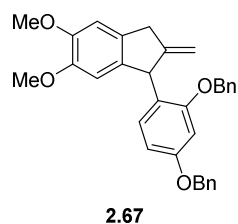


To a cooled (0 °C) solution of methyl ester **2.65** (1.1:1 mixture of diastereomers 0.277 g, 0.528 mmol) in THF (40.0 mL) was added  $\text{LiAlH}_4$  (40.0 mg, 1.06 mmol) portion wise over 5 minutes, with vigorous stirring. The reaction mixture was warmed to 23 °C and then heated at reflux. Upon consumption of the methyl ester (1 h), the mixture was cooled to 23 °C. After, aqueous 0.4 M NaOH (40 mL) was added and the mixture stirred for 5 min.  $\text{H}_2\text{O}$  (80 mL) was added to help solubilize the aluminum salts. The resulting mixture was then filtered through tightly packed Celite, and the pad was rinsed with EtOAc (3 × 50 mL). The biphasic mixture was poured into a separatory funnel, and the aqueous phase extracted with EtOAc (3 x 50 mL). The combined organic fractions were dried ( $\text{MgSO}_4$ ), and concentrated *in vacuo*. The resulting crude yellow solid was purified by flash chromatography (20:80 – 40:60 EtOAc:hexanes) to afford alcohol **2.66** an inseparable 1:1 mixture of diastereomers as a white solid (0.246 g, 94%).

$R_f$  = 0.28 (40:60 EtOAc:hexanes, stains bluish-purple by *p*-anis dip stain). mp = 48–55 °C.  $^1\text{H}$  NMR (600 MHz,  $\text{CDCl}_3$ )  $\delta$  7.52 – 7.30 (m, 19H), 6.82 (d,  $J$  = 8.5 Hz, 1H), 6.81 (s, 1H), 6.77 (s, 1H), 6.72 (s, 1H), 6.69 (d,  $J$  = 2.4 Hz, 1H), 6.57 (s, 1H), 6.52 (dd,  $J$  = 8.6, 2.6 Hz, 1H), 6.51 (s, 1H), 6.48 – 6.42 (m, 1H), 6.37 (d,  $J$  = 8.5 Hz, 1H), 5.19 – 5.05 (m, 4H), 5.03 (s, 2H), 5.01 (s, 2H), 4.86 (d,  $J$  = 8.0 Hz, 1H), 4.51 (d,  $J$  = 6.7 Hz, 1H), 3.89 (s, 3H), 3.88 (s, 3H), 3.77 (s, 3H), 3.75 (s,

3H), 3.63 (q,  $J = 5.5$  Hz, 2H), 3.38 (s, 1H), 3.24 (t,  $J = 10.0$  Hz, 1H), 3.00 (dt,  $J = 14.8, 7.5$  Hz, 2H), 2.84 (dd,  $J = 15.3, 7.8$  Hz, 1H), 2.69 (dd,  $J = 15.5, 7.0$  Hz, 1H), 2.63 (dd,  $J = 15.3, 9.5$  Hz, 1H), 2.49 (h,  $J = 6.5$  Hz, 1H), 2.27 (d,  $J = 9.5$  Hz, 1H), 1.73 (s, 1H); The absence of 1H from the 7.52 – 7.30 region is likely due to differences in relaxation delay times. With longer relaxation delay (d1 = 15 s), the integration for the 7.52 – 7.30 region is 20H.  $^{13}\text{C}$  NMR (151 MHz,  $\text{CDCl}_3$ )  $\delta$  158.56, 158.52, 157.1, 156.6, 148.37, 148.35, 148.29, 148.23, 137.7, 136.9, 136.85, 136.83, 136.4, 136.2, 135.0, 134.9, 130.4, 129.2, 128.8, 128.7, 128.6, 128.4, 128.3, 128.08, 128.06, 127.8, 127.6, 125.9, 122.5, 108.3, 107.6, 107.3, 106.4, 106.0, 100.9, 100.4, 71.0, 70.6, 70.22, 70.20, 65.4, 64.0, 56.1, 56.01, 56.00, 52.6, 48.2, 46.3, 44.3, 34.5, 33.9; IR (ATR) 3513, 2932, 1605, 1582, 1500, 1292, 1248, 1216, 1165, 1090, 1024, 735  $\text{cm}^{-1}$ ; HRMS (ESI)  $m/z$  calcd for  $\text{C}_{32}\text{H}_{32}\text{O}_5\text{Na}$  [ $\text{M} + \text{Na}$ ] $^+$  519.2147, found 519.2148.

#### 1-(2,4-Bis(benzyloxy)phenyl)-5,6-dimethoxy-2-methylene-2,3-dihydro-1H-indene, **2.67**



A flame-dried flask was charged with alcohol **2.66** (0.300 g, 0.604 mmol), 2-nitrophenyl selenocyanate (0.837 g, 3.02 mmol.) and THF (2.0 mL). The heterogeneous solution was stirred briefly prior to adding  $\text{P}(n\text{-Bu})_3$  (0.75 mL, 3.02 mmol) dropwise over 30 min via syringe pump. Upon addition, the heterogeneous solution turned red in color. At 30 min, additional THF (1.0 mL) was added to ensure proper stirring of the slurry. The mixture was stirred at 23 °C and monitored by TLC. At 3.5 h, the mixture was concentrated *in vacuo* and subjected to flash chromatography (15:85 – 40:60 EtOAc:hexanes) to afford a yellow oil that was carried on to the next step without further purification. The yellow oil was dissolved in THF (2.0 mL) and then cooled (0 °C) and stirred. Degassed 30% (w/w)  $\text{H}_2\text{O}_2$  (142  $\mu\text{L}$ , 6.04 mmol) was then added dropwise. Upon completion (5.5 h), the cooled mixture was quenched with saturated aqueous  $\text{Na}_2\text{S}_2\text{O}_3$  (0.15 mL) and stirred

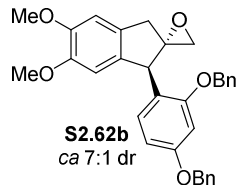


vigorously for 5 min. The mixture was partitioned between H<sub>2</sub>O (20 mL) and EtOAc (20 mL). The layers were separated and the aqueous extracted with EtOAc (2 × 15 mL), and ether (1 × 15 mL). The combined organic layers were washed with saturated NaHCO<sub>3</sub> (1 × 50 mL), brine (1 × 50 mL), dried (Na<sub>2</sub>SO<sub>4</sub>), and concentrated *in vacuo*. The crude oil was purified by flash chromatography (2.5:0:97.5 – 2.5:8:89.5 NEt<sub>3</sub>:EtOAc:hexanes) to yield alkene **2.67** as a yellow oil (0.161 g) containing a small amount (4 mol %, 4 wt. %, by <sup>1</sup>H NMR) of bis(*o*-nitrophenyl) diselenide (54% yield of **2.67**).

$R_f = 0.28$  (20:80 EtOAc:hexanes, stains blue by *p*-anis dip stain). <sup>1</sup>H NMR (600 MHz, CDCl<sub>3</sub>) δ 7.45 – 7.40 (m, 2H), 7.41 – 7.36 (m, 2H), 7.37 – 7.27 (m, 6H), 6.87 (d,  $J = 8.4$  Hz, 1H), 6.73 (s, 1H), 6.66 (d,  $J = 2.4$  Hz, 1H), 6.53 (s, 1H), 6.50 (dd,  $J = 8.4, 2.4$  Hz, 1H), 5.30 (s, 1H), 5.04 (d,  $J = 3.8$  Hz, 3H), 5.02 (s, 2H), 4.90 (q,  $J = 2.4$  Hz, 1H), 3.87 (s, 3H), 3.72 (s, 3H), 3.67 (d,  $J = 2.8$  Hz, 2H); <sup>13</sup>C NMR (151 MHz, CDCl<sub>3</sub>) δ 158.5, 157.2, 154.3, 148.4, 148.3, 137.7, 137.02, 136.98, 133.4, 130.0, 128.6, 128.4, 128.0, 127.8, 127.6, 127.3, 126.6, 108.3, 107.8, 107.2, 105.7, 100.7, 70.17, 70.15, 56.01, 55.98, 49.6, 38.8. IR (ATR) 3064, 3031, 1710, 1656, 1606, 1501, 1168, 1026, 735, 697 cm<sup>-1</sup>; HRMS (ESI)  $m/z$  calcd for C<sub>32</sub>H<sub>30</sub>O<sub>4</sub>Na [M + Na]<sup>+</sup> 501.2042, found 501.2034.

*Data for bis(o-nitrophenyl) diselenide for comparison.* Peaks present in <sup>1</sup>H and <sup>13</sup>C NMR of compound **2.67**: <sup>1</sup>H NMR (600 MHz, CDCl<sub>3</sub>) δ 8.36 (dd,  $J = 8.2, 1.4$  Hz, 2H), 7.91 (dd,  $J = 8.2, 1.3$  Hz, 2H), 7.50 (ddd,  $J = 8.3, 7.1, 1.5$  Hz, 2H), 7.46 – 7.41 (m, 2H of impurity and overlapping m, 50 H of **2.67**). <sup>13</sup>C NMR (151 MHz, CDCl<sub>3</sub>) δ 134.8, 131.6, 128.8, 127.6, 126.4. Previously reported data:<sup>8</sup> <sup>1</sup>H NMR (400 MHz, CDCl<sub>3</sub>): δ 8.37 (d, 2H,  $J = 4$  Hz), 7.92 (d, 2H,  $J = 8$  Hz), 7.50–7.52 (m, 2H), 7.42–7.46 (m, 2H). <sup>13</sup>C NMR (101 MHz, CDCl<sub>3</sub>): δ 134.8, 131.6, 128.8, 127.6, 126.4.

### 1-(2,4-Bis(benzyloxy)phenyl)-5,6-dimethoxy-1,3-dihydrospiro[indene-2,2'-oxirane], **S2.62b**



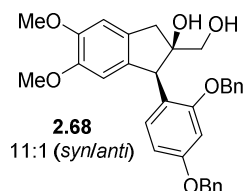
A sample of alkene **2.67** (0.1037g, 0.287 mmol) was dissolved in DCM (0.72 mL) at 23 °C. Purified *m*-CPBA (51.0 mg, 0.296 mmol) was added in one portion. The reaction was driven to completion by adding *m*-CPBA (0.296 mmol) at 1 h 15 min, and again at 2.5 h. Additional DCM (0.70 mL) was added at 2.5 h to ensure proper stirring. At 3.5 h, the reaction was quenched with aqueous 10% (w/w) Na<sub>2</sub>SO<sub>3</sub> (3 mL). The mixture was stirred vigorously for 5 min and then partitioned between H<sub>2</sub>O (10 mL) and DCM (10 mL). The layers were separated and the aqueous extracted with DCM (2 × 10 mL). The combined organic layers were washed with 5% (w/w) NaHCO<sub>3</sub> (1 × 25 mL), dried (Na<sub>2</sub>SO<sub>4</sub>), purged with N<sub>2</sub> for 20 min, and then concentrated *in vacuo* to afford a yellow brown oil. The oil was purified by flash chromatography (10:90 – 20:80 EtOAc:hexanes) to yield epoxide **S2.62b** as an inseparable 7.6:1 mixture of diastereomers as a yellow oil (42.2 mg) containing a small amount (8 mol %, 2 wt. % by <sup>1</sup>H NMR) of EtOAc (29% yield of **S2.62b**). Peaks for the major diastereomer are reported below. X-ray Data Collection, Structure Solution and Refinement for **S2.62b** is provided in Appendix B.

R<sub>f</sub> = 0.21 (20:80 EtOAc:hexanes, stains purple by *p*-anis dip stain). Major diastereomer: <sup>1</sup>H NMR (600 MHz, CDCl<sub>3</sub>) δ 7.44 – 7.26 (m, 10H), 7.20 (d, *J* = 7.2 Hz, 2H), 6.83 (d, *J* = 8.3 Hz, 1H), 6.70 (s, 1H), 6.61 (d, *J* = 2.4 Hz, 1H), 6.52 (s, 1H), 6.48 (dd, *J* = 8.4, 2.4 Hz, 1H), 5.01 (s, 3H), 4.98 – 4.88 (m, 2H), 4.60 (s, 1H), 3.88 (s, 3H), 3.72 (s, 3H), 3.28 (dd, *J* = 17.0, 3.9 Hz, 1H), 2.94 (d, *J* = 17.1 Hz, 1H), 2.75 (d, *J* = 4.8 Hz, 1H), 2.72 (d, *J* = 4.8 Hz, 1H); <sup>13</sup>C NMR (151 MHz, CDCl<sub>3</sub>) δ 159.0, 157.2, 148.6, 148.5, 136.9, 136.6, 136.3, 132.1, 130.4, 128.6, 128.4, 128.1, 127.9, 127.6, 127.3, 123.1, 107.7, 107.2, 105.4, 100.8, 70.2, 70.1, 68.6, 56.0, 55.97, 51.8, 51.2, 38.8. IR

(ATR) 3065, 3028, 3010, 2991, 2960, 2908, 2863, 2834, 1608, 1582, 1501, 1172, 1084, 1028, 739, 692  $\text{cm}^{-1}$ ; HRMS (ESI)  $m/z$  calcd for  $\text{C}_{32}\text{H}_{30}\text{O}_5\text{Na}$   $[\text{M} + \text{Na}]^+$  517.1991, found 517.1999.

**1-(2,4-Bis(benzyloxy)phenyl)-2-(hydroxymethyl)-5,6-dimethoxy-2,3-dihydro-1*H*-inden-2-ol,**

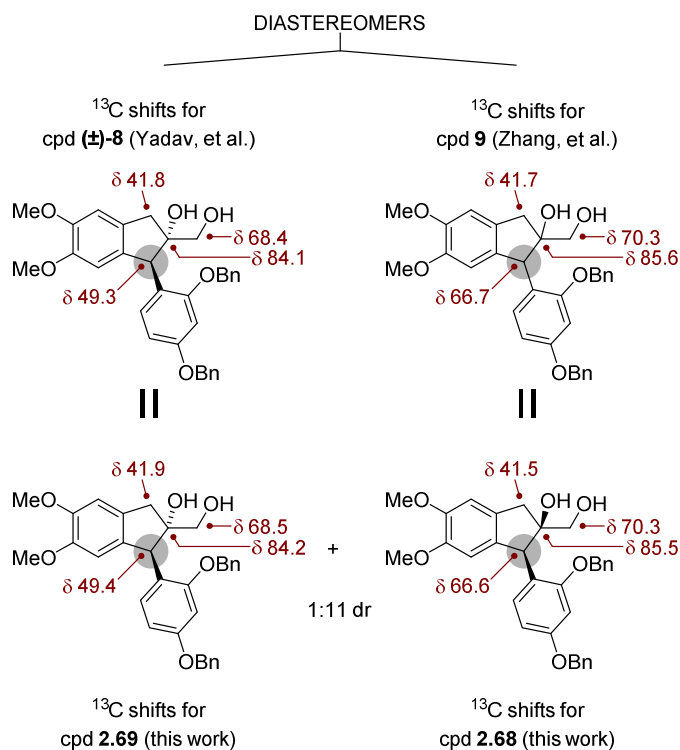
**2.68 (11:1 *syn/anti*)**



To a cooled (0 °C) solution of alkene **2.67** (9.0 mg, 18.8  $\mu\text{mol}$ ) and NMO (6.6 mg, 56.4  $\mu\text{mol}$ ) in DCM (0.22 mL) was added  $\text{OsO}_4$  (6.0  $\mu\text{L}$ , 0.94  $\mu\text{mol}$ , 4 wt. % in  $\text{H}_2\text{O}$ ). The mixture was stirred at 0 °C for 5 h, and then warmed to 23 °C to stir for an additional 14 h. After, the mixture was quenched with 5 wt. %  $\text{NaHSO}_3$  (4.0 mL) and stirred for 15 min. The layers were separated and the aqueous extracted with DCM (3  $\times$  10 mL). The combined organic layers were dried ( $\text{MgSO}_4$ ), and concentrated *in vacuo* to afford a crude orange solid. The solid was purified by flash chromatography (20:80 – 40:60 EtOAc:hexanes) to afford diols *syn*-**17** and *anti*-**18** as an inseparable 11:1 mixture of diastereomers as a white solid (8.5 mg, 89%). Peaks for the major *syn*-**2.68** diol are reported below. The *anti*-**2.69** diol has been previously characterized.<sup>9</sup>

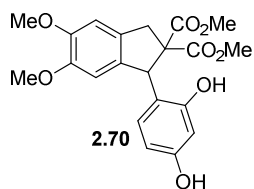
$R_f$  = 0.15 (50:50 EtOAc/hexanes; stains pink by *p*-anis dip stain). Major peaks:  $^1\text{H}$  NMR (600 MHz,  $\text{CDCl}_3$ )  $\delta$  7.52 – 7.31 (m, 10H and m, 1 H), 6.82 (s, 1H), 6.74 (s, 1H), 6.59 (s, 1H), 6.48 (s, 2H), 5.19 (d,  $J$  = 11.2 Hz, 1H), 5.09 (d,  $J$  = 11.4 Hz, 1H), 5.06 (s, 1H), 5.02 (s, 2H), 4.82 (s, 0.09H, *anti*), 4.74 (s, 1H, *syn*), 3.89 (s, 3H), 3.78 (s, 3H), 3.31 (d,  $J$  = 11.5 Hz, 1H), 3.25 (d,  $J$  = 11.7 Hz, 1H), 3.13 (s, 1H), 3.06 (d,  $J$  = 16.0 Hz, 1H), 2.83 (d,  $J$  = 16.0 Hz, 1H), 2.43 (s, 1H);  $^{13}\text{C}$  NMR (151 MHz,  $\text{CDCl}_3$ )  $\delta$  158.8, 156.8, 148.7, 148.6, 136.7, 135.8, 135.4, 133.2, 129.6, 128.9, 128.7, 128.6, 128.1, 127.9, 127.6, 127.6, 121.7, 108.7, 107.9, 106.7, 101.2, 85.5, 71.3, 70.3, 70.3, 66.6, 56.0, 53.9, 41.4. IR (ATR) 3350, 2938, 2921, 2851, 1608, 1584, 1504, 1215, 1175, 1094  $\text{cm}^{-1}$ ; HRMS (ESI)  $m/z$  calcd for  $\text{C}_{32}\text{H}_{32}\text{O}_6\text{Na}$   $[\text{M} + \text{Na}]^+$  535.2097, found 535.2098.

**Assignment of Stereochemistry of Major (2.68) and Minor (2.69) Diols by Correlation with <sup>13</sup>C Data for Diol Stereoisomers prepared by Zhang and Yadav**



The relative stereochemistry of diol stereoisomers **2.68** and **2.69** were assigned by comparison to the diastereomeric diols prepared by Yadav<sup>9</sup> and Zhang.<sup>10</sup> Yadav secured the stereochemistry of his diol, compound (±)-**8**, by converting it to the final product, (±)-brazilin. Zhang mis-assigned the same stereochemistry to his diol, compound **9**, prepared by a different route. Zhang's diol is clearly a diastereomer of the Yadav diol. Minor diol **2.69** in this work corresponds to Yadav's diol; major diol **2.68** in this work corresponds to Zhang's diol.

**Dimethyl 1-(2,4-dihydroxyphenyl)-5,6-dimethoxy-1,3-dihydro-2*H*-indene-2,2-dicarboxylate, **2.70**.**

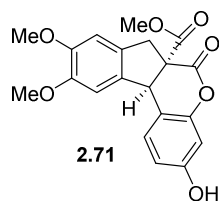


A reaction mixture containing 1-arylidane **2.57** (1.5 g, 2.57 mmol) and 20 wt.% Pd(OH)<sub>2</sub>/C (442 mg, 0.629 mmol) in a solution of 1:1 MeOH/THF (88.0 mL) was evacuated and backfilled with H<sub>2</sub> (× 3). 1-Arylidane **2.57**

was consumed within 30 min. The flask was evacuated and backfilled with N<sub>2</sub> (× 3), and the reaction mixture diluted with EtOAc (40 mL). The heterogenous mixture was filtered through tightly packed Celite and the pad washed with EtOAc (3 × 50 mL). The organic was concentrated *in vacuo* to afford a black solid. The solid was purified by flash chromatography (45:55 EtOAc:hexanes) to yield resorcinol **2.70** and chromanone **2.71** (1.08 g) as an inseparable 2.1:1 mixture. This mixture was used in the next step without further purification. In a different run, an analytical sample of resorcinol **2.70** was obtained by chromatography.

R<sub>f</sub> = 0.18 (50:50 EtOAc:hexanes). mp = 138–142 °C (shrinkage begins at 80 °C; sharp melt at 138–142 °C). <sup>1</sup>H NMR (500 MHz, CDCl<sub>3</sub>) δ 8.38 (s, 1H), 6.78 (s, 1H), 6.61 (d, *J* = 8.5 Hz, 1H), 6.50 (d, *J* = 2.6 Hz, 1H), 6.42 (s, 1H), 6.29 (dd, *J* = 8.5, 2.6 Hz, 1H), 5.41 (s, 1H), 5.15 (s, 1H), 3.89 (s, 3H), 3.86 (s, 3H), 3.80 (d, *J* = 16.3 Hz, 1H), 3.73 (s, 3H), 3.30 (d, *J* = 16.3 Hz, 1H), 3.19 (s, 3H); <sup>13</sup>C NMR (126 MHz, CDCl<sub>3</sub>) δ 175.9, 170.0, 157.1, 156.4, 149.1, 148.7, 133.1, 132.2, 130.2, 117.6, 108.2, 107.6, 106.7, 104.2, 67.2, 56.1, 56.0, 53.9, 52.4, 50.3, 39.6; IR (ATR) 3418, 2953, 1713, 1621, 1505, 1454, 1262, 1216, 1112, 1087, 1055, 975 cm<sup>-1</sup>; HRMS (ESI) *m/z* calcd for C<sub>21</sub>H<sub>22</sub>O<sub>8</sub>Na [M + Na]<sup>+</sup> 425.1212, found 425.1212.

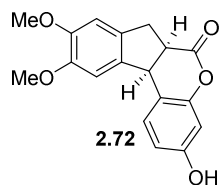
**Methyl 3-hydroxy-9,10-dimethoxy-6-oxo-7,11b-dihydroindeno[2,1-c]chromene-6a(6H)-carboxylate, 2.71.**



A solution of the 2.1:1 mixture of resorcinol **2.70** and chromanone **2.71** (1.08 g) described above, and *p*-toluenesulfonic acid hexahydrate (133 mg, 0.772 mmol) in toluene (103 mL) was heated at reflux. When resorcinol **2.70** was no longer detected by TLC (1 h), the mixture was cooled to 23 °C and partitioned between EtOAc (50 mL) and saturated aqueous NaHCO<sub>3</sub> (100 mL). The layers were separated and the organic layer washed sequentially with H<sub>2</sub>O and brine. The organic was then dried (MgSO<sub>4</sub>) and concentrated *in vacuo* to afford a peach solid that was purified by flash chromatography (40:60 – 60:40 EtOAc:hexanes) to afford chromanone **2.71** as a peach solid (0.889 g, 93% over two steps).

$R_f = 0.14$  (40:60 EtOAc:hexanes). mp = 188–190 °C. <sup>1</sup>H NMR (500 MHz, CDCl<sub>3</sub>) δ 7.27 (d,  $J = 2.0$  Hz, 1H), 6.79 (s, 1H), 6.75 (dd,  $J = 8.2, 2.5$  Hz, 1H), 6.65 (d,  $J = 2.5$  Hz, 1H), 6.42 (s, 1H), 5.95 (s, 1H), 4.72 (s, 1H), 3.92 (d,  $J = 15.2$  Hz, 1H), 3.85 (s, 3H), 3.75 (s, 3H), 3.72 (s, 3H), 3.64 (d,  $J = 15.2$  Hz, 1H); <sup>13</sup>C NMR (126 MHz, CDCl<sub>3</sub>) δ 169.8, 167.4, 156.7, 151.0, 149.5, 149.0, 132.2, 130.7, 129.8, 112.4, 112.2, 107.7, 106.5, 104.6, 61.3, 56.10, 56.09, 53.5, 50.5, 40.5; IR (ATR) 3432, 2953, 1737, 1629, 1503, 1457, 1306, 1244, 1160 cm<sup>-1</sup>; HRMS (ESI)  $m/z$  calcd for C<sub>20</sub>H<sub>18</sub>O<sub>7</sub>Na [M + Na]<sup>+</sup> 393.0950, found 393.0944.

**3-Hydroxy-9,10-dimethoxy-7,11b-dihydroindeno[2,1-c]chromen-6(6aH)-one, 2.72.**



All glassware was oven-dried or flame-dried. A 5 mL round-bottom flask half-filled with KCl was placed under vacuum, and flame-dried until the salt no longer adhered to the flask wall. All materials were kept under N<sub>2</sub>. DMSO was stored over 3 Å molecular sieves in a Schlenk flask. Chromanone **2.71** (50 mg, 0.135 mmol) and KCl (106 mg, 1.42 mmol) were quickly added to a 10 mL round-bottom flask. The flask was

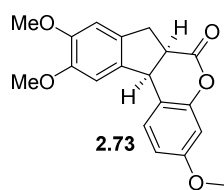
connected to a condenser. The set-up was evacuated, backfilled with N<sub>2</sub> and capped tightly with a rubber septum. A steady stream of N<sub>2</sub> was added through the top of the condenser. Anhydrous DMSO (2.7 mL) was then added through the top of the condenser. The mixture was heated at 160 °C and stirred for 2 h 40 min. At 2 h 40 min, the reaction was removed from the oil bath and cooled to 23 °C while stirring. Then, brine (4.0 mL) was added, causing a precipitate to form. Additional brine (1.0 mL) was added if no precipitate formed. The mixture was briefly stirred and then poured into a separatory funnel containing brine (15 mL). The aqueous layer was extracted with EtOAc (3 × 15 mL) and the combined organic layers then washed with water (3 × 50 mL). The organic layer was dried (Na<sub>2</sub>SO<sub>4</sub>), and concentrated *in vacuo*.

This reaction was performed six times in parallel to bring up material as scaling the reaction led to lower yields, on average. Combining reactions producing identical <sup>1</sup>H NMR led to fraction A and fraction B. These were purified separately by flash chromatography (25:75 – 40:60 EtOAc:hexanes). Fraction A and B afforded phenol **2.72** as a yellow solid (45 mg, 18%) and (18 mg, 7%) respectively. The phenol, **2.72**, from fraction A and B were triturated, separately, with distilled hexanes to afford analytical samples for characterization (38 mg, 15%) and (15 mg, 6%) respectively, for a combined yield of 53 mg (21%). <sup>1</sup>H and <sup>13</sup>C NMR for both samples were identical.

R<sub>f</sub> = 0.08 (30:70 EtOAc:hexanes). R<sub>f</sub> = 0.23 (40:60 EtOAc:hexanes). <sup>1</sup>H NMR (499 MHz, CDCl<sub>3</sub>) δ 7.26 (s, 1H), 6.82 (s, 1H), 6.72 (d, *J* = 8.3 Hz, 1H), 6.63 (s, 1H), 6.60 (s, 1H), 6.08 (s, 1H), 4.41 (d, *J* = 7.3 Hz, 1H), 3.85 (s, 3H), 3.79 (s, 3H), 3.63 – 3.52 (m, 2H), 3.25 (dd, *J* = 15.3, 7.0 Hz, 1H); <sup>13</sup>C NMR (126 MHz, CDCl<sub>3</sub>) δ 170.6, 156.4, 151.3, 149.1, 148.7, 134.3, 132.6, 129.7, 113.3, 112.2, 108.0, 107.0, 104.4, 56.2, 56.1, 44.7, 44.3, 35.5; IR (ATR) 3402, 2947, 1720, 1634, 1601, 1503, 1449, 1348, 1297, 1227, 1160, 1081, 852 cm<sup>-1</sup>; HRMS (ESI) *m* / *z* calcd for

$C_{18}H_{16}O_5Na$   $[M + Na]^+$  335.0895, found 335.0898;  $^1H$  NMR data of same sample, at a different time, with resolved peaks.  $^1H$  NMR (499 MHz,  $CDCl_3$ )  $\delta$  7.26 (s, 1H), 6.82 (s, 1H), 6.72 (dd,  $J = 8.3, 2.5$  Hz, 1H), 6.63 (d,  $J = 2.5$  Hz, 1H), 6.60 (s, 1H), 5.55 (s, 1H), 4.41 (d,  $J = 7.3$  Hz, 1H), 3.85 (s, 3H), 3.79 (s, 3H), 3.58 (dd,  $J = 15.3, 2.7$  Hz, 1H), 3.51 (td,  $J = 7.2, 2.7$  Hz, 1H), 3.25 (dd,  $J = 15.2, 7.0$  Hz, 1H). The main byproduct results from in-situ methylation of phenol **2.72** to afford chromanone **2.73** (127 mg, 48%).

**3,9,10-Trimethoxy-7,11b-dihydroindeno[2,1-c]chromen-6(6aH)-one, 2.73.**



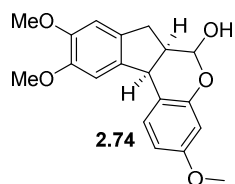
A partial sample of phenol **2.72** (47 mg, 0.15 mmol), described above, anhydrous  $K_2CO_3$  (63 mg, 0.45 mmol), and dimethyl sulfate (43  $\mu$ L, 0.45 mmol) in acetone (7.5 mL) were heated at reflux and monitored for consumption of phenol **2.72**. At 2 h, additional dimethyl sulfate (0.45 mmol) was added. At 5 h, additional  $K_2CO_3$  (0.45 mmol) was added. Within 9 h, phenol **2.72** was consumed as determined by TLC. After the reaction was cooled to 23  $^{\circ}C$ , the solvent was removed *in vacuo*. The residue was partitioned between  $H_2O$  (10 mL) and EtOAc (10 mL). The layers were separated and the aqueous extracted with EtOAc (2  $\times$  10 mL). The combined organic layers were dried ( $MgSO_4$ ), and concentrated *in vacuo* to afford a mixture that was purified by flash chromatography (25:75 EtOAc: hexanes) to yield chromanone **2.73** as a pale yellow solid (44 mg, 90%).

$R_f = 0.23$  (30:70 EtOAc:hexanes).  $R_f = 0.35$  (40:60 EtOAc:hexanes). mp = 145–149  $^{\circ}C$ .  $^1H$  NMR (600 MHz,  $CDCl_3$ )  $\delta$  7.30 (d,  $J = 8.4$  Hz, 1H), 6.82 (s, 1H), 6.78 (dd,  $J = 8.4, 2.6$  Hz, 1H), 6.61 (d,  $J = 2.6$  Hz, 1H), 6.60 (s, 1H), 4.42 (d,  $J = 7.3$  Hz, 1H), 3.85 (s, 3H), 3.81 (s, 3H), 3.80 (s, 3H), 3.58 (dd,  $J = 15.3, 2.8$  Hz, 1H), 3.51 (td,  $J = 7.2, 2.8$  Hz, 1H), 3.25 (dd,  $J = 15.1, 7.2$  Hz, 1H);  $^{13}C$  NMR (151 MHz,  $CDCl_3$ )  $\delta$  170.1, 160.0, 151.4, 149.1, 148.7, 134.2, 132.5, 129.4, 113.4, 111.0, 107.9, 106.9, 102.5, 56.14, 56.07, 55.5, 44.8, 44.3, 35.5; IR (ATR) 1754, 1626, 1588,



1504, 1154, 1103, 1080, 829  $\text{cm}^{-1}$ ; HRMS (ESI)  $m/z$  calcd for  $\text{C}_{19}\text{H}_{18}\text{O}_5\text{Na}$   $[\text{M} + \text{Na}]^+$  349.1052, found 349.1049.

### 3,9,10-Trimethoxy-6,6a,7,11b-tetrahydroindeno[2,1-c]chromen-6-ol, **2.74**

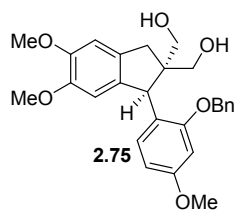


To a cooled ( $-78\text{ }^\circ\text{C}$ ) solution of chromanone **2.73** (40.0 mg, 0.123 mmol) in DCM (0.82 mL) was added DIBAL-H (0.13 mL, 0.129 mmol, 1M in THF) dropwise over three minutes. Stirring continued at  $-78\text{ }^\circ\text{C}$  until chromanone **2.73** was no longer detected by TLC. Within 15 min, a light-yellow solid appeared. At 1 h, additional DCM (1.0 mL) was added to solubilize the yellow solid. The mixture was warmed to  $23\text{ }^\circ\text{C}$  at 3 h when no reaction progress was detected. Stirring at  $23\text{ }^\circ\text{C}$  for 1 h did not result in any observable effect by TLC. At 4 h and 6 h, the flask was briefly cooled ( $-78\text{ }^\circ\text{C}$ ) and DIBAL-H (0.123 mmol) added dropwise over five minutes. By 7 h, there was approximately 5% chromanone **2.73** remaining and the reaction was briefly cooled ( $-78\text{ }^\circ\text{C}$ ), quenched with  $\text{H}_2\text{O}$  (3.0 mL), and warmed to  $23\text{ }^\circ\text{C}$ . The mixture was extracted with  $\text{Et}_2\text{O}$  ( $3 \times 15\text{ mL}$ ) and the combined organic layers washed with brine ( $1 \times 15\text{ mL}$ ), dried ( $\text{Na}_2\text{SO}_4$ ), and concentrated *in vacuo* to afford a crude white solid. The crude mixture was purified by flash chromatography (25:75 EtOAc:hexanes) to yield lactol **2.74** as an inseparable 5.8:1 mixture of diastereomers as a white solid (19.4 mg, 48%). The major side-products resulted from over-reduction. The  $^{13}\text{C}$  NMR was obtained using lactol **2.74** from a different run.

$R_f = 0.10$  (25:75 EtOAc:hexanes).  $R_f = 0.15$  (30:70 EtOAc:hexanes).  $R_f = 0.24$  (40:60 EtOAc:hexanes).  $^1\text{H}$  NMR (500 MHz,  $\text{CDCl}_3$ )  $\delta$  7.30 (d,  $J = 8.6\text{ Hz}$ , 1H), 6.90 (s, 1H), 6.77 (s, 1H), 6.61 (dd,  $J = 8.5, 2.5\text{ Hz}$ , 1H), 6.45 (d,  $J = 2.5\text{ Hz}$ , 1H), 5.11 (t,  $J = 5.9\text{ Hz}$ , 1H), 4.33 (d,  $J = 7.1\text{ Hz}$ , 1H), 3.87 (s, 3H), 3.85 (s, 3H), 3.77 (s, 3H), 3.12 (dd,  $J = 15.6, 7.3\text{ Hz}$ , 1H), 3.08 – 2.97 (m, 2H), 2.85 – 2.74 (m, 1H);  $^{13}\text{C}$  NMR (151 MHz,  $\text{CDCl}_3$ )  $\delta$  159.3, 152.4, 148.6, 148.3, 137.0,

132.4, 129.8, 115.6, 108.6, 108.2, 107.7, 102.3, 94.2, 56.2, 56.1, 55.3, 44.1, 42.4, 33.6; IR (ATR) 3446, 2930, 2850, 1617, 1582, 1501, 1302, 1258, 1222, 1198, 1158, 1125, 1031, 843, 734  $\text{cm}^{-1}$ . HRMS (ESI)  $m/z$  calcd for  $\text{C}_{19}\text{H}_{20}\text{O}_5\text{Na}$   $[\text{M} + \text{Na}]^+$  351.1208, found 351.1208.  $^1\text{H}$  NMR data of same sample containing resolved peaks of major diastereomer:  $^1\text{H}$  NMR (500 MHz,  $\text{CDCl}_3$ )  $\delta$  7.30 (d,  $J = 8.5$  Hz, 1H), 6.90 (s, 1H), 6.77 (s, 1H), 6.61 (dd,  $J = 8.5, 2.6$  Hz, 1H), 6.45 (d,  $J = 2.6$  Hz, 1H), 5.11 (t,  $J = 6.0$  Hz, 1H), 4.33 (d,  $J = 7.2$  Hz, 1H), 3.87 (s, 3H), 3.84 (s, 3H), 3.77 (s, 3H), 3.12 (dd,  $J = 15.7, 7.3$  Hz, 1H), 3.03 (dd,  $J = 15.7, 4.7$  Hz, 1H), 2.98 (d,  $J = 5.8$  Hz, 1H), 2.79 (dt,  $J = 12.0, 7.0$  Hz, 1H).

**(1-(2-(Benzyloxy)-4-methoxyphenyl)-5,6-dimethoxy-2,3-dihydro-1H-indene-2,2-diyl)-dimethanol, 2.75**



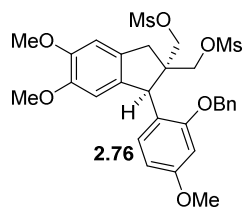
In one portion,  $\text{LiAlH}_4$  (300 mg, 7.89 mmol) was added to a stirring, chilled (0  $^\circ\text{C}$ ) solution of 1-arylidane **2.58** (1.00 g, 1.97 mmol) in THF (22.0 mL).

Additional THF (14.0 mL) was added to rinse the  $\text{LiAlH}_4$  off the walls of the flask. The reaction was stirred (23  $^\circ\text{C}$ ) and quenched with saturated aqueous potassium sodium tartrate solution (65.0 mL) upon consumption of 1-arylidane **2.58** (1 h 10 min). The mixture was stirred vigorously for 15 min and then extracted with EtOAc ( $3 \times 75$  mL). The combined organic layers were dried ( $\text{Na}_2\text{SO}_4$ ) and concentrated *in vacuo* to afford a peach solid. The solid was dissolved in minimal EtOAc with light heating. After cooling to 23  $^\circ\text{C}$ , the solution was chilled (0  $^\circ\text{C}$ ) and room temperature hexanes was added slowly, until a cloudy suspension remained in the solution while swirling. The persistent cloudy suspension was kept cool (0  $^\circ\text{C}$ ) until the amount of precipitate forming remained unchanged. The resulting suspension was filtered to yield geminal alcohol **2.75** as a white solid (635 mg, 71%). The additional peaks in the  $^1\text{H}$  NMR are determined

to be of rotamers and not impurities. This was the assignment based on the 1D NOE data obtained for 1-arylidane **2.58**.

$R_f = 0.19$  (50:50 EtOAc:hexanes, stains purple by *p*-anis dip stain).  $^1\text{H}$  NMR (500 MHz,  $\text{CDCl}_3$ )  $\delta$  7.49 (d,  $J = 7.0$  Hz, 2H), 7.43 (t,  $J = 7.4$  Hz, 2H), 7.39 – 7.33 (m, 1H), 6.77 (s, 1H), 6.65 (d,  $J = 2.4$  Hz, 1H), 6.51 – 6.48 (m, 2H), 6.41 (dd,  $J = 8.5, 2.4$  Hz, 1H), 5.18 (d,  $J = 11.1$  Hz, 1H), 5.09 (d,  $J = 11.1$  Hz, 1H), 4.65 (s, 1H), 3.88 (s, 3H), 3.79 (s, 3H), 3.75 (s, 3H), 3.73 (d,  $J = 4.4$  Hz, 1H), 3.65 (dd,  $J = 11.0, 4.6$  Hz, 1H), 3.41 – 3.37 (m, 2H), 2.73 (s, 2H), 2.60 (d,  $J = 6.2$  Hz, 1H), 2.33 (t,  $J = 6.1$  Hz, 1H);  $^{13}\text{C}$  NMR (126 MHz,  $\text{CDCl}_3$ )  $\delta$  159.5, 156.6, 148.45, 148.36, 136.8, 135.9, 133.6, 130.7, 128.8, 128.5, 127.9, 122.2, 108.5, 107.6, 105.6, 100.1, 71.1, 68.7, 67.0, 56.0, 55.4, 54.3, 46.9, 37.0; IR (ATR) 3230, 2933, 1606, 1584, 1503, 1216, 1162, 1093, 1043  $\text{cm}^{-1}$ ; HRMS (ESI)  $m/z$  calcd for  $\text{C}_{27}\text{H}_{30}\text{O}_6\text{Na}$   $[\text{M} + \text{Na}]^+$  473.1940, found 473.1929.

**(1-(2-(benzyloxy)-4-methoxyphenyl)-5,6-dimethoxy-2,3-dihydro-1*H*-indene-2,2-diyl)bis(methylene) dimethanesulfonate, 2.76**

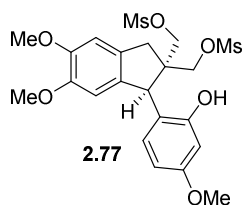


To a stirring, chilled (0 °C) solution of a separate batch of alcohol **2.75** (0.976 g, 2.16 mmol) in DCM (15.5 mL) was added  $\text{NEt}_3$  (0.700 mL, 5.05 mmol) and mesyl chloride (0.391 mL, 5.05 mmol).  $\text{NEt}_3$  and mesyl chloride were purified prior to use. The yellow reaction mixture was kept chilled for the duration of the reaction. At 1.5 h, mesyl chloride (0.100 mL, 1.29 mmol) was added and at 2 h,  $\text{NEt}_3$  (0.200 mL, 1.43 mmol) was added to drive complete consumption of starting alcohol. At 2.5 h, the starting alcohol was no longer detectable by TLC. The mixture was then diluted with DCM (15 mL) and washed with chilled portions of  $\text{H}_2\text{O}$  (1  $\times$  30 mL) and aqueous 5%  $\text{HCl}$  (1  $\times$  30 mL). Then, the organic was washed with saturated aqueous  $\text{NaHCO}_3$  (1  $\times$  30 mL) and brine (1  $\times$  30 mL). The organic layer was dried ( $\text{MgSO}_4$ ), and concentrated *in vacuo* to afford a crude pink solid that was purified by

flash chromatography (10:90 to 30:70 EtOAc:toluene) to yield bis(mesylate) **2.76** as a fluffy white solid (1.29 g, 95%). The additional peaks in the  $^1\text{H}$ NMR are determined to be due to rotamers using the method of Ley and co-workers. Major peaks for bis-mesylate **2.76** and minor peaks of rotamer, are reported below.

Major peaks:  $R_f = 0.39$  (30:70 EtOAc:toluene, stains pink by *p*-anis dip stain).  $^1\text{H}$  NMR (600 MHz,  $\text{CDCl}_3$ )  $\delta$  7.53 (d,  $J = 7.4$  Hz, 2H), 7.44 (t,  $J = 7.2$  Hz, 2H), 7.36 (t,  $J = 7.4$  Hz, 1H), 6.76 (s, 1H), 6.60 (d,  $J = 3.1$  Hz, 1H), 6.50 (s, 2H), 6.37 (dd,  $J = 7.6, 3.8$  Hz, 1H), 5.15 (d,  $J = 11.3$  Hz, 1H), 5.09 (d,  $J = 11.3$  Hz, 1H), 4.81 (s, 1H), 4.23 (s, 2H), 4.08 (d,  $J = 9.7$  Hz, 1H), 3.89 (d,  $J = 2.6$  Hz, 4H), 3.78 – 3.77 (m, 3H), 3.77 – 3.75 (m, 3H), 2.99 (d,  $J = 16.4$  Hz, 1H), 2.87 (d,  $J = 16.5$  Hz, 1H), 2.79 – 2.76 (m, 3H), 2.74 – 2.70 (m, 3H);  $^{13}\text{C}$  NMR (151 MHz,  $\text{CDCl}_3$ )  $\delta$  160.0, 157.4, 149.1, 149.0, 136.7, 135.3, 131.9, 130.4, 128.8, 128.3, 128.0, 120.0, 108.4, 107.4, 104.9, 99.7, 71.2, 70.6, 70.2, 56.05, 56.02, 55.4, 50.8, 47.0, 38.0, 36.9, 36.8; Minor peaks of rotamer:  $^1\text{H}$  NMR (600 MHz,  $\text{CDCl}_3$ )  $\delta$  7.35 (s, 1H), 7.25 – 7.18 (m, 3H), 6.87 (d,  $J = 7.2$  Hz, 2H), 6.48 (s, 4H), 6.41 (s, 1H), 4.78 (d,  $J = 11.1$  Hz, 1H), 4.54 (d,  $J = 10.9$  Hz, 1H), 4.19 (d,  $J = 8.6$  Hz, 2H), 4.00 (d,  $J = 9.2$  Hz, 1H), 3.90 (s, 2H), 3.83 (s, 3H), 3.79 (d,  $J = 2.3$  Hz, 4H), 3.74 (s, 3H), 3.05 – 3.02 (m, 3H), 2.64 (d,  $J = 2.3$  Hz, 4H);  $^{13}\text{C}$  NMR (151 MHz,  $\text{CDCl}_3$ )  $\delta$  160.7, 157.9, 148.6, 148.5, 135.6, 134.9, 133.5, 131.7, 128.3, 128.2, 128.1, 120.5, 107.3, 104.7, 100.6, 71.5, 70.5, 70.3, 60.4, 56.1, 55.9, 55.7, 55.4, 49.3, 39.0, 37.3, 36.3; IR (ATR) 3026, 2937, 2836, 1607, 1504, 1352, 1253, 1171, 1038, 949, 826  $\text{cm}^{-1}$ ; HRMS (ESI)  $m/z$  calcd for  $\text{C}_{29}\text{H}_{34}\text{O}_{10}\text{S}_2\text{Na}$   $[\text{M} + \text{Na}]^+$  629.1491, found 629.1509.

**(1-(2-Hydroxy-4-methoxyphenyl)-5,6-dimethoxy-2,3-dihydro-1H-indene-2,2-diyl)bis(methylene) dimethanesulfonate, 2.77**



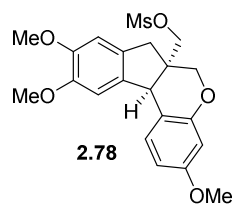
To a 40 mL amber vial containing 20% wt. Pd(OH)<sub>2</sub>/C (316 mg, 0.45 mmol) was added a solution of bis-mesylate **2.76** (1.12 g, 1.83 mmol) in THF (3.2 mL). Methanol was dried (Na<sub>2</sub>SO<sub>4</sub>) briefly, and then added (3.2 mL) to the mixture. The reaction vessel was evacuated and backfilled with H<sub>2</sub> (× 3). After debenzylation was complete (1.5 h), the mixture was filtered through a tightly packed Celite pad. The pad was rinsed with EtOAc (3 × 25 mL) and the organic concentrated *in vacuo*. The crude pink solid was purified by flash chromatography (60:40 EtOAc:hexanes) to yield product **2.77** as a white solid (940 mg, 99%) which was used without any further purification. Rotamers are present in the <sup>1</sup>H NMR as determined by the published method of Ley and co-workers.<sup>7</sup> <sup>1</sup>H and <sup>13</sup>C NMR in two different solvents at two different temperatures results in peak resolution and splitting.

R<sub>f</sub> = 0.21 (60:40 EtOAc:hexanes, stains red by *p*-anis dip stain). <sup>1</sup>H NMR (600 MHz, CDCl<sub>3</sub>) (20:80 mixture of rotamers) δ 7.26 (s, 1H), 7.14 (d, *J* = 8.3 Hz, 0.2H), 6.77 (s, 1H), 6.58 (s, 0.2H), 6.55 – 6.52 (m, 1H), 6.45 (apparent d, *J* = 7.8 Hz, 0.8H), 6.43 – 6.40 (m, 0.9H), 6.39 – 6.34 (m, 0.8H), 6.31 (apparent s, 0.2H), 5.59 (br s, 0.8H), 4.73 (apparent s, 0.8H), 4.68 (s, 0.2H), 4.39 – 4.31 (m, 1.6H), 4.30 – 4.21 (m, 0.6H), 4.16 (apparent d, *J* = 9.4 Hz, 0.2H), 4.08 (apparent d, *J* = 9.5 Hz, 0.8H), 4.02 (apparent d, *J* = 8.8 Hz, 0.2H), 3.93 (apparent d, *J* = 9.6 Hz, 0.9H), 3.91 – 3.87 (m, 3H), 3.78 – 3.72 (m, 6H), 3.22 (apparent d, *J* = 16.6 Hz, 0.2H), 3.07 (s, 3H), 3.02 (apparent d, *J* = 16.3 Hz, 0.8H), 2.95 (apparent d, *J* = 16.6 Hz, 0.2H), 2.90 (overlapping d, 0.8H), 2.87 (s, 2.8H), 2.76 (s, 0.5H); <sup>13</sup>C NMR (151 MHz, CDCl<sub>3</sub>) (20:80 mixture of rotamers) δ 160.8, 159.7, 155.8, 154.6, 149.9, 149.7, 149.1, 149.1, 135.0, 133.4, 132.7, 131.6, 131.2, 130.6, 128.3, 117.8, 117.0, 108.4, 107.8, 107.6, 107.4, 106.9, 106.5, 103.5, 102.2, 71.4, 71.0, 70.5, 70.2, 56.1,

56.0, 55.4, 55.3, 54.8, 50.9, 49.7, 47.1, 38.9, 37.8, 37.4, 37.0, 36.6;  $^{13}\text{C}$  NMR major peaks:  $\delta$  159.7, 154.6, 149.15, 149.12, 135.0, 131.6, 130.6, 128.3, 117.8, 108.4, 107.4, 106.5, 102.2, 71.4, 70.5, 56.1, 56.0, 55.3, 50.9, 47.1, 37.8, 37.4, 37.0.  $^{13}\text{C}$  NMR minor peaks:  $\delta$  160.8, 155.8, 149.9, 149.7, 133.4, 132.7, 131.2, 117.0, 107.8, 107.6, 106.9, 103.5, 71.0, 70.2, 55.4, 54.8, 49.7, 38.9, 36.6; IR (ATR) 3429, 2936, 1614, 1505, 1351, 1172, 957, 835  $\text{cm}^{-1}$ ; HRMS (ESI)  $m/z$  calcd for  $\text{C}_{22}\text{H}_{28}\text{O}_{10}\text{S}_2\text{Na}$   $[\text{M} + \text{Na}]^+$  539.1022, found 539.1005.

### (3,9,10-trimethoxy-7,11b-dihydroindeno[2,1-c]chromen-6a(6H)-yl)methyl

#### methanesulfonate, **2.78**

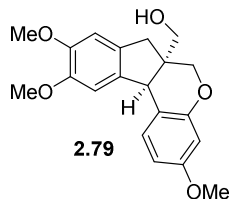


To a stirring solution of phenol **2.77** (0.900 g, 1.74 mmol) in THF (22.0 mL) at 0 °C was added un-rinsed 60% NaH/mineral oil (73.0 mg, 1.83 mmol) in one portion. Upon consumption of phenol **2.77** (2 h), the reaction was quenched with 20 mL of  $\text{H}_2\text{O}$ . The resulting mixture was extracted with EtOAc ( $3 \times 50$  mL) and the combined organic layers dried ( $\text{MgSO}_4$ ) and concentrated *in vacuo* to afford a fluffy pink solid. Purification by two rounds of flash chromatography (40:60 EtOAc:hexanes; then, 4:96 – 30:70 EtOAc:toluene) yielded partially purified mesyl chromane product **2.78** as a white fluffy solid (660 mg) containing (34 mol %, 10 wt. % by  $^1\text{H}$  NMR) of toluene (81% yield of **2.78**). Upon standing under vacuum, this compound turns pink in color. This sample was carried on to the next step without further purification.

$R_f = 0.35$  (50:50 EtOAc:hexanes, stains pink by *p*-anis dip stain).  $^1\text{H}$  NMR (500 MHz,  $\text{CDCl}_3$ )  $\delta$  7.29 (d,  $J = 8.5$  Hz, 1H), 6.79 (s, 1H), 6.74 (s, 1H), 6.64 (dd,  $J = 8.4, 2.6$  Hz, 1H), 6.45 (d,  $J = 2.6$  Hz, 1H), 4.42 (d,  $J = 9.9$  Hz, 1H), 4.33 (d,  $J = 9.9$  Hz, 1H), 4.12 (dd,  $J = 11.4, 1.3$  Hz, 1H), 4.03 (s, 1H), 3.85 (s, 3H), 3.83 (s, 3H), 3.78 (s, 3H), 3.70 (d,  $J = 11.3$  Hz, 1H), 3.20 (d,  $J = 16.0$  Hz, 1H), 3.03 (s, 3H), 2.66 (d,  $J = 16.0$  Hz, 1H).  $^{13}\text{C}$  NMR (126 MHz,  $\text{CDCl}_3$ )  $\delta$  159.5, 154.5,

148.8, 148.5, 136.1, 130.9, 130.8, 129.0 (toluene), 128.2 (toluene), 125.3 (toluene), 113.9, 108.7, 108.4, 107.6, 102.0, 71.4, 66.4, 56.1, 56.08, 55.3, 45.4, 45.0, 38.0, 37.1; IR (ATR) 2925, 2852, 1503, 1355, 1174, 957, 845, 730  $\text{cm}^{-1}$ ; HRMS (ESI)  $m/z$  calcd for  $\text{C}_{21}\text{H}_{24}\text{O}_7\text{SNa}$   $[\text{M} + \text{Na}]^+$  443.1140, found 443.1143.

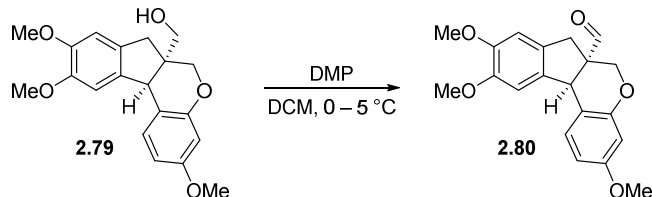
**(3,9,10-Trimethoxy-7,11b-dihydroindeno[2,1-c]chromen-6a(6H)-yl)methanol, 2.79**



To a cooled (0 °C) solution of mesyl chromane **2.78** containing (34 mol %, 10 wt. % by  $^1\text{H}$  NMR) of toluene (660 mg, 90% wt/wt, 1.41 mmol of **2.78**) in THF (32 mL), described above, was added  $\text{LiAlH}_4$  (238 mg, 6.27 mmol) in one portion. The solution warmed to 23 °C and then heated at reflux. Upon consumption of mesyl chromane **2.78** (2 h), the reaction was cooled (0 °C) and slowly quenched with 20 mL of saturated aqueous potassium sodium tartrate. The solution was stirred at 23 °C for 15 min and then extracted with EtOAc (3  $\times$  50 mL). The combined organic layers were dried ( $\text{Na}_2\text{SO}_4$ ), concentrated *in vacuo*, and purified by flash chromatography (30:70 – 50:50 EtOAc:hexanes) to yield alcohol **2.79** as a beige fluffy solid (440 mg, 90%).

$R_f$  = 0.30 (50:50 EtOAc:hexanes; stains pink by *p*-anis dip stain).  $^1\text{H}$  NMR (600 MHz,  $\text{CDCl}_3$ )  $\delta$  7.29 (dd,  $J$  = 8.5, 0.8 Hz, 1H), 6.81 (d,  $J$  = 0.9 Hz, 1H), 6.74 (s, 1H), 6.61 (dd,  $J$  = 8.4, 2.6 Hz, 1H), 6.43 (d,  $J$  = 2.6 Hz, 1H), 4.16 (dd,  $J$  = 11.1, 1.3 Hz, 1H), 3.98 (s, 1H), 3.86 (d,  $J$  = 10.9 Hz, 1H), 3.84 (s, 3H), 3.83 (s, 3H), 3.77 (s, 3H), 3.74 (d,  $J$  = 10.8 Hz, 1H), 3.68 (d,  $J$  = 11.1 Hz, 1H), 3.13 (d,  $J$  = 15.8 Hz, 1H), 2.61 (d,  $J$  = 15.9 Hz, 1H);  $^{13}\text{C}$  NMR (151 MHz,  $\text{CDCl}_3$ )  $\delta$  159.3, 154.9, 148.5, 148.3, 137.2, 131.7, 130.9, 115.1, 108.5, 108.2, 107.8, 101.8, 67.2, 65.2, 56.1, 56.07, 55.3, 46.9, 45.3, 37.8; IR (ATR) 3502, 2931, 2833, 1502, 1160, 1134, 1125, 1086, 1034, 846, 730  $\text{cm}^{-1}$ ; HRMS (ESI)  $m/z$  calcd for  $\text{C}_{20}\text{H}_{22}\text{O}_5\text{Na}$   $[\text{M} + \text{Na}]^+$  365.1365, found 365.1371.

### 3,9,10-Trimethoxy-7,11b-dihydroindeno[2,1-c]chromene-6a(6H)-carbaldehyde, **2.80**



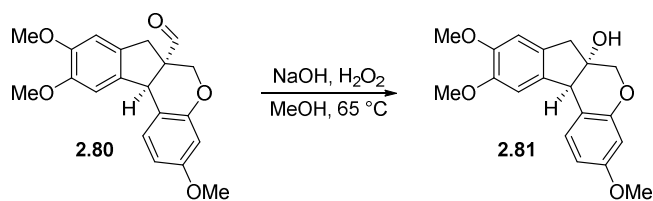
Dess–Martin periodinane (105 mg, 0.24 mmol, 98%) was added in one portion to a solution of alcohol **2.79** (76 mg, 0.22 mmol) in dichloromethane (1.1 mL) at 0 °C. The reaction was stirred at 23 °C until alcohol was no longer observed by TLC (45 min). The reaction was quenched with saturated aqueous Na<sub>2</sub>S<sub>2</sub>O<sub>3</sub> (3.0 mL) and stirred vigorously for 15 min. The solution was purged with N<sub>2</sub> gas (1.5 h) and extracted with degassed EtOAc (3 × 15 mL). The combined organic layers were dried (Na<sub>2</sub>SO<sub>4</sub>), concentrated *in vacuo*, and purified by flash chromatography (30:70 EtOAc:hexanes). The fractions containing product were collected and purged with N<sub>2</sub> before concentrating *in vacuo* to afford aldehyde **2.80** as an amorphous, fluffy red solid (67 mg) containing a small amount (13 mol %, 4 wt. % by <sup>1</sup>H NMR) of EtOAc (86% yield of **2.80**).

R<sub>f</sub> = 0.25 (40:60 EtOAc:hexanes; stains pink-orange by *p*-anis dip stain). <sup>1</sup>H NMR (600 MHz, CDCl<sub>3</sub>) δ 9.86 (s, 1H), 7.34 (d, *J* = 8.5 Hz, 1H), 6.85 (s, 1H), 6.74 (s, 1H), 6.63 (dd, *J* = 8.5, 2.6 Hz, 1H), 6.44 (d, *J* = 2.5 Hz, 1H), 4.56 (s, 1H), 4.45 (dd, *J* = 11.4, 1.2 Hz, 1H), 3.84 (s, 6H), 3.82 (d, *J* = 11.3 Hz, 1H), 3.76 (s, 3H), 3.31 (d, *J* = 15.9 Hz, 1H), 2.71 (d, *J* = 15.9 Hz, 1H); <sup>13</sup>C NMR (151 MHz, CDCl<sub>3</sub>) δ 201.9, 159.5, 154.8, 148.9, 148.8, 135.9, 130.4, 129.7, 114.0, 108.8, 108.2, 107.7, 102.0, 65.8, 56.6, 56.10, 56.07, 55.3, 44.1, 35.7; IR (ATR) 2924, 2834, 1725, 1286, 1269, 1086, 1034, 908, 731, 698 cm<sup>-1</sup>; HRMS (ESI) *m/z* calcd for C<sub>20</sub>H<sub>20</sub>O<sub>5</sub>Na [M + Na]<sup>+</sup> 363.1208, found 363.1201.



***O*-Trimethylbrazilin (3,9,10-trimethoxy-7,11b-dihydroindeno[2,1-*c*]chromen-6a(6*H*)-ol),**

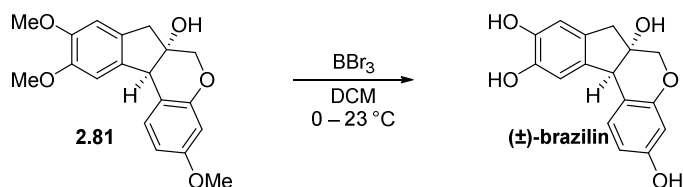
**2.81**



To a stirring solution of aldehyde **2.80** (78 mg, 0.23 mmol) in anhydrous MeOH (3.3 mL) was added NaOH (42 mg, 1.06 mmol) in one portion. Then, degassed aqueous 30% (w/w) H<sub>2</sub>O<sub>2</sub> (152  $\mu$ L, 1.49 mmol) was added. The yellow, cloudy reaction mixture was then heated and stirred at 65 °C until aldehyde **2.80** was no longer observed by TLC. Upon completion, the reaction was cooled (23°C) and then concentrated *in vacuo*. The residue was partitioned between DCM (15 mL) and H<sub>2</sub>O (15 mL) (both degassed). The layers were separated and the aqueous was extracted with DCM (3  $\times$  15 mL). The combined organic layers were washed with brine (1  $\times$  20 mL), dried (MgSO<sub>4</sub>), and purged with N<sub>2</sub> (45 min). The solution was then concentrated and purified by flash chromatography using degassed solvents (40:60 EtOAc:hexanes) to yield *O*-trimethylbrazilin **2.81** as a beige fluffy solid (31.9 mg, 42%, >95% purity).

$R_f = 0.19$  (40:60 EtOAc:hexanes; stains pink by *p*-anis dip stain).  $R_f = 0.28$  (50:50 EtOAc:hexanes; stains pink by *p*-anis dip stain). <sup>1</sup>H NMR (600 MHz, Chloroform-*d*)  $\delta$  7.29 (d,  $J = 8.3$  Hz, 1H), 6.78 (s, 1H), 6.73 (s, 1H), 6.65 (dd,  $J = 8.6, 1.9$  Hz, 1H), 6.48 (d,  $J = 2.0$  Hz, 1H), 4.11 (s, 1H), 4.02 (dd,  $J = 11.2, 1.8$  Hz, 1H), 3.84 (s, 3H), 3.83 – 3.79 (s, 3H and d,  $J = 11.4$  Hz, 1H), 3.77 (s, 3H), 3.24 (d,  $J = 15.7$  Hz, 1H), 2.87 (d,  $J = 15.7$  Hz, 1H); <sup>13</sup>C NMR (151 MHz, Chloroform-*d*)  $\delta$  159.4, 154.4, 148.7, 148.4, 136.1, 131.1, 130.6, 114.4, 108.9, 108.4, 107.7, 102.0, 77.5, 70.3, 56.10, 56.06, 55.3, 50.5, 41.4; IR (ATR) 3309, 2917, 1619, 1579, 1503, 1157, 1034, 763 cm<sup>-1</sup>; HRMS (ESI)  $m/z$  calcd for C<sub>19</sub>H<sub>20</sub>O<sub>5</sub>Na [M + Na]<sup>+</sup> 351.1208, found 351.1208.

**(±)-Brazilin (7,11b-dihydroindeno[2,1-c]chromene-3,6a,9,10(6H)-tetraol)**



A solution of BBr<sub>3</sub> (0.49 mL, 0.49 mmol, 1 M in DCM) was added dropwise via syringe pump over 10 min to a cooled (–78 °C) solution of *O*-trimethylbrazilin **2.81** (31.9 mg, 0.097 mmol) in DCM (3.04 mL). The resulting bright red solution was stirred at –78 °C for 2 h and then 18 h at 23 °C. The reaction was quenched with degassed H<sub>2</sub>O (3.0 mL) and stirred vigorously for 5–10 min. The biphasic mixture was then partitioned between degassed H<sub>2</sub>O (30 mL) and degassed EtOAc (15 mL). The layers were separated and the aqueous extracted with degassed EtOAc (2 × 15 mL) and degassed DCM (1 × 20 mL). The combined organic layers were dried (MgSO<sub>4</sub>) and concentrated *in vacuo* to afford red oil. The red oil was purified by flash chromatography (50:50 EtOAc:hexanes) to afford (±)-brazilin as a red oil (18.8 mg, 68%, >95% purity) that solidifies upon standing.

$R_f = 0.09$  (50:50 EtOAc:hexanes, stains pink by *p*-anis dip stain).  $R_f = 0.36$  (80:20 EtOAc:hexanes, stains pink by *p*-anis dip stain).  $R_f = 0.38$  (10:90 MeOH/CHCl<sub>3</sub>, stains pink by *p*-anis dip stain). <sup>1</sup>H NMR (600 MHz, Methanol-*d*<sub>4</sub>) δ 7.18 (d, *J* = 8.3 Hz, 1H), 6.71 (s, 1H), 6.60 (s, 1H), 6.47 (dd, *J* = 8.3, 2.5 Hz, 1H), 6.29 (d, *J* = 2.4 Hz, 1H), 3.96 (s, 1H), 3.93 (d, *J* = 11.4 Hz, 1H), 3.69 (d, *J* = 11.3 Hz, 1H), 3.02 (d, *J* = 15.5 Hz, 1H), 2.77 (d, *J* = 15.6 Hz, 1H); <sup>13</sup>C NMR (151 MHz, Methanol-*d*<sub>4</sub>) δ 157.9, 155.7, 145.6, 145.3, 137.4, 132.2, 131.3, 115.5, 112.9, 112.4, 109.9, 104.3, 78.1, 70.8, 51.0, 49.0 (CD<sub>3</sub>OD), 42.9; IR (ATR) 3275, 2922, 1620, 1598, 1505, 1462, 1298, 1156, 1116, 1036, 844 cm<sup>-1</sup>; HRMS (ESI) *m/z* calcd for C<sub>16</sub>H<sub>13</sub>O<sub>5</sub> [M – H]<sup>-</sup> 285.0763, found 285.0758.

## References

1. Pangborn, A. B.; Giardello, M. A.; Grubbs, R. H.; Rosen, R. K.; Timmers, F. J. Safe and convenient procedure for solvent purification. *Organometallics* **1996**, *15*, 1518–1520.
2. Armarego, W. L. F.; Chai, C. L. L., *Purification of Laboratory Chemicals*. 5<sup>th</sup> ed.; Elsevier: 2013; p 608.
3. Ziegler, F. E.; Chliwner, I.; Fowler, K. W.; Kanfer, S. J.; Kuo, S. J.; Sinha, N. D. The ambient temperature Ullmann reaction and its application to the total synthesis of (±)-steganacin. *J. Am. Chem. Soc.* **1980**, *102*, 790–798.
4. (a) Sangeetha, S.; Muthupandi, P.; Sekar, G. Copper-Catalyzed Domino Synthesis of 2-Arylthiochromanones through Concomitant C-S Bond Formations Using Xanthate as Sulfur Source. *Org. Lett.* **2015**, *17*, 6006–6009; (b) Fu, M.; Lin, D.; Deng, Y.; Zhang, X.-Q.; Liu, Y.; Lai, C.; Zeng, W. Pd-catalyzed tandem homocoupling–aldol–dehydration of ortho-acylphenyl iodides. *RSC Adv.* **2014**, *4*, 23595–23603.
5. Aggarwal, V. K.; Alonso, E.; Bae, I.; Hynd, G.; Lydon, K. M.; Palmer, M. J.; Patel, M.; Porcelloni, M.; Richardson, J.; Stenson, R. A.; Studley, J. R.; Vasse, J. L.; Winn, C. L. A new protocol for the in situ generation of aromatic, heteroaromatic, and unsaturated diazo compounds and its application in catalytic and asymmetric epoxidation of carbonyl compounds. Extensive studies to map out scope and limitations, and rationalization of diastereo- and enantioselectivities. *J. Am. Chem. Soc.* **2003**, *125*, 10926–10940.
6. (a) Maekawa, T.; Hara, R.; Odaka, H.; Kimura, H.; Mizufune, H.; Fukatsu, K. 1,2-azole derivatives with hypoglycemic and hypolipidemic activity WO 03/099793 A1, Dec. 4, 2003; (b) Lin, C. F.; Yang, J. S.; Chang, C. Y.; Kuo, S. C.; Lee, M. R.; Huang, L. J. Synthesis and anticancer activity of benzyloxybenzaldehyde derivatives against HL-60 cells. *Bioorg. Med. Chem.* **2005**, *13*, 1537–1544.
7. Hu, D. X.; Grice, P.; Ley, S. V. Rotamers or diastereomers? An overlooked NMR solution. *J. Org. Chem.* **2012**, *77*, 5198–5202.
8. Raj, M.; Wu, H.; Blosser, S. L.; Vittoria, M. A.; Arora, P. S. Aldehyde capture ligation for synthesis of native peptide bonds. *J. Am. Chem. Soc.* **2015**, *137*, 6932–6940.
9. Yadav, J. S.; Mishra, A. K.; Das, S. Formal synthesis of (±)-brazilin and total synthesis of (±)-brazilane. *Tetrahedron* **2014**, *70*, 7560–7566.
10. Pan, C. X.; Guan, Y. F.; Zhang, H. B. Synthesis of a Brazilin Analog. *Acta Chim. Sinica* **2012**, *70*, 183–189.

## Chapter 3

### Total Synthesis of the Indano[2,1-*c*]chromans, (±)-Pestalachloride C and (±)-Pestalachloride D via a Knoevenagel-Hetero-Diels–Alder Cyclization

#### Plant-Derived Indano[2,1-*c*]chromans

Indano[2,1-*c*]chromans have unknowingly held the attention of humans for over two millennia (Figure 3-1).<sup>1</sup> The red extracts of sappanwood were mentioned in writings from as early as the 2<sup>nd</sup> century. Crystals of the key constituent of these extracts, brazilin, were reported in 1808, but the indano[2,1-*c*]chroman structure was not inferred until 1901<sup>2</sup> and correctly deduced in 1908.<sup>3</sup> Plant-based indano[2,1-*c*]chromans, including (+)-brazilin,<sup>4</sup> (+)-3'-*O*-methylbrazilin,<sup>4</sup> (±)-4'-*O*-methylbrazilin,<sup>4</sup> (+)-brazilane,<sup>4b</sup> caesalpiniafenol E,<sup>4b</sup> neoprotosappanin,<sup>5</sup> (+)-haematoxylin – still used as a common cell stain – (–)-isohaematoxylin,<sup>6</sup> and the protosappanins<sup>5a</sup>,<sup>7</sup> are widely believed to arise from the C15 chalcone biosynthetic pathway.<sup>8</sup>

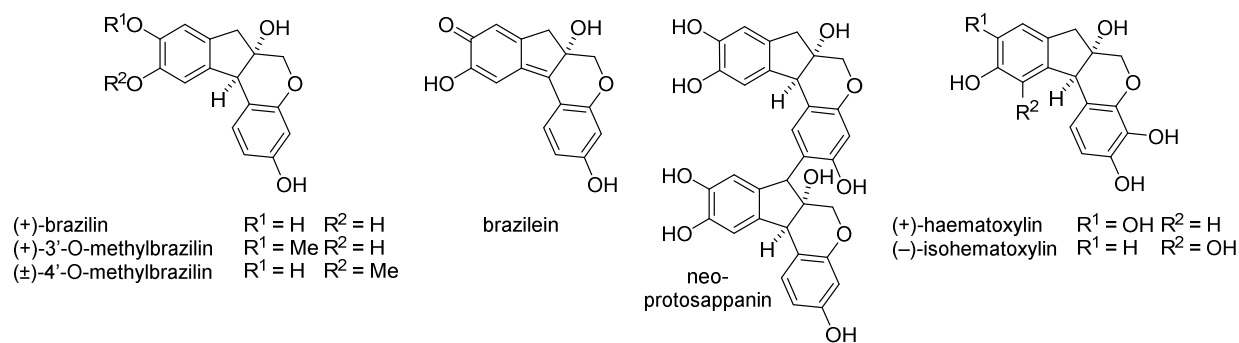
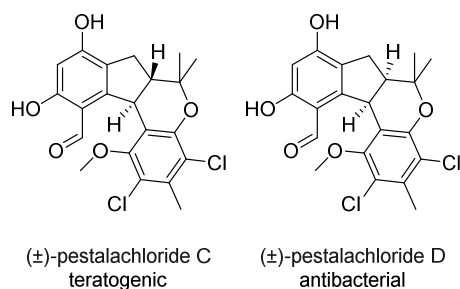


Figure 3-1. Indano[2,1-*c*]chromans from plants.

## Fungus-Derived Indano[2,1-*c*]chromans

In 2008, a new indano[2,1-*c*]chroman, (±)-pestalachloride C was isolated from an endophytic plant fungus, *Pestalotiopsis adusta* (L416) (Figure 3-2).<sup>9</sup> Che and co-workers elucidated the structure of (±)-pestalachloride C by NMR experiments and by single-crystal X-ray crystallographic analysis, and showed that it shared the indano[2,1-*c*]chroman core of brazilin and hematoxylin. However, (±)-pestalachloride C is structurally richer than the plant-derived indano[2,1-*c*]chromans, containing an *anti*-annulated dihydrobenzopyran, an aromatic aldehyde, high oxygenation, and a chlorinated dihydrobenzopyran.



**Figure 3-2.** New racemic indano[2,1-*c*]chromans from marine fungi.

The distinct, congested structure is further distinguished by its occurrence as a racemate.<sup>10</sup> A variety of other natural products have also been isolated as a racemates suggesting non-enzymatic biosynthetic origins – for example, isopestacin,<sup>11</sup> pestacin,<sup>12</sup> sporothrins A and B, and<sup>13</sup> longamide.<sup>14</sup> When tested for antifungal activity by Che and co-workers, (±)-pestalachloride C did not exhibit any noticeable inhibition ( $IC_{50} > 100$   $\mu$ M) against the plant pathogenic fungi *Fusarium culmorum*, *Gibberella zeae*, and *Verticillium albo-atrum*. No other studies were conducted by Che and co-workers.

In 2013, Shao, Wang and co-workers isolated both (±)-pestalachloride C and a new epimer, (±)-pestalachloride D – also a as racemate – from a marine-derived fungus (of the *Pestalotiopsis*

sp.) extracted from a *Sarcophyton* sp soft coral.<sup>15</sup> The ( $\pm$ ) designation for optical rotation will be omitted from the rest of this chapter when discussing the pestalachlorides. Pestalachlorides C and D were isolated in a 3.6:1 ratio. The structure of pestalachloride D is identical to pestalachloride C but differs in that it features a *syn* annulated dihydrobenzopyran ring system. Both pestalachlorides C and D are easily distinguished by the proton NMR coupling constant,  $J = 11.2$  Hz and  $J = 6.0$  Hz, respectively, and chemical shift of the benzhydryl methine proton. This simple stereochemical inversion of a carbon-hydrogen bond imparts staggeringly different bioactivities for these molecules.

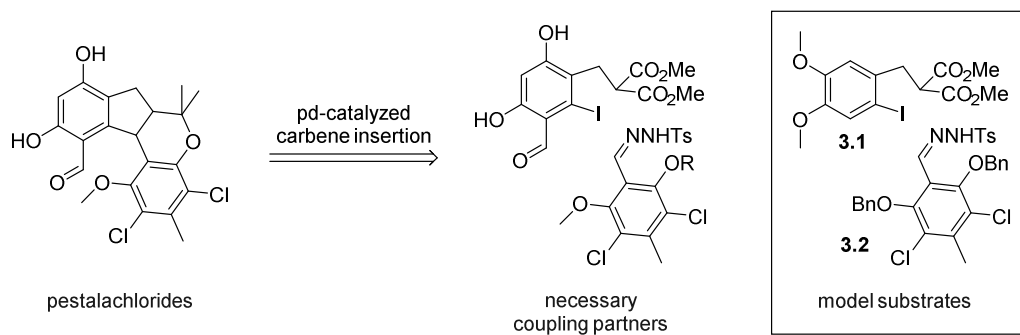
Shao, Wang and co-workers tested pestalachlorides C and D for teratogenic effects utilizing a zebrafish (*D. rerio*) embryo teratogenicity assay. The *syn*-isomer, pestalachloride D, exhibited no teratogenicity up to the assay limit of 50  $\mu\text{g/mL}$ , whereas the *anti*-isomer, pestalachloride C, exhibited teratogenic effects in zebrafish embryos at multiple stages – including egg coagulation, nonspontaneous movements, abnormal heartbeat, organ malformation, delayed hatching, and embryonic death. The authors speculate that the *anti*-configuration is potentially what contributes to the teratogenic effects of pestalachloride C. A variety of selective teratogens such as retinoic acid, thalidomide, lenalidomide, pomalidomide, apremilast, vismodegib, and sotidegib have found use as drugs against cancer and other diseases.<sup>16</sup> A concise route to pestalachlorides C and D would facilitate assessment of their therapeutic potential.

### **Palladium-Carbenylative Insertion Result**

Extending our success in the synthesis of ( $\pm$ )-brazilin, we sought to apply our palladium-catalyzed carbene insertion to highly functionalized indano[2,1-*c*]chromans like those found in the pestalachlorides.<sup>17</sup> The palladium-catalyzed reaction creates a central point of disconnection to

access these 1-arylidanes, and we envisioned utilizing the method to develop a convergent synthesis of pestalachlorides C and D.

The carbenylative insertion reaction to synthesize pestalachlorides would require highly congested and functionalized coupling partners (Scheme 3-1). Based on our previously published work, it was unclear whether a highly congested *N*-tosylhydrazone would participate in the coupling reaction, or whether an aryl iodide containing a nucleophilic and electrophilic center would present a problem. We opted to use aryl iodide **3.1** and *N*-tosylhydrazone **3.2** for an initial model reaction.



**Scheme 3-1.** Coupling partners necessary for carbenylative insertion reaction.

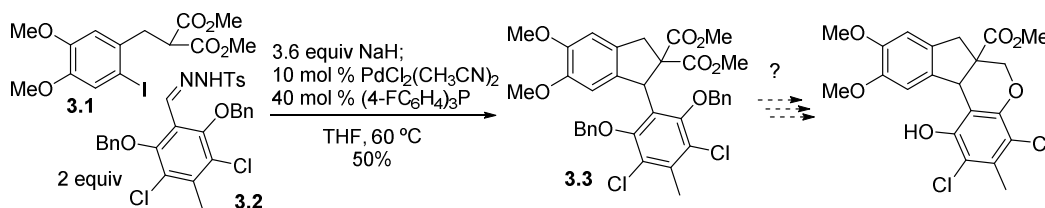
The synthesis of *N*-tosylhydrazone **3.2** began with Lewis acid-catalyzed formylation of 4,6-dichloro-5-methyl resorcinol with dichloromethyl methyl ether to afford an inseparable mixture of *C*-formylated and *O*-formylated side-products (Scheme 3-2); the formate esters were hydrolyzed upon subsequent reactions.



**Scheme 3-2.** Synthesis of *N*-tosylhydrazone **3.2**.

The inseparable mixture was carried on through the next two steps prior to purification. *O*-Benzoylation with benzyl bromide and potassium carbonate followed by condensation with *p*-toluenesulfonyl hydrazide generated *N*-tosylhydrazone **3.2** ready for use as a carbene precursor in the palladium-catalyzed carbenylation reaction.

The palladium-catalyzed carbenylative insertion reaction of aryl iodide **3.1** and *N*-tosylhydrazone **3.2** led to modest yields of the highly congested arylindane **3.3**, even when two equivalents of the *N*-tosylhydrazone were used (Scheme 3-3).



**Scheme 3-3.** Palladium-catalyzed carbenylative insertion model reaction with chlorinated *N*-tosylhydrazone **3.2**.

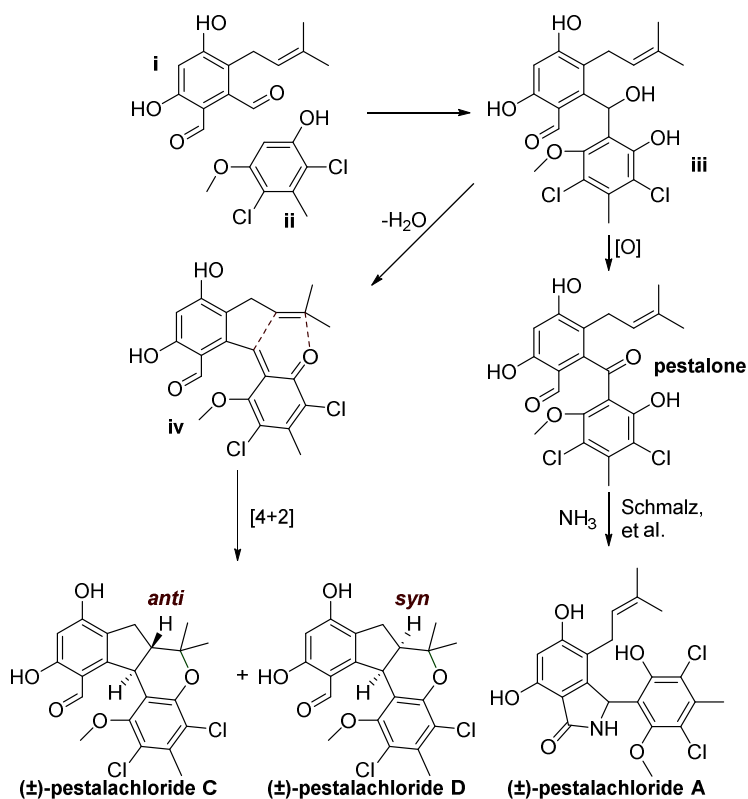
Preparative layer chromatography was necessary to remove impurities of close polarity to obtain a pure sample of arylindane **3.3**. Given the modest yields of this reaction using optimized conditions, we were unsure we could carry through a formyl group or masked formyl group through without further dramatic reduction of the yield. Given the challenges associated with this carbene insertion route, we sought inspiration from nature to synthesize pestalachloride C and D.

### Proposed Biosynthesis of the Pestalachlorides

The biosynthesis of pestalone<sup>18</sup> and pestalachlorides A, C and D seem to be related. In 2010, Schmalz and co-workers published a synthesis of pestalone and demonstrated its facile conversion to pestalachloride A by simply treating the natural product pestalone with aqueous ammonia (Scheme 3-4).<sup>19</sup> In their isolation paper, Shao, Wang and co-workers proposed a



compelling hypothesis for the biosynthesis of pestalone, pestalachloride C, and the new stereoisomeric natural product pestalachloride D.<sup>15</sup> The hypothesis accounts for the fact that pestalone is co-isolated with pestalachloride C and D from the marine-derived fungus.



**Scheme 3-4.** Shao, Wang and co-workers' proposed biosynthesis of pestalachlorides and pestalone.

The proposed biosynthesis involves a cascade reaction starting with condensation of the *o*-phthalaldehyde **i** with the resorcinol **ii** to generate a benzhydrol **iii** with two potential fates – dehydration or oxidation. Dehydration of benzhydrol **iii** produces a highly reactive *o*-quinone methide **iv** which could undergo an inverse electron demand hetero Diels–Alder cycloaddition to afford the *anti*-isomer pestalachloride C, or the *syn*-isomer pestalachloride D (Figure 3-3).

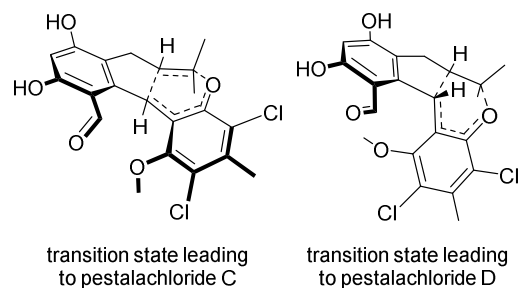


**Figure 3-3.** Depiction of transition states leading to pestalachloride C and D.

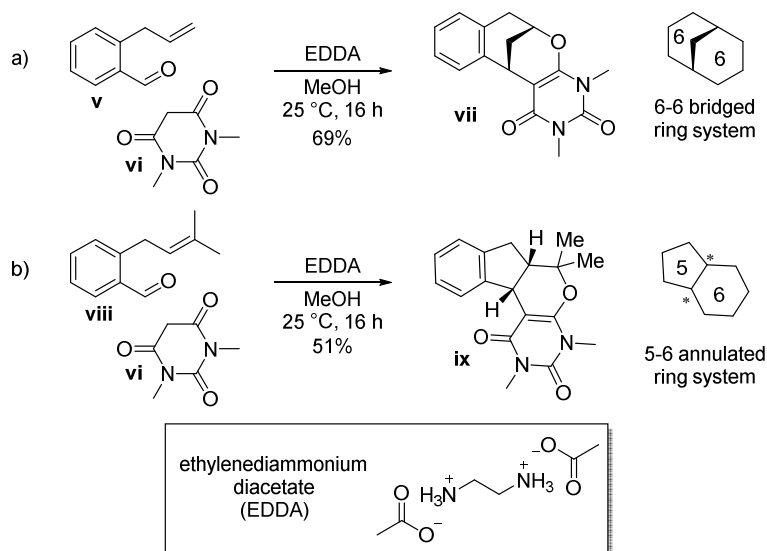
Alternatively, oxidation of benzhydrol **iii** would directly generate pestalone and then pestalachloride A in the presence of ammonia (Scheme 3-4). The involvement of aldiminium intermediates in the biosynthesis of pestalachloride A suggests a potential role for iminium intermediates in the formation of pestalachlorides C and D through a non-enzymatic biosynthetic process.

### **Proposed Biosynthesis Relation to Knoevenagel/hetero-Diels–Alder Tietze Cascade Reactions**

Shao, Wang and co-workers' hypothesis to access the indano[2,1-*c*]chromans pestalachloride C and D is related to the Knoevenagel/hetero-Diels–Alder (KHDA) cascade reactions developed by Tietze and co-workers.<sup>20</sup> Tietze and co-workers carried out seminal work applying this domino reaction to the synthesis of 6-6 annulated ring structures and have shown that the stereochemistry of the ring fusion (either *syn* or *anti*) is highly dependent on the structure of the starting materials.<sup>21</sup>

For example, in 2001, Tietze and co-workers published a Knoevenagel/hetero-Diels–Alder cascade catalyzed by the diamine catalyst ethylenediammonium diacetate (10 mol % EDDA), presumably via an iminium ion intermediate (Scheme 3-5).<sup>22</sup> Depending on the structure of the electrophile, Tietze and co-workers showed the reaction generates two types of fused barbituric

acid derivatives. The allyl substrate **v** afforded bridged tetralin **vii**, whereas the prenyl-substituted substrate **viii** afforded exclusively the *syn*-fused indane **ix** (Scheme 3-5).



**Scheme 3-5.** Knoevenagel/hetero-Diels–Alder products depend on structure of starting materials.

Pestalachlorides C and D contain a 5-6 *anti*-annulated and *syn*-annulated ring system, respectively. It was unclear whether any *anti*-fused indane was observed or isolated. Lee and co-workers have applied the Tietze conditions to aromatic nucleophiles to generate cannabinoids and related 6-6 annulated ring systems.<sup>23</sup> The facile generation of tetracycles related to indano[2,1-*c*]chromans under organocatalytic conditions strongly supports Shao, Wang and co-workers' proposed biosynthesis, but the stereoselectivity and sensitivity to substituents on the electrophile left us uncertain that the domino reaction could be applied to a total synthesis of *both* the *syn*-isomer, pestalachloride D, and the *anti*-isomer, pestalachloride C.

Other workers have shown that quinone methide intermediates derived from benzylic alcohols can undergo intramolecular hetero Diels–Alder reactions to generate mixtures of *syn*- and *anti*-fused cyclopenta[*c*]chromans in which the *syn*-fused chromans are generally preferred.<sup>24</sup> Conflicted by the strong precedent and lingering questions, we set out to test the cascade reaction

underlying the Shao, Wang and co-workers biosynthetic hypothesis as an approach to pestalachlorides C and D.

### Initial Results of KHDA to Construct the Indano[2,1-*c*]chroman Core

Prior to the synthesis of pestalachlorides C and D, we utilized the Tietze conditions on a model system, 2-prenylbenzaldehyde<sup>25</sup> and commercially available orcinol, to establish if the cyclization reaction generated the indano[2,1-*c*]chroman core present in pestalachlorides C and D. When we utilized 10 mol % EDDA and methanol at room temperature, no reaction was observed.

Utilizing EDDA as an organocatalyst, and triethylamine and xylenes at reflux as co-solvents, which has previously been reported to synthesize 6-6 annulated dihydrobenzopyrans,<sup>23b</sup> we observed conversion to the indano[2,1-*c*]chroman core by the presence of a doublet signal in the 4–5 ppm region corresponding to the benzhydryl methine proton of the 5-6 ring juncture. The same proton appears as a doublet for pestalachlorides C and D at 4.26 and 4.72 ppm, respectively.<sup>15</sup> Additionally, based on the respective coupling constants of the peaks we identified two stereoisomers – both *syn*- and *anti*- diastereomers were synthesized (Figure 3-4).

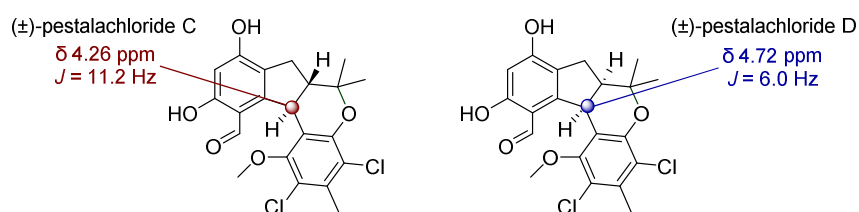


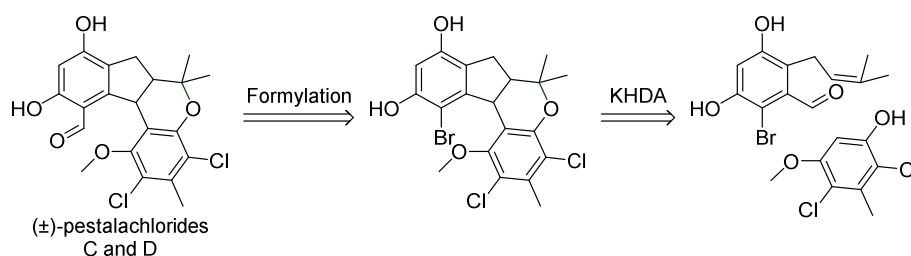
**Figure 3-4.** Characteristic proton shifts and coupling constants of pestalachloride C and D.

The doublet closest to 5.0 ppm was assigned the *syn*-configuration based on a smaller coupling constant of 8.0 Hz, relative to the other doublet near 4.0 ppm. The doublet at 4.0 ppm was assigned the *anti*-configuration based on its large coupling constant of 13.0 Hz. These coupling constants mirror closely to that of the same protons on pestalachloride D ( $J = 6.0$  Hz) and

pestalachloride C ( $J = 11.2$  Hz), respectively. By comparison to pestalachlorides C and D, our model reaction established that the reaction proceeds and generates both diastereomers of the indano[2,1-*c*]chroman core.

### Total Synthesis Results and Discussion

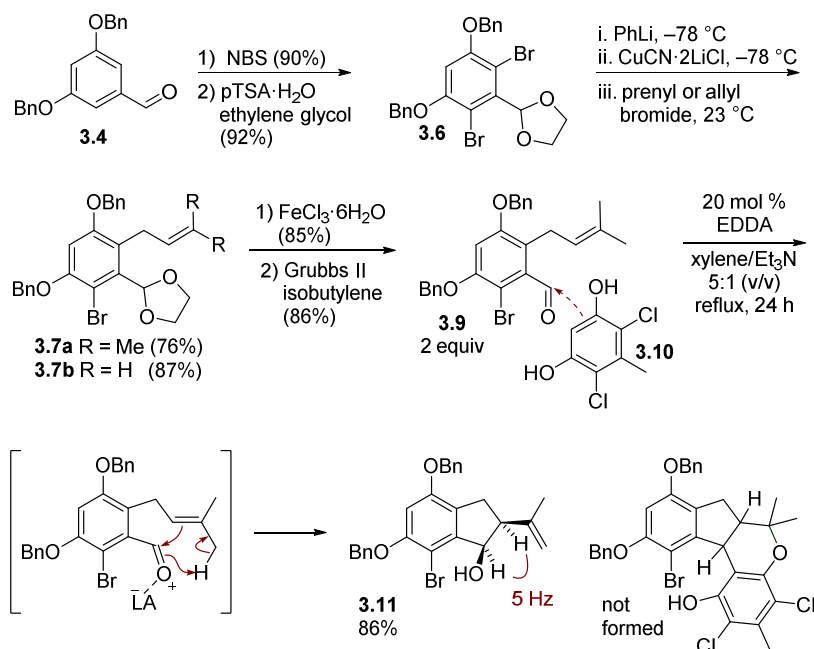
Shao, Wang and co-workers' biosynthetic hypothesis towards pestalachlorides C and D requires a regioselective Knoevenagel condensation with just one of the two aldehydes of *o*-phthalaldehyde **i** (Scheme 3-4). To ensure condensation with the correct aldehyde, we opted to introduce the second formyl group at a later stage into the fully formed indane ring system (Scheme 3-6). We anticipated the need for a functional handle like bromine to allow installation of the aldehyde into a crowded position.



**Scheme 3-6.** Initial approach towards pestalachlorides C and D involved late-stage introduction of formyl group.

Confident in the Knoevenagel/hetero-Diels–Alder reaction, we focused our efforts in synthesizing the functionalized aldehyde **3.8** (Scheme 3-7). To that end, we converted commercially available benzaldehyde **3.4** into an *o,o'*-dibromobenzaldehyde (**3.5** omitted) and masked the aldehyde to give acetal **3.6**. One of the two bromines was converted to the cyanocuprate through lithium-halogen exchange with 1.2 equivalents of phenyllithium, and the cuprate was then coupled with prenyl bromide to afford acetal **3.7a**. The juxtaposition of aldehyde and prenyl group

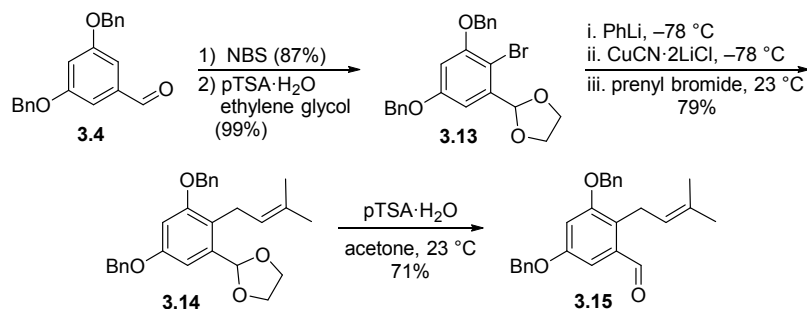
in **3.7a** is precarious. All attempts to deprotect the acetal led to complex mixtures arising from Prins reactions. We found it expedient to carry out the cuprate coupling with allyl bromide to afford allylbenzene derivative **3.7b**. After revealing the aldehyde (**3.8** omitted), we gently converted the allyl group to a prenyl group using Grubbs metathesis with isobutylene to afford prenyl benzaldehyde **3.9**.



**Scheme 3-7.** Premature intramolecular carbonyl-ene process competes with the Knoevenagel-hetero-Diels–Alder cascade reaction.

The 4,6-dichloro-5-methyl resorcinol **3.10** nucleophile was obtained through the regioselective chlorination of commercially available orcinol.<sup>26</sup> Sadly, we were unable to engage the resorcinol **3.10** in the Knoevenagel/hetero-Diels–Alder cascade due to the competing intramolecular carbonyl-ene process. Under some conditions, the undesired indane **3.11** was formed stereoselectively in high yield. A *syn*-orientation of the substituents on indane **3.11** has been tentatively assigned based on the 5 Hz vicinal coupling constant<sup>27</sup> and on the preference for intramolecular carbonyl-ene reactions to afford *syn*-cyclopentanol in saturated systems.<sup>28</sup>

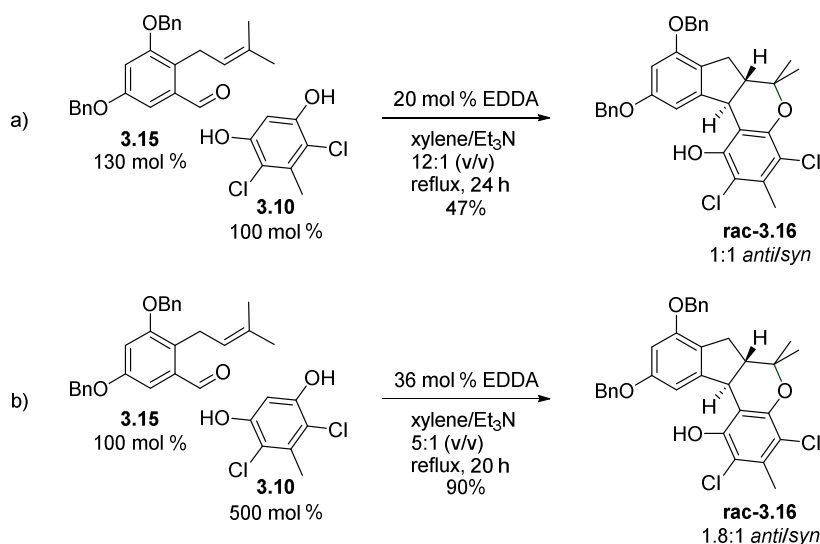
We hypothesized that the *ortho* bromo substituent of aldehyde **3.9** might be accelerating the undesired carbonyl-ene reaction and set out to synthesize a less crowded benzaldehyde lacking the *ortho* bromo substituent to test in the cascade reaction (Scheme 3-8). Benzaldehyde **3.15** was synthesized as described in Scheme 3-7. The desired monobromide **3.13** was prepared from aldehyde **3.4** by monobromination and protection of the aldehyde (**3.12** omitted) as an acetal. As before, aryl bromide **3.13** was converted to the cyanocuprate and coupled with prenyl bromide to afford dioxolane **3.14**. This time, the acetal was receptive to deprotection under mildly acidic conditions at incomplete conversion. The desired aldehyde **3.15** could be obtained in 71% yield. The allylation, acid catalyzed deprotection, and Grubbs metathesis could still be applied to synthesize the desired aldehyde **3.15**. However, the process would take longer and the cost of incomplete conversion with the route outlined in Scheme 3-8 more than compensates for the choice.



**Scheme 3-8.** Synthesis of less crowded benzaldehyde **3.15** for Knoevenagel-hetero-Diels–Alder reaction.

Knoevenagel condensation followed by Diels–Alder reaction under less basic conditions of aldehyde **3.15** and the limiting reagent resorcinol **3.10**, gave a 1:1 mixture of indano[2,1-*c*]chromans **3.16** in modest yields (Scheme 3-9a). We found that the yield of chroman **3.16** was improved by changing the limiting reagent to the aldehyde and using excess equivalents of the resorcinol reagent (Scheme 3-9b). Under these conditions, we were pleased to not only see an

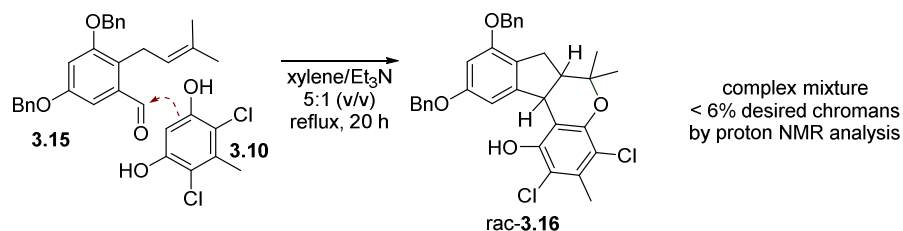
improvement in the yield (90%), but also in the *anti/syn* ratio (1.8:1) favoring the desired diastereomer that would lead to the teratogenic compound, pestalachloride C. More equivalents of the resorcinol **3.10** led to faster reaction times which could contribute to the diastereomeric ratio observed.



**Scheme 3-9.** Knoevenagel/hetero-Diels–Alder reaction. (a) Initial results. (b) Optimized results.

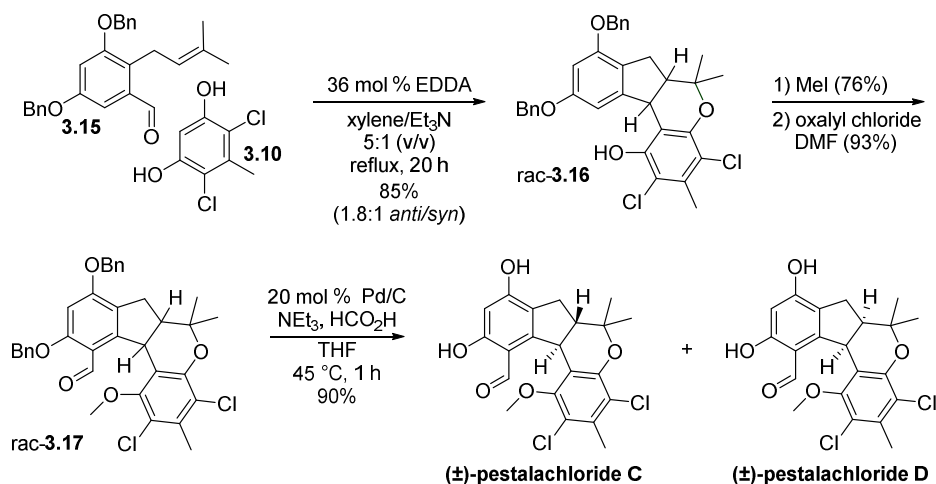
It was unclear whether the EDDA catalyst was generating an iminium ion intermediate or simply acting as a Brønsted acid catalyst. Based on our failed attempts to deprotect the dioxolane precursors containing the pendant prenyl group, we suspected that acid-catalyzed Prins cyclization would out-pace acid-catalyzed condensation of the aldehyde with the orcinol. As expected, when we treated aldehyde **3.15** and resorcinol **3.10** with benzoic acid, no indano[2,1-*c*]chromans formed, but the corresponding indanols from Prins reactions were present – by  $^1\text{H}$  NMR the doublet indicating a prenyl group was absent, and new peaks corresponding to aliphatic, vinyl, and methyl protons were present. When the EDDA was excluded and only triethylamine was added, aldehyde **3.15** and resorcinol **3.10** generated a complex mixture containing less than 6% of the desired indano[2,1-*c*]chromans **3.16** as determined by  $^1\text{H}$  NMR analysis (Scheme 3-10).





**Scheme 3-10.** Basic conditions led to complex mixtures of side products and byproducts.

In the presence of EDDA, which promotes iminium ion formation, the reaction is much more efficient, and the Knoevenagel/hetero-Diels–Alder cascade generates the indano[2,1-*c*]chromans **3.16** in 85–90% yields in about 90% purity (Scheme 3-11). The *anti*- and *syn*- isomers are formed in a 1.4–1.6:1 ratio, depending on the equivalents of resorcinol used and reaction time. After chromatographic purification, the ratio was 1.8:1, probably due to slight chromatographic loss of the *syn*-isomer. Despite slight differences in solubility based on chromatographic loss, the diastereomers were inseparable, and the mixture was carried on through the synthetic route. Although the solvents and temperatures are abiotic, the success of this cascade reaction is consistent with a biosynthetic route that involves a non-enzymatic cascade reaction.



**Scheme 3-11.** Total synthesis of pestalachlorides C and D through a Knoevenagel/hetero-Diels–Alder cascade reaction of benzaldehyde **3.15** and resorcinol **3.10**.

We were pessimistic that an aldehyde could be introduced at the more hindered position of the indane aromatic ring of compound **3.16**. Fortunately, Vilsmeier-Haack reaction of phenol **3.15** was found to introduce the formyl group at the desired position, but the resulting mixture of seven-membered ring hemiacetals and hydroxyaldehydes proved unwieldy. The fortuitous and surprising regioselectivity in the formylation was initially attributed to a directing effect from the phenolic hydroxyl group on the dichloroorecinol ring.

We were surprised to find that *O*-methylation of the dichlorochroman phenol **3.16** was still followed by a highly regioselective Vilsmeier-Haack formylation at the hindered position to afford carbaldehyde **3.17**. Attempts to cleave the benzyl ethers of carbaldehyde **3.17** under typical hydrogenolysis conditions with hydrogen gas were accompanied by concomitant reduction of the benzaldehyde moiety of **3.17** to a methyl group, but when formate was used as the reductant, deprotection proceeded cleanly to afford a mixture of (±)-pestalachloride C and (±)-pestalachloride D in a 1.6:1 ratio in 83–90% yield. The isomers were readily separable by reverse phase HPLC.

Hydroxylated flavonoids are known to exert weak teratogenic effects, anti-melanogenic activity, and to inhibit proliferation of melanoma.<sup>29</sup> We tested (±)-pestalachlorides C and D against the A375 melanoma cell lines and found pestalachloride D to be slightly more potent with IC<sub>50</sub>s of 12.4±2.4 μM and 7.1±0.6 μM, respectively. We were surprised to find that the activity of pestalachlorides C and D did not match the teratogenic bioactivity.

## Conclusion

The ready formation of pestalachlorides C and D through a Tietze cascade reaction, involving Knoevenagel reactions of dienophiles tethered to aldehydes followed by hetero Diels–Alder cycloaddition of a quinone methide intermediate, supports the Shao, Wang and co-workers' biosynthetic hypothesis for these racemic natural products. It adds to the growing list of related

Knoevenagel/hetero-Diels–Alder cascade reactions that parallel biosynthetic pathways.<sup>30,31</sup> Late stage introduction of the formyl group allows the assembly ( $\pm$ )-pestalachlorides C and D in a facile and concise manner utilizing a Knoevenagel/hetero-Diels–Alder cascade cyclization reaction.

## References

1. Dapson, R. W.; Bain, C. L. Brazilwood, sappanwood, brazilin and the red dye brazilin: from textile dyeing and folk medicine to biological staining and musical instruments. *Biotech. Histochem.* **2015**, *90*, 401–423.
2. Gilbody, A. W.; Perkin, W. H.; Yates, J. CXLVI.—Brazilin and haematoxylin. Part I. *J. Chem. Soc., Trans.* **1901**, *79*, 1396–1411.
3. Perkin, W. H.; Robinson, R. XLVI.—Brazilin and haematoxylin. Part VIII. Synthesis of brazilinic acid, the lactones of dihydrobrazilinic and dihydrohaematoxylinic acids anhydrobrazilic acid, etc. The constitution of brazilin, haematoxylin, and their derivatives. *J. Chem. Soc., Trans.* **1908**, *93*, 489–517.
4. (a) Namikoshi, M.; Nakata, H.; Yamada, H.; Nagai, M.; Saitoh, T. Homoisoflavonoids and related compounds. II. Isolation and absolute configurations of 3,4-dihydroxylated homoisoflavans and brazilins from *Caesalpinia sappan* L. *Chem. Pharm. Bull.* **1987**, *35*, 2761–2773; (b) Min, B. S.; Cuong, T. D.; Hung, T. M.; Min, B. K.; Shin, B. S.; Woo, M. H. Compounds from the Heartwood of *Caesalpinia sappan* and their Anti-inflammatory Activity. *Bioorg. Med. Chem. Lett.* **2012**, *22*, 7436–7439.
5. (a) Nguyen, M. T.; Awale, S.; Tezuka, Y.; Tran, Q. L.; Kadota, S. Xanthine oxidase inhibitors from the heartwood of Vietnamese *Caesalpinia sappan*. *Chem. Pharm. Bull.* **2005**, *53*, 984–988; (b) Chen, F.-Z.; Zhao, Q.; Yan, J.; Guo, X.-Q.; Song, Q.; Yao, Q.; Gou, X.-J. Antioxidant Activity and Antioxidant Mechanism of Brazilin and Neoprotosappanin from *Caesalpinia sappan* Lignum. *Asian J. Chem.* **2014**, *26*, 4979–4981.
6. Lin, L. G.; Xie, H.; Li, H. L.; Tong, L. J.; Tang, C. P.; Ke, C. Q.; Liu, Q. F.; Lin, L. P.; Geng, M. Y.; Jiang, H.; Zhao, W. M.; Ding, J.; Ye, Y. Naturally occurring homoisoflavonoids function as potent protein tyrosine kinase inhibitors by c-Src-based high-throughput screening. *J. Med. Chem.* **2008**, *51*, 4419–4429.
7. Masuda, H.; Ohtani, K.; Mizutani, K.; Ogawa, S.; Kasai, R.; Tanaka, O. Chemical Study on *Haematoxylon Campechianum* - a Sweet Principle and New Dibenz[*b,d*]oxocin Derivatives. *Chem. Pharm. Bull.* **1991**, *39*, 1382–1384.
8. (a) Dewick, P. M. Biosynthesis of the 3-benzylchroman-4-one eucomin in *Eucomis bicolor*. *Phytochemistry* **1975**, *14*, 983–988; (b) Nagai, M.; Nagumo, S.; Eguchi, I.; Lee, S. M.; Suzuki, T. Sappanchalcone from *Caesalpinia sappan* L., the proposed biosynthetic precursor of brazilin. *Yakugaku Zasshi* **1984**, *104*, 935–938; (c) Nagai, M.; Nagumo, S.; Lee, S.-M.; Eguchi, I.; Kawai, K.-I. Protosappanin A, a novel biphenyl compound from Sappan Lignum. *Chem. Pharm. Bull.* **1986**, *34*, 1–6; (d) Lin, L. G.; Liu, Q. Y.; Ye, Y. Naturally Occurring Homoisoflavonoids and Their Pharmacological Activities. *Planta Med.* **2014**, *80*, 1053–1066 and references therein.
9. Li, E.; Jiang, L.; Guo, L.; Zhang, H.; Che, Y. Pestalochlorides A–C, antifungal metabolites from the plant endophytic fungus *Pestalotiopsis adusta*. *Bioorg. Med. Chem.* **2008**, *16*, 7894–7899.
10. Zask, A.; Ellestad, G. Biomimetic syntheses of racemic natural products. *Chirality* **2018**, *30*, 157–164 and references cited therein.
11. Strobel, G.; Ford, E.; Worapong, J.; Harper, J. K.; Arif, A. M.; Grant, D. M.; Fung, P. C. W.; Ming Wah Chau, R. Isopestacin, an isobenzofuranone from *Pestalotiopsis microspora*, possessing antifungal and antioxidant activities. *Phytochemistry* **2002**, *60*, 179–183.

12. Harper, J. K.; Arif, A. M.; Ford, E. J.; Strobel, G. A.; Porco, J. A.; Tomer, D. P.; Oneill, K. L.; Heider, E. M.; Grant, D. M. Pestacin: a 1,3-dihydro isobenzofuran from *Pestalotiopsis microspora* possessing antioxidant and antimycotic activities. *Tetrahedron* **2003**, *59*, 2471–2476.
13. Wen, L.; Cai, X.; Xu, F.; She, Z.; Chan, W. L.; Vrijmoed, L. L.; Jones, E. B.; Lin, Y. Three metabolites from the mangrove endophytic fungus *Sporothrix* sp. (#4335) from the South China Sea. *J. Org. Chem.* **2009**, *74*, 1093–1098.
14. Umeyama, A.; Ito, S.; Yuasa, E.; Arihara, S.; Yamada, T. A New Bromopyrrole Alkaloid and the Optical Resolution of the Racemate from the Marine Sponge *Homaxinella* sp. *J. Nat. Prod.* **1998**, *61*, 1433–1434.
15. Wei, M. Y.; Li, D.; Shao, C. L.; Deng, D. S.; Wang, C. Y. (±)-Pestalachloride D, an antibacterial racemate of chlorinated benzophenone derivative from a soft coral-derived fungus *Pestalotiopsis* sp. *Mar Drugs* **2013**, *11*, 1050–1060.
16. Blagosklonny, M. V. Teratogens as Anticancer Drugs. *Cell Cycle* **2005**, *4*, 1518–1521.
17. Gutman, E. S.; Arredondo, V.; Van Vranken, D. L. Cyclization of  $\eta^3$ -Benzylpalladium Intermediates Derived from Carbene Insertion. *Org. Lett.* **2014**, *16*, 5498–5501.
18. Cueto, M.; Jensen, P. R.; Kauffman, C.; Fenical, W.; Lobkovsky, E.; Clardy, J. Pestalone, a New Antibiotic Produced by a Marine Fungus in Response to Bacterial Challenge. *J. Nat. Prod.* **2001**, *64*, 1444–1446.
19. Slavov, N.; Cvengroš, J.; Neudörfl, J.-M.; Schmalz, H.-G. Total synthesis of the marine antibiotic pestalone and its surprisingly facile conversion into pestalalactone and pestalachloride A. *Angew. Chem. Int. Ed.* **2010**, *49*, 7588–7591.
20. (a) Tietze, L. F.; Ketschau, G., Hetero Diels–Alder reactions in organic chemistry. In *Stereoselective Heterocyclic Synthesis I*, Metz, P., Ed. Springer, Berlin, Heidelberg: Berlin, Heidelberg, 1997; Vol. 189, pp 1–120; (b) Tietze, L. F.; Beifuss, U. Sequential Transformations in Organic Chemistry: A Synthetic Strategy with a Future. *Angew. Chem. Int. Ed.* **1993**, *32*, 131–163; (c) Tietze, L. F. Domino Reactions in Organic Synthesis. *Chem. Rev.* **1996**, *96*, 115–136; (d) Tietze, L. F.; Modi, A. Multicomponent domino reactions for the synthesis of biologically active natural products and drugs. *Med. Res. Rev.* **2000**, *20*, 304–322; (e) Tietze, L. F.; Haunert, F., Domino Reaction in Organic Synthesis. An Approach to Efficiency, Elegance, Ecological Benefit, Economic Advantage and Preservation of Our Resources in Chemical Transformations. In *Stimulating Concepts in Chemistry*, Vögtle, F.; Stoddart, J. F.; Shibasaki, M., Eds. Wiley-VCH Verlag GmbH & Co. KGaA: Weinheim, FRG, 2005; pp 39–64; (f) Tietze, L. F.; Rackelmann, N. Domino reactions in the synthesis of heterocyclic natural products and analogs. *Pure Appl. Chem.* **2004**, *76*, 1967–1983; (g) Tietze, L. F. Domino-Reactions: the Tandem-Knoevenagel-Hetero-Diels–Alder Reaction and Its Application in Natural Product Synthesis. *J. Heterocycl. Chem.* **1990**, *27*, 47–69.
21. (a) Tietze, L. F.; Bachmann, J.; Wichmann, J.; Zhou, Y. F.; Raschke, T. Efficient biomimetic synthesis of indole alkaloids of the vallesiachotamine group by a domino Knoevenagel hetero Diels–Alder hydrogenation sequence. *Liebigs Ann. Recl.* **1997**, 881–886; (b) Tietze, L. F.; Meier, H.; Nutt, H. Inter- and intramolecular hetero Diels–Alder reactions, 28. Synthesis of (±)-secologanin aglucone O-ethyl ether and derivatives by tandem Knoevenagel hetero Diels–Alder Reaction. *Liebigs Ann. Chem.* **1990**, 253–260; (c) Tietze, L. F.; Meier, H.; Nutt, H. Intermolecular and Intramolecular Hetero Diels–Alder Reactions, 25. The Tandem Knoevenagel Hetero Diels–Alder Reaction with a

- Formylacetic Acid Equivalent. Synthesis of Dihydropyranocarboxylates. *Chem. Ber.* **1989**, *122*, 643–650; (d) Tietze, L. F.; Brumby, T.; Pretor, M.; Remberg, G. Intramolecular Hetero-Diels–Alder Reaction of Alkylidenepyrazolone and Benzylidenepyrazolone and Benzylideneisoxazolones. Investigations toward the Conformation of the Transition State. *J. Org. Chem.* **1988**, *53*, 810–820.
22. Tietze, L. F.; Ott, C.; Hauer, F. Efficient and regioselective synthesis of bridged ring systems by domino Knoevenagel - hetero-Diels–Alder reaction. *Can. J. Chem.* **2001**, *79*, 1511–1514.
  23. (a) Lee, Y. R.; Xia, L. Efficient one-pot synthetic approaches for cannabinoid analogues and their application to biologically interesting (–)-hexahydrocannabinol and (+)-hexahydrocannabinol. *Tetrahedron Lett.* **2008**, *49*, 3283–3287; (b) Lee, Y. R.; Kim, Y. M.; Kim, S. H. Efficient one-pot synthesis of benzopyranobenzopyrans and naphthopyranobenzopyrans by domino aldol-type reaction/hetero Diels–Alder reaction of resorcinols and naphthols. *Tetrahedron* **2009**, *65*, 101–108.
  24. (a) Shrestha, K. S.; Honda, K.; Asami, M.; Inoue, S. Facile Synthesis of the Fused 6-6-5 Ring System Containing Chroman Ring from 2-(1-Hydroxy-5-alkenyl)phenol Derivatives via Intramolecular Inverse-Electron-Demand Diels–Alder Reaction. *Bull. Chem. Soc. Jpn.* **1999**, *72*, 73–83; (b) Hug, R.; Hansen, H. J.; Schmid, H. Thermische Cyclodehydratisierung von Salicylalkoholen; eine einfache Synthese von 4-substituierten 2H-Chromenen. *Helv. Chim. Acta* **1972**, *55*, 1675–1691.
  25. (a) Ashby, E. C.; Coleman, D.; Gamasa, M. Single-electron transfer in the Cannizzaro reaction. *J. Org. Chem.* **1987**, *52*, 4079–4085; (b) Padwa, A.; Lipka, H.; Watterson, S. H.; Murphree, S. S. Phenylsulfonyl ene-allenes as efficient precursors to bicyclic systems via intramolecular [2 + 2]-cycloaddition reactions. *J. Org. Chem.* **2003**, *68*, 6238–6250.
  26. Kaiser, F.; Schmalz, H.-G. Synthetic analogues of the antibiotic pestalone. *Tetrahedron* **2003**, *59*, 7345–7355.
  27. (a) Agrawal, P. K.; Schneider, H.-J.; Malik, M. S.; Rastogi, S. N. <sup>13</sup>C NMR shifts and conformations of substituted indans. *Organic Magnetic Resonance* **1983**, *21*, 146–150; (b) Guo, X. X.; Sawano, T.; Nishimura, T.; Hayashi, T. Rhodium-catalyzed enantioselective alkynylative cyclization of allenyl aldehydes with terminal alkynes. *Tetrahedron: Asymmetry* **2010**, *21*, 1730–1736; (c) Wu, A.; Cremer, D.; Auer, A. A.; Gauss, J. Extension of the Karplus Relationship for NMR Spin–Spin Coupling Constants to Nonplanar Ring Systems: Pseudorotation of Cyclopentane. *J. Phys. Chem. A* **2002**, *106*, 657–667.
  28. Grachan, M. L.; Tudge, M. T.; Jacobsen, E. N. Enantioselective Catalytic Carbonyl–Ene Cyclization Reactions. *Angew. Chem. Int. Ed.* **2008**, *47*, 1469–1472.
  29. (a) Liu-Smith, F.; Meyskens, F. L. Molecular mechanisms of flavonoids in melanin synthesis and the potential for the prevention and treatment of melanoma. *Mol. Nutr. Food Res.* **2016**, *60*, 1264–1274; (b) Veselinovic, J. B.; Kocic, G. M.; Pavic, A.; Nikodinovic-Runic, J.; Senerovic, L.; Nikolic, G. M.; Veselinovic, A. M. Selected 4-phenyl hydroxycoumarins: in vitro cytotoxicity, teratogenic effect on zebrafish (*Danio rerio*) embryos and molecular docking study. *Chem. Biol. Interact.* **2015**, *231*, 10–17.
  30. (a) Yang, B.; Gao, S. Recent advances in the application of Diels–Alder reactions involving *o*-quinodimethanes, aza-*o*-quinone methides and *o*-quinone methides in natural product total synthesis. *Chem. Soc. Rev.* **2018**, *47*, 7926–7953; (b) Spivey, A.; Nielsen, C.; Abas, H. Stereoselective Reactions of *ortho*-Quinone Methide and *ortho*-Quinone Methide Imines and Their Utility in Natural Product Synthesis. *Synthesis* **2018**, *50*, 4008–4018; (c)

- Ai, W. Y.; Liao, D. H.; Lei, X. G. Applications of *ortho*-Quinone Methides in the Synthesis of Natural Products. *Chin. J. Org. Chem.* **2015**, *35*, 1615–1626; (d) Willis, N. J.; Bray, C. D. *ortho*-Quinone methides in Natural Product Synthesis. *Chemistry* **2012**, *18*, 9160–9173; (e) Tietze, L. F.; Rackelmann, N., The Domino-Knoevenagel-Hetero-Diels–Alder Reaction and Related Transformations. In *Multicomponent Reactions*, Zhu, J.; Bienaymé, H., Eds. Wiley-VCH: Weinheim, Germany, 2005; pp 121–168.
31. (a) Casiraghi, G.; Cornia, M.; Casnati, G.; Fava, G. G.; Belicchi, M. F. A one-step highly stereocontrolled synthesis of (–)- and (+)-hexahydrocannabinol and related compounds. *J. Chem. Soc., Chem. Commun.* **1986**, 271–273; (b) Lawrence, A. L.; Adlington, R. M.; Baldwin, J. E.; Lee, V.; Kershaw, J. A.; Thompson, A. L. A short biomimetic synthesis of the meroterpenoids guajadial and psidial A. *Org. Lett.* **2010**, *12*, 1676–1679; (c) Newton, C. G.; Tran, D. N.; Wodrich, M. D.; Cramer, N. One-Step Multigram-Scale Biomimetic Synthesis of Psiguajadial B. *Angew. Chem. Int. Ed.* **2017**, *56*, 13776–13780; (d) Spence, J. T.; George, J. H. Structural reassignment of cytosporolides A–C via biomimetic synthetic studies and reinterpretation of NMR data. *Org. Lett.* **2011**, *13*, 5318–5321; (e) Spence, J. T.; George, J. H. Total Synthesis of Peniphenones A–D via Biomimetic Reactions of a Common *o*-Quinone Methide Intermediate. *Org. Lett.* **2015**, *17*, 5970–5973; (f) Lam, H. C.; Phan, Q. D.; Sumbly, C. J.; George, J. H. Biomimetic Synthesis of Hyperjapones F–I. *Aust. J. Chem.* **2018**, *71*, 649–654; (g) Dethlefsen, D. H.; B. V. K.; Maiti, R. Biomimetic total syntheses of chromane meroterpenoids, guajadial B and C, guapsidial A and psiguajadial D. *Org. Biomol. Chem.* **2018**, *16*, 4793–4796; (h) Takao, K.; Noguchi, S.; Sakamoto, S.; Kimura, M.; Yoshida, K.; Tadano, K. Total Synthesis of (+)-Cytosporolide A via a Biomimetic Hetero-Diels–Alder Reaction. *J. Am. Chem. Soc.* **2015**, *137*, 15971–15977; (i) Chapman, L. M.; Beck, J. C.; Lacker, C. R.; Wu, L.; Reisman, S. E. Evolution of a Strategy for the Enantioselective Total Synthesis of (+)-Psiguajadial B. *J. Org. Chem.* **2018**, *83*, 6066–6085.

## Supporting Information

### General Information and Reagents

**Reactions and materials:** Unless otherwise specified, all reactions were performed under an atmosphere of dry N<sub>2</sub> gas. Anhydrous solvents and reagents, where applicable, were transferred using Schlenk technique. Toluene, tetrahydrofuran (THF), diethyl ether (Et<sub>2</sub>O), and dichloromethane (CH<sub>2</sub>Cl<sub>2</sub>) were dried by passage through alumina according to the procedure of Grubbs and co-workers.<sup>1</sup> All other solvents were purified according to reported procedures.<sup>2</sup> Triethylamine (NEt<sub>3</sub>) was distilled from calcium hydride prior to use in reactions or in purification methods. *p*-Toluenesulfonic acid monohydrate, 99%, (*p*TSA·H<sub>2</sub>O) (CAS 6192-52-5) was recrystallized from benzene prior to use to yield a wet, white crystalline solid. Xylenes (Fisher), acetone Optima™ (Fisher), extra-dry CH<sub>3</sub>CN (Acros), 3,5-dibenzyloxybenzaldehyde (Ark Pharm), and orcinol (Sigma or Alfa Aesar) were used without prior purification.

Ethylenediammonium diacetate (EDDA) was prepared fresh using the following procedure: “A 150 mL beaker, containing 100 mL dry ether and 12.0 g (0.2 mol) of ethylenediamine, is placed in an ice-bath and a solution of 24.0 g (0.4 mol) glacial acetic acid in 20 mL ether is added with stirring at such a rate as to prevent boiling of the ether. The solution is left to crystallize overnight, then filtered with suction, the crystals washed with ether and recrystallized from approximately 50 mL MeOH. Yield after drying in a vacuum desiccator is around 27.5 g (75%) of colorless needles, mp 114°C.<sup>3</sup> EDDA was stored in an amber bottle under argon and kept in a vacuum desiccator when not in use. <sup>1</sup>H and <sup>13</sup>C spectral data for EDDA was consistent with that previously reported.<sup>4</sup>



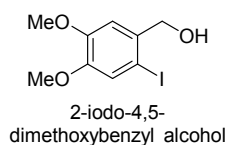
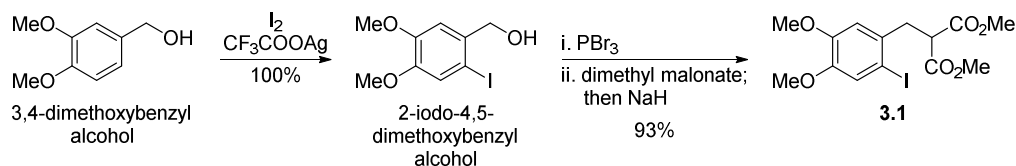
**Analysis and Purification:** All reactions were monitored by thin-layer chromatography (TLC) and visualized by UV (254 nm) illumination and by  $\text{KMnO}_4$  and *p*-anisaldehyde (*p*-anis) dip stains. The *p*-anis stain was prepared by adding 25 mL of concentrated sulfuric acid to a chilled solution of 95% ethanol (676 mL, made from 200 proof ethanol and de-ionized water). Glacial acetic acid (7.5 mL) and *p*-anisaldehyde (99%, 18.4 mL) were then added to afford a colorless solution. The stain was stored at 0 °C. Analytical TLC was performed using EMD Millipore 0.25 mm Silica gel 60 F<sub>254</sub> 20 × 20 cm plates (EM1.05715.0001). Preparative layer chromatography (PLC) was performed using EMD Millipore PLC Plates F<sub>254</sub>, 500 μm thick, 200 × 200 mm, 60 Å pore size (EM1.05744.0001). “Flash” chromatography on silica gel was performed using Agela Technologies Flash Silica sorbent (40-63 μm) silica gel of 230-400 mesh (CS605025-P).

**Identity:** Unless otherwise noted, <sup>1</sup>H and <sup>13</sup>C NMR spectral data were recorded at 23 °C using a Bruker Avance 500 or 600 MHz spectrometer equipped with a cryoprobe. All spectra were calibrated to tetramethylsilane (0.00 ppm). The NMR data are reported as follows: chemical shift in ppm (δ), multiplicity (br = broad, app = apparent, s = singlet, d = doublet, t = triplet, q = quartet and m = multiplet), coupling constants (Hz), and integration. NMR data was processed using Mestrelab Research MestReNova 11.0.2 software, using automatic baseline correction and automatic phasing. Infrared spectroscopy data was acquired using a PerkinElmer Spectrum Two IR Spectrometer or a Thermo Scientific iD5 ATR (Nicolet iS5) Spectrometer. Mass spectra were obtained using a Waters (Micromass) LCT premier with a TOF analyzer using the ionization method indicated to obtain accurate mass. Melting points were taken on a Thermo Scientific Electrothermal Mel-Temp<sup>®</sup> apparatus (Model No. 1001D) using a mercury thermometer and values reported are uncorrected. Chemical names found in the supporting information were generated using PerkinElmer ChemBioDraw Ultra 13.0 software.

## Experimental Procedures

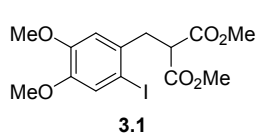
### Synthesis of Compound 3.1

Compound **3.1** was prepared according to the following synthetic route:



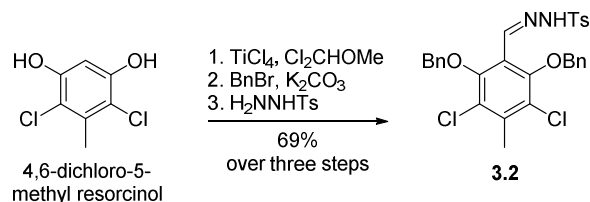
2-iodo-4,5-dimethoxybenzyl alcohol was synthesized according to literature procedure,<sup>5</sup> with modifications. A flame-dried round-bottom flask wrapped in aluminum foil was charged with 3,4-dimethoxybenzyl alcohol (1.00 g, 5.94

mmol), CF<sub>3</sub>COOAg (weighed in the dark) (1.44 g, 6.54 mmol), and CHCl<sub>3</sub> (4.5 mL) and then cooled to -5 °C. Finely ground I<sub>2</sub> (1.66 g, 6.54 mmol) was dissolved in CHCl<sub>3</sub> (9.0 mL) and added dropwise via syringe over 5 – 10 min yielding a yellow heterogeneous mixture. Any remaining I<sub>2</sub> was transferred via spatula. After 1 h, the reaction mixture was filtered through tightly packed Celite<sup>®</sup> to remove the silver salts. The pad was rinsed with CHCl<sub>3</sub> (3 × 50 mL). The filtrate was washed with saturated aqueous Na<sub>2</sub>S<sub>2</sub>O<sub>3</sub> (1 × 150 mL), dried (MgSO<sub>4</sub>), filtered, and concentrated *in vacuo* to yield a crude solid. Purification by column chromatography (20:80 – 50:50 EtOAc:hexanes) afforded 2-iodo-4,5-dimethoxybenzyl alcohol as a white solid (1.75 g, 100%). R<sub>f</sub> = 0.13 (20:80 EtOAc:hexanes, stains purple by *p*-anis dip stain). mp = 104–105 °C. <sup>1</sup>H NMR (600 MHz, Chloroform-*d*) δ 7.22 (s, 1H), 7.01 (s, 1H), 4.62 (d, *J* = 6.1 Hz, 2H), 3.88 (s, 3H), 3.86 (s, 3H), 2.07 (t, *J* = 6.1 Hz, 1H); <sup>13</sup>C NMR (151 MHz, Chloroform-*d*) δ 149.5, 148.9, 135.2, 121.5, 111.7, 85.4, 69.1, 56.2, 56.0; IR (ATR) 3479, 1499, 1462, 1437, 1255, 1153 cm<sup>-1</sup>; HRMS (ESI) *m/z* calcd for C<sub>9</sub>H<sub>11</sub>IO<sub>3</sub>Na [M + Na]<sup>+</sup> 316.9651, found 316.9636.



2-iodo-4,5-dimethoxybenzyl alcohol (1.75 g, 5.94 mmol) was then dissolved in  $\text{CH}_2\text{Cl}_2$  (59.0 mL) and treated with  $\text{PBr}_3$  (1.11 mL, 11.9 mmol) according to literature procedure,<sup>6</sup> with modifications. The reaction mixture was stirred for 16 h at 23 °C and then concentrated *in vacuo*. The resulting crude oil was neutralized using saturated aqueous  $\text{NaHCO}_3$  and extracted with  $\text{CH}_2\text{Cl}_2$  (3 × 30 mL). The combined organic extracts were dried ( $\text{Na}_2\text{SO}_4$ ), filtered, and concentrated *in vacuo* to afford a crude white solid. Dimethyl malonate (23.7 mL, 208 mmol) and THF (6.0 mL) were then added, and the mixture was stirred vigorously until the crude solid solubilized. Then, 60%  $\text{NaH}$ /mineral (0.949 g, 23.7 mmol) was added in portions over five minutes. After 1 h 15 min, the heterogenous yellow mixture was quenched with saturated aqueous  $\text{NH}_4\text{Cl}$  (50.0 mL) and extracted with  $\text{CH}_2\text{Cl}_2$  (3 × 50 mL). The combined organic layers were dried ( $\text{Na}_2\text{SO}_4$ ), filtered, and concentrated *in vacuo*. Excess dimethyl malonate was removed by vacuum distillation to yield a crude yellow solid. Purification by column chromatography (15:85 – 20:80 EtOAc:hexanes) afforded aryl iodide **3.1** as a white solid (2.25 g, 93%).  $R_f = 0.35$  (30:70 EtOAc:hexanes, stains pink-sienna by *p*-anis dip stain). mp = 88–89 °C.  $^1\text{H}$  NMR (600 MHz, Chloroform-*d*)  $\delta$  7.21 (s, 1H), 6.77 (s, 1H), 3.84 (s, 3H), 3.83 (s, 3H), 3.80 (t,  $J = 7.8$  Hz, 1H), 3.71 (s, 6H), 3.27 (d,  $J = 7.9$  Hz, 2H);  $^{13}\text{C}$  NMR (151 MHz, Chloroform-*d*)  $\delta$  169.0, 149.2, 148.5, 132.5, 121.7, 113.3, 88.1, 56.1, 55.9, 52.6, 51.8, 39.0; IR (ATR) 2951, 1734, 1506, 1255, 1215, 1163, 1026  $\text{cm}^{-1}$ ; HRMS (ESI)  $m/z$  calcd for  $\text{C}_{14}\text{H}_{17}\text{IO}_6\text{H}$  [ $\text{M} + \text{H}$ ]<sup>+</sup> 409.0148, found 409.0163.

### Synthesis of Compound 3.2



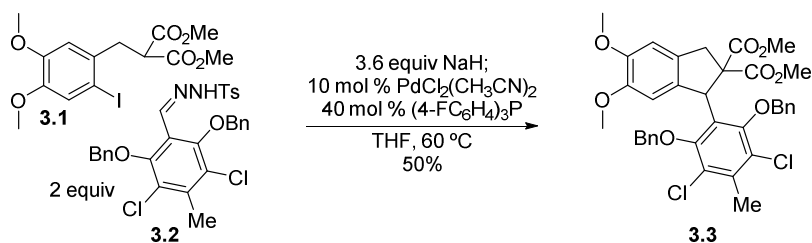
4,6-dichloro-5-methyl resorcinol (0.500 g, 2.59 mmol) and dichloromethyl methyl ether (1.03 mL, 11.4 mmol) were stirred for 45 min in CH<sub>2</sub>Cl<sub>2</sub> (8.60 mL) at -10 °C. While stirring at -10 °C, TiCl<sub>4</sub> (1.42 mL, 12.9 mmol, 98%) was added dropwise as a solution in CH<sub>2</sub>Cl<sub>2</sub> (2.40 mL). The resulting red solution was stirred for 1 h at -10 °C and then quenched by adding approximately 250 mL of equal volumes of ice-cold 3 M HCl and CHCl<sub>3</sub>. The resulting biphasic mixture was stirred vigorously at 23 °C for 2 – 6 h until the red-orange emulsion cleared. The aqueous layer was then extracted with CHCl<sub>3</sub> (3 × 100 mL) and the combined organic extracts were washed with water, dried (MgSO<sub>4</sub>), filtered, and concentrated *in vacuo* to afford 0.597 g of a crude yellow solid. The solid was dissolved in EtOAc and passed through a column packed with silica gel (5:95 then 10:90 EtOAc:hexanes) to afford a white solid mixture that was used in the next step without any further purification.

The white solid mixture was then treated with anhydrous K<sub>2</sub>CO<sub>3</sub> (4.29 g, 31.1 mmol), acetone (5.20 mL), and benzyl bromide (1.85 mL, 15.5 mmol) and heated at reflux for 6 h. Upon completion, the slurry was filtered through a pad of tightly packed Celite<sup>®</sup> and the pad rinsed with acetone (3 × 50 mL). The organic solution was concentrated *in vacuo* and the resulting oil was dissolved in EtOAc (50 mL) and sequentially washed with saturated aqueous NaHCO<sub>3</sub> (50 mL), 3 M HCl (50 mL), and brine (50 mL). The organic layer was dried (Na<sub>2</sub>SO<sub>4</sub>), filtered, concentrated *in vacuo*, and triturated with hexanes to remove excess benzyl bromide. Trituration with hexanes afforded 0.891 g of a white solid mixture that was used in the next step without further purification.

The 0.891 g of white solid mixture was dissolved in THF (4.5 mL) and stirred at 0 °C. Once cool, *p*-toluenesulfonyl hydrazide (1.02 g, 5.33 mmol, 97%) was then added in one portion. The heterogeneous mixture was warmed to ambient temperature and stirred for 30 min. Upon completion, the reaction mixture was concentrated *in vacuo* and purified by column

chromatography (10:90 – 15:85 EtOAc:hexanes) to afford *N*-tosylhydrazone **3.2** as a white solid (1.02 g, 69% over three steps).  $R_f = 0.30$  (20:80 EtOAc:hexanes, stains yellow by *p*-anis dip stain). mp = 157–158 °C.  $^1\text{H}$  NMR (600 MHz, Chloroform-*d*)  $\delta$  7.94 (s, 1H), 7.69 (d,  $J = 1.4$  Hz, 1H), 7.61 (dd,  $J = 8.3, 1.7$  Hz, 2H), 7.43 (d,  $J = 7.9$  Hz, 4H), 7.39 – 7.30 (m, 6H), 7.03 (d,  $J = 7.9$  Hz, 2H), 4.91 (s, 4H), 2.53 (d,  $J = 1.6$  Hz, 3H), 2.28 (s, 3H);  $^{13}\text{C}$  NMR (151 MHz, Chloroform-*d*)  $\delta$  152.3, 144.1, 141.6, 138.3, 136.3, 135.2, 129.6, 128.50, 128.48, 128.41, 128.38, 127.8, 126.1, 121.8, 76.0, 21.5, 18.7; IR (ATR) 3178, 2923, 1596, 1575, 1366, 1337, 1162, 1085, 953  $\text{cm}^{-1}$ ; HRMS (ESI)  $m/z$  calcd for  $\text{C}_{29}\text{H}_{26}\text{Cl}_2\text{N}_2\text{O}_4\text{SNa}$   $[\text{M} + \text{Na}]^+$  591.0888, found 591.0865.

### Synthesis of Compound 3.3

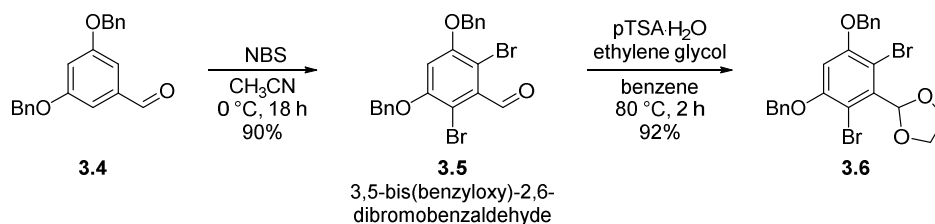


Aryl indane **3.3** was synthesized according to literature procedure.<sup>7</sup> To a stirring solution of NaH (17.6 mg, 0.441 mmol, 60% dispersion in mineral oil) in THF (2.0 mL) at  $-10$  °C was added a pre-stirred solution of compound **3.1** (50.0 mg, 0.122 mmol) and *N*-tosylhydrazone **3.2** (0.140 g, 0.240 mmol) in THF (0.70 mL). Additional THF (1.40 mL) was used to transfer any remaining reagent solution. The heterogeneous solution was stirred at 23 °C for 20 min before adding a pre-stirred solution of  $\text{PdCl}_2(\text{CH}_3\text{CN})_2$  (3.2 mg, 0.012 mmol) and  $(4\text{-FC}_6\text{H}_4)_3\text{P}$  (15.5 mg, 0.049 mmol) in THF (0.70 mL). Additional THF (1.40 mL) was used to transfer any remaining catalyst solution. The reaction was then heated at 60 °C. Within 30 min, *N*-tosylhydrazone **3.2** had been consumed. The reaction mixture was cooled to 23 °C and then passed through a pad of silica that was rinsed with  $\text{Et}_2\text{O}$  ( $3 \times 15$  mL). The filtrate was concentrated *in vacuo* and passed through

a silica gel column (10:90 then 30:70 EtOAc:hexanes) to afford an orange-red oil. This oil was further purified by preparative layer chromatography. The plate was developed twice with 15:85 EtOAc:hexanes, and then three times with 20:80 EtOAc:hexanes to yield aryl indane **3.3** as a peach amorphous solid (40.7 mg, 50%).  $R_f = 0.22$  (20:80 EtOAc:hexanes, stains brown by *p*-anis dip stain).  $^1\text{H NMR}$  (600 MHz, Chloroform-*d*)  $\delta$  7.75 – 7.72 (m, 2H), 7.45 (t,  $J = 7.5$  Hz, 2H), 7.41 – 7.36 (m, 1H), 7.31 (dd,  $J = 8.0, 6.5$  Hz, 2H), 7.29 – 7.26 (m, 1H), 7.23 – 7.19 (m, 2H), 6.52 (s, 1H), 6.35 (s, 1H), 6.15 (s, 1H), 5.15 (d,  $J = 9.9$  Hz, 1H), 5.02 (d,  $J = 9.9$  Hz, 1H), 4.75 (d,  $J = 11.6$  Hz, 1H), 4.14 (d,  $J = 16.5$  Hz, 1H), 3.76 (s, 6H), 3.68 (s, 3H), 3.44 (s, 3H), 3.19 (d,  $J = 16.7$  Hz, 1H), 2.88 (d,  $J = 11.6$  Hz, 1H), 2.52 (s, 3H);  $^{13}\text{C NMR}$  (151 MHz, Chloroform-*d*)  $\delta$  173.0, 169.6, 152.8, 152.2, 148.7, 148.6, 137.7, 136.6, 135.6, 134.6, 132.2, 130.8, 129.1, 128.7, 128.5, 127.8, 127.2, 125.9, 125.4, 125.1, 107.4, 107.3, 75.3, 72.9, 65.5, 56.2, 55.8, 53.3, 52.3, 48.1, 41.3, 18.3; IR (ATR) 2950, 2928, 2359, 1735, 1241, 1221, 1089  $\text{cm}^{-1}$ ; HRMS (ESI)  $m/z$  calcd for  $\text{C}_{36}\text{H}_{34}\text{Cl}_2\text{O}_8\text{Na}$   $[\text{M} + \text{Na}]^+$  687.1528, found 687.1537.

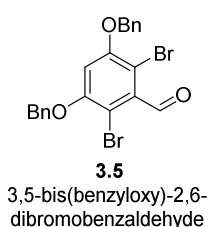
### Synthesis of Compound 3.6

Compound 3.6 was prepared using the following synthetic route:



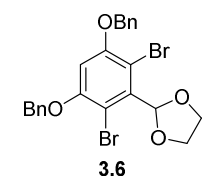
3,5-bis(benzyloxy)-2,6-dibromobenzaldehyde was synthesized according to literature procedure,<sup>8</sup> with modifications. A solution of *N*-bromosuccinimide (NBS) (1.24 g, 7.22 mmol) in  $\text{CH}_3\text{CN}$  (11.0 mL) was added via syringe pump over 1 h at 0 °C to a stirring solution of 3,5-bis(benzyloxy)benzaldehyde **3.4** (0.997 g, 3.13 mmol) in dry  $\text{CH}_3\text{CN}$  (24.0 mL). As the reaction

progressed, a precipitate formed. The mixture was warmed to 23 °C and stirred overnight. Upon completion, the pink precipitate was filtered, rinsed with cold CH<sub>3</sub>CN (80 mL), and dried *in vacuo* to afford 3,5-bis(benzyloxy)-2,6-dibromobenzaldehyde **3.5** as a pink solid (1.31 g, 90%).



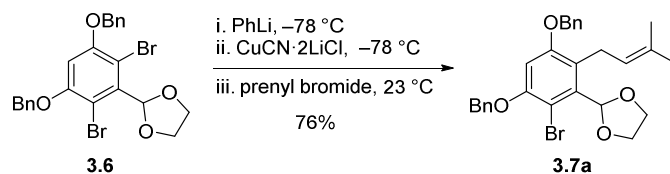
$R_f = 0.30$  (10:90 EtOAc:hexanes). mp = 159–160 °C; <sup>1</sup>H NMR (600 MHz, Chloroform-*d*) δ 10.20 (s, 1H), 7.39 (d,  $J = 4.4$  Hz, 8H), 7.34 (m, 2H), 6.67 (s, 1H), 5.09 (s, 4H); <sup>13</sup>C NMR (151 MHz, Chloroform-*d*) δ 191.6, 155.3, 135.9, 135.5, 128.8, 128.4, 127.0, 104.9, 103.8, 71.6; IR (ATR) 2909, 2869, 1696, 1569, 1327, 1232, 950, 826, 726, 691 cm<sup>-1</sup>; HRMS (ESI)  $m/z$  calcd for C<sub>21</sub>H<sub>16</sub>Br<sub>2</sub>O<sub>3</sub>Na [M + Na]<sup>+</sup> 496.9364, found 496.9384.

2-(3,5-bis(benzyloxy)-2,6-dibromophenyl)-1,3-dioxolane **3.6** was synthesized according to literature procedure,<sup>9</sup> with modifications. Using a Dean-Stark apparatus, dibromobenzaldehyde **3.5** (2.00 g, 4.20 mmol), *p*TSA·H<sub>2</sub>O (80.0 mg, 0.420 mmol), and ethylene glycol (1.17 mL, 21.0 mmol) were heated at reflux in benzene (35.0 mL) for 2 h. Upon completion, the reaction was cooled to 23 °C, quenched with saturated aqueous NaHCO<sub>3</sub> (50 mL), stirred for 15 min, and extracted with EtOAc (3 × 30 mL). The combined organic extracts were washed with brine (100 mL), dried (Na<sub>2</sub>SO<sub>4</sub>), filtered, and concentrated *in vacuo* to afford a crude solid. Trituration with chilled Et<sub>2</sub>O yielded dibromodioxolane **3.6** as a white solid (2.02 g, 92%).



$R_f = 0.23$  (10:90 EtOAc:hexanes, stains brown by *p*-anis dip stain). mp = 166–167 °C; <sup>1</sup>H NMR (600 MHz, Chloroform-*d*) δ 7.42 – 7.34 (m, 8H), 7.35 – 7.29 (m, 2H), 6.58 (s, 1H), 6.57 (s, 1H), 5.06 (s, 4H), 4.42 – 4.32 (m, 2H), 4.15 – 4.03 (m, 2H); <sup>13</sup>C NMR (151 MHz, Chloroform-*d*) δ 155.1, 155.1, 136.0, 134.2, 128.7, 128.3, 128.2, 127.0, 127.0, 107.3, 104.6, 102.6, 71.6, 65.9; IR (ATR) 3032, 2893, 1571, 1227 cm<sup>-1</sup>; HRMS (ESI)  $m/z$  calcd for C<sub>23</sub>H<sub>20</sub>Br<sub>2</sub>O<sub>4</sub>Na [M + Na]<sup>+</sup> 540.9626, found 540.0056.

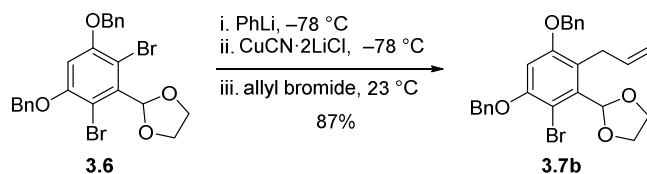
## Synthesis of Compound 3.7a



2-(3,5-Bis(benzyloxy)-2-bromo-6-(3-methylbut-2-en-1-yl)phenyl)-1,3-dioxolane, **3.7a**, was prepared as follows: Phenyllithium (1.9 M in dibutyl ether, 0.180 mL, 0.348 mmol) was added dropwise via syringe to a stirring solution of dibromodioxolane **3.6** (0.151 g, 0.290 mmol) in THF (1.90 mL) at  $-78\text{ }^{\circ}\text{C}$ . The resulting yellow solution was stirred for 30 min at  $-78\text{ }^{\circ}\text{C}$  before adding CuCN·2LiCl (1 M in THF, 87.0  $\mu\text{L}$ , 0.087 mmol) and prenyl bromide (0.134 mL, 1.16 mmol, 96%) sequentially via syringe. The reaction was then stirred at  $23\text{ }^{\circ}\text{C}$  until complete. The reaction was quenched with a 1:1 mixture of 50% brine and 50% aqueous  $\text{NH}_3$  (10 mL), stirred for an additional 15 min, and then extracted with EtOAc ( $3 \times 15\text{ mL}$ ). The combined organic extracts were dried ( $\text{MgSO}_4$ ), filtered and concentrated *in vacuo*. The resulting crude solid was triturated with hexane and a small amount of  $\text{Et}_2\text{O}$  to afford prenyl dioxolane **3.7a** as a white solid (0.114 g, 76%).  $R_f = 0.30$  (10:90 EtOAc:hexanes, stains dark violet/black by *p*-anis dip stain). mp =  $143\text{--}144\text{ }^{\circ}\text{C}$ ;  $^1\text{H NMR}$  (600 MHz, Chloroform-*d*)  $\delta$  7.43 – 7.28 (m, 10H), 6.55 (s, 1H), 6.40 (s, 1H), 5.12 (ddt,  $J = 9.3, 5.7, 2.8\text{ Hz}$ , 1H), 5.04 (s, 2H), 4.97 (s, 2H), 4.26 – 4.19 (m, 2H), 4.05 – 4.00 (m, 2H), 3.50 (d,  $J = 6.5\text{ Hz}$ , 2H), 1.65 (d,  $J = 1.7\text{ Hz}$ , 3H), 1.58 (d,  $J = 1.4\text{ Hz}$ , 3H);  $^{13}\text{C NMR}$  (151 MHz, Chloroform-*d*)  $\delta$  156.9, 153.7, 136.7, 136.6, 133.2, 130.6, 128.6, 128.5, 127.9, 127.3, 127.1, 126.2, 124.0, 106.7, 104.2, 101.7, 71.6, 70.6, 65.1, 25.7, 24.7, 17.9; IR (ATR) 2871, 1591, 1573, 1322, 1164, 1051, 962, 732, 694  $\text{cm}^{-1}$ ; HRMS (ESI)  $m/z$  calcd for  $\text{C}_{28}\text{H}_{29}\text{BrO}_4\text{Na}$  [ $\text{M} + \text{Na}$ ] $^+$  531.1147, found 531.1147.



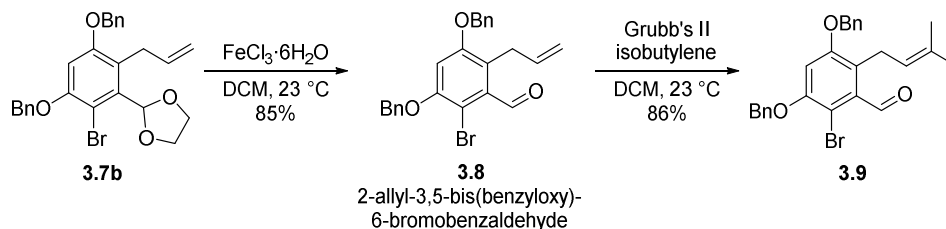
## Synthesis of Compound 3.7b



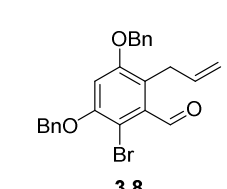
2-(2-Allyl-3,5-bis(benzyloxy)-6-bromophenyl)-1,3-dioxolane, **3.7b**, was prepared as follows: Phenyllithium (1.9 M in dibutyl ether, 1.21 mL, 2.31 mmol) was added dropwise via syringe to a stirring solution of dibromodioxolane **3.6** (1.00 g, 1.92 mmol) in THF (12.8 mL) at  $-78\text{ }^{\circ}\text{C}$ . The resulting yellow solution was stirred for 30 min at  $-78\text{ }^{\circ}\text{C}$  before adding CuCN·2LiCl (1 M in THF, 0.576 mL, 0.576 mmol) and allyl bromide (0.665 mL, 7.68 mmol) sequentially via syringe. The reaction was then stirred at  $23\text{ }^{\circ}\text{C}$  until complete. The reaction was quenched with a 1:1 mixture of 50% brine and 50% aqueous  $\text{NH}_3$  (30 mL), stirred for an additional 15 min, and then extracted with EtOAc ( $3 \times 30\text{ mL}$ ). The combined organic extracts were dried ( $\text{MgSO}_4$ ), filtered and concentrated *in vacuo*. The resulting crude solid was triturated with cold  $\text{Et}_2\text{O}$  to afford a fraction of allyl dioxolane **3.7b** as a white solid (0.759 g, 82%) and another fraction that was purified by column chromatography (5:95 EtOAc:hexanes) to afford additional allyl dioxolane **3.7b** (49.6 mg, 5%).  $R_f = 0.29$  (10:90 EtOAc:hexanes, stains violet by *p*-anis dip stain). mp =  $119\text{--}120\text{ }^{\circ}\text{C}$ ;  $^1\text{H NMR}$  (600 MHz, Chloroform-*d*)  $\delta$  7.45 – 7.26 (m, 10H), 6.58 (s, 1H), 6.39 (s, 1H), 5.96 (ddt,  $J = 16.7, 11.8, 6.1\text{ Hz}$ , 1H), 5.06 (s, 2H), 4.98 (s, 2H), 4.97 – 4.91 (m, 2H), 4.29 – 4.17 (m, 2H), 4.09 – 3.99 (m, 2H), 3.58 (dd,  $J = 5.9, 1.9\text{ Hz}$ , 2H);  $^{13}\text{C NMR}$  (151 MHz, Chloroform-*d*)  $\delta$  157.0, 154.0, 137.6, 136.7, 136.5, 133.4, 128.6, 128.6, 128.0, 127.9, 127.11, 127.08, 124.2, 114.7, 106.9, 104.3, 101.7, 71.5, 70.6, 65.0, 29.6; IR (ATR) 3031, 2887, 2322, 1591, 1573, 1322, 1053, 733, 694  $\text{cm}^{-1}$ ; HRMS (ESI)  $m/z$  calcd for  $\text{C}_{26}\text{H}_{25}\text{BrO}_4\text{Na}$  [ $\text{M} + \text{Na}$ ] $^+$  503.0834, found 503.0842.

## Synthesis of Compound 3.9

Compound 3.9 was prepared using the following synthetic route:



To a stirring solution of allyl dioxolane **3.7b** (0.759 g, 1.58 mmol) in CH<sub>2</sub>Cl<sub>2</sub> (26.0 mL) was added FeCl<sub>3</sub>·6H<sub>2</sub>O (1.49 g, 5.53 mmol) at 23 °C. The reaction was stirred for 1 h and quenched by addition of saturated aqueous NaHCO<sub>3</sub> (40 mL). After stirring for 15 min, the solution was extracted with CH<sub>2</sub>Cl<sub>2</sub> (3 × 30 mL). The combined organic extracts were washed with brine, dried (MgSO<sub>4</sub>), filtered, and concentrated *in vacuo*. The crude yellow solid was purified by column chromatography (2.5:97.5 EtOAc:hexanes) to afford 2-allyl-3,5-bis(benzyloxy)-6-bromobenzaldehyde **3.8** as a white solid (0.584 g, 85%).

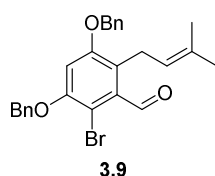


**3.8**  
2-allyl-3,5-bis(benzyloxy)-6-bromobenzaldehyde

$R_f = 0.38$  (10:90 EtOAc:hexanes, stains pink/violet by *p*-anis dip stain). mp = 95–96 °C; <sup>1</sup>H NMR (600 MHz, Chloroform-*d*) δ 10.45 (s, 1H), 7.45 – 7.32 (m, 10H), 6.70 (s, 1H), 5.94 (ddt, *J* = 16.5, 10.1, 6.2 Hz, 1H), 5.10 (s, 2H), 5.02 (s, 2H), 4.97 – 4.91 (m, 2H), 3.65 (dt, *J* = 6.2, 1.6 Hz, 2H); <sup>13</sup>C NMR (151 MHz, Chloroform-*d*) δ 194.5, 156.8, 154.0, 136.7, 136.2, 136.0, 134.6, 128.7, 128.7, 128.2, 128.2, 127.1, 127.1, 124.1, 115.1, 107.2, 103.7, 71.6, 70.9, 29.1; IR (ATR) 2933, 2869, 1693, 1312, 1168, 736, 695 cm<sup>-1</sup>; HRMS (ESI) *m/z* calcd for C<sub>24</sub>H<sub>21</sub>BrO<sub>3</sub>Na [M + Na]<sup>+</sup> 461.0555, found 461.0560.

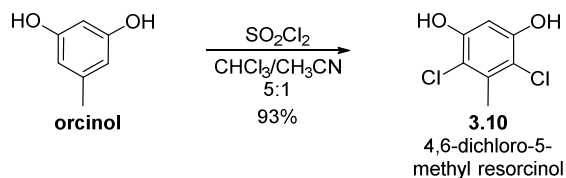
3,5-Bis(benzyloxy)-2-bromo-6-(3-methylbut-2-en-1-yl)benzaldehyde, **3.9**, was prepared as follows: To a flame-dried 25 mL Schlenk tube was added allyl benzaldehyde **3.8** (50.0 mg, 0.114

mmol) and Grubbs Catalyst™ 2nd Generation (4.9 mg, 0.0057 mmol). The tube was evacuated and backfilled with N<sub>2</sub> gas. It was then submerged in a -78 °C bath and isobutylene (2.85 mL, 28.6 mmol) and CH<sub>2</sub>Cl<sub>2</sub> (3.80 mL) were then added. The tube was sealed and stirred at 23 °C for three days. On the third day, the vessel was cooled to -78 °C and opened to release ethylene gas. Isobutylene and CH<sub>2</sub>Cl<sub>2</sub> were then removed by rotary evaporation at 0 °C. The resulting dark brown/pink solid was filtered through a silica plug (6 inches in length) using 5:95 NEt<sub>3</sub>:hexanes to yield a mixture of allyl benzaldehyde **3.7b** and prenyl benzaldehyde **3.9** in a 1:9 ratio. This mixture was re-submitted to the same reaction and work-up conditions to afford a brown-yellow oil that solidified upon standing under vacuum. The final product obtained was a mixture of allyl benzaldehyde **3.7b** and prenyl benzaldehyde **3.9** in a 1:34 ratio as a light brown solid (46.0 mg, 86%).



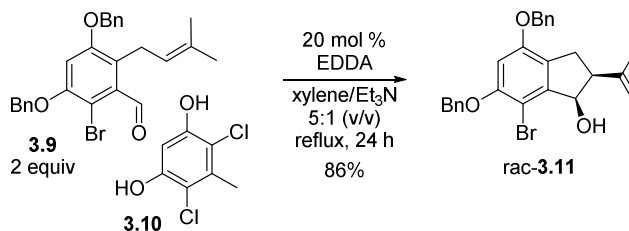
$R_f = 0.39$  (10:90 EtOAc:hexanes, stains blue/violet by *p*-anis dip stain). mp = 103–104 °C; <sup>1</sup>H NMR (600 MHz, Chloroform-*d*) δ 10.43 (s, 1H), 7.43 – 7.30 (m, 11H), 6.67 (s, 1H), 5.11 – 5.06 (m, 3H), 5.01 (s, 2H), 3.57 (d, *J* = 6.8 Hz, 1H), 1.65 (d, *J* = 1.4 Hz, 3H), 1.62 (d, *J* = 1.4 Hz, 3H); <sup>13</sup>C NMR (151 MHz, Chloroform-*d*) δ 194.7, 156.7, 153.7, 136.2, 136.1, 134.8, 132.0, 128.7, 128.7, 128.7, 128.2, 127.3, 127.1, 127.1, 126.1, 122.7, 106.6, 103.6, 71.6, 70.9, 25.8, 24.3, 18.0; IR (ATR) 2919, 2906, 2866, 2851, 1691, 1590, 1567, 1321, 1168, 726, 695 cm<sup>-1</sup>; HRMS (ESI) *m/z* calcd for C<sub>26</sub>H<sub>25</sub>BrO<sub>3</sub>Na [M + Na]<sup>+</sup> 487.0885, found 487.0876.

## Synthesis of Compound 3.10



4,6-dichloro-5-methyl resorcinol, **3.10**, was prepared as follows: A two-necked round-bottom flask containing orcinol (97%, 9.59 g, 74.9 mmol) and a 5:1 solution of  $\text{CHCl}_3/\text{CH}_3\text{CN}$  (407.5 mL) was submerged in an ice-water bath. A solution of  $\text{SO}_2\text{Cl}_2$  (12.7 mL, 153.6 mmol, 97%) in  $\text{CHCl}_3$  (40.0 mL) was added dropwise into the reaction flask over 30 – 40 min via an addition funnel. The reaction was stirred at 23 °C until orcinol had been consumed as determined by TLC. The reaction was quenched with 10% NaOH (200 mL), stirred for an additional 40 min at 23 °C, and then acidified with 1 M HCl (400 mL) to achieve a pH of 3–4. The acidified mixture was extracted with  $\text{CH}_2\text{Cl}_2$  (4 × 150 mL) and the combined organic extracts were washed with brine (1 × 100 mL), dried ( $\text{MgSO}_4$ ), filtered, and concentrated *in vacuo*. The resulting solid was triturated with  $\text{CH}_2\text{Cl}_2$  and filtered to afford pure product as white needles. The filtrate was concentrated *in vacuo* and triturated at least two more times to produce two more pure batches of 4,6-dichloro-5-methyl resorcinol **3.10** (12.3 g, 85%) and one impure batch that was further purified by column chromatography (20:80 EtOAc:hexanes) to afford additional 4,6-dichloro-5-methyl resorcinol **3.10** as a white solid (1.12 g, 8%) for a total combined yield of 93%.  $R_f = 0.26$  (20:80 EtOAc:hexanes, stains faintly by *p*-anis dip stain). mp = 168–169 °C.  $^1\text{H}$  and  $^{13}\text{C}$  spectral data is consistent with that previously reported.<sup>10</sup>  $^1\text{H}$  NMR (600 MHz, Chloroform-*d*)  $\delta$  6.63 (s, 1H), 5.58 (s, 2H), 2.45 (s, 3H);  $^{13}\text{C}$  NMR (151 MHz, Chloroform-*d*)  $\delta$  150.9, 134.2, 112.7, 101.0, 18.0; HRMS (ESI):  $m/z$  calcd for  $\text{C}_7\text{H}_5\text{Cl}_2\text{O}_2$  [ $\text{M} - \text{H}$ ] $^-$  190.9667, found 190.9667.

## Synthesis of Compound rac-3.11

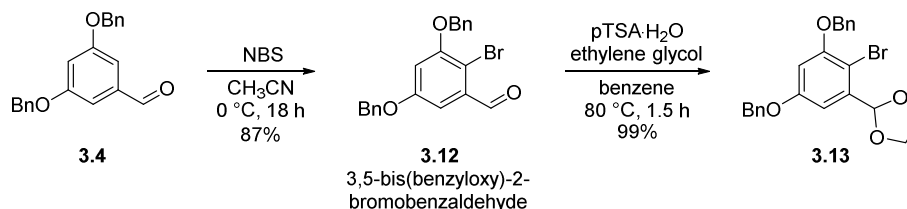


4,6-Bis(benzyloxy)-7-bromo-2-(prop-1-en-2-yl)-2,3-dihydro-1H-inden-1-ol, rac-**3.11**, was prepared as follows: To a stirring solution of prenyl benzaldehyde **3.9** (10.0 mg, 21.4  $\mu\text{mol}$ ) and 4,6-dichloro-5-methyl resorcinol **3.10** (2.1 mg, 10.8  $\mu\text{mol}$ ) in xylenes (110  $\mu\text{L}$ ) was added EDDA (0.4 mg, 2.18  $\mu\text{mol}$ ) and NEt<sub>3</sub> (21.7  $\mu\text{L}$ , 0.156 mmol) at 23 °C. The reaction mixture was heated at reflux for 24 h. Evaporation of the solvent afforded a brown oil that was purified by column chromatography (20:80 EtOAc:hexanes) to afford racemic indane **3.11** as a brown oil (8.6 mg, 86%, >80% purity).  $R_f$  = 0.35 (20:80 EtOAc:hexanes, stains blue by *p*-anis dip stain). <sup>1</sup>H NMR (600 MHz, Chloroform-*d*)  $\delta$  7.47 – 7.29 (m, 10H), 6.49 (s, 1H), 5.22 (dd,  $J$  = 5.3, 3.9 Hz, 1H), 5.11 (d,  $J$  = 1.6 Hz, 1H), 5.08 (s, 2H), 5.04 – 4.98 (m, 3H), 3.14 (td,  $J$  = 12.7, 5.0 Hz, 1H), 3.05 – 2.94 (m, 2H), 1.96 (s, 3H), 1.83 (d,  $J$  = 3.9 Hz, 1H); <sup>13</sup>C NMR (151 MHz, Chloroform-*d*)  $\delta$  154.9, 154.6, 150.9, 145.8, 143.2, 136.62, 136.59, 128.65, 128.60, 128.1, 128.0, 127.2, 127.1, 126.0, 113.0, 101.04, 101.03, 76.0, 71.8, 70.4, 51.6, 30.6, 22.9. IR (ATR) 3502, 2918, 2851, 1580, 1326, 1164, 733, 694  $\text{cm}^{-1}$ ; HRMS (ESI)  $m/z$  calcd for C<sub>26</sub>H<sub>25</sub>BrO<sub>3</sub>Na [M + Na]<sup>+</sup> 487.0885, found 487.0890. Additional <sup>1</sup>H and <sup>13</sup>C data taken in C<sub>6</sub>D<sub>6</sub>: <sup>1</sup>H NMR (500 MHz, C<sub>6</sub>D<sub>6</sub>)  $\delta$  7.36 (d,  $J$  = 7.5 Hz, 2H), 7.23 (d,  $J$  = 7.5 Hz, 2H), 7.21 – 7.17 (m, 2H), 7.15 – 7.03 (m, 4H), 6.32 (s, 1H), 5.18 (d,  $J$  = 5.5 Hz, 1H), 4.95 (s, 1H), 4.85 (s, 1H), 4.79 (s, 2H), 4.71 – 4.60 (m, 2H), 3.16 (dd,  $J$  = 15.5, 10.2 Hz, 1H), 2.98 (dd,  $J$  = 15.5, 7.3 Hz, 1H), 2.63 (q,  $J$  = 7.2 Hz, 1H), 1.75 (s, 3H); <sup>13</sup>C NMR

(151 MHz, C<sub>6</sub>D<sub>6</sub>)  $\delta$  155.4, 155.0, 151.7, 147.1, 143.6, 137.3, 137.3, 128.8, 128.8, 128.3, 128.1, 128.0, 127.6, 127.4, 126.3, 112.7, 101.8, 100.9, 76.6, 71.7, 70.4, 51.9, 50.3, 31.1, 22.8.

### Synthesis of Compound 3.13

Compound 3.13 was prepared using the following synthetic route:



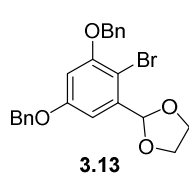
In one portion, NBS (0.123 g, 0.691 mmol) was added at 0 °C to a stirring solution of 3,5-bis(benzyloxy)benzaldehyde **3.4** (0.200 g, 0.628 mmol) in dry CH<sub>3</sub>CN (4.80 mL). The mixture was warmed to 23 °C and stirred overnight. As the reaction progressed, a precipitate formed. The reaction was then concentrated *in vacuo* and purified by column chromatography (8:92 EtOAc:hexanes) to afford 3,5-bis(benzyloxy)-2-bromobenzaldehyde **3.12** (0.218 mg, 87%) as a beige solid.

**3.12**  
3,5-bis(benzyloxy)-2-bromobenzaldehyde

$R_f = 0.37$  (10:90 EtOAc:hexanes). <sup>1</sup>H and <sup>13</sup>C spectral data is consistent with that previously reported.<sup>9</sup> <sup>1</sup>H NMR (600 MHz, Chloroform-*d*)  $\delta$  10.42 (s, 1H), 7.46 (d,  $J = 7.2$  Hz, 2H), 7.44 – 7.36 (m, 6H), 7.38 – 7.31 (m, 2H), 7.15 (d,  $J = 2.8$  Hz, 1H), 6.84 (d,  $J = 2.8$  Hz, 1H), 5.14 (s, 2H), 5.06 (s, 2H); <sup>13</sup>C NMR (151 MHz, Chloroform-*d*)  $\delta$  192.0, 158.9, 156.2, 135.9, 135.8, 134.8, 128.72, 128.70, 128.4, 128.2, 127.7, 127.0, 110.0, 108.0, 105.1, 71.2, 70.6; IR (ATR) 3059, 3034, 2865, 1684, 1578 cm<sup>-1</sup>; HRMS (ESI)  $m/z$  calculated for C<sub>21</sub>H<sub>17</sub>BrO<sub>3</sub>Na [M + Na]<sup>+</sup> 419.0259, found 419.0247.

2-(3,5-Bis(benzyloxy)-2-bromophenyl)-1,3-dioxolane, **3.13**, was synthesized as follows:  
Using a Dean-Stark apparatus, 3,5-bis(benzyloxy)-2-bromobenzaldehyde **3.12** (4.00 g, 10.1

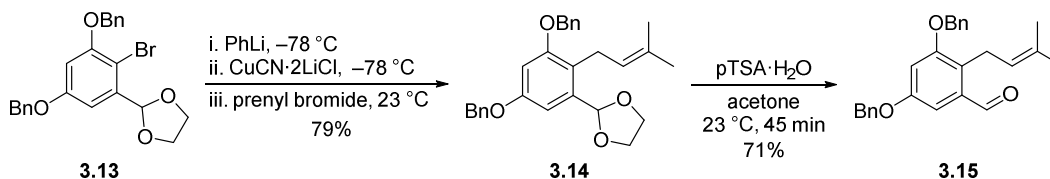
mmol), *p*TSA·H<sub>2</sub>O (192 mg, 1.01 mmol), and ethylene glycol (2.82 mL, 50.3 mmol) were heated at reflux in benzene (84.0 mL) for 4 h. Upon completion, the reaction was cooled to 23 °C, quenched with saturated aqueous NaHCO<sub>3</sub> (100 mL), stirred for 15 min, and extracted with EtOAc (3 × 50 mL). The combined organic layers were washed with brine (1 × 75 mL), dried (Na<sub>2</sub>SO<sub>4</sub>), filtered, concentrated *in vacuo*, and purified by column chromatography (10:90 EtOAc:hexanes) to yield dioxolane **3.13** as a white solid (4.43 g, 99%).



$R_f = 0.19$  (10:90 EtOAc:hexanes). mp = 95–96 °C; <sup>1</sup>H and <sup>13</sup>C spectral data is consistent with that previously reported.<sup>9</sup> <sup>1</sup>H NMR (600 MHz, Chloroform-*d*) δ 7.45 (d, *J* = 7.1 Hz, 2H), 7.42 – 7.35 (m, 6H), 7.36 – 7.29 (m, 2H), 6.90 (d, *J* = 2.8 Hz, 1H), 6.61 (d, *J* = 2.8 Hz, 1H), 6.15 (s, 1H), 5.10 (s, 2H), 5.03 (s, 2H), 4.15 – 4.09 (m, 2H), 4.09 – 4.04 (m, 2H); <sup>13</sup>C NMR (151 MHz, Chloroform-*d*) δ 158.8, 155.9, 138.6, 136.5, 136.3, 128.64, 128.59, 128.2, 128.0, 127.6, 127.0, 105.1, 104.6, 103.0, 102.5, 71.0, 70.4, 65.4.; IR (ATR) 2968, 2883, 1593, 1167, 728, 693 cm<sup>-1</sup>; HRMS (ESI) *m/z* calcd for C<sub>23</sub>H<sub>21</sub>BrO<sub>4</sub>Na [M + Na]<sup>+</sup> 463.0521, found 463.0522.

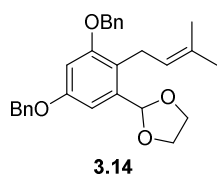
### Synthesis of Compound 3.15

Compound **3.15** was synthesized using the following synthetic route:



2-(3,5-Bis(benzyloxy)-2-(3-methylbut-2-en-1-yl)phenyl)-1,3-dioxolane, **3.14**, was prepared as follows: Phenyllithium (1.9 M in dibutyl ether, 0.420 mL, 0.800 mmol,) was added dropwise via

syringe to a stirring solution of dioxolane **3.13** (221 mg, 0.500 mmol) in THF (3.40 mL) at  $-78$  °C. The resulting yellow solution was stirred at  $-78$  °C for 30 min before adding CuCN·2LiCl (1 M in THF, 0.150 mL, 0.150 mmol) and prenyl bromide (96%, 0.240 mL, 2.00 mmol) sequentially via syringe. The reaction was then stirred at 23 °C until complete at which point it was quenched by addition of a 1:1 mixture of 50% brine and 50% aqueous NH<sub>3</sub> (30 mL), stirred for an additional 15 min, and then extracted with EtOAc (3 × 20 mL). The combined organic layers were dried (MgSO<sub>4</sub>), filtered, concentrated *in vacuo*, and purified by column chromatography (5:2.5:92.5 to 5:5:95 EtOAc:hexanes) to yield prenyl dioxolane **3.14** as a white solid (172 mg, 79%).

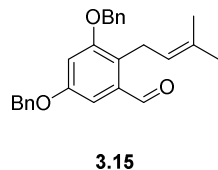


$R_f = 0.31$  (10:90 EtOAc:hexanes, stains violet by *p*-anis dip stain). mp = 77–78 °C. <sup>1</sup>H NMR (600 MHz, Chloroform-*d*)  $\delta$  7.44 – 7.28 (m, 10H), 6.87 (d,  $J = 2.5$  Hz, 1H), 6.59 (d,  $J = 2.5$  Hz, 1H), 5.97 (s, 1H), 5.16 – 5.11 (m, 1H), 5.02 (d,  $J = 2.0$  Hz, 4H), 4.15 – 4.11 (m, 2H), 4.05 – 4.00 (m, 2H), 3.47 (d,  $J = 6.8$  Hz, 2H), 1.65 (d,  $J = 1.5$  Hz, 3H), 1.65 (d,  $J = 1.4$  Hz, 3H); <sup>13</sup>C NMR (151 MHz, Chloroform-*d*)  $\delta$  157.8, 157.6, 137.1, 137.1, 137.1, 130.8, 128.6, 128.4, 128.0, 127.74, 127.69, 127.3, 123.5, 122.2, 102.9, 101.4, 101.2, 70.3, 70.2, 65.3, 25.7, 24.2, 17.8; IR (ATR) 2875, 1602, 1161, 1045 cm<sup>-1</sup>; HRMS (ESI)  $m/z$  calcd for C<sub>28</sub>H<sub>30</sub>O<sub>4</sub>Na [M + Na]<sup>+</sup> 453.2042, found 453.2059.

3,5-Bis(benzyloxy)-2-(3-methylbut-2-en-1-yl)benzaldehyde, **3.15**, was prepared as follows: To a solution of prenyl dioxolane **3.14** (0.395 g, 0.916 mmol) in acetone (18.0 mL) was added *p*TSA·H<sub>2</sub>O (19.0 mg, 0.100 mmol) and stirred at 23 °C. The reaction was quenched at exactly 45 min by addition of saturated aqueous NaHCO<sub>3</sub> solution followed by rotary evaporation to remove acetone. The residue was extracted with EtOAc (3 × 30 mL) and the combined organic extracts were washed with brine (1 × 75 mL), dried (Na<sub>2</sub>SO<sub>4</sub>), filtered, and concentrated *in vacuo*. The

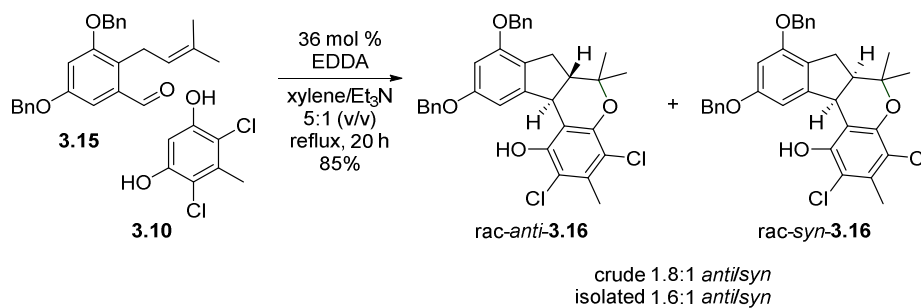


resulting crude solid was purified by column chromatography (5:2.5:92.5 NEt<sub>3</sub>:EtOAc:hexanes) to yield prenyl benzaldehyde **3.15** as a white solid (249 mg, 71%).



$R_f = 0.43$  (10:90 EtOAc:hexanes, stains blue/violet by *p*-anis dip stain). mp = 71–72 °C. <sup>1</sup>H NMR (600 MHz, Chloroform-*d*)  $\delta$  10.32 (s, 1H), 7.46 – 7.36 (m, 8H), 7.35 – 7.31i (m, 2H), 7.09 (d,  $J = 2.5$  Hz, 1H), 6.81 (d,  $J = 2.5$  Hz, 1H), 5.13 (tdd,  $J = 6.8, 2.9, 1.5$  Hz, 1H), 5.06 (d,  $J = 1.9$  Hz, 4H), 3.74 (d,  $J = 6.8$  Hz, 2H), 1.67 (d,  $J = 1.3$  Hz, 3H), 1.66 (d,  $J = 1.5$  Hz, 3H); <sup>13</sup>C NMR (151 MHz, Chloroform-*d*)  $\delta$  191.7, 157.9, 157.8, 136.5, 135.1, 131.7, 128.7, 128.6, 128.2, 128.0, 127.70, 127.68, 127.3, 123.4, 106.7, 104.1, 70.6, 70.3, 25.7, 22.9, 17.9; IR (ATR) 2909, 2867, 1672, 1600, 1285, 1153, 695 cm<sup>-1</sup>; HRMS (ESI)  $m/z$  calcd for C<sub>26</sub>H<sub>26</sub>O<sub>3</sub>Na [M + Na]<sup>+</sup> 409.1780, found 409.1772.

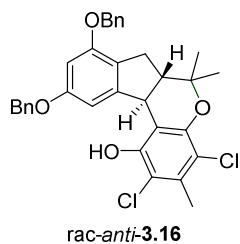
### Synthesis of Racemic Compound *anti*-**3.16** and *syn*-**3.16**



8,10-Bis(benzyloxy)-2,4-dichloro-3,6,6-trimethyl-6,6a,7,11b-tetrahydroindeno[2,1-*c*]-chromen-1-ol, *rac*-**3.16**, was prepared as follows: In the following order, prenyl benzaldehyde **3.15** (0.228 g, 0.595 mmol), 4,6-dichloro-5-methyl resorcinol **3.10** (0.574 g, 2.975 mmol), xylenes (12.0 mL), and EDDA (38.2 mg, 0.214 mmol) were added to a flame-dried flask equipped with a stir bar. The initial colorless heterogenous solution was stirred at 23 °C under a N<sub>2</sub> atmosphere before adding NEt<sub>3</sub> (2.41 mL, 17.3 mmol) in one portion via syringe. The reaction was heated at reflux

for 20 h and then cooled to 23 °C before it was placed in an ice-bath for 15 min. The resulting heterogenous solution was filtered. The filtrate was concentrated *in vacuo* to yield a crude brown-red oil containing indano[2,1-*c*]chromans rac-**3.16** as a 1.8:1 mixture of *anti/syn* diastereomers. Partial purification by column chromatography (5:95 EtOAc:hexanes) afforded indano[2,1-*c*]chromans rac-**3.16** as an inseparable 1.6:1 mixture of *anti/syn* diastereomers as a white solid (0.285 g, 85%, in about 90% purity).  $R_f = 0.40$  (10:90 EtOAc:hexanes; stains blue by *p*-anis dip stain). About 18 mg of this mixture was taken on directly to the methylation to obtain a yield for the two-step procedure.

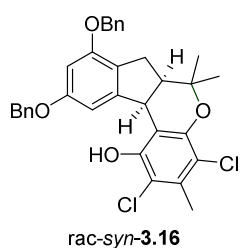
The majority of the sample was triturated with ether to afford a 16:1 *anti/syn* mixture of rac-**3.16**, free of other impurities, as a white solid (0.1474 g). The filtrate was concentrated to afford 0.1172 g of a waxy solid enriched in the *syn*-isomer of rac-**3.16**. Successive attempts to purify the waxy solid by silica gel chromatography with toluene and then 5:95 – 7.5:92.5 ether/hexanes were unsuccessful. Impurities were removed by two rounds of preparative TLC (80:20 toluene:hexane and then 10:90 acetone:hexane to afford a 2.5:1 *syn/anti* mixture of rac-**3.16** (94.7 mg). The combined yield of racemic *syn*- and *anti*-**3.16** from these two batches was 0.2421 g (72%).



rac-*anti*-**3.16** (major signals taken from a 16:1 *anti/syn* mixture):  $^1\text{H}$  NMR (500 MHz, Chloroform-*d*)  $\delta$  7.46 – 7.36 (m, 9H), 7.36 – 7.29 (m, 2H), 6.49 (d,  $J = 2.1$  Hz, 1H), 5.82 (s, 1H), 5.09 – 5.03 (m, 4H), 4.04 (dd,  $J = 10.9, 3.4$  Hz, 1H), 2.93 (dd,  $J = 12.5, 7.7$  Hz, 1H), 2.45 (s, 3H), 2.42 – 2.33 (m, 2H),

1.53 (s, 3H), 1.28 (s, 3H);  $^{13}\text{C}$  NMR (126 MHz, Chloroform-*d*)  $\delta$  159.0, 155.0, 150.0, 147.8, 146.3, 137.5, 137.1, 133.1, 128.6, 128.56, 128.5, 127.92, 127.89, 127.5, 127.40, 127.37, 127.3, 123.5, 115.5, 112.1, 110.8, 106.3, 98.7, 79.1, 70.7, 70.1, 55.5, 43.2, 28.0, 27.9, 20.3, 18.0; IR (ATR) 3482,

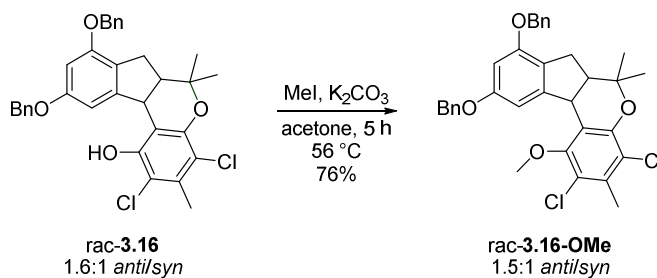
2979, 1593, 1151, 1082, 1038, 818, 780, 726, 700  $\text{cm}^{-1}$ ; HRMS (ESI)  $m/z$  calcd for  $\text{C}_{33}\text{H}_{30}\text{Cl}_2\text{O}_4\text{Na}$   $[\text{M} + \text{Na}]^+$  583.1419, found 583.1409.



**rac-syn-3.16** (major signals taken from a 1:2.5 *anti/syn* mixture):  $^1\text{H}$  NMR (500 MHz, Chloroform-*d*)  $\delta$  7.47 – 7.23 (m, 10H), 7.05 (d,  $J = 2.2$  Hz, 1H), 6.43 (d,  $J = 2.2$  Hz, 1H), 5.56 (s, 1H), 5.03 – 4.95 (m, 4H), 4.48 (d,  $J = 8.0$  Hz, 1H), 3.01 (dd,  $J = 15.8, 8.1$  Hz, 1H), 2.92 (d,  $J = 7.9$  Hz, 1H), 2.73 (q,  $J = 8.0$  Hz, 1H), 2.38 (s, 3H), 1.31 (s, 3H), 1.29 (s, 3H);  $^{13}\text{C}$  NMR (126 MHz, Chloroform-*d*)  $\delta$

158.8, 154.9, 148.8, 148.2, 146.1, 137.5, 137.1, 132.5, 128.5, 128.5, 127.9, 127.8, 127.4, 127.2, 123.1, 115.3, 112.3, 110.8, 105.5, 99.4, 77.3, 70.4, 69.9, 48.2, 41.2, 29.6, 25.5, 25.4, 17.7; IR (ATR) 3502, 2977, 2932, 1599, 1297, 1149, 1133, 1083, 734, 696  $\text{cm}^{-1}$ ; HRMS (ESI)  $m/z$  calcd for  $\text{C}_{33}\text{H}_{30}\text{Cl}_2\text{O}_4\text{Na}$   $[\text{M} + \text{Na}]^+$  583.1419, found 583.1417.

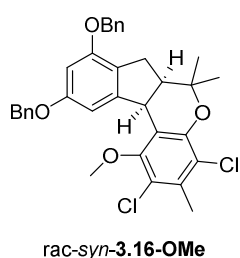
### Synthesis of Racemic Compound 3.16-OMe



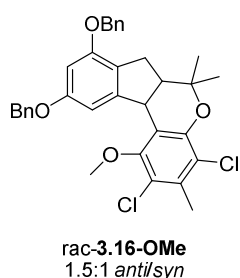
8,10-Bis(benzyloxy)-2,4-dichloro-1-methoxy-3,6,6-trimethyl-6,6a,7,11b-tetrahydroindeno[2,1-*c*]chromene, **rac-3.16-OMe**, was prepared as follows:

The crude mixture (90% pure) of 1.6:1 *anti/syn* of compound **rac-3.16** was subjected to methylation. Methyl iodide (91.0  $\mu\text{L}$ , 1.46 mmol) was added to a solution of indano[2,1-*c*]chromans **rac-3.16** (18.2 mg, 0.0324 mmol) and anhydrous  $\text{K}_2\text{CO}_3$  (101 mg, 0.729 mmol) in acetone (0.46 mL). The reaction was then heated at reflux and additional amounts of MeI (32.0

$\mu\text{L}$ , 0.518 mmol) were added every half hour for the reaction to achieve full consumption of starting material. At 3 h, the reaction was complete by TLC and was cooled to 23 °C. The reaction mixture was then filtered through a pipette silica plug and the plug washed with  $\text{CH}_2\text{Cl}_2$  ( $3 \times 2$  mL). The resulting organic layer was concentrated *in vacuo* and purified by column chromatography (3:97 EtOAc:hexanes) to afford partially purified indano[2,1-*c*]chromans rac-**3.16-OMe** as an inseparable 1.6:1 mixture of *anti/syn* diastereomers as a yellow oil (19.1 mg). Trituration with hexanes afforded an analytical sample of rac-*syn*-isomer **3.16-OMe** (2.3 mg) as a white solid. The filtrate, enriched in *anti*-isomer of rac-**3.16-OMe** was concentrated *in vacuo* (14 mg) and subjected to preparative TLC with 10:90 acetone:hexanes (developed twice) to afford an *anti/syn* mixture of indano[2,1-*c*]chromans rac-**3.16-OMe** as a fluffy white solid (11.9 mg). The batches were combined to afford a 1.5:1 *anti/syn* mixture of rac-**3.16-OMe** (14.2 mg, 76%).



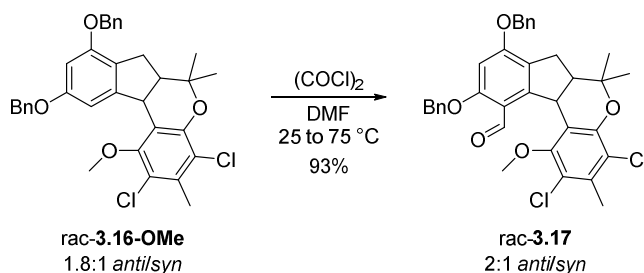
rac-*syn*-**3.16-OMe**:  $^1\text{H}$  NMR (600 MHz, Chloroform-*d*)  $\delta$  7.45 – 7.28 (m, 10H), 7.05 (d,  $J = 2.1$  Hz, 1H), 6.41 (d,  $J = 2.0$  Hz, 1H), 5.06 – 4.93 (m, 4H), 4.49 (d,  $J = 8.0$  Hz, 1H), 3.85 (s, 3H), 3.04 (dd,  $J = 15.9, 8.0$  Hz, 1H), 2.91 (dd,  $J = 15.9, 6.5$  Hz, 1H), 2.78 (td,  $J = 8.0, 6.6$  Hz, 1H), 2.44 (s, 3H), 1.54 (s, 3H), 1.37 (s, 3H), 1.18 (s, 3H);  $^{13}\text{C}$  NMR (151 MHz, Chloroform-*d*)  $\delta$  159.3, 154.9, 153.3, 148.6, 146.5, 137.2, 137.1, 134.2, 128.5, 127.88, 127.85, 127.8, 127.3, 122.8, 120.3, 119.3, 117.9, 104.7, 99.5, 77.5, 70.4, 69.9, 59.8, 47.6, 41.5, 29.9, 25.9, 24.8, 17.8.



1.5:1 *anti/syn*- rac-**3.16-OMe**:  $R_f = 0.44$  (10:90 EtOAc:hexanes, stains blue/violet by *p*-anis dip stain).  $^1\text{H}$  NMR (600 MHz, Chloroform-*d*)  $\delta$  7.58 – 7.55 (m, 1.5H), 7.49 – 7.28 (m, 25H), 7.05 (d,  $J = 2.1$  Hz, 1H), 6.51 (d,  $J = 2.1$  Hz, 1.5H), 6.41 (d,  $J = 2.1$  Hz, 1H), 5.08 – 5.03 (m, 6H), 5.03 – 4.96 (m, 4H), 4.49 (d,  $J = 8.0$  Hz, 1H), 4.05 (d,  $J = 12.6$  Hz, 1.5H), 3.85 (s, 3H), 3.61 (s, 4.5H), 3.04 (dd,  $J$

= 15.9, 8.1 Hz, 1H), 2.94 (dd,  $J = 13.5, 5.8$  Hz, 1.5H), 2.93 – 2.87 (m, 1H), 2.81 – 2.74 (m, 1H), 2.48 (s, 4.5H), 2.44 (s, 3H), 2.43 – 2.37 (m, 1.5H), 2.34 (td,  $J = 12.2, 5.7$  Hz, 1.7H), 1.53 (s, 4.5H), 1.37 (s, 3H), 1.32 (s, 4.5H), 1.18 (s, 3H);  $^{13}\text{C}$  NMR (151 MHz, Chloroform-*d*)  $\delta$  159.3, 159.28, 155.1, 154.9, 153.3, 152.7, 149.6, 148.6, 146.5, 145.6, 137.3, 137.2, 137.15, 137.1, 134.6, 134.2, 128.6, 128.54, 128.52, 128.51, 127.9, 127.88, 127.85, 127.8, 127.7, 127.4, 127.3, 123.2, 122.8, 120.28, 120.26, 119.5, 119.3, 118.0, 117.9, 105.4, 104.7, 99.5, 99.1, 79.1, 77.5, 70.4, 70.39, 70.0, 69.9, 59.8, 59.75, 55.5, 47.6, 43.5, 41.5, 29.9, 28.1, 27.9, 25.9, 24.8, 20.6, 18.0, 17.8; IR (ATR) 3031, 2973, 2931, 2871, 2359, 2343, 1136, 1086, 734, 695  $\text{cm}^{-1}$ ; HRMS (ESI)  $m/z$  calculated for  $\text{C}_{34}\text{H}_{32}\text{Cl}_2\text{O}_4\text{Na}$   $[\text{M} + \text{Na}]^+$  597.1575, found 597.1554.

### Synthesis of Racemic Compound 3.17



8,10-Bis(benzyloxy)-2,4-dichloro-1-methoxy-3,6,6-trimethyl-6,6a,7,11b-tetrahydroindeno[2,1-*c*]-chromene-11-carbaldehyde, **rac-3.17**, was prepared as follows:

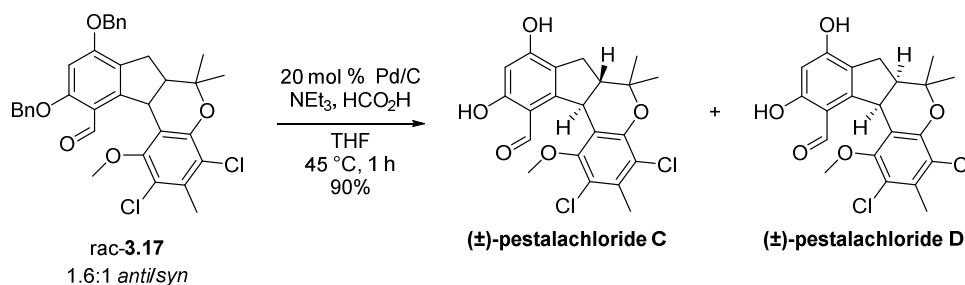
To a flame-dried flask equipped with a stir-bar was added anhydrous 1,2-dichloroethane (9.15 mL) and oxalyl chloride (0.196 mL, 2.28 mmol). The solution was cooled in an ice-water bath. Anhydrous DMF (0.226 mL, 2.92 mmol) was then added dropwise. Gas evolution occurred, and a white precipitate formed. The solution was stirred for 30 min at 23 °C before adding 1.8:1 *anti/syn* mixture of indano[2,1-*c*]chromans **rac-3.16-OMe** (0.194 g, 0.336 mmol) as a solution in  $\text{CH}_3\text{CN}$  (0.5 M). Additional  $\text{CH}_3\text{CN}$  (1.92 mL) was used to transfer any remaining compound to

the reaction flask. With a condenser attached, the flask was heated to 75 °C while stirring. After 4 to 5 h at 75 °C, the resulting orange solution was quenched by addition of water (11.0 mL) and further vigorous stirring at 75 °C for 1 h. The reaction flask was then cooled to 23 °C and the mixture transferred to a separatory funnel. The mixture was extracted with EtOAc (3 × 30 mL) and the combined organic extracts were washed with water (3 × 50 mL), dried (Na<sub>2</sub>SO<sub>4</sub>), filtered, and concentrated *in vacuo*. The crude material was purified by column chromatography (15:85 EtOAc:hexanes) to afford carbaldehyde rac-**3.17** as an inseparable 3:1 mixture of *anti/syn* isomers as a beige solid (0.115 g, 56%) and an impure fraction that was further purified (10:90 – 20:80 EtOAc:hexanes) to afford additional carbaldehyde rac-**3.17** as an inseparable 1.2:1 mixture of *anti/syn* isomers as beige solid (74.4 mg, 37%).  $R_f = 0.34$  (*anti*) (15:85 EtOAc:hexanes).  $R_f = 0.41$  (*syn*) (15:85 EtOAc:hexanes). Both stain blue by *p*-anis dip stain. The total yield is 189.4 mg (93%) of *anti/syn* isomers in a 2:1 ratio This reaction was run multiple times; final *anti/syn* ratios varied from 1.6-2.0:1 after chromatography due to losses in chromatography.

1.2:1 *anti/syn*- rac-**3.17**: <sup>1</sup>H NMR (600 MHz, Chloroform-*d*) δ 10.51 (s, 1.2H), 10.50 (s, 1H), 7.46 – 7.29 (m, 21H), 6.53 (s, 1H), 6.36 (s, 1H), 5.20 (d,  $J = 6.7$  Hz, 1H), 5.21 – 4.93 (m, 9H), 4.41 (d,  $J = 11.9$  Hz, 1.2H), 3.56 (s, 3H), 3.06 – 2.98 (m, 5H), 2.86 – 2.80 (m, 1H), 2.80 – 2.70 (m, 2H), 2.59 (ddd,  $J = 15.0, 11.6, 1.7$  Hz, 1.2H), 2.43 (s, 3.4H), 2.38 (s, 3H), 2.20 (td,  $J = 11.8, 8.4$  Hz, 1.2H), 1.53 (s, 3.6H), 1.52 (s, 3H), 1.40 (s, 3.5H), 1.36 (s, 3H); <sup>13</sup>C NMR (151 MHz, Chloroform-*d*) δ 191.5, 189.1, 161.7, 161.2, 158.6, 158.4, 154.5, 149.4, 148.7, 148.6, 147.2, 143.3, 136.33, 136.30, 136.2, 136.0, 134.8, 132.7, 128.74, 128.72, 128.6, 128.4, 128.24, 128.2, 128.1, 127.41, 127.4, 127.30, 127.26, 125.8, 124.9, 122.4, 120.9, 120.1, 119.2, 119.02, 119.0, 115.7, 96.8, 96.6, 82.2, 75.6, 71.3, 71.26, 70.2, 70.0, 61.6, 61.1, 57.1, 50.3, 47.0, 39.1, 29.8, 28.4, 27.8, 27.0, 24.5, 23.6, 17.9, 17.8; IR (ATR) 3064, 3031, 2974, 2928, 2857, 2359, 2343, 1678, 1589, 1455,

1385, 1335, 1321, 1119, 1096, 736, 697  $\text{cm}^{-1}$ ; HRMS (ESI)  $m/z$  calcd for  $\text{C}_{35}\text{H}_{32}\text{Cl}_2\text{O}_5$   $[\text{M} + \text{Na}]^+$  625.1525, found 625.1518.

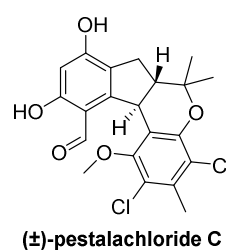
### Synthesis of ( $\pm$ )-Pestalachloride C and ( $\pm$ )-Pestalachloride D



To a Schlenk tube was added a 1.6:1 mixture of *anti/syn* carbaldehyde **rac-3.17** (18.8 mg, 31.1  $\mu\text{mol}$ ) and THF (0.207 mL). The solution was stirred until all the carbaldehyde **rac-3.17** was dissolved. Then,  $\text{NEt}_3$  (17.4  $\mu\text{L}$ , 0.124 mmol) was added directly to the solution. In a similar fashion, 88% formic acid solution (7.05  $\mu\text{L}$ , 0.164 mmol) was added followed by 10% Pd/C (6.63 mg, 6.22  $\mu\text{mol}$ ). The tube was sealed, heated at 35 °C, and stirred. The temperature was increased to 45 °C over 10 min and the reaction was left to stir until deemed complete by TLC (~40 min to 1 h). Prior to taking a small sample for TLC, the tube was cooled to 23 °C. (When taking a TLC sample, gas evolution was observed. In instances where no gas was observed upon taking a TLC sample, no debenzoylation was observed). Upon reaction completion, the reaction mixture was diluted with EtOAc and filtered through a pad of silica gel and Celite<sup>®</sup>. The pad was washed with EtOAc (3  $\times$  15 mL) and the resulting organic layer was concentrated *in vacuo* to yield a crude mixture of ( $\pm$ )-pestalachlorides C and D in a 1.6:1 ratio. Purification by flash chromatography (15:85 EtOAc:hexanes) afforded an inseparable 1.8:1 mixture of ( $\pm$ )-pestalachloride C and ( $\pm$ )-pestalachloride D as a white solid (11.9 mg, 90%). On a 0.12 mmol scale the yield of pestalachlorides C and D was 83%.

Separation of (±)-pestalachlorides C and D was achieved by preparative reverse-phase HPLC using a Rainin Dynamax SD-200 solvent delivery system: stationary phase – Phenomenex Luna 5 μm C18(2) 100 Å 250 x 21.20 mm column; mobile phase – isocratic 10:90 H<sub>2</sub>O/MeOH at a flow rate of 10 mL/min; peak detection was performed using a Dynamax UV-1 variable wavelength UV/Visible absorbance detector at a wavelength of 254 nm. Spectral data is consistent with that previously reported for isolated (±)-pestalachloride C in deuterated acetone and in deuterated chloroform,<sup>11</sup> and for isolated (±)-pestalachloride D in deuterated chloroform.<sup>11a</sup>

### Pestalachloride C Characterization



(±)-pestalachloride C:  $R_f = 0.22$  (20:80 EtOAc:hexanes). Stains violet by *p*-anis dip stain. <sup>1</sup>H NMR (600 MHz, Chloroform-*d*) δ 11.91 (s, 1H), 9.77 (s, 1H), 6.32 (s, 1H), 5.65 (s, 1H), 4.26 (d,  $J = 11.6$  Hz, 1H), 3.13 (s, 3H), 3.01 (dd,  $J = 14.6, 8.4$  Hz, 1H), 2.65 (ddd,  $J = 14.6, 11.3, 1.8$  Hz, 1H), 2.48 (s, 3H), 2.30 (td,  $J = 11.5, 8.4$  Hz, 1H), 1.57 (s, 3H), 1.45 (s, 3H); <sup>13</sup>C NMR (151 MHz, Chloroform-*d*) δ 193.2, 164.2, 158.3, 149.4, 149.1, 145.2, 133.9, 127.0, 123.1, 122.4, 121.4, 113.1, 102.5, 82.2, 61.0, 57.7, 45.3, 29.7, 28.2, 23.7, 17.9; IR (ATR) 3308 (br), 3080 (br), 2927, 1636, 1615, 1447, 1372, 1272, 1218, 1136, 1095 cm<sup>-1</sup>; HRMS (ESI)  $m/z$  calcd for C<sub>21</sub>H<sub>20</sub>Cl<sub>2</sub>O<sub>5</sub>Na [M + Na]<sup>+</sup> 445.0586, found 447.0571.

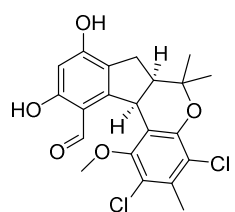
(±)-pestalachloride C: <sup>1</sup>H NMR (600 MHz, Acetone-*d*<sub>6</sub>) δ 11.94 (s, 1H), 9.78 (s, 1H), 6.35 (s, 1H), 4.43 (d,  $J = 11.7$  Hz, 1H), 3.13 (s, 3H), 3.08 (dd,  $J = 14.8, 8.4$  Hz, 1H), 2.65 (ddd,  $J = 14.8, 11.3, 1.8$  Hz, 1H), 2.46 (s, 3H), 2.43 (ddd,  $J = 11.5, 11.46, 8.4$  Hz, 1H), 1.59 (s, 3H), 1.45 (s, 3H); <sup>13</sup>C NMR (151 MHz, Acetone-*d*<sub>6</sub>) δ 194.2, 165.3, 161.5, 150.9, 150.3, 146.0, 133.8, 129.0, 124.3, 123.0, 121.6, 113.2, 102.5, 83.6, 61.6, 57.9, 46.0, 30.0, 29.1, 23.8, 18.0.



### Comparison of Natural and Synthetic Pestalachloride C

(±)-pestalachloride C (CDCl <sub>3</sub> )		(±)-pestalachloride C (acetone- <i>d</i> <sub>6</sub> )	
natural product δ <sub>H</sub> (J in Hz) <sup>a,11a</sup>	synthetic δ <sub>H</sub> (J in Hz) <sup>b</sup>	natural product δ <sub>H</sub> (J in Hz) <sup>c,11b</sup>	synthetic δ <sub>H</sub> (J in Hz) <sup>d</sup>
11.91, brs	11.91, s	11.92, s	11.94, s
9.76, s	9.77, s	9.76, s	9.78, s
6.32, s	6.32, s	6.34, s	6.35, s
–	5.65, brs	–	–
4.26 d (11.5)	4.26, d (11.6)	4.41, d (12)	4.43, d (11.7)
3.13, s	3.13, s	3.11, s	3.13, s
3.01, dd (14.6, 8.4)	3.01, dd (14.6, 8.4)	3.06, dd (15, 8.0)	3.08, dd (14.8, 8.4)
2.64 ddd (14.6, 11.3, 1.4)	2.65, ddd (14.6, 11.3, 1.8)	2.64, ddd (15, 11, 1.5)	2.65, ddd (14.8, 11.3, 1.8)
2.48, s	2.48, s	2.45, s	2.46, s
2.30 ddd (11.5, 11.3, 8.4)	2.3, td (11.5, 11.4, 8.4)	2.42, ddd (12, 11, 8.0)	2.43, ddd (11.5, 11.4, 8.4)
1.57, s	1.57, s	1.58, s	1.59, s
1.44, s	1.45, s	1.44, s	1.45, s
natural product δ <sub>C</sub>	synthetic δ <sub>C</sub>	natural product δ <sub>C</sub>	synthetic δ <sub>C</sub>
193.1	193.2	194.2	194.2
164.3	164.2	165.2	165.3
158.6	158.3	161.4	161.5
149.4	149.4	150.8	150.9
149.2	149.1	150.2	150.3
145.1	145.2	146.0	146.0
133.9	133.9	133.8	133.8
127.0	127.0	129.0	129.0
123.1	123.1	124.2	124.3
122.5	122.4	123.0	123.0
121.4	121.4	121.6	121.6
113.1	113.1	113.2	113.2
102.5	102.5	102.5	102.5
82.2	82.2	83.5	83.6
61.0	61.0	61.5	61.6
57.7	57.7	57.9	57.9
45.3	45.3	45.9	46.0
29.7	29.7	29.6	30.0
28.2	28.2	29.0	29.1
23.7	23.7	23.8	23.8
17.9	17.9	17.9	18.0
<sup>a</sup> Recorded at 400 MHz for <sup>1</sup> H and 100 MHz for <sup>13</sup> C		<sup>c</sup> Recorded at 500 MHz for <sup>1</sup> H and 100 MHz for <sup>13</sup> C	
<sup>b</sup> Recorded at 600 MHz for <sup>1</sup> H and 151 MHz for <sup>13</sup> C		<sup>b</sup> Recorded at 600 MHz for <sup>1</sup> H and 151 MHz for <sup>13</sup> C	

## Pestalachloride D Characterization



(±)-pestalachloride D:  $R_f = 0.20$  (20:80 EtOAc:hexanes). Stains purple by *p*-anis dip stain.  $^1\text{H}$  NMR (600 MHz, Chloroform-*d*)  $\delta$  11.75 (s, 1H), 10.22 (s, 1H), 6.20 (s, 1H), 5.36 (brs, 1H), 4.72 (d,  $J = 6.1$  Hz, 1H), 3.59 (s, 3H), 2.84 – 2.73 (m, 3H), 2.42 (s, 3H), 1.56 (s, 3H), 1.39 (s, 3H);  $^{13}\text{C}$  NMR (151 MHz, Chloroform-*d*)  $\delta$  193.5, 163.6, 158.4, 154.0, 150.1, 148.6, 135.7, 121.4, 120.1, 119.5, 114.0, 113.1, 102.1, 75.5, 60.3, 51.1, 38.8, 27.4, 26.9, 24.7, 18.0; IR (ATR) 3313, 2925, 1634, 1558, 1540, 1369, 1292, 1244, 1215, 1164, 1153, 1139, 1093  $\text{cm}^{-1}$ ; HRMS (ESI)  $m/z$  calcd for  $\text{C}_{21}\text{H}_{20}\text{Cl}_2\text{O}_5\text{Na}$  [ $\text{M} + \text{Na}$ ] $^+$  445.0586, found 447.0575.

## Comparison of Natural and Synthetic Pestalachloride D

(±)-pestalachloride D ( $\text{CDCl}_3$ )			
natural product $\delta_{\text{H}}$ ( $J$ in Hz) <sup>a,b11a</sup>	synthetic $\delta_{\text{H}}$ ( $J$ in Hz) <sup>a,c</sup>	natural product $\delta_{\text{C}}$	synthetic $\delta_{\text{C}}$
11.74, brs	11.75, s	193.4	193.5
10.21, s	10.22, s	163.6	163.6
6.20, s	6.20, s	158.5	158.4
–	5.36, brs	154.0	154.0
4.71, d (6.0)	4.72, d (6.1)	150.0	150.1
3.59, s	3.59, s	148.5	148.6
2.81, m (overlapped signal)	2.79, m	135.6	135.7
2.81, m (overlapped signal)	2.79, m	121.4	121.4
2.42, s	2.42, s	120.0	120.1
1.55, s	1.56, s	119.4	119.5
1.38, s	1.39, s	114.0	114.0
		112.9	113.1
		102.1	102.1
		75.6	75.5
		60.2	60.3
		51.1	51.1
		38.7	38.8
		27.5	27.4
		26.8	26.9
		24.6	24.7
		17.9	18.0

<sup>a</sup> Recorded at 400 MHz for  $^1\text{H}$  and 100 MHz for  $^{13}\text{C}$

<sup>b</sup> Recorded at 600 MHz for  $^1\text{H}$  and 151 MHz for  $^{13}\text{C}$

# HPLC Chromatogram for Pestalachlorides C and D

Analytical Column Sample Chromatogram:

Date: Tue, Oct 30, 2018 10:04 PM

Data: VA-4-130-C1\_analytical\_90MeOH\_2

Sample: VA-4-130-C1

Stationary Phase: Phenomenex Luna C18(2) 5 micron

250x4.6 mm

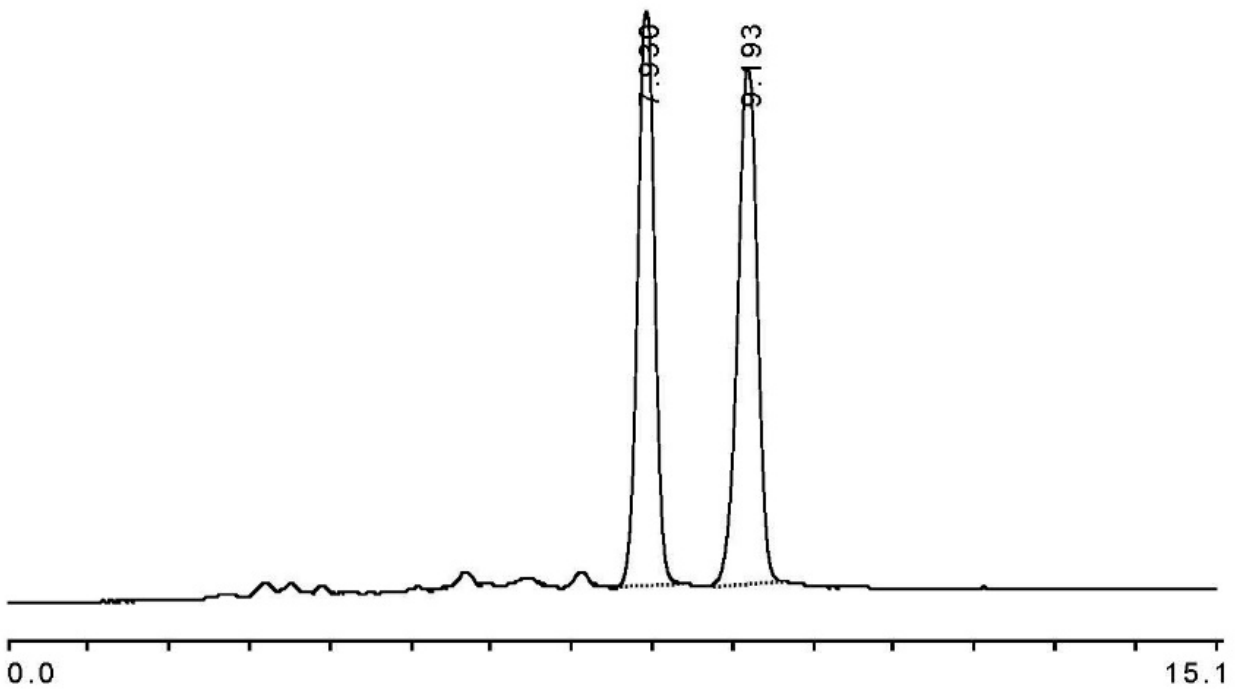
Mobile Phase: 10%H2O/90%MeOH 0.8mL/min 2.01kpsi

Method: analytical isocratic 90\_MeOH

Inject Vol: 25

Sampling Int: 0.1 Seconds

Data:



Analysis: Channel A

Peak No.	Time	Type	Height(μV)	Area(μV-sec)	Area%
1	7.930	N	42572	535391	48.224
2	9.193	N	38105	574825	51.775
Total Area				1110216	99.999

Preparative Column Sample Chromatogram:

Date: Fri, Aug 10, 2018 7:20 PM

Data: VA-4-130\_iso\_90\_MeOH

Sample: VA-4-130-C1

Phenomenex Luna C18(2) 100 Angstrom 5u 250x21.4 mm

Mobile Phase: Isocratic 10 H2O/ 90 MeOH 10mL/min

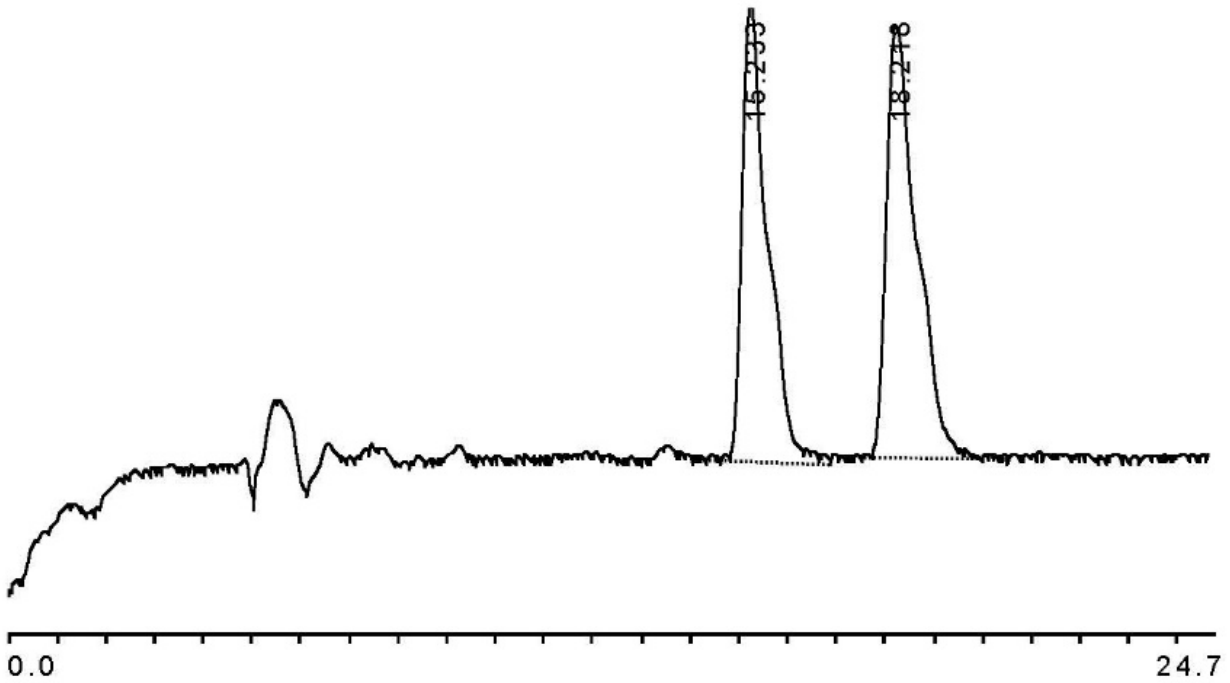
Processing File: VA-4-130-C1-an-75

Method: prep isocratic 90\_MeOH

Inject Vol: 50

Sampling Int: 0.1 Seconds

Data:



Analysis: Channel A

Peak No.	Time	Type	Height( $\mu$ V)	Area( $\mu$ V-sec)	Area%
1	15.233	* N	2578	85126	47.065
2	18.218	* N	2436	95743	52.934
Total Area				180869	99.999

## Biological Assay – Inhibitory effect of Pestalachlorides C and D on A375 Human Melanoma Cells

**Method:** A375 melanoma cells were seeded in a 96-well plate on day 1. Cells were treated with Pestalachloride C or Pestalachloride D on day 2 at concentrations of serial dilution (0.125, 0.25, 0.5, 1.0, 2.0, 4.0, 8.0, 16.0, 32.0 and 64.0 mM) for three days. Cells treated with 0.1% DMSO was used as control. 72 hours after incubation with drugs, cells were subjected to MTT assay.<sup>12</sup> Absorbance at 570 nm with 650 nm reference absorbance (subtraction) were read by a plate reader (BioTek Synergy 2) as survival indices. MTT readings were normalized to control cells. Survival curve was based on normalized survival fractions and plotted by GraphPad Prism 6 software.

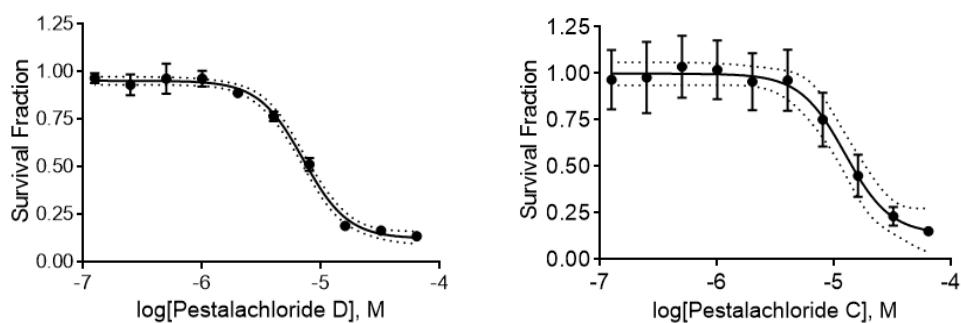


**Figure legend:** Quadruplicate A375 cells were seeded and treated with various concentrations of Pestalachloride C or Pestalachloride D for three days. Relative survival fractions were calculated and plotted. The dotted lines indicate 95% confidence intervals of the true means of the regression. The  $IC_{50}$ s for Pestalachloride C and Pestalachloride D are  $12.4 \pm 3.4$  mM and  $7.1 \pm 0.6$  mM, respectively. Left Panel, Pestalachloride D; Right panel: Pestalachloride C. Note: this is to test whether these drugs can kill melanoma cells. Both show relatively good killing effect.

## References

1. Pangborn, A. B.; Giardello, M. A.; Grubbs, R. H.; Rosen, R. K.; Timmers, F. J. Safe and convenient procedure for solvent purification. *Organometallics* **1996**, *15*, 1518–1520.
2. Armarego, W. L. F.; Chai, C. L. L., *Purification of Laboratory Chemicals*. 5<sup>th</sup> ed.; Elsevier: 2013; p 608.
3. Rhodium Ethylenediammonium diacetate. <https://erowid.org/archive/rhodium/chemistry/edda.html> (accessed June 16).
4. Roberts, K. M.; Tormos, J. R.; Fitzpatrick, P. F. Characterization of unstable products of flavin- and pterin-dependent enzymes by continuous-flow mass spectrometry. *Biochemistry* **2014**, *53*, 2672–2679.
5. Cossy, J.; Tresnard, L.; Pardo, D. G. Radical Cyclizations – Synthesis of  $\gamma$ -Lycorane. *Eur. J. Org. Chem.* **1999**, *1999*, 1925–1933.
6. Ruiz, J.; Ardeo, A.; Ignacio, R.; Sotomayor, N.; Lete, E. An efficient entry to pyrrolo[1,2-*b*]isoquinolines and related systems through Parham cyclisation. *Tetrahedron* **2005**, *61*, 3311–3324.
7. Gutman, E. S.; Arredondo, V.; Van Vranken, D. L. Cyclization of  $\eta^3$ -Benzylpalladium Intermediates Derived from Carbene Insertion. *Org. Lett.* **2014**, *16*, 5498–5501.
8. Liao, Y.-R.; Kuo, P.-C.; Huang, S.-C.; Liang, J.-W.; Wu, T.-S. An efficient total synthesis of Benzocamphorin H and its anti-inflammatory activity. *Tetrahedron Lett.* **2012**, *53*, 6202–6204.
9. Carreras, J.; Gopakumar, G.; Gu, L.; Gimeno, A.; Linowski, P.; Petuškova, J.; Thiel, W.; Alcarazo, M. Polycationic Ligands in Gold Catalysis: Synthesis and Applications of Extremely  $\pi$ -Acidic Catalysts. *J. Am. Chem. Soc.* **2013**, *135*, 18815–18823.
10. Kaiser, F.; Schmalz, H.-G. Synthetic analogues of the antibiotic pestalone. *Tetrahedron* **2003**, *59*, 7345–7355.
11. (a) Wei, M. Y.; Li, D.; Shao, C. L.; Deng, D. S.; Wang, C. Y. ( $\pm$ )-Pestalachloride D, an antibacterial racemate of chlorinated benzophenone derivative from a soft coral-derived fungus *Pestalotiopsis* sp. *Mar Drugs* **2013**, *11*, 1050–1060; (b) Li, E.; Jiang, L.; Guo, L.; Zhang, H.; Che, Y. Pestalachlorides A–C, antifungal metabolites from the plant endophytic fungus *Pestalotiopsis adusta*. *Bioorg. Med. Chem.* **2008**, *16*, 7894–7899.
12. Liu, F.; Singh, A.; Yang, Z.; Garcia, A.; Kong, Y.; Meyskens, F. L., Jr. MiTF links Erk1/2 kinase and p21 CIP1/WAF1 activation after UVC radiation in normal human melanocytes and melanoma cells. *Molecular Cancer* **2010**, *9*, 214.

## Chapter 4

### **Enantioselective Palladium-Catalyzed Carbene Insertion into the N–H Bonds of Aromatic Heterocycles**

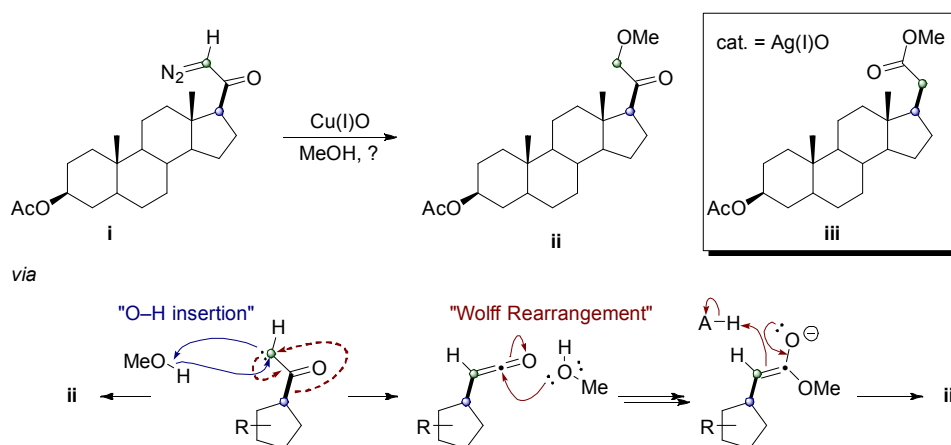
#### **Early History of Metal-Catalyzed Carbene Insertions of Diazo Compounds into Heteroatom–H Bonds (X–H)**

Catalytic carbene insertion processes are an attractive method to form new bonds between heteroatoms and  $sp^3$ -hybridized carbon (e.g., C–O and C–N). The process connects two different molecules, by way of a newly formed electrophilic-metal-carbene coupling partner, and results in a newly formed  $sp^3$  hybridized carbon linkage center. This has been an attractive method to functionalize X–H bonds of compounds such as alcohols and nitrogen-containing heterocycles, and is an area of continuous investigation. Diazo compounds have long been used to generate metal-carbene intermediates that are utilized in various organic transformations<sup>1</sup> such as C–X bond formation.<sup>2</sup>

Early formal carbene insertions into the X–H bonds of heteroatoms were achieved by thermal decomposition and photochemical treatment of diazo compounds.<sup>2a</sup> In 1902, Wolff discovered that photochemical treatment of diazo compounds afforded rearrangement products resulting from ketene formation<sup>3</sup> and later reported silver-ion catalyzed the rearrangements of diazoketones.<sup>4</sup> This rearrangement is known as the Wolff rearrangement.

In 1906, Silberrad and Roy demonstrated the first transition-metal-catalyzed decomposition of diazocarbonyl compounds utilizing copper dust – opening new chemical space for transformations involving metals and diazo compounds.<sup>5</sup> In 1950, Casanova and Reichstein

reported the first formal carbene insertion into a heteroatom–H bond (Scheme 4-1). After treating steroidal diazoketone **i** with copper oxide, they observed methoxyketone **ii** resulting from O–H insertion; on the other hand, Wolff rearrangement products were obtained when silver oxide was used.<sup>6</sup>

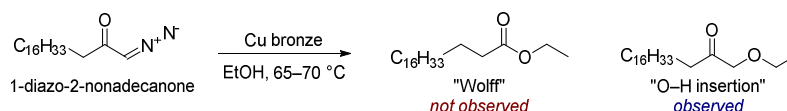


**Scheme 4-1.** First synthetic transformation involving transition-metal-catalyzed insertion of diazo compounds into O–H bond.

The first detailed report and systematic study on insertion into X–H bonds was by Yates in 1952 when he inadvertently stumbled upon non-rearranged products from a copper-catalyzed diazo decomposition.<sup>7</sup> Yates was trying to find a more efficient catalyst than silver oxide for the decomposition of diazo compounds in the Wolff rearrangement reaction and was interested in copper. Copper had been suggested as a suitable replacement for silver to decompose diazoketones with rearrangement, but few instances were disclosed in the literature. Yates notes that in the few cases where copper had been utilized to effect the Wolff rearrangement, “either the yields have been abnormally low or the conditions have been abnormally forced.” At the time, the low yields and harsh conditions was most likely due to catalytic X–H insertion side-reactions as a major product, and other catalytic side-reactions of a copper-carbene complexes, such as cross-couplings,

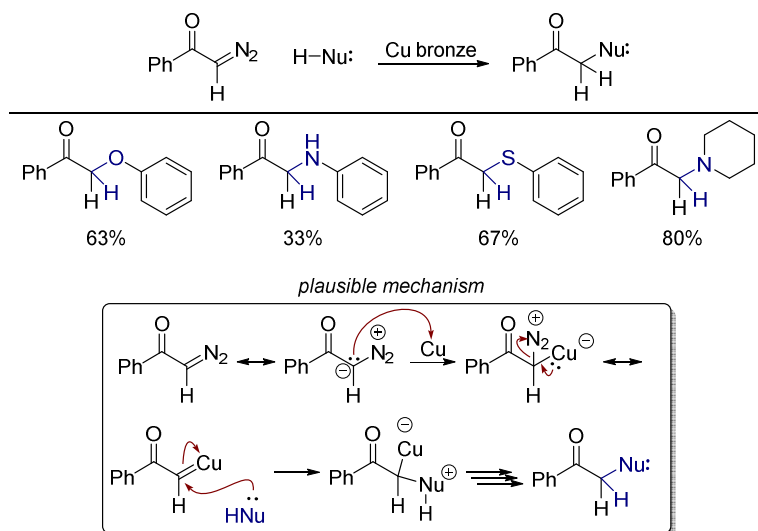


cyclopropanation, and C–H insertion.<sup>8</sup> In his study to investigate the copper-bronze catalyzed decomposition of 1-diazo-2-nonadecanone in ethanolic solution, he found copper to increase the rate of diazo decomposition, but obtained 1-ethoxy-2-nonadecanone instead of the Wolff rearrangement product ethyl nonadecanoate (Scheme 4-2).



**Scheme 4-2.** Copper-bronze-catalyzed investigation of diazo decomposition by Yates leads to products resulting from O–H insertion.

Once Yates established that the products from the copper-catalyzed decomposition of diazoketones in alcoholic solvents involved formal carbene insertions into the O–H bonds of the solvent instead of Wolff rearrangement, he investigated this heterogeneous reaction in the presence of other substrates such as phenol, thiophenol, aniline, and piperidine using  $\alpha$ -diazacetophenone as the carbene precursor (Scheme 4-3). In each of the cases studied, no Wolff rearrangement product was observed, prompting the authors to formulate a proposed mechanism involving carbene intermediates followed by an insertion (Scheme 4-3). It is likely the carbene intermediate exists as a copper-carbene complex following the copper-catalyzed decomposition of diazo compound. The copper-carbene complex can then undergo an insertion reaction with the nucleophile.

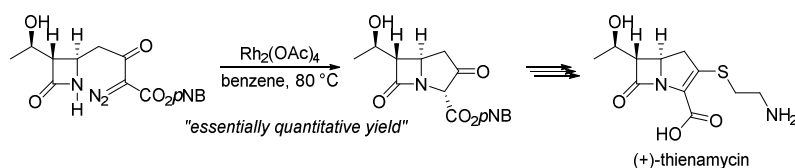


**Scheme 4-3.** Copper-catalyzed insertion of  $\alpha$ -diazoacetophenone into the X–H bonds of aromatic heterocycles and piperidine. Mechanistic consideration proposed.

This report by Yates was first to associate a reaction mechanism involving carbene-type intermediates to explain the formation of these unrearranged products. Following this seminal work, studies on copper-catalyzed decomposition of diazo compounds blossomed – Takebayashi and co-workers reported the reactions in different alcoholic solvents of diazoketones with various metal chelates;<sup>9</sup> Saegusa and co-workers examined the reactions of thiols, alcohols, and amines with diazo compounds by cupric chloride, cuprous chloride, or cuprous cyanide;<sup>10</sup> and Nozaki, Noyori and co-workers investigated copper-catalyzed decomposition of diazo compounds in asymmetric reactions which led them to propose a copper-stabilized carbene intermediate.<sup>11</sup>

The field of catalytic X–H insertion reactions took off when Teyssié, Hubert and co-workers reported their findings on rhodium(II) acetate as a highly efficient catalyst for the decomposition of ethyl diazoacetate and its facile O–H insertion reactions, which, shortly thereafter, they expanded to insertion into S–H and N–H bonds.<sup>12</sup> The utility of this transformation was convincingly demonstrated by workers at Merck in the industrial synthesis of the carbapen-2-

em ring system of (+)-thienamycin in which the key step is an intramolecular rhodium-catalyzed carbene insertion into an amide N–H bond (Scheme 4-4).<sup>13</sup> This was an instrumental accomplishment as it demonstrated the highly efficient transformation as applied to generating strained ring systems and its application in a total synthesis. Rapoport and co-workers then elegantly applied this intramolecular variant to the synthesis of four-, five-, and six- membered oxygen, sulfur, and nitrogen heterocycles.<sup>14</sup>



**Scheme 4-4.** Practical application of N–H insertion catalyzed by rhodium(II) acetate.

### General Mechanistic Model of Metal-Catalyzed Insertion of Diazo Compounds into X–H Bonds

The general, simplified mechanism of heteroatom X–H insertion of carbene derived from a diazo compound catalyzed by a metal is depicted in Figure 4-1. Depending on the identity of the metal, the catalytic cycle can vary in the rate-determining step, or even the mechanism of insertion. In general, however, it is typically accepted that diazo compound first attacks the metal catalyst (i) to generate metal complex (ii). The metal will then catalyze the decomposition of the diazo compound by extrusion of nitrogen gas (step B) resulting in metal-carbene intermediate iii.

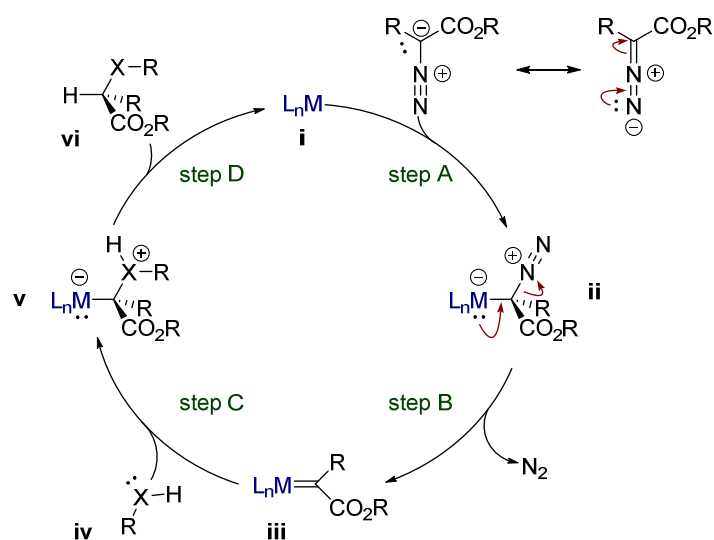


**Figure 4-1.** General mechanism of X–H insertion of diazo compound catalyzed by palladium(0), rhodium(II), copper(I) and other metals.

A heteroatom nucleophile containing an X–H bond then reacts with the metal-carbene complex to generate a zwitterionic C-bound enolate **v**. This zwitterionic intermediate may also be present as an O-bound enolate, or the metal may even dissociate from the enolate to afford a free ylide (Figure 4-2). The dominant species varies, but in general, proton transfer and metal dissociation to regenerate the catalyst affords the formal insertion product **vi**.

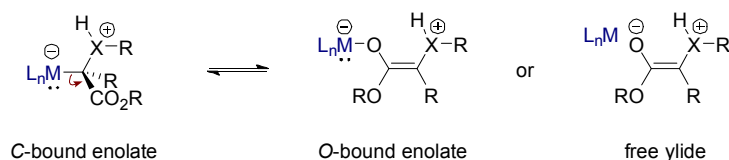


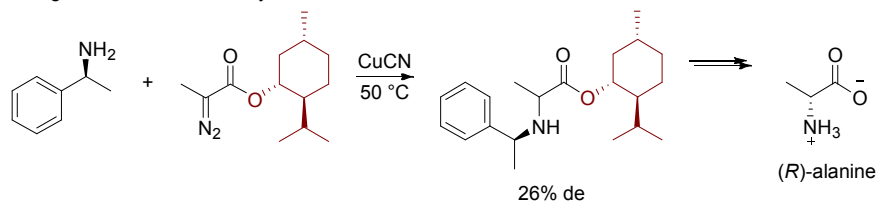
**Figure 4-2.** Depictions of possible ylide intermediates in metal catalyzed X–H insertion.

A review by Gillingham and Fei highlights mechanistic considerations for this insertion process involving copper(I), rhodium(II), and iron(III) metal catalysts.<sup>15</sup> An enantioselective or diastereoselective method can be envisioned for this insertion process by way of chiral additives, chiral substrates or auxiliaries, or chiral ligands.

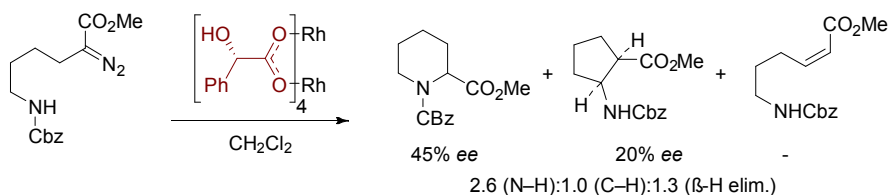
## Asymmetric Metal-Catalyzed Insertions of Diazo Compounds into X–H Bonds

The earliest report of an asymmetric insertion reaction, by way of a chiral auxiliary approach, was reported in 1971. Kagan and co-workers noted that copper(I) cyanide-catalyzed the insertion reaction into the N–H bonds of amines containing chiral ester side-chains to afford amino acids in up to 26% optical purity (Scheme 4-5a).<sup>16</sup> With the emergence of rhodium(II) acetate as an optimal catalyst for X–H insertion in 1973, the literature expanded with examples of rhodium(II)-catalyzed reactions. In 1996, McKervery and co-workers reported an intramolecular rhodium(II)-catalyzed insertion of diazo compounds into the N–H bonds of a pendant aliphatic amine in up to 45% *ee* (Scheme 4-5b).<sup>17</sup>

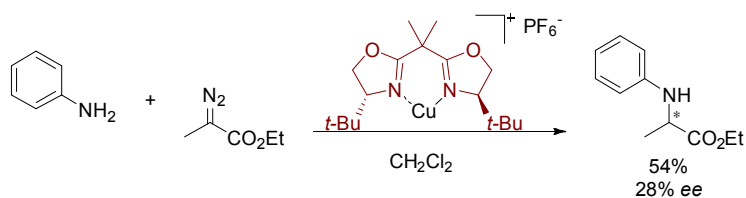
a) 1970: Kagan et. al, chiral auxiliary



b) 1996: McKervery et. al, chiral ligand



c) 2004: Jørgensen et. al, chiral ligand



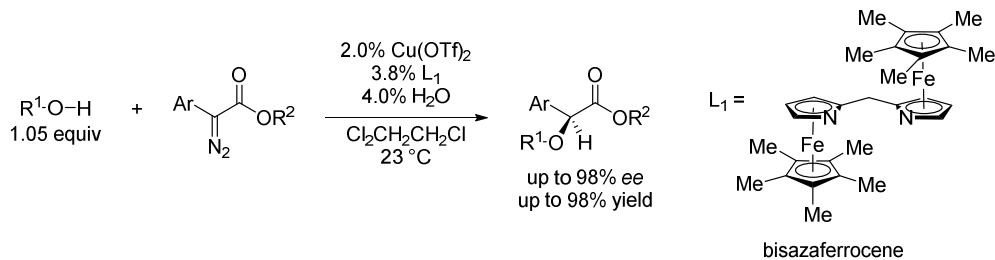
**Scheme 4-5.** Some early examples of asymmetric X–H insertion.

The asymmetric rhodium(II)-catalyzed variants, however, typically resulted in low *de* or *ee* and were plagued by side-reactions resulting from competitive C–H insertion, or beta-hydride

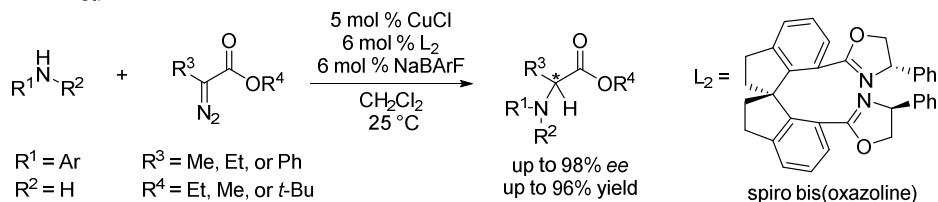
elimination. Intermolecular reactions utilizing rhodium(II) catalysts were less promising, resulting in *ees* as high as 9% for N–H insertion reactions<sup>18</sup> and 8% for O–H insertions into water.<sup>19</sup> The potential of copper-catalysis in the asymmetric variant of the insertion reaction saw a resurgence in the field and was re-evaluated when Jørgensen and co-workers demonstrated that N–H insertions catalyzed by copper(I)-bisoxazoline ligands could be realized in up to 28% *ee* in 2004 (Scheme 4-5c).<sup>20</sup> Shortly thereafter, highly efficient insertions into O–H and N–H bonds catalyzed by copper were reported (Scheme 4-6).

Fu and co-workers reported a highly efficient O–H insertion between alpha-aryldiazoesters and various alkyl alcohols catalyzed by copper(II) triflates in up to 98% yield and 98% *ee* using a chiral bisazaferrocene ligand (Scheme 4-6a).<sup>21</sup> Notably, Fu reported that a small amount of water was necessary for higher enantioselectivity and that the *ee* correlated linearly with catalyst *ee*.

a) 2006: Fu et. al.



b) 2007: Zhou et. al.



**Scheme 4-6.** First reports of highly efficient O–H and N–H catalytic insertions of diazo compounds catalyzed by copper catalysts.

Zhou and co-workers reported an efficient enantioselective insertion of various alkyl diazo esters into the N–H bonds of anilines catalyzed by copper(I) chloride in similar yields and *ees*

using a chiral spiro-bis(oxazoline) ligand.<sup>22</sup> They noticed that more coordinating counterions negatively influenced *ee*, while non-coordinating counterions like NaBARF dramatically improved the *ee*.

The high yields and higher *ees* with minimal side reactions made copper a more attractive catalyst than rhodium for the asymmetric version of this insertion process. Since McKervey's initial report, the examples of copper-,<sup>23</sup> rhodium-,<sup>24</sup> and iron-catalyzed<sup>25</sup> insertion reactions into O–H and N–H bonds of phenols and anilines, respectively, have grown extensively. Additionally, the field of asymmetric copper,<sup>26</sup> rhodium,<sup>27</sup> iron,<sup>28</sup> and even ruthenium<sup>29</sup> catalysis of N–H, O–H, and X–H insertion has seen considerable progress and development in the past couple of years.<sup>15</sup>

30

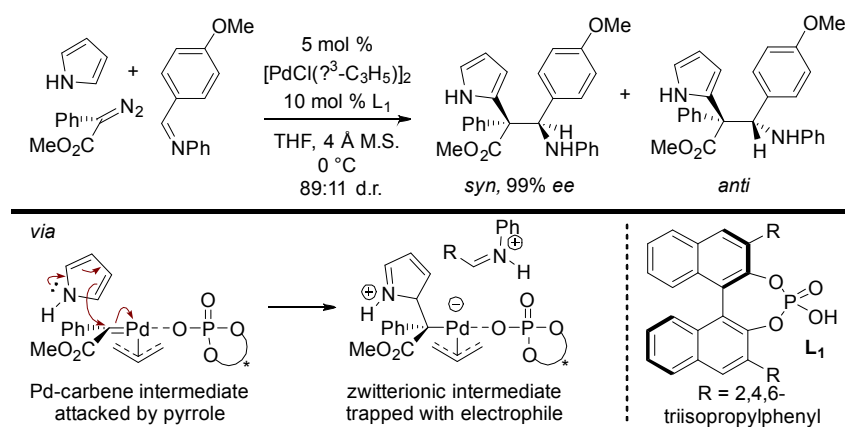
### **Asymmetric Palladium-Catalyzed X–H Insertions with Diazo Compounds**

Palladium has been an indispensable transition metal catalyst in providing powerful and reliable methods to form new C–C, C–N, and C–X bonds in cross-coupling reactions with aryl halides.<sup>31</sup> Palladium has been well known to catalyze cyclopropanation of alkenes in the presence of diazo compounds, but a new wave of carbene reactivity was discovered in 2001 when Van Vranken and co-workers reported a cross-coupling reaction involving a palladium-carbene migratory insertion.<sup>32</sup> Palladium has proven efficient in the construction of new C–C and C–X bonds in the recent years through reactions with diazo compounds<sup>33</sup> and their applications in cross-coupling reactions.<sup>34</sup> Despite these significant developments, the examples of asymmetric palladium-catalyzed cross-coupling reactions involving carbene intermediates generated from diazo decomposition have slowly emerged.

In 2012, Van Vranken and co-workers reported mixed results achieving absolute stereocontrol of an intermolecular palladium-catalyzed carbene insertion cross-coupling reaction

to generate allylic amines.<sup>35</sup> Using various chiral phosphine ligands, higher *ees* were observed to correlate with lower yields. Either a reasonable yield of allylic amine was obtained (54%) with low *ee* (14%), or a low yield was obtained (6%) with moderate *ee* (64%), suggesting that it was possible to control the stereochemistry of a cross-coupling reaction involving palladium-carbene intermediates by using chiral ligands.

In 2013, Hu and co-workers reported the first highly enantioselective cross-coupling reaction of diazo compounds, imines, and pyrrole catalyzed by a palladium catalyst – demonstrating for the first time that stereocontrol can be achieved in a palladium-carbenoid-mediated reaction (Scheme 4-7).<sup>36</sup> Enantioselection was achieved by using a chiral phosphoric acid,<sup>37</sup> which provides an asymmetric environment for nucleophilic attack of the electrophilic iminium. Hu and co-workers provide a more detailed plausible mechanism that considers the conformational analysis that leads to *syn* and *anti* products from imine trapping.



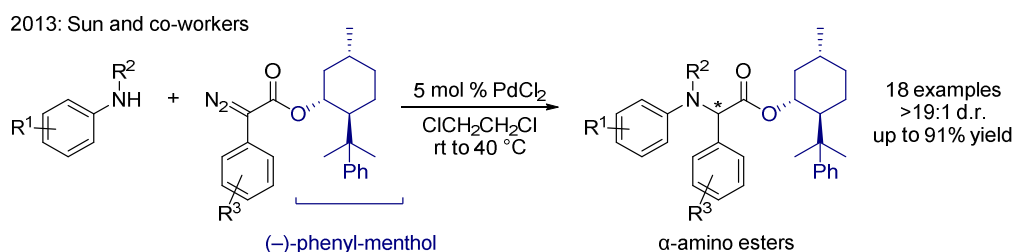
**Scheme 4-7.** First example of enantioselective palladium-catalyzed carbene insertion via zwitterionic intermediate trapping with imine.

No reaction is observed when the palladium catalyst is omitted from the reaction conditions. In the presence of palladium catalyst without chiral phosphoric acid, only trace



amounts of product are observed, implicating that both reagents are necessary for the success of the reaction. The possibility of asymmetric induction for palladium-carbene mediated reactions provided the opportunity for asymmetric X–H insertion reaction development.

The first asymmetric insertion of a palladium-catalyzed carbene insertion into the N–H bond of aniline was reported by Sun and co-workers and was accomplished by utilizing a chiral auxiliary (Scheme 4-8).<sup>38</sup> Sun and co-workers used palladium(II) precatalysts and chiral  $\alpha$ -aryl- $\alpha$ -diazoesters to insert into aniline N–H bonds, obtaining  $\alpha$ -aminoesters.



**Scheme 4-8.** First asymmetric palladium-catalyzed insertion of diazo compounds into N–H bonds.

Various anilines and *N*-methylanilines underwent reaction with the chiral  $\alpha$ -aryl- $\alpha$ -diazoesters to afford chiral amino ester derivatives. The reaction also worked with  $\alpha$ -aryl- $\alpha$ -diazoester compounds resulting in products of N–H insertion, but without stereo-induction. Other alkyl amines, such as benzylamine, aminopiperidine, and 2-(aminomethyl)aniline, did not react under the reaction conditions to give the corresponding N–H insertion reactions.

Shortly thereafter in 2014, the field of enantioselective palladium-catalyzed insertion into X–H bonds saw major advances. Zhou, Zhu and co-workers published an enantioselective palladium-catalyzed carbene insertion of  $\alpha$ -aryl- $\alpha$ -diazoesters into the O–H bonds of phenols (Table 4-1).<sup>39</sup>

2014: Zhou, Zhu, and co-workers

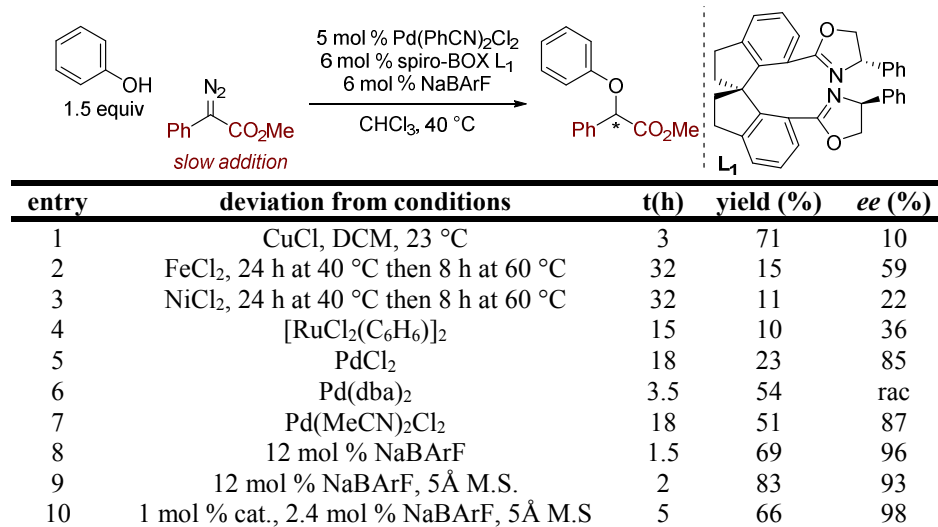


**Table 4-1.** Selected entries of Zhou, Zhu and co-workers' screening conditions for optimization of insertion into phenol.

Enantioselection was achieved by using a chiral spiro-bis(oxazoline) ligand **L**<sub>1</sub> and with slow addition of diazo compound over 2 h. Zhou, Zhu and co-workers showed that copper(I)-, iron(II)-, nickel(II)-, and ruthenium(II)-based catalysts resulted in either poor *ee*<sup>40</sup> (entry 1), or poor yield with some stereo-induction (entries 2–4). They demonstrated that palladium(II) chloride precatalyst was more effective than these other metals at obtaining product in higher enantioselectivity (entry 5), but was unstable and would form palladium black under the conditions. A palladium(0) precatalyst gave higher yields in less time, but no stereo-induction (entry 6).

When bis(acetonitrile) palladium(II) dichloride was used they obtained 51% yield and 87% *ee* (entry 7). They obtained a slightly improved *ee* (92%) and similar yield when they used bis(benzonitrile)dichloropalladium(II) instead. Changing the stoichiometry of NaBARF from 6 to 12 mol % resulted in shorter reaction times, slightly better yields, and higher *ee* (entry 8). NaBARF is essential to the reaction. In the absence of NaBARF, yields dropped to less than 10%. The role

of NaBARF is unclear, but Zhou, Zhu and co-workers postulate that “the bulky and noncoordinating BARF anion of the of resulting palladium catalyst may increase its [the catalyst’s] Lewis acidity and stability.” A potential role for sodium cations was not ruled out.

Side products were observed to arise from competitive insertion into the O–H bonds of water. The yields were improved by adding molecular sieves to the reaction to sequester adventitious water (entry 9). High enantioselectivity is retained with lower catalyst loading, but the reaction requires longer times and results in lower yields of insertion products (entry 10). Using a chiral PyBOX ligand instead of a spiro-BOX one gave much lower enantioselectivity (19% vs 98% *ee*).

Overall, Zhou, Zhu and co-workers demonstrated that a palladium(II) precatalyst was more effective than other metals for enantioselective carbene insertion into the O–H bonds of phenols, using  $\alpha$ -aryl- $\alpha$ -diazoesters as palladium carbene precursors and a chiral spiro-bis(oxazoline) ligand. The addition of molecular sieves prevents side-products resulting from the insertion into the O–H bond of water, and although its role is unclear, NaBARF is necessary for achieving higher reactivity and enantioselectivity.

Nearly at the same time, Feng, Liu and co-workers reported the enantioselective N–H insertion reaction of anilines and  $\alpha$ -alkyl- $\alpha$ -diazoesters catalyzed by palladium(0) precatalysts and a chiral guanidine co-catalyst **L**<sub>2</sub> (Table 4-2).<sup>41</sup> In these conditions, the diazo compound is added in one portion to the reaction mixture instead of slow addition over 2 h. The main catalysts known for X–H insertion, copper(I) chloride, rhodium(II) diacetate, and iron(II) perchlorate, afforded product in good yields and promising *ees*, except in the case of iron, which afforded racemic products (entries 1–3). A balance between yield and enantioselection was achieved when a palladium(II) precatalyst was used (entry 4). Interestingly, a slightly better yield and *ee* was

obtained when the amount of chiral guanidine was reduced to 2 mol %, but no further improvement was seen with lower amounts of the guanidine (entries 4–6).

2014: Feng, Liu and co-workers

entry	deviation from conditions	yield (%)	ee (%)
1	10 mol % CuCl	99	71
2	Rh <sub>2</sub> (OAc) <sub>4</sub>	60	70
3	10 mol % Fe(ClO <sub>4</sub> ) <sub>2</sub> ·6H <sub>2</sub> O	99	0
4	none	86	88
5	2 mol % L <sub>2</sub>	86	90
6	1 mol % L <sub>2</sub>	86	87

**Table 4-2.** Selected entries of Feng, Liu and co-workers' screening conditions for optimization of insertion into anilines.

Feng, Liu and co-workers note that  $\alpha$ -aryl- $\alpha$ -diazoesters and other  $\alpha$ -alkyl-substituted- $\alpha$ -diazoesters were poor substrates in the N–H insertion reaction. In those cases, the aniline substrate was not consumed. However, they showed that both primary and secondary anilines work well under the optimized conditions.

In 2015, the separate group of Zhou and co-workers reported an enantioselective insertion of  $\alpha$ -aryl- $\alpha$ -diazoesters into the O–H bonds of phenol and the C3–H bonds of *N*-substituted indoles utilizing an axially chiral 2,2'-bipyridine ligand (**L**<sub>3</sub>) and palladium(II) precatalyst (Table 4-3).<sup>42,43</sup> This was the first report of an enantioselective palladium-catalyzed carbene insertion at the C3–H position of indoles. Copper(I) chloride, palladium(II) chloride, and bis(acetonitrile)palladium(II) chloride were efficient precatalysts in the reaction, but better enantioselection and slightly better yields were achieved by using the palladium(II) precatalyst (entries 1–4). The reaction tolerates chlorinated solvents and hydrocarbon-based solvents like toluene (entries 5–7). In order to

maintain high *ees*, the addition of NaBARF is crucial – products are obtained, but in 8% *ee* in its absence (entry 8).

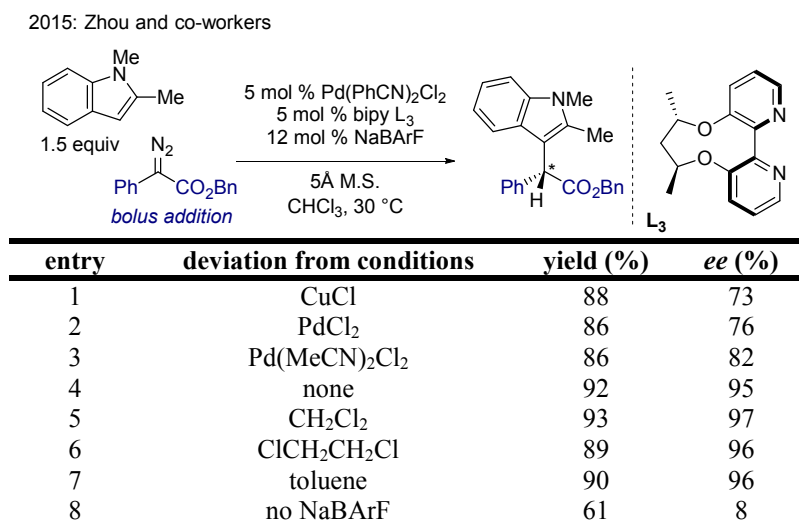
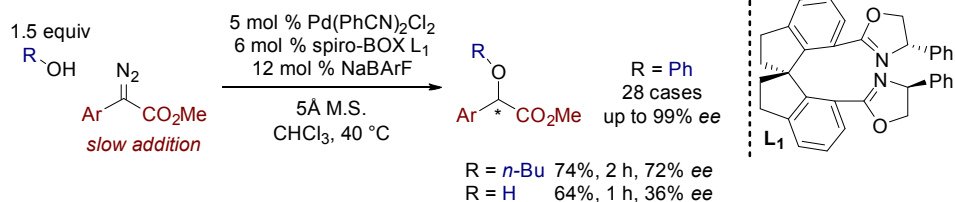
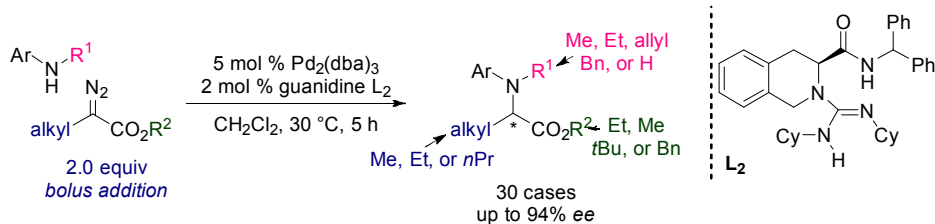


**Table 4-3.** Zhou and co-workers selected screening conditions for C–H insertion into *N*-substituted indoles.

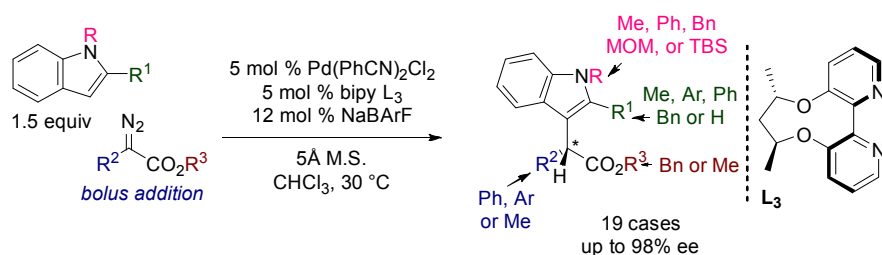
2014: Zhou, Zhu and co-workers



2014: Feng, Liu and co-workers



2015: Zhou and co-workers



**Scheme 4-9.** Side by side comparisons of previously published work in asymmetric palladium-catalyzed carbene insertion into X–H bonds utilizing chiral ligands.

The seminal work published by Zhou, Zhou, and Feng was instrumental in pioneering the new applicability of palladium for insertion of carbene groups into O–H, N–H, and C–H bonds (Scheme 4-9). However, the examples were limited to phenols and anilines, and it was unclear whether such insertions could be applied to the N–H bonds of aromatic heterocycles relevant to many biologically active molecules.

### ***N*-Substituted Aromatic Nitrogen Heterocycles via Transition Metal Catalysis**

*N*-Substituted aromatic nitrogen heterocycles are prevalent in many synthetic pharmaceutical drugs: purines (abacavir), indazoles (ibrutinib), indoles (vincamine), and

carbazoles (midostaurin) (Figure 4-3). *N*-Alkylindoles (fluvastatin, vincamine) and *N*-alkylcarbazoles (midostaurin, rimcazole) present a particular challenge for synthesis due to the low nucleophilicity of the parent NH group.

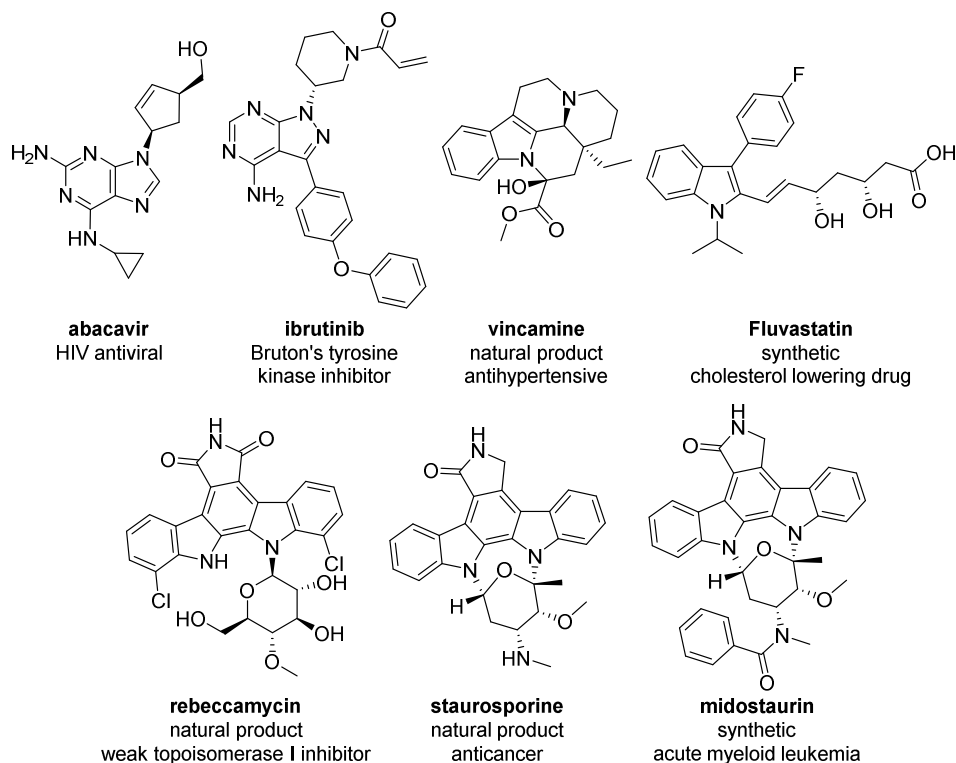


**Figure 4-3.** Examples of *N*-substituted aromatic nitrogen heterocycles in pharmaceutical drugs.

Alkylating the free N–H of aromatic nitrogen heterocycles like indoles, pyrazoles, and triazoles, in a regioselective manner, while creating a new C–N stereogenic center, would provide access to derivatives of *N*-alkylindoles and *N*-alkylcarbazoles of more potency.

For example, *N*-alkylindoles with stereocenters adjacent to the indole nitrogen, such as human norepinephrine reuptake inhibitor **4.0a**, are pharmacophores for important biological targets (Figure 4-4).<sup>44</sup> Such *N*-substituted indoles are commonly accessed through inefficient and challenging substitution reactions with an electrophilic coupling partner, usually alkyl halides<sup>45</sup> or secondary alcohols via Mitsunobu conditions.<sup>46</sup> These methods are highly substrate dependent –

steric and electronic factors play a major role in the success of the reaction – and require enantioenriched starting material<sup>47</sup> or chiral resolution to obtain products with the desired stereochemistry.<sup>44c, 48</sup>

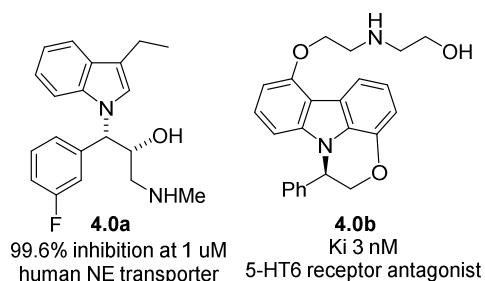


**Figure 4-4.** Biologically active *N*-alkylindoles with stereocenters adjacent to nitrogen.

Alternatively, *N*-substituted carbazoles such as 5-HT<sub>6</sub> receptor antagonist **4.0b** may be synthesized through enantioselective reductive amination, but require a late-stage Fischer indolization to construct the heterocycle.<sup>49</sup> This late-stage construction of the aromatic heterocycle has also been applied to indoles via Fischer indole synthesis of chiral hydrazines,<sup>50</sup> oxidation of chiral *N*-alkylated indolines,<sup>51</sup> or by reduction of chiral *N*-alkyl isatins.<sup>52</sup>

As of August, 2019, a search for transformations in which the free N–H of indole overall underwent an asymmetric alkylation identified 207 reports. Of those reports, 172 described single step asymmetric alkylations, of which more than half were substitution reactions. A little under 12% were metal-catalyzed asymmetric alkylations – an underwhelming amount considering the invaluable contributions transition metal catalysis has been in the synthesis of pharmaceutical drugs.<sup>53</sup>

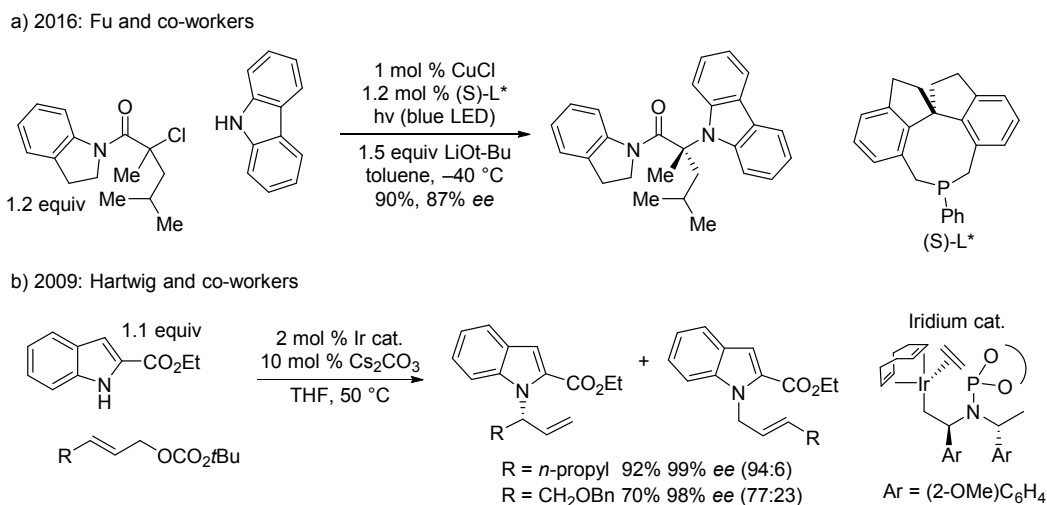
Transition metal catalysis provides access to new electrophilic cross-coupling partners to expand the scope of alkylated derivatives of N–H heterocycles, without the need for late-stage



functionalization to install the heterocyclic core by providing a way to derivatize the heterocyclic core directly.

For example, the coupling of sterically hindered alkyl halides to carbazoles has been achieved using radicals as a cross-coupling partners to generate sterically encumbered, chiral C–N bonds (Scheme 4-10a).<sup>54</sup> The method works well for simple carbazole substrates and 3-substituted indoles in good yield and high *ee*, but requires synthesis of specialized tertiary alkyl chlorides, and does not tolerate aliphatic amine and aldehyde functional groups.

*N*-alkylation of indoles has also been achieved through asymmetric metal-catalyzed activation of allylic substrates to generate electrophilic allyl cross-coupling partner to afford chiral *N*-allyl indole products, but often suffers from regioselectivity issues (Scheme 4-10b).<sup>55</sup> Both branched and linear *N*-allyl products are obtained, and the ratio is highly dependent on the allyl carbonate, as seen with the *O*-benzyl substituted allyl carbonate (Scheme 4-10b). Selectively alkylating the nitrogen over C2 and C3 is challenging, but typically, as in this case, *N*-alkylation is favored over C2 and C3 by attenuating the nucleophilicity at those positions with electron withdrawing groups at C2 or C3 of indole. A 2016 report circumvented these issues by designing a C2-substituted indole with pendant allyl carbonate, favoring an intramolecular allylation reaction to form a six-membered ring.<sup>55a</sup>



**Scheme 4-10.** Selected examples of typical asymmetric alkylations of indole catalyzed by metals.

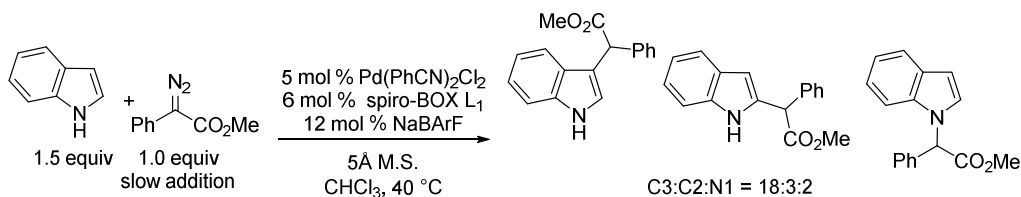
Electrophilic metal-carbene complexes, generated by the metal-catalyzed decomposition of diazo compounds, have been used as cross-coupling partners to functionalize heteroatom X–H since the 1900's. In the 1970's, asymmetric versions were developed using copper and rhodium catalysts. The utility of palladium in these processes was not highlighted until 2013 and since then has been shown to perform as well, if not better, than the rhodium and copper catalysts. However, these transition-metal catalyzed cross-coupling reactions with an electrophilic metal-carbene complex have been limited to phenols and anilines and, at the time of this work, had not been demonstrated with indoles or carbazoles, despite their prevalence in natural products and pharmaceutical drugs. Given the prevalence of *N*-alkylated indole backbone in pharmaceutical drugs, having new methods to access them by direct use of the heterocycle in a cross-coupling reaction would allow for facile one step functionalization/derivatization.

This chapter describes the development of a palladium-catalyzed reaction for asymmetric insertion of a carbene functional group, derived from a diazo compound, into the N–H bond of the aromatic heterocycles: indoles and carbazoles. It adds to the underexplored nature of metal-

carbenes generated from diazo compounds, as electrophilic cross-coupling partner with unadulterated indole and carbazoles. This work represented the first example of a palladium-catalyzed carbene insertion into the N–H bonds of aromatic heterocycles, such as indoles and carbazoles, to obtain  $\alpha$ -(*N*-indolyl)- $\alpha$ -arylesters and  $\alpha$ -(*N*-carbazolyl)- $\alpha$ -arylesters, using  $\alpha$ -aryl- $\alpha$ -diazoesters as palladium carbene precursors in which enantioselection was achieved by way of a chiral PyBOX ligand. This new method was applied towards the synthesis of the core of a bioactive carbazole derivative in a concise manner.

## Results and Discussion

After an initial discovery by my colleague Udara Premachandra, I worked as a team with Stanley Hiew and Eugene Gutman to explore and optimize the palladium-catalyzed insertion of carbene groups into the N–H bonds of aromatic heterocycles. Our studies began with an examination of the intrinsic regioselectivity for palladium-catalyzed carbene insertion with unprotected indole and methyl phenyldiazoacetate (Scheme 4-11). Under the conditions reported by Zhou, Zhu and co-workers for O–H insertion – slow addition of the limiting diazo reagent and chiral spiro-BOX ligand – I observed insertion at the indole C3, C2, and N1 position in an 18:3:2 ratio ( $^1\text{H}$  NMR), respectively. While insertion at C3 was favored, we were pleased to observe that N–H insertion was also a viable process.



**Scheme 4-11.** Intrinsic regioselectivity of unsubstituted indole.

Udara Premachandra, Stanley Hiew, and I optimized the N–H insertion conditions using carbazole substrate **4.1a** and methyl phenyldiazoacetate **4.2a** (Table 4-4).

entry	Pd cat.	X	Y	solvent	L*	t(h)	yield (%) <sup>e</sup>	ee (%) <sup>f</sup>
1 <sup>a</sup>	A	5	12	CHCl <sub>3</sub>	L <sub>1</sub>	2	64	83
2 <sup>b</sup>	B	5	-	DCM	L <sub>2</sub>	5	100	5
3 <sup>c</sup>	A	5	12	CHCl <sub>3</sub>	L <sub>1</sub>	2	88	76
4	A	5	12	CHCl <sub>3</sub>	L <sub>2</sub>	2	85	13
5	A	5	12	CHCl <sub>3</sub>	L <sub>3</sub>	2	nr	-
6	A	5	12	CHCl <sub>3</sub>	L <sub>4</sub>	2	94	15
7	A	5	12	CHCl <sub>3</sub>	L <sub>5</sub>	16	94	90
8	A	5	12	CHCl <sub>3</sub>	L <sub>6</sub>	2	99	97
9	B	2.5	12	CHCl <sub>3</sub>	L <sub>6</sub>	0.2	97	66
10	-	-	12	CHCl <sub>3</sub>	L <sub>6</sub>	22	nd	-
11 <sup>d</sup>	A	5	-	CHCl <sub>3</sub>	L <sub>6</sub>	96	34	ndt
12	A	1	12	CHCl <sub>3</sub>	L <sub>6</sub>	4	98	97
13	A	0.5	12	CHCl <sub>3</sub>	L <sub>6</sub>	20	91	95
14	A	5	12	DCE	L <sub>6</sub>	4	100	96
15	A	5	12	PhMe	L <sub>6</sub>	4	95	95
16	A	5	12	THF	L <sub>6</sub>	4	0	-

<sup>a</sup> catalyst A = Pd(PhCN)<sub>2</sub>Cl<sub>2</sub>; catalyst B = Pd<sub>2</sub>dba<sub>3</sub>. <sup>a</sup> See Scheme 4-11. 1.5 equiv of **4.1a** with slow addition of 1.0 equiv of **4.2a**. <sup>b</sup> 2 equiv of diazo, 2 mol % guanidine co-catalyst, no NaBARF, no 5 Å M.S. <sup>c</sup> Bolus addition of excess diazo **4.2a**. <sup>d</sup> 1.5 equiv of carbazole, 1 equiv of diazo compound. <sup>e</sup> Isolated yield. <sup>f</sup> Determined by normal phase HPLC using ChiralPak OD-H column and IPA/hexanes solvent system. nd = not detected. ndt = not determined.

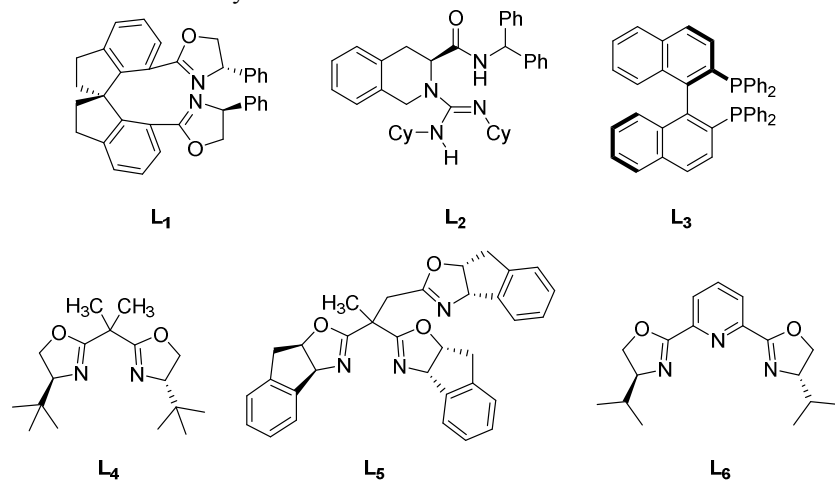


**Table 4-4.** Reaction optimization for carbazole **4.1a**.

When I applied Zhou, Zhu and co-workers' O–H insertion conditions using chiral spiro-BOX **L1** to carbazole **4.1a**, the N–H insertion product  $\alpha$ -(*N*-carbozoyl)- $\alpha$ -phenylacetate **4.3aa** was obtained in 64% yield and 83% *ee* (Table 4-4, entry 1). As a comparison, application of Feng, Liu and co-workers' N–H insertion conditions using a palladium(0) precatalyst, chiral guanidine additive **L2**, and bolus addition of excess diazo compound, gave insertion product **4.3aa** in quantitative yield, but in substantially lower *ee* (entry 2). In general, both palladium(0) and palladium(II) species can competently catalyze the insertion reaction into the N–H bond of carbazole, but high levels of asymmetric induction are only achieved with a palladium(II) catalyst and chiral ligand.

A higher yield of carbazole insertion product **4.3aa** was obtained with bolus addition of excess methyl phenyldiazoacetate (1.5 equiv), although in slightly lower *ee* (entry 1 and 3). With moderate yields in hand, we sought a more efficient ligand that would improve the *ee* of the carbazole insertion product. Utilizing 6 mol % of chiral guanidine **L2** as co-catalyst afforded product in comparable 85% yield, but in only in 15% *ee* (entry 4). In the presence of guanidine, additional side-products formed that were not isolated, but presumably resulted from C–H insertion via electrophilic aromatic substitution onto the electron-rich carbazole rings. When (*R*)-BINAP was used, the reaction was completely shut down – the starting carbazole, **4.1a**, was not consumed and no N–H insertion product was observed (entry 5).

Both the bidentate bis(oxazoline) ligand **L4** and the tri-coordinate bis(oxazoline) ligand **L5** afforded N–H insertion products in 94% yield. Surprisingly, however, the bidentate ligand **L4** gave much lower asymmetric induction compared to the tri-coordinate ligand **L5**, and took one-eighth the time to reach completion (entries 6 and 7). The optimal ligand for this insertion reaction was found to be isopropyl-bis(oxazoline) ligand with a pyridine spacer ((*S,S*)-*i*Pr-PyBOX) **L6**,

affording insertion product **4.3aa** in 99% yield and 97% *ee* (entry 8). Using (*R,R*)-*i*Pr-PyBOX afforded product in 95% yield and –94% *ee* (not shown). Under these optimized conditions, using a palladium(0) precatalyst, Pd<sub>2</sub>(dba)<sub>3</sub>, afforded product in 97% yield in one-fifth the time, but surprisingly gave product in 66% *ee*, thus supporting the highly advantageous nature of using palladium(II), a more electrophilic, reactive metal that can better coordinate to the chiral ligand (entry 9).

In the absence of palladium catalyst and ligand, no N–H insertion product was detected by <sup>1</sup>H NMR even after 22 h (entry 10). When NaBARF was excluded from the reaction and the carbazole was present in excess (carbazole/diazo = 1.5:1), N–H insertion product was detected but only in 32% <sup>1</sup>H NMR yield after 96 hours (entry 11). Changing the catalyst loadings from 5 to 1 to 0.1 mol % resulted in longer reaction times (2, 4, 20 h, respectively), but still generated product in high yield and *ee* (entries 8, 12, 13). My colleague, Stanley Hiew, investigated the solvent effects on the reaction and found that other chlorinated solvents and toluene worked well for the reaction (entries 14, 15), but the reaction did not proceed in more coordinating solvents such as THF (entry 16).

With the optimized conditions (entry 8), my colleagues and I explored the scope of the reaction with other diazo compounds and *N*-heterocycles. We first explored the scope of diazo compounds, synthesized by Stanley Hiew, in the N–H insertion reaction (Figure 4-5). Aryl substituents were generally tolerated on the methyl  $\alpha$ -aryldiazoacetate substrates **4.2b-e**, forming carbazole insertion products **4.3ab-4.3ae**. Halogen aryl substituents on the diazo substrate are tolerated, but result in slightly lower yields and incomplete conversion (**4.3ab**); halogen substitution at the *ortho*-position of the diazo was detrimental to substrate yield, but N–H insertion products were still obtained in a moderate 87% *ee* (**4.3ae**). *Para*-substitution with an electron-

donating methoxy group accelerated the reaction, with carbazole **4.1a** fully consumed in 30 minutes. In contrast, an electron-withdrawing *para*-nitro group slowed the reaction significantly, affording a low yield of **4.3ad** after 24 h at 55°C. Not surprisingly, the easily enolizable *para*-nitro analogue **4.3ad** was obtained as the racemate.

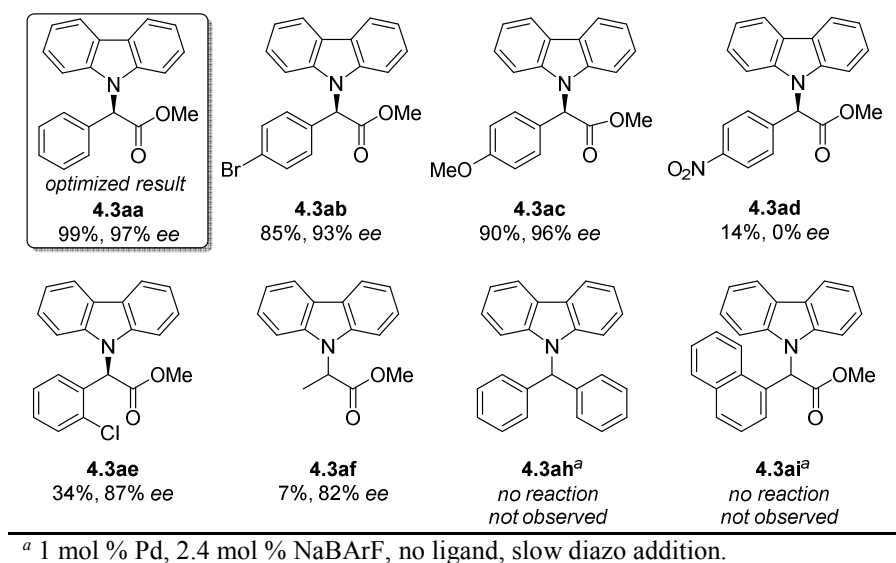
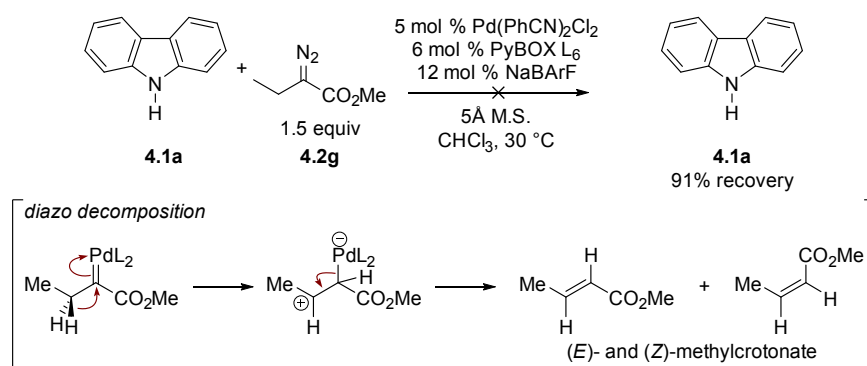


**Figure 4-5.** Scope of diazo compounds in N–H insertion with carbazole.

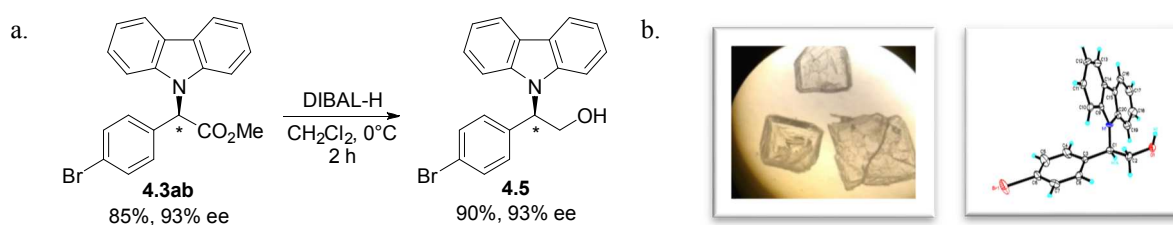
My colleague, Stanley Hiew and I investigated and showed that  $\alpha$ -alkyl- $\alpha$ -diazoesters were poor substrates in the reaction. When methyl  $\alpha$ -diazopropanoate was used, N–H insertion product **4.3af** was obtained in 7% yield after 14 h while still maintaining high *ee* (Figure 4-5). In general,  $\alpha$ -alkyl- $\alpha$ -diazoesters were poor substrates due to palladium-catalyzed decomposition. For example, methyl  $\alpha$ -diazobutanoate **4.3ag** formed (*E*)- and (*Z*)-methylcrotonate as major products and no insertion reaction was observed (Scheme 4-12). Carbazole **4.1a** was recovered in 91% yield after chromatography. In the absence of carbazole, methyl  $\alpha$ -diazobutanoate was consumed in approximately 3 h at 40 °C and (*E*)- and (*Z*)-methylcrotonate were still obtained. Similar results were obtained with indole **4.6c** (see note in supporting information).



**Scheme 4-12.** Decomposition of methyl  $\alpha$ -diazobutanoate.

Diazodiphenyl methane and methyl  $\alpha$ -(naphthyl)diazoacetate were also poor substrates for the reaction due to palladium-catalyzed decomposition of the diazo compound (Figure 4-5). Under slightly modified reaction conditions used to produce racemic material, no reaction occurred and the expected products were not observed (**4.3ah** and **4.3ai**). Slow addition was necessary for these diazo compounds due to their immediate decomposition by palladium catalyst.

The carbazolyl insertion products were not amenable to crystallization, but I found that suitable crystals could be obtained from their corresponding alcohols. The absolute stereochemistry of **4.3ab** was secured by X-ray crystallographic analysis of the corresponding alcohol **4.5** following DIBAL-H reduction (Scheme 4-13). The absolute configuration of alcohol **4.5** and analogous insertion products were assigned (*R*) based on the X-ray structure.<sup>56</sup>



**Scheme 4-13.** (a) Absolute stereochemistry assigned by X-ray analysis of alcohol **4.5**. (b) View of crystals through microscope lens (left) X-ray crystal structure (right).



Stanley Hiew, Eugene Gutman, and I then turned our attention to different carbazole substrates (Figure 4-6). Halogen substituents on the carbazole substrate are tolerated, but bromine substituents led to slightly lower yields and incomplete conversion, possibly due to catalyst deactivation resulting from oxidative addition (**4.3ba**).

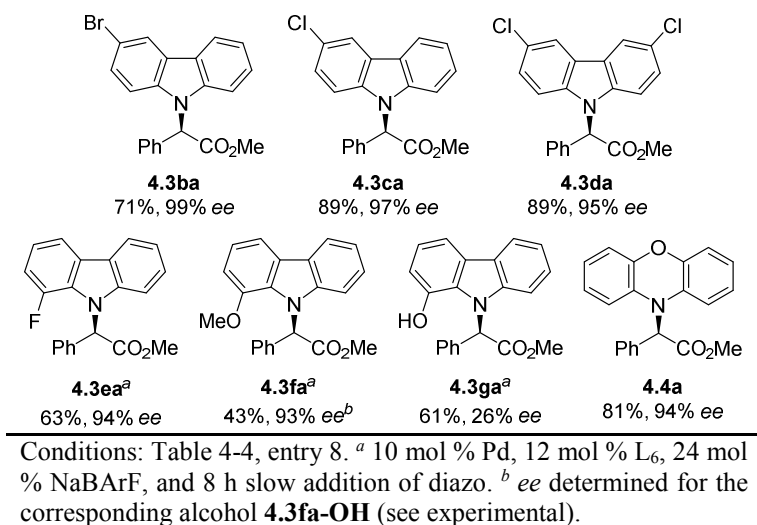
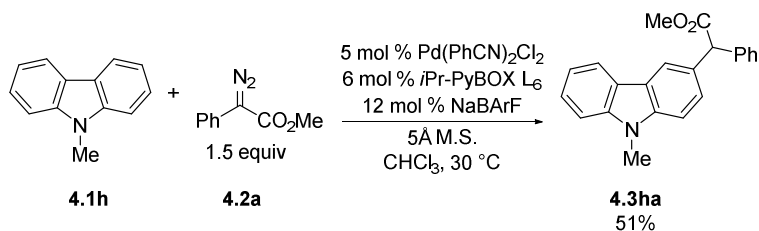


**Figure 4-6.** Reaction scope with various carbazoles.

1-Substituted carbazoles were challenging, affording products **4.3ea-4.3ga** in yields below 30% under standard conditions – however, Stanley Hiew found that higher temperatures, higher catalyst loadings, and slow addition of the diazo compound led to reasonable yields. Above 40°C, competitive formation of fumarate side products was observed. Slow addition of diazo reduced fumarate formation, although up to two equivalents were required.

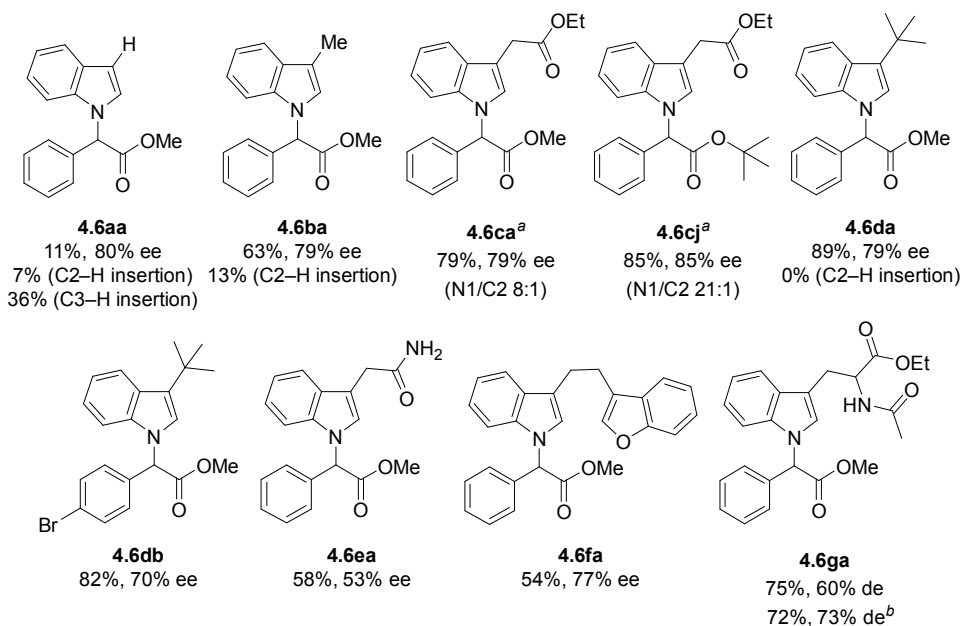
With hindered 1-methoxycarbazole **4.1f**, the corresponding product **4.3fa** was accompanied by an inseparable mixture of over-insertion products, presumably due to reaction with the electron-rich aromatic ring. Indeed, when Eugene Gutman subjected 9-*N*-methylcarbazole **4.1h** to the reaction conditions, the C3-H insertion product was obtained in 51% yield (Scheme 4-14).<sup>57</sup>



**Scheme 4-14.** Insertion reaction of 9-*N*-methylcarbazole **4.1h**.

With 1-hydroxycarbazole **4.1g**, the N–H insertion product **4.3ga** was obtained in up to 61% yield and 4:1 selectivity over the O–H insertion product.<sup>23c</sup> The *ee* for **4.3ga** was highly variable (0 to 49%) depending on reaction conditions and is attributed to the proximal O–H acting as an achiral proton donor. Electron deficient aromatic substrates such as 1-nitrocarbazole and 3-nitrocarbazole did not react under standard conditions or even after heating at 45 °C for 8 h. It is possible that the lower nucleophilicity, as well as the low solubility of those substrates in chloroform, contributed to the poor performance. Aniline-like heterocycles such as phenoxazine also worked well, affording **4.4a** in 81% yield and 94% *ee*, but with some C–H insertion products; the corresponding phenothiazine led only to decomposition products.<sup>58</sup>

I revisited unsubstituted indole using the conditions optimized for carbazole and methyl  $\alpha$ -phenyldiazoacetate. Once more, indole **4.6a** gave primarily C3–H insertion product, and approximately equal amounts of C2–H and N–H insertion products, with double-insertion at the N1 and C3 position as the major side-product (Figure 4-7).



<sup>a</sup> Yield of an inseparable N1/C2 product mixture. Ratio obtained by <sup>1</sup>H NMR analysis.

<sup>b</sup> (*R,R*)-*i*Pr-PyBOX.

**Figure 4-7.** Indole substrate scope.

Substitution the C3 position led to preferential insertion at N1, but C2–H insertion was still obtained. Increasing the steric environment at the C3 position improved selectivity for N–H over C2–H insertion (**4.6aa**<**4.6ba**<**4.6ca**). Using the bulkier *tert*-butyl phenyldiazoacetate improved selectivity for N–H insertion, but C2–H insertion was still detectable by <sup>1</sup>H NMR (**4.6cj**). Stanley Hiew showed no C2–H insertion was observed when 3-*tert*-butylindole was the substrate (**4.6da**) and that indole substrates containing substituents with hydrogen-bonding groups led to poorer *ee* (**4.6ea** and **4.6ga**). A crystal structure of 3-*tert*-butyl indole **4.6db** was obtained as the racemate, by Stanley Hiew, and confirms the new C–N bond formed from this insertion process (Figure 4-8).<sup>59</sup>

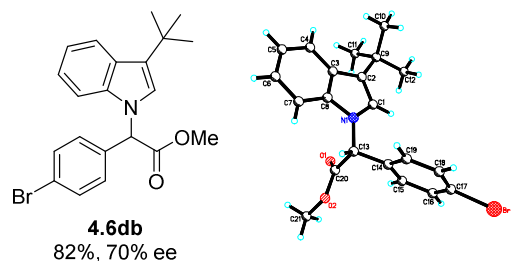
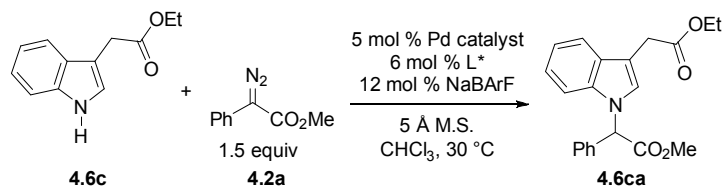


**Figure 4-8.** X-ray crystal structure of indole **4.6db**.

Indole substrates generally exhibited lower *ees* than carbazole substrates. I screened different ligand classes with ethyl-3-indoleacetate **4.6d** as the model substrate to identify if there was a more suitable ligand for indole substrates (Table 4-5). In general, spiro-BOX L<sub>1</sub>, chiral guanidine L<sub>2</sub>, BOX L<sub>4</sub>, BOX L<sub>5</sub> and BOX L<sub>7</sub> (not shown – similar to L<sub>4</sub>) did not improve the *ee* of product **4.6ca**.



entry	L*	deviation from conditions	t(h)	N1:C2 <sup>a</sup>	yield (%) <sup>b</sup>	<i>ee</i> (%)
1	L <sub>6</sub>	-	18	8:1	79	79
2	L <sub>1</sub>	-	6	16:1	89	69
3	L <sub>2</sub>	-	0.75	13:1	71	rac
4	L <sub>4</sub>	-	1.5	8:1	76	2
5	L <sub>5</sub>	6 h at 30 °C, then 18 h at 50 °C	24	6:1	68 <sup>c</sup>	34 <sup>d</sup>
6	L <sub>7</sub>	( <i>S</i> )-BTBBPh-SaBOX <sup>e</sup>	0.75	7.4:1	47	6
7	L <sub>6</sub>	<i>t</i> -butyl phenyldiazoacetate	14	21:1	85	85

<sup>a</sup> Ratio determined by <sup>1</sup>H NMR of isolated product after chromatography. <sup>b</sup> Isolated yield of an inseparable mixture of N–H/C2–H insertion products. <sup>c</sup> Yield determined by <sup>1</sup>H NMR using 1,4-dimethoxybenzene as a standard. <sup>d</sup> *ee* determined from a sample collected mid-fraction from column chromatography. <sup>e</sup> CAS = 1428328-51-1.

**Table 4-5.** Effects of different ligands on N–H insertion with ethyl-3-indoleacetate **4.6c**.

Spiro-BOX L<sub>1</sub> gave overall better results – the reaction was complete within 6 h, the selectivity for N–H over C2–H insertion improved, and a higher yield was obtained (entry 1 and 2), but enantioselectivity suffered and dropped to 69% *ee*. In the presence of chiral guanidine

additive L<sub>2</sub>, BOX L<sub>4</sub>, and BOX L<sub>7</sub>, the reaction was complete in less than an hour resulting in moderate selectivity and yields, but in drastically lower *ees* (entry 3, 4, and 6). These results suggest poor ligand-palladium complexation, which could be the reason for lower *ees* if the stereo-induction step involves a metal-bound chiral complex. Tri-coordinate BOX L<sub>5</sub> caused a decrease in the rate of reaction, necessitating higher temperatures or longer times to reach completion, but afforded mediocre results (entry 5). The only modification resulting in slightly improved *ee* was using the bulkier *tert*-butyl phenyldiazoacetate (entry 6) to generate insertion product **4.6cj** (see Figure 4-8 for structure).

Other aromatic heterocycles with sp<sup>2</sup> lone pairs (e.g. imidazole, indazole, and pyrazole) were poor substrates for the reaction (Figure 4-9). For example, pyrazole afforded racemic insertion product **4.7a** in 32% yield. The presence of unreacted starting material suggests catalyst deactivation due to over-ligation by the substrate and the sp<sup>2</sup> hybridized nitrogen atoms. Aliphatic amines were briefly investigated. Piperidine afforded product **4.8a** in 40% yield. Derivative **4.9a** and P2Y<sub>12</sub> antagonist **4.9e** ((±)-clopidogrel) were obtained in 59% and 79% yield, respectively. Aliphatic amines are basic enough to racemize the products; the *ee* of carbazole product **4aa** declined to 25% after 2 h under the reaction conditions with 50 mol% piperidine.

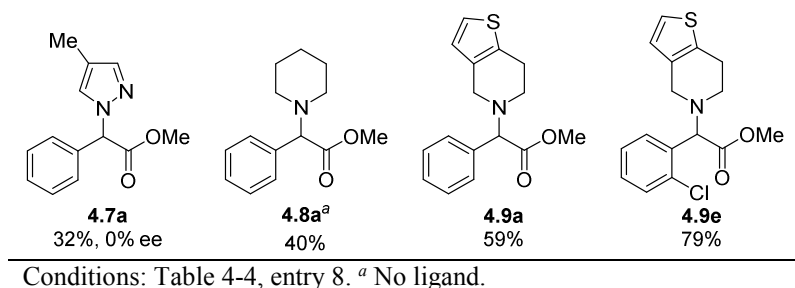


**Figure 4-9.** Examples of other N–H heterocycles investigated for this reaction.

I applied the N–H insertion reaction towards the synthesis of the core of 5-HT<sub>6</sub> receptor antagonist **4.11** (Figure 4-10). Oxazinocarbazole **4.10** was synthesized by DIBAL–H reduction of

**4.3fa** to the alcohol, mesylation, and a one-step thermal cyclization/dealkylation. This concise synthesis highlights the powerful palladium-catalyzed N–H insertion reaction described herein, avoiding a lengthy synthesis of oxazinocarbazoles that involves a late-stage Fischer indolization.

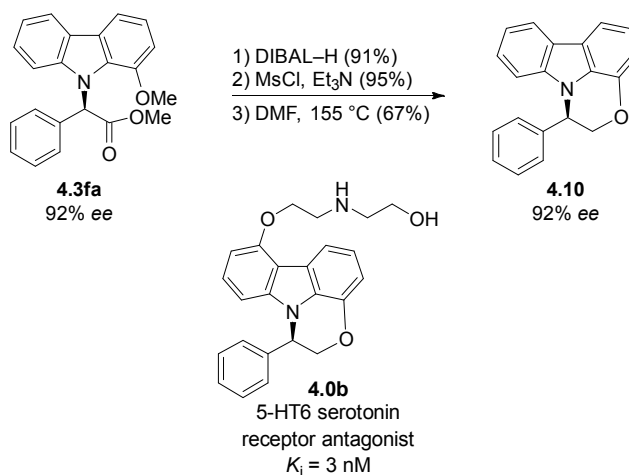


**Figure 4-10.** Synthesis of the core of 5-HT<sub>6</sub> receptor antagonist **4.0b**.

## Conclusion

In summary, I helped to develop a powerful enantioselective palladium-catalyzed carbene insertion into the N–H bonds of aromatic heterocycles using (*S,S*)-*i*Pr-PyBOX and a palladium(II) precatalyst. *N*-Alkylated products were obtained in good to excellent yields and up to 99% *ee*. A product of the reaction was carried through a series of further transformations without erosion of *ee* to synthesize the core of a potent 5-HT<sub>6</sub> antagonist.

Our success has already inspired further developments. After the publication of this palladium-catalyzed N–H insertion reaction into carbazoles and indoles, two publications were reported investigating enantioselective palladium-catalyzed C–H functionalization of pyrroles using 2,2'-bipyridine ligand,<sup>60</sup> and enantioselective N–H insertion into carbazoles using copper(I) chloride or iron(II) triflate using an axially chiral 2,2'-biimidazole ligands.<sup>61</sup>

## References

- (a) Doyle, M. P.; McKervey, M. A.; Ye, T., X–H Insertion Reactions of Diazocarbonyl Compounds (X = N, O, S, Se, P, Halogen). In *Modern Catalytic Methods for Organic Synthesis with Diazo Compounds: From Cyclopropanes to Ylides*, John Wiley & Sons, Inc.: New York, 1998; pp 433–486; (b) Doyle, M. P.; McKervey, M. A.; Ye, T., *Modern Catalytic Methods for Organic Synthesis with Diazo Compounds: From Cyclopropanes to Ylides*. John Wiley & Sons, Inc.: New York, 1998; p 652; (c) Kirmse, W., *Carbene Chemistry*. 2<sup>nd</sup> ed.; Academic Press: New York, 1971; Vol. 1; (d) Kirmse, W., In *Advances in Carbene Chemistry*, Brinker, U., Ed. JAI Press: Greenwich, CT, 1994; Vol. 1, pp 1–57; (e) Maas, G., Transition-metal catalyzed decomposition of aliphatic diazo compounds — New results and applications in organic synthesis. In *Organic Synthesis, Reactions and Mechanisms. Topics in Current Chemistry, vol 137.*, Springer: Berlin, Heidelberg, 1987; pp 75–253; (f) Regitz, M.; Maas, G., *Diazo Compounds. Properties and Synthesis*. Academic Press: New York, 1986; p 596.
- (a) Miller, D. J.; Moody, C. J. Synthetic Applications of the O–H Insertion Reactions of Carbenes and Carbenoids Derived from Diazocarbonyl and Related Diazo Compounds. *Tetrahedron* **1995**, *51*, 10811–10843 and references therein; (b) Ye, T.; McKervey, M. A. Organic Synthesis with  $\alpha$ -Diazo Carbonyl Compounds. *Chem. Rev.* **1994**, *94*, 1091–1160; (c) Shapiro, E. A.; Dyatkin, A. B.; Nefedov, O. M. Carbene reactions of diazoesters with  $\sigma$ -bonds as an effective method for the alkoxy-carbonylmethylenation of organic compounds. *Russ. Chem. Rev.* **1993**, *62*, 447–472; (d) Marchand, A. P.; Brockway, N. M. Carbalkoxycarbenes. *Chem. Rev.* **1974**, *74*, 431–469.
- Wolff, L. Ueber Diazoanhydride. *Liebigs Annalen* **1902**, *325*, 129–195.
- (a) Wolff, L.; Krüche, R. Über Diazoanhydride (1,2,3-Oxydiazole oder Diazoxyde) und Diazoketone. *Liebigs Annalen* **1912**, *394*, 23–59; (b) Kirmse, W. 100 Years of the Wolff Rearrangement. *Eur. J. Org. Chem.* **2002**, *2002*, 2193–2256.
- Silberrad, O.; Roy, C. S. XXIV.—Gradual decomposition of ethyl diazoacetate. *J. Chem. Soc., Trans.* **1906**, *89*, 179–182.
- (a) Casanova, R.; Reichstein, T. Methoxyketone aus Diazoketonen. Steroide, 5. Mitteilung. *Helv. Chim. Acta* **1950**, *33*, 417–422; (b) Casanova, R.; Reichstein, T. 17-Iso-allopregnan. Steroide, 1. Mitteilung. *Helv. Chim. Acta* **1949**, *32*, 647–656.
- Yates, P. The Copper-catalyzed Decomposition of Diazoketones. *J. Am. Chem. Soc.* **1952**, *74*, 5376–5381.
- (a) Brenna, S.; Ardizzioia, G. A. Carbene Transfer and Carbene Insertion Reactions Catalyzed by a Mixed-Ligand Copper(I) Complex. *Eur. J. Org. Chem.* **2018**, *2018*, 3336–3342; (b) Minnick, J. L.; Domyati, D.; Ammons, R.; Tahsini, L. C–X (X = N, O) Cross-Coupling Reactions Catalyzed by Copper-Pincer Bis(*N*-Heterocyclic Carbene) Complexes. *Front. Chem.* **2019**, *7*.
- Takebayashi, M.; Ibata, T.; Kohara, H.; Kim, B. H. Reactions of Diazoketones in the Presence of Metal Chelates. I. Reactions in Alcohols. *Bull. Chem. Soc. Jpn.* **1967**, *40*, 2392–2397.
- (a) Saegusa, T.; Ito, Y.; Kobayashi, S.; Hirota, K.; Shimizu, T. Synthetic reaction by complex catalyst III. Copper catalyzed *N*-alkylation of amine with diazoalkane. *Tetrahedron Lett.* **1966**, *7*, 6131–6134; (b) Saegusa, T.; Ito, Y.; Kobayashi, S.; Hirota, K.;

- Shimizu, T. Synthetic reactions by complex catalysts. VIII. Copper-catalyzed reactions of thiol and alcohol with diazoacetate. *J. Org. Chem.* **1968**, *33*, 544–547.
11. Nozaki, H.; Takaya, H.; Moriuti, S.; Noyori, R. Homogeneous catalysis in the decomposition of diazo compounds by copper chelates. *Tetrahedron* **1968**, *24*, 3655–3669.
  12. (a) Paulissen, R.; Hayez, E.; Hubert, A. J.; Teyssie, P. Transition metal catalysed reactions of diazocompounds - part III a one-step synthesis of substituted furanes and esters. *Tetrahedron Lett.* **1974**, *15*, 607–608; (b) Paulissen, R.; Reimlinger, H.; Hayez, E.; Hubert, A. J.; Teyssié, P. Transition metal catalysed reactions of diazocompounds - II insertion in the hydroxylic bond. *Tetrahedron Lett.* **1973**, *14*, 2233–2236.
  13. (a) Ratcliffe, R. W.; Salzmann, T. N.; Christensen, B. G. A novel synthesis of the carbapen-2-em ring system. *Tetrahedron Lett.* **1980**, *21*, 31–34; (b) Salzmann, T. N.; Ratcliffe, R. W.; Christensen, B. G.; Bouffard, F. A. A stereocontrolled synthesis of (+)-thienamycin. *J. Am. Chem. Soc.* **1980**, *102*, 6161–6163.
  14. Moyer, M. P.; Feldman, P. L.; Rapoport, H. Intramolecular N–H, O–H, and S–H insertion reactions. Synthesis of heterocycles from  $\alpha$ -diazo  $\beta$ -keto esters. *J. Org. Chem.* **1985**, *50*, 5223–5230.
  15. Gillingham, D.; Fei, N. Catalytic X–H insertion reactions based on carbenoids. *Chem. Soc. Rev.* **2013**, *42*, 4918–4931.
  16. Nicoud, J.-F.; Kagan, H. B. Une nouvelle synthese asymetrique de l'alanine par insertion d'un carbene sur une liaison N–H. *Tetrahedron Lett.* **1971**, *12*, 2065–2068.
  17. García, C. F.; McKervey, M. A.; Ye, T. Asymmetric catalysis of intramolecular N–H insertion reactions of  $\alpha$ -diazocarbonyls. *Chem. Commun.* **1996**, 1465–1466.
  18. Buck, R. T.; Moody, C. J.; Pepper, A. G. N–H Insertion reactions of rhodium carbenoids. Part 4. New chiral dirhodium(II) carboxylate catalysts. *Arkivoc* **2002**, *2002*, 16–33.
  19. Bulugahapitiya, P.; Landais, Y.; Parra-Rapado, L.; Planchenault, D.; Weber, V. A Stereospecific Access to Allylic Systems Using Rhodium(II)–Vinyl Carbenoid Insertion into Si–H, O–H, and N–H Bonds. *J. Org. Chem.* **1997**, *62*, 1630–1641.
  20. Bachmann, S.; Fielenbach, D.; Jørgensen, K. A. Cu(I)-carbenoid- and Ag(I)-Lewis acid-catalyzed asymmetric intermolecular insertion of  $\alpha$ -diazo compounds into N–H bonds. *Org. Biomol. Chem.* **2004**, *2*, 3044–3049.
  21. Maier, T. C.; Fu, G. C. Catalytic enantioselective O–H insertion reactions. *J. Am. Chem. Soc.* **2006**, *128*, 4594–4595.
  22. Liu, B.; Zhu, S. F.; Zhang, W.; Chen, C.; Zhou, Q. L. Highly enantioselective insertion of carbenoids into N–H bonds catalyzed by copper complexes of chiral spiro bisoxazolines. *J. Am. Chem. Soc.* **2007**, *129*, 5834–5835.
  23. (a) Tishinov, K.; Fei, N.; Gillingham, D. Cu(I)-catalysed N–H insertion in water: a new tool for chemical biology. *Chem. Sci.* **2013**, *4*, 4401–4406; (b) Ramakrishna, K.; Sivasankar, C. Synthesis of Aminobenzoic Acid Derivatives via Chemoselective Carbene Insertion into the –NH Bond Catalyzed by Cu(I) Complex. *J. Org. Chem.* **2016**, *81*, 6609–6616; (c) Ramakrishna, K.; Murali, M.; Sivasankar, C. Chemoselective Carbene insertion into the N–H Bond over O–H Bond Using a Well-Defined Single Site (P-P)Cu(I) Catalyst. *Org. Lett.* **2015**, *17*, 3814–3817; (d) Ding, D.; Lv, X.; Li, J.; Xu, G.; Ma, B.; Sun, J. Copper-catalyzed N–H insertion and oxidative aromatization cascade: facile synthesis of 2-arylaminophenols. *Chem. Asian J.* **2014**, *9*, 1539–1542; (e) Ramakrishna, K.; Sivasankar, C. Phosphine ligands stabilized Cu(I) catalysts for carbene insertion into the N–H bond. *J. Organomet. Chem.* **2016**, *805*, 122–129; (f) Morilla, M. E.; Molina, M. J.; Díaz-Requejo,



- M. M.; Belderrain, T. R.; Nicasio, M. C.; Trofimenko, S.; Pérez, P. J. Copper-Catalyzed Carbene Insertion into O–H Bonds: High Selective Conversion of Alcohols into Ethers. *Organometallics* **2003**, *22*, 2914–2918.
24. (a) Muthusamy, S.; Srinivasan, P. Facile chemoselective rhodium carbenoid N–H insertion reactions: synthesis of 3-arylamino- or 3-heteroaryl piperidin-2-ones. *Tetrahedron Lett.* **2005**, *46*, 1063–1066; (b) Moody, C. J.; Swann, E. N–H Insertion Reactions of Rhodium Carbenoids: A Modified Bischler Indole Synthesis. *Synlett* **1998**, *1998*, 135–136; (c) Nicolle, S. M.; Hayes, C. J.; Moody, C. J. Alkyl halide-free heteroatom alkylation and epoxidation facilitated by a recyclable polymer-supported oxidant for the in-flow preparation of diazo compounds. *Chem. Eur. J.* **2015**, *21*, 4576–4579; (d) Gibe, R.; Kerr, M. A. Convenient Preparation of Indolyl Malonates via Carbenoid Insertion. *J. Org. Chem.* **2002**, *67*, 6247–6249; (e) Shi, G.-q.; Zhi-yao, C.; Wei-ling, C. Rhodium-mediated insertion of CF<sub>3</sub>-substituted carbenoid into O–H: An efficient method for the synthesis of  $\alpha$ -trifluoromethylated alkoxy- and aryloxyacetic acid derivatives. *Tetrahedron* **1995**, *51*, 5011–5018; (f) Nelson, T. D.; Song, Z. J.; Thompson, A. S.; Zhao, M.; DeMarco, A.; Reamer, R. A.; Huntington, M. F.; Grabowski, E. J. J.; Reider, P. J. Rhodium-carbenoid-mediated intermolecular O–H insertion reactions: a dramatic additive effect. Application in the synthesis of an ascomycin derivative. *Tetrahedron Lett.* **2000**, *41*, 1877–1881; (g) Nagai, K.; Sunazuka, T.; Omura, S. Synthesis of 4"-alkoxy avermectin derivatives using rhodium carbenoid-mediated O–H insertion reaction. *Tetrahedron Lett.* **2004**, *45*, 2507–2509; (h) Liao, M.; Dong, S.; Deng, G.; Wang, J. Synthesis of oxygen-containing heterocyclic compounds based on the intramolecular O–H insertion and Wolff rearrangement of  $\alpha$ -diazocarbonyl compounds. *Tetrahedron Lett.* **2006**, *47*, 4537–4540.
25. (a) Mbuvi, H. M.; Klobukowski, E. R.; Roberts, G. M.; Woo, L. K. O–H insertion and tandem N–H insertion/cyclization reactions using an iron porphyrin as catalyst with diazo compounds as carbene sources. *J. Porphyr. Phthalocyanines* **2010**, *14*, 284–292; (b) Aviv, I.; Gross, Z. Iron(III) corroles and porphyrins as superior catalysts for the reactions of diazoacetates with nitrogen- or sulfur-containing nucleophilic substrates: synthetic uses and mechanistic insights. *Chem. Eur. J.* **2008**, *14*, 3995–4005; (c) Baumann, L. K.; Mbuvi, H. M.; Du, G.; Woo, L. K. Iron Porphyrin Catalyzed N–H Insertion Reactions with Ethyl Diazoacetate. *Organometallics* **2007**, *26*, 3995–4002; (d) Gross, Z.; Aviv, I. Iron Corroles and Porphyrins as Very Efficient and Highly Selective Catalysts for the Reactions of  $\alpha$ -Diazo Esters with Amines. *Synlett* **2006**, *2006*, 951–953; (e) Ma, C.; Xing, D.; Zhai, C.; Che, J.; Liu, S.; Wang, J.; Hu, W. Iron porphyrin-catalyzed three-component reaction of ethyl diazoacetate with aliphatic amines and  $\beta,\gamma$ -unsaturated  $\alpha$ -keto esters. *Org. Lett.* **2013**, *15*, 6140–6143; (f) Nicolas, I.; Roisnel, T.; Maux, P. L.; Simonneaux, G. Asymmetric intermolecular cyclopropanation of alkenes by diazoketones catalyzed by Halterman iron porphyrins. *Tetrahedron Lett.* **2009**, *50*, 5149–5151.
26. (a) Zhao, X.; Zhang, Y.; Wang, J. Recent developments in copper-catalyzed reactions of diazo compounds. *Chem. Commun.* **2012**, *48*, 10162–10173; (b) Le Maux, P.; Simonneaux, G. Enantioselective insertion of carbenoids into N–H bonds catalyzed by chiral bicyclobisoxazoline copper(I) complexes. *Tetrahedron* **2015**, *71*, 9333–9338; (c) Le Maux, P.; Carrié, D.; Jehan, P.; Simonneaux, G. Asymmetric O–H insertion reaction of carbenoids catalyzed by chiral bicyclobisoxazoline copper(I) and (II) complexes. *Tetrahedron* **2016**, *72*, 4671–4675; (d) Song, X.-G.; Ren, Y.-Y.; Zhu, S.-F.; Zhou, Q.-L. Enantioselective Copper-Catalyzed Intramolecular N–H Bond Insertion: Synthesis of Chiral 2-

- Carboxytetrahydroquinolines. *Adv. Synth. Catal.* **2016**, *358*, 2366–2370; (e) Hou, Z.; Wang, J.; He, P.; Wang, J.; Qin, B.; Liu, X.; Lin, L.; Feng, X. Highly enantioselective insertion of carbenoids into N-H bonds catalyzed by copper(I) complexes of binol derivatives. *Angew. Chem. Int. Ed.* **2010**, *49*, 4763–4766; (f) Lee, E. C.; Fu, G. C. Copper-catalyzed asymmetric N–H insertion reactions: couplings of diazo compounds with carbamates to generate  $\alpha$ -amino acids. *J. Am. Chem. Soc.* **2007**, *129*, 12066–12067; (g) Chen, C.; Zhu, S. F.; Liu, B.; Wang, L. X.; Zhou, Q. L. Highly enantioselective insertion of carbenoids into O–H bonds of phenols: an efficient approach to chiral  $\alpha$ -aryloxy-carboxylic esters. *J. Am. Chem. Soc.* **2007**, *129*, 12616–12617; (h) Jiang, N.; Wang, J.; Chan, A. S. C. Diastereoselective intermolecular O–H insertions by Cu(II)-mediated carbenoids derived from phenyldiazoacetamide. *Tetrahedron Lett.* **2001**, *42*, 8511–8513.
27. (a) Im, C. Y.; Okuyama, T.; Sugimura, T. Stereoselective Formation of a Chiral Ether by Intramolecular O–H Insertion Reaction of a Metal Carbenoid Generated from Diazoacetate. *Eur. J. Org. Chem.* **2008**, *2008*, 285–294; (b) Xu, B.; Zhu, S. F.; Xie, X. L.; Shen, J. J.; Zhou, Q. L. Asymmetric N–H insertion reaction cooperatively catalyzed by rhodium and chiral spiro phosphoric acids. *Angew. Chem. Int. Ed.* **2011**, *50*, 11483–11486; (c) Xu, X.; Zavalij, P. Y.; Doyle, M. P. Synthesis of tetrahydropyridazines by a metal-carbene-directed enantioselective vinylogous N-H insertion/Lewis acid-catalyzed diastereoselective Mannich addition. *Angew. Chem. Int. Ed.* **2012**, *51*, 9829–9833; (d) Xu, B.; Zhu, S. F.; Zuo, X. D.; Zhang, Z. C.; Zhou, Q. L. Enantioselective N–H insertion reaction of  $\alpha$ -aryl  $\alpha$ -diazoketones: an efficient route to chiral  $\alpha$ -aminoketones. *Angew. Chem. Int. Ed.* **2014**, *53*, 3913–3916; (e) Doyle, M. P.; Yan, M. Chiral catalyst enhancement of diastereocontrol for O–H insertion reactions of styryl- and phenyldiazoacetate esters of pantolactone. *Tetrahedron Lett.* **2002**, *43*, 5929–5931.
28. Zhu, S.-F.; Cai, Y.; Mao, H.-X.; Xie, J.-H.; Zhou, Q.-L. Enantioselective iron-catalysed O–H bond insertions. *Nat. Chem.* **2010**, *2*, 546–551.
29. Deng, Q. H.; Xu, H. W.; Yuen, A. W.; Xu, Z. J.; Che, C. M. Ruthenium-catalyzed one-pot carbenoid N–H insertion reactions and diastereoselective synthesis of prolines. *Org. Lett.* **2008**, *10*, 1529–1532.
30. (a) Burtoloso, A. C. B.; Santiago, J. V.; Bernardim, B.; Talero, A. G. Advances in the Enantioselective Metal-catalyzed N–H and O–H Insertion Reactions with Diazocarbonyl Compounds. *Current Organic Synthesis* **2015**, *12*, 650–659; (b) Zhu, S. F.; Zhou, Q. L. Transition-metal-catalyzed enantioselective heteroatom-hydrogen bond insertion reactions. *Acc. Chem. Res.* **2012**, *45*, 1365–1377; (c) Moody, C. J. Enantioselective insertion of metal carbenes into N-H bonds: a potentially versatile route to chiral amine derivatives. *Angew. Chem. Int. Ed.* **2007**, *46*, 9148–9150.
31. (a) Tsuji, J., *Palladium Reagents and Catalysts: New Perspectives for the 21st Century*. John Wiley & Sons, Ltd: Chichester, UK, 2004; (b) King, A. O.; Yasuda, N., Palladium-Catalyzed Cross-Coupling Reactions in the Synthesis of Pharmaceuticals. In *Organometallics in Process Chemistry*, 2004; pp 205–245; (c) de Meijere, A.; Diederich, F., *Metal-Catalyzed Cross-Coupling Reactions*. 2<sup>nd</sup> ed.; Wiley-VCH: Weinheim, 2004; Vol. 1; (d) Tsuji, J., *Palladium in Organic Synthesis*. Springer Berlin Heidelberg: 2005; Vol. 14; (e) Negishi, E.-i., *Handbook of Organopalladium Chemistry for Organic Synthesis*. John Wiley & Sons, Inc.: New York, USA, 2002; Vol. 1 and 2; (f) Molnár, Á., *Palladium-Catalyzed Coupling Reactions: Practical Aspects and Future Developments*. Wiley-VCH: Weinheim, Germany, 2013; (g) Johansson Seechurn, C. C. C.; Kitching, M.

- O.; Colacot, T. J.; Snieckus, V. Palladium-catalyzed cross-coupling: a historical contextual perspective to the 2010 Nobel Prize. *Angew. Chem. Int. Ed.* **2012**, *51*, 5062–5085; (h) Johansson, C. C. C.; Colacot, T. J. Metal-catalyzed  $\alpha$ -arylation of carbonyl and related molecules: novel trends in C–C bond formation by C–H bond functionalization. *Angew. Chem. Int. Ed.* **2010**, *49*, 676–707.
32. Greenman, K. L.; Carter, D. S.; Van Vranken, D. L. Palladium-catalyzed insertion reactions of trimethylsilyldiazomethane. *Tetrahedron* **2001**, *57*, 5219–5225.
33. (a) Zhang, Y.; Wang, J. Recent Developments in Pd-Catalyzed Reactions of Diazo Compounds. *Eur. J. Org. Chem.* **2011**, *2011*, 1015–1026; (b) Zhang, Z.; Wang, J. Recent studies on the reactions of  $\alpha$ -diazocarbonyl compounds. *Tetrahedron* **2008**, *64*, 6577–6605; (c) Pena-Lopez, M.; Beller, M. Functionalization of Unactivated C(sp<sup>3</sup>)-H Bonds Using Metal-Carbene Insertion Reactions. *Angew. Chem. Int. Ed.* **2017**, *56*, 46–48; (d) Albéniz, A. C. Reactive Palladium Carbenes: Migratory Insertion and Other Carbene-Hydrocarbyl Coupling Reactions on Well-Defined Systems. *Eur. J. Inorg. Chem.* **2018**, *2018*, 3693–3705.
34. (a) Xia, Y.; Qiu, D.; Wang, J. Transition-Metal-Catalyzed Cross-Couplings through Carbene Migratory Insertion. *Chem. Rev.* **2017**, *117*, 13810–13889; (b) Xia, Y.; Zhang, Y.; Wang, J. Catalytic Cascade Reactions Involving Metal Carbene Migratory Insertion. *ACS Catal.* **2013**, *3*, 2586–2598; (c) Liu, Z.; Wang, J. Cross-coupling reactions involving metal carbene: from C=C/C–C bond formation to C–H bond functionalization. *J. Org. Chem.* **2013**, *78*, 10024–10030; (d) Xiao, Q.; Zhang, Y.; Wang, J. Diazo compounds and *N*-tosylhydrazones: novel cross-coupling partners in transition-metal-catalyzed reactions. *Acc. Chem. Res.* **2013**, *46*, 236–247; (e) Barluenga, J.; Valdes, C. Tosylhydrazones: new uses for classic reagents in palladium-catalyzed cross-coupling and metal-free reactions. *Angew. Chem. Int. Ed.* **2011**, *50*, 7486–7500; (f) Valdés, C.; Barroso, R.; Cabal, M. Pd-catalyzed Auto-Tandem Cascades Based on *N*-Sulfonylhydrazones: Hetero- and Carbocyclization Processes. *Synthesis* **2017**, *28*, 4434–4447.
35. Khanna, A.; Maung, C.; Johnson, K. R.; Luong, T. T.; Van Vranken, D. L. Carbenylative amination with *N*-tosylhydrazones. *Org. Lett.* **2012**, *14*, 3233–3235.
36. Zhang, D.; Qiu, H.; Jiang, L.; Lv, F.; Ma, C.; Hu, W. Enantioselective palladium(II) phosphate catalyzed three-component reactions of pyrrole, diazoesters, and imines. *Angew. Chem. Int. Ed.* **2013**, *52*, 13356–13360.
37. (a) Mukherjee, S.; List, B. Chiral counteranions in asymmetric transition-metal catalysis: highly enantioselective Pd/Bronsted acid-catalyzed direct  $\alpha$ -allylation of aldehydes. *J. Am. Chem. Soc.* **2007**, *129*, 11336–11337; (b) Jiang, G.; List, B. Direct asymmetric  $\alpha$ -allylation of aldehydes with simple allylic alcohols enabled by the concerted action of three different catalysts. *Angew. Chem. Int. Ed.* **2011**, *50*, 9471–9474; (c) Ohmatsu, K.; Ito, M.; Kunieda, T.; Ooi, T. Exploiting the modularity of ion-paired chiral ligands for palladium-catalyzed enantioselective allylation of benzofuran-2(3*H*)-ones. *J. Am. Chem. Soc.* **2013**, *135*, 590–593; (d) Tao, Z. L.; Zhang, W. Q.; Chen, D. F.; Adele, A.; Gong, L. Z. Pd-catalyzed asymmetric allylic alkylation of pyrazol-5-ones with allylic alcohols: the role of the chiral phosphoric acid in C–O bond cleavage and stereocontrol. *J. Am. Chem. Soc.* **2013**, *135*, 9255–9258.
38. Liu, G.; Li, J.; Qiu, L.; Liu, L.; Xu, G.; Ma, B.; Sun, J. Palladium-catalyzed carbenoid based N–H bond insertions: application to the synthesis of chiral  $\alpha$ -amino esters. *Org. Biomol. Chem.* **2013**, *11*, 5998–6002.

39. Xie, X. L.; Zhu, S. F.; Guo, J. X.; Cai, Y.; Zhou, Q. L. Enantioselective palladium-catalyzed insertion of  $\alpha$ -Aryl- $\alpha$ -diazoacetates into the O–H bonds of phenols. *Angew. Chem. Int. Ed.* **2014**, *53*, 2978–2981.
40. This result was taken from and previously reported by Chen, C. and co-workers. See reference 26g.
41. Zhu, Y.; Liu, X.; Dong, S.; Zhou, Y.; Li, W.; Lin, L.; Feng, X. Asymmetric N–H insertion of secondary and primary anilines under the catalysis of palladium and chiral guanidine derivatives. *Angew. Chem. Int. Ed.* **2014**, *53*, 1636–1640.
42. Gao, X.; Wu, B.; Huang, W. X.; Chen, M. W.; Zhou, Y. G. Enantioselective palladium-catalyzed C–H functionalization of indoles using an axially chiral 2,2'-bipyridine ligand. *Angew. Chem. Int. Ed.* **2015**, *54*, 11956–11960.
43. Zhou, Zhu and co-workers published an enantioselective O–H insertion utilizing slow addition of diazo compound and a chiral spiro-BOX ligand. Zhou and co-workers used bolus diazo addition and an axially chiral 2,2'-bipyridyl ligand.
44. (a) Mahaney, P. E.; Kim, C. Y.; Coghlan, R. D.; Cohn, S. T.; Heffernan, G. D.; Huselton, C. A.; Terefenko, E. A.; Vu, A. T.; Zhang, P.; Burroughs, K. D.; Cosmi, S. A.; Bray, J. A.; Johnston, G. H.; Deecher, D. C.; Trybulski, E. J., Structure–activity relationships of the 1-amino-3-(1*H*-indol-1-yl)-3-phenylpropan-2-ol series of monoamine reuptake inhibitors. In *Bioorg. Med. Chem. Lett.*, 2009; Vol. 19, pp 5807–5810; (b) Kim, C. Y.; Mahaney, P. E.; Trybulski, E. J.; Zhang, P.; Terefenko, E. A.; McComas, C. C. Phenylaminopropanol derivatives and methods of their use. US 2005/0222148 A1, Oct. 6, 2005; (c) Crespo, A.; Lan, P.; Mal, R.; Ogawa, A.; Shen, H.; Sinclair, P. J.; Sun, Z.; Bunte, E. K. V.; Wu, Z.; Liu, K.; DeVita, R. J.; Shen, D.-m.; Shu, M.; Tan, J. Q.; Qi, C.; Wang, Y.; Beresis, R. Mineralocorticoid receptor antagonists. US 9,403,807 B2, Aug. 2, 2016; (d) Bagley, S.; Greenlee, W. J.; Dhanoa, D. S.; Patchett, A. A. Angiotensin II antagonists incorporating a substituted indole or dihydroindole. US 5,175,164, Dec. 29, 1992.
45. Martinborough, E.; Neubert, T.; Whitney, T.; Lehsten, D.; Hampton, T.; Zimmerman, N.; Termin, A. P. Ion channel modulators and methods of use. US 8,193,194 B2, Jun. 5, 2012.
46. (a) Fitzpatrick, S.; Hardy, C. S.; Waters, M. G.; Lai, E. Method of treating atherosclerosis, dyslipidemias and related conditions. WO/2006/089309 A2, Aug. 24, 2006; (b) Norris, D. J.; DeLucca, G. V.; Gavai, A. V.; Lee, F. Y.; Tokarski, J. S. Tricyclic compounds as anticancer agents. US 9,458,156, B2, Oct. 4, 2016.
47. (a) Loakes, D.; Hill, F.; Brown, D. M.; Ball, S.; Reeve, M. A.; Robinson, P. S. 5'-Tailed Octanucleotide Primers for Cycle Sequencing. *Nucleosides and Nucleotides* **1999**, *18*, 2685–2695; (b) Wasserman, H. H.; Xia, M.; Carr, A. J.; Han, W. T.; Siegel, M. G. Generation of Penems, Carbapenems and Aza Analogs of Cephems by the Addition of Heterocycles and Other Building Blocks to Azetidinones. *Tetrahedron* **2000**, *56*, 5621–5629.
48. Li, L.; Beaulieu, C.; Guay, D.; Sturino, C.; Wang, Z. Fluoro-methanesulfonyl-substituted cycloalkanoindoles and their use as prostaglandin d2 antagonists. WO 2004/103970 A1, Dec. 2, 2004.
49. Tenbrink, R. E. Oxazinocarbazoles for the treatment of CNS diseases. US 6,821,970 B2, Nov. 23, 2004.
50. Xu, K.; Gilles, T.; Breit, B. Asymmetric synthesis of *N*-allylic indoles via regio- and enantioselective allylation of aryl hydrazines. *Nat. Commun.* **2015**, *6*, 1–7.
51. Dou, X.; Yao, W.; Jiang, C.; Lu, Y. Enantioselective *N*-alkylation of isatins and synthesis of chiral *N*-alkylated indoles. *Chem. Commun.* **2014**, *50*, 11354–11357.

52. Liu, W. B.; Zhang, X.; Dai, L. X.; You, S. L. Asymmetric *N*-allylation of indoles through the iridium-catalyzed allylic alkylation/oxidation of indolines. *Angew. Chem. Int. Ed.* **2012**, *51*, 5183–5187.
53. (a) Busacca, C. A.; Fandrick, D. R.; Song, J. J.; Senanayake, C. H., Transition Metal Catalysis in the Pharmaceutical Industry. In *Applications of Transition Metal Catalysis in Drug Discovery and Development*, Crawley, M. L.; Trost, B. M., Eds. John Wiley & Sons, Inc.: Hoboken, New Jersey, 2012; pp 1–24; (b) Shen, H. C., Selected Applications of Transition Metal-Catalyzed Carbon-Carbon Cross-Coupling Reactions in the Pharmaceutical Industry. In *Applications of Transition Metal Catalysis in Drug Discovery and Development*, Crawley, M. L.; Trost, B. M., Eds. John Wiley & Sons, Inc.: Hoboken, New Jersey, 2012; pp 25–95; (c) Yin, J., Selected Applications of Pd- and Cu-Catalyzed Carbon–Heteroatom Cross-Coupling Reactions in the Pharmaceutical Industry. In *Applications of Transition Metal Catalysis in Drug Discovery and Development*, Crawley, M. L.; Trost, B. M., Eds. John Wiley & Sons, Inc.: Hoboken, New Jersey, 2012; pp 97–163; (d) Taylor, A. P.; Robinson, R. P.; Fobian, Y. M.; Blakemore, D. C.; Jones, L. H.; Fadeyi, O. Modern advances in heterocyclic chemistry in drug discovery. *Org. Biomol. Chem.* **2016**, *14*, 6611–6637; (e) Blakemore, D. C.; Castro, L.; Churcher, I.; Rees, D. C.; Thomas, A. W.; Wilson, D. M.; Wood, A. Organic synthesis provides opportunities to transform drug discovery. *Nat. Chem.* **2018**, *10*, 383–394.
54. (a) Kainz, Q. M.; Matier, C. D.; Bartoszewicz, A.; Zultanski, S. L.; Peters, J. C.; Fu, G. C. Asymmetric copper-catalyzed C–N cross-couplings induced by visible light. *Science* **2016**, *351*, 681–684; (b) Bissember, A. C.; Lundgren, R. J.; Creutz, S. E.; Peters, J. C.; Fu, G. C. Transition-metal-catalyzed alkylations of amines with alkyl halides: photoinduced, copper-catalyzed couplings of carbazoles. *Angew. Chem. Int. Ed.* **2013**, *52*, 5129–5133.
55. (a) Ye, K. Y.; Cheng, Q.; Zhuo, C. X.; Dai, L. X.; You, S. L. An Iridium(I) *N*-Heterocyclic Carbene Complex Catalyzes Asymmetric Intramolecular Allylic Amination Reactions. *Angew. Chem. Int. Ed.* **2016**, *55*, 8113–8116; (b) Stanley, L. M.; Hartwig, J. F. Iridium-catalyzed regio- and enantioselective *N*-allylation of indoles. *Angew. Chem. Int. Ed.* **2009**, *48*, 7841–7844; (c) Trost, B. M.; Krische, M. J.; Berl, V.; Grenzer, E. M. Chemo-, regio-, and enantioselective Pd-catalyzed allylic alkylation of indolocarbazole pro-aglycons. *Org. Lett.* **2002**, *4*, 2005–2008; (d) Chen, L. Y.; Yu, X. Y.; Chen, J. R.; Feng, B.; Zhang, H.; Qi, Y. H.; Xiao, W. J. Enantioselective direct functionalization of indoles by Pd/sulfoxide-phosphine-catalyzed *N*-allylic alkylation. *Org. Lett.* **2015**, *17*, 1381–1384; (e) Trost, B. M.; Osipov, M.; Dong, G. Palladium-catalyzed dynamic kinetic asymmetric transformations of vinyl aziridines with nitrogen heterocycles: rapid access to biologically active pyrroles and indoles. *J. Am. Chem. Soc.* **2010**, *132*, 15800–15807; (f) Trost, B. M.; Zhang, T.; Sieber, J. D. Catalytic asymmetric allylic alkylation employing heteroatom nucleophiles: a powerful method for C–X bond formation. *Chem. Sci.* **2010**, *1*, 427–440.
56. See CCDC 1519937 for supplementary crystallographic data of alcohol compound 4.5 free of charge at [www.ccdc.cam.ac.uk/data\\_request/cif](http://www.ccdc.cam.ac.uk/data_request/cif) from The Cambridge Crystallographic Data Centre.
57. (a) Tayama, E.; Yanaki, T.; Iwamoto, H.; Hasegawa, E. Copper(II) Triflate Catalyzed Intermolecular Aromatic Substitution of *N,N*-Disubstituted Anilines with Diazo Esters. *Eur. J. Org. Chem.* **2010**, *2010*, 6719–6721; (b) Tayama, E.; Ishikawa, M.; Iwamoto, H.; Hasegawa, E. Copper(II)–acid co-catalyzed intermolecular substitution of electron-rich aromatics with diazoesters. *Tetrahedron Lett.* **2012**, *53*, 5159–5161; (c) Yang, J. M.; Cai,

- Y.; Zhu, S. F.; Zhou, Q. L. Iron-catalyzed arylation of  $\alpha$ -aryl- $\alpha$ -diazoesters. *Org. Biomol. Chem.* **2016**, *14*, 5516–5519.
58. Co-worker Eugene Gutman performed reactions with halogenated carbazoles, phenoxazine, and phenothiazine.
59. See CCDC 1520167 for supplementary crystallographic data of compound 4.6db, free of charge at [www.ccdc.cam.ac.uk/data\\_request/cif](http://www.ccdc.cam.ac.uk/data_request/cif) from The Cambridge Crystallographic Data Centre.
60. Shen, H.-Q.; Liu, C.; Zhou, J.; Zhou, Y.-G. Enantioselective palladium-catalyzed C–H functionalization of pyrroles using an axially chiral 2,2'-bipyridine ligand. *Org. Chem. Front.* **2018**, *5*, 611–614.
61. Shen, H. Q.; Wu, B.; Xie, H. P.; Zhou, Y. G. Preparation of Axially Chiral 2,2'-Biimidazole Ligands through Remote Chirality Delivery and Their Application in Asymmetric Carbene Insertion into N–H of Carbazoles. *Org. Lett.* **2019**, *21*, 2712–2717.

## Supporting Information

### General Information and Reagents

**Reactions and materials:** Unless otherwise specified, all reactions were performed under an atmosphere of dry N<sub>2</sub> gas. Anhydrous solvents and reagents, where applicable, were transferred using Schlenk technique. Toluene, tetrahydrofuran (THF), diethyl ether (Et<sub>2</sub>O), and dichloromethane (CH<sub>2</sub>Cl<sub>2</sub>) were dried by passage through alumina according to the procedure of Grubbs and co-workers.<sup>1</sup> All other solvents were purified according to reported procedures.<sup>2</sup> Unless otherwise noted, all reagents were commercially obtained and used without prior purification. Indole **4.6a**, 3-methylindole **4.6b**, ethyl-3-indoleacetate **4.6c**, and indole-3-acetamide **4.6e** were commercially available and used without prior purification. 3-(2-(benzofuran-3-yl)ethyl)-1H-indole **4.6f** and *N*-acetyl-*L*-tryptophan ethyl ester **4.6g** were synthesized previously by Van Vranken group members and their synthesis and characterization have previously been reported.<sup>3</sup>

**Analysis and Purification:** All reactions were monitored by thin-layer chromatography (TLC) and visualized by UV (254 nm) illumination and by KMnO<sub>4</sub> and *p*-anisaldehyde (*p*-anis) dip stains. The *p*-anis stain was prepared by adding 25 mL of concentrated sulfuric acid to a chilled solution of 95% ethanol (676 mL, made from 200 proof ethanol and de-ionized water). Glacial acetic acid (7.5 mL) and *p*-anisaldehyde (99%, 18.4 mL) were then added to afford a colorless solution. The stain was stored at 0 °C.

Analytical TLC was performed using EMD Millipore 0.25 mm Silica gel 60 F<sub>254</sub> 20 × 20 cm plates (EM1.05715.0001). Preparative layer chromatography (PLC) was performed using EMD Millipore PLC Plates F<sub>254</sub>, 500 μm thick, 200 × 200 mm, 60 Å pore size (EM1.05744.0001).

“Flash” chromatography on silica gel was performed using Agela Technologies Flash Silica sorbent (40-63  $\mu\text{m}$ ) silica gel of 230-400 mesh (CS605025-P).

Enantiomeric excess (*ee*) was determined by HPLC. Waters Acrodisc filters were used to filter HPLC samples (P/N WAT200520). A Chiralcel Technologies normal phase CHIRALPAK AD (0.46cm $\varnothing$   $\times$  25cm) chiral column was used on an Agilent Technologies Series 1100 HPLC instrument. The instrument comprises a series 1100 auto-sampler, a series 1100 binary pump system, a series 1100 diode array detector, and a series 1100 COLCOM. Data analysis was performed using ChemStation for LC 3D systems Rev. B.04.01.

A Chiralcel Technologies normal phase CHIRALCEL OD-H (0.46cm $\varnothing$   $\times$  25cm) chiral column was used on a Shimadzu Prominence Modular HPLC instrument. The instrument comprises two solvent delivery units (LC-20AD), a UV-VIS detector (SPD-20AV), an on-line degassing unit (DGU-20A-5R), and a system controller (CBM-20A LITE w/network switch). Analysis was performed on LabSolutions software version 5.52 copyright of Shimadzu Corporation.

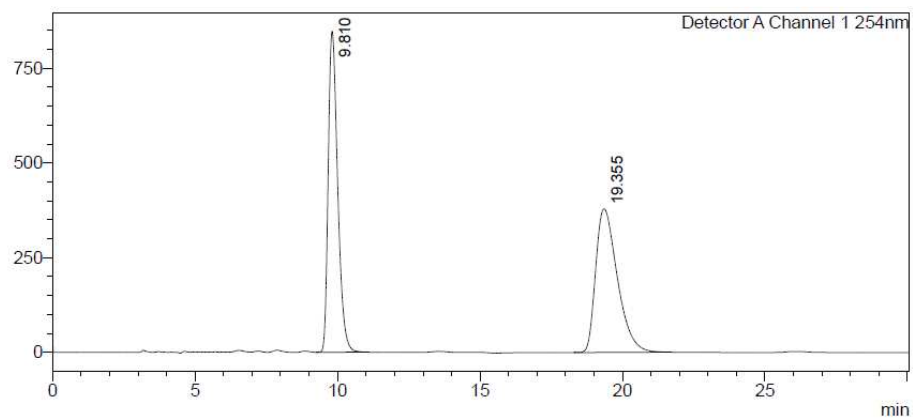
**Identity:** Unless otherwise noted,  $^1\text{H}$  and  $^{13}\text{C}$  NMR spectral data were recorded at 23  $^\circ\text{C}$  using a Bruker Avance 500 or 600 MHz spectrometer equipped with a cryoprobe. All spectra were calibrated to tetramethylsilane (0.00 ppm). The NMR data are reported as follows: chemical shift in ppm ( $\delta$ ), multiplicity (br = broad, app = apparent, s = singlet, d = doublet, t = triplet, q = quartet and m = multiplet), coupling constants (Hz), and integration. NMR data was processed using Mestrelab Research MestReNova 11.0.2 software, using automatic baseline correction and automatic phasing. Infrared spectroscopy data was acquired using a PerkinElmer Spectrum Two IR Spectrometer. Mass spectra were obtained using a Waters (Micromass) LCT premier with a TOF analyzer using the ionization method indicated to obtain accurate mass. Melting points were



taken on a Thermo Scientific Electrothermal Mel-Temp<sup>®</sup> apparatus (Model No. 1001D) using a mercury thermometer and values reported are uncorrected. Chemical names found in the supporting information were generated using PerkinElmer ChemBioDraw Ultra 13.0 software.

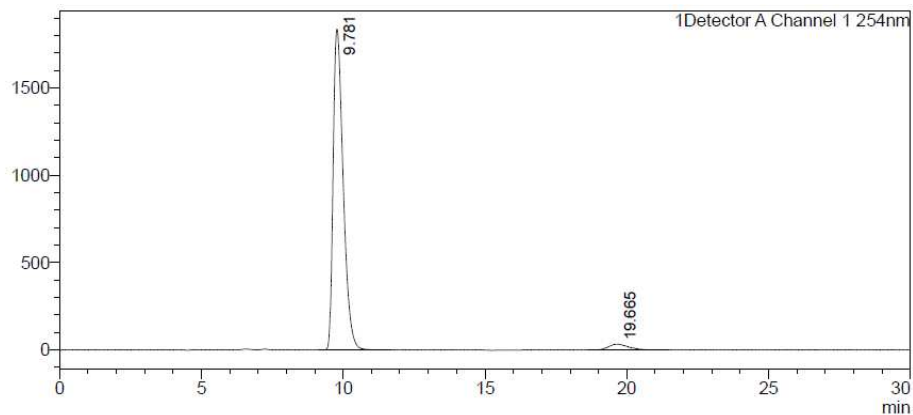
## Representative HPLC Traces

Representative HPLC traces are shown below for racemic and chiral compound **4.3ab**. Information including choice of chiral column, eluent, flow rate, and enantiomeric excess are provided in the Analytical Data section of the supporting information.



Peak Table

Peak#	Ret. Time	Area	Conc.	Mark	Area%
1	9.810	19668736	49.682	M	49.682
2	19.355	19920681	50.318	M	50.318
Total		39589417			100.000

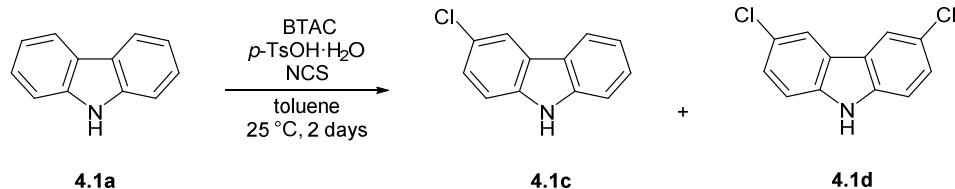


<Peak Table>

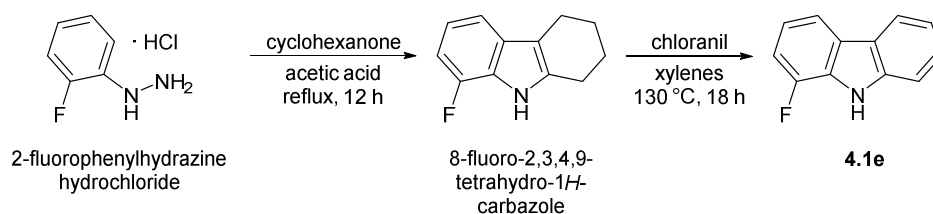
Peak#	Ret. Time	Height	Conc.	Area	Area%	Unit	Mark
1	9.781	1836172	96.446	45368762	96.446		M
2	19.665	32990	3.554	1671767	3.554		M
Total		1869161		47040530	100.000		

## Experimental Procedures

### Procedures for the Synthesis of Carbazole and Indole Substrates 4.1b–4.1g, 4.6d.



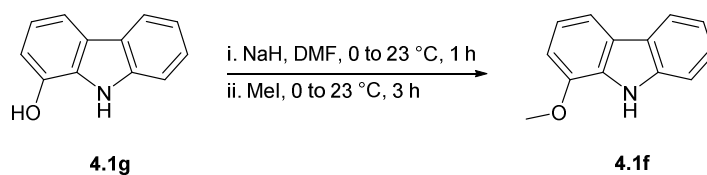
3-chloro-9*H*-carbazole (**4.1c**) and 3,6-Dichloro-9*H*-carbazole (**4.1d**) were synthesized according to a previously reported procedure by Chen and co-workers, with minor modification.<sup>4</sup> A flame-dried 100 mL round-bottom flask equipped with stir bar was charged with carbazole **4.1a** (1.0 g, 6.0 mmol, 95% grade), benzyltriethylammonium chloride (0.063 g, 0.30 mmol), and *p*-toluenesulfonic acid monohydrate (0.57 g, 3.0 mmol). The flask was then charged with toluene (30 mL) and allowed to stir open to air for two days. *N*-Chlorosuccinimide (1.6 g, 12.0 mmol) was added in four portions over two days. The reaction mixture was poured into saturated aqueous NaHCO<sub>3</sub> (100 mL) and the aqueous phase was extracted with ether (3 × 75 mL). The combined organic phase was washed with de-ionized water (3 × 75 mL), dried over Na<sub>2</sub>SO<sub>4</sub>, and concentrated *in vacuo* to obtain a yellow oil. The crude product was purified by flash chromatography on silica gel (15:85 EtOAc:hexanes) to afford 3-chloro-9*H*-carbazole **4.1c** as a tan solid (92 mg, 8%) as well as 3,6-Dichloro-9*H*-carbazole **4.1d** as a tan solid (0.680 g, 48%). Spectroscopic data for both compounds matched known reported data.<sup>5</sup>



1-fluoro-9H-carbazole (**4.1e**) was synthesized in two steps according to literature procedure with minor modification.<sup>6</sup>

**Step 1:** A 100 mL round-bottom flask was charged with 2-fluorophenylhydrazine hydrochloride (3.0 g, 18.5 mmol), cyclohexanone (2.3 mL, 22.2 mmol), and acetic acid (30 mL). The flask was fitted with a reflux condenser and the reaction mixture heated at reflux for 12 h. The mixture was cooled to room temperature, diluted with H<sub>2</sub>O (250 mL), and extracted with ether (3 × 100 mL). The combined organic layers were washed with H<sub>2</sub>O (3 × 75 mL) and brine (75 mL), dried over Na<sub>2</sub>SO<sub>4</sub>, and concentrated *in vacuo*. The crude product was purified by flash chromatography on silica gel (1<sup>st</sup> column = 50:50 ether:hexanes; 2<sup>nd</sup> column = 10:90 ether:hexanes). Pure fractions were combined and concentrated *in vacuo* to obtain 8-fluoro-2,3,4,9-tetrahydro-1H-carbazole as white cubic crystals (569 mg, 3.0 mmol, 16%).  $R_f = 0.81$  (50:50 ether:hexanes);  $R_f = 0.43$  (10:90 ether:hexanes). <sup>1</sup>H NMR data agrees with previously reported values.<sup>7</sup> Data for <sup>13</sup>C and IR have not been reported and are included here. <sup>1</sup>H NMR (500 MHz, CDCl<sub>3</sub>) δ 7.81 (br s, 1H), 7.21 (app d,  $J = 7.8$  Hz, 1H), 7.00 – 6.92 (m, 1H), 6.86 – 6.77 (m, 1H), 2.83 – 2.58 (m, 4H), 2.00 – 1.75 (m, 4H); <sup>13</sup>C NMR (125 MHz, CDCl<sub>3</sub>) 149.2 (d,  $J = 242.4$  Hz), 134.9, 131.6 (d,  $J = 5.5$  Hz), 123.5 (d,  $J = 12.6$  Hz), 119.3 (d,  $J = 6.2$  Hz), 113.5 (d,  $J = 3.1$  Hz), 111.0, 106.1 (d,  $J = 16.4$  Hz), 23.2, 23.14, 23.08, 21.0; IR (ATR) 3380, 2931, 2848, 1232, 774, 725 cm<sup>-1</sup>; HRMS (ESI)  $m/z$  calcd for C<sub>12</sub>H<sub>11</sub>FN [M – Na]<sup>-</sup> 188.0876, found 188.0870.

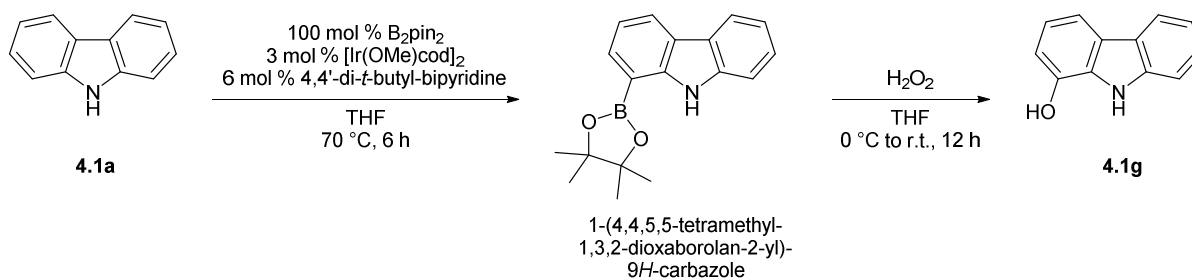
**Step 2:** An oven-dried 50 mL round-bottom flask equipped with stir bar was charged with 8-fluoro-2,3,4,9-tetrahydro-1*H*-carbazole (500 mg, 2.61 mmol), chloranil (1.41 g, 5.74 mmol), and anhydrous xylenes (15 mL). The flask was fitted with a reflux condenser and then submerged in a heated (130 °C) oil bath for 18 h. The reaction mixture was cooled to room temperature, diluted with ether (150 mL), and washed with aqueous 0.5 M NaOH (2 × 75 mL), H<sub>2</sub>O (75 mL), and brine (75 mL). The organic layer was dried over Na<sub>2</sub>SO<sub>4</sub> and concentrated *in vacuo*. The crude product was purified by flash chromatography on silica gel (1<sup>st</sup> column = 25:75 DCM:hexanes; 2<sup>nd</sup> column = 8:92 ether:hexanes) to obtain 1-fluoro-9*H*-carbazole **4.1e** as a white solid (318 mg, 1.72 mmol, 66%). Spectroscopic data matched known reported data.<sup>8</sup>  $R_f = 0.28$  (25:75 DCM:hexanes);  $R_f = 0.32$  (8:92 ether:hexanes). <sup>1</sup>H NMR (500 MHz, CDCl<sub>3</sub>) δ 8.17 (br s, 1H), 8.06 (d,  $J = 7.8$  Hz, 1H), 7.85 – 7.80 (m, 1H), 7.48 – 7.41 (m, 2H), 7.30 – 7.22 (m, 1H), 7.18 – 7.10 (m, 2H); <sup>13</sup>C NMR (125 MHz, CDCl<sub>3</sub>) δ 149.1 (d,  $J = 242.8$  Hz), 139.5, 127.5 (d,  $J = 13.1$  Hz), 126.8 (d,  $J = 5.7$  Hz), 126.5, 123.2 (d,  $J = 2.7$  Hz), 120.6, 120.0, 119.7 (d,  $J = 5.9$  Hz), 116.0 (d,  $J = 3.4$  Hz), 111.1, 110.9 (d,  $J = 16.2$  Hz); HRMS (ESI)  $m/z$  calcd for C<sub>12</sub>H<sub>7</sub>FN [M–Na]<sup>–</sup> 184.0563, found 184.0555.



1-methoxy-9*H*-carbazole (**4.1f**) was synthesized according to a patented procedure for a similar carbazole.<sup>9</sup> A 250 mL oven-dried round bottom flask was charged with 9*H*-carbazol-1-ol **4.1g** (850 mg, 4.64 mmol) and anhydrous DMF (50 mL). The flask was cooled in an ice-water bath for 10 min while stirring. To the flask was added in a single portion NaH (240 mg, 6.0 mmol, 60% dispersion in mineral oil). The reaction was warmed to room temperature and stirred for one hour.

Next, the flask was again cooled in an ice-water bath for 10 min and iodomethane (375  $\mu$ L, 6.0 mmol) was added. The reaction was warmed to room temperature and stirred for 3 h. Work-up and purification according to literature procedure yielded 1-methoxy-9*H*-carbazole **4.1f** as a beige solid (801 mg, 88%). Spectroscopic data matched known reported data.<sup>8, 10</sup>

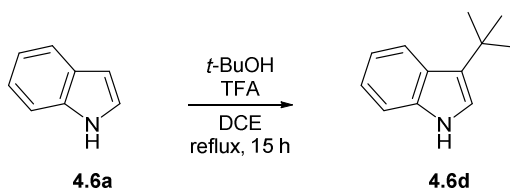
9*H*-carbazol-1-ol (**4.1g**) was synthesized according to a two-step procedure by Sperry and co-workers, with modifications.<sup>11</sup>



**Step 1:** A oven-dried 500 mL round-bottom flask was charged with carbazole **4.1a** (6 g, 36.0 mmol), 4,4'-di-*tert*-butyl-bipyridine (193 mg, 0.72 mmol), [Ir(OMe)cod]<sub>2</sub> (238 mg, 0.36 mmol), and dry THF (200 mL). The mixture was stirred at room temperature for 10 minutes until a dark red, homogeneous solution was obtained. The flask was submerged in a 70 °C oil bath. Bis(pinacolato)-diboron (3.04 g, 12.0 mmol) was dissolved in dry THF (20 mL) and this solution was added over 1.5 h using a syringe pump. After addition, the reaction mixture was stirred at 70 °C for an additional 4.5 h, for a total reaction time of 6 h. The reaction mixture was cooled to room temperature and concentrated *in vacuo*. The crude product was purified by flash chromatography on silica gel (8:92 EtOAc:hexanes), concentrated, and dried *in vacuo* to obtain 1-(4,4,5,5-tetramethyl-1,3,2-dioxaborolan-2-yl)-9*H*-carbazole as a white solid (1.86 g, 26%).  $R_f = 0.43$  (8:92 EtOAc:hexanes); <sup>1</sup>H NMR<sup>11</sup> and <sup>13</sup>C NMR<sup>12</sup> spectroscopic data match previously reported data. (<sup>1</sup>H NMR conflicts with ref. [12]). <sup>1</sup>H NMR (500 MHz, CDCl<sub>3</sub>)  $\delta$  9.15 (s, 1H), 8.18 (d,  $J = 8.2$  Hz, 1H), 8.07 (d,  $J = 7.8$  Hz, 1H), 7.86 (dd,  $J = 7.2, 1.2$  Hz, 1H), 7.49 (d,  $J = 8.1$  Hz,

1H), 7.41 (ddd,  $J = 8.2, 7.1, 1.2$  Hz, 1H), 7.28 – 7.18 (m, 2H), 1.42 (s, 12H);  $^{13}\text{C}$  NMR (125 MHz,  $\text{CDCl}_3$ )  $\delta$  145.1, 139.3, 132.8, 125.7, 123.7, 122.9, 122.3, 120.3, 119.1, 118.7, 110.6, 84.0, 25.0.

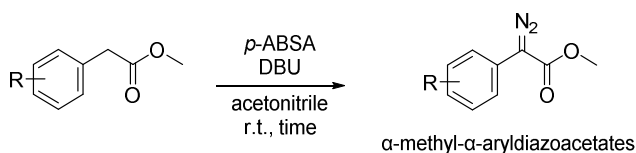
**Step 2:** 1-(4,4,5,5-tetramethyl-1,3,2-dioxaborolan-2-yl)-9H-carbazole (1.80 g, 6.13 mmol) was dissolved in THF (75 mL). The reaction was cooled in an ice-water bath for 10 min while stirring. Into the flask was syringed 30 wt % aqueous hydrogen peroxide (1.9 mL, 18.4 mmol). The mixture was allowed to warm to room temperature and stirred for 12 h. The mixture was concentrated *in vacuo*, purified by flash chromatography on silica gel (30:70 EtOAc:hexanes), concentrated, and dried *in vacuo* to obtain a light brown solid. The solid was recrystallized from hot benzene under nitrogen. Upon cooling to room temperature, a few drops of hexanes were added to initiate crystallization. The mother liquor was removed via syringe, and the solid washed twice with cold hexanes. The solid was dried *in vacuo* to obtain 9H-carbazol-1-ol **4.1g** as flaky white crystals (920 mg, 82%).  $R_f = 0.28$  (30:70 EtOAc:hexanes). Spectroscopic data matched known reported data.<sup>10</sup>  $^{13}\text{C}$  NMR data has not been reported.  $^1\text{H}$  NMR (500 MHz,  $\text{CDCl}_3$ )  $\delta$  8.24 (s, 1H), 8.07 (d,  $J = 8.3$  Hz, 1H), 7.70 (d,  $J = 7.9$  Hz, 1H), 7.52 – 7.40 (m, 2H), 7.25 (ddd,  $J = 8.0, 7.0, 1.2$  Hz, 1H), 7.09 (t,  $J = 7.8$  Hz, 1H), 6.84 (dd,  $J = 7.6, 0.7$  Hz, 1H), 5.00 (s, 1H);  $^{13}\text{C}$  NMR (125 MHz,  $\text{CDCl}_3$ ) 141.0, 139.4, 129.0, 126.0, 125.3, 123.6, 120.6, 119.7, 119.5, 113.3, 111.0, 110.7.



3-(*tert*-Butyl)-1H-indole **4.6d** was synthesized according to a patented procedure.<sup>13</sup> Indole **4.6a** (3.0 g, 25.6 mmol) was used to obtain compound **4.6d** as an amorphous pale pink solid (312 mg, 7%). Pure compound **4.6d** containing residual toluene (<5 mol %) was isolated following three rounds of flash chromatography on silica gel (1<sup>st</sup> column = 10:90 EtOAc:hexanes; 2<sup>nd</sup> column =

5:95 – 10:90 EtOAc:hexanes; 3<sup>rd</sup> column = 40:60 toluene:hexanes).  $R_f = 0.32$  (10:90 EtOAc:hexanes);  $R_f = 0.22$  (5:95 EtOAc:hexanes);  $R_f = 0.31$  (40:60 toluene:hexanes).  $^1\text{H NMR}$  (500 MHz,  $\text{CDCl}_3$ )  $\delta$  7.82 (dd,  $J = 8.0, 1.1$  Hz, 1H), 7.70 (br s, 1H), 7.30 (dd,  $J = 8.1, 1.0$  Hz, 1H), 7.16 (ddd,  $J = 8.1, 7.0, 1.2$  Hz, 1H), 7.09 (ddd,  $J = 8.2, 7.0, 1.2$  Hz, 1H), 6.86 (d,  $J = 2.5$  Hz, 1H), 1.45 (s, 9H).  $^{13}\text{C NMR}$  (126 MHz,  $\text{CDCl}_3$ )  $\delta$  137.1, 126.7, 125.8, 121.4, 121.2, 119.2, 118.7, 111.3, 31.6, 30.7; IR (ATR): 3394, 2962, 2863, 1616, 1459, 1360, 1123, 1100, 737  $\text{cm}^{-1}$ .

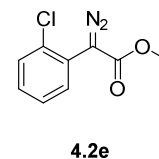
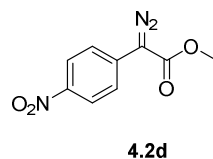
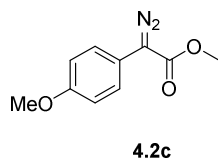
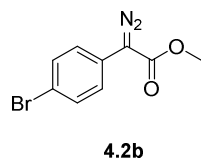
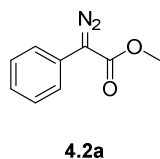
### General Procedure for Synthesis of $\alpha$ -Aryl- $\alpha$ -Diazoesters 4.2a–



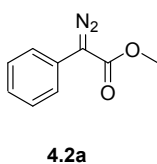
$\alpha$ -Methyl- $\alpha$ -aryldiazoacetates **4.2a–4.2e** were synthesized according to the following patented procedure.<sup>14</sup> An oven-dried round-bottom flask equipped with stir bar was charged with the  $\alpha$ -methyl- $\alpha$ -arylacetate (1.0 equiv) and *p*-acetamidobenzenesulfonyl azide (1.1 equiv). Dry acetonitrile was added to obtain a 0.25 M solution in aryl acetate. The flask was cooled in an ice-water bath for 10 minutes while stirring. A 1.5 M solution of DBU (1.2 equiv) in acetonitrile was syringed into the flask. The flask was allowed to warm to room temperature and stirred until aryl acetate was no longer detected by TLC. Next, the reaction mixture was diluted with three times its volume of ether, then washed sequentially with 50 mL each of saturated aqueous  $\text{NH}_4\text{Cl}$  and  $\text{H}_2\text{O}$  ( $\times 2$ ). The organic layer was dried with  $\text{Na}_2\text{SO}_4$ , concentrated, and purified by flash chromatography on silica gel to afford the target  $\alpha$ -aryldiazoacetate product.

### Characterization for $\alpha$ -Aryl- $\alpha$ -Diazoesters 4.2a–4.2e

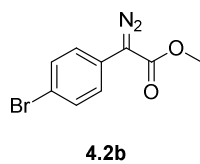




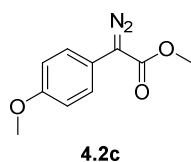
Synthesis and characterization for **2a-c**, **e**<sup>15</sup> and **2d**<sup>16</sup> has been previously reported.



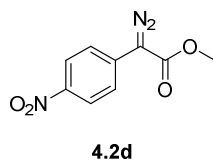
**4.2a:** <sup>1</sup>H NMR (600 MHz, CDCl<sub>3</sub>) δ 7.48 (d, *J* = 8.5 Hz, 2H), 7.38 (t, *J* = 8.0 Hz, 2H), 7.18 (t, *J* = 7.4 Hz, 1H), 3.86 (s, 3H); <sup>13</sup>C NMR (126 MHz, CDCl<sub>3</sub>) δ 165.6, 128.9, 125.8, 125.5, 123.9, 52.0.



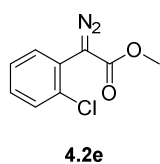
**4.2b:** <sup>1</sup>H NMR (500 MHz, CDCl<sub>3</sub>) δ 7.50 (d, *J* = 8.7 Hz, 2H), 7.36 (d, *J* = 8.7 Hz, 2H), 3.87 (s, 3H); <sup>13</sup>C NMR (126 MHz, CDCl<sub>3</sub>) δ 165.2, 132.0, 125.3, 124.7, 119.3, 52.1.



**4.2c:** <sup>1</sup>H NMR (500 MHz, CDCl<sub>3</sub>) δ 7.38 (d, *J* = 9.0 Hz, 2H), 6.95 (d, *J* = 9.0 Hz, 2H), 3.85 (s, 2H), 3.81 (s, 3H).



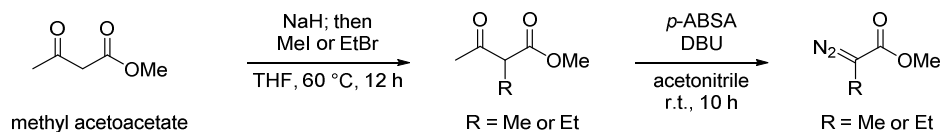
**4.2d:** <sup>1</sup>H NMR (500 MHz, CDCl<sub>3</sub>) δ 8.24 (d, *J* = 9.1 Hz, 2H), 7.67 (d, *J* = 9.1 Hz, 2H), 3.91 (s, 3H); <sup>13</sup>C NMR (126 MHz, CDCl<sub>3</sub>) δ 164.1, 145.0, 133.8, 124.3, 123.1, 52.4.



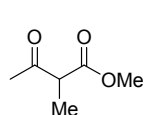
**4.2e:** <sup>1</sup>H NMR (500 MHz, CDCl<sub>3</sub>) δ 7.54 (dd, *J* = 7.8, 1.7 Hz, 1H), 7.42 (dd, *J* = 7.8, 1.6 Hz, 1H), 7.32 (td, *J* = 7.6, 1.5 Hz, 1H), 7.28 (dd, *J* = 7.9, 1.8 Hz, 1H), 3.84 (s, 3H); <sup>13</sup>C NMR (126 MHz, CDCl<sub>3</sub>) δ 165.9, 133.8, 132.3, 130.1, 129.6, 127.1, 123.9, 52.3.

### Procedure for Synthesis of $\alpha$ -Alkyl- $\alpha$ -Diazoesters

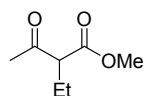
$\alpha$ -Alkyl- $\alpha$ -diazoesters compounds were synthesized from methyl acetoacetate in two steps. A previously reported procedure for the first step was used with some modification.<sup>17</sup>



**Step 1:** An oven-dried 100 mL round-bottom flask equipped with stir bar was evacuated and backfilled with argon. The flask was charged with NaH (0.48 g, 12 mmol, 60% dispersion in mineral oil) and THF (25 mL). The suspension was cooled in an ice-water bath for 10 minutes while stirring. A solution of methyl acetoacetate (1.75 g, 15 mmol) in THF (5 mL) was then added to the flask over 10 minutes. The flask was warmed to room temperature and stirred for 30 minutes. Iodomethane (1.42 g, 10 mmol) was then added and the flask submerged in a 60 °C oil bath for 12 h. After 12 h, the flask was cooled in an ice-water bath for 10 minutes, and saturated aqueous NH<sub>4</sub>Cl (15 mL) was added. The mixture was diluted with ether (30 mL) and H<sub>2</sub>O (30 mL). The resulting layers were separated and the aqueous layer extracted with additional ether (50 mL). The organic layers were combined and washed with brine, dried over Na<sub>2</sub>SO<sub>4</sub>, and concentrated *in vacuo*. The resulting oil was further purified by flash chromatography on silica gel (30:70 ether:hexanes) to obtain methyl 2-methyl-3-oxobutanoate (methyl 2-methylacetoacetate) as a colorless oil (678 mg, 52%). Spectroscopic data was consistent with previous reports.<sup>18</sup>

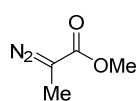


**methyl 2-methyl-3-oxobutanoate:** <sup>1</sup>H NMR (500 MHz, CDCl<sub>3</sub>) δ 3.77 (s, 3H), 3.55 (q, *J* = 7.2 Hz, 1H), 2.27 (s, 3H), 1.38 (d, *J* = 7.2 Hz, 3H); <sup>13</sup>C NMR (500 MHz, CDCl<sub>3</sub>) δ 203.6, 171.0, 53.4, 52.4, 28.5, 12.8.

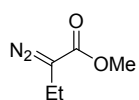


**methyl 2-ethyl-3-oxobutanoate:** Methyl 2-ethyl-3-oxobutanoate was synthesized as outlined in Step 1 above, except ethyl bromide (1.09 g, 10 mmol) was used instead of iodomethane. The product was obtained as a colorless oil (1.02 g, 71 %). <sup>1</sup>H NMR (500 MHz, CDCl<sub>3</sub>) δ 3.74 (s, 3H), 3.36 (t, *J* = 7.4 Hz, 1H), 2.23 (s, 3H), 2.00 – 1.81 (m, 2H), 0.94 (t, *J* = 7.5 Hz, 3H); <sup>13</sup>C NMR (125 MHz, CDCl<sub>3</sub>) δ 203.3, 170.3, 61.2, 52.3, 28.9, 21.7, 11.9.

Step 2:<sup>14</sup> An oven-dried round-bottom flask equipped with stir bar was charged with methyl 2-methyl-3-oxobutanoate (622 mg, 4.78 mmol), *p*-acetamidobenzenesulfonyl azide (1.26 g, 5.25 mmol), and dry acetonitrile (15 mL). The flask was cooled in an ice-water bath for 10 minutes while stirring. A solution of DBU (872 mg, 5.73 mmol) in dry acetonitrile (5 mL) was then syringed into the flask. The flask was allowed to warm to room temperature and stirred for 10 h. The reaction mixture was diluted with ether (60 mL) and then washed with saturated aqueous NH<sub>4</sub>Cl (30 mL) and brine (30 mL). The organic layer was dried over Na<sub>2</sub>SO<sub>4</sub>, concentrated, and purified by flash chromatography on silica gel (10:90 ether:hexanes) to obtain methyl 2-diazopropanoate as a yellow oil (263 mg, 48%). The product was volatile, so was concentrated to ~2 mL *in vacuo* and the remaining solvent evaporated under a gentle stream of argon. Spectroscopic data was consistent with previous reports.<sup>19</sup>

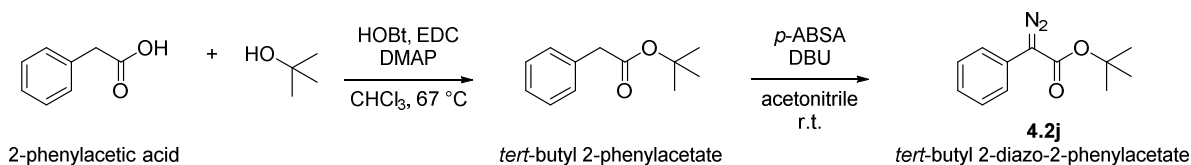


**methyl 2-diazopropanoate:** <sup>1</sup>H NMR (500 MHz; CDCl<sub>3</sub>) 3.77 (3H, s), 1.97 (3H, s); <sup>13</sup>C NMR (125 MHz CDCl<sub>3</sub>) δ 52.0, 8.5. Resonances from C=N<sub>2</sub> and C=O not observed.



**methyl 2-ethyl-3-oxobutanoate:** Methyl 2-diazobutanoate was synthesized as outlined in Step 2 above, except methyl 2-ethyl-3-oxobutanoate (912 mg, 6.33 mmol) was used instead of methyl 2-methyl-3-oxobutanoate and all other reagents scaled proportionally. The product was obtained as a yellow oil (620 mg, 76 %). <sup>1</sup>H NMR (500 MHz, CDCl<sub>3</sub>) δ 3.76 (s, 3H), 2.36 (q, *J* = 7.5 Hz, 2H), 1.14 (t, *J* = 7.5 Hz, 3H); <sup>13</sup>C NMR (125 MHz, CDCl<sub>3</sub>) δ 51.9, 16.6, 12.0. Resonances from C=N<sub>2</sub> and C=O not observed.

### Synthesis of *tert*-Butyl 2-Diazo-2-Phenylacetate 4.2j

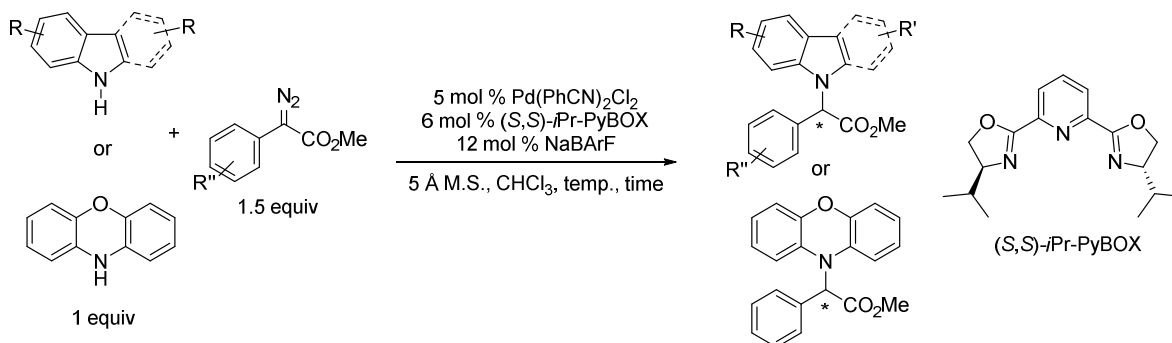


***tert*-Butyl-2-phenylacetate** was synthesized according to literature procedure with modified equivalents of reagents.<sup>20</sup> Phenylacetic acid (1.08 g, 7.93 mmol), anhydrous HOBt (1.33 g, 7.93 mmol), EDC (HCl salt) (1.52 g, 7.93 mmol), and CHCl<sub>3</sub> (30 mL) were stirred at room temperature for 30 min before adding DMAP (3.87 g, 31.7 mmol) and *tert*-butyl alcohol (3.0 mL, 31.7 mmol). The reaction was then stirred at reflux for 18 h. After 18 h, excess solvent was evaporated and the resulting yellow oil was dissolved in ether. The organic phase was then washed with 10% (w/v) aqueous NaHCO<sub>3</sub> (× 2), 10% (w/v) aqueous citric acid (× 2), 10% (w/v) aqueous K<sub>2</sub>CO<sub>3</sub> (× 2), and brine (× 2). The resulting organic phase was dried over Na<sub>2</sub>SO<sub>4</sub>, filtered, concentrated *in vacuo*, and purified by flash chromatography on silica gel (5:95 ether:hexanes) to afford *tert*-butyl-2-phenylacetate as a colorless oil (0.343 g, 23%). Spectroscopic data was consistent with previous reports.<sup>20</sup>

*tert*-Butyl-2-diazo-2-phenylacetate **4.2j** was synthesized according to literature procedure.<sup>21</sup> *tert*-Butyl-2-phenylacetate (0.343 g, 1.78 mmol) and *p*-acetamidobenzenesulfonyl azide (0.530 g, 2.14 mmol) were dissolved in anhydrous acetonitrile (5.4 mL). DBU (0.37 mL, 2.49 mmol) was added dropwise and the resulting mixture was stirred at room temperature for 24 h. Incomplete conversion of starting material resulted. The mixture was diluted with water and extracted with ether (× 3). The combined organic extracts were washed with 10% (w/v) aqueous NH<sub>4</sub>Cl (×3), brine (× 1) and dried over MgSO<sub>4</sub>. The resulting yellow-orange oil was purified by flash chromatography on silica gel (5:95 ether:hexanes) to afford *tert*-butyl 2-diazo-2-phenylacetate **4.2j**

as a clear yellow-orange oil (0.170 g, 43%). Spectroscopic data was consistent with previous reports.<sup>16</sup>

### General Experimental Procedure A: Palladium-Catalyzed Insertion with Aromatic *N*-Heterocycles

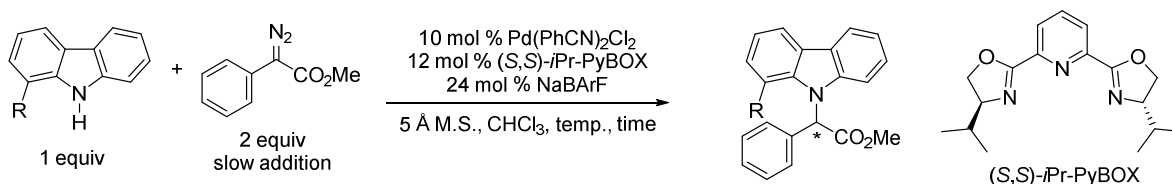


To a flame-dried round-bottom flask equipped with a stir bar was added the aromatic *N*-heterocycle substrate (1 equiv),  $\text{Pd}(\text{PhCN})_2\text{Cl}_2$  (5 mol %),  $(S,S)$ -*iPr*-PyBOX (6 mol %), NaBARF (12 mol %), and 5 Å MS (approximately 1 g/mmol of the heterocycle). To a separate flame-dried pear-shaped flask was added the  $\alpha$ -aryldiazoester (1.5 equiv). Both flasks were evacuated for 10 min and then backfilled with nitrogen gas. Distilled  $\text{CHCl}_3$  (stored over 4 Å MS) was added to the round-bottom flask to obtain a heterocycle concentration of 200 mM. The round-bottom flask was submerged in an oil bath of specified temperature for 5 min (see Analytical Data section below for reaction temperature). The  $\alpha$ -aryldiazoester was dissolved in  $\text{CHCl}_3$  to afford a 750 mM solution, and this solution was transferred in one portion to the round-bottom flask. Additional  $\text{CHCl}_3$  was used to rinse the pear-shaped flask and ensure complete transfer of the  $\alpha$ -aryldiazoester and to achieve a final heterocycle concentration of 75 mM. The reaction was stirred until consumption of either the heterocycle or  $\alpha$ -aryldiazoester as determined by TLC. Upon completion, the reaction flask was cooled to room temperature and the mixture diluted with  $\text{CHCl}_3$ . Then, the mixture was filtered through a pad of Celite®, and the pad washed three times with  $\text{CHCl}_3$ . The filtrate was

concentrated *in vacuo* and the residue purified via flash chromatography on silica gel to afford the target compounds.

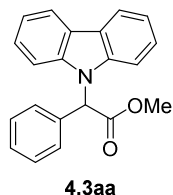
A slightly modified procedure was used for aliphatic amine substrates, please refer to the Analytical Data section for those examples.

### General Experimental Procedure B: Palladium-Catalyzed Insertion with 1-Substituted Carbazoles



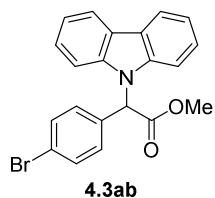
To a flame-dried round-bottom flask equipped with a stir bar was added the 1-substituted carbazole substrate (1 equiv), Pd(PhCN)<sub>2</sub>Cl<sub>2</sub> (10 mol %), (S,S)-iPr-PyBOX (12 mol %), NaBARF (24 mol %), and 5 Å MS (approximately 1g/mmol of carbazole). To a separate flame-dried pear-shaped flask was added the  $\alpha$ -aryldiazoester (2 equiv). Both flasks were evacuated for 10 min, and backfilled with nitrogen gas. To the round-bottom flask was added CHCl<sub>3</sub> to obtain a 100 mM solution with respect to the carbazole substrate. The  $\alpha$ -aryldiazoester was dissolved in CHCl<sub>3</sub> to obtain a 300 mM solution. The round-bottom flask was submerged in an oil bath for 5 min (see Analytical Data section below for reaction temperature) and the diazo solution added over 8 hours using a syringe pump. After addition, the reaction was stirred for some additional time (see Analytical Data section) until consumption of either the 1-substituted carbazole or  $\alpha$ -aryldiazoester as determined by TLC. Upon completion, the reaction mixture was cooled to room temperature and diluted with CHCl<sub>3</sub>. The mixture was then filtered through a pad of Celite® and the pad washed three times with CHCl<sub>3</sub>. The filtrate was concentrated *in vacuo* and the residue purified via flash chromatography on silica gel to afford the target compounds.

### Analytical Data for Insertion Products 4.3aa–4.3ai



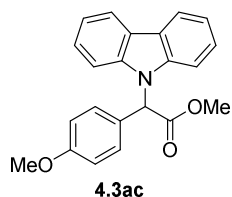
Methyl 2-(9*H*-carbazol-9-yl)-2-phenylacetate, **4.3aa**: Example using general procedure A. A flame-dried, 5 mL round-bottom flask equipped with stir bar was charged with 9*H*-carbazole **4.1a** (31.4 mg, 0.19 mmol, 1 equiv), Pd(PhCN)<sub>2</sub>Cl<sub>2</sub> (3.6 mg, 0.009 mmol, 5 mol %), (*S,S*)-*i*Pr-PyBOX (3.4 mg, 0.01 mmol, 6 mol %), NaBARF (20 mg, 0.02 mmol, 12 mol %), and 5 Å MS (190 mg). To a separate flame-dried pear-shaped flask was added methyl α-phenyldiazoacetate **4.2a** (49.6 mg, 0.28 mmol, 1.5 equiv). Both flasks were evacuated for 10 min and then backfilled with nitrogen gas. Distilled CHCl<sub>3</sub> (1.1 mL) was added to the round-bottom flask to obtain a carbazole concentration of 200 mM. The round-bottom flask was submerged in a 30 °C oil bath for 5 min while stirring. Next, the methyl α-phenyldiazoacetate **4.2a** was dissolved in CHCl<sub>3</sub> (0.4 mL) to obtain a 750 mM solution, and this solution was transferred in one portion to the round-bottom flask. Additional CHCl<sub>3</sub> (1.0 mL) was used to rinse the pear-shaped flask and ensure complete transfer of the diazo substrate and to achieve a final heterocycle concentration of 75 mM. The reaction mixture was stirred at 30 °C for 2 h. By this time, no carbazole was detected by TLC. The crude product was purified by flash chromatography on silica gel (5:95 ether:hexanes) to obtain insertion compound **4.3aa** as a pale beige solid (55.6 mg, 99%, 97% *ee*). *R<sub>f</sub>* = 0.37 (20:80 ether:hexanes); The *ee* was measured utilizing the Shimadzu HPLC instrument using a chiral stationary phase [Chiralcel OD-H, 2-propanol:hexanes = 8/92, 1.0 mL/min, λ = 254 nm], *t<sub>R</sub>* = 9.50 min (major), 19.04 min (minor); <sup>1</sup>H NMR (500 MHz, CDCl<sub>3</sub>) δ 8.11 (dd, *J* = 8.0, 1.2 Hz, 2H), 7.36 (td, *J* = 7.5, 7.1, 1.2 Hz, 2H), 7.34 – 7.30 (m, 3H), 7.27 – 7.26 (m, 2H), 7.25 – 7.21 (m, 4H), 6.62 (s, 1H), 3.78 (s, 3H); <sup>13</sup>C NMR (126 MHz, CDCl<sub>3</sub>) δ 169.8, 140.2, 134.0, 128.7, 128.3, 127.4, 125.8, 123.5, 120.3, 119.7, 110.1, 60.3, 52.8; IR (ATR) 3036,

2920, 2851, 1741, 1449, 1205  $\text{cm}^{-1}$ . HRMS (ESI)  $m/z$  calcd for  $\text{C}_{21}\text{H}_{17}\text{NO}_2\text{Na}$   $[\text{M} + \text{Na}]^+$  338.1157, found 338.1144.



Methyl 2-(4-bromophenyl)-2-(9H-carbazol-9-yl)acetate, **4.3ab**: Using general procedure A, 9H-carbazole **4.1a** (95%, 21.1 mg, 0.12 mmol) was reacted with methyl 2-(4-bromophenyl)-2-diazoacetate **4.2b** (45.9 mg, 0.18 mmol) for 8 h.

The crude product was purified by flash chromatography on silica gel (20:80 ether:hexanes) to obtain insertion product **4.3ab** as pale yellow solid (40.4 mg, 85%, 93% *ee*).  $R_f = 0.31$  (20:80 ether:hexanes); The *ee* was measured utilizing the Shimadzu HPLC instrument using a chiral stationary phase [Chiralcel OD-H, 2-propanol:hexanes = 8/92, 1.0 mL/min,  $\lambda = 254$  nm],  $t_R = 9.78$  min (major), 19.67 min (minor);  $^1\text{H}$  NMR (500 MHz,  $\text{CDCl}_3$ )  $\delta$  8.11 (d,  $J = 7.7$  Hz, 2H), 7.43 (d,  $J = 8.6$  Hz, 2H), 7.38 (t,  $J = 7.2$  Hz, 2H), 7.30 – 7.19 (m, 4H), 7.10 (d,  $J = 8.4$  Hz, 2H), 6.52 (s, 1H), 3.75 (s, 3H);  $^{13}\text{C}$  NMR (125 MHz,  $\text{CDCl}_3$ )  $\delta$  169.3, 140.0, 133.0, 131.8, 129.1, 125.9, 123.6, 122.5, 120.4, 120.0, 109.9, 59.6, 52.9; IR (ATR): 3061, 2949, 1745, 1483, 1451, 1198, 1171, 996, 749, 724  $\text{cm}^{-1}$ ; HRMS (ESI)  $m/z$  calcd for  $\text{C}_{21}\text{H}_{16}\text{BrNO}_2\text{Na}$   $[\text{M} + \text{Na}]^+$  416.0262, found 416.0247.

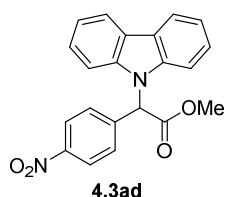


Methyl 2-(9H-carbazol-9-yl)-2-(4-methoxyphenyl)acetate, **4.3ac**: Using general procedure A, 9H-carbazole **4.1a** (95%, 21.1 mg, 0.12 mmol) was reacted with methyl 2-diazo-2-(4-methoxyphenyl)acetate **4.2c** (37.1 mg, 0.18

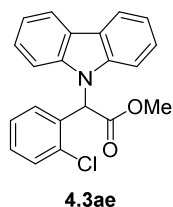
mmol) for 30 min. The crude product was purified by flash chromatography on silica gel (1<sup>st</sup> column = 15:85 ether:hexanes; 2<sup>nd</sup> column = 25:75 ether:hexanes) to obtain insertion product **4.3ac** as a pale orange solid (37.3 mg, 90%, 96% *ee*).  $R_f = 0.15$  (15:85 ether:hexanes);  $R_f = 0.29$  (25:75 ether:hexanes); The *ee* was measured utilizing the Shimadzu HPLC instrument using a chiral stationary phase [Chiralcel OD-H, 2-propanol:hexanes = 12/88, 1.0 mL/min,  $\lambda = 254$  nm],  $t_R = 11.45$  min (major), 21.95 min (minor);  $^1\text{H}$  NMR (500 MHz,  $\text{CDCl}_3$ )  $\delta$  8.10 (d,  $J = 7.6$  Hz, 2H),



7.36 (t,  $J = 7.2$  Hz, 2H), 7.30 – 7.20 (m, 4H), 7.16 (d,  $J = 8.8$  Hz, 2H), 6.84 (d,  $J = 8.8$  Hz, 2H), 6.57 (s, 1H), 3.78 (s, 3H), 3.76 (s, 3H);  $^{13}\text{C}$  NMR (125 MHz,  $\text{CDCl}_3$ )  $\delta$  170.1, 159.5, 140.2, 128.7, 125.9, 125.8, 123.5, 120.3, 119.7, 114.0, 110.2, 59.8, 55.3, 52.7; IR (ATR): 3010, 2951, 2837, 1743, 1612, 1598, 1512, 1450, 1175, 750,  $722.7\text{ cm}^{-1}$ ; HRMS (ESI)  $m/z$  calcd for  $\text{C}_{22}\text{H}_{19}\text{NO}_3\text{Na}$   $[\text{M} + \text{Na}]^+$  368.1263, found 368.1256.



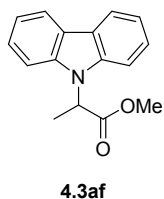
Methyl 2-(9H-carbazol-9-yl)-2-(4-nitrophenyl)acetate, **4.3ad**: Using general procedure A, 9H-carbazole **4.1a** (95%, 21.1 mg, 0.12 mmol) was reacted with methyl 2-diazo-2-(4-nitrophenyl)acetate **4.2d** (39.8 mg, 0.18 mmol) at 55 °C for 30 h. The crude product was purified by flash chromatography on silica gel (1<sup>st</sup> column = 50:50 ether:hexanes; 2<sup>nd</sup> column = 70:30 DCM:hexanes) to obtain insertion product **4.3ad** as pale yellow solid (6.1 mg, 14%, 0% *ee*).  $R_f = 0.44$  (50:50 ether:hexanes);  $R_f = 0.39$  (70:30 DCM:hexanes); The *ee* was measured utilizing the Shimadzu HPLC instrument using a chiral stationary phase [Chiralcel OD-H, 2-propanol:hexanes = 15/85, 1.0 mL/min,  $\lambda = 254$  nm],  $t_R = 16.91$  min (equal), 24.08 min (equal);  $^1\text{H}$  NMR (500 MHz,  $\text{CDCl}_3$ )  $\delta$  8.14 (t,  $J = 8.0$  Hz, 4H), 7.44 – 7.35 (m, 4H), 7.29 (t,  $J = 7.5$  Hz, 2H), 7.21 (d,  $J = 8.3$  Hz, 2H), 6.61 (s, 1H), 3.76 (s, 3H);  $^{13}\text{C}$  NMR (125 MHz,  $\text{CDCl}_3$ )  $\delta$  168.7, 147.8, 141.1, 139.8, 128.5, 126.2, 123.8, 123.7, 120.6, 120.3, 109.6, 59.5, 53.2; IR (ATR): 3050, 2952, 1743, 1520, 1451, 1344, 1203, 750,  $723\text{ cm}^{-1}$ ; HRMS (ESI)  $m/z$  calcd for  $\text{C}_{21}\text{H}_{15}\text{N}_2\text{O}_4$   $[\text{M} - \text{H}]^-$  359.1032, found 359.1041.



Methyl 2-(9H-carbazol-9-yl)-2-(2-chlorophenyl)acetate, **4.3ae**: Using general procedure A, 9H-carbazole **4.1a** (95%, 16.7 mg, 0.095 mmol) was reacted with methyl 2-(2-chlorophenyl)-2-diazoacetate **4.2e** (31.5 mg, 0.15 mmol) at 30 °C for 2.5 h. The crude product was purified by flash chromatography on silica gel (4:96 EtOAc:hexanes) to afford insertion product **4.3ae** as a clear oil (11.3 mg, 34%, 87% *ee*).  $R_f = 0.65$  (25:75

EtOAc:hexanes); The *ee* was measured utilizing the Shimadzu HPLC instrument using a chiral stationary phase [Chiralcel OD-H, 2-propanol:hexanes = 1/99, 1.0 mL/min,  $\lambda$  = 254 nm],  $t_R$  = 22.60 min (major), 24.84 min (minor);  $^1\text{H}$  NMR (500 MHz,  $\text{CDCl}_3$ )  $\delta$  8.13 (d,  $J$  = 7.7 Hz, 2H), 7.46 (d,  $J$  = 8.4 Hz, 1H), 7.41 (t,  $J$  = 7.2 Hz, 2H), 7.34 – 7.26 (m, 5H), 7.16 – 7.11 (m, 2H), 6.77 (s, 1H), 3.76 (s, 3H);  $^{13}\text{C}$  NMR (125 MHz,  $\text{CDCl}_3$ )  $\delta$  168.7, 140.3, 134.1, 132.7, 129.9, 128.4, 127.0, 126.1, 123.5, 120.4, 120.0, 109.5, 59.1, 53.1; IR (ATR) 2923, 2852, 1746, 1451, 747  $\text{cm}^{-1}$ ; HRMS (ESI)  $m/z$  calcd for  $\text{C}_{21}\text{H}_{16}\text{ClNO}_2\text{Na}$  [ $\text{M} + \text{Na}$ ] $^+$  372.0767, found 372.0760.

### Supplementary Reactions: Reactions of Carbazole 4.1a with $\alpha$ -Alkyl- $\alpha$ -Diazoesters

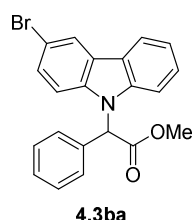


**methyl 2-(9H-carbazol-9-yl)propanoate:** Using general procedure A, carbazole **4.1a** (25.1 mg, 0.15 mmol) was reacted with methyl 2-diazopropanoate (25.7 mg, 0.23 mmol) at 30 °C for 14 h. The resulting red oil was purified by flash chromatography on silica gel (10:90 ether:hexanes) followed by preparative thin-layer chromatography (10:90 acetone:hexanes) to afford methyl 2-(9H-carbazol-9-yl)propanoate **4.3af** as a white film (2.7 mg, 7%, 82% *ee*).  $R_f$  = 0.32 (10:90 acetone:hexanes); The *ee* was measured utilizing Shimadzu HPLC instrument using a chiral stationary phase [Chiralcel OD-H, 2-propanol:hexanes = 7.5/92.5, 1.0 mL/min,  $\lambda$  = 254 nm],  $t_R$  = 15.53 min (major), 16.82 min (minor);  $^1\text{H}$  NMR (500 MHz,  $\text{CDCl}_3$ )  $\delta$  8.11 (dt,  $J$  = 7.8, 1.0 Hz, 2H), 7.45 (ddd,  $J$  = 8.3, 7.1, 1.2 Hz, 2H), 7.37 (d,  $J$  = 8.2 Hz, 2H), 7.25 (t,  $J$  = 7.4 Hz, 2H), 5.43 (q,  $J$  = 7.3 Hz, 1H), 3.69 (s, 3H), 1.83 (d,  $J$  = 7.3 Hz, 3H);  $^{13}\text{C}$  NMR (126 MHz,  $\text{CDCl}_3$ )  $\delta$  171.6, 139.5, 129.5, 125.8, 123.4, 120.5, 119.4, 109.1, 52.7, 52.0, 15.4; IR (ATR) 3048, 2925, 1740, 1453, 1236, 1226, 748, 722  $\text{cm}^{-1}$ ; HRMS (ESI)  $m/z$  calcd for  $\text{C}_{16}\text{H}_{15}\text{NO}_2\text{Na}$  [ $\text{M} + \text{Na}$ ] $^+$  276.1000, found 276.0994.

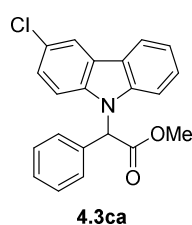
Note: No N-H insertion was observed in the reaction of methyl 2-diazobutanoate with either carbazole **4.1a** or ethyl-3-indoleacetate **4.6c**. Rather, we observe (*E*) and (*Z*)-methylcrotonate as

major byproducts, which result from palladium-catalyzed decomposition of the diazo substrate. Most of the starting materials were recovered following chromatography (91% carbazole **4.1a** and 82% ethyl-3-indoleacetate **4.6c**). Indeed, (*E*) and (*Z*)-methylcrotonate were still obtained when carbazole **4.1a** or ethyl-3-indoleacetate **4.6c** was excluded from the reaction; in the absence of heterocycle, methyl 2-diazobutanoate was consumed within ~3 hours at 40 °C.

### Analytical Data for Insertion Products 4.3ba–4.3ai

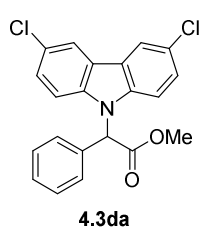


Methyl 2-(3-bromo-9*H*-carbazol-9-yl)-2-phenylacetate, **4.3ba**: Using general procedure A, 3-bromo-9*H*-carbazole **4.1b** (97%, 73.5 mg, 0.29 mmol) was reacted with methyl 2-diazo-2-phenylacetate **4.2a** (79.3 mg, 0.45 mmol) at 30 °C for 7 h. The crude product was purified by flash chromatography on silica gel (15:85 EtOAc:hexanes) to obtain insertion product **4.3ba** as a clear oil (81.9 mg, 71%, 99% *ee*).  $R_f = 0.41$  (20:80 EtOAc:hexanes); The *ee* was measured utilizing the Shimadzu HPLC instrument using a chiral stationary phase [Chiralcel OD-H, 2-propanol:hexanes = 8/92, 1.0 mL/min,  $\lambda = 254$  nm],  $t_R = 8.90$  min (major), 13.75 min (minor);  $^1\text{H}$  NMR (500 MHz,  $\text{CDCl}_3$ )  $\delta$  8.21 (d,  $J = 1.9$  Hz, 1H), 8.06 (d,  $J = 7.7$  Hz, 1H), 7.43 – 7.39 (m, 2H), 7.35 – 7.32 (m, 3H), 7.29 – 7.26 (m, 2H), 7.21 – 7.19 (m, 2H), 7.07 (d,  $J = 8.7$  Hz, 1H), 6.58 (s, 1H), 3.79 (s, 3H);  $^{13}\text{C}$  NMR (125 MHz,  $\text{CDCl}_3$ )  $\delta$  169.5, 140.6, 138.7, 133.6, 128.8, 128.5, 128.4, 127.3, 126.6, 125.4, 123.0, 122.5, 120.5, 120.2, 112.7, 112.1, 110.1, 60.4, 52.8; IR (ATR) 3056, 2950, 1745, 1444, 1270, 1201, 731  $\text{cm}^{-1}$ ; HRMS (ESI)  $m/z$  calcd for  $\text{C}_{21}\text{H}_{16}\text{BrNO}_2\text{Na}$  [ $\text{M} + \text{Na}$ ] $^+$  416.0262, found 416.0262.



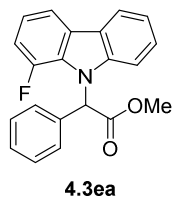
Methyl 2-(3-chloro-9*H*-carbazol-9-yl)-2-phenylacetate, **4.3ca**: Using general procedure A, 3-chloro-9*H*-carbazole **4.1c** (24.0 mg, 0.12 mmol) was reacted with methyl 2-diazo-2-phenylacetate **4.2a** (31.4 mg, 0.18 mmol) at 30 °C for 2 h. The crude product was purified by flash chromatography on silica gel (25:75

ether:hexanes) to obtain insertion product **4.3ca** as a clear oil (33.6 mg, 89%, 97% *ee*).  $R_f = 0.46$  (30:70 ether:hexanes); The *ee* was measured utilizing the Shimadzu HPLC instrument using a chiral stationary phase [Chiralcel OD-H, 2-propanol:hexanes = 8/92, 1.0 mL/min,  $\lambda = 254$  nm],  $t_R = 8.46$  min (major), 12.35 min (minor);  $^1\text{H NMR}$  (500 MHz,  $\text{CDCl}_3$ )  $\delta$  8.09 – 8.03 (m, 2H), 7.40 (t,  $J = 7.4$  Hz, 1H), 7.35 – 7.25 (m, 6H), 7.21 – 7.17 (m, 2H), 7.11 (d,  $J = 8.8$  Hz, 1H), 6.58 (s, 1H), 3.78 (s, 3H);  $^{13}\text{C NMR}$  (125 MHz,  $\text{CDCl}_3$ )  $\delta$  169.5, 140.8, 138.4, 133.6, 128.8, 128.5, 127.3, 126.5, 125.8, 125.3, 124.8, 122.6, 120.5, 120.1, 120.0, 111.6, 110.1, 60.4, 52.8; IR (ATR) 3063, 2924, 2951, 1745, 1473, 1446, 1201, 745  $\text{cm}^{-1}$ ; HRMS (ESI)  $m/z$  calcd for  $\text{C}_{21}\text{H}_{16}\text{ClNO}_2\text{Na}$  [ $\text{M} + \text{Na}$ ] $^+$  372.0767, found 372.0759.

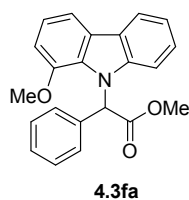


Methyl 2-(3,6-dichloro-9H-carbazol-9-yl)-2-phenylacetate, **4.3da**: Using general procedure A, 3,6-dichloro-9H-carbazole **4.1d** (22.6 mg, 0.10 mmol) was reacted with methyl 2-diazo-2-phenylacetate **4.2a** (25.3 mg, 0.14 mmol) for 3.5 h at 30 °C. The crude product was purified by flash chromatography on silica gel

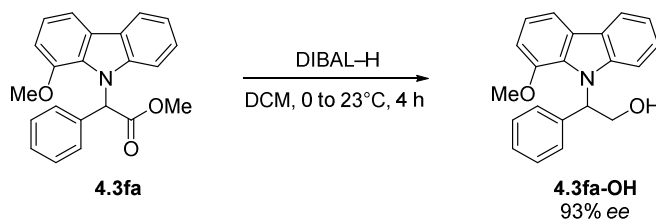
(30:70 ether:hexanes) to obtain insertion product **4.3da** as a clear oil (32.8 mg, 89%, 95% *ee*).  $R_f = 0.41$  (30:70 ether:hexanes); The *ee* was measured utilizing the Shimadzu HPLC instrument using a chiral stationary phase [Chiralcel OD-H, 2-propanol:hexanes = 2/98, 1.5 mL/min,  $\lambda = 254$  nm],  $t_R = 9.40$  min (minor), 10.29 min (major);  $^1\text{H NMR}$  (500 MHz,  $\text{CDCl}_3$ )  $\delta$  8.00 (d,  $J = 2.1$  Hz, 2H), 7.35 – 7.31 (m, 5H), 7.19 – 7.17 (m, 2H), 7.15 (d,  $J = 8.8$  Hz, 2H), 6.54 (s, 1H), 3.80 (s, 3H);  $^{13}\text{C NMR}$  (125 MHz,  $\text{CDCl}_3$ )  $\delta$  169.3, 139.0, 133.3, 128.9, 128.7, 127.2, 126.6, 125.7, 123.8, 120.2, 111.5, 60.6, 52.9; IR (ATR) 2952, 2921, 1745, 1474, 1434, 1203, 864, 792, 734  $\text{cm}^{-1}$ ; HRMS (ESI)  $m/z$  calcd for  $\text{C}_{21}\text{H}_{15}\text{Cl}_2\text{NO}_2\text{Na}$  [ $\text{M} + \text{Na}$ ] $^+$  406.0378, found 406.0382.



Methyl 2-(1-fluoro-9*H*-carbazol-9-yl)-2-phenylacetate, **4.3ea**: Example using general procedure B. A flame-dried, 5 mL round-bottom flask equipped with stir bar was charged with 1-fluoro-9*H*-carbazole **4.1e** (38.3 mg, 0.21 mmol, 1 equiv), Pd(PhCN)<sub>2</sub>Cl<sub>2</sub> (7.6 mg, 0.020 mmol, 10 mol %), (*S,S*)-*i*Pr-PyBOX (7.2 mg, 0.024 mmol, 12 mol %), NaBARF (42.5 mg, 0.048 mmol, 24 mol %), and 5 Å MS (196 mg). To a separate flame-dried pear-shaped flask was added  $\alpha$ -methyl- $\alpha$ -phenyldiazoacetate **4.2a** (74.0 mg, 0.42 mmol, 2 equiv). Both flasks were evacuated for 10 min and then backfilled with nitrogen gas. Distilled CHCl<sub>3</sub> (2.1 mL) was added to the round-bottom flask to obtain a 100 mM solution with respect to 1-fluoro-9*H*-carbazole **4.1e**. The  $\alpha$ -methyl- $\alpha$ -phenyldiazoacetate **4.2a** was dissolved in CHCl<sub>3</sub> (1.4 mL) to obtain a 300 mM solution. The round-bottom flask was submerged in an oil bath pre-heated to 43 °C, and the contents stirred for 5 min. Then, the methyl phenyldiazoacetate solution was added to the reaction mixture over 8 hours via syringe pump, followed by 2.5 h additional stirring. The crude product was purified by flash chromatography on silica gel (15:85 ether:hexanes) to obtain insertion compound **4.3ea** as a white solid (43.1 mg, 63%, 94% *ee*). *R*<sub>f</sub> = 0.32 (15:85 ether:hexanes); The *ee* was measured utilizing the Shimadzu HPLC instrument using a chiral stationary phase [Chiralcel OD-H, 2-propanol:hexanes = 8/92, 1.0 mL/min,  $\lambda$  = 254 nm], *t*<sub>R</sub> = 6.68 min (major), 9.78 min (minor); <sup>1</sup>H NMR (500 MHz, CDCl<sub>3</sub>)  $\delta$  8.06 (d, *J* = 7.8 Hz, 1H), 7.92 – 7.84 (m, 1H), 7.37 – 7.26 (m, 6H), 7.26 – 7.20 (m, 3H), 7.19 (m, 3H), 3.78 (s, 3H); <sup>13</sup>C NMR (125 MHz, CDCl<sub>3</sub>)  $\delta$  169.8, 149.4 (d, *J* = 241.9 Hz), 140.3, 134.9, 128.5, 128.2, 127.9 (d, *J* = 8.0 Hz), 127.4, 127.3 (d, *J* = 4.7 Hz), 126.4, 123.7 (d, *J* = 2.0 Hz), 120.4, 120.2, 120.1 (d, *J* = 6.8 Hz), 116.1 (d, *J* = 3.4 Hz), 112.4 (d, *J* = 19.6 Hz), 111.3, 61.7 (d, *J* = 7.9 Hz), 52.8; IR (ATR): 3070, 2943, 1744, 1574, 1457, 1431, 1338, 1211, 748, 736 cm<sup>-1</sup>; HRMS (ESI) *m/z* calcd for C<sub>21</sub>H<sub>16</sub>FNO<sub>2</sub>Na [M + Na]<sup>+</sup> 356.1063, found 356.1081.

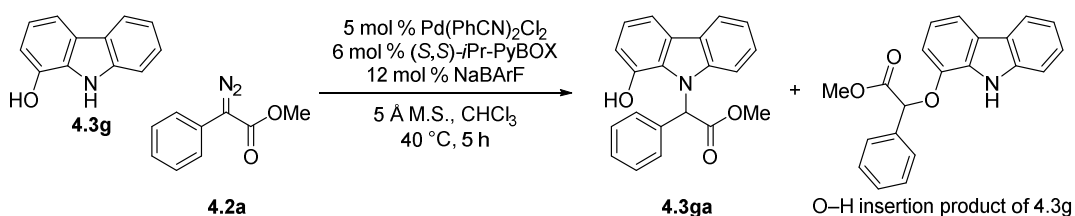


Methyl 2-(1-methoxy-9*H*-carbazol-9-yl)-2-phenylacetate, **4.3fa**: Using general procedure B, 1-methoxy-9*H*-carbazole **4.1f** (700 mg, 3.55 mmol) was reacted with  $\alpha$ -methyl- $\alpha$ -phenyldiazoacetate **4.2a** (1.25 g, 7.10 mmol) at 40 °C. The diazo solution was added via syringe pump over 8 h, followed by 1 h additional stirring. The crude product was purified by flash chromatography on silica gel (1<sup>st</sup> column = 30:70 ether:hexanes; 2<sup>nd</sup> column = 30:70 ether:hexanes) to obtain insertion product **4.3fa** as a colorless oil that solidifies upon drying *in vacuo* (529 mg, 43%).  $R_f$  = 0.31 (toluene);  $R_f$  = 0.38 (30:70 ether:hexanes); The *ee* was determined by analyzing the reduced product (see next paragraph). <sup>1</sup>H NMR (500 MHz, CDCl<sub>3</sub>)  $\delta$  8.05 (d,  $J$  = 7.8 Hz, 1H), 7.73 (d,  $J$  = 7.8 Hz, 1H), 7.47 (br, 1H), 7.35 – 7.23 (m, 6H), 7.21 – 7.15 (m, 2H), 7.11 (d,  $J$  = 8.3 Hz, 1H), 6.93 (d,  $J$  = 7.9 Hz, 1H), 3.86 (s, 3H), 3.71 (s, 3H); <sup>13</sup>C NMR (125 MHz, CDCl<sub>3</sub>)  $\delta$  170.4, 146.7, 140.1, 135.9, 129.8, 128.3, 127.7, 127.5, 125.6, 125.3, 123.8, 120.2, 120.2, 119.6, 113.1, 111.2, 107.8, 61.5, 55.6, 52.5; IR (ATR): 3058, 2950, 2838, 1740, 1579, 1455, 1430, 1261, 1204, 1014, 735 cm<sup>-1</sup>; HRMS (ESI)  $m/z$  calculated for C<sub>22</sub>H<sub>19</sub>NO<sub>3</sub>Na [M + Na]<sup>+</sup> 368.1263, found 368.1255.

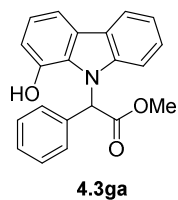


2-(1-methoxy-9*H*-carbazol-9-yl)-2-phenylethan-1-ol, **4.3fa-OH**: An oven-dried 100 mL round-bottom flask equipped with stir bar was charged with compound **4.3fa** (293 mg, 0.85 mmol, 1 equiv), evacuated, backfilled with nitrogen, and sealed with a rubber septum. Through the septum was injected dry CH<sub>2</sub>Cl<sub>2</sub> (20 mL). The flask was submerged in an ice-water bath for 10 min while stirring. Through the septum was injected DIBAL-H (2.6 mL, 1 M in hexanes, 2.55 mmol, 3 equiv). The ice-water bath was allowed to warm to room temperature and the reaction stirred for

4 h. Next, the flask was cooled for 10 min in an ice-water bath. Methanol (0.5 mL) was added dropwise to quench unreacted DIBAL–H and the reaction mixture diluted with ether (25 mL). To the mixture was added a saturated solution of sodium potassium tartrate (5 mL) and stirred vigorously at room temperature for 2 h. The ether layer was collected. Additional ether (30 mL) was added to the aqueous layer and the mixture stirred vigorously for 15 min. The ether layers were combined and concentrated *in vacuo*. The crude product was purified by flash chromatography on silica gel (30:70 EtOAc:hexanes) to obtain the corresponding alcohol **4.3fa-OH** (246 mg, 91%, 93% *ee*).  $R_f = 0.41$  (30:70 EtOAc:hexanes); The *ee* was measured utilizing the Shimadzu HPLC instrument using a chiral stationary phase [Chiralcel OD-H, 2-propanol:hexanes = 50/50, 0.5 mL/min,  $\lambda = 254$  nm],  $t_R = 14.07$  min (major), 44.20 min (minor);  $^1\text{H}$  NMR (500 MHz,  $\text{CDCl}_3$ )  $\delta$  8.02 (d,  $J = 7.9$  Hz, 1H), 7.70 (d,  $J = 7.8$  Hz, 1H), 7.52 – 6.67 (m, 11H), 4.62 – 4.41 (m, 2H), 3.82 (s, 2H);  $^{13}\text{C}$  NMR (125 MHz,  $\text{CDCl}_3$ )  $\delta$  146.7, 138.8, 130.7, 128.5, 127.1, 126.4, 125.3, 124.2, 120.3, 119.9, 119.3, 113.0, 112.1, 108.1, 62.9, 60.3, 55.7; IR (ATR): 3343 (br), 3054, 2932, 2835, 1576, 1454, 1427, 1328, 1259, 1217  $\text{cm}^{-1}$ . HRMS (ESI)  $m/z$  calcd for  $\text{C}_{21}\text{H}_{19}\text{NO}_2\text{Na}$   $[\text{M} + \text{Na}]^+$  340.1313, found 340.1325.

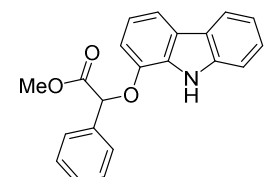


Using general procedure, A, 9*H*-carbazol-1-ol **4.1g** (55.0 mg, 0.30 mmol) was reacted with  $\alpha$ -methyl- $\alpha$ -phenyldiazoacetate **4.2a** (79.2 mg, 0.45 mmol) at 40 °C for 5 h. The crude product was purified by flash chromatography on silica gel (1<sup>st</sup> column = 30:70 ether:hexanes; 2<sup>nd</sup> column = 50:50 ether:hexanes) to obtain N–H insertion product **4.3ga** as a white solid (60.8 mg, 61%, 26% *ee*) and O–H insertion product as a colorless oil (14.9 mg, 15%).



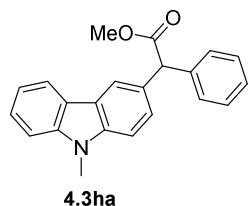
Methyl 2-(1-hydroxy-9*H*-carbazol-9-yl)-2-phenylacetate **4.3ga**:  $R_f = 0.15$  (30:70 ether:hexanes);  $R_f = 0.33$  (50:50 ether:hexanes); The *ee* was measured utilizing the

Shimadzu HPLC instrument using a chiral stationary phase [Chiralcel OD-H, 2-propanol:hexanes = 10/90, 1.0 mL/min,  $\lambda = 254$  nm],  $t_R = 12.10$  min (major), 36.38 min (minor);  $^1\text{H}$  NMR (500 MHz, acetone- $d_6$ ) 9.10 (br, 1H), 8.10 (d,  $J = 7.8$  Hz, 1H), 7.78 (s, 1H), 7.71 (dd,  $J = 7.8, 0.9$  Hz, 1H), 7.40 (d,  $J = 7.6$  Hz, 2H), 7.34 – 7.20 (m, 5H), 7.19 – 7.13 (m, 1H), 7.08 (t,  $J = 7.7$  Hz, 1H), 6.98 (dd,  $J = 7.7, 0.9$  Hz, 1H), 3.74 (s, 3H);  $^{13}\text{C}$  NMR (126 MHz, acetone- $d_6$ )  $\delta$  170.9, 144.5, 141.1, 137.5, 130.1, 129.0, 128.7, 128.4, 126.5, 126.2, 124.9, 121.2, 120.9, 120.2, 113.1, 112.8, 112.4, 62.1, 52.7, 29.8 (acetone- $d_6$ ); IR (ATR): 3413 (br), 3057, 2951, 1722, 1585, 1455, 1338, 1268, 1215, 742  $\text{cm}^{-1}$ ; HRMS (ESI)  $m/z$  calcd for  $\text{C}_{21}\text{H}_{17}\text{NO}_3\text{Na}$   $[\text{M} + \text{Na}]^+$  354.1106, found 354.1113.



Methyl 2-((9*H*-carbazol-1-yl)oxy)-2-phenylacetate (O–H insertion product of 4.3g):  $R_f = 0.33$  (30:70 ether:hexanes);  $R_f = 0.52$  (50:50 ether:hexanes);

$^1\text{H}$  NMR (500 MHz,  $\text{CDCl}_3$ )  $\delta$  8.65 (br, 1H), 8.04 (d,  $J = 7.8$  Hz, 1H), 7.72 (d,  $J = 7.8$  Hz, 1H), 7.65 (d,  $J = 6.6$  Hz, 2H), 7.54 – 7.36 (m, 5H), 7.24 – 7.17 (m, 1H), 7.08 (t,  $J = 7.8$  Hz, 1H), 6.84 (d,  $J = 7.8$  Hz, 1H), 5.82 (s, 1H), 3.75 (s, 3H);  $^{13}\text{C}$  NMR (125 MHz,  $\text{CDCl}_3$ )  $\delta$  170.7, 143.3, 139.4, 135.5, 130.6, 129.2, 128.9, 127.2, 125.9, 125.0, 123.5, 120.5, 119.5, 119.4, 114.4, 111.0, 109.3, 79.7, 52.7; IR (ATR): 3414 (br), 3060, 2952, 1743, 1577, 1455, 1234, 1099, 743  $\text{cm}^{-1}$ ; HRMS (ESI)  $m/z$  calcd for  $\text{C}_{21}\text{H}_{17}\text{NO}_3\text{Na}$   $[\text{M} + \text{Na}]^+$  354.1106, found 354.1114.

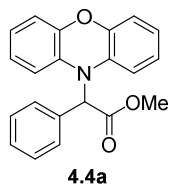


Methyl 2-(9-methyl-9*H*-carbazol-3-yl)-2-phenylacetate **4.3ha**: Using general procedure A, 9-methylcarbazole **4.1h** (36.2 mg, 0.20 mmol) was reacted with  $\alpha$ -methyl- $\alpha$ -phenyldiazoacetate **4.2a** (52.8 mg, 0.30 mmol) at 30 °C for 5 h.

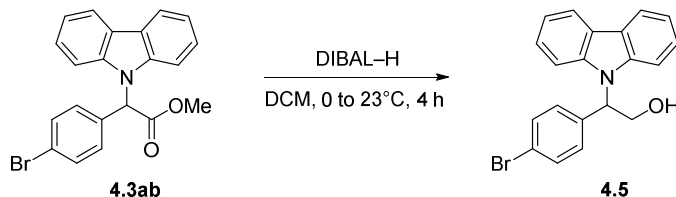
The crude product was purified by flash chromatography on silica gel (15:85 EtOAc:hexanes) to



obtain C–H insertion product **4.3ha** as a red oil (33.5 mg, 51%).  $R_f = 0.46$  (20:80 EtOAc:hexanes);  $^1\text{H NMR}$  (500 MHz,  $\text{CDCl}_3$ )  $\delta$  8.06 – 8.05 (m, 2H), 7.48 – 7.43 (m, 2H), 7.38 – 7.31 (m, 6H), 7.27 – 7.24 (m, 1H), 7.21 (t,  $J = 7.5$  Hz, 1H), 5.24 (s, 1H), 3.83 (s, 3H), 3.77 (s, 3H);  $^{13}\text{C NMR}$  (125 MHz,  $\text{CDCl}_3$ )  $\delta$  173.6, 141.3, 140.2, 139.5, 129.0, 128.5, 127.1, 126.4, 125.8, 122.9, 122.6, 120.4, 120.3, 118.9, 108.6, 108.5, 57.0, 52.3, 29.1; IR (ATR) 3026, 2948, 1732, 1602, 1494, 1471, 1146, 730  $\text{cm}^{-1}$ ; HRMS (ESI)  $m/z$  calcd for  $\text{C}_{22}\text{H}_{19}\text{NO}_2\text{Na}$   $[\text{M} + \text{Na}]^+$  352.1313, found 352.1326.



Methyl 2-(10*H*-phenoxazin-10-yl)-2-phenylacetate **4.4a**: Using general procedure A, phenoxazine **4.4a** (19.8 mg, 0.11 mmol) was reacted with  $\alpha$ -methyl- $\alpha$ -phenyldiazoacetate **4.2a** (28.6 mg, 0.16 mmol) at 30 °C for 15 min. The crude product was purified by flash chromatography on silica gel (10:90 ether:hexanes) to obtain compound **4.4a** as a white solid (36.5 mg, 81%, 94% *ee*).  $R_f = 0.59$  (20:80 ether:hexanes); The *ee* was measured utilizing the Shimadzu HPLC instrument using a chiral stationary phase [Chiralcel OD-H, 2-propanol:hexanes = 2/98, 1.0 mL/min,  $\lambda = 254$  nm],  $t_R = 7.86$  min (major), 9.53 min (minor);  $^1\text{H NMR}$  (500 MHz,  $\text{CDCl}_3$ )  $\delta$  7.43 (d,  $J = 8.1$  Hz, 2H), 7.37 (t,  $J = 7.4$  Hz, 2H), 7.34 – 7.31 (m, 1H), 6.79 (dd,  $J = 7.8, 1.6$  Hz, 2H), 6.75 (td,  $J = 7.6, 1.5$  Hz, 2H), 6.70 (td,  $J = 7.6, 1.7$  Hz, 2H), 6.36 (dd,  $J = 7.9, 1.4$  Hz, 2H), 5.71 (s, 1H), 3.76 (s, 3H);  $^{13}\text{C NMR}$  (125 MHz,  $\text{CDCl}_3$ )  $\delta$  170.3, 146.8, 133.8, 133.3, 128.6, 128.0, 127.7, 123.4, 122.1, 115.7, 114.2, 64.0, 52.9; IR (ATR) 3056, 2922, 1744, 1484, 1207, 1131  $\text{cm}^{-1}$ ; HRMS (ESI)  $m/z$  calcd for  $\text{C}_{21}\text{H}_{17}\text{NO}_3\text{Na}$   $[\text{M} + \text{Na}]^+$  354.1106, found 354.1113.

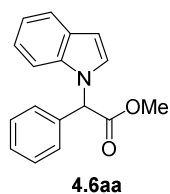


2-(4-Bromophenyl)-2-(9*H*-carbazol-9-yl)ethan-1-ol, **4.5** was synthesized according to a modified procedure used by Lee and co-workers.<sup>22</sup> Compound **3ab** (880 mg, 2.2 mmol, 1 equiv) was added to a round-bottom flask containing a stir bar. The flask was evacuated, backfilled with nitrogen, and capped with a septum. Through the septum was added dry DCM (15 mL). The solution was stirred and cooled to 0 °C. Upon cooling, DIBAL-H (8.9 mL, 1M in hexanes, 4 equiv) was added through the septum. The resulting solution was stirred for 25 min until consumption of starting material as determined by TLC. Upon completion, the solution was cooled to 0 °C and MeOH was added dropwise to quench unreacted DIBAL-H. The reaction was warmed to room temperature and saturated sodium potassium tartrate was added (7 mL/3.5 mmol). The reaction was stirred vigorously for 5 hours before extracting with EtOAc (3 × 20 mL). The combined organic extracts were washed with brine (3 × 30 mL) and dried with MgSO<sub>4</sub>. The dried organic layer was concentrated *in vacuo* and purified by flash chromatography on silica gel (20:80 ether:hexanes) to afford the corresponding alcohol **4.5** as a white solid (0.741 g, 90%, 93% *ee*).  $R_f = 0.21$  (30:70 ether:hexanes); The *ee* was determined by utilizing the Shimadzu HPLC instrument using a chiral stationary phase [Chiralcel OD-H, 2-propanol:hexanes = 30/70, 1.0 mL/min,  $\lambda = 254$  nm],  $t_R = 12.03$  min (major), 18.24 min (minor); <sup>1</sup>H NMR (600 MHz, CDCl<sub>3</sub>)  $\delta$  8.09 (dt,  $J = 7.6, 1.1$  Hz, 2H), 7.40 (d,  $J = 8.6$  Hz, 2H), 7.34 (td,  $J = 7.6, 1.3$  Hz, 2H), 7.23 (td,  $J = 7.5, 1.0$  Hz, 4H), 7.07 (d,  $J = 8.5$  Hz, 2H), 5.90 (dd,  $J = 8.6, 5.2$  Hz, 1H), 4.54 (ddd,  $J = 11.5, 8.6, 4.4$  Hz, 1H), 4.46 (ddd,  $J = 11.6, 8.4, 5.3$  Hz, 1H), 1.58 (dd,  $J = 8.4, 4.4$  Hz, 1H); <sup>13</sup>C NMR (151 MHz, CDCl<sub>3</sub>)  $\delta$  140.1, 136.0, 131.9, 128.4, 125.8, 123.5, 121.8, 120.4, 119.6, 110.2, 62.3, 58.8. IR (ATR) 3320, 1593, 1480, 1449, 747, 721 cm<sup>-1</sup>.

Crystallization procedure for **4.5**: Alcohol **4.5** was crystallized by the vapor diffusion method using DCM and hexanes. 50 mg of **4.5** was added to a 2-dram vial and dissolved in 0.5

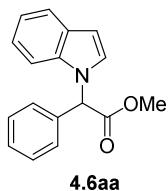
mL of dry DCM (filtered through a Waters Acrodisc Syringe Filter, 13 mm, 0.45  $\mu\text{m}$  Nylon). The open vial was placed in a larger 20 mL vial containing 5 mL hexanes (HPLC grade). The larger vial was sealed and left undisturbed for two days. After two days, colorless cubic crystals formed, from which an X-ray structure was obtained. The absolute stereochemistry was determined as (*R*). X-ray data was uploaded to the Cambridge Crystallographic Data Centre (CCDC) Database (deposition number: 1519937).

### Analytical Data for Indole Based Heterocycles 4.6aa–4.6ga

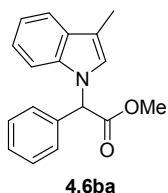


Methyl 2-(1*H*-indol-1-yl)-2-phenylacetate, **4.6aa**: Using general procedure A, indole **4.6a** (70.2 mg, 0.60 mmol) was reacted with  $\alpha$ -methyl- $\alpha$ -phenyldiazoacetate **4.2a** (158.6 mg, 0.90 mmol). The general procedure was modified so that the reaction was halted 15 minutes after adding the diazo solution, with indole only partially reacted. The reaction mixture was immediately diluted with  $\text{CHCl}_3$  (2 mL) and filtered through a pad of Celite®. (Longer reaction times led to products resulting from over-insertion). The crude product was purified by flash chromatography on silica gel (8:92 ether:hexanes) to obtain compound **4.6aa** as a colorless oil (17.4 mg, 11%, 80% *ee*). The ratio of N–H/C2–H/C3–H insertion at 15 min was 1.0:0.8:3.0 as determined by  $^1\text{H}$  NMR analysis.  $R_f = 0.49$  (20:80 ether:hexanes); The *ee* was measured utilizing the Shimadzu HPLC instrument using a chiral stationary phase [Chiralcel OD-H, 2-propanol:hexanes = 3/97, 1.0 mL/min,  $\lambda = 254$  nm],  $t_R = 11.29$  min (major), 12.62 min (minor);  $^1\text{H}$  NMR (600 MHz,  $\text{CDCl}_3$ )  $\delta$  7.63 (dt,  $J = 7.9, 0.9$  Hz, 1H), 7.41 – 7.36 (m, 3H), 7.36 – 7.31 (m, 3H), 7.22 (t,  $J = 8.3$  Hz, 1H), 7.16 – 7.10 (m, 2H), 6.53 (d,  $J = 3.3$  Hz, 1H), 6.26 (s, 1H), 3.80 (s, 3H);  $^{13}\text{C}$  NMR (151 MHz,  $\text{CDCl}_3$ )  $\delta$  170.1, 136.4, 134.6, 129.1, 129.0, 128.8, 128.06, 126.7, 121.9, 121.2, 120.1, 109.0, 102.5, 62.0, 52.8; IR (ATR) 3030, 952, 2923, 1745, 1457, 1310,

1197, 1168, 737  $\text{cm}^{-1}$ ; HRMS (ESI)  $m/z$  calcd for  $\text{C}_{17}\text{H}_{15}\text{NO}_2\text{Na}$   $[\text{M} + \text{Na}]^+$  288.1000, found 288.1013.

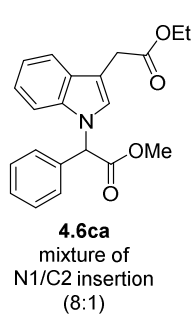


Methyl 2-(1*H*-indol-1-yl)-2-phenylacetate, **4.6aa**: Using Zhu's conditions<sup>23</sup>, indole **4.6a** (35.2 mg, 0.30 mmol) was reacted with  $\alpha$ -methyl- $\alpha$ -phenyldiazoacetate **4.2a** (35.1 mg, 0.20 mmol). Diazo solution (0.28 M in  $\text{CHCl}_3$ , 0.35 mL/min) was added slowly via syringe pump to the reaction mixture containing indole **4.6a**,  $\text{Pd}(\text{PhCN})_2\text{Cl}_2$  (3.8 mg, 0.01 mmol), (*S*)-Ph-SpiroBOX (6.1 mg, 0.012 mmol),  $\text{NaBARF}$  (21.3 mg, 0.024 mmol), and 5 Å M.S. in  $\text{CHCl}_3$  (2 mL) at 40 °C. Over-insertion products began to form within 1.5 h as determined by TLC. At this point, 0.5 mL of diazo solution had been added and the reaction was halted. The reaction mixture was immediately diluted with  $\text{CHCl}_3$  (1 mL) and filtered through a pad of Celite®. The crude reaction mixture was analyzed by  $^1\text{H}$  NMR. The ratio of N1-H/C2-H/C3-H insertion was determined to be 2:3:18.

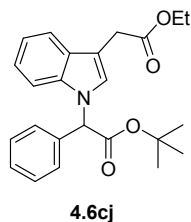


Methyl 2-(3-methyl-1*H*-indol-1-yl)-2-phenylacetate, **4.6ba**: Using general procedure A, 3-methylindole **4.6a** (98%, 13.4 mg, 0.1 mmol) was reacted with  $\alpha$ -methyl- $\alpha$ -phenyldiazoacetate **4.2a** (26.4 mg, 0.15 mmol) at 30 °C for 1 h. The general procedure was modified slightly so that the 3-methylindole solution was stirred at 30 °C for 15 min instead of 5 min before adding the diazo solution. The crude product was purified by flash chromatography on silica gel (5:95 ether:hexanes) to obtain insertion product **4.6ba** as an off-white oil (17.5 mg, 63%, 79% *ee*).  $R_f$  = 0.35 (10:90 ether:hexanes); The *ee* was measured utilizing the Agilent HPLC instrument using a chiral stationary phase [Chiralpak AD, 2-propanol:hexanes = 5/95, 1.0 mL/min,  $\lambda$  = 254 nm],  $t_R$  = 6.38 min (major), 7.52 min (minor);  $^1\text{H}$  NMR (500 MHz,  $\text{CDCl}_3$ )  $\delta$  7.57 (d,  $J$  = 7.8 Hz, 1H), 7.41 – 7.36 (m, 3H), 7.34 – 7.28 (m, 3H), 7.21 (t,  $J$  = 7.4 Hz, 1H), 7.14 (t,  $J$  = 7.4 Hz, 1H), 6.88 (s, 1H), 6.21 (s, 1H), 3.79 (s, 3H), 2.28 (s,

3H);  $^{13}\text{C}$  NMR (126 MHz,  $\text{CDCl}_3$ )  $\delta$  170.3, 136.8, 134.9, 129.1, 129.0, 128.8, 128.0, 124.1, 121.9, 119.4, 119.2, 111.6, 108.8, 77.3, 77.0, 76.8, 61.7, 52.7, 9.7; IR (ATR) 3030, 2918, 1747, 1459, 1194, 1169  $\text{cm}^{-1}$ ; HRMS (ESI)  $m/z$  calcd for  $\text{C}_{18}\text{H}_{17}\text{NO}_2\text{Na}$   $[\text{M} + \text{Na}]^+$  302.1157, found 302.1145.



Methyl 2-(3-(2-ethoxy-2-oxoethyl)-1*H*-indol-1-yl)-2-phenylacetate, **4.6ca**: Using general procedure A, ethyl-3-indoleacetate **4.6c** (99%, 20.5 mg, 0.1 mmol) was reacted with  $\alpha$ -methyl- $\alpha$ -phenyldiazoacetate **4.2a** (26.4 mg, 0.15 mmol) at 30 °C for 18 h. The general procedure was modified slightly so that the ethyl-3-indoleacetate solution was stirred at 30 °C for 15 min instead of 5 min before adding the diazo solution. The crude product was purified by flash chromatography on silica gel (10:90 – 20:80 ether:hexanes) to obtain an inseparable mixture of N–H/C2–H insertion products in an 8:1 ratio as a pale-yellow oil (28.0 mg, 79%, 79% *ee*);  $R_f$  = 0.23 (20:80 ether:hexanes); The *ee* was measured utilizing the Agilent HPLC instrument using a chiral stationary phase [Chiralpak AD, 2-propanol:hexanes = 30/70, 1.0 mL/min,  $\lambda$  = 254 nm], N1–H insertion  $t_R$  = 6.38 min (major), 7.52 min (minor); C2–H insertion  $t_R$  = 8.07 min (equal), 9.18 min (equal); Major peaks are reported for  $^1\text{H}$  and  $^{13}\text{C}$  NMR. See attached NMR for other peaks resulting from C2-H insertion product present in minor amounts;  $^1\text{H}$  NMR (500 MHz,  $\text{CDCl}_3$ )  $\delta$  7.63 (d,  $J$  = 7.8 Hz, 1H), 7.41 – 7.37 (m, 3H), 7.37 – 7.28 (m, 4H), 7.23 (dd,  $J$  = 13.4, 6.1 Hz, 1H), 7.15 (t,  $J$  = 7.4 Hz, 1H), 7.09 (s, 1H), 6.22 (s, 1H), 4.12 (q,  $J$  = 7.1 Hz, 2H), 3.79 (s, 3H), 3.71 (s, 2H), 1.22 (t,  $J$  = 7.1 Hz, 3H). Note: An extra proton is reported presumably due to the C2–H insertion product overlapping in the aromatic region with the N–H insertion product;  $^{13}\text{C}$  NMR (126 MHz,  $\text{CDCl}_3$ )  $\delta$  171.8, 170.0, 136.7, 134.4, 129.1, 129.0, 128.9, 128.2, 128.1, 127.7, 125.5, 122.2, 120.0, 119.5, 109.1, 108.4, 61.9, 60.7, 52.8, 31.5, 14.2; IR (ATR) 2953, 1737, 1460, 1167  $\text{cm}^{-1}$ ; HRMS (ESI)  $m/z$  calcd for  $\text{C}_{21}\text{H}_{21}\text{NO}_4\text{Na}$   $[\text{M} + \text{Na}]^+$  374.1368, found 374.1379.

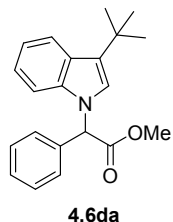


*tert*-Butyl 2-(3-(2-ethoxy-2-oxoethyl)-1H-indol-1-yl)-2-phenylacetate, **4.6cj**:

Using general procedure A, ethyl-3-indoleacetate **4.6c** (99%, 20.5 mg, 0.1 mmol) was reacted with *tert*-butyl 2-diazo-2-phenylacetate **4.2j** (32.7 mg, 0.15 mmol) at

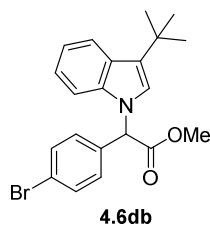
30 °C for 14 h. The general procedure was modified slightly so that the ethyl-3-

indoleacetate solution was stirred at 30 °C for 10 min instead of 5 min before adding the diazo solution. The crude product was purified by flash chromatography on silica gel (10:90 ether:hexanes) to obtain an inseparable mixture of N–H/C2–H insertion products in a 21:1 ratio as a pale-yellow oil (33.7 mg, 85%, 85% *ee*);  $R_f = 0.28$  (20:80 ether:hexanes); The *ee* was measured utilizing the Agilent HPLC instrument using a chiral stationary phase [Chiralpak AD, 2-propanol:hexanes = 20/70, 1.0 mL/min,  $\lambda = 254$  nm], N1–H insertion  $t_R = 4.43$  min (major), 4.89 min (minor); C2–H insertion  $t_R = 5.68$  min (equal), 6.91 min (equal); Major peaks are reported for  $^1\text{H}$  and  $^{13}\text{C}$  NMR. See attached NMR for other peaks resulting from C2-H insertion product present in minor amounts;  $^1\text{H}$  NMR (600 MHz,  $\text{CDCl}_3$ )  $\delta$  7.63 (dt,  $J = 8.0, 0.9$  Hz, 1H), 7.42 – 7.34 (m, 5H), 7.32 (d,  $J = 8.3$  Hz, 1H), 7.21 (ddd,  $J = 8.2, 7.0, 1.2$  Hz, 1H), 7.14 (ddd,  $J = 7.9, 7.1, 1.0$  Hz, 1H), 7.07 (s, 1H), 6.08 (s, 1H), 4.11 (q,  $J = 7.1$  Hz, 2H), 3.70 (dd,  $J = 3.0, 0.9$  Hz, 2H), 1.44 (s, 9H), 1.21 (t,  $J = 7.2$  Hz, 3H);  $^{13}\text{C}$  NMR (151 MHz,  $\text{CDCl}_3$ )  $\delta$  171.8, 168.6, 136.8, 135.0, 129.0, 128.7, 128.1, 125.7, 122.0, 119.8, 119.4, 109.2, 108.1, 82.9, 62.7, 60.6, 31.6, 27.9, 14.2; IR (ATR) 2978, 1731, 1460, 1367, 1141  $\text{cm}^{-1}$ ; HRMS (ESI)  $m/z$  calcd for  $\text{C}_{24}\text{H}_{27}\text{NO}_4\text{Na}$  [ $\text{M} + \text{Na}$ ] $^+$  416.1838, found 416.1844.



Methyl 2-(3-(*tert*-butyl)-1H-indol-1-yl)-2-phenylacetate, **4.6da**: Using general procedure A, 3-(*tert*-butyl)-1H-indole **4.6d** (20.5 mg, 0.12 mmol) was reacted with  $\alpha$ -methyl- $\alpha$ -phenyldiazoacetate **4.2a** (31.3 mg, 0.18 mmol) for 4 h. The crude product was purified by flash chromatography on silica gel (10:90 ether:hexanes)

to obtain insertion product **4.6da** as a white solid (33.8 mg, 89%, 79% *ee*);  $R_f = 0.33$  (10:90 ether:hexanes); The *ee* was measured utilizing the Shimadzu HPLC instrument using a chiral stationary phase [Chiralcel OD-H, 2-propanol:hexanes = 0.3/99.7, 1.0 mL/min,  $\lambda = 254$  nm],  $t_R = 14.27$  min (minor), 15.54 min (major);  $^1\text{H NMR}$  (500 MHz,  $\text{CDCl}_3$ )  $\delta$  7.82 (d,  $J = 8.0$  Hz, 1H), 7.41 – 7.34 (m, 3H), 7.33 – 7.29 (m, 3H), 7.18 (t,  $J = 7.2$  Hz, 1H), 7.11 (t,  $J = 7.2$  Hz, 1H), 6.87 (s, 1H), 6.21 (s, 1H), 3.80 (s, 3H), 1.40 (s, 9H);  $^{13}\text{C NMR}$  (125 MHz,  $\text{CDCl}_3$ )  $\delta$  170.2, 137.6, 134.9, 129.0, 128.8, 128.0, 126.9, 126.4, 121.8, 121.6, 121.4, 119.1, 109.2, 61.8, 52.7, 31.6, 30.7; IR (ATR) 2953, 1749, 1462, 1197, 1166, 736  $\text{cm}^{-1}$ ; HRMS (ESI)  $m/z$  calcd for  $\text{C}_{21}\text{H}_{22}\text{BrNO}_2\text{Na}$  [ $\text{M} + \text{Na}$ ] $^+$  344.1627, found 344.1638.

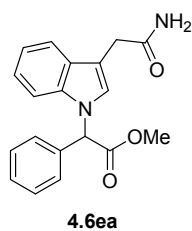


Methyl 2-(4-bromophenyl)-2-(3-(tert-butyl)-1H-indol-1-yl)acetate, **4.6db**:

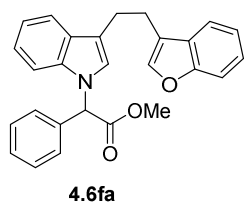
Using general procedure A, 3-(*tert*-butyl)-1H-indole **4.6d** (153 mg, 0.88 mmol) was reacted with methyl 2-(4-bromophenyl)-2-diazoacetate **4.2b** (337 mg, 1.32 mmol) for 10 h. The crude product was purified by flash chromatography on

silica gel (10:90 ether:hexanes) to obtain insertion product **4.6db** as a white solid (288 mg, 82%, 70% *ee*);  $R_f = 0.31$  (10:90 ether:hexanes); The *ee* was measured utilizing the Shimadzu HPLC instrument using a chiral stationary phase [Chiralcel OD-H, 2-propanol:hexanes = 1/99, 1.0 mL/min,  $\lambda = 254$  nm],  $t_R = 7.15$  min (minor), 8.07 min (major);  $^1\text{H NMR}$  (500 MHz,  $\text{CDCl}_3$ )  $\delta$  7.82 (d,  $J = 8.0$  Hz, 1H), 7.50 (d,  $J = 8.5$  Hz, 2H), 7.26 (d,  $J = 8.3$  Hz, 1H), 7.20 – 7.05 (m, 4H), 6.87 (s, 1H), 6.15 (s, 1H), 3.80 (s, 3H), 1.41 (s, 9H);  $^{13}\text{C NMR}$  (125 MHz,  $\text{CDCl}_3$ )  $\delta$  169.7, 137.5, 134.0, 132.1, 129.5, 126.9, 126.9, 123.0, 121.7, 121.6, 121.5, 119.2, 109.2, 61.2, 52.9, 31.7, 30.7; IR (ATR) 2964, 1748, 1201, 1174, 734  $\text{cm}^{-1}$ ; HRMS (ESI)  $m/z$  calcd for  $\text{C}_{21}\text{H}_{22}\text{BrNO}_2\text{Na}$  [ $\text{M} + \text{Na}$ ] $^+$  422.0732, found 422.0742.

Compound **4.6db** was crystallized as the racemate from scalemic material by slow evaporation from methanol. X-ray data was uploaded to the Cambridge Crystallographic Data Centre (CCDC) Database (deposition number: 1520167).



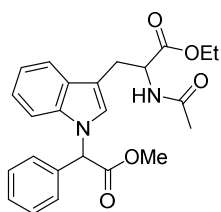
Methyl 2-(3-(2-amino-2-oxoethyl)-1*H*-indol-1-yl)-2-phenylacetate, **4.6ea**: Using general procedure A, indole-3-acetamide **4.6e** (21.7 mg, 0.12 mmol) was reacted with  $\alpha$ -methyl- $\alpha$ -phenyldiazoacetate **4.2a** (32.9 mg, 0.19 mmol) at 40 °C for 25 h. The crude product was purified by flash chromatography on silica gel (EtOAc) to obtain insertion compound **4.6ea** as a white solid (22.4 mg, 58%, 53% *ee*);  $R_f = 0.37$  (EtOAc); The *ee* was measured utilizing the Agilent HPLC instrument using a chiral stationary phase [Chiralpak AD, 2-propanol:hexanes = 30/70, 1.0 mL/min,  $\lambda = 254$  nm],  $t_R = 7.21$  min (major), 9.68 min (minor);  $^1\text{H}$  NMR (500 MHz,  $\text{CDCl}_3$ )  $\delta$  7.59 (d,  $J = 7.9$  Hz, 1H), 7.46 – 7.40 (m, 3H), 7.39 – 7.33 (m, 3H), 7.28 (t,  $J = 7.7$  Hz, 1H), 7.20 (t,  $J = 7.5$  Hz, 1H), 7.04 (s, 1H), 6.24 (s, 1H), 5.62 (br s, 1H), 5.43 (br s, 1H), 3.81 (s, 3H), 3.67 (s, 2H);  $^{13}\text{C}$  NMR (125 MHz,  $\text{CDCl}_3$ )  $\delta$  173.9, 170.0, 137.1, 134.1, 129.3, 128.2, 127.8, 126.1, 122.8, 120.6, 119.3, 109.28, 109.27, 61.9, 52.9, 33.0; IR (ATR) 3390, 3196, 2951, 1742, 1652, 1205, 1168, 743  $\text{cm}^{-1}$ ; HRMS (ESI)  $m/z$  calcd for  $\text{C}_{19}\text{H}_{18}\text{N}_2\text{O}_3\text{Na}$  [ $\text{M} + \text{Na}$ ] $^+$  345.1215, found 345.1216.



Methyl 2-(3-(2-(benzofuran-3-yl)ethyl)-1*H*-indol-1-yl)-2-phenylacetate, **4.6fa**: Using general procedure A, 3-(2-(benzofuran-3-yl)ethyl)-1*H*-indole **4.6f** (31.4 mg, 0.12 mmol) was reacted with  $\alpha$ -methyl- $\alpha$ -phenyldiazoacetate **4.2a** (32.3 mg, 0.18 mmol) at 40 °C for 2 h. The crude product was purified by flash chromatography on silica gel (10:90 ether:hexanes) to obtain insertion product **4.6fa** as a pale yellow oil (26.5 mg, 54%, 77% *ee*);  $R_f = 0.18$  (10:90 ether:hexanes); The *ee* was measured utilizing the Shimadzu HPLC instrument using a chiral stationary phase [Chiralcel OD-H, 2-



propanol:hexanes = 5/95, 1.0 mL/min,  $\lambda$  = 254 nm],  $t_r$  = 14.63 min (minor), 16.62 min (major);  $^1\text{H}$  NMR (500 MHz,  $\text{CDCl}_3$ )  $\delta$  7.63 (d,  $J$  = 7.8 Hz, 1H), 7.52 (d,  $J$  = 7.7 Hz, 1H), 7.45 (d,  $J$  = 8.2 Hz, 1H), 7.40 – 7.35 (m, 3H), 7.33 (t,  $J$  = 4.1 Hz, 2H), 7.30 – 7.25 (m, 3H), 7.25 – 7.18 (m, 2H), 7.15 (t,  $J$  = 7.5 Hz, 1H), 6.88 (s, 1H), 6.22 (s, 1H), 3.79 (s, 3H), 3.14 – 3.08 (m, 2H), 3.06 – 3.00 (m, 2H);  $^{13}\text{C}$  NMR (125 MHz,  $\text{CDCl}_3$ )  $\delta$  170.2, 155.2, 141.3, 136.9, 134.7, 129.0, 128.9, 128.24, 128.21, 127.9, 124.02, 123.99, 122.2, 122.0, 120.2, 119.7, 119.6, 119.2, 115.8, 111.4, 109.1, 61.8, 52.8, 25.1, 24.3; IR (ATR) 3055, 2949, 2852, 1746, 1452, 1195, 1169, 739  $\text{cm}^{-1}$ ; HRMS (ESI)  $m/z$  calcd for  $\text{C}_{27}\text{H}_{23}\text{NO}_3\text{Na}$  [ $\text{M} + \text{Na}$ ] $^+$  432.1576, found 432.1576.



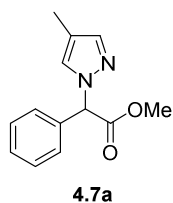
**4.6ga**

Ethyl  $N^\alpha$ -acetyl-1-(2-methoxy-2-oxo-1-phenylethyl)tryptophanate, **4.6ga**:

Using general procedure A,  $N$ -acetyl- $L$ -tryptophan ethyl ester **4.6g** (31.8 mg, 0.12 mmol) was reacted with  $\alpha$ -methyl- $\alpha$ -phenyldiazoacetate **4.2a** (32.3 mg, 0.18 mmol) at 40 °C for 21 h. The crude product was purified by flash

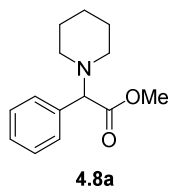
chromatography on silica gel (1<sup>st</sup> column = 60:40 ether:hexanes; 2<sup>nd</sup> column = 90:10 ether:hexanes; 3<sup>rd</sup> column = 20:80 ether:DCM) to obtain insertion product **4.6ga** as pale yellow oil (36.9 mg, 75%, 60% *de*).  $R_f$  = 0.07 (60:40 ether:hexanes);  $R_f$  = 0.28 (90:10 ether:hexanes);  $R_f$  = 0.40 (20:80 ether:DCM). The diastereomeric excess was determined by  $^1\text{H}$  NMR analysis of the crude product by integration of peaks at 6.86 and 6.84 ppm.  $^1\text{H}$  NMR (500 MHz,  $\text{CDCl}_3$ )  $\delta$  7.53 (d,  $J$  = 7.7 Hz, 1H), 7.44 – 7.35 (m, 3H), 7.35 – 7.27 (m, 3H), 7.22 (ddd,  $J$  = 8.2, 7.1, 1.1 Hz, 1H), 7.14 (ddd,  $J$  = 8.0, 7.1, 1.0 Hz, 1H), 6.85 (s, 1H), 6.22 (s, 1H), 5.98 (d,  $J$  = 7.7 Hz, 1H), 4.87 (dt,  $J$  = 7.9, 5.1 Hz, 1H), 3.98 (dq,  $J$  = 10.8, 7.2 Hz, 1H), 3.87 (dq,  $J$  = 10.7, 7.1 Hz, 1H), 3.80 (s, 3H), 3.27 (qd,  $J$  = 14.6, 4.8 Hz, 2H), 1.95 (s, 3H), 1.08 (t,  $J$  = 7.2 Hz, 3H);  $^{13}\text{C}$  NMR (125 MHz,  $\text{CDCl}_3$ ) 171.7, 170.0, 169.6, 136.7, 134.6, 129.1, 129.0, 128.8, 128.1, 125.4, 122.3, 120.1, 119.2, 110.1, 109.0, 61.6,

61.4, 53.2, 52.8, 27.6, 23.2, 14.0; IR (ATR): 3300 (br), 3056, 2982, 1737, 1659, 1460, 1197, 732  $\text{cm}^{-1}$ ; HRMS (ESI)  $m/z$  calcd for  $\text{C}_{24}\text{H}_{26}\text{N}_2\text{O}_5\text{Na}$   $[\text{M} + \text{Na}]^+$  445.1740, found 445.1721.



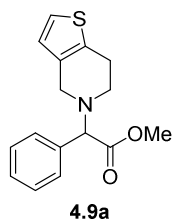
Methyl 2-(4-methyl-1*H*-pyrazol-1-yl)-2-phenylacetate, **4.7a**: Using general procedure A, 4-methyl-1*H*-pyrazole **4.7** (22.3 mg, 0.27 mmol) was reacted with  $\alpha$ -methyl- $\alpha$ -phenyldiazoacetate **4.2a** (22.3 mg, 0.41 mmol) at 55 °C for 30 h. The crude product was purified by flash chromatography on silica gel (1<sup>st</sup> column = 20:80 ether:hexanes; 2<sup>nd</sup> column = 50:50 ether:hexanes) to obtain insertion product **4.7a** as a white solid (20.3 mg, 32%, 0% *ee*);  $R_f$  = 0.35 (50:50 ether:hexanes); The *ee* was measured utilizing the Shimadzu HPLC instrument using a chiral stationary phase [Chiralcel OD-H, 2-propanol:hexanes = 8/92, 1.0 mL/min,  $\lambda$  = 254 nm],  $t_R$  = 9.56 min (equal), 19.38 min (equal);  $^1\text{H}$  NMR (500 MHz,  $\text{CDCl}_3$ )  $\delta$  7.46 – 7.35 (m, 6H), 7.14 (s, 1H), 6.16 (s, 1H), 3.80 (s, 3H), 2.03 (s, 3H);  $^{13}\text{C}$  NMR (125 MHz,  $\text{CDCl}_3$ )  $\delta$  169.7, 140.5, 134.0, 129.3, 129.2, 128.4, 127.9, 116.6, 67.8, 52.9, 890; IR (ATR) 2950, 1740, 1432, 1210, 978, 742  $\text{cm}^{-1}$ ; HRMS (ESI)  $m/z$  calcd for  $\text{C}_{13}\text{H}_{14}\text{N}_2\text{O}_2\text{Na}$   $[\text{M} + \text{Na}]^+$  253.0953, found 253.0957.

### General Procedures for the Palladium-Catalyzed Insertion with Aliphatic Amines



Methyl 2-phenyl-2-(piperidin-1-yl)acetate, **4.8a**: A flame-dried, 5 mL round-bottom flask equipped with stir bar was charged with  $\text{Pd}(\text{PhCN})_2\text{Cl}_2$  (3.3 mg, 0.009 mmol, 5 mol %), NaBARF (18.7 mg, 0.021 mmol, 12 mol %), and 5 Å MS (170 mg). To a separate flame-dried, 5 mL pear-shaped flask was added  $\alpha$ -methyl- $\alpha$ -phenyldiazoacetate **4.2a** (45.7 mg, 0.26 mmol, 1.5 equiv). Both flasks were evacuated for 10 min and backfilled with nitrogen gas. Distilled  $\text{CHCl}_3$  (1.1 mL) was added to the flask containing catalyst and stirred for 5 min at 30 °C. Piperidine (21  $\mu\text{mL}$ , 0.21 mmol, 1 equiv) was injected into the flask via syringe. Next,  $\text{CHCl}_3$  (0.3 mL) was added to the flask containing methyl 2-diazo-2-phenylacetate.

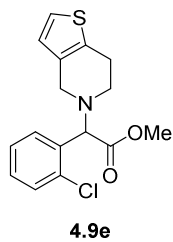
Additional CHCl<sub>3</sub> (0.9 mL) was used to ensure complete transfer of the diazo substrate. The flask was stirred at 30 °C for 48 h. Then, the reaction mixture was cooled to room temperature and diluted with CHCl<sub>3</sub>. The mixture was filtered through a pad of Celite® and washed three times with CHCl<sub>3</sub>. The filtrate was concentrated and the residue purified by flash chromatography on silica gel (10:90 EtOAc:hexanes) to obtain insertion product **4.8a** as a clear oil (16.2 mg, 40%); *R<sub>f</sub>* = 0.43 (20:80 EtOAc:hexanes); <sup>1</sup>H NMR (500 MHz, CDCl<sub>3</sub>) δ 7.43 (d, *J* = 7.2 Hz, 2H), 7.35 – 7.28 (m, 3H), 3.97 (s, 1H), 3.68 (s, 3H), 2.44 – 2.27 (m, 4H), 1.59 (p, *J* = 5.5 Hz, 4H), 1.43 (p, *J* = 6.2 Hz, 2H); <sup>13</sup>C NMR (125 MHz, CDCl<sub>3</sub>) δ 172.4, 136.1, 128.8, 128.5, 128.2, 75.0, 52.5, 52.0, 25.7, 24.3; IR (ATR) 2926, 2851, 1736, 1453, 1152, 747, 697 cm<sup>-1</sup>; HRMS (ESI) *m/z* calcd for C<sub>14</sub>H<sub>19</sub>NO<sub>2</sub>Na [M + Na]<sup>+</sup> 256.1313, found 256.1304.



Methyl 2-(6,7-dihydrothieno[3,2-*c*]pyridin-5(4*H*)-yl)-2-phenylacetate, **4.9a**: A flame-dried, 10 mL round-bottom flask equipped with stir bar was charged with Pd(PhCN)<sub>2</sub>Cl<sub>2</sub> (4.1 mg, 0.011 mmol, 5 mol %), (*S,S*)-*i*Pr-PyBOX (3.9 mg, 0.013 mmol, 6 mol %), NaBARF (23.0 mg, 0.026 mmol, 12 mol %), and 5 Å MS (200

mg). To a second flame-dried, 5 mL pear-shaped flask was added α-methyl-α-phenyldiazoacetate **4.2a** (57.0 mg, 0.32 mmol, 1.5 equiv). To a third flame-dried, 5 mL pear-shaped flask was added 4,5,6,7-tetrahydrothieno[3,2-*c*]pyridine (30.0 mg, 0.22 mmol, 1 equiv). All three flasks were evacuated for 10 min and backfilled with nitrogen gas. Distilled CHCl<sub>3</sub> (0.9 mL) was added to the flask containing catalyst and the resulting solution stirred for 5 min at 25 °C. Next, CHCl<sub>3</sub> (0.5 mL) was added to the flask containing 4,5,6,7-tetrahydrothieno[3,2-*c*]pyridine; the resulting solution was added via syringe to the catalyst solution. Additional CHCl<sub>3</sub> (0.5 mL) was used to ensure complete transfer of the pyridine substrate and the reaction mixture stirred for an additional 5 min at 30 °C. Finally, CHCl<sub>3</sub> (0.5 mL) was used to dissolve methyl 2-diazo-2-phenylacetate and

the resulting solution transferred to the reaction mixture. Additional CHCl<sub>3</sub> (0.5 mL) was used to ensure complete transfer of the diazo substrate. The reaction was stirred at 30 °C for 18 h. The reaction mixture was cooled to room temperature, diluted with CHCl<sub>3</sub>, and filtered through a pad of Celite®. The pad was washed three times with CHCl<sub>3</sub>. The filtrate was concentrated and the residue purified by flash chromatography on silica gel (8:92 EtOAc:hexanes) to obtain insertion product **4.9a** as a clear oil (36.8 mg, 60%).  $R_f = 0.57$  (20:80 EtOAc:hexanes); <sup>1</sup>H NMR (500 MHz, CDCl<sub>3</sub>) δ 7.49 (dd,  $J = 7.8, 1.6$  Hz, 2H), 7.38 – 7.32 (m, 3H), 7.05 (d,  $J = 5.1$  Hz, 1H), 6.65 (d,  $J = 5.2$  Hz, 1H), 4.30 (s, 1H), 3.72 (s, 3H), 3.64 (app d,  $J = 14.3$  Hz, 1H), 3.60 (app d,  $J = 14.3$  Hz, 1H), 2.92 – 2.76 (m, 4H); <sup>13</sup>C NMR (125 MHz, CDCl<sub>3</sub>) δ 172.0, 135.9, 133.3, 133.2, 128.8, 128.7, 128.5, 125.2, 122.7, 72.9, 52.1, 51.0, 48.3, 25.3; IR (ATR) 2949, 2921, 2841, 1737, 1651, 1453, 1433, 1162, 732, 697 cm<sup>-1</sup>; HRMS (ESI)  $m/z$  calcd for C<sub>16</sub>H<sub>17</sub>NO<sub>2</sub>SNa [M + Na]<sup>+</sup> 310.0878, found 310.0869.



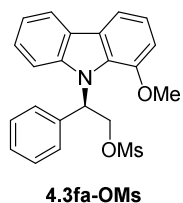
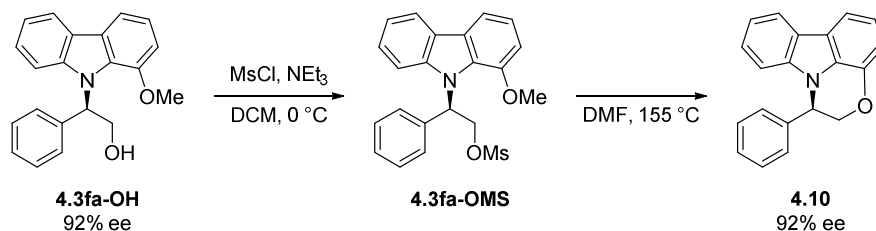
Methyl 2-(2-chlorophenyl)-2-(6,7-dihydrothieno[3,2-*c*]pyridin-5(4*H*)-yl)acetate,

**4.9e** (± clopidogrel): A flame-dried, 10 mL round-bottom flask equipped with stir bar was charged with Pd(PhCN)<sub>2</sub>Cl<sub>2</sub> (5.7 mg, 0.015 mmol, 5 mol %), (*S,S*)-*i*Pr-PyBOX (5.4 mg, 0.018 mmol, 6 mol %), NaBARF (32.0 mg, 0.036 mmol, 12 mol %), and 5 Å MS (300 mg). To a second flame-dried, 5 mL, pear-shaped flask was added methyl 2-(2-chlorophenyl)-2-diazoacetate **4.2e** (94.5 mg, 0.45 mmol, 1.5 equiv). To a third flame-

dried, 5 mL pear-shaped flask was added 4,5,6,7-tetrahydrothieno[3,2-*c*]pyridine (42.0 mg, 0.30 mmol, 1 equiv). All three flasks were evacuated for 10 min and backfilled with nitrogen gas. Distilled CHCl<sub>3</sub> (1.2 mL) was added to the flask containing catalyst and the resulting solution stirred for 5 min at 30 °C. Next, CHCl<sub>3</sub> (0.7 mL) was added to the flask containing 4,5,6,7-tetrahydrothieno[3,2-*c*]pyridine; the resulting solution was added via syringe to the round-bottom

flask. Additional  $\text{CHCl}_3$  (0.7 mL) was used to ensure complete transfer of the pyridine substrate, and the reaction mixture stirred for an additional 5 min at 25 °C. Finally,  $\text{CHCl}_3$  (0.7 mL) was used to dissolve the diazo substrate and the resulting solution transferred to the reaction mixture. Additional  $\text{CHCl}_3$  (0.7 mL) was used to ensure complete transfer of the diazo substrate. The reaction was stirred at 30 °C for 15 h. The reaction mixture was cooled to room temperature, diluted with  $\text{CHCl}_3$ , and filtered through a pad of Celite®. The pad was washed three times with  $\text{CHCl}_3$ . The filtrate was concentrated and the residue purified by flash chromatography on silica gel (15:85 ether:hexanes) to obtain compound **4.9e** as a pale, yellow oil (76.6 mg, 79%).  $R_f = 0.40$  (20:80 EtOAc:hexanes);  $^1\text{H}$  NMR (500 MHz,  $\text{CDCl}_3$ )  $\delta$  7.70 (dd,  $J = 7.4, 2.2$  Hz, 1H), 7.41 (dd,  $J = 7.4, 1.9$  Hz, 1H), 7.32 – 7.26 (m, 2H), 7.06 (d,  $J = 5.2$  Hz, 1H), 6.67 (d,  $J = 5.1$  Hz, 1H), 4.92 (s, 1H), 3.76 (d,  $J = 14.3$  Hz, 1H), 3.63 (d,  $J = 14.2$  Hz, 1H), 2.88 (s, 4H);  $^{13}\text{C}$  NMR (126 MHz,  $\text{CDCl}_3$ )  $\delta$  171.3, 134.7, 133.8, 133.29, 133.26, 130.0, 129.8, 129.4, 127.2, 125.2, 122.7, 67.9, 52.2, 50.7, 48.3, 25.5; IR (ATR) 2951, 2921, 2844, 1738, 1433, 1164, 752  $\text{cm}^{-1}$ ; HRMS (ESI)  $m/z$  calcd for  $\text{C}_{16}\text{H}_{16}\text{ClNO}_2\text{SNa}$  [ $\text{M} + \text{Na}$ ] $^+$  344.0488, found 344.0472.

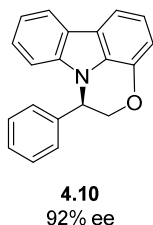
### Procedures and Analytical Data for Synthesis of Compound 4.10



2-(1-methoxy-9H-carbazol-9-yl)-2-phenylethyl methanesulfonate, **4.3fa-OMS** was prepared from reaction of **4.3fa-OH** by adapting reaction conditions from a patented procedure.<sup>24</sup> A solution of 2-(1-methoxy-9H-carbazol-9-yl)-2-

phenylethan-1-ol **4.3fa-OH** (20 mg, 0.06 mmol, 1.0 equiv) in DCM (1.1 mL) was treated with

NEt<sub>3</sub> (17.5  $\mu$ L, 0.13 mmol, 2 equiv) at 0 °C. Mesyl chloride (7.3  $\mu$ L, 0.09 mmol, 1.5 equiv) was then added and the resulting solution was stirred for 20 min at 0 °C. The reaction was quenched with aqueous saturated NaHCO<sub>3</sub> (2 mL). The resulting mixture was extracted with DCM (3  $\times$  10 mL) and the combined organic layers were dried with Na<sub>2</sub>SO<sub>4</sub>. The organic layer was concentrated and purified by flash chromatography on silica gel (20:80 EtOAc:hexanes) to afford 2-(1-methoxy-9H-carbazol-9-yl)-2-phenylethyl methanesulfonate **4.3fa-OMs** as a white solid (24 mg, 95%). *R*<sub>f</sub> = 0.22 (toluene); <sup>1</sup>H NMR (600 MHz, CDCl<sub>3</sub>)  $\delta$  8.05 (d, *J* = 7.8 Hz, 1H), 7.72 (d, *J* = 7.8 Hz, 1H), 7.43 – 7.25 (br m, 6H), 7.20 (t, *J* = 7.8 Hz, 3H), 7.11 – 6.61 (br s, 2H), 5.52 – 4.91 (br m, 2H), 3.94 (br s, 3H), 2.31 (br s, 2H); <sup>13</sup>C NMR (150 MHz, CDCl<sub>3</sub>)  $\delta$  146.7, 137.1, 130.4, 128.80 127.7, 126.3, 125.6, 120.5, 119.7, 113.0, 112.3, 108.2, 68.6, 57.1, 55.7, 37.0; IR (ATR) 3029, 2634, 1453, 1428, 1356, 1329, 1260, 1218, 1172 cm<sup>-1</sup>; HRMS (ESI) *m/z* calcd for C<sub>22</sub>H<sub>21</sub>NO<sub>4</sub>SNa [M + Na]<sup>+</sup> 418.1089, found 418.1092.



1-phenyl-1,2-dihydro-[1,4]oxazino[2,3,4-*jk*]carbazole **4.10** was synthesized by heating **4.3fa-OMs** (12.1 mg, 0.031 mmol, 1 equiv) at 155 °C in DMF (0.5 mL) for 8 h. After 8 h, the reaction was allowed to cool to room temperature and then diluted with de-ionized H<sub>2</sub>O (1 mL) and extracted with EtOAc (3  $\times$  10 mL). The combined organic layers were washed with H<sub>2</sub>O (3  $\times$  10 mL) and dried with Na<sub>2</sub>SO<sub>4</sub>. The resulting organic layers were concentrated and purified using preparative layer chromatography (5:95 EtOAc:hexanes) to afford compound **4.10** as a pale white film (6 mg, 67%, 92% *ee*). *R*<sub>f</sub> = 0.58 (30:70 EtOAc:hexanes). The *ee* was measured utilizing the Shimadzu HPLC instrument using a chiral stationary phase [Chiralcel OD-H, 2-propanol:hexanes = 5/95, 1.0 mL/min,  $\lambda$  = 254 nm], *t*<sub>R</sub> = 8.57 min (major), 14.94 min (minor); <sup>1</sup>H NMR (600 MHz, CDCl<sub>3</sub>)  $\delta$  8.09 (dt, *J* = 7.7, 0.9 Hz, 1H), 7.70 (dd, *J* = 7.9, 0.7 Hz, 1H), 7.38 – 7.31 (m, 3H), 7.24 – 7.20 (m, 1H), 7.20 – 7.17 (m, 3H),

7.15 (d,  $J = 7.8$  Hz, 1H), 6.98 (dd,  $J = 7.8, 0.7$  Hz, 1H), 6.80 (dd,  $J = 8.0, 1.0$  Hz, 1H), 5.51 (dd,  $J = 5.5, 3.4$  Hz, 1H), 4.63 (dd,  $J = 11.3, 3.4$  Hz, 1H), 4.52 (dd,  $J = 11.3, 5.5$  Hz, 1H);  $^{13}\text{C}$  NMR (150 MHz,  $\text{CDCl}_3$ )  $\delta$  142.6, 139.2, 136.9, 129.0, 128.9, 128.6, 127.1, 125.5, 123.9, 122.8, 121.2, 119.9, 119.4, 113.4, 110.3, 109.8, 71.8, 56.6; IR (ATR) 3057, 2920, 1636, 1587, 1500, 1450, 1234, 742  $\text{cm}^{-1}$ ; HRMS (ESI)  $m/z$  calcd for  $\text{C}_{20}\text{H}_{15}\text{NOH}$  [ $\text{M} + \text{H}$ ] 286.1232, found 286.1227.

### Direct Synthesis of 1-phenyl-1,2-dihydro-[1,4]oxazino[2,3,4-*jk*]carbazole 4.10 from 4.3fa-OH

A flame-dried 5 mL, single-necked, round-bottom flask equipped with a rubber septum and magnetic stir bar was charged with 2-(1-methoxy-9*H*-carbazol-9-yl)-2-phenylethan-1-ol **4.3fa-OH** (20.0 mg, 0.06 mmol). The flask was purged and backfilled with nitrogen three times, charged with dry DCM (0.5 mL), cooled to  $-78$  °C in a dry ice/acetone bath, and charged with pyridine (12  $\mu\text{L}$ , 0.07 mmol) while stirring. After 10 min,  $\text{TiF}_2\text{O}$  (5.6  $\mu\text{L}$ , 0.07 mmol) was added via syringe. The reaction mixture was stirred at  $-78$  °C for 45 min and then allowed to warm to room temperature over 1 h. Half-saturated aqueous ammonium chloride (5 mL) was then added, and the resulting mixture was extracted with DCM ( $3 \times 5$  mL). The combined organic layers were washed with brine ( $1 \times 25$  mL), dried over  $\text{Na}_2\text{SO}_4$ , and concentrated *in vacuo* to afford a yellow oil. The oil was purified by flash chromatography on silica gel (3:97 EtOAc:hexanes) to afford compound **4.10** as a pale white film (7.7 mg, 43%, 93% *ee*).

## References

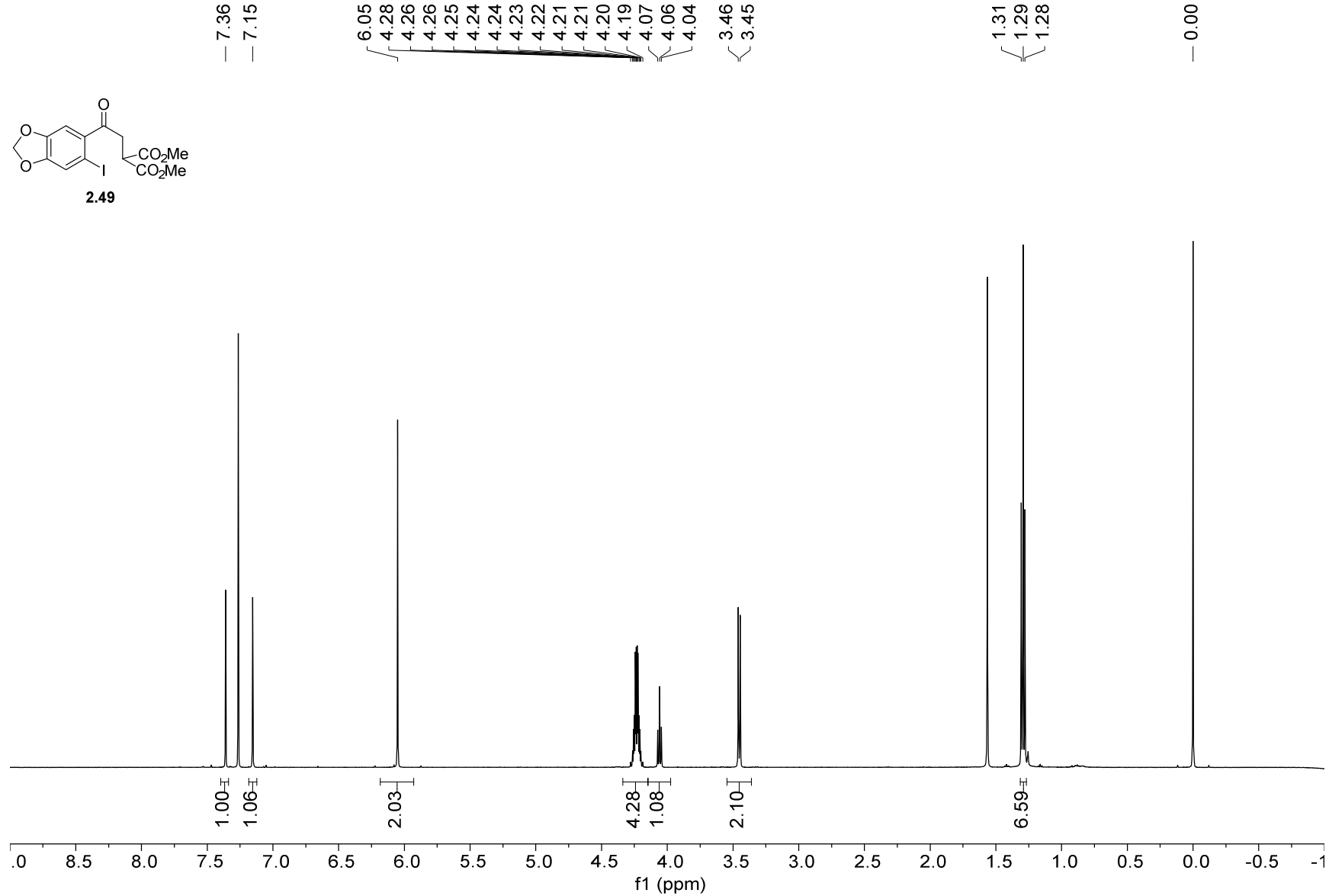
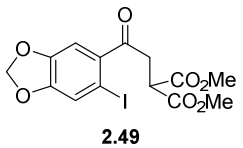
1. Pangborn, A. B.; Giardello, M. A.; Grubbs, R. H.; Rosen, R. K.; Timmers, F. J. Safe and convenient procedure for solvent purification. *Organometallics* **1996**, *15*, 1518–1520.
2. Armarego, W. L. F.; Chai, C. L. L., *Purification of Laboratory Chemicals*. 5<sup>th</sup> ed.; Elsevier: 2013; p 608.
3. (a) Gilbert, E. J.; Chisholm, J. D.; Van Vranken, D. L. Conformational Control in the Rebeccamycin Class of Indolocarbazole Glycosides. *J. Org. Chem.* **1999**, *64*, 5670–5676; (b) Biggs, B.; Presley, A. L.; Van Vranken, D. L. The retro-Mannich cleavage of  $\delta_1, \delta_1'$ -tryptophan dimers. *Bioorg. Med. Chem.* **1998**, *6*, 975–981.
4. Huang, J.; Chen, J.; Xiong, X.; Chen, Z. Imidazolium Salt Catalyzed *para*-Selective Halogenation of Electron-Rich Arenes. *Synlett* **2015**, *26*, 2831–2834.
5. (a) Bonesi, S. M.; Erra-Balsells, R. On the synthesis and isolation of chlorocarbazoles obtained by chlorination of carbazoles. *J. Heterocycl. Chem.* **1997**, *34*, 877–889; (b) Bonesi, S. M.; Ponce, M. A.; Erra-Balsells, R. A study of substituent effect on  $^1\text{H}$  and  $^{13}\text{C}$  NMR spectra of mono, di and poly substituted carbazoles. *J. Heterocycl. Chem.* **2005**, *42*, 867–875.
6. Allen, F. L.; Suschitzky, H. 786. Heterocyclic fluorine compounds. Part I. Monofluoro-1:2:3:4-tetrahydrocarbazoles and monofluorocarbazoles. *J. Chem. Soc.* **1953**, 3845–3849.
7. Chen, J.; Hu, Y. Microwave-Assisted One-Pot Synthesis of 1,2,3,4-Tetrahydrocarbazoles. *Synth. Commun.* **2006**, *36*, 1485–1494.
8. (a) Ackermann, L.; Althammer, A. Domino N–H/C–H bond activation: palladium-catalyzed synthesis of annulated heterocycles using dichloro(hetero)arenes. *Angew. Chem. Int. Ed.* **2007**, *46*, 1627–1629; (b) Ackermann, L.; Althammer, A.; Mayer, P. Palladium-Catalyzed Direct Arylation-Based Domino Synthesis of Annulated *N*-Heterocycles Using Alkenyl or (Hetero)Aryl 1,2-Dihalides. *Synthesis* **2009**, *2009*, 3493–3503.
9. (a) Balasubramanian, G.; Gharat, L. A.; Lakdawala, A. D.; Anupindi, R. R. Tricyclic Compounds Useful for the Treatment of Inflammatory and Allergic Disorders: Process for Their Preparation and Pharmaceutical Compositions Containing Them. WO 2004/037805 A1, May 6., 2004; (b) Balasubramanian, G.; Gharat, L. A.; Lakdawala, A. D.; Anupindi, R. R. Tricyclic Compounds Useful for the Treatment of Inflammatory and Allergic Disorders: Process for Their Preparation and Pharmaceutical Compositions Containing Them. US 7,238,725 B2, Jul. 3, 2007.
10. Martin, T.; Moody, C. J. A New Route to 1-Oxygenated Carbazoles - Synthesis of the Carbazole Alkaloids Murrayafoline-a and Murrayaquinone-A. *J. Chem. Soc., Perkin Trans. 1* **1988**, 235–240.
11. Eastabrook, A. S.; Wang, C.; Davison, E. K.; Sperry, J. A procedure for transforming indoles into indolequinones. *J. Org. Chem.* **2015**, *80*, 1006–1017.
12. Robbins, D. W.; Boebel, T. A.; Hartwig, J. F. Iridium-catalyzed, silyl-directed borylation of nitrogen-containing heterocycles. *J. Am. Chem. Soc.* **2010**, *132*, 4068–4069.
13. (a) Allen, J. R.; Amegadzie, A. K.; Gardinier, K. M.; Gregory, G. S.; Hitchcock, S. A.; Hoogestraat, P. J.; Jones, W. D., Junior; Smith, D. L. CB1 Modulator Compounds. WO 2005/066126 A1, Jul 21, 2005; (b) Allen, J. R.; Amegadzie, A. K.; Gardinier, K. M.; Gregory, G. S.; Hitchcock, S. A.; Hoogestraat, P. J.; Jones, W. D., Junior; Smith, D. L. CB1 Modulator Compounds. US 7,595,339 B2, Sep. 29, 2009.



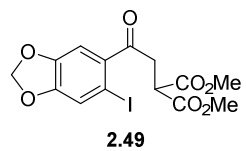
14. (a) Davies, H. M. L.; Chennamadhavuni, S.; Martin, T. J.; Childers, S. R. Cyclopropyl derivatives and methods of use. WO 2012/145234 A2, Oct. 26, 2012; (b) Davies, H. M. L.; Chennamadhavuni, S.; Martin, T. J.; Childers, S. R. Cyclopropyl derivatives and methods of use. 10,207,984 B2, Feb. 19, 2019.
15. Tayama, E.; Saito, S. Copper-Catalyzed Regiospecific and 1,2-Regioselective Cyclopropanation of (1Z)-1-Amino- and (1Z)-1-Oxy-1,3-butadienyl Derivatives. *Synlett* **2015**, 26, 1880–1884.
16. Chan, W. W.; Yeung, S. H.; Zhou, Z.; Chan, A. S.; Yu, W. Y. Ruthenium catalyzed directing group-free C2-selective carbenoid functionalization of indoles by  $\alpha$ -aryldiazoesters. *Org. Lett.* **2010**, 12, 604–607.
17. Gao, L.; Kang, B. C.; Ryu, D. H. Catalytic asymmetric insertion of diazoesters into aryl-CHO bonds: highly enantioselective construction of chiral all-carbon quaternary centers. *J. Am. Chem. Soc.* **2013**, 135, 14556–14559.
18. Lee, M.; Kim, D. H. Syntheses and Kinetic Evaluation of Racemic and Optically Active 2-Benzyl-2-methyl-3,4-epoxybutanoic Acids as Irreversible Inactivators for Carboxypeptidase A. *Bior. Med. Chem.* **2002**, 10, 913–922.
19. Bartrum, H. E.; Blakemore, D. C.; Moody, C. J.; Hayes, C. J. Rapid access to  $\alpha$ -alkoxy and  $\alpha$ -amino acid derivatives through safe continuous-flow generation of diazoesters. *Chemistry* **2011**, 17, 9586–9589.
20. Cárdenas, J.; Morales-Serna, J.; Vera, A.; Paleo, E.; García-Ríos, E.; Gaviño, R.; García de la Mora, G. Using Benzotriazole Esters as a Strategy in the Esterification of Tertiary Alcohols. *Synthesis* **2010**, 2010, 4261–4267.
21. Muthusamy, S.; Sivaguru, M. Atom-economical access to highly substituted indenenes and furan-2-ones via tandem reaction of diazo compounds and propargyl alcohols. *Org. Lett.* **2014**, 16, 4248–4251.
22. Lee, C. L.; Loh, T. P. Gram-scale synthesis of (-)-epibatidine. *Org. Lett.* **2005**, 7, 2965–2967.
23. (a) Xie, X. L.; Zhu, S. F.; Guo, J. X.; Cai, Y.; Zhou, Q. L. Enantioselective palladium-catalyzed insertion of  $\alpha$ -Aryl- $\alpha$ -diazoacetates into the O–H bonds of phenols. *Angew. Chem. Int. Ed.* **2014**, 53, 2978–2981; (b) Xie, X.-L.; Zhu, S.-F.; Guo, J.-X.; Cai, Y.; Zhou, Q.-L. Enantioselective Palladium-Catalyzed Insertion of  $\alpha$ -Aryl- $\alpha$ -diazoacetates into the O–H Bonds of Phenols. *Angew. Chem.* **2014**, 126, 3022–3025.
24. Li, L.; Beaulieu, C.; Guay, D.; Sturino, C.; Wang, Z. Fluoro-methanesulfonyl-substituted cycloalkanoindoles and their use as prostaglandin d2 antagonists. WO 2004/103970 A1, Dec. 2, 2004.

## **Appendix A: Chapter 2 – NMR**

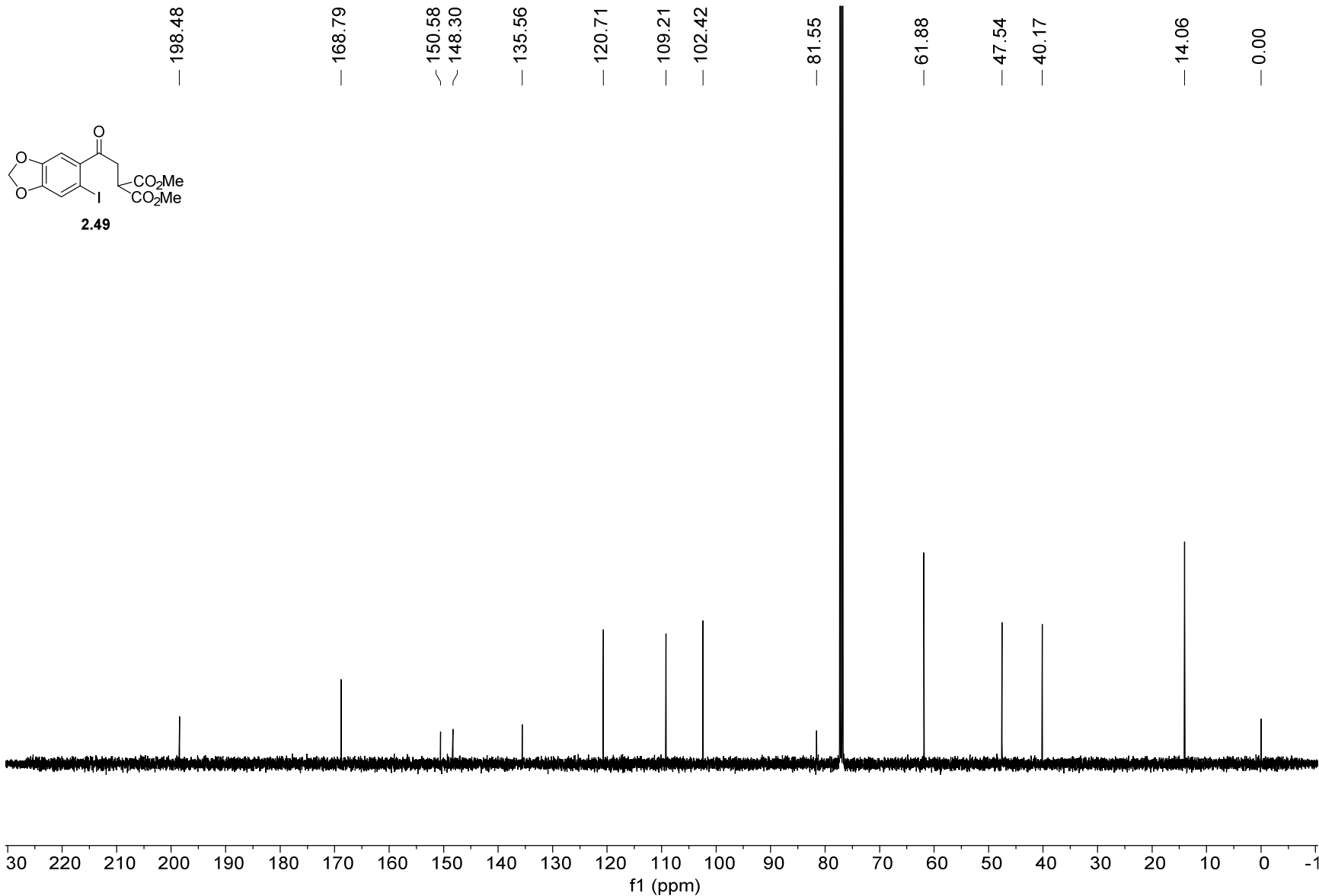
1H NMR — 500 MHz — CDCl3 — 298.0 K



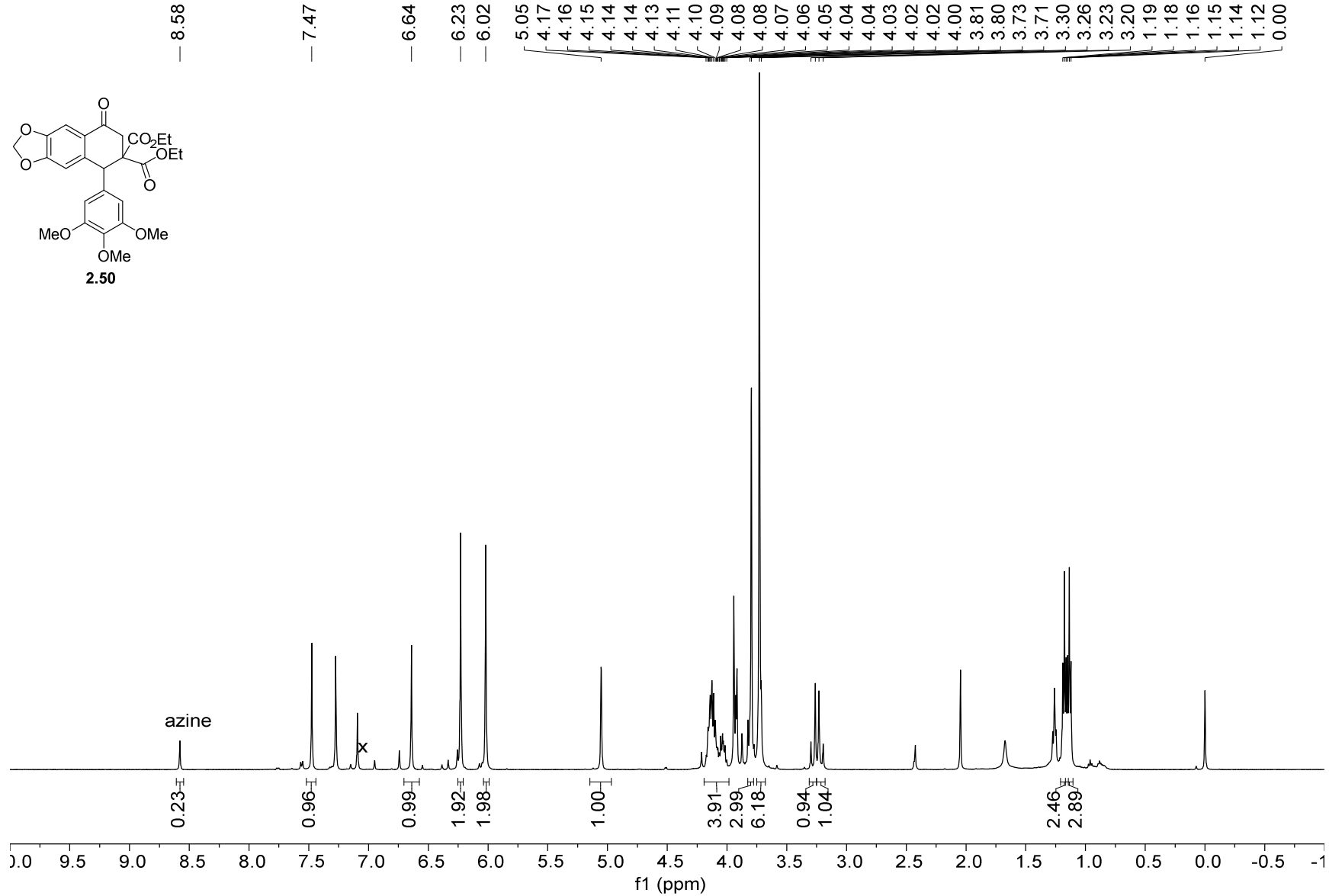
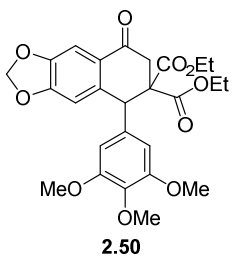
13C NMR — 126 MHz — CDCl3 — 298.0 K



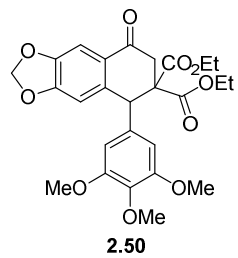
— 198.48 — 168.79 — 150.58 — 148.30 — 135.56 — 120.71 — 109.21 — 102.42 — 81.55 — 61.88 — 47.54 — 40.17 — 14.06 — 0.00



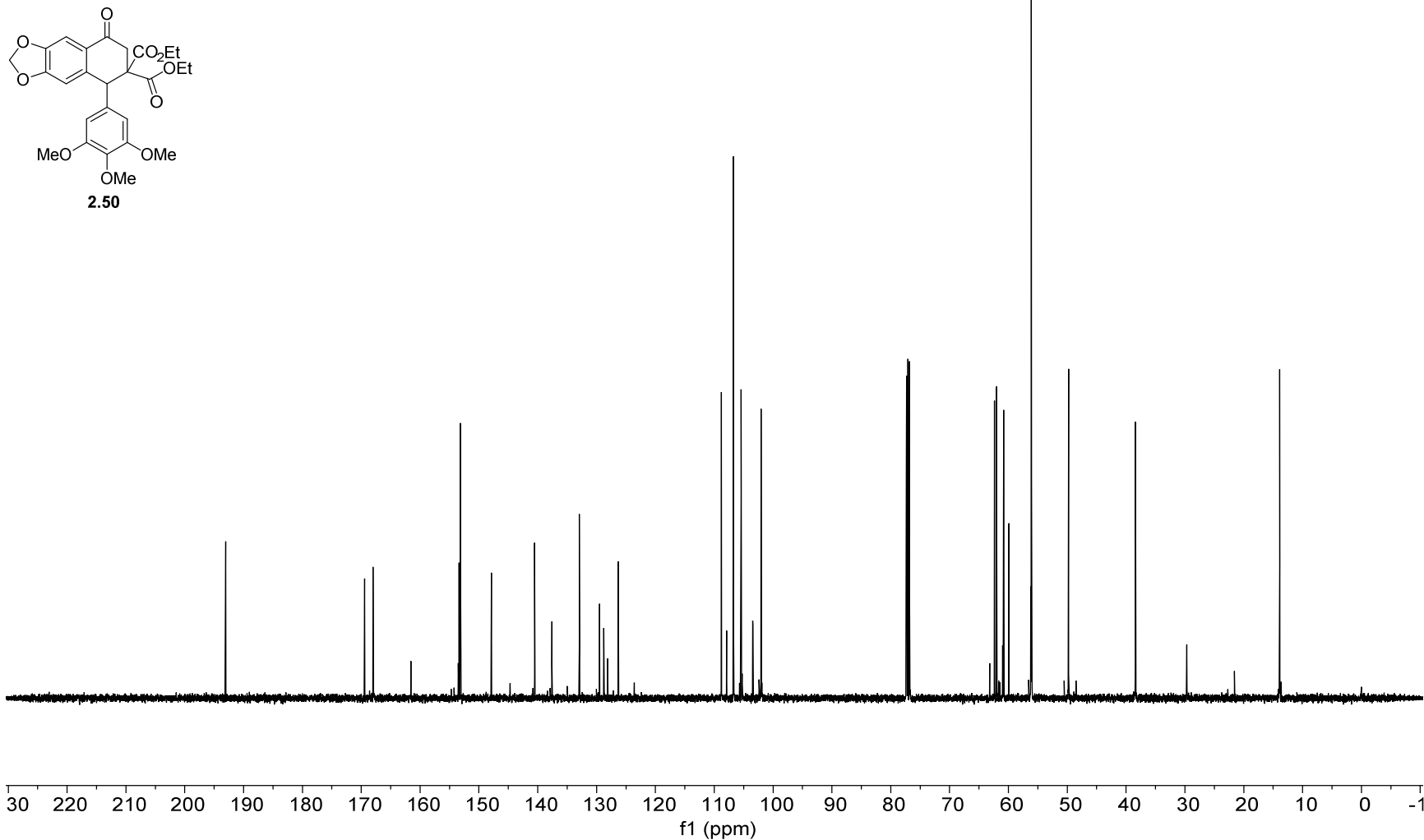
1H NMR — 500 MHz — CDCl3 — 298.0 K



13C NMR — 126 MHz — CDCl3 — 298.0 K

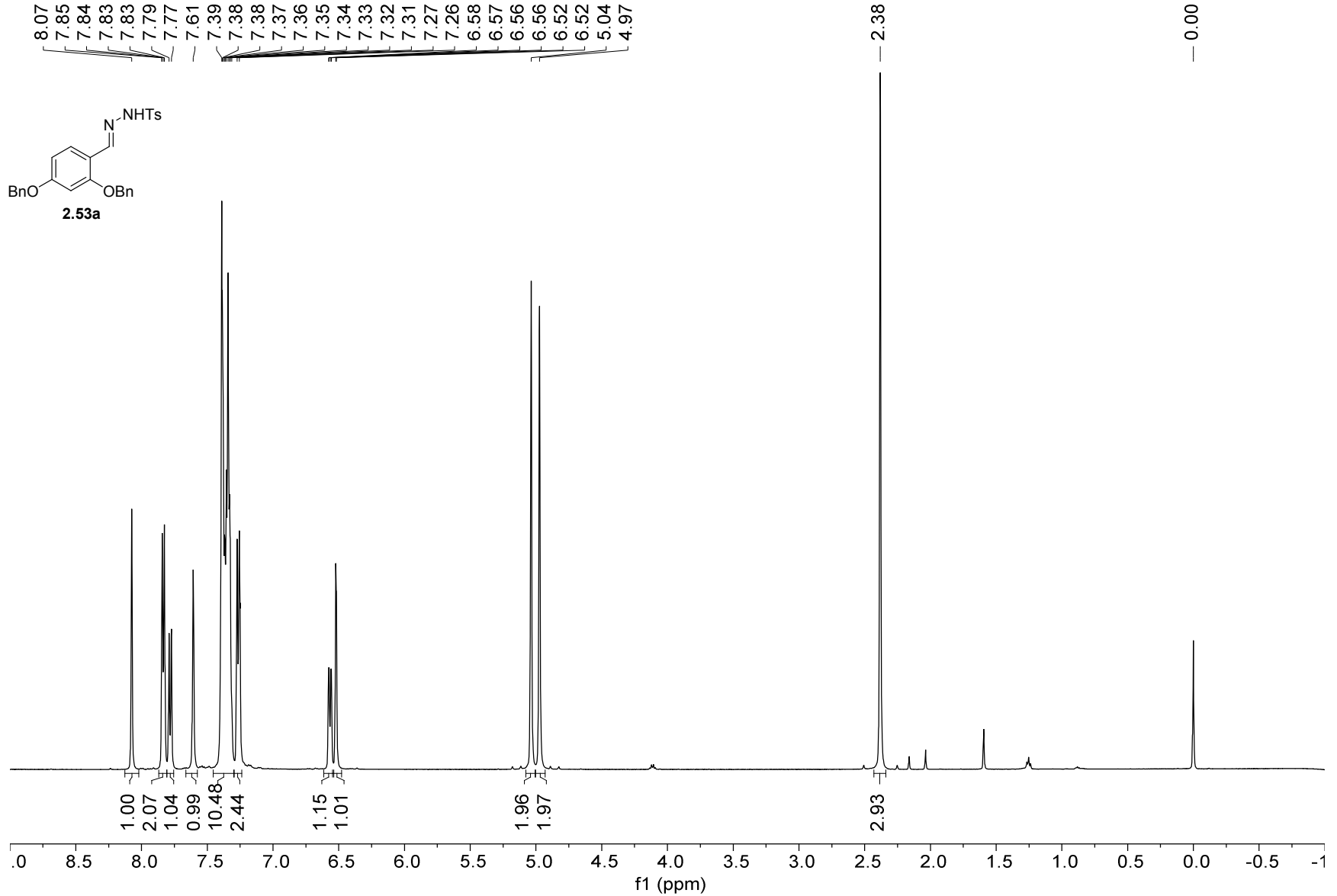
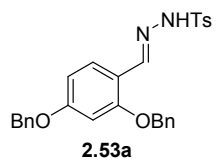


193.05  
169.45  
167.98  
153.36  
153.14  
147.89  
140.54  
137.60  
132.93  
129.50  
128.78  
126.33  
108.80  
107.90  
106.75  
105.45  
103.45  
102.05  
62.37  
62.01  
60.81  
59.93  
56.10  
49.78  
38.41  
13.90  
13.83  
-0.00

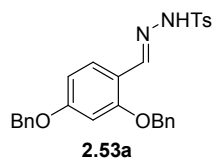


232

1H NMR — 500 MHz — CDCl3T — 298.0 K



13C NMR — 126 MHz — CDCl3 — 298.0 K



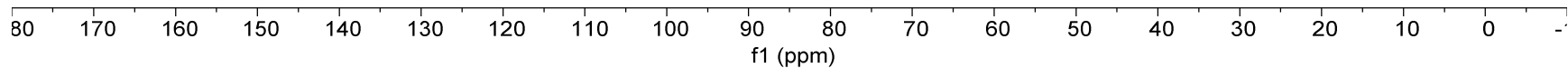
161.91  
158.32  
143.99  
143.96  
136.32  
136.12  
135.44  
129.57  
128.70  
128.67  
128.28  
128.21  
127.95  
127.83  
127.53  
115.24  
106.90  
100.06

70.42  
70.19

21.58

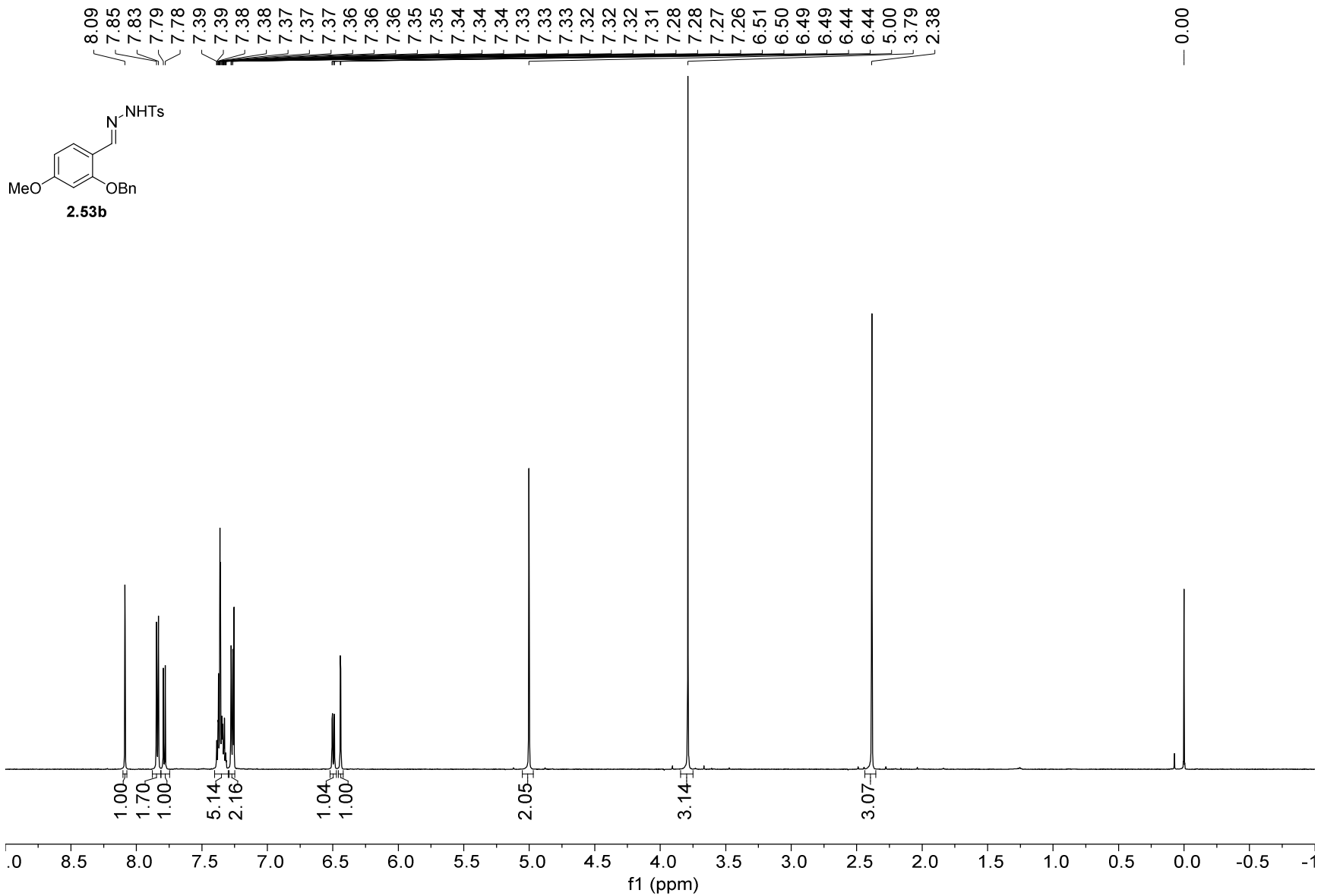
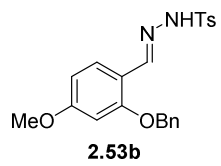
0.00

233



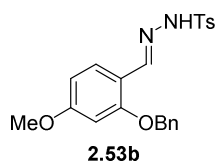


1H NMR — 600 MHz — CDCl3T — 298.0 K

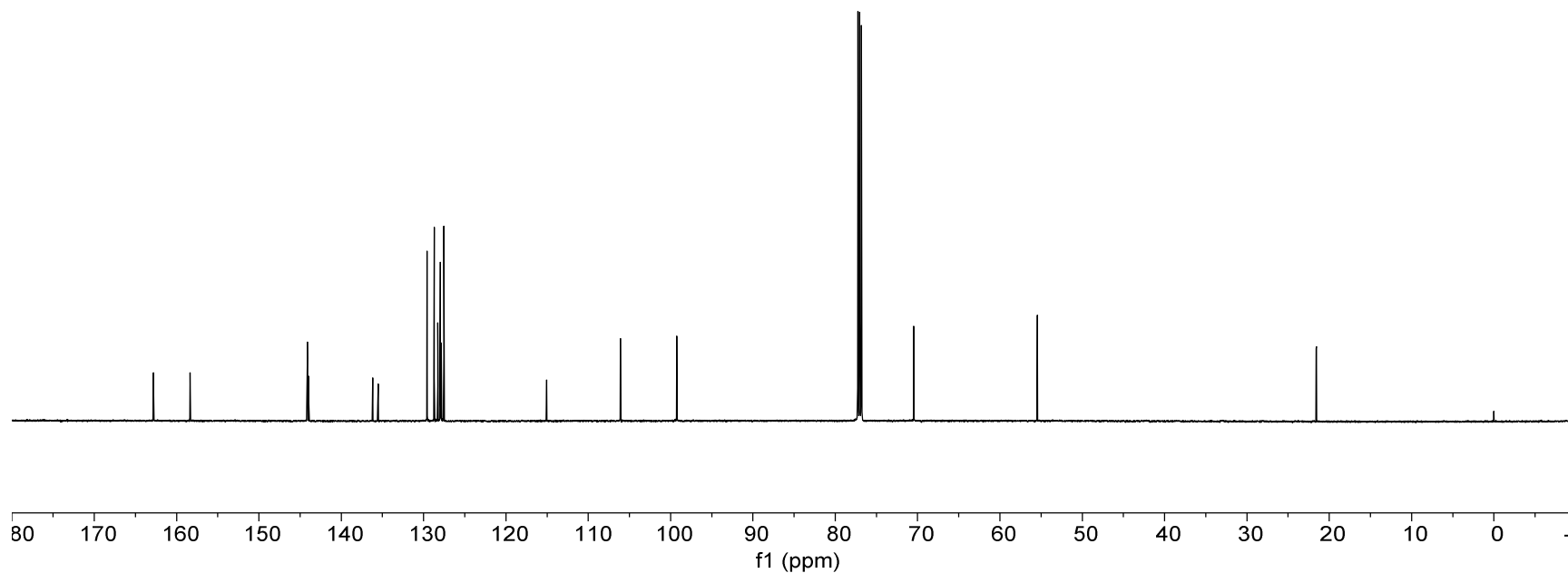


13C NMR — 151 MHz — CDCl3T — 298.0 K

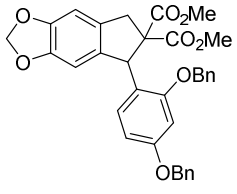
— 162.80 — 158.37 — 144.13 143.96 — 136.18 135.49 — 129.57 128.71 128.28 127.96 127.86 127.53 115.07 — 106.08 — 99.25 — 70.46 — 55.46 — 21.58 — -0.00



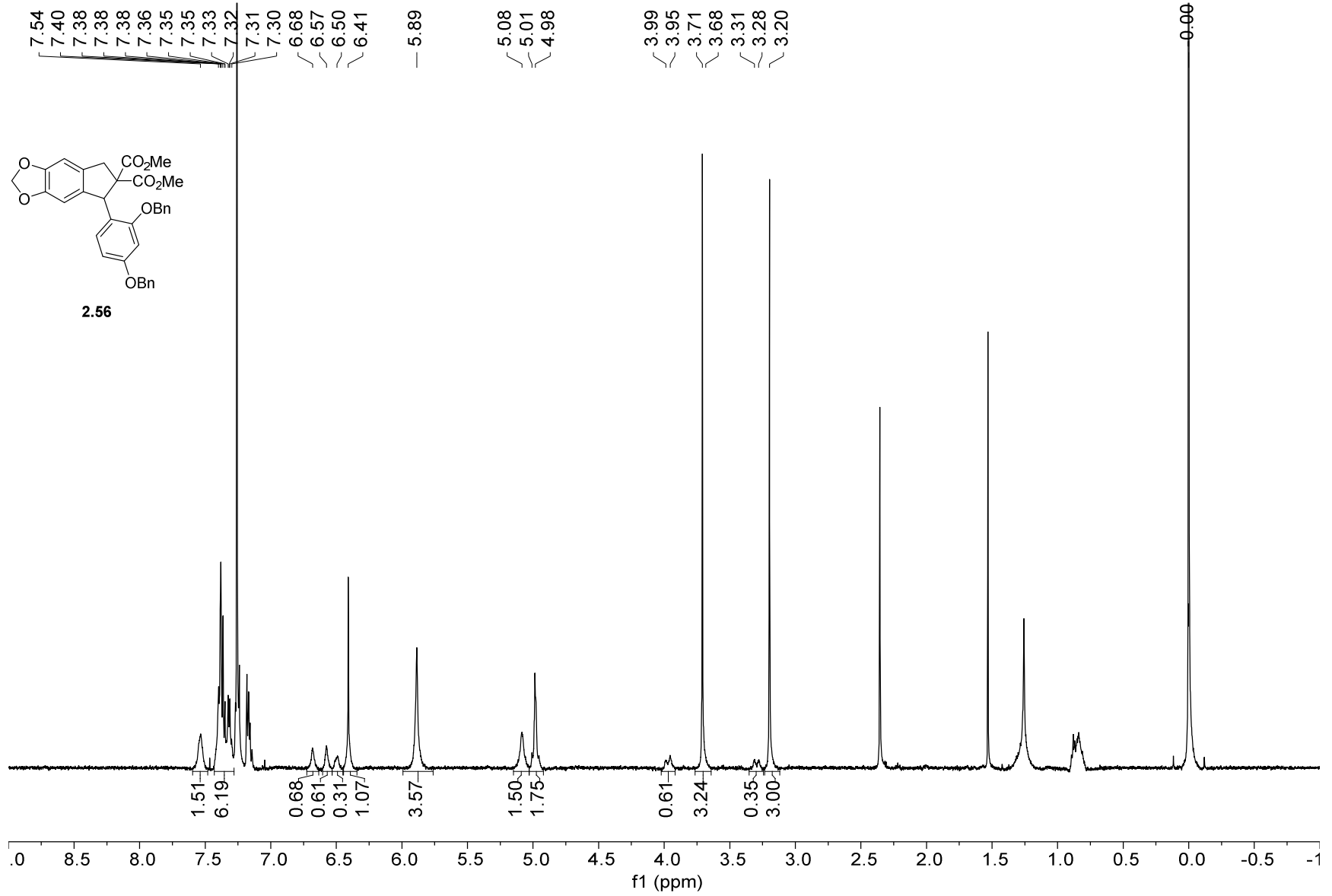
235



1H NMR — 499 MHz — CDCl3T — 298.0 K



2.56



13C NMR — 126 MHz — CDCl3 — 298.0 K

172.32  
170.02

158.85  
157.04

147.41

137.17

136.84

132.51

130.38

128.58

128.47

128.02

127.73

127.60

127.03

122.11

105.53

104.28

101.05

100.32

70.17

70.03

66.27

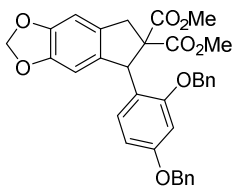
52.89

52.03

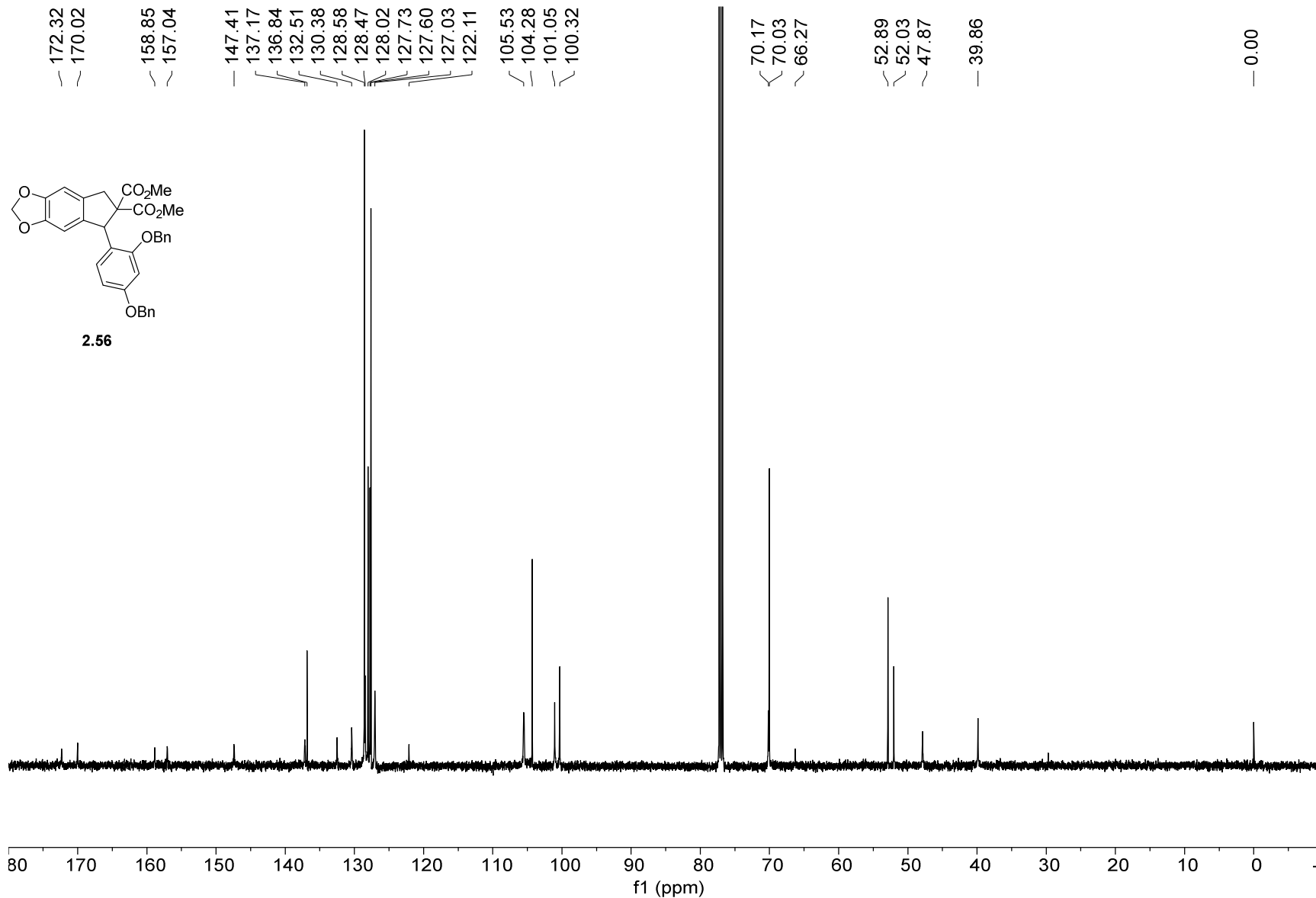
47.87

39.86

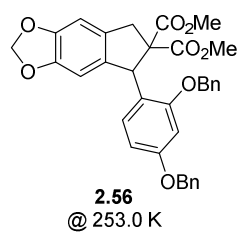
0.00



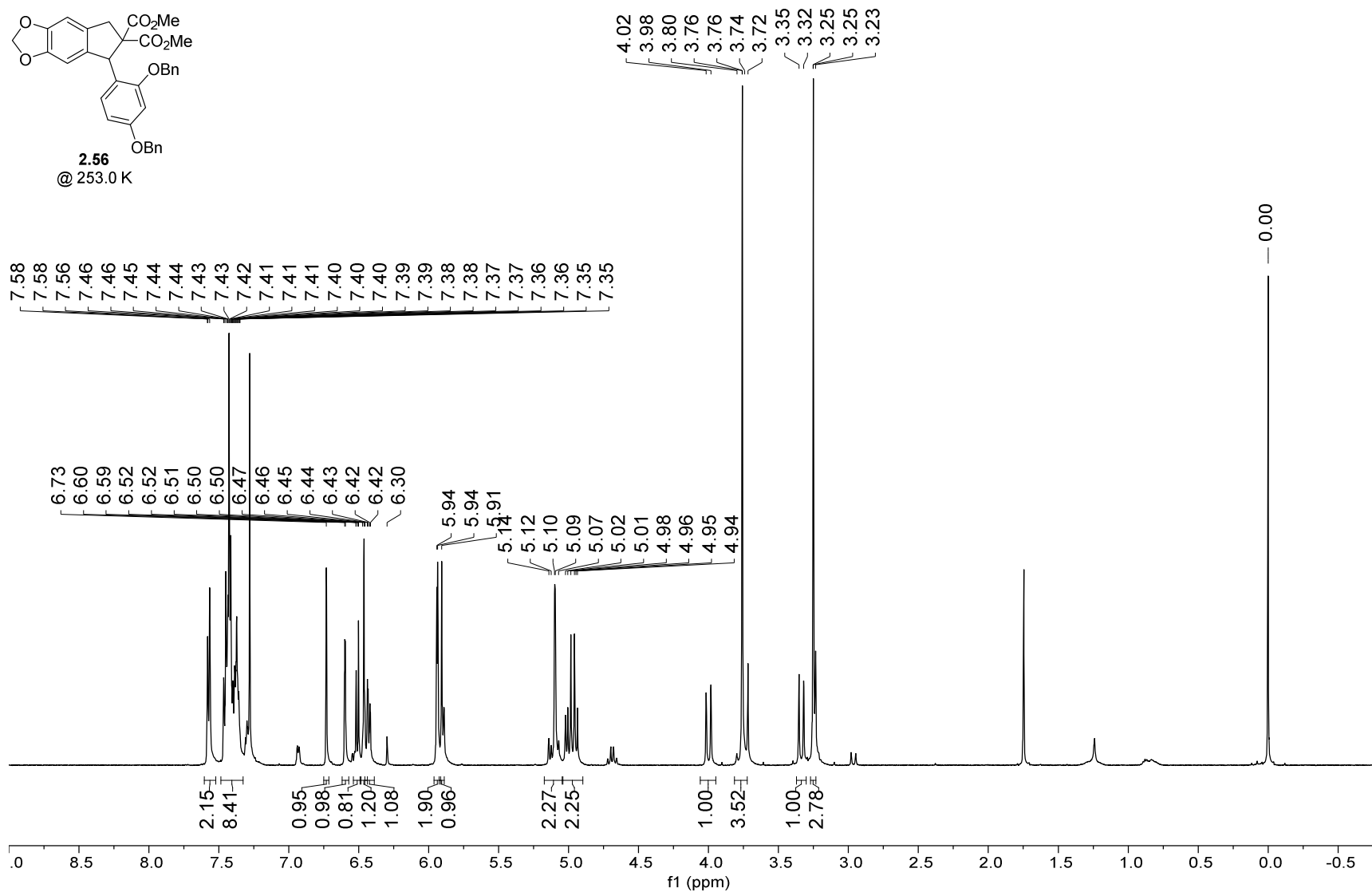
2.56



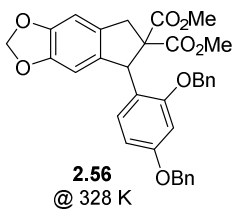
<sup>1</sup>H NMR — 499 MHz — CDCl<sub>3</sub>T — 253.0 K



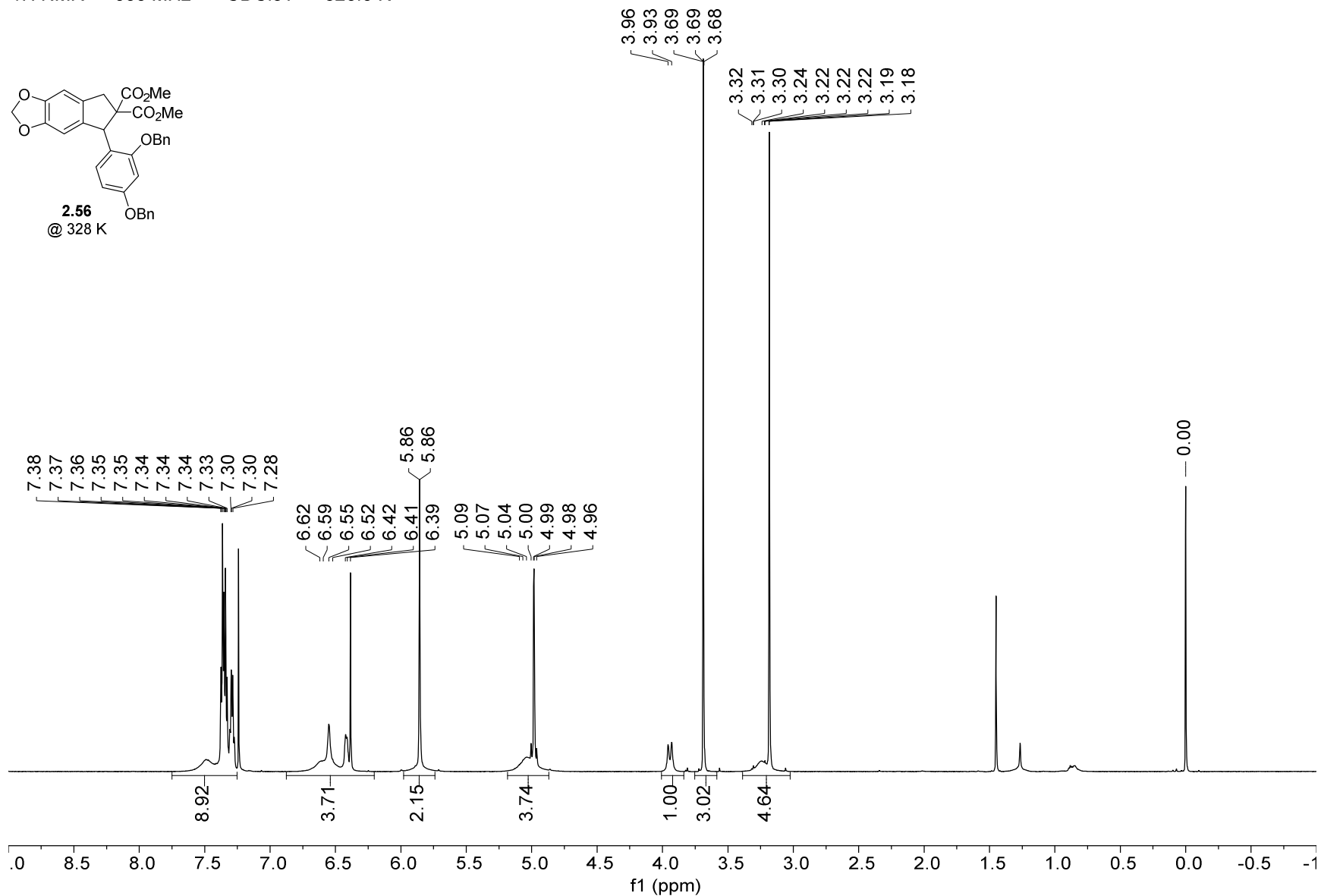
238



1H NMR — 600 MHz — CDCl3T — 328.0 K

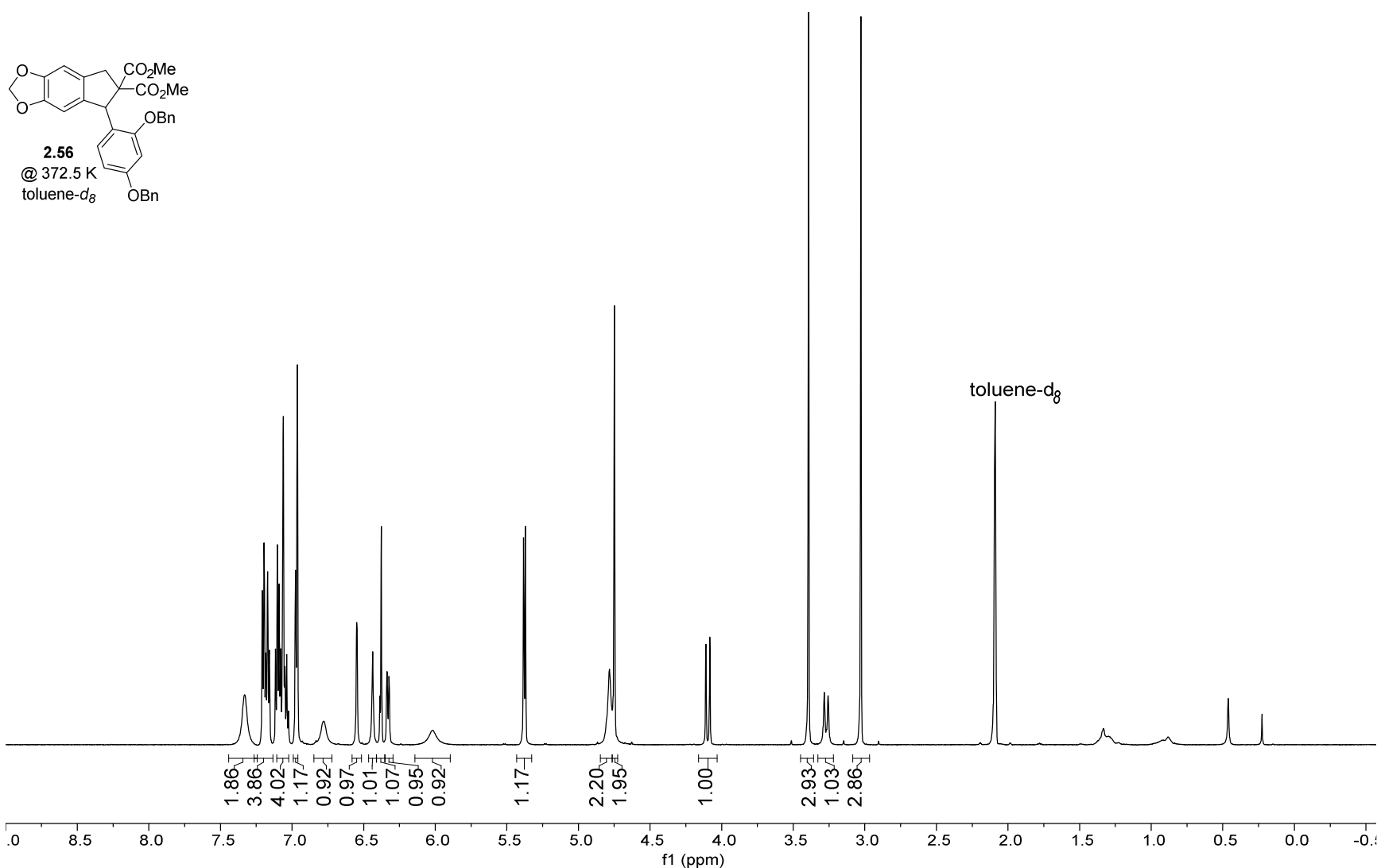
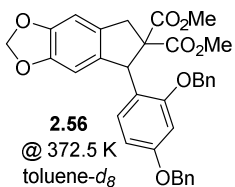


239



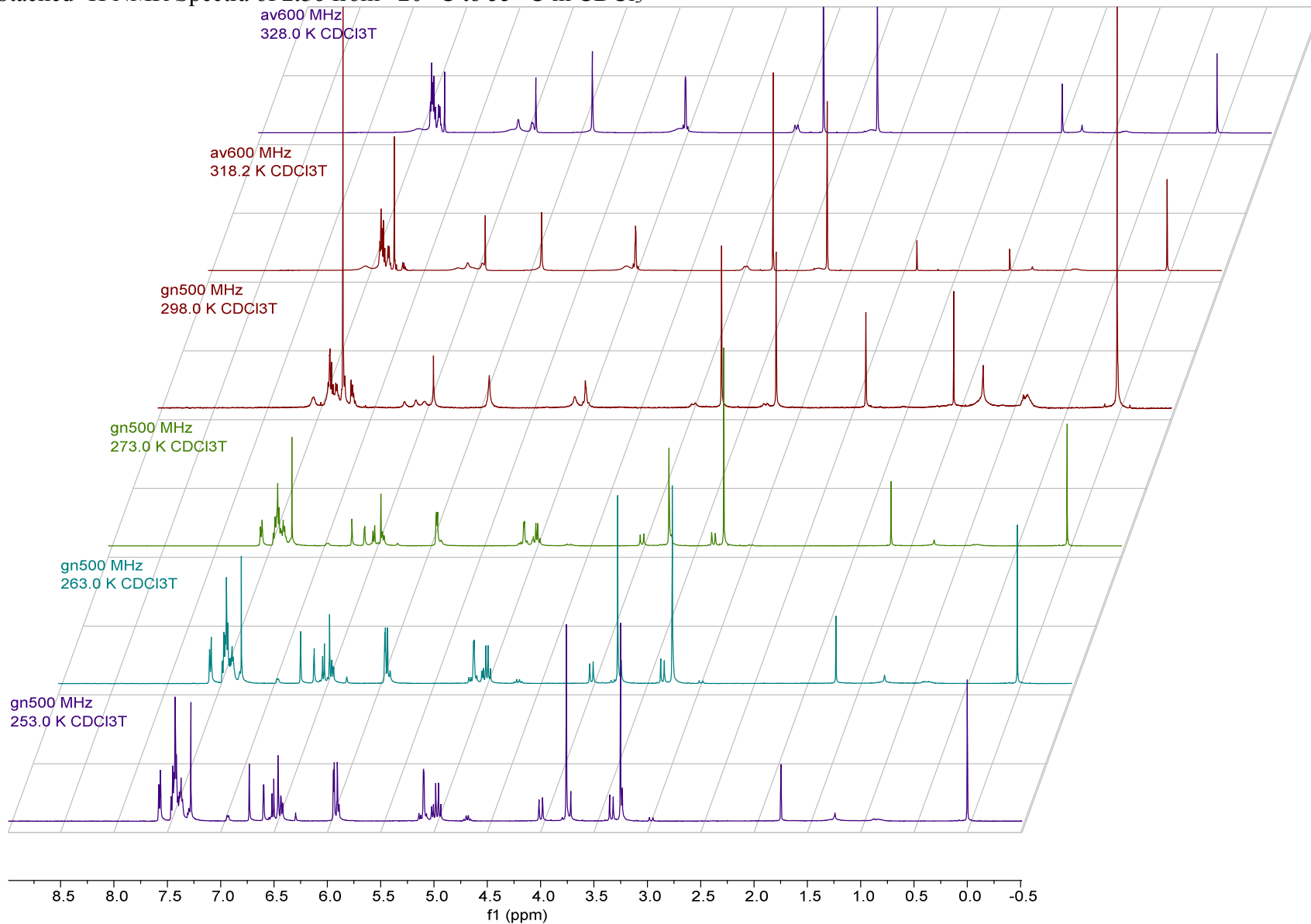
1H NMR — 600 MHz — Tol — 372.5 K

7.21  
7.20  
7.18  
7.17  
7.16  
7.09  
7.09  
7.08  
7.06  
7.06  
7.05  
7.05  
7.04  
6.98  
6.97  
6.97  
6.96  
6.55  
6.55  
6.44  
6.38  
6.34  
5.39  
5.38  
5.38  
5.37  
5.37  
5.37  
4.78  
4.75  
4.11  
4.08  
3.41  
3.39  
3.39  
3.28  
3.27  
3.26  
3.03  
3.03  
2.10  
2.09  
2.09  
2.09



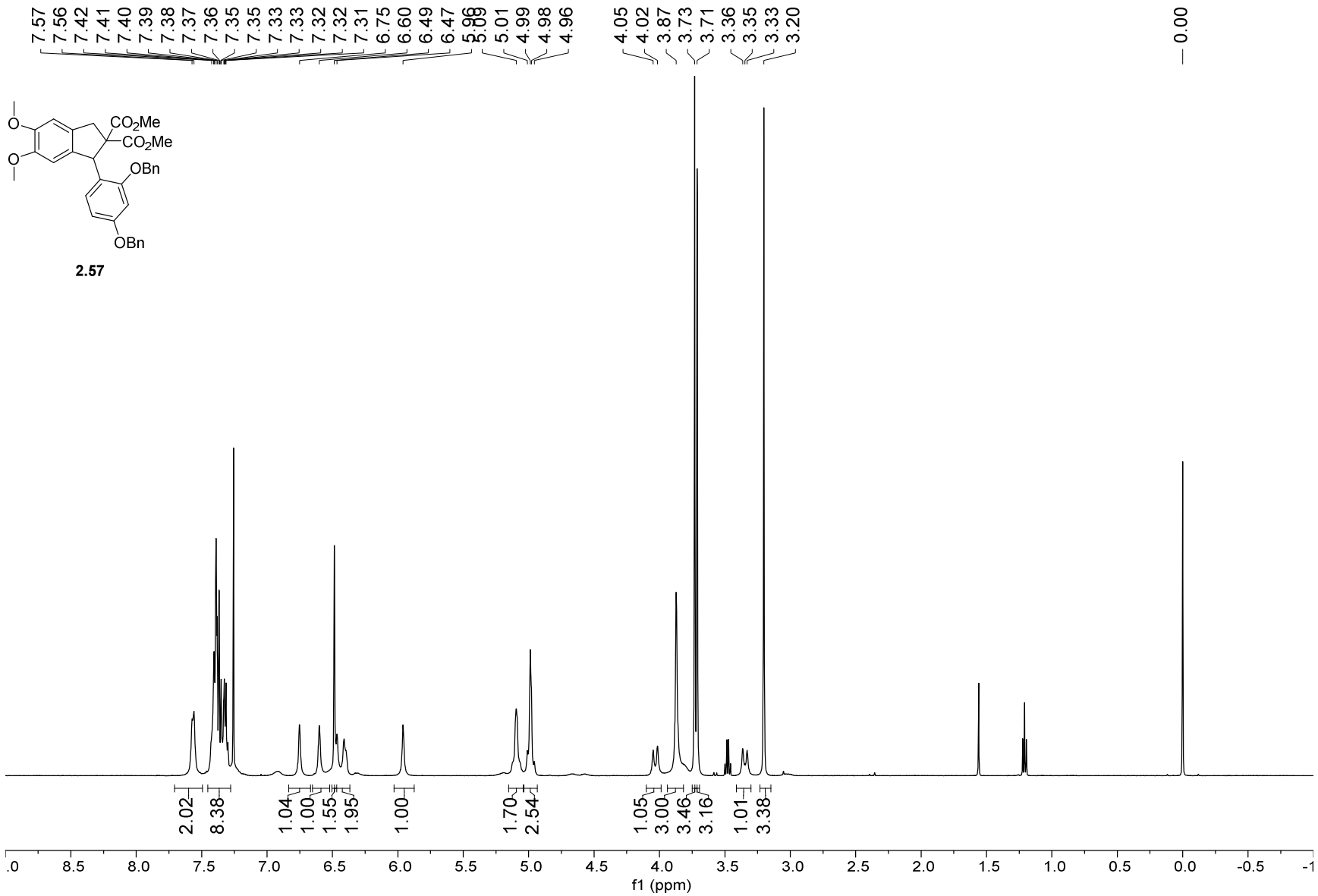
Stacked  $^1\text{H}$  NMR Spectra of **2.56** from  $-20\text{ }^\circ\text{C}$  to  $55\text{ }^\circ\text{C}$  in  $\text{CDCl}_3$

241



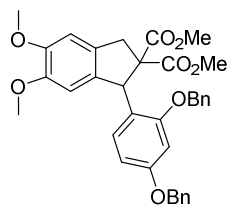


1H NMR — 500 MHz — CDCl3T — 298.0 K

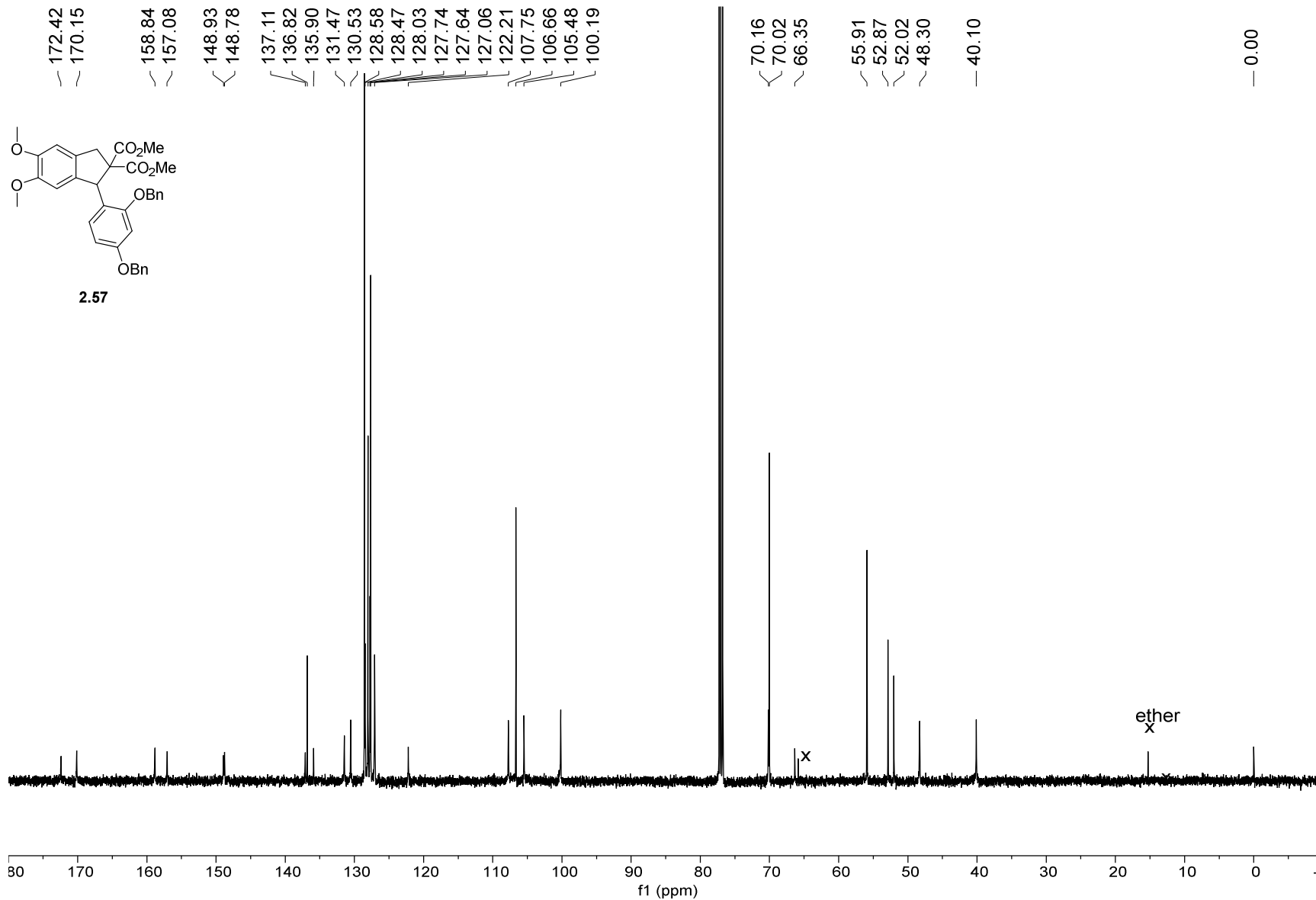


13C NMR — 126 MHz — CDCl3 — 298.0 K

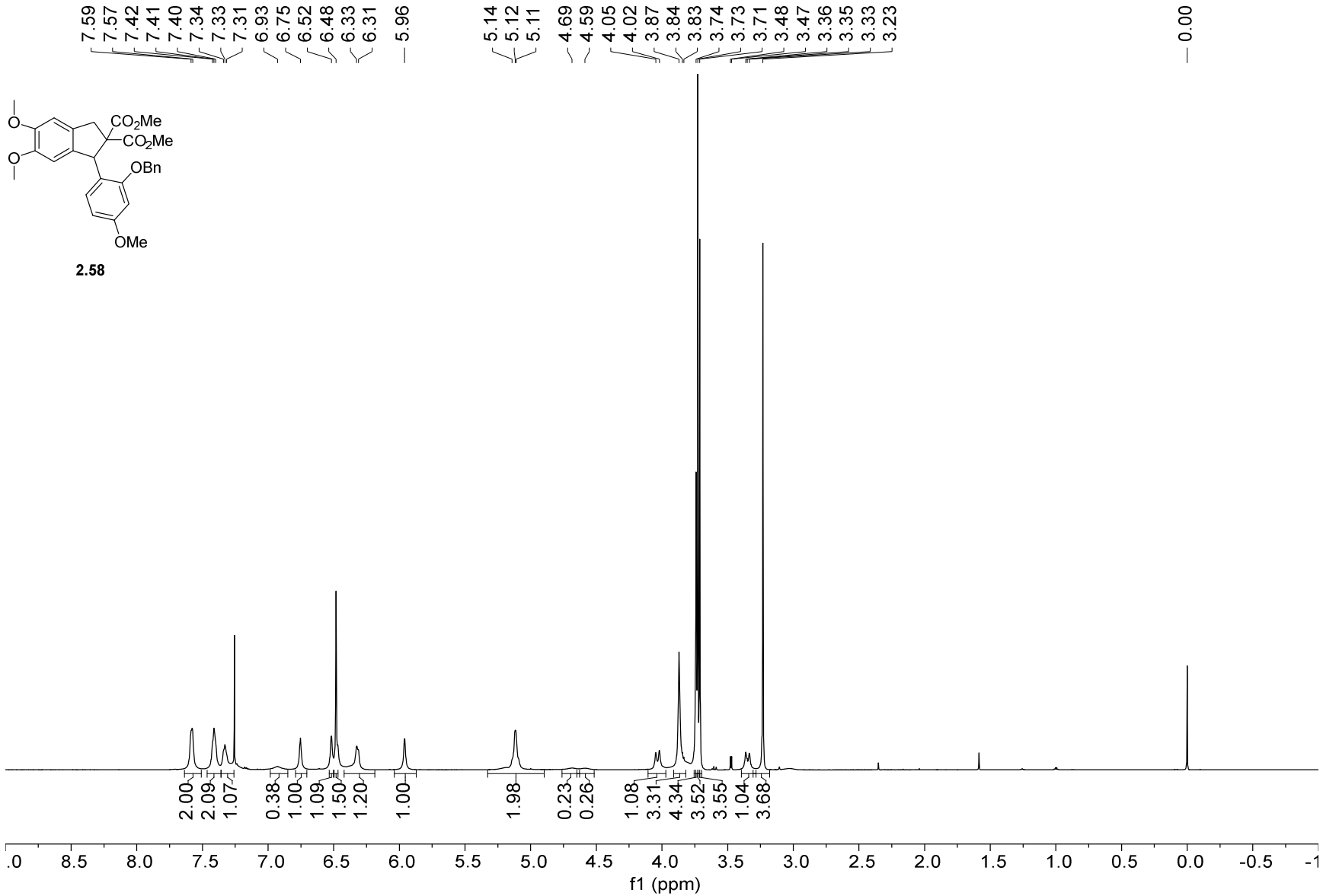
172.42  
170.15  
158.84  
157.08  
148.93  
148.78  
137.11  
136.82  
135.90  
131.47  
130.53  
128.58  
128.47  
128.03  
127.74  
127.64  
127.06  
122.21  
107.75  
106.66  
105.48  
100.19  
70.16  
70.02  
66.35  
55.91  
52.87  
52.02  
48.30  
40.10  
0.00



2.57



1H NMR — 600.13 MHz — CDCl3T — 298.3 K



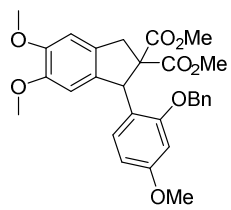
13C NMR — 150.92 MHz — CDCl3T — 298.0 K

172.43  
170.14  
159.67  
157.09  
148.95  
148.80  
137.16  
136.00  
131.46  
130.55  
128.47  
127.74  
127.09  
121.97

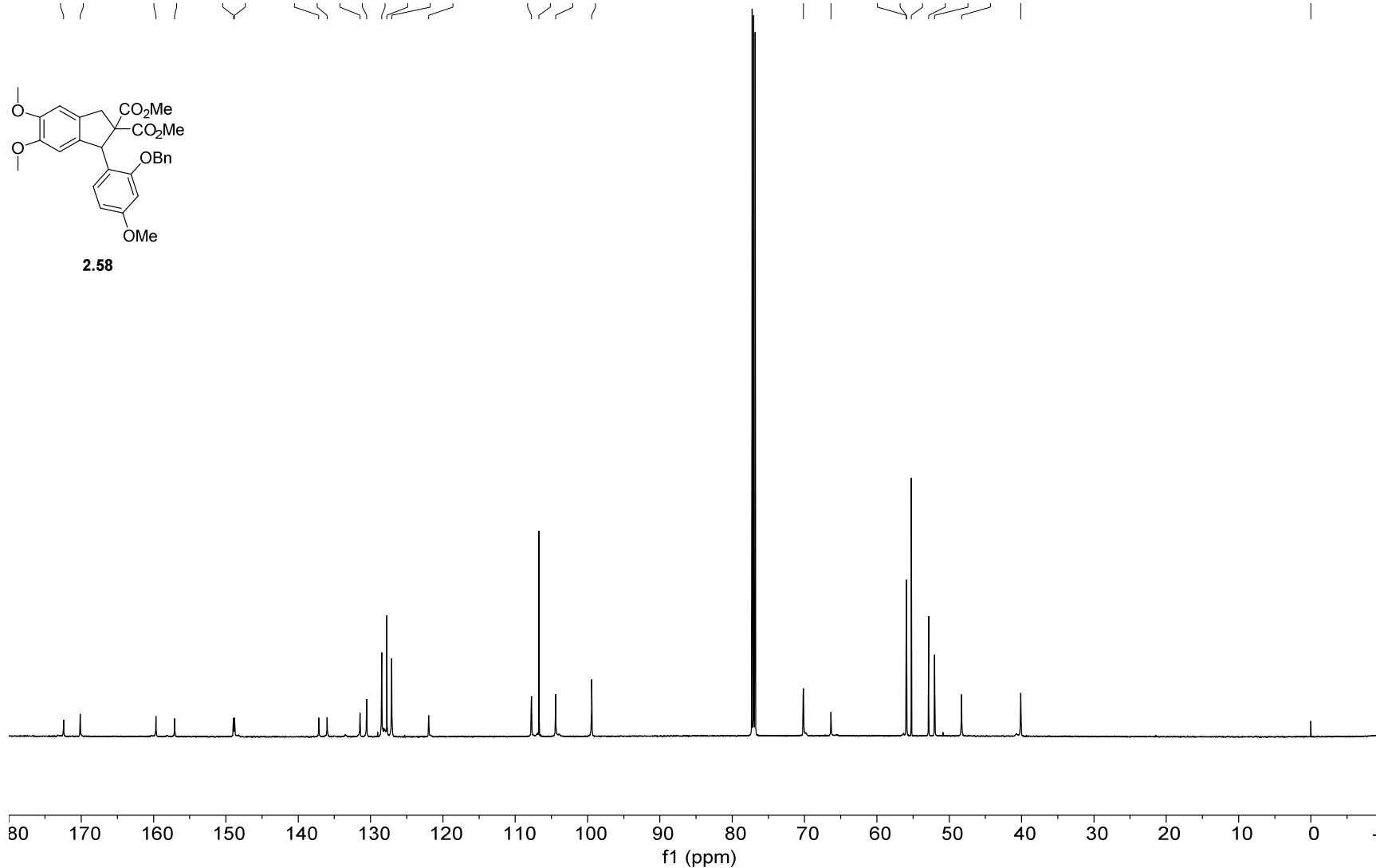
107.76  
106.71  
104.42  
99.42

70.17  
66.35  
55.93  
55.90  
55.23  
52.85  
52.02  
48.29  
40.11

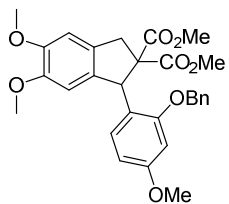
0.00



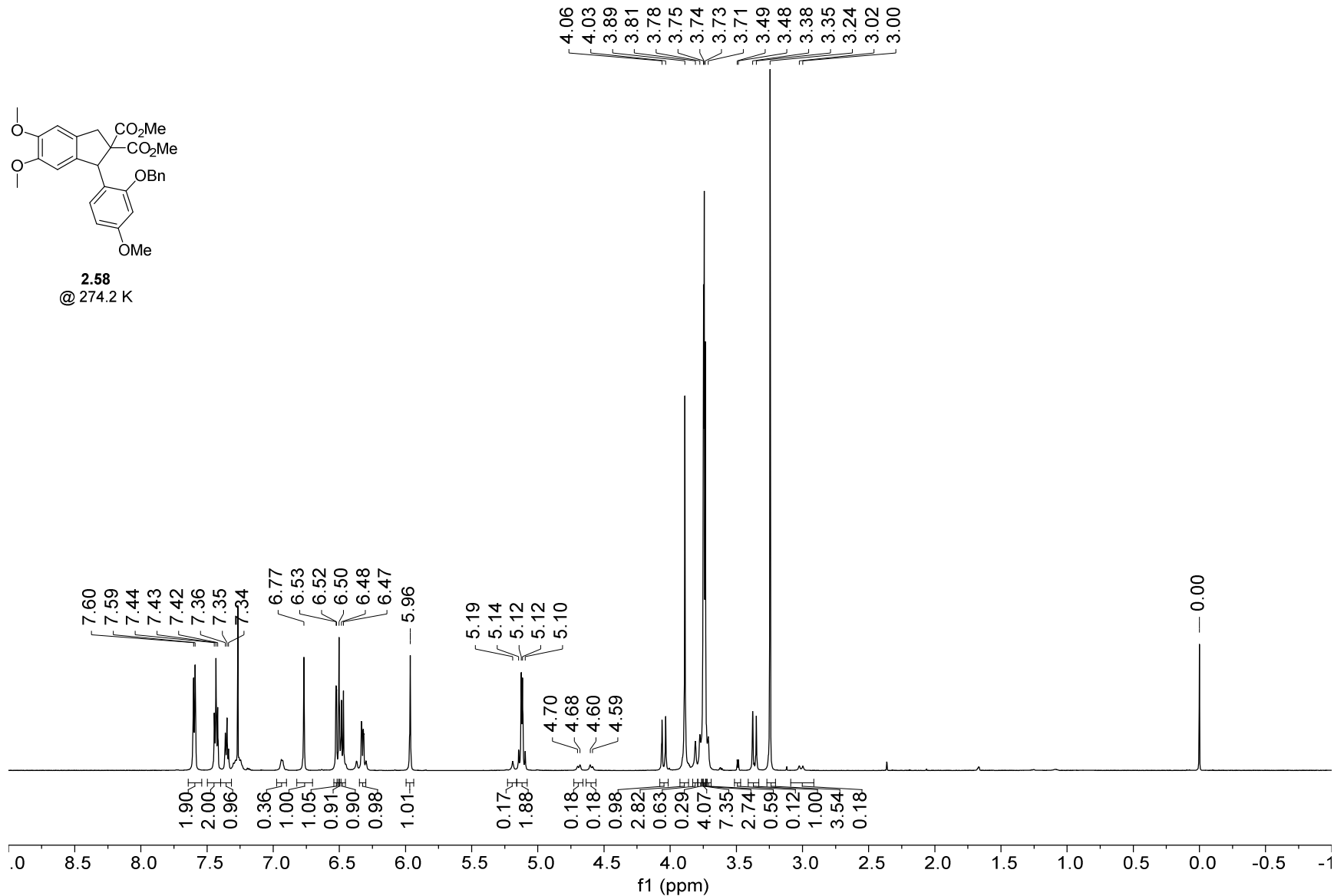
2.58



1H NMR — 600.13 MHz — CDCl3T — 274.2 K



2.58  
@ 274.2 K



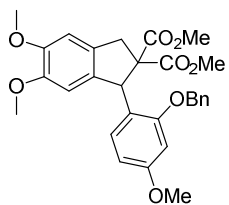
13C NMR — 150.92 MHz — CDCl3T — 274.2 K

172.43  
170.16  
159.49  
156.83  
148.64  
148.49  
136.99  
135.71  
131.22  
130.47  
128.47  
127.73  
126.93  
121.61

107.33  
106.32  
104.01  
99.16

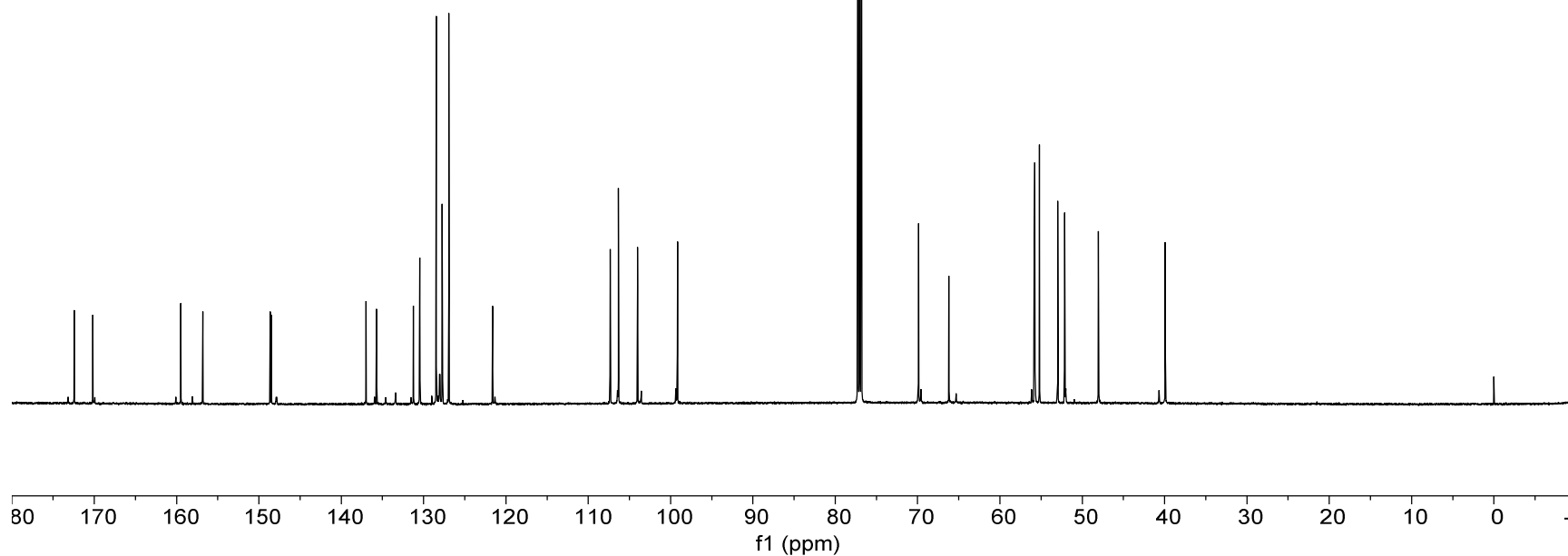
69.89  
66.19  
55.82  
55.76  
55.19  
52.96  
52.14  
48.03  
39.92

-0.00

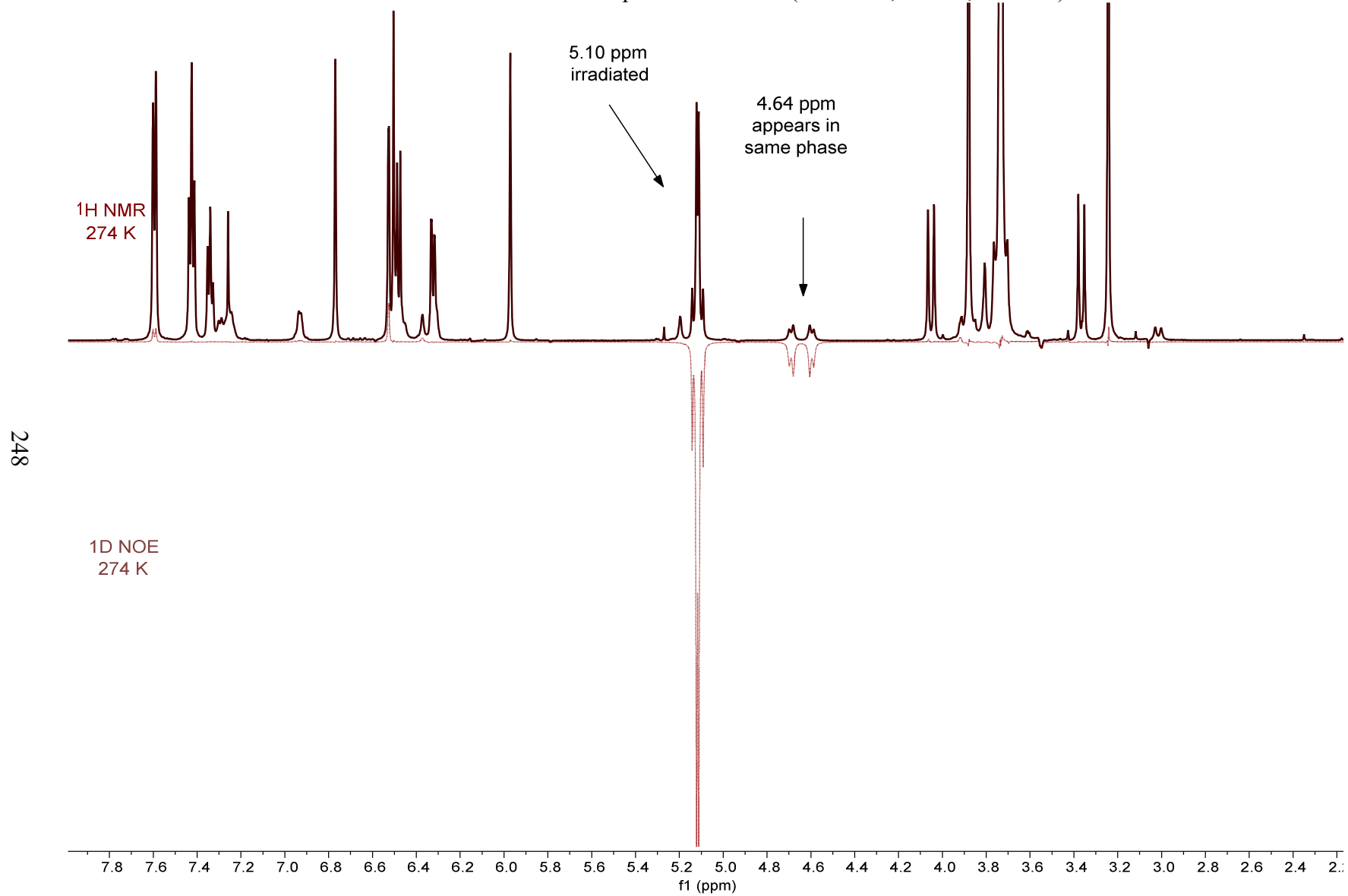


2.58  
@ 274.2 K

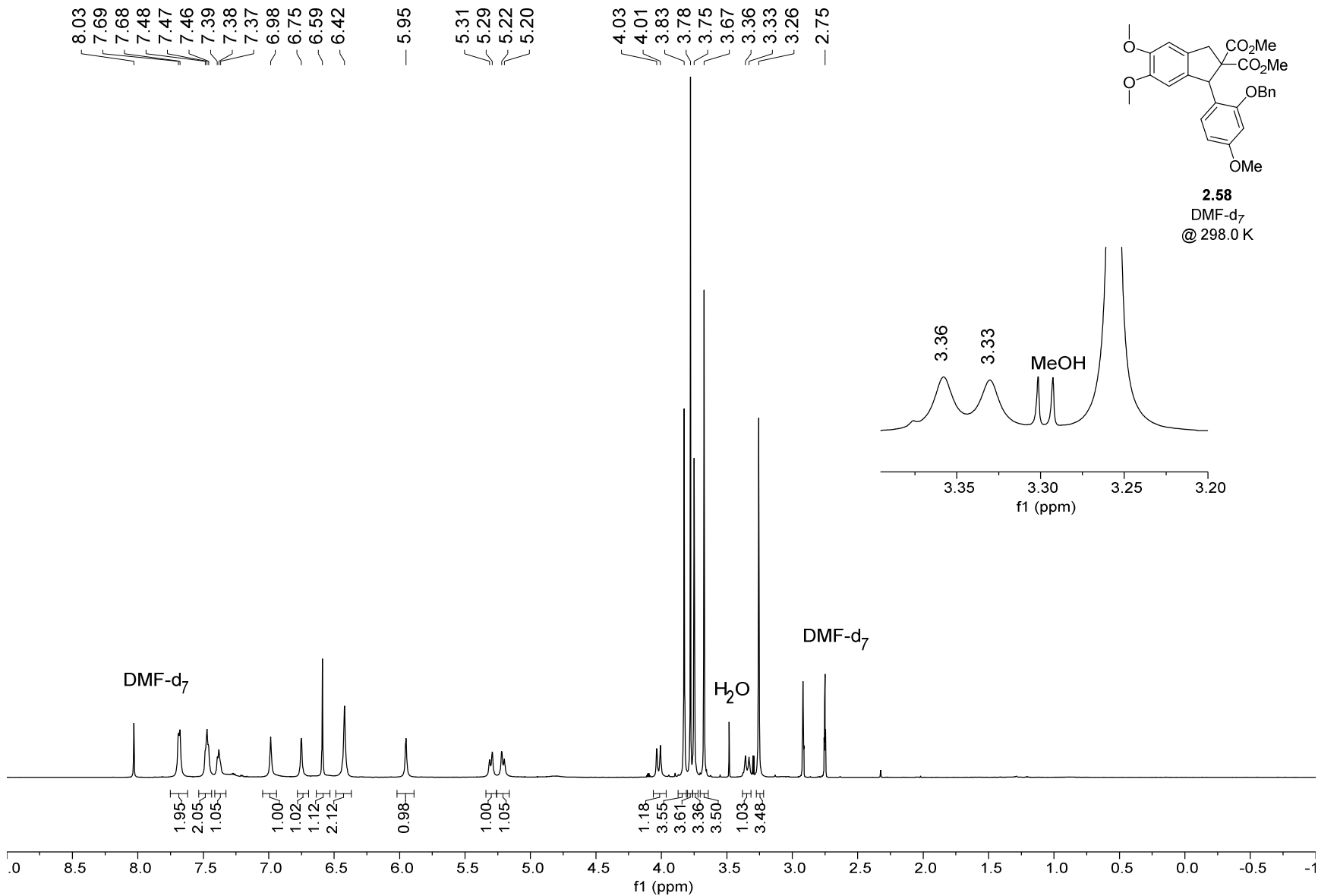
247



$^1\text{H}$  NMR and 1D NOE Experiment of **2.58** (600 MHz,  $\text{CDCl}_3$ , 274.0 K)



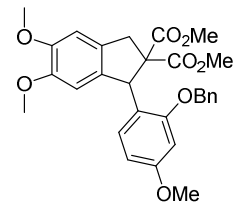
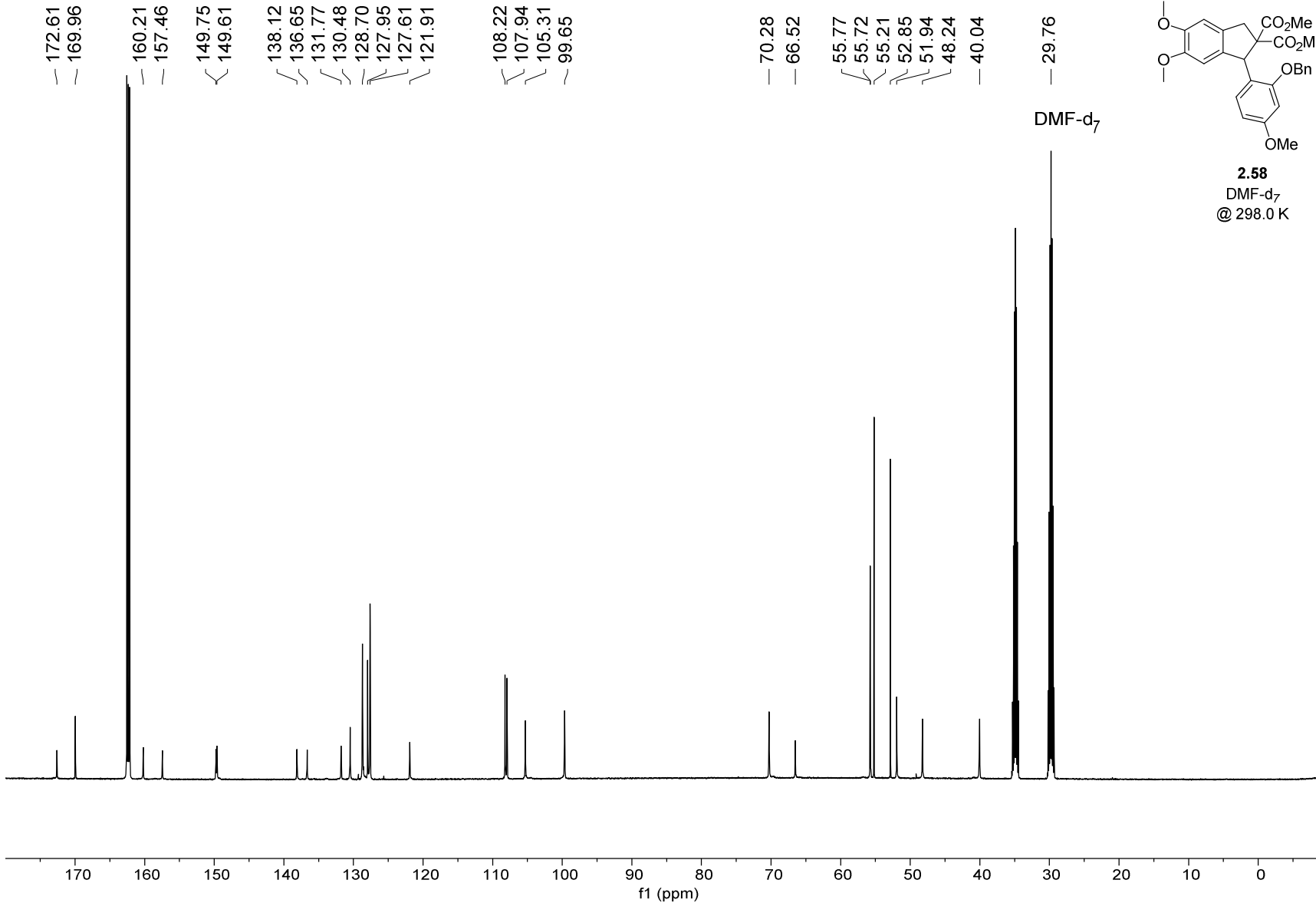
1H NMR — 600 MHz — DMF — 298.0 K





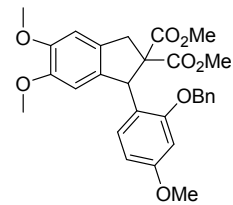
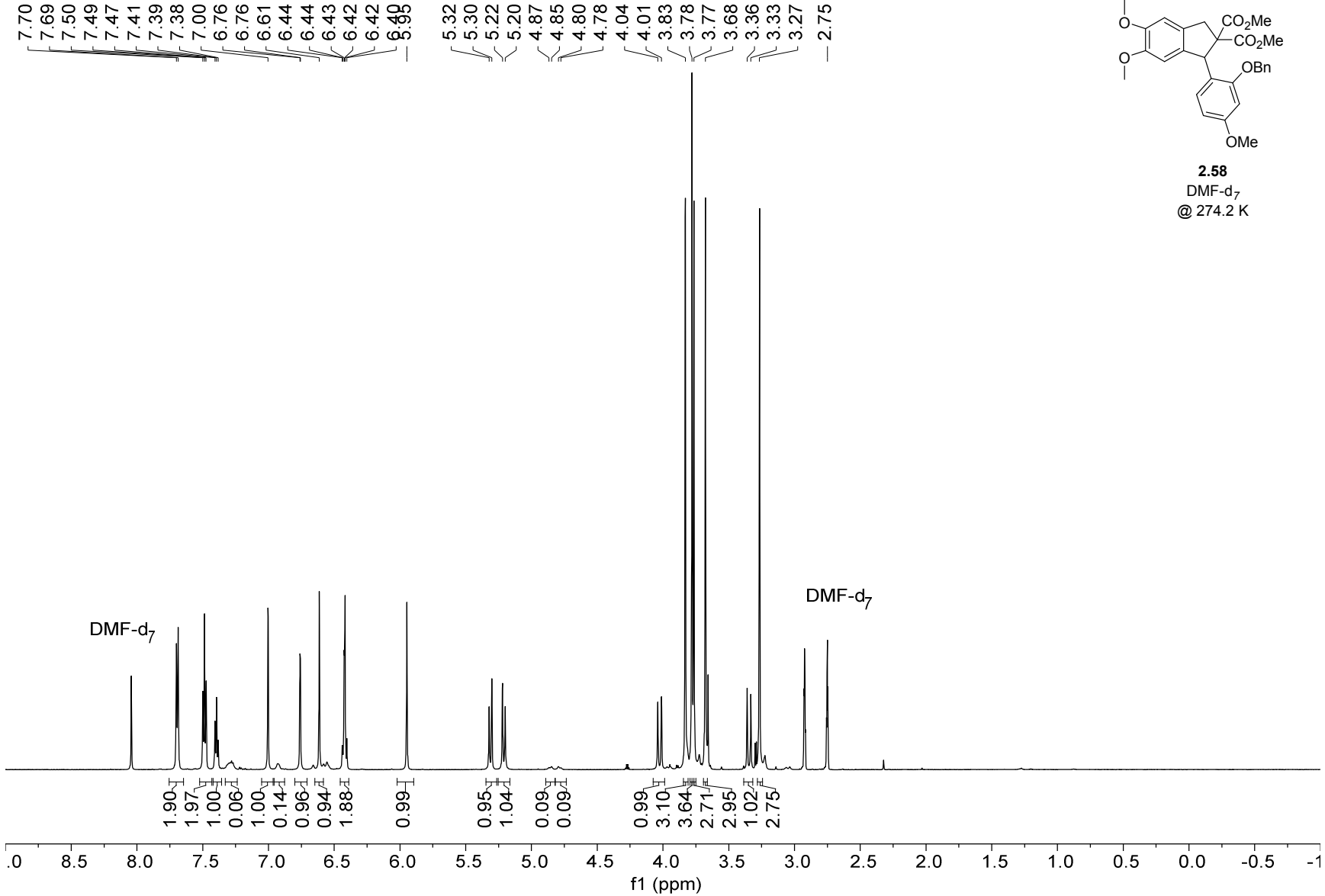
250

13C NMR — 151 MHz — DMF — 298.0 K



**2.58**  
DMF-d<sub>7</sub>  
@ 298.0 K

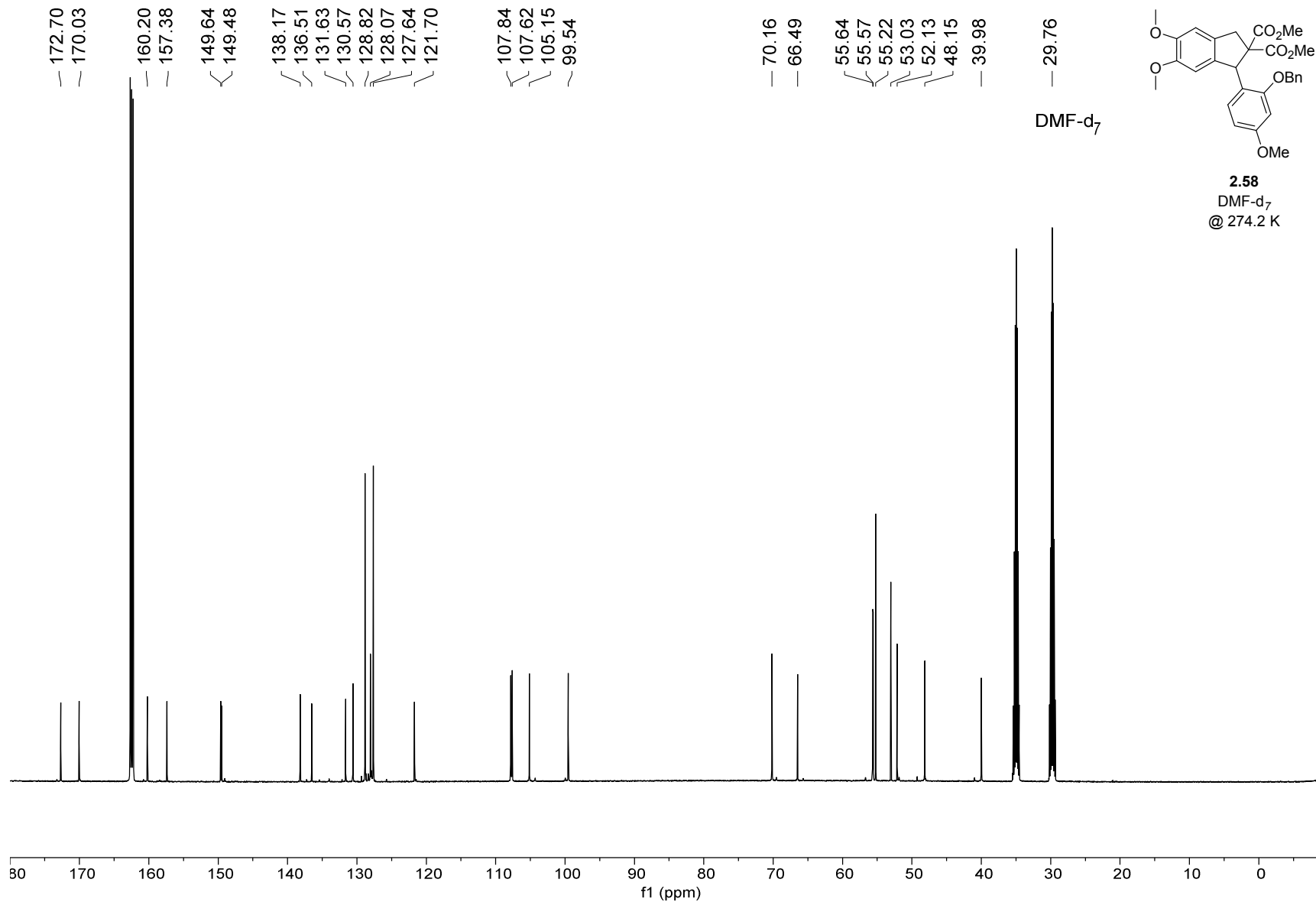
1H NMR — 600 MHz — DMF — 274.2 K



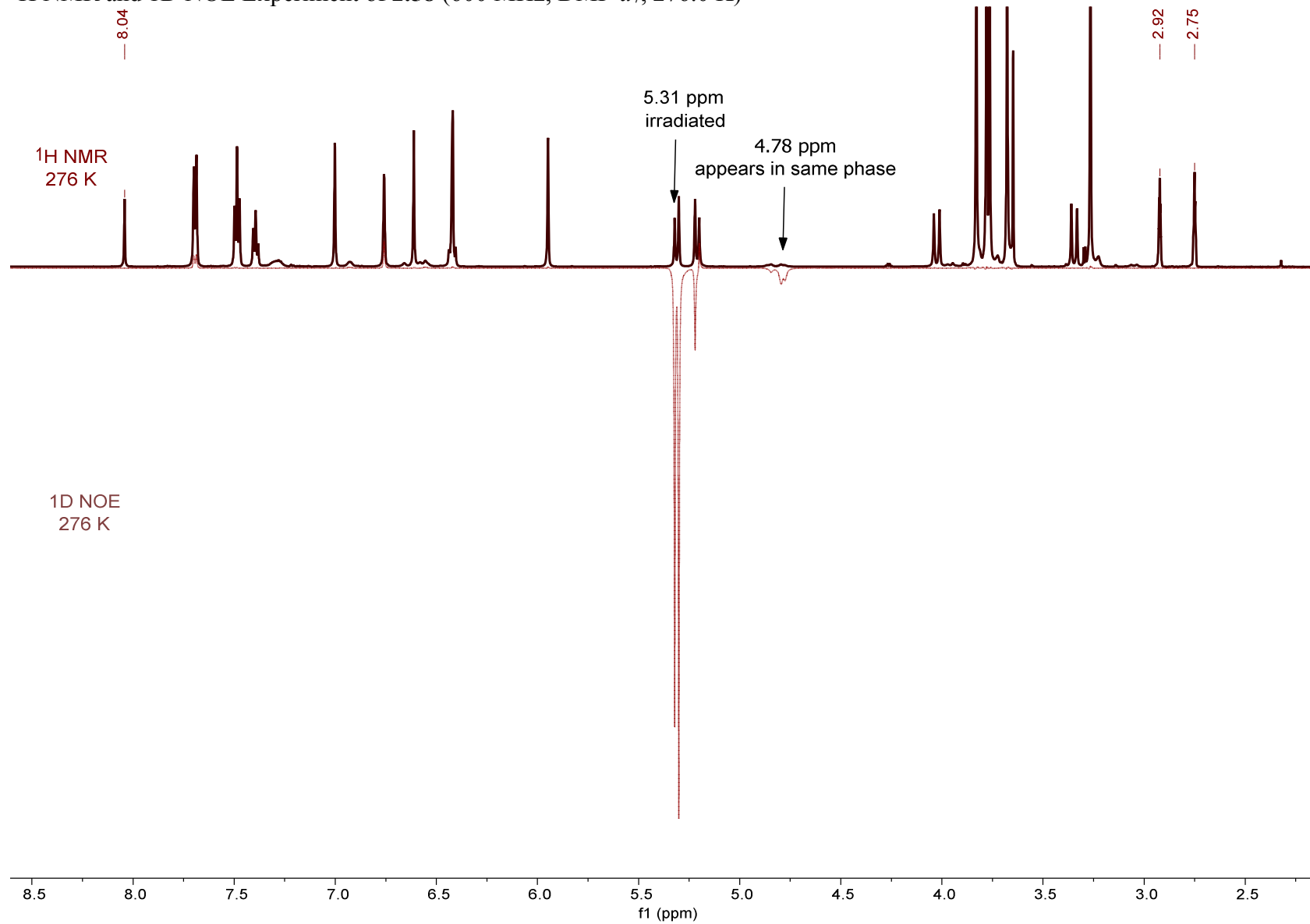
**2.58**  
DMF-d<sub>7</sub>  
@ 274.2 K

252

13C NMR — 151 MHz — DMF — 274.2 K

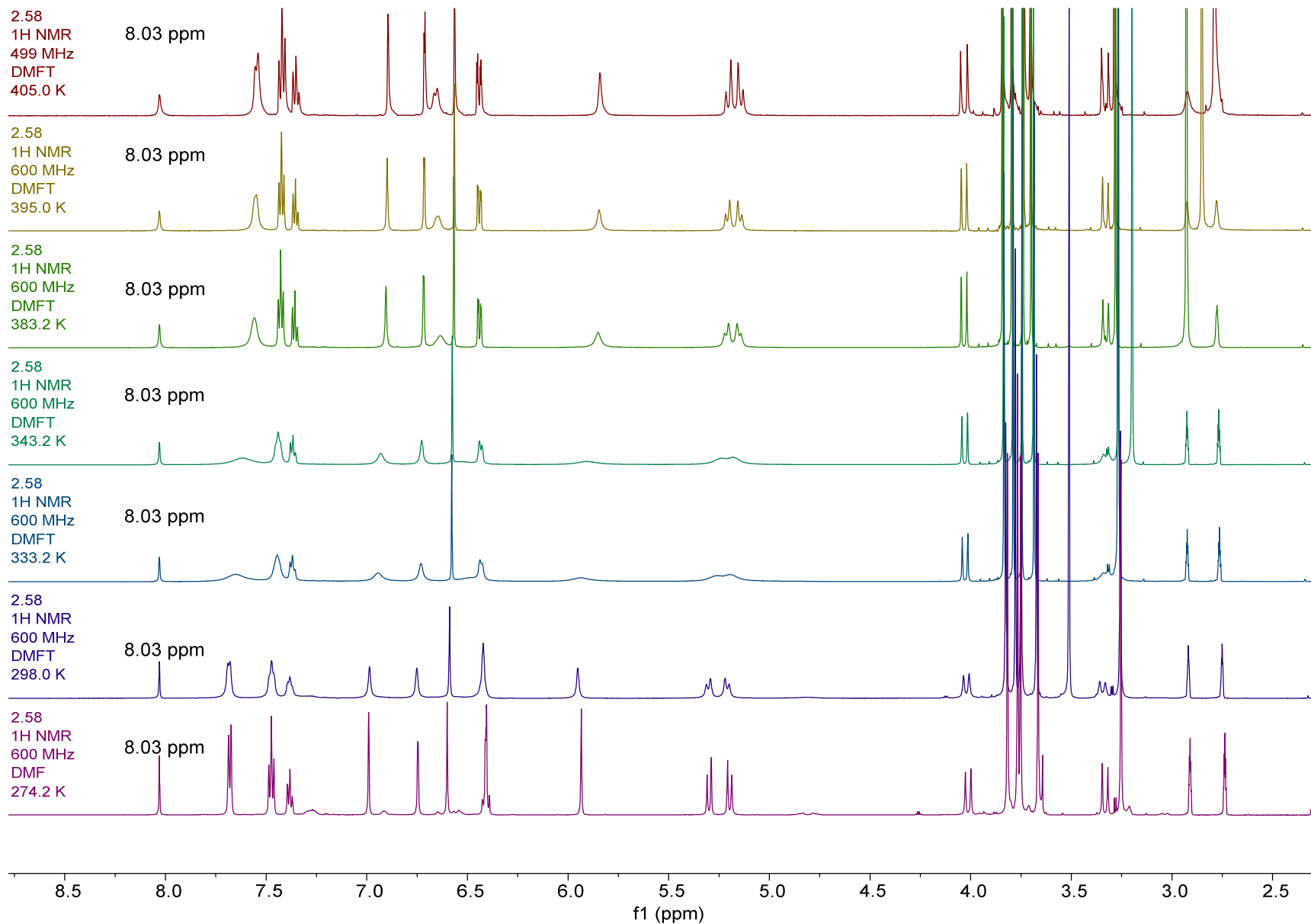


<sup>1</sup>H NMR and 1D NOE Experiment of **2.58** (600 MHz, DMF-*d*<sub>7</sub>, 276.0 K)

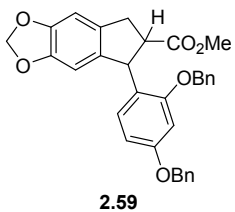


253

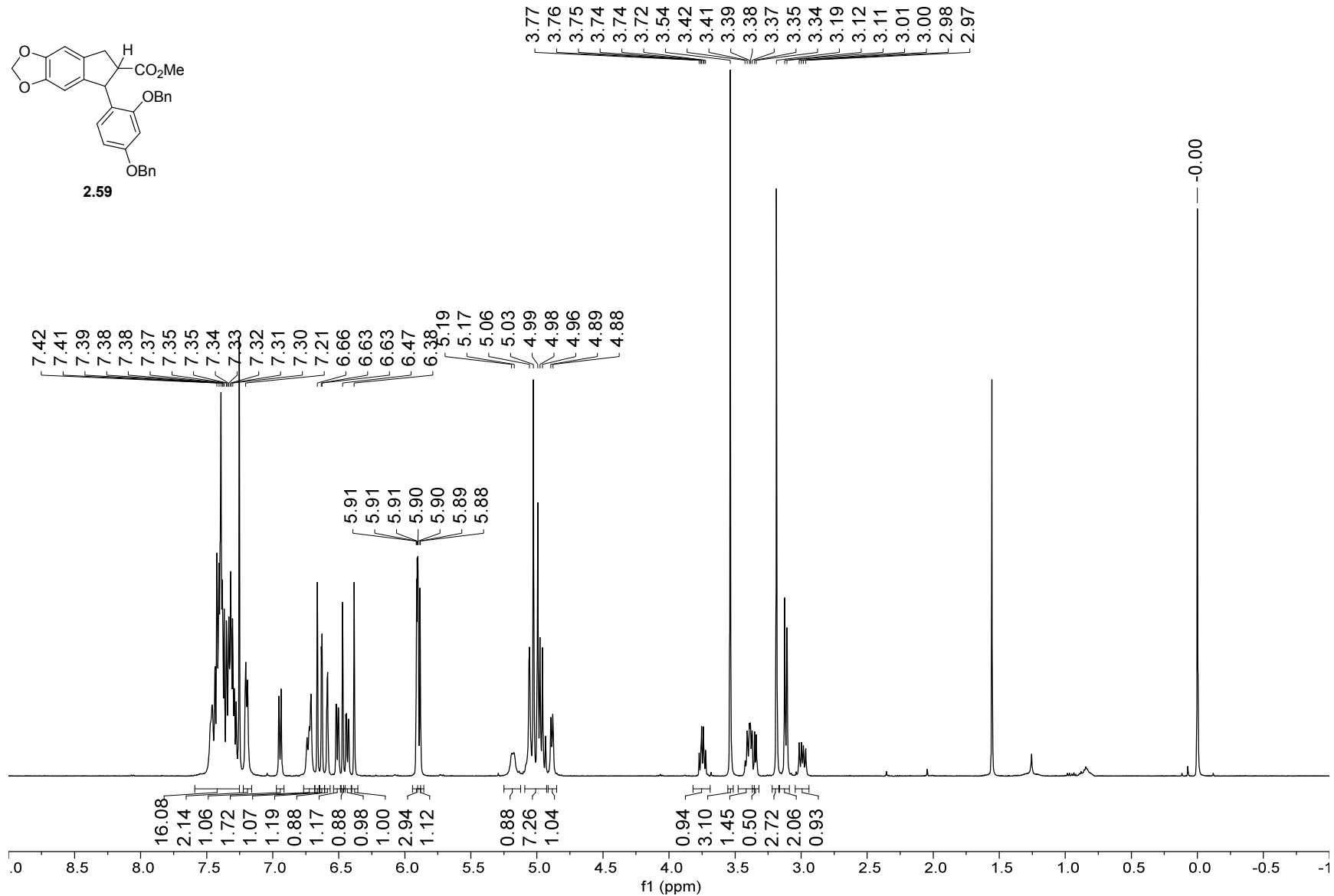
254



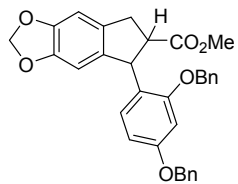
1H NMR — 500 MHz — CDCl3T — 298.0 K



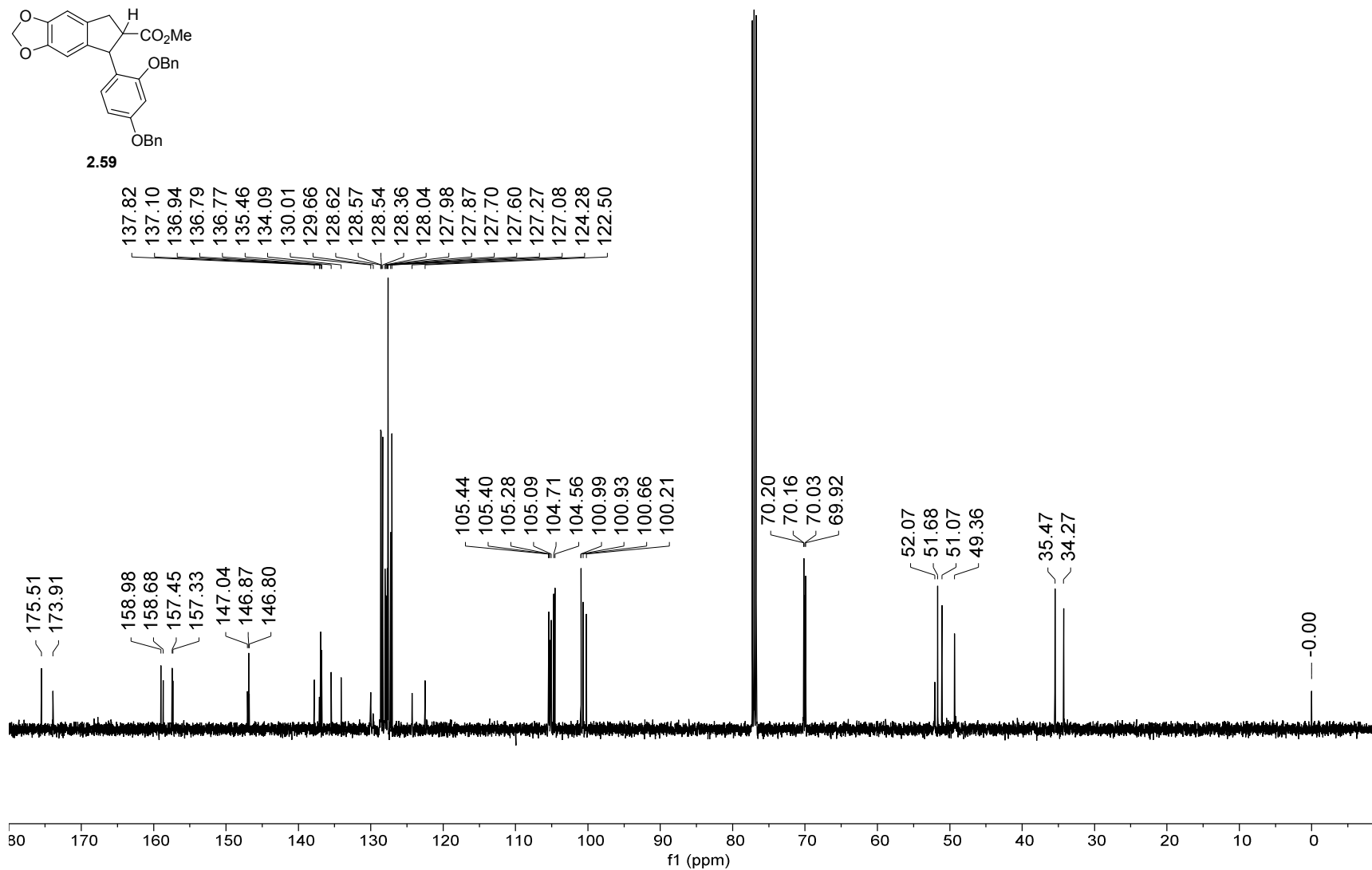
255



13C NMR — 126 MHz — CDCl3 — 298.0 K



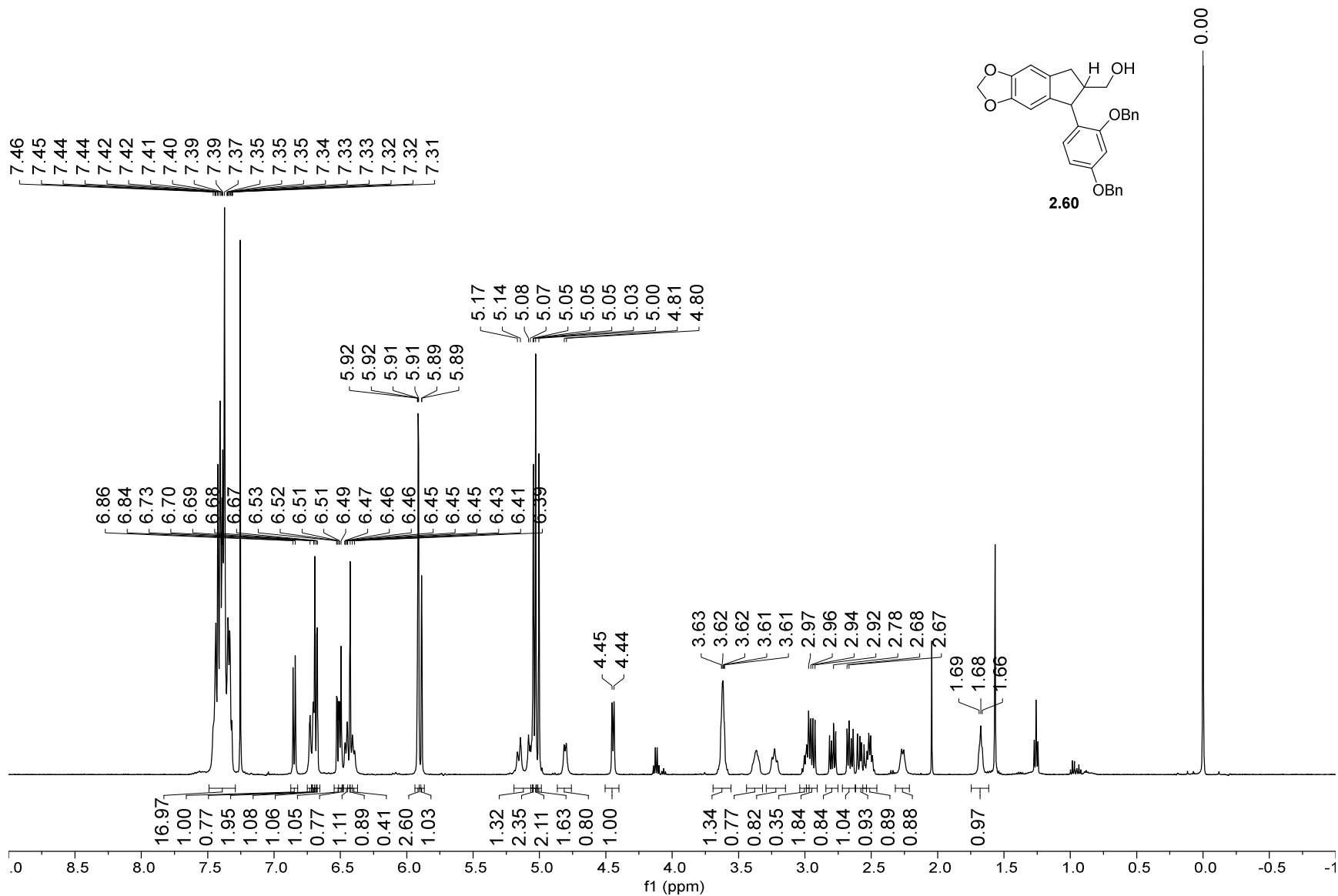
2.59



256

1H NMR — 500 MHz — CDCl3T — 298.0 K

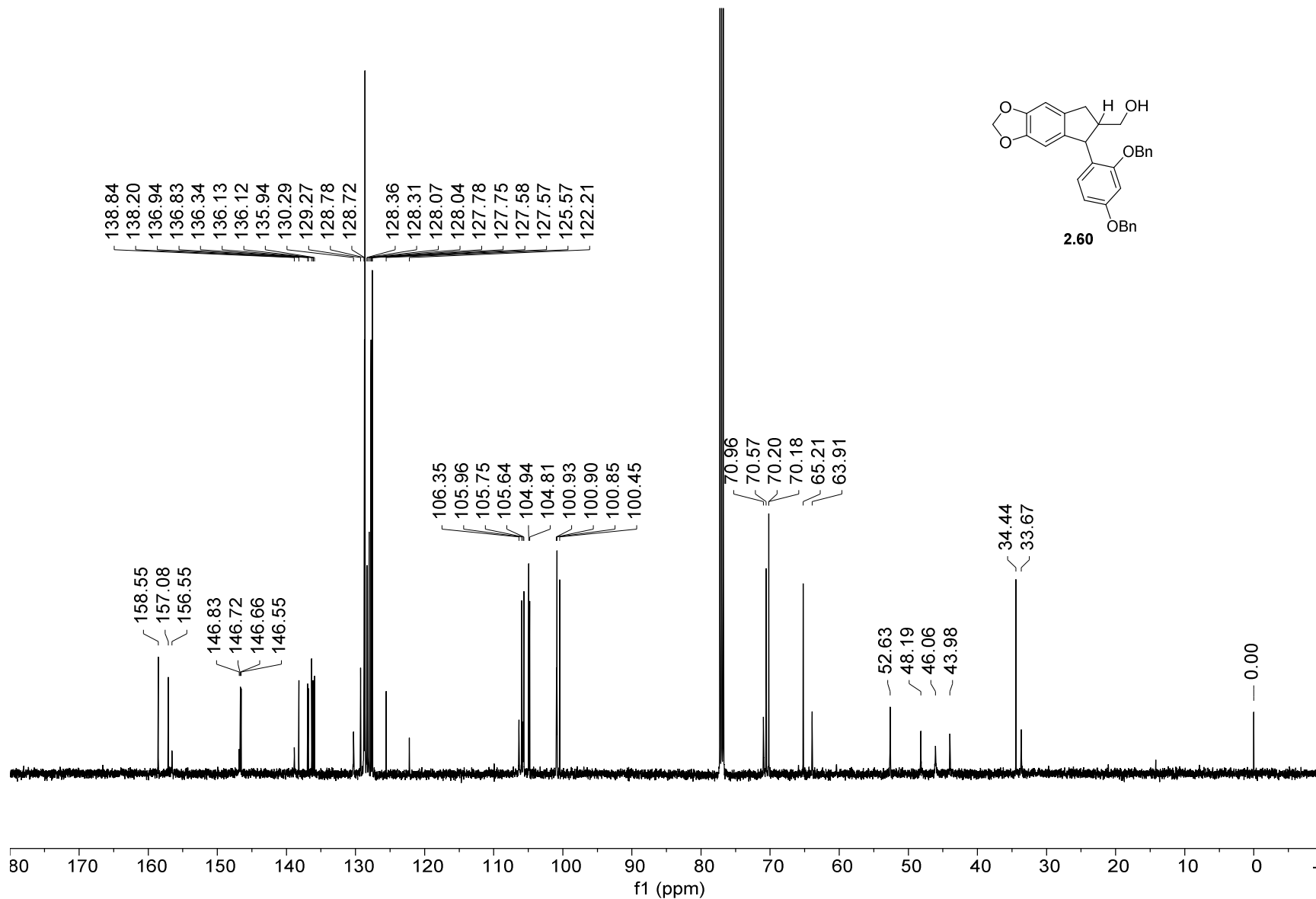
257





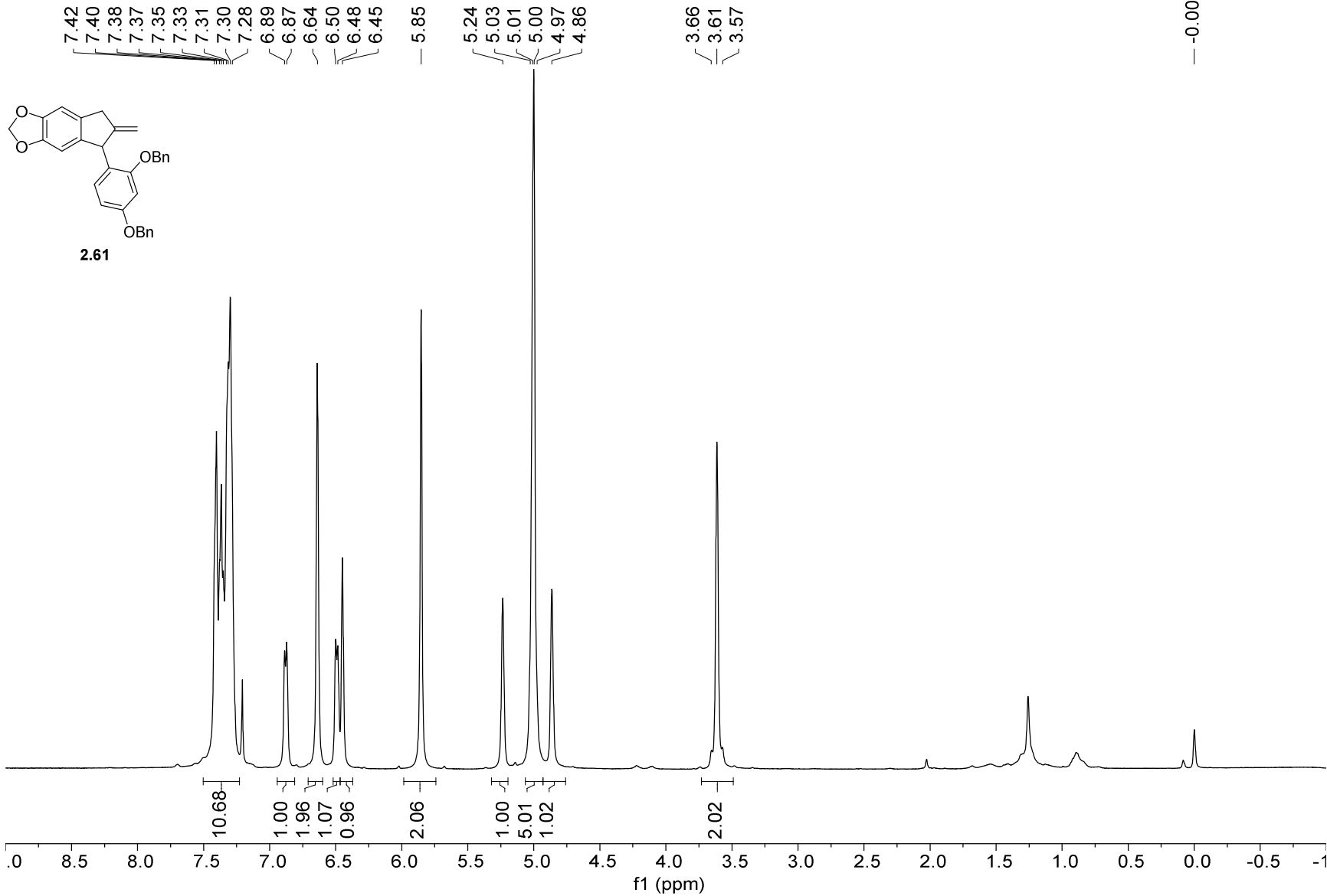
13C NMR — 126 MHz — CDCl3 — 298.0 K

258



259

1H NMR — 500 MHz — CDCl3T — 298.2 K



13C NMR — 126 MHz — CDCl3 — 298.2 K

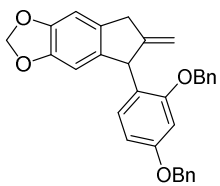
158.57  
157.22  
154.15  
146.67  
138.97  
137.05  
136.93  
134.26  
130.09  
128.58  
128.43  
127.98  
127.78  
127.58  
127.29  
126.36  
108.31  
105.75  
105.27  
104.56  
100.74  
100.70

70.19  
70.15

49.48

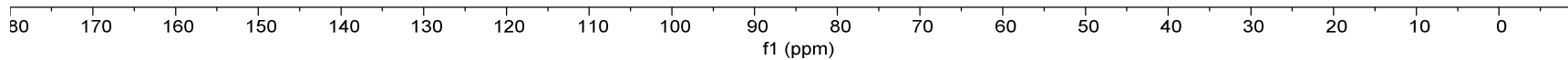
38.83

-0.00



2.61

260





13C NMR — 126 MHz — CDCl3 — 298.0 K

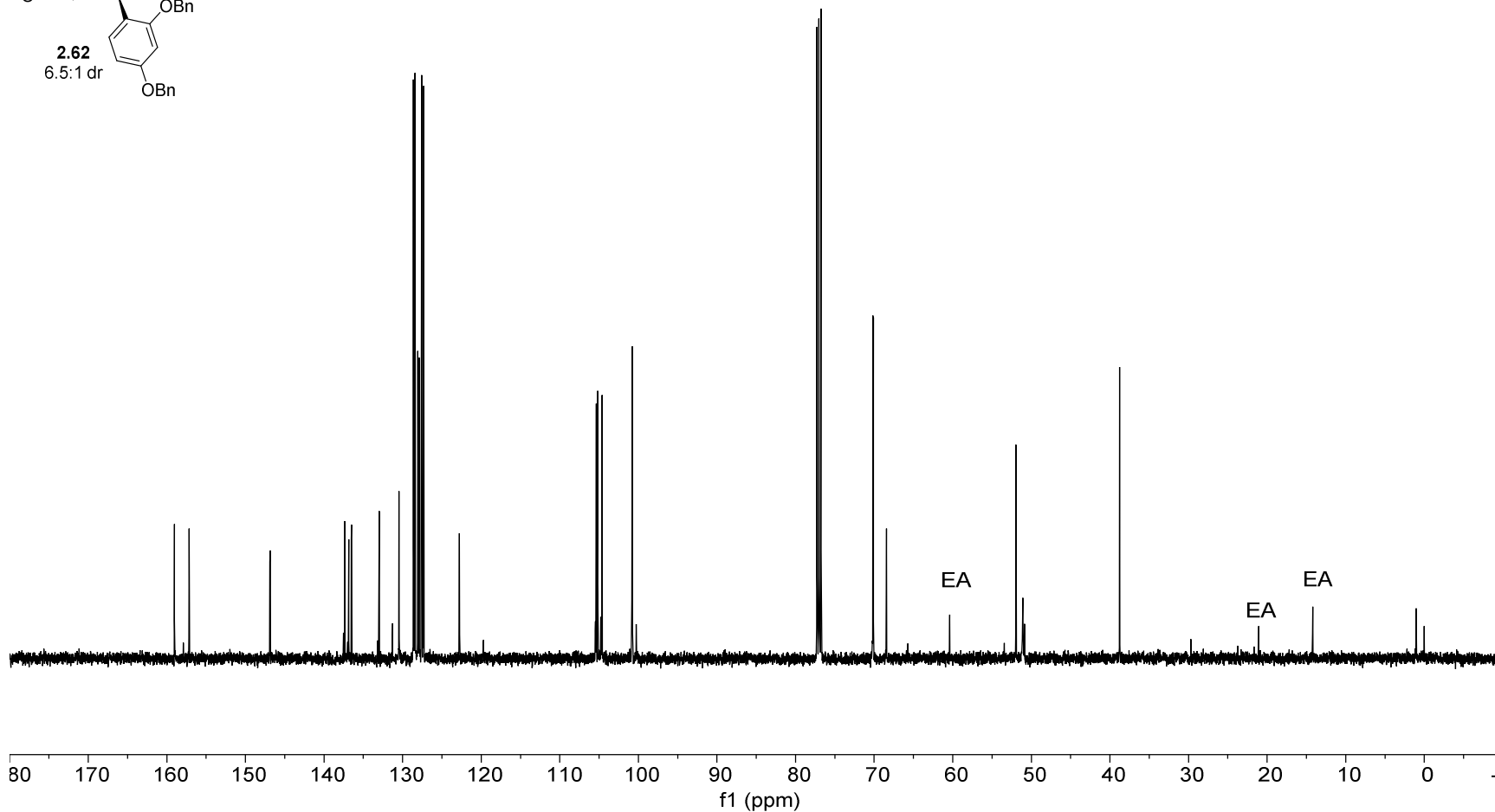
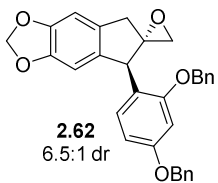
159.04  
157.18  
146.90  
146.85  
137.37  
136.86  
136.51  
132.98  
130.46  
128.62  
128.43  
128.06  
127.89  
127.59  
127.34  
122.77  
105.37  
105.18  
104.62  
100.82  
100.78

70.16  
70.09  
68.43

51.95  
51.09

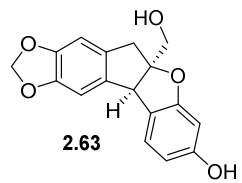
38.76

0.00

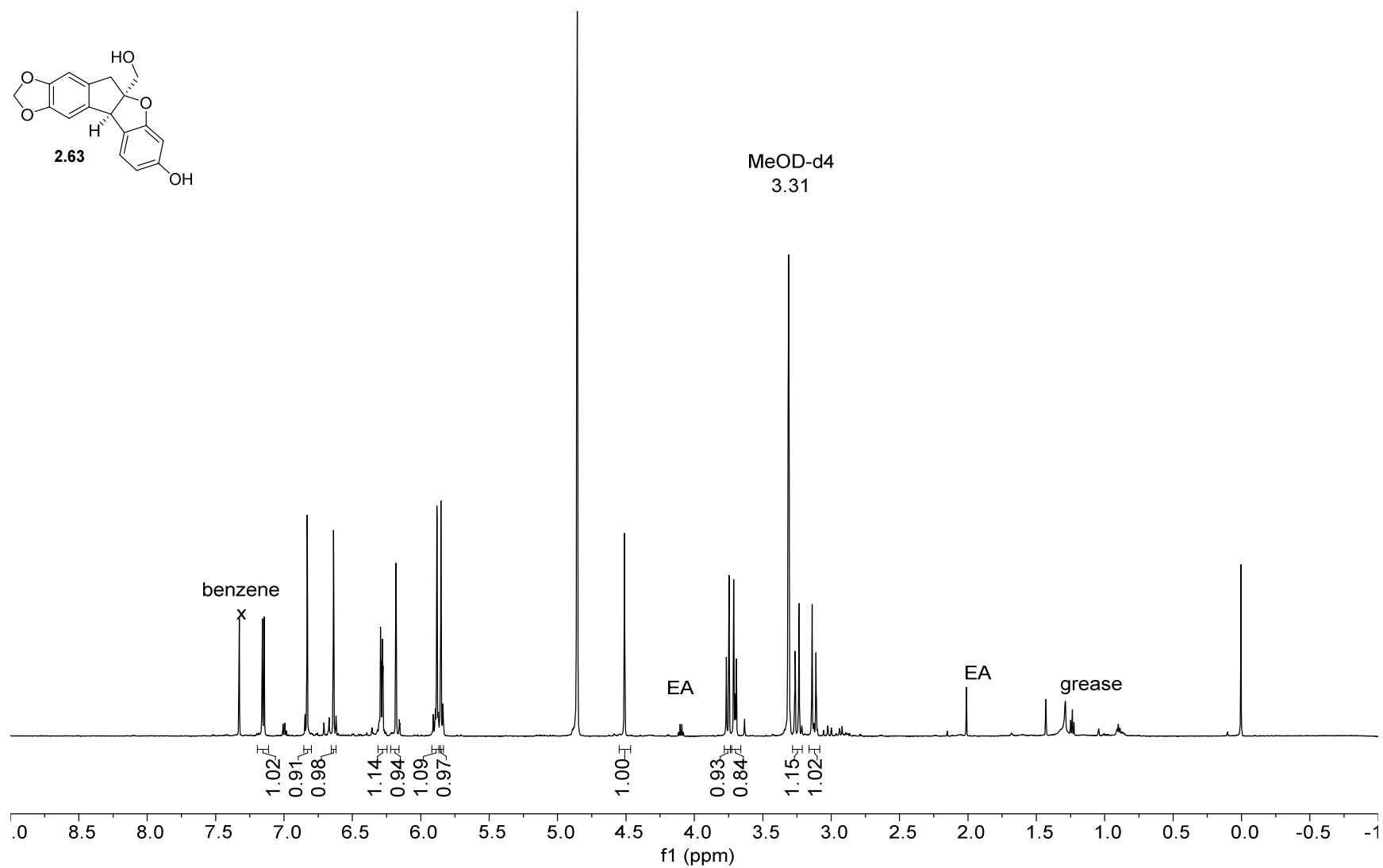


263

1H NMR — 600 MHz — CD3ODT — 298.0 K

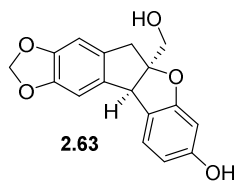


7.33 7.33 7.16 7.14 6.83 6.64 6.29 6.29 6.28 6.28 6.18 6.18 5.88 5.88 5.85 5.85  
4.51 3.77 3.75 3.71 3.69 3.31 3.26 3.23 3.14 3.11

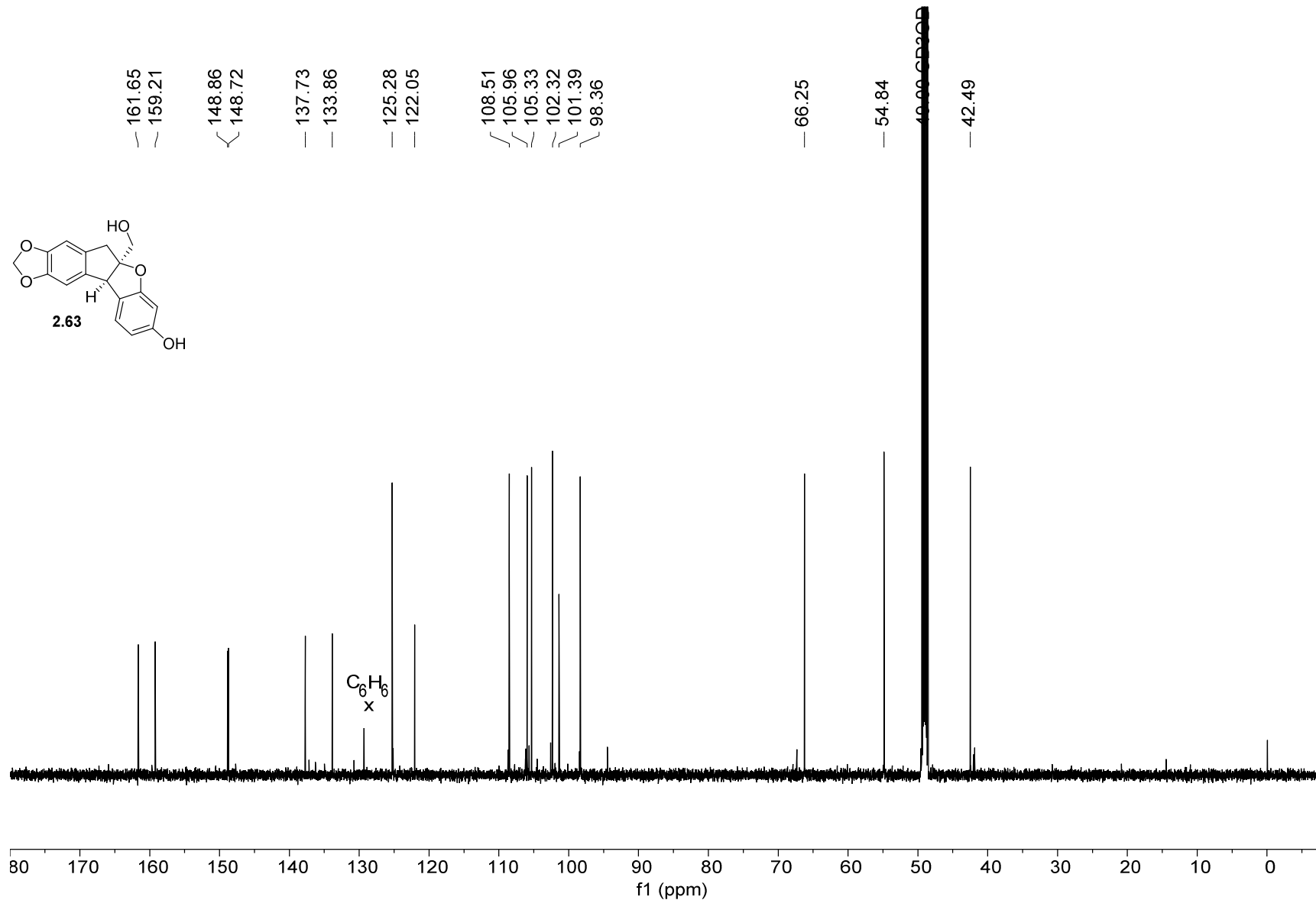


13C NMR — 151 MHz — CD3ODT — 298.0 K

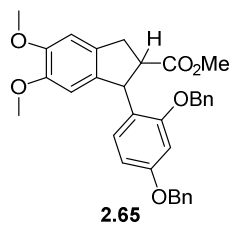
161.65  
159.21  
148.86  
148.72  
137.73  
133.86  
125.28  
122.05  
108.51  
105.96  
105.33  
102.32  
101.39  
98.36  
66.25  
54.84  
42.49



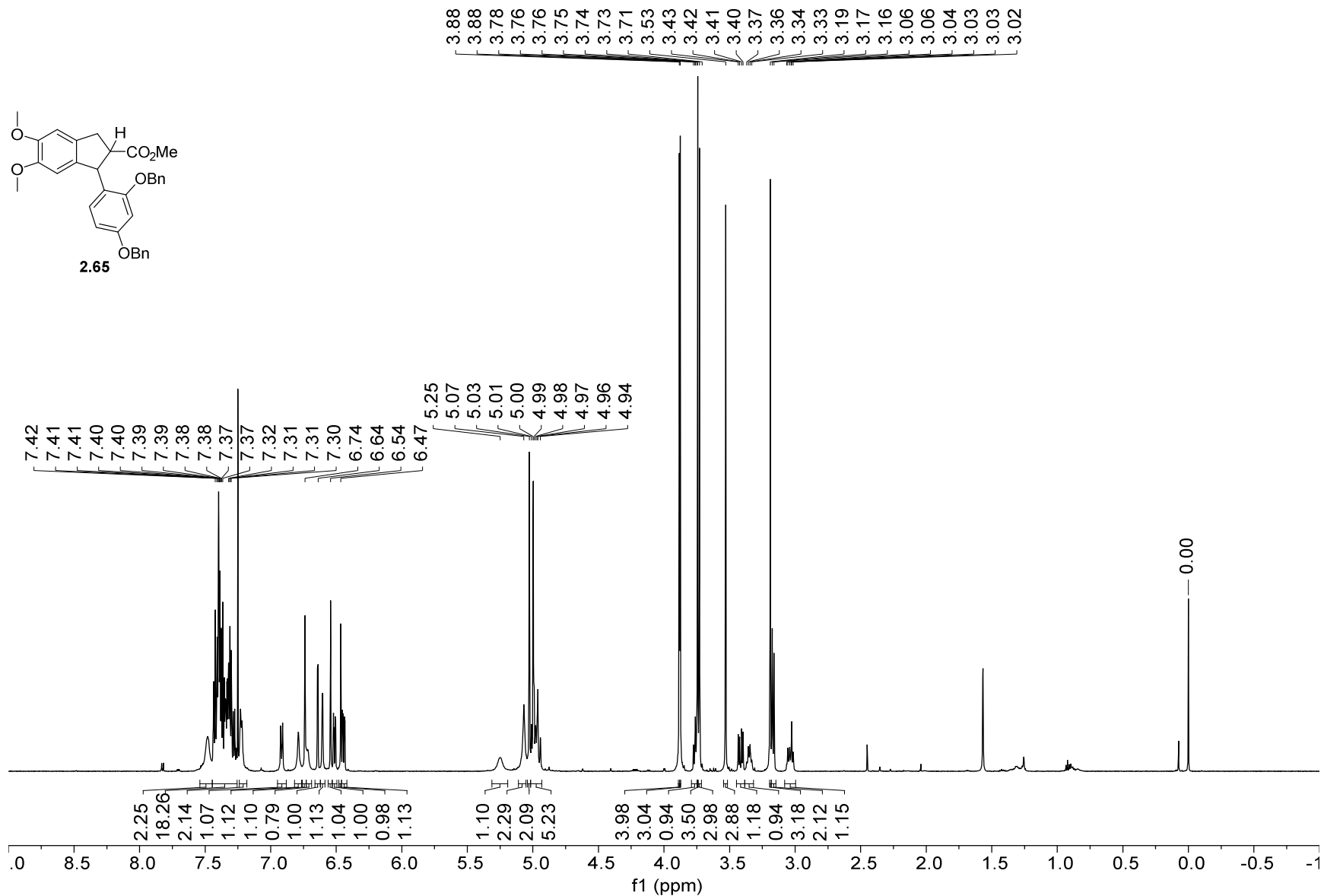
264



1H NMR — 600 MHz — CDCl3T — 298.0 K

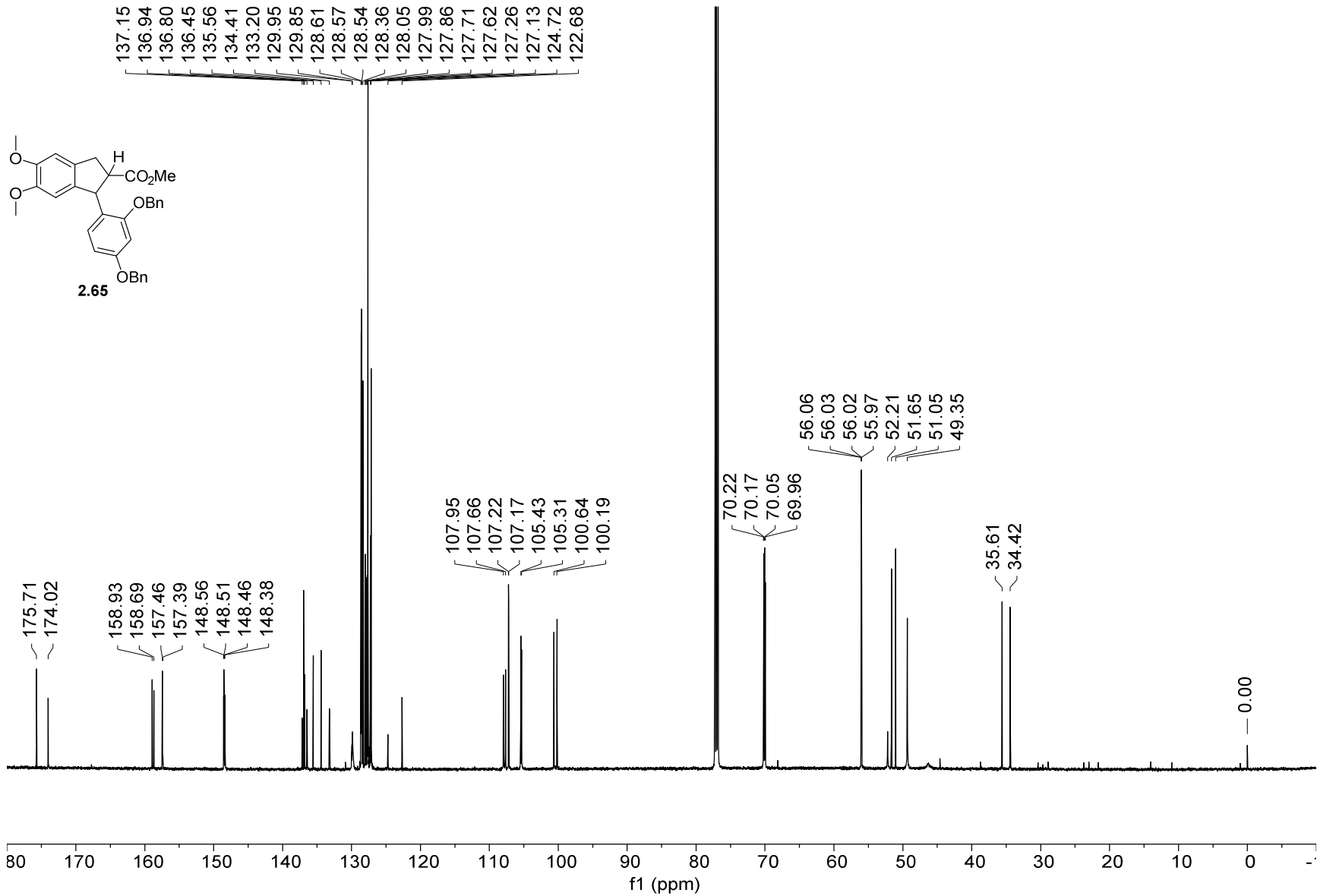


265

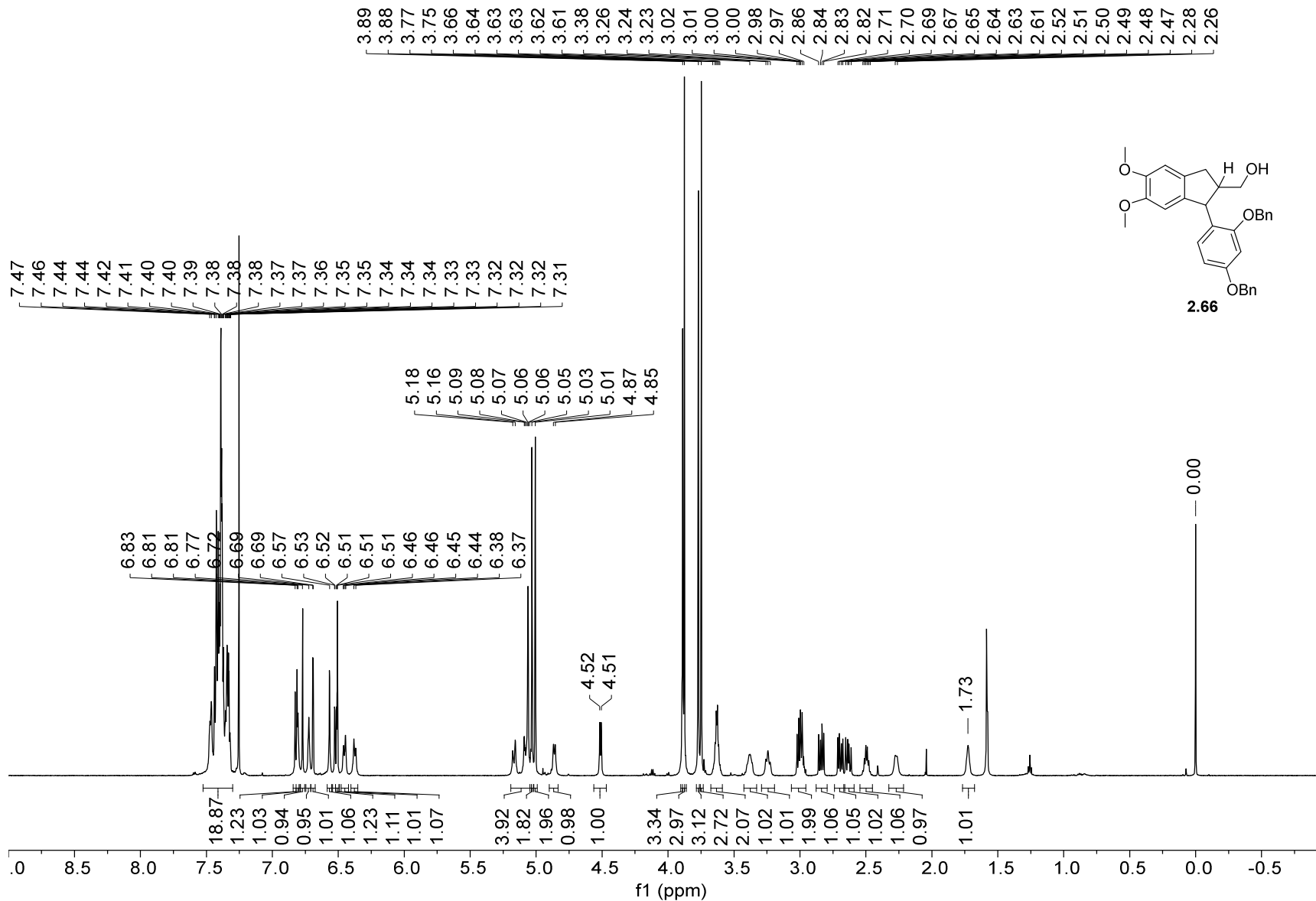




<sup>13</sup>C NMR — 151 MHz — CDCl<sub>3</sub>T — 298.0 K

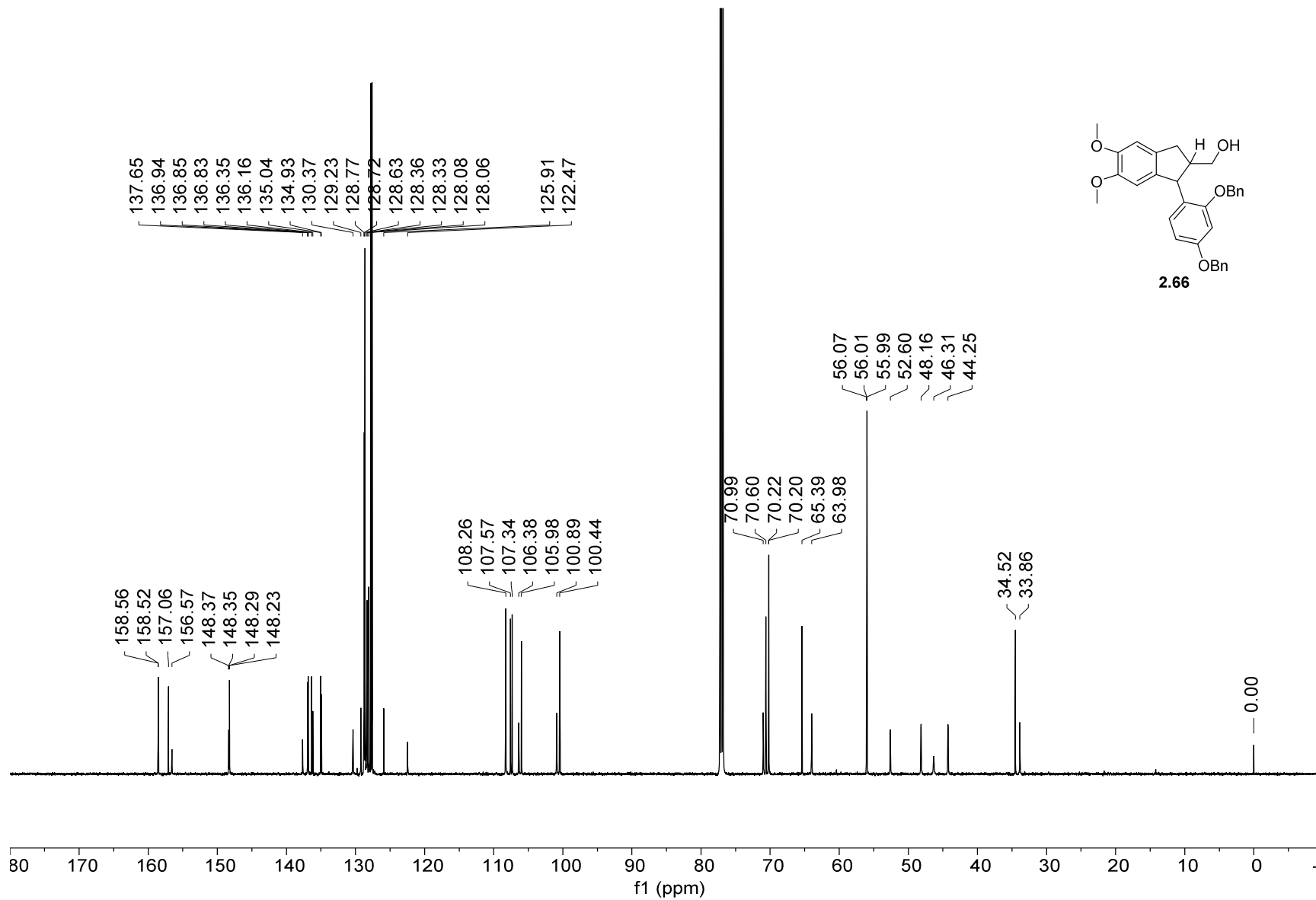


<sup>1</sup>H NMR — 600 MHz — CDCl<sub>3</sub>T — 298.0 K

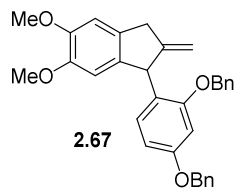


13C NMR — 151 MHz — CDCl3T — 298.0 K

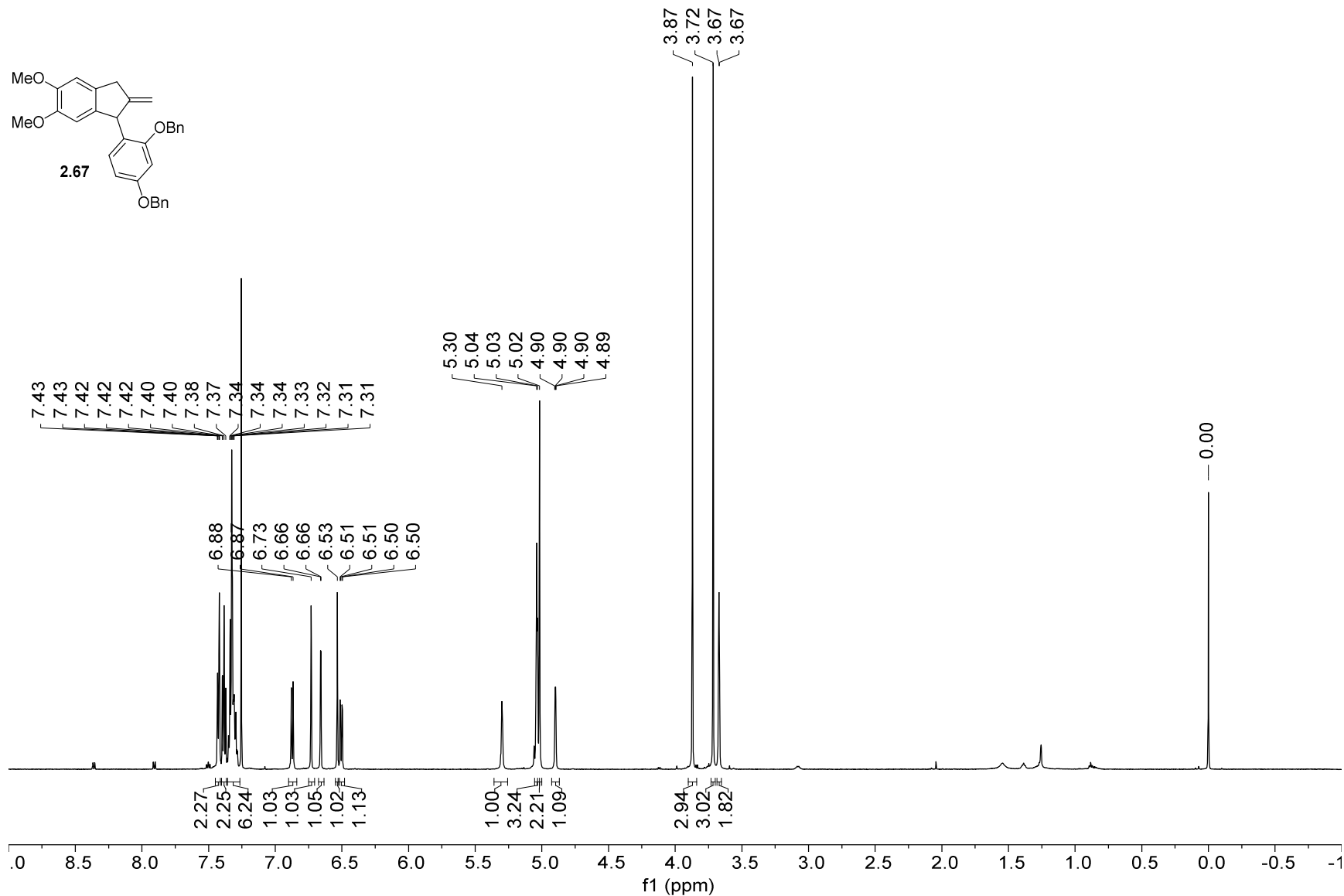
268



1H NMR — 600 MHz — CDCl3T — 298.1 K

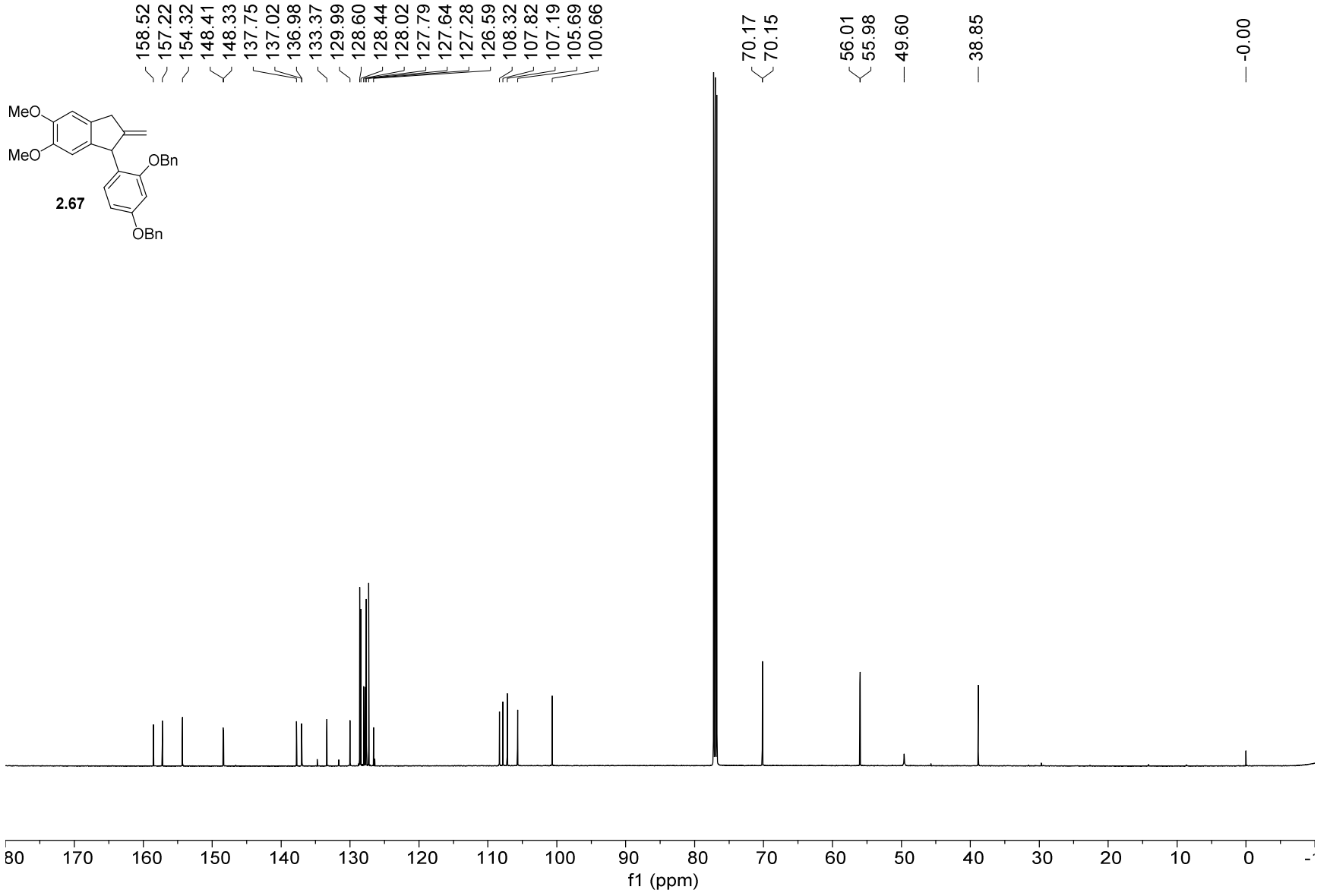


269

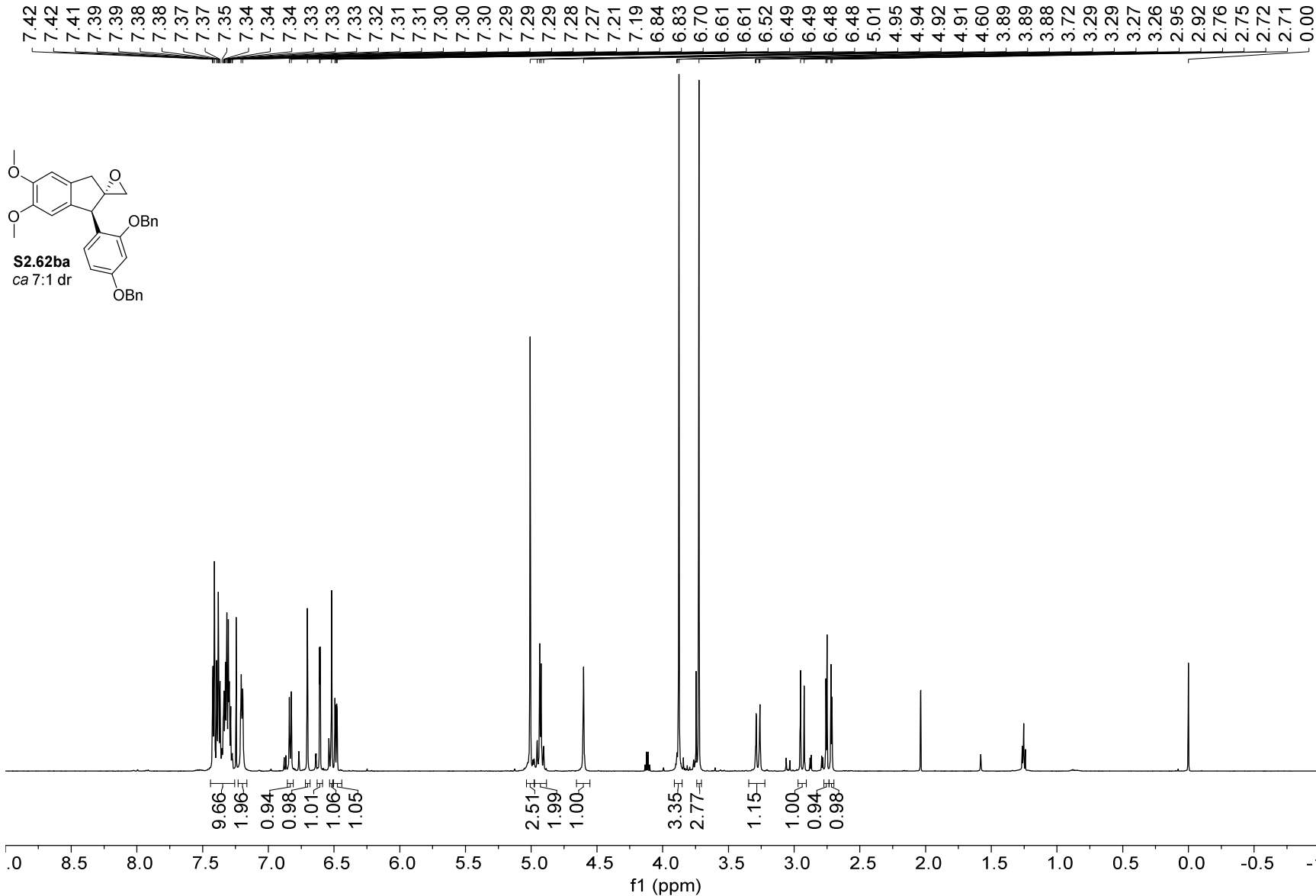


270

13C NMR — 151 MHz — CDCl3T — 298.0 K



<sup>1</sup>H NMR — 600 MHz — CDCl<sub>3</sub>T — 298.0 K



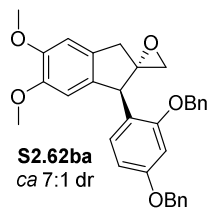
13C NMR — 151 MHz — CDCl3T — 298.0 K

158.98  
157.21  
148.59  
148.54  
136.87  
136.58  
136.28  
132.10  
130.36  
128.61  
128.41  
128.06  
127.86  
127.60  
127.33  
123.06  
107.67  
107.20  
105.44  
100.79

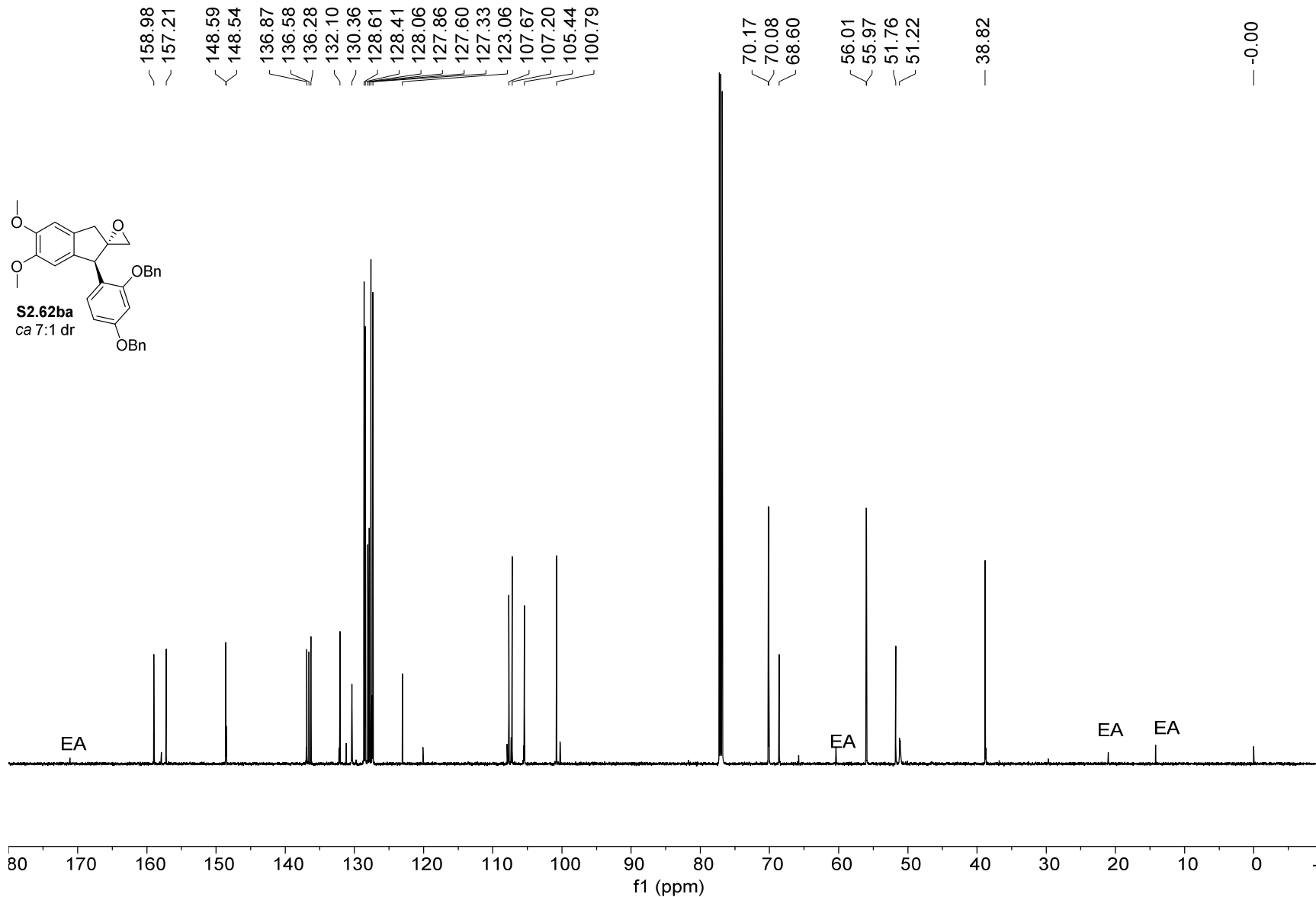
70.17  
70.08  
68.60  
56.01  
55.97  
51.76  
51.22

38.82

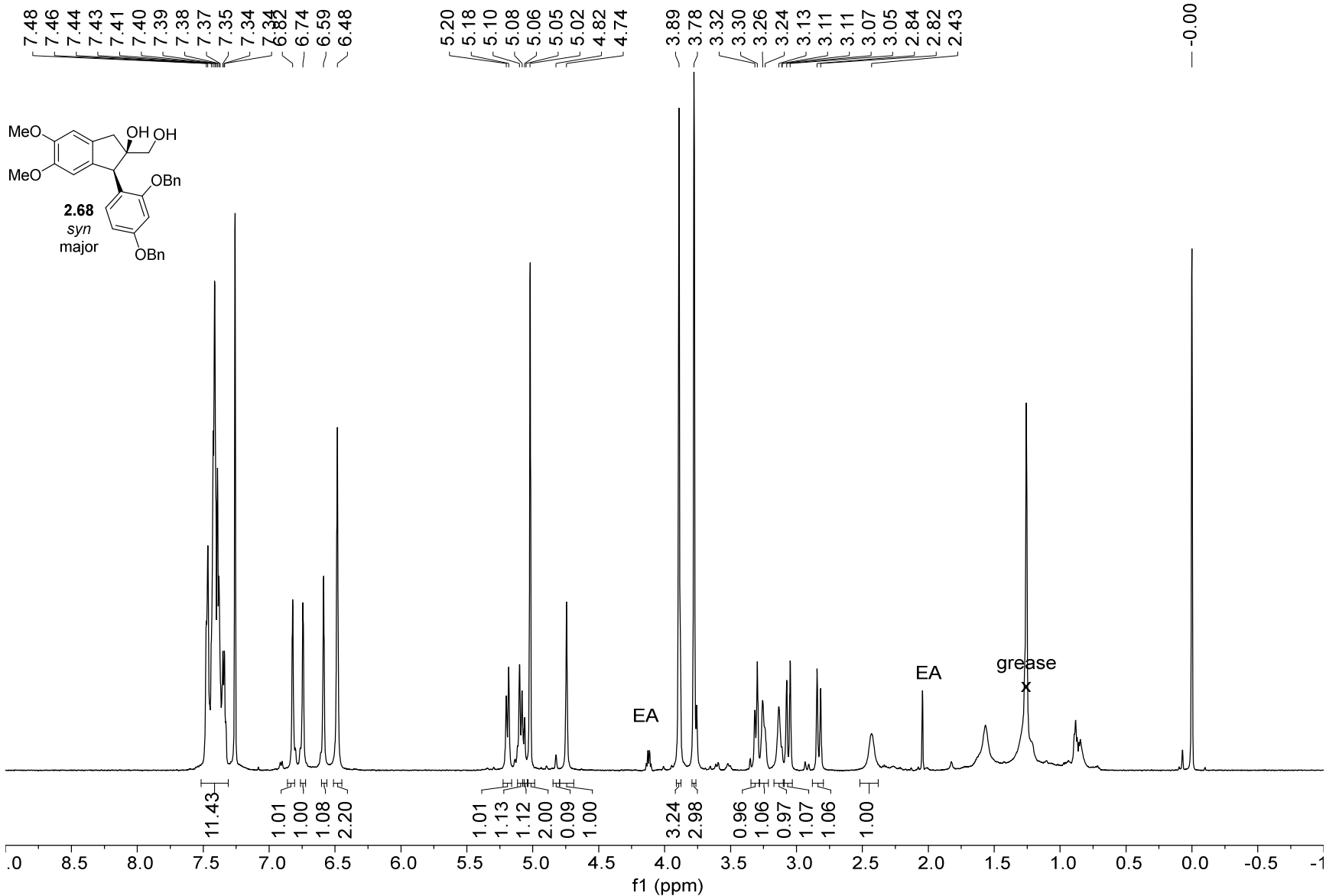
-0.00



272



1H NMR — 600 MHz — CDCl3T — 298.0 K



273



13C NMR — 151 MHz — CDCl3T — 298.0 K

158.83  
156.80  
148.73  
148.59  
136.70  
135.76  
135.39  
133.16  
129.59  
128.92  
128.67  
128.60  
128.15  
127.86  
127.63  
127.59  
121.66  
108.72  
107.90  
106.72  
101.19

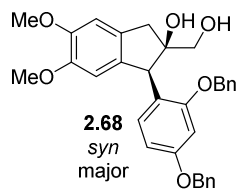
85.52

71.30  
70.28  
70.25  
66.58

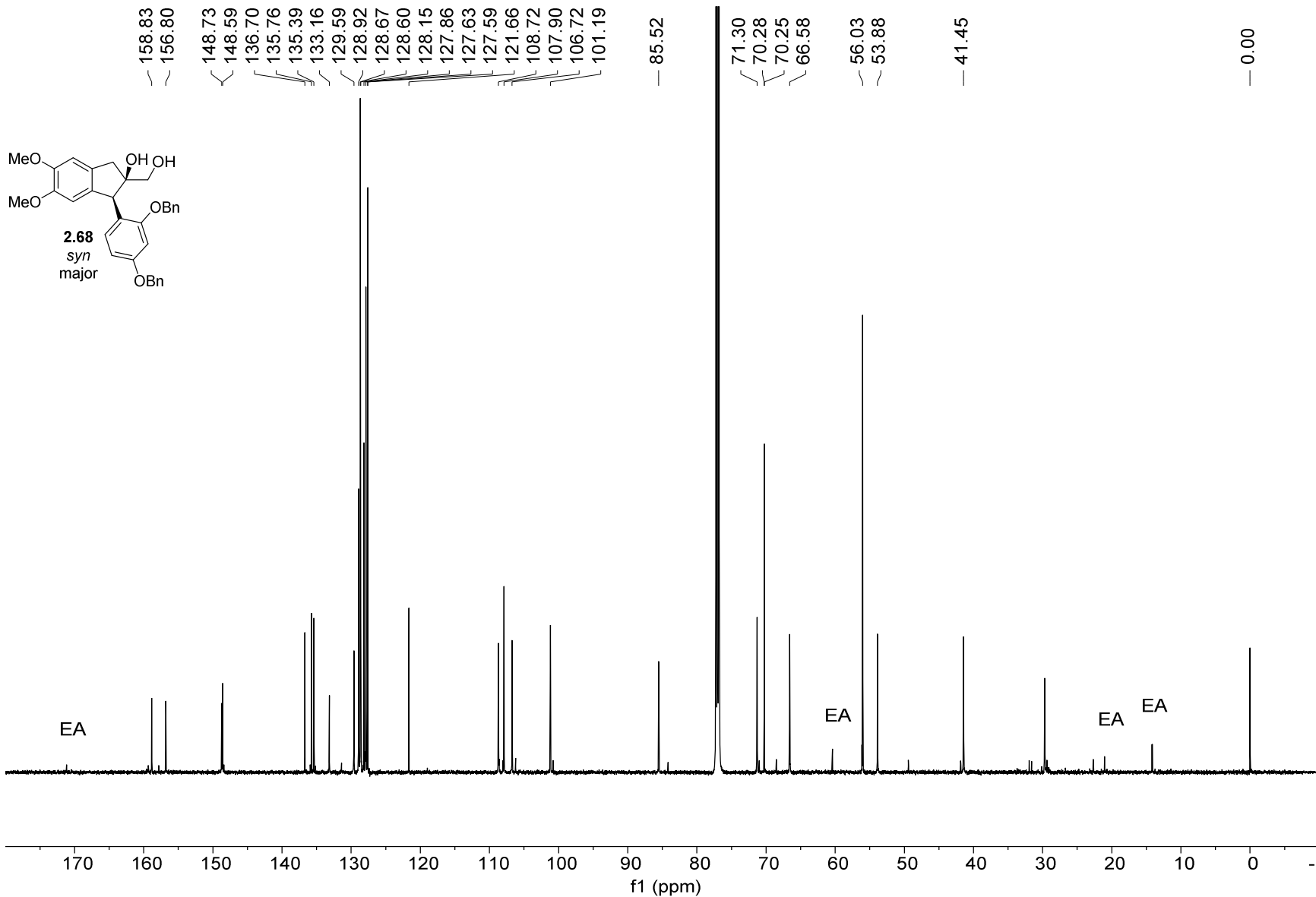
56.03  
53.88

41.45

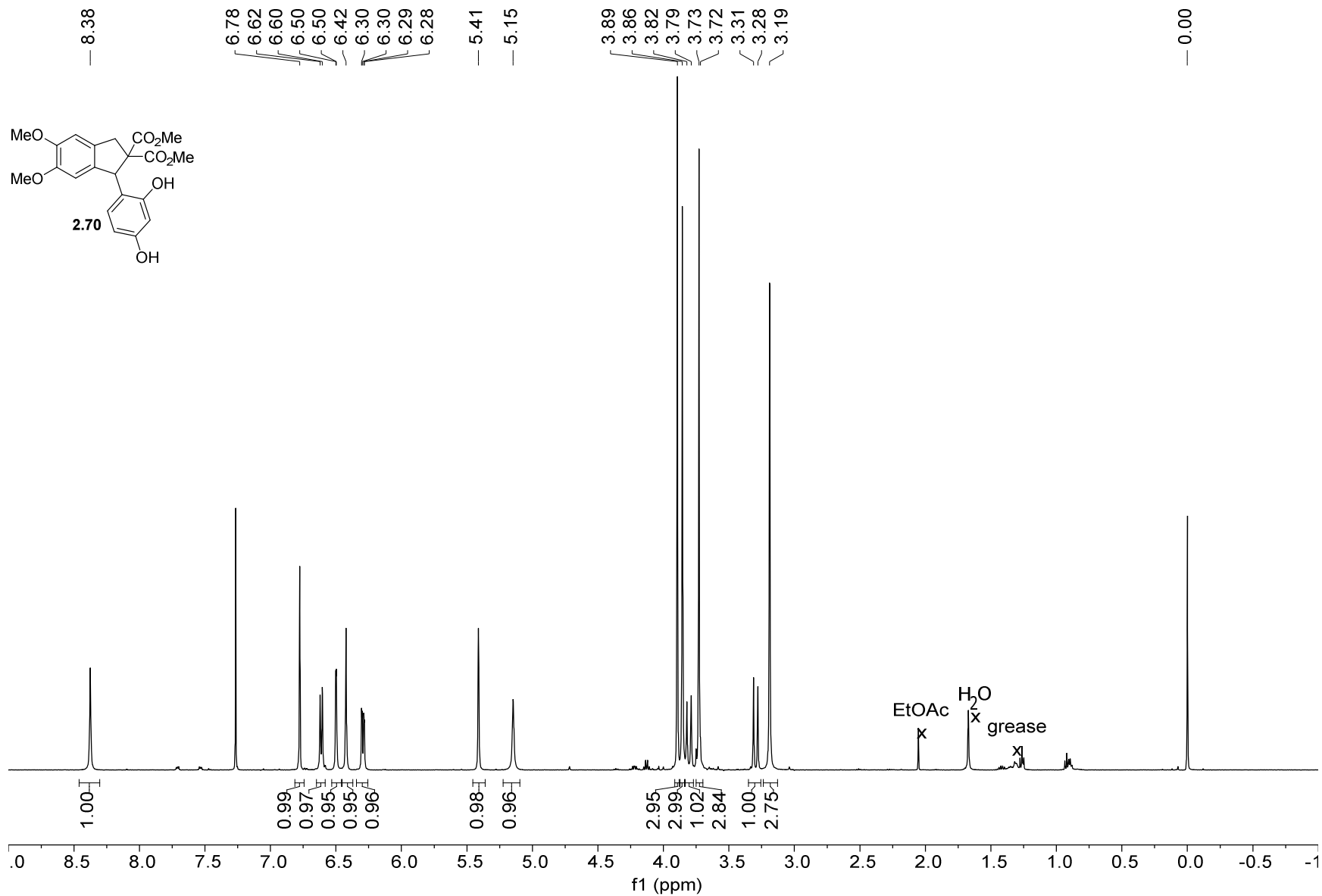
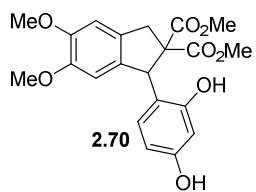
0.00



274



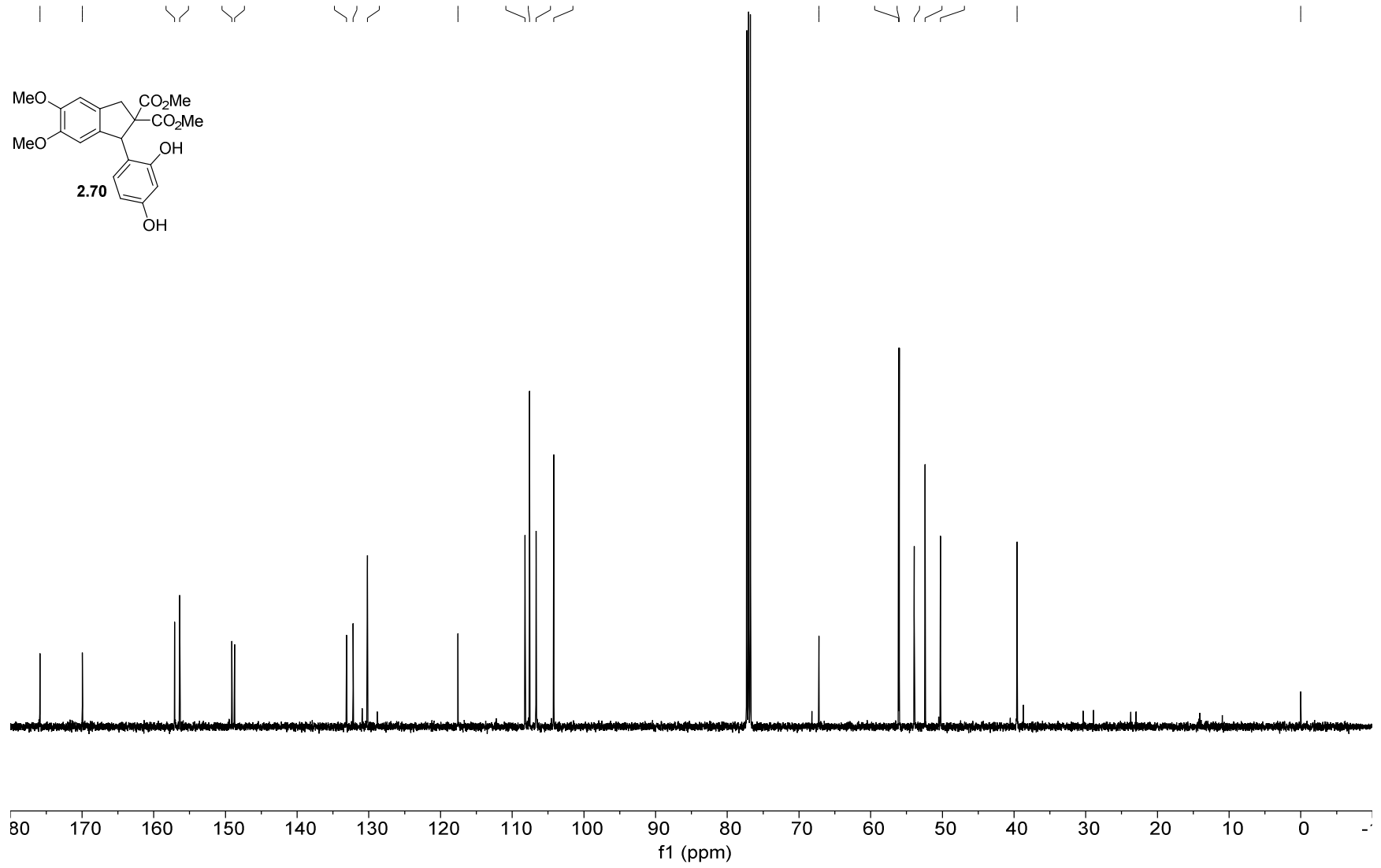
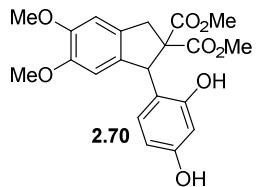
1H NMR — 500 MHz — CDCl3T — 298.0 K



275

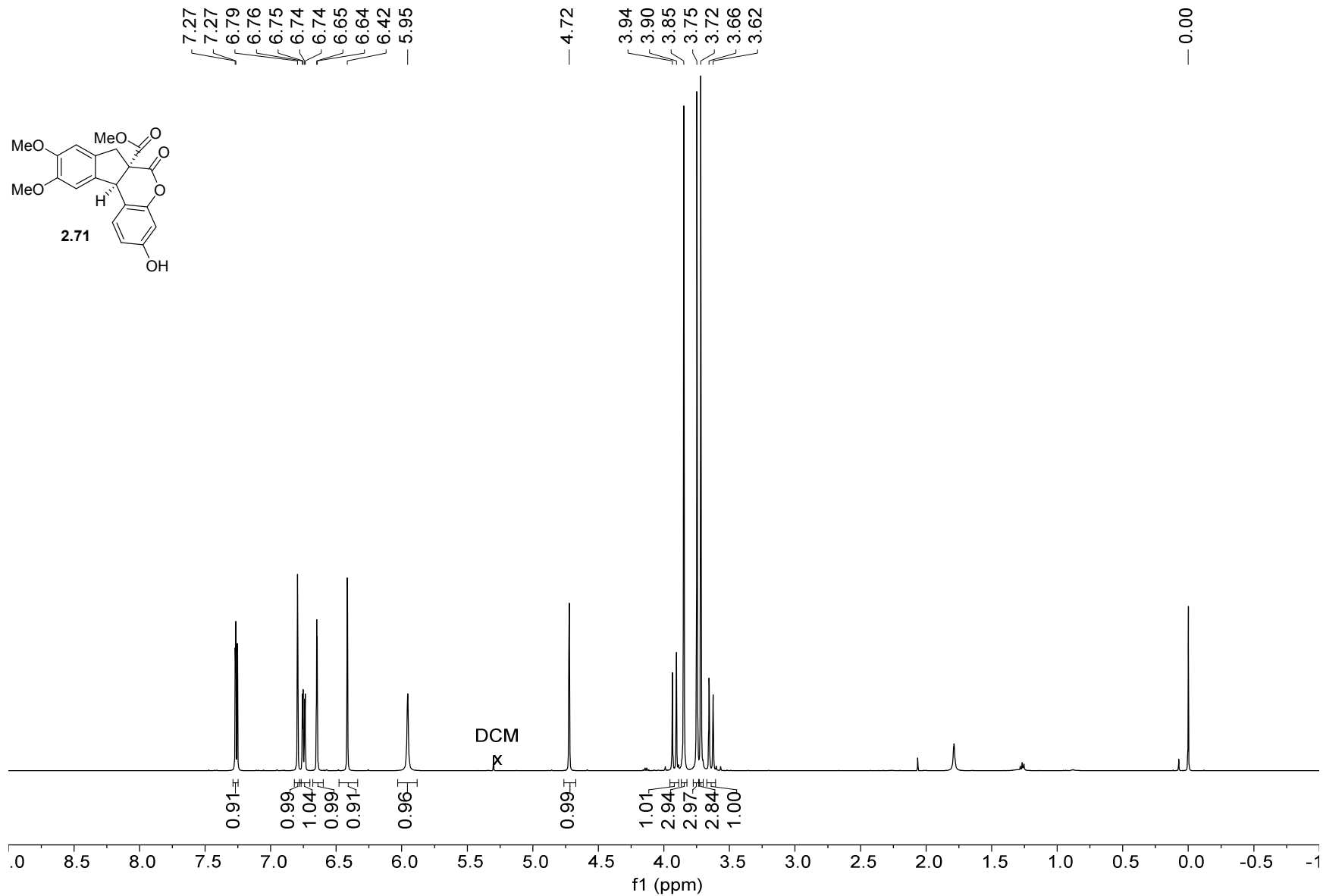
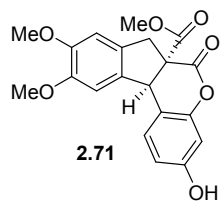
13C NMR — 126 MHz — CDCl3 — 298.0 K

— 175.86 — 169.95 — 157.08 — 156.37 — 149.10 — 148.73 — 133.12 — 132.19 — 130.20 — 117.56 — 108.20 — 107.60 — 106.65 — 104.21 — 67.22 — 56.09 — 56.01 — 53.92 — 52.42 — 50.27 — 39.58 — 0.00



277

1H NMR — 500 MHz — CDCl3T — 298.0 K



13C NMR — 126 MHz — CDCl3 — 298.0 K

169.85  
167.43

156.67  
151.00  
149.48  
149.05

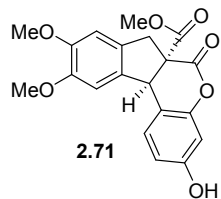
132.15  
130.74  
129.75

112.37  
112.22  
107.74  
106.55  
104.57

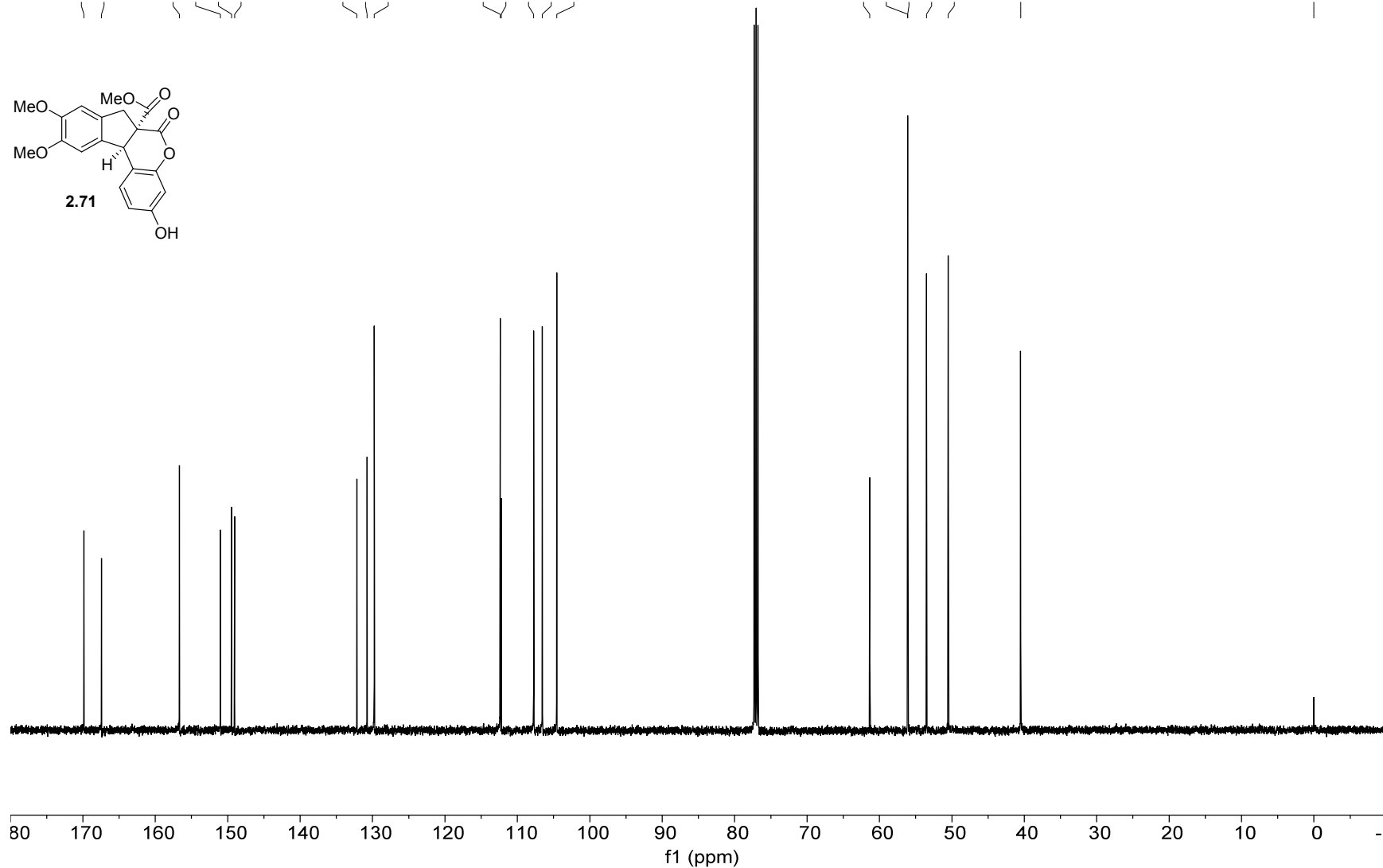
61.34  
56.10  
56.09  
53.50  
50.50

40.51

-0.00

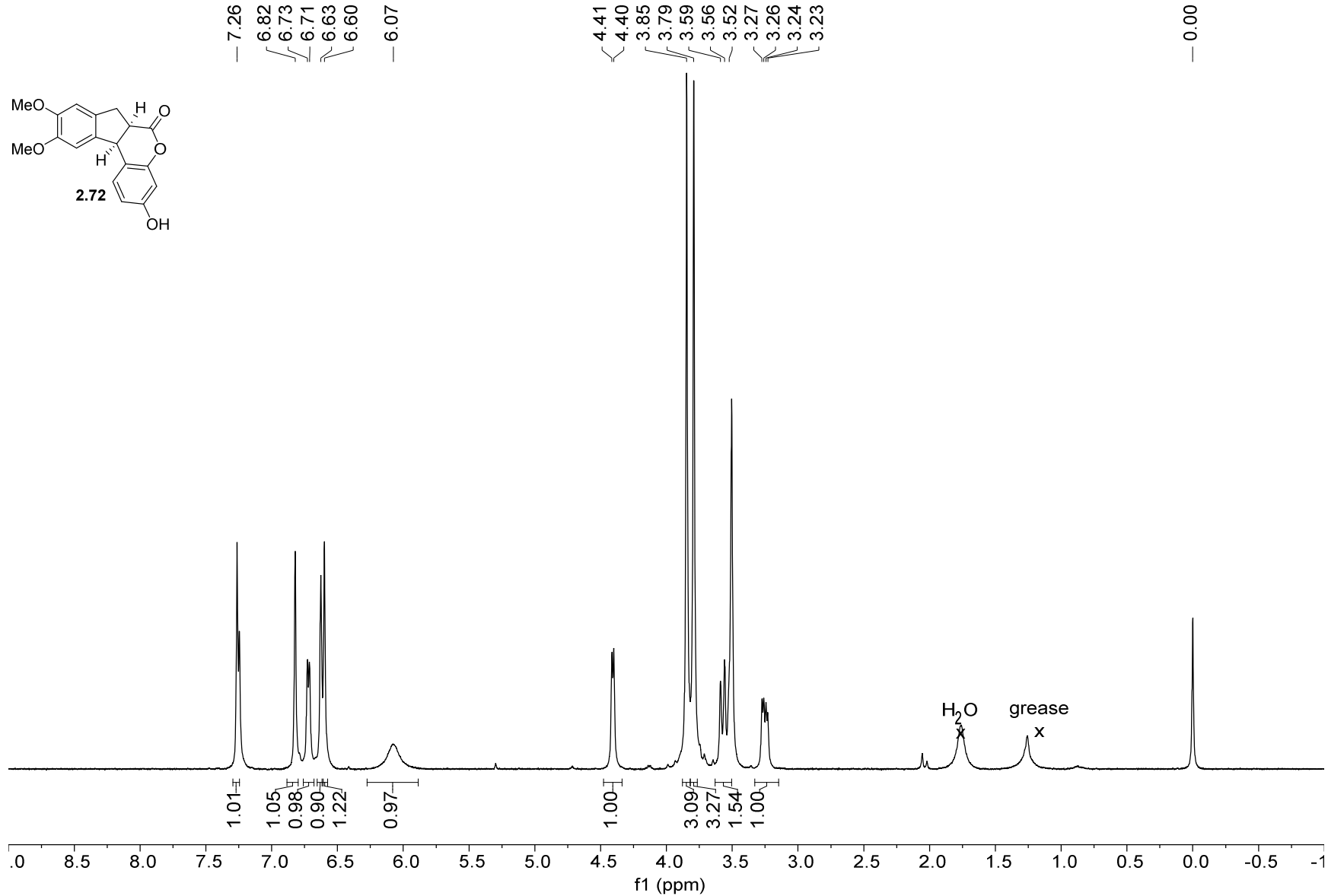
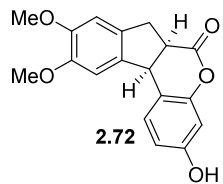


278

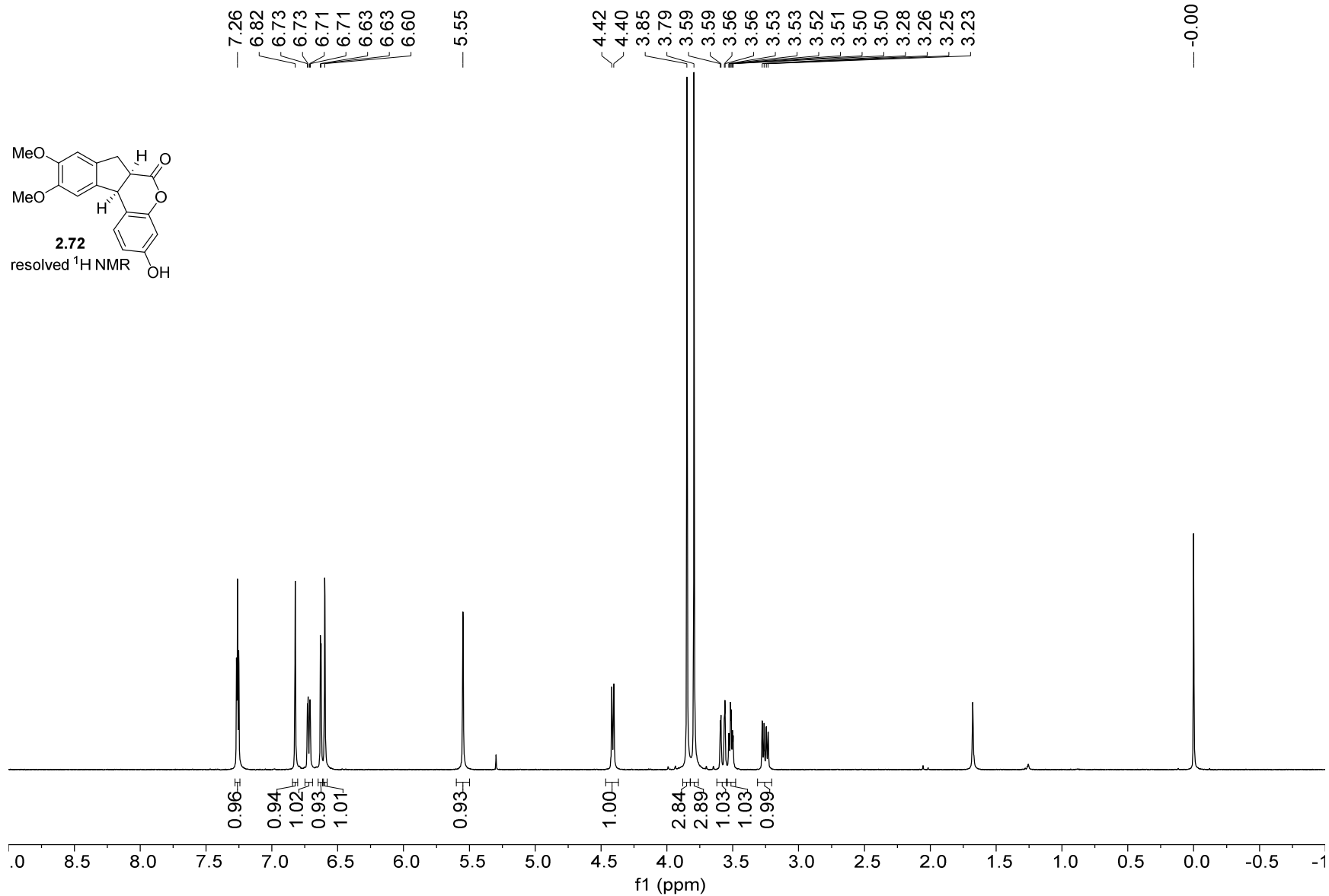
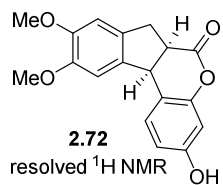


279

1H NMR — 499 MHz — CDCl3T — 298.0 K



1H NMR — 499 MHz — CDCl3T — 298.0 K



13C NMR — 126 MHz — CDCl3 — 298.0 K

— 170.65

— 156.38

— 151.27

— 149.10

— 148.73

— 134.27

— 132.55

— 129.68

— 113.28

— 112.17

— 108.01

— 107.03

— 104.38

— 56.17

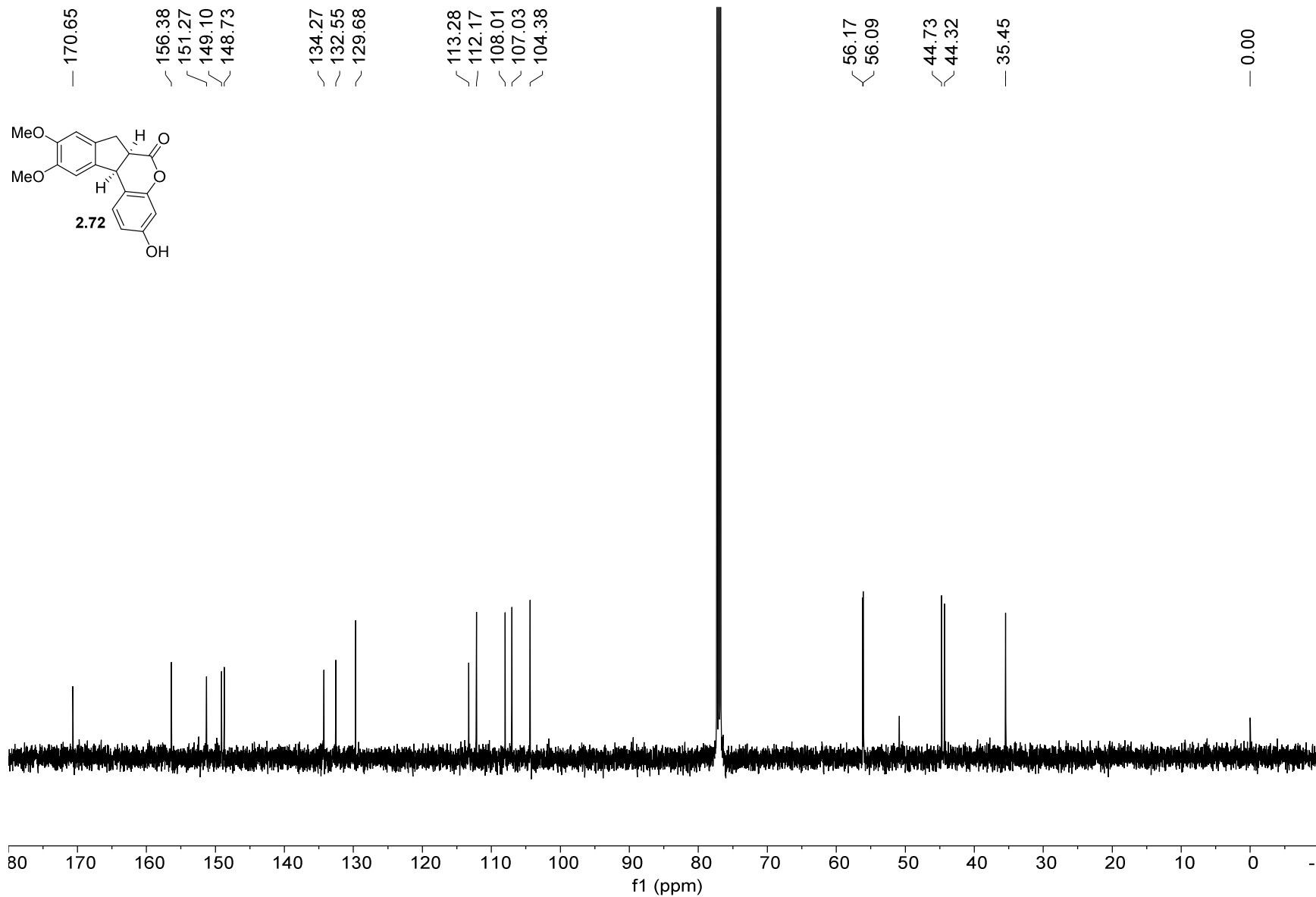
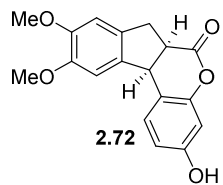
— 56.09

— 44.73

— 44.32

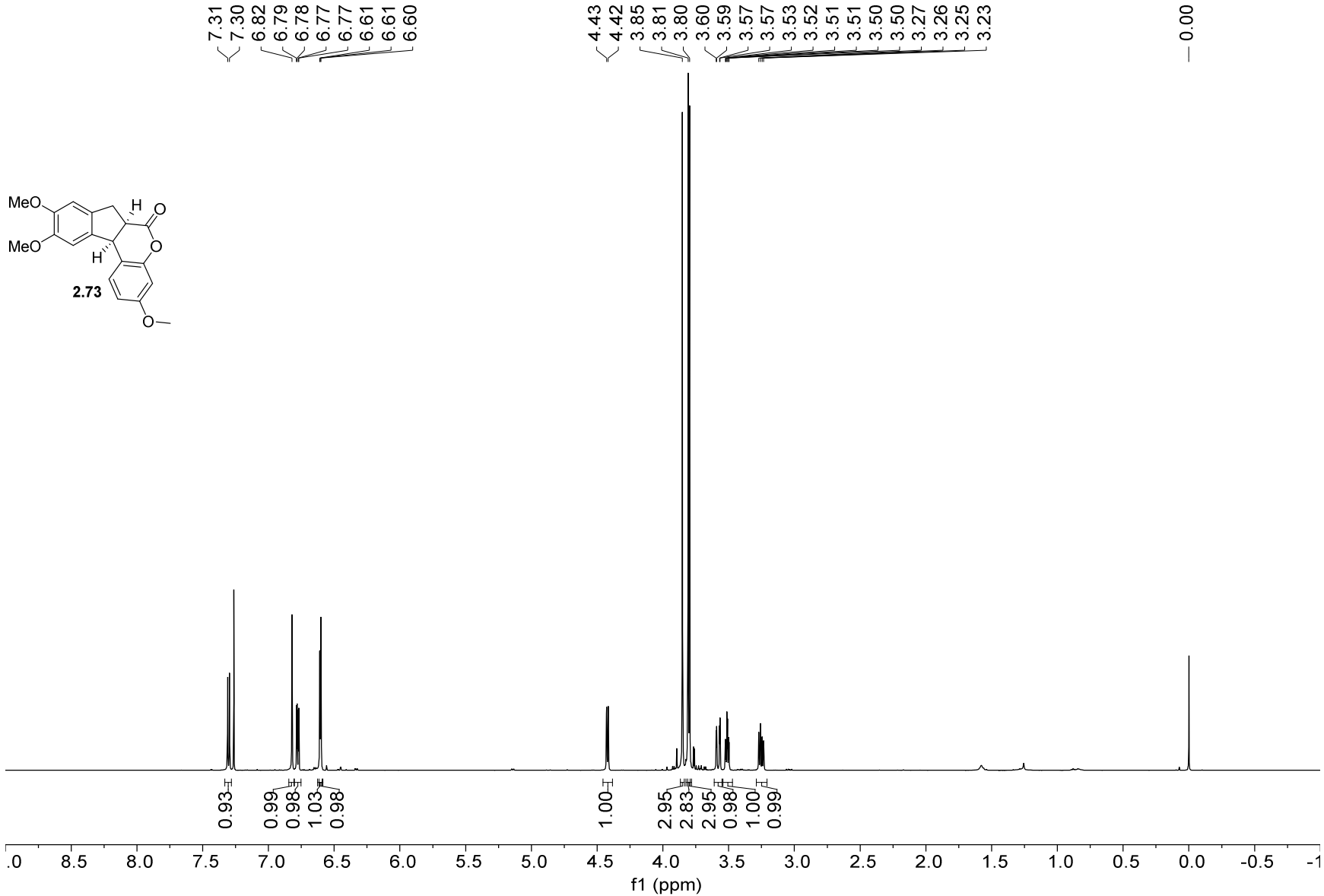
— 35.45

— 0.00





1H NMR — 600 MHz — CDCl3T — 298.0 K



13C NMR — 151 MHz — CDCl3T — 298.0 K

— 170.13

— 159.97

151.44

149.09

148.73

134.24

132.55

129.44

113.40

111.03

107.95

106.94

102.47

56.14

56.07

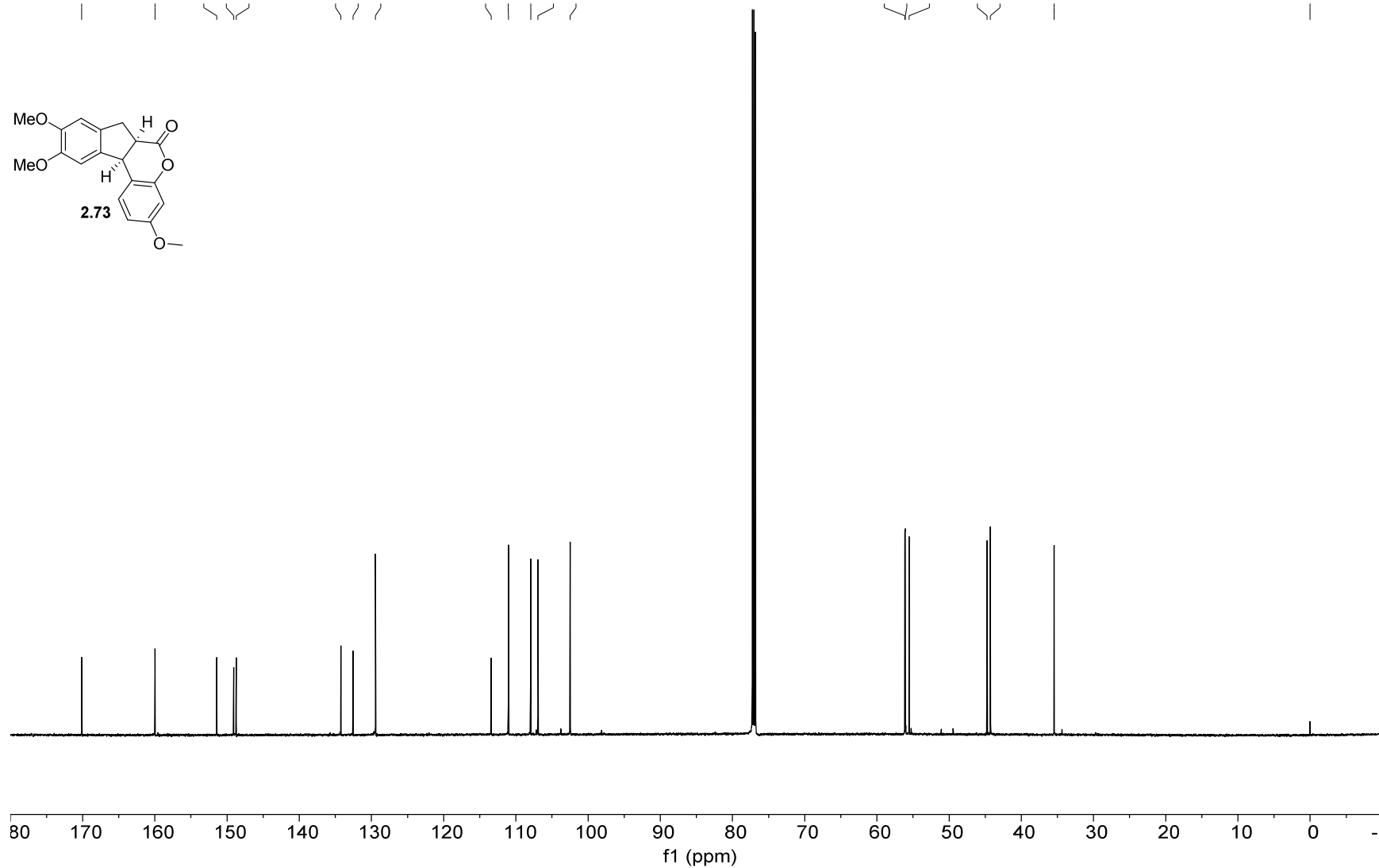
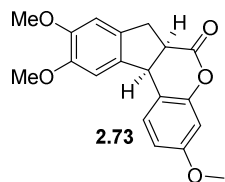
55.54

44.75

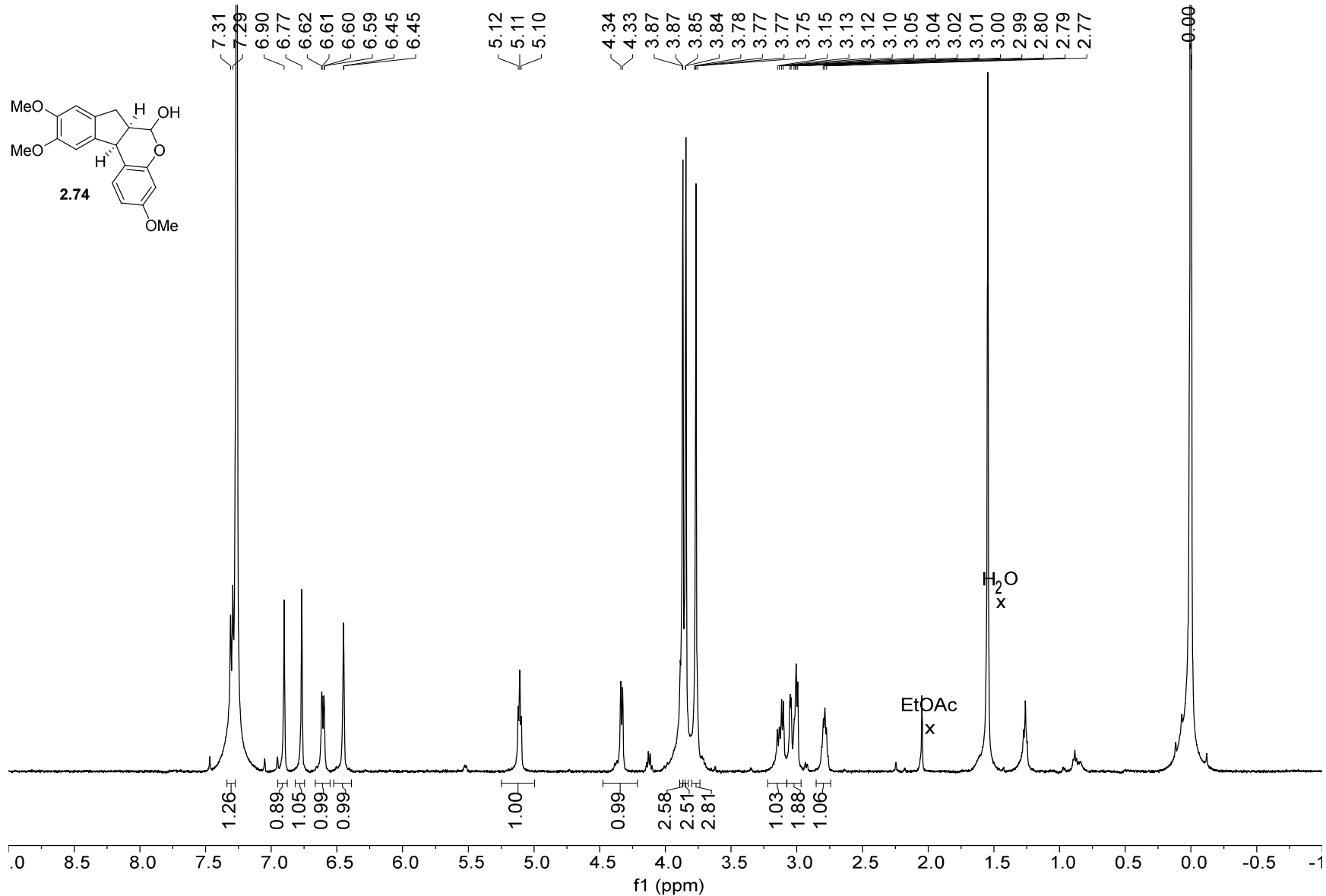
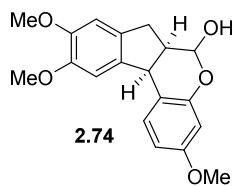
44.28

— 35.47

— 0.00



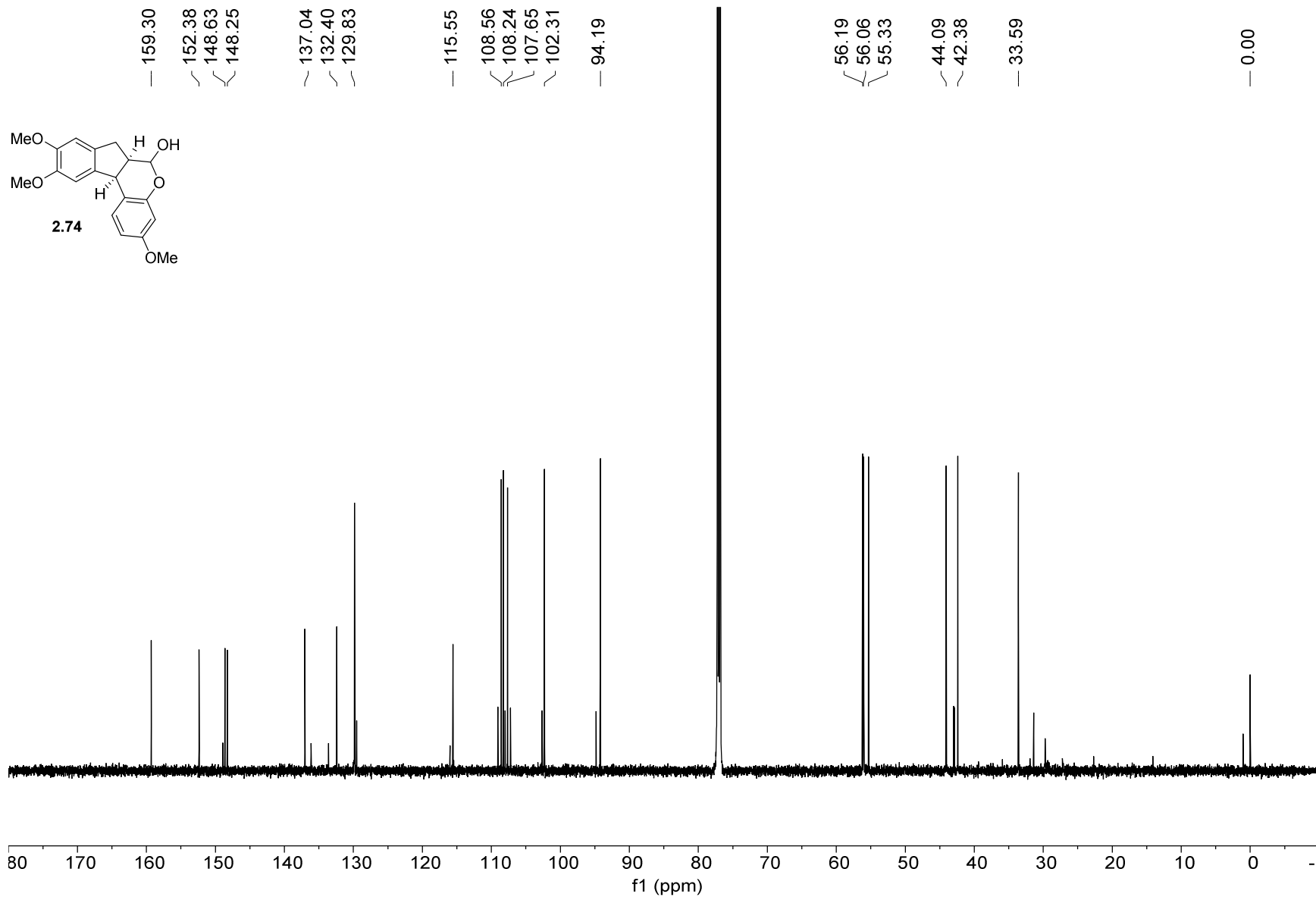
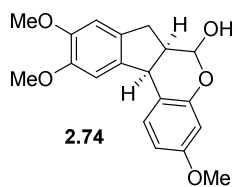
1H NMR — 500 MHz — CDCl3T — 298.0 K



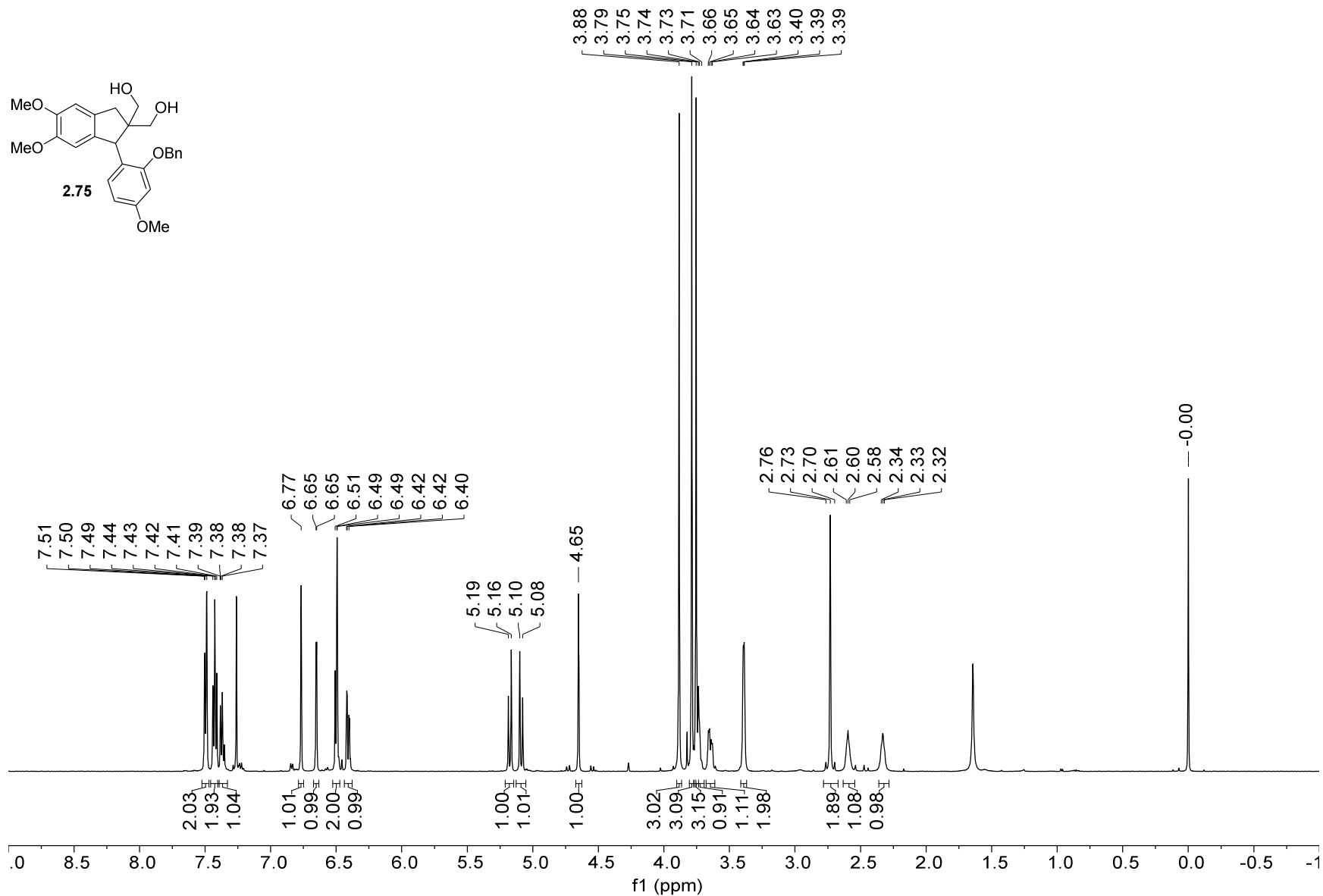
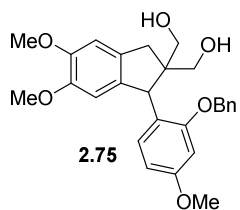


13C NMR — 151 MHz — CDCl3T — 298.0 K

— 159.30  
— 152.38  
— 148.63  
— 148.25  
— 137.04  
— 132.40  
— 129.83  
— 115.55  
— 108.56  
— 108.24  
— 107.65  
— 102.31  
— 94.19  
— 56.19  
— 56.06  
— 55.33  
— 44.09  
— 42.38  
— 33.59  
— 0.00

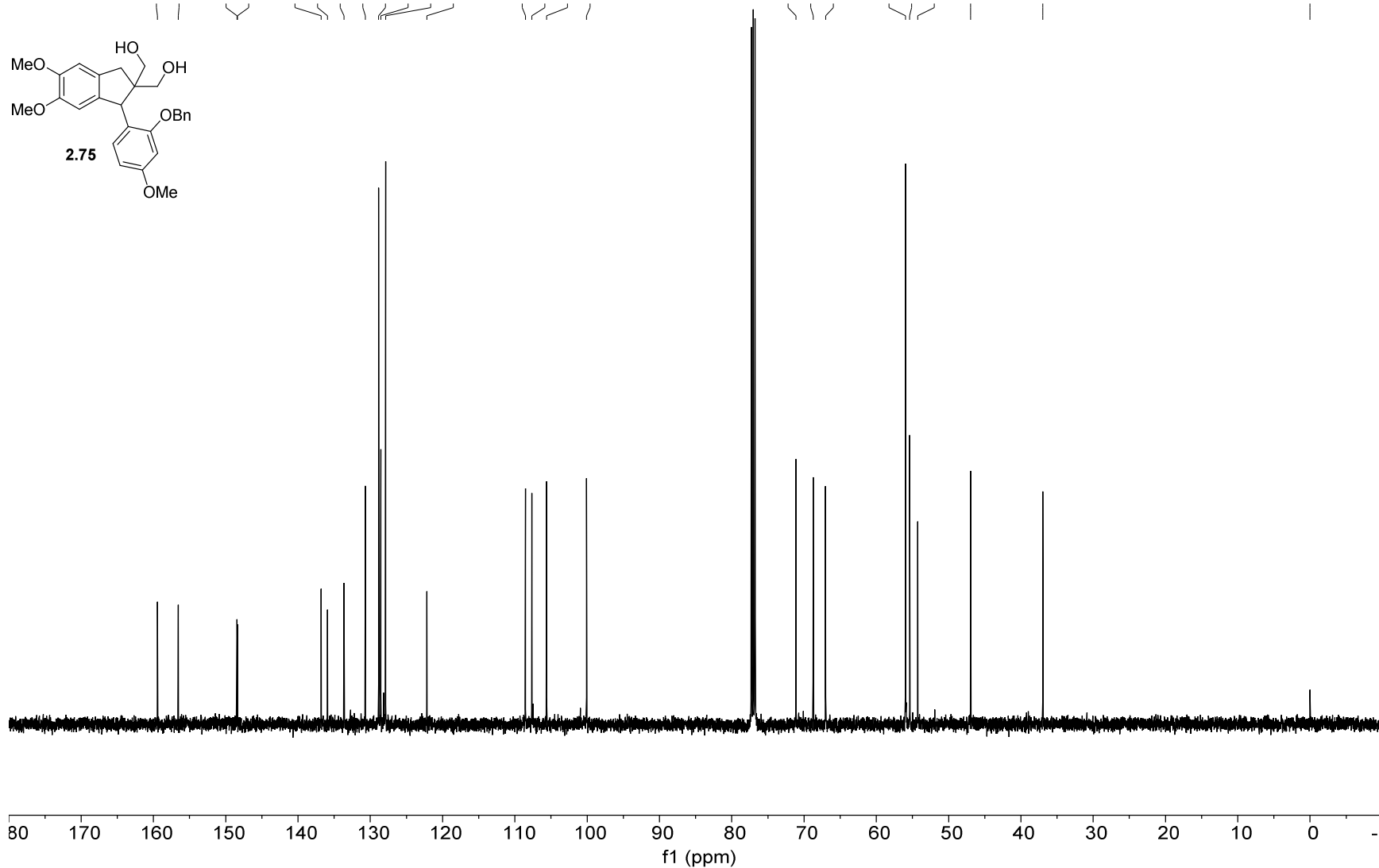
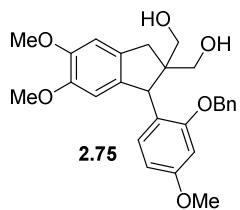


1H NMR — 500.22 MHz — CDCl3T — 298.0 K

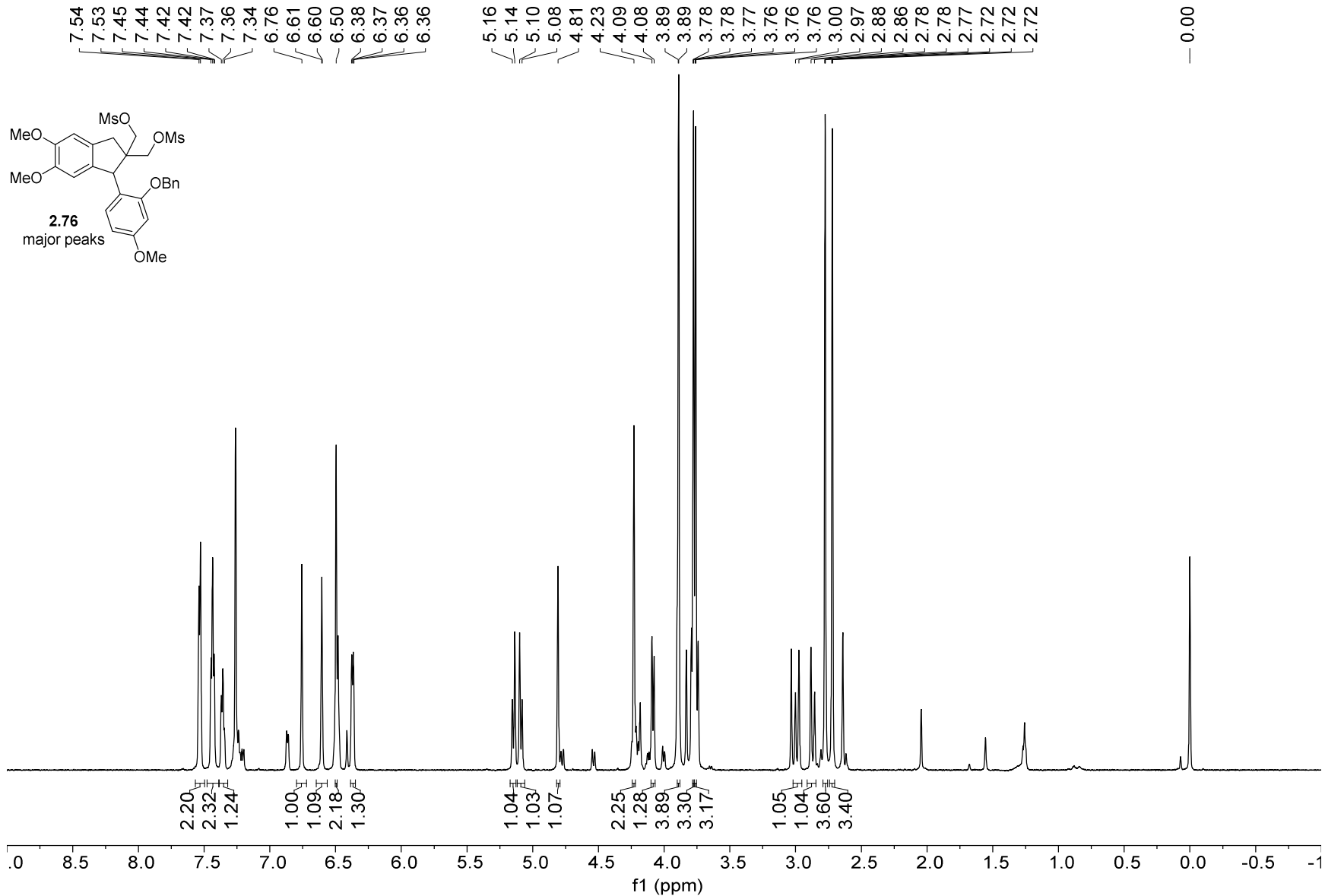
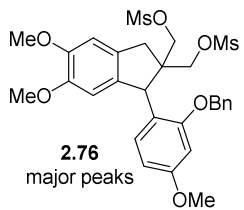


13C NMR — 125.79 MHz — CDCl3 — 298.0 K

159.45  
156.58  
148.45  
148.36  
136.79  
135.92  
133.62  
130.69  
128.84  
128.54  
127.88  
122.17  
108.54  
107.65  
105.62  
100.07  
71.13  
68.73  
67.02  
55.97  
55.38  
54.27  
46.95  
36.96  
-0.00

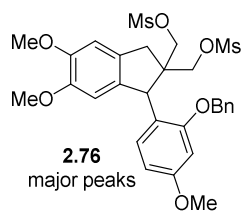


1H NMR — 600 MHz — CDCl3T — 298.0 K





13C NMR — 151 MHz — CDCl3T — 298.0 K



159.97  
157.44  
149.05  
149.01  
136.68  
135.35  
131.87  
130.42  
128.85  
128.29  
128.03  
120.00

108.41  
107.37  
104.94  
99.65

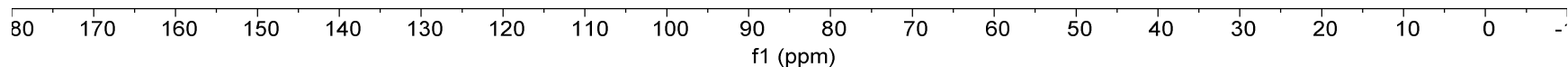
71.23  
70.56  
70.23

56.05  
56.02  
55.37  
50.81  
47.01

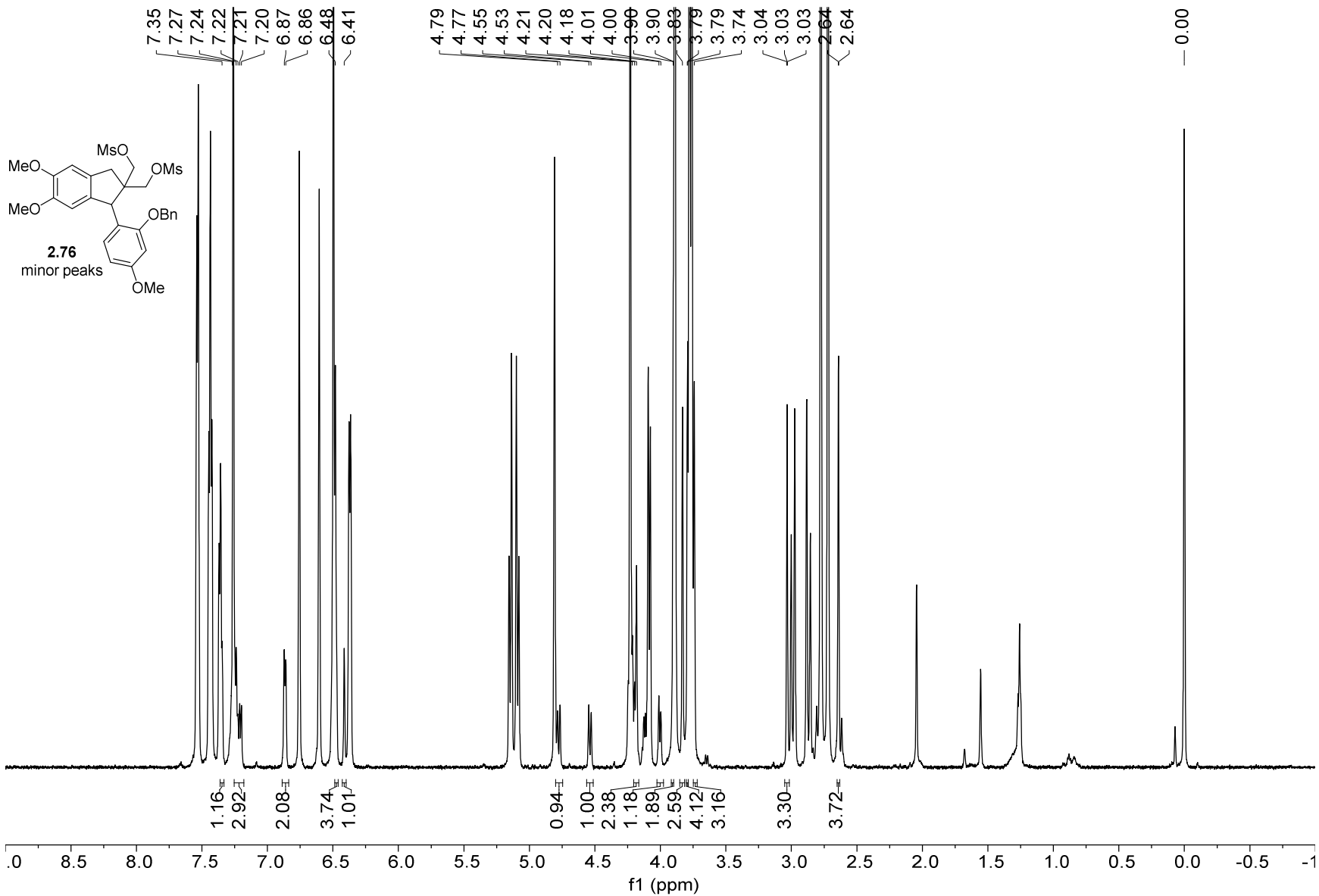
38.01  
36.87  
36.81

-0.00

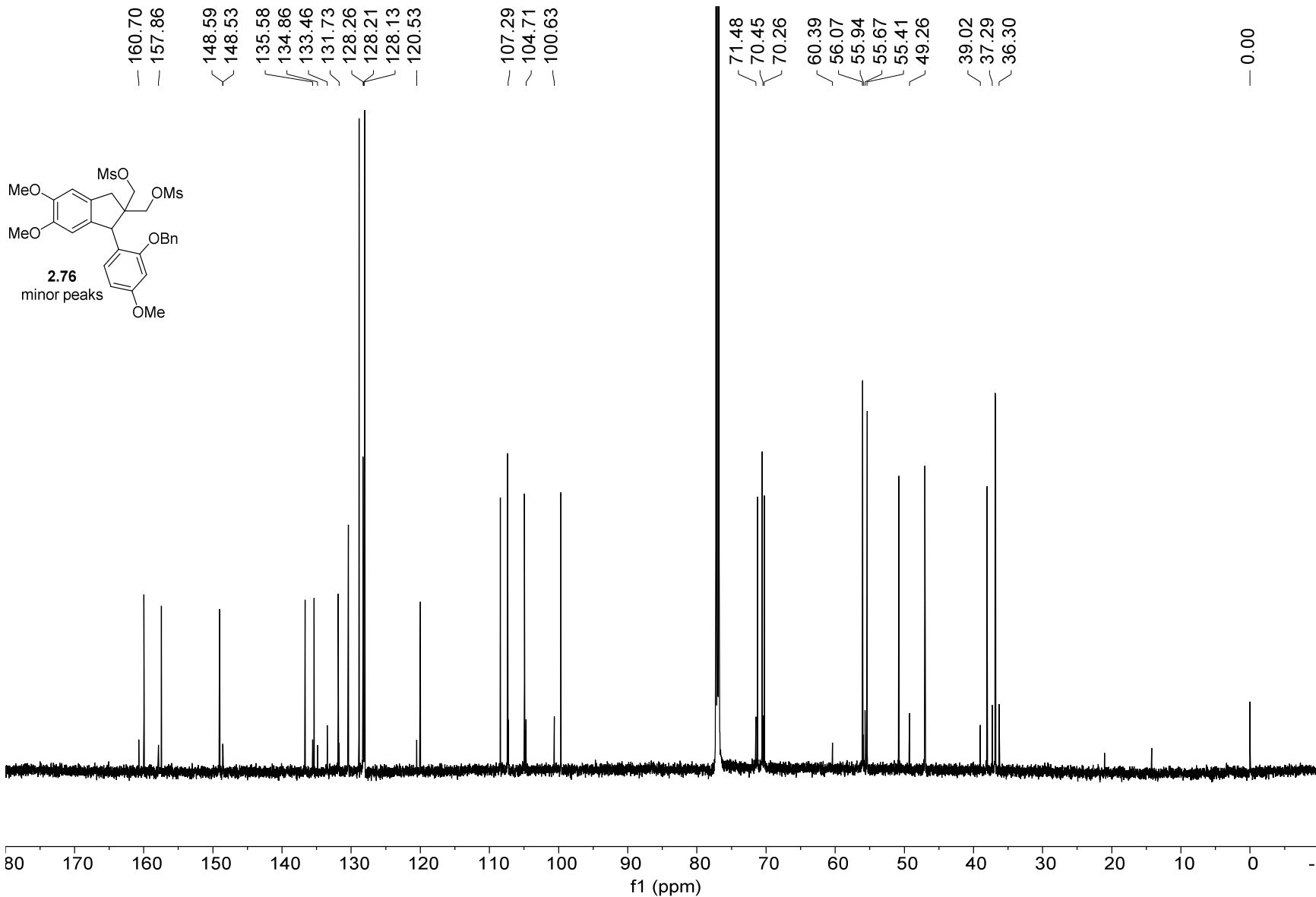
290



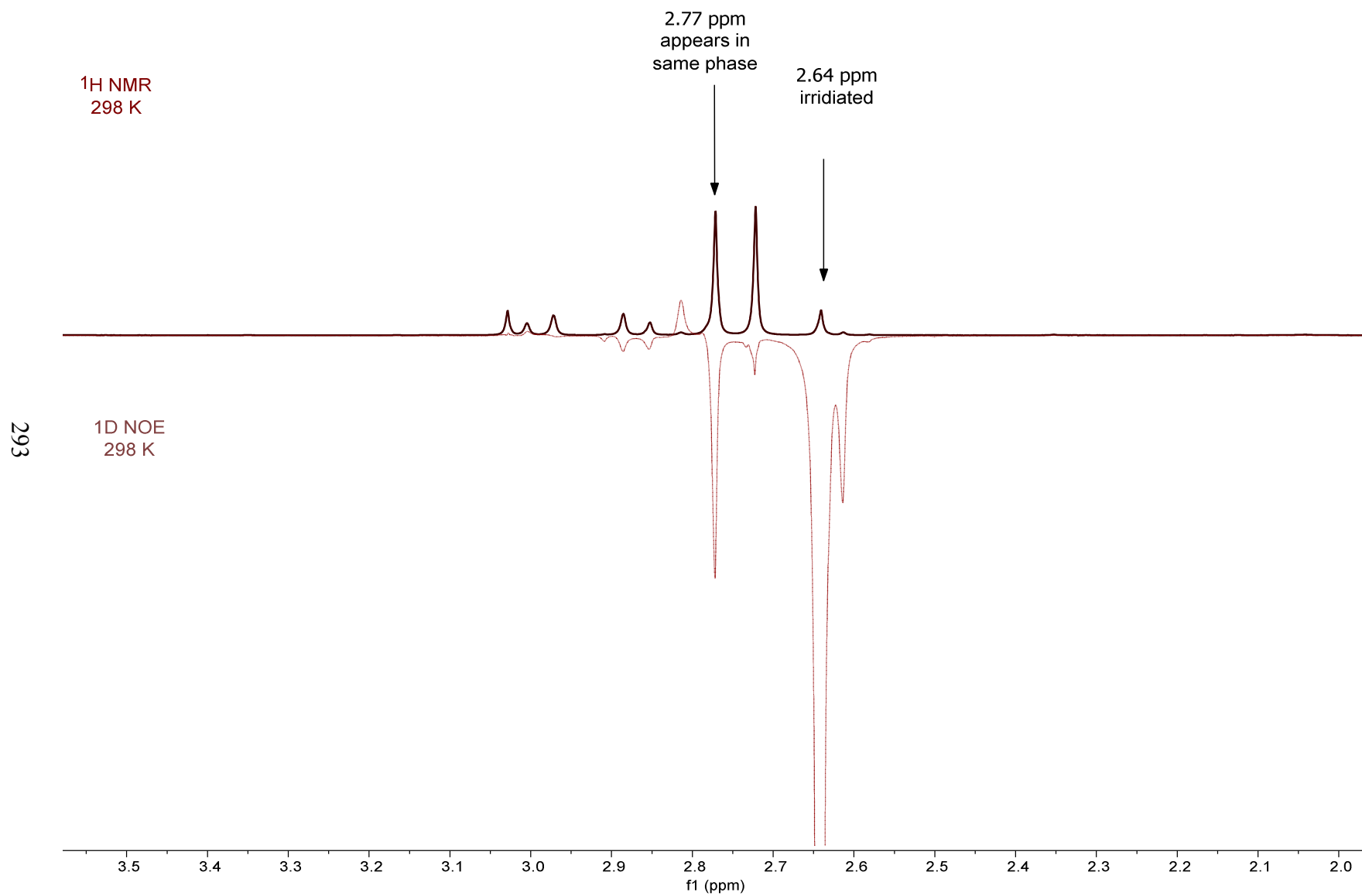
1H NMR — 600 MHz — CDCl3T — 298.0 K



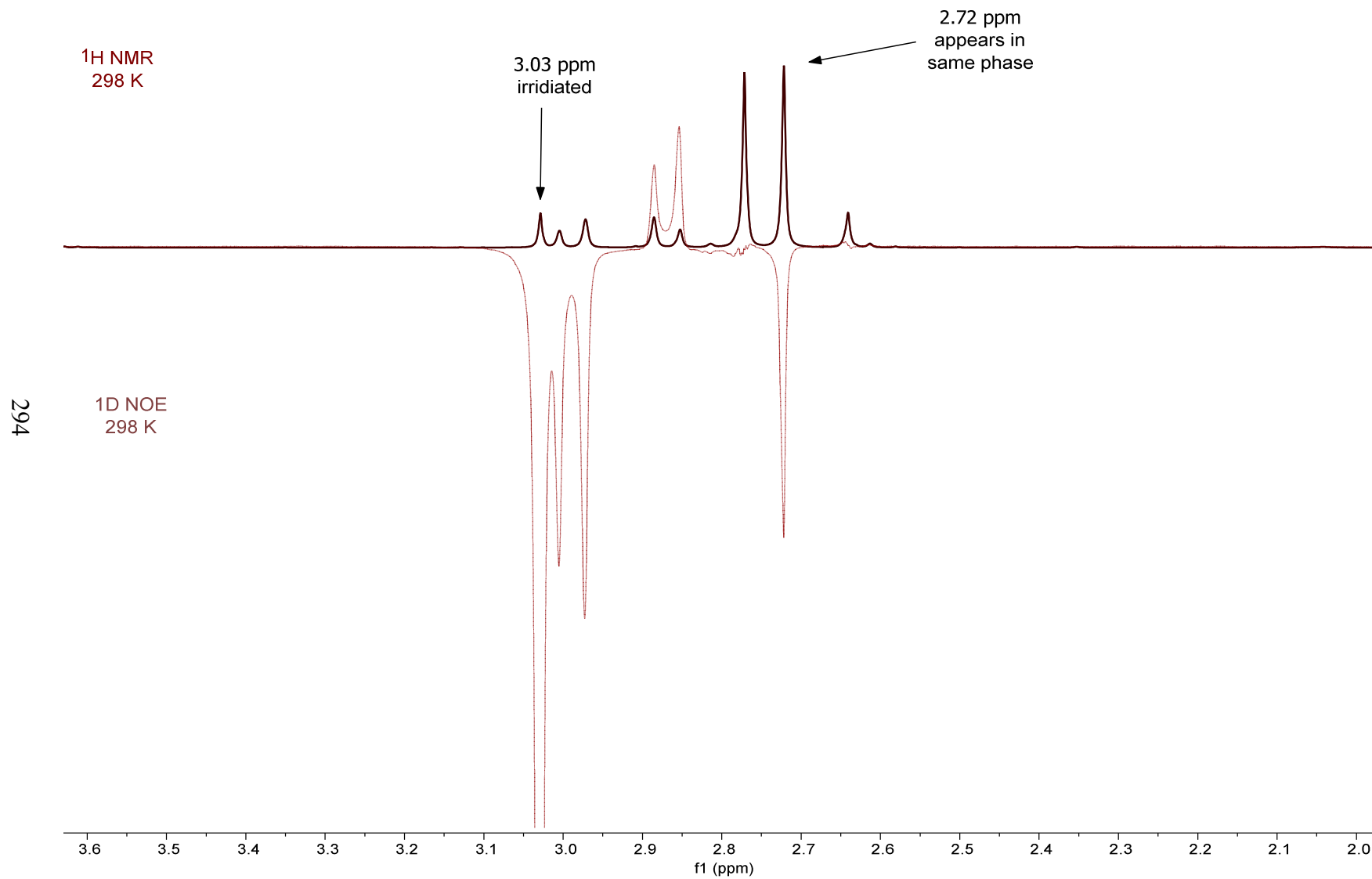
13C NMR — 151 MHz — CDCl3T — 298.0 K



$^1\text{H}$  NMR and 1D NOE Experiments of **2.76** (500 MHz,  $\text{CDCl}_3$ , 298.0 K)

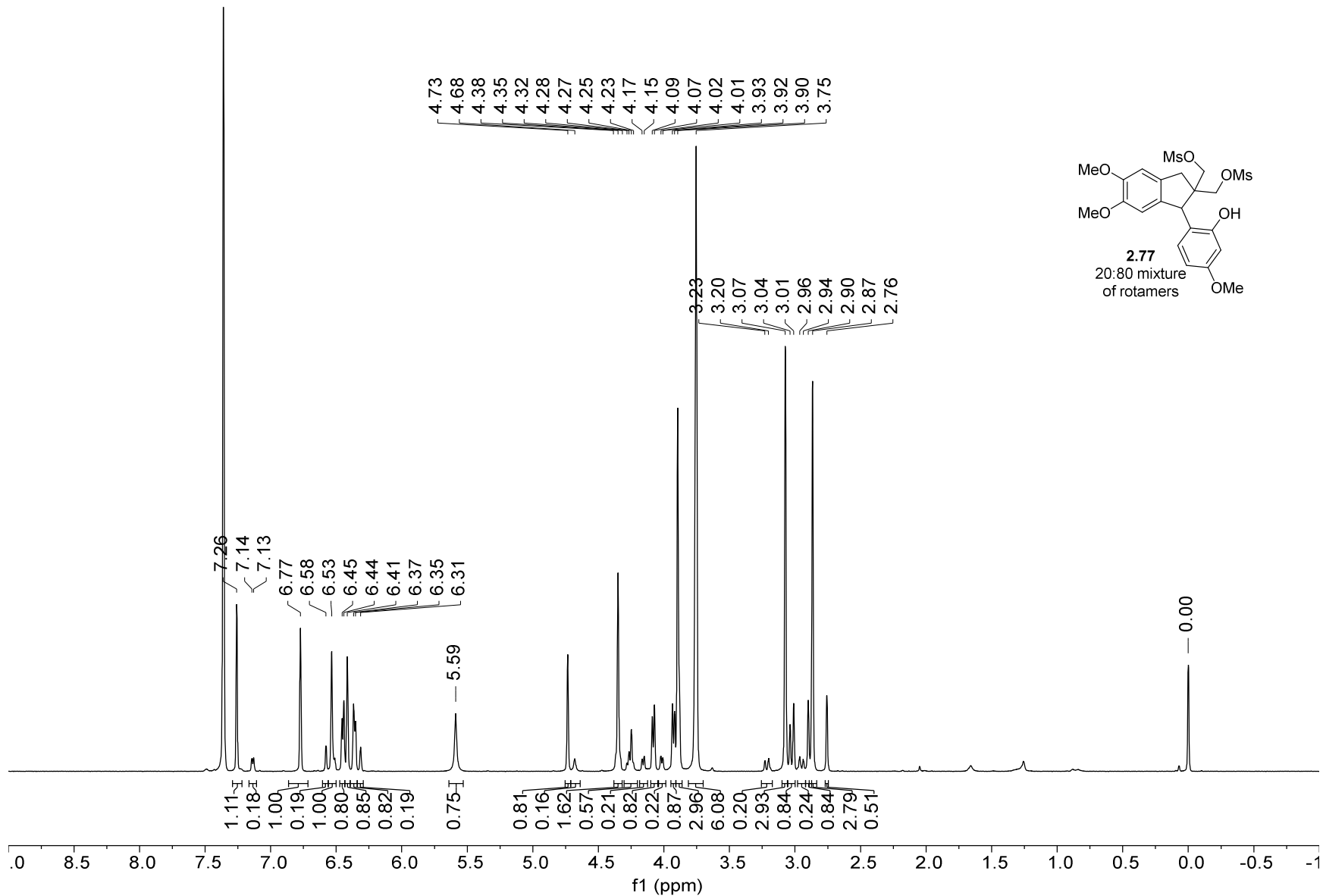


<sup>1</sup>H NMR and 1D NOE Experiments of **2.76** (500 MHz, CDCl<sub>3</sub>, 298.0 K)

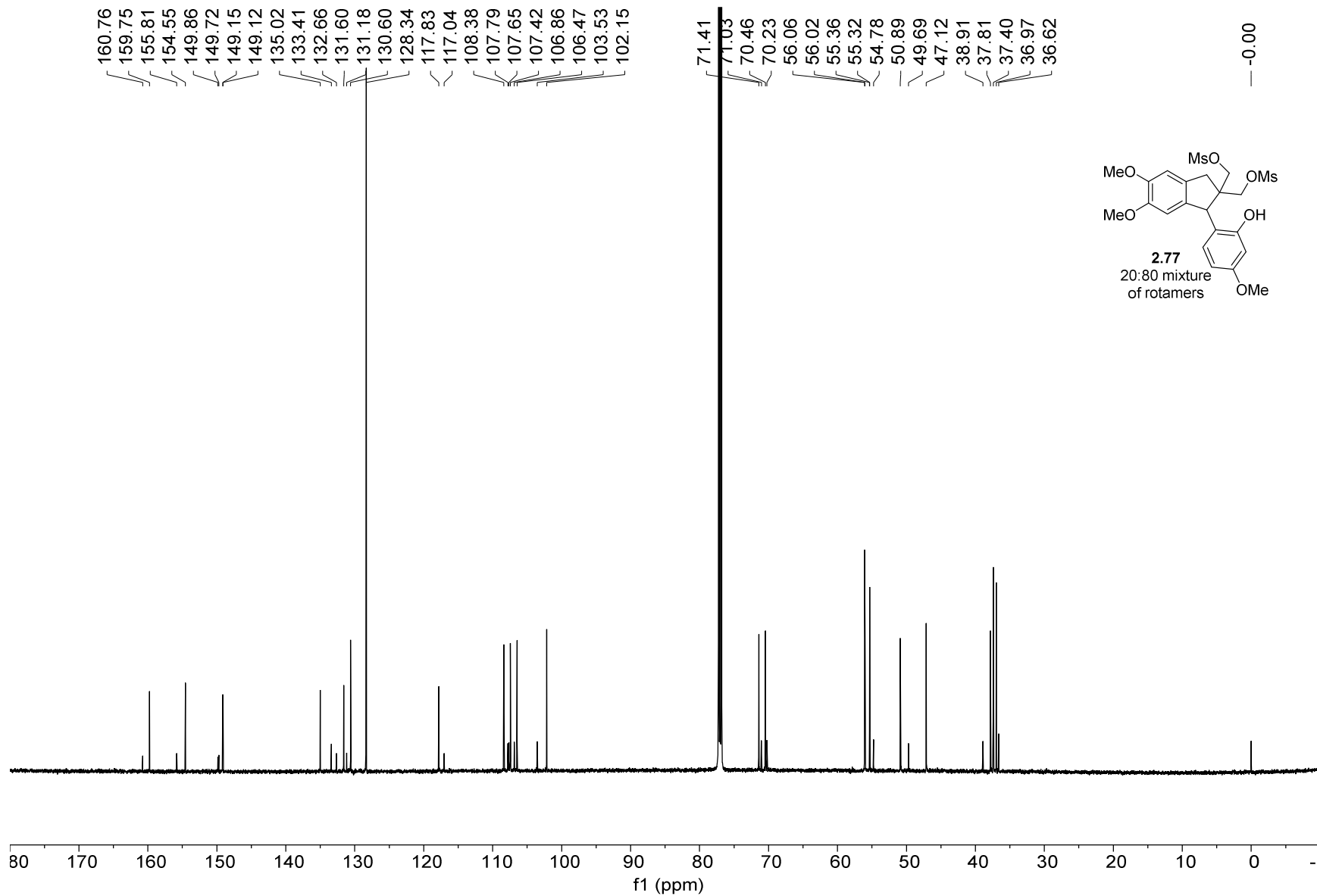


1H NMR — 600.13 MHz — CDCl3T — 298.0 K

295

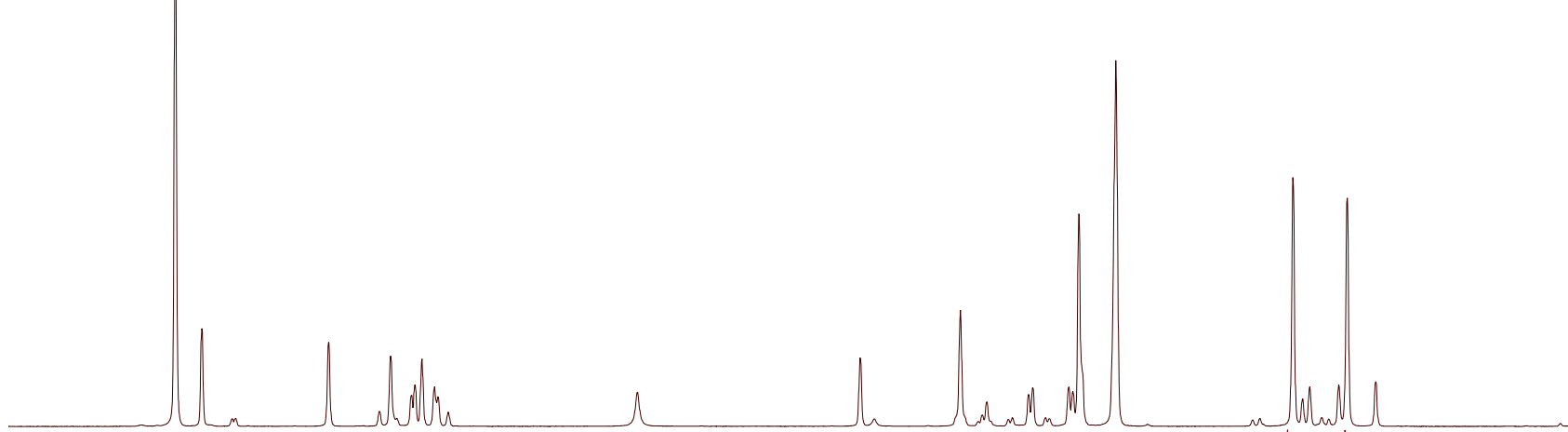


13C NMR — 150.92 MHz — CDCl3T — 298.0 K

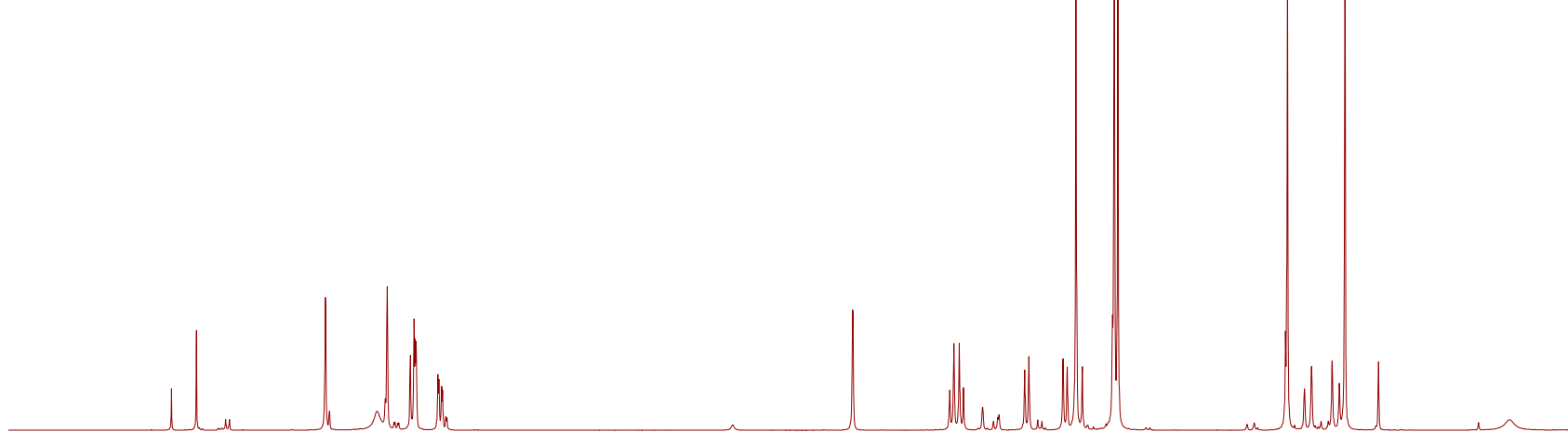


<sup>1</sup>H NMR Experiments of **2.77** (600 MHz, CDCl<sub>3</sub>) at 298.0 K and 276.0 K

600 MHz CDCl<sub>3</sub> 298.0 K



600 MHz CDCl<sub>3</sub> 276.0 K

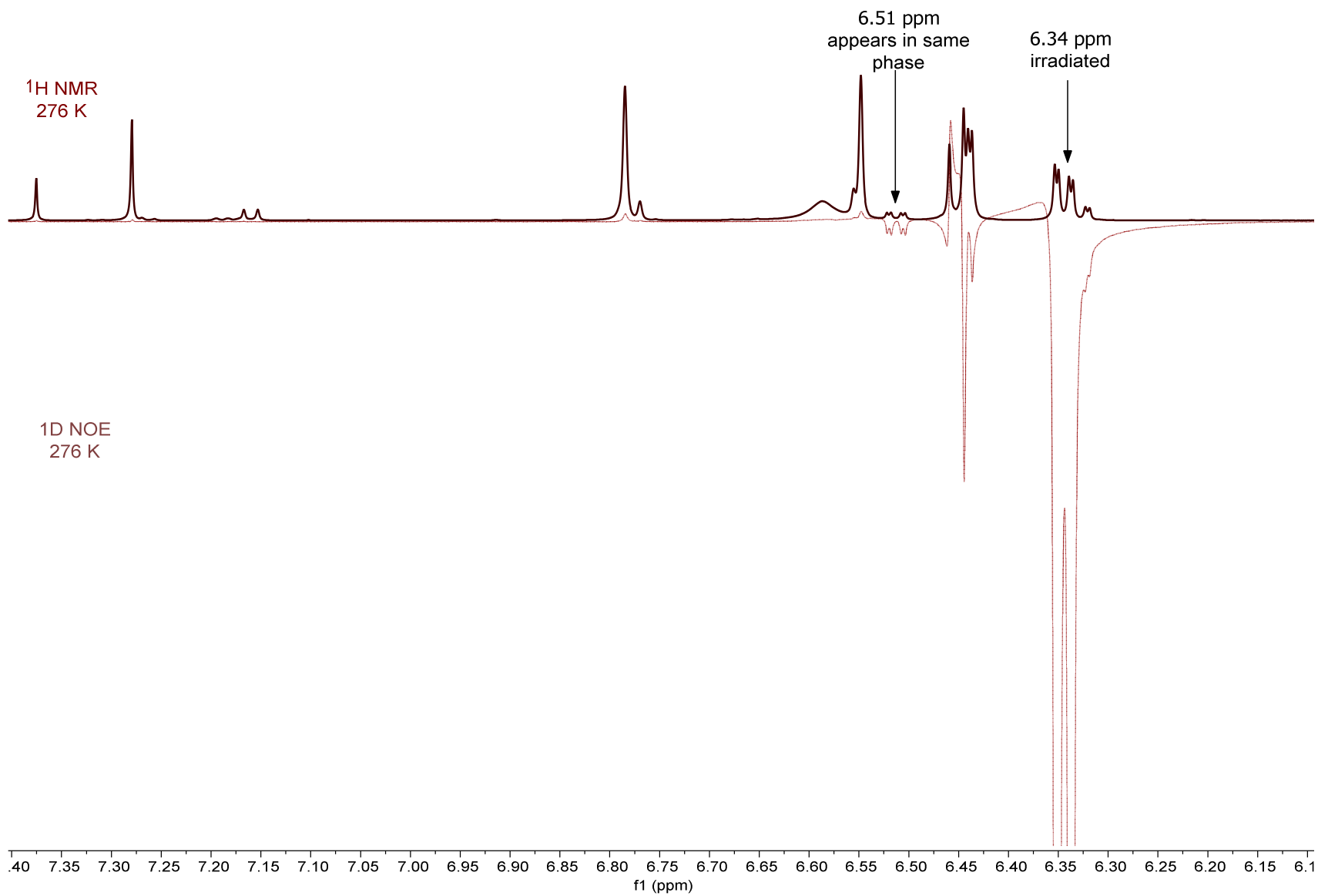


297

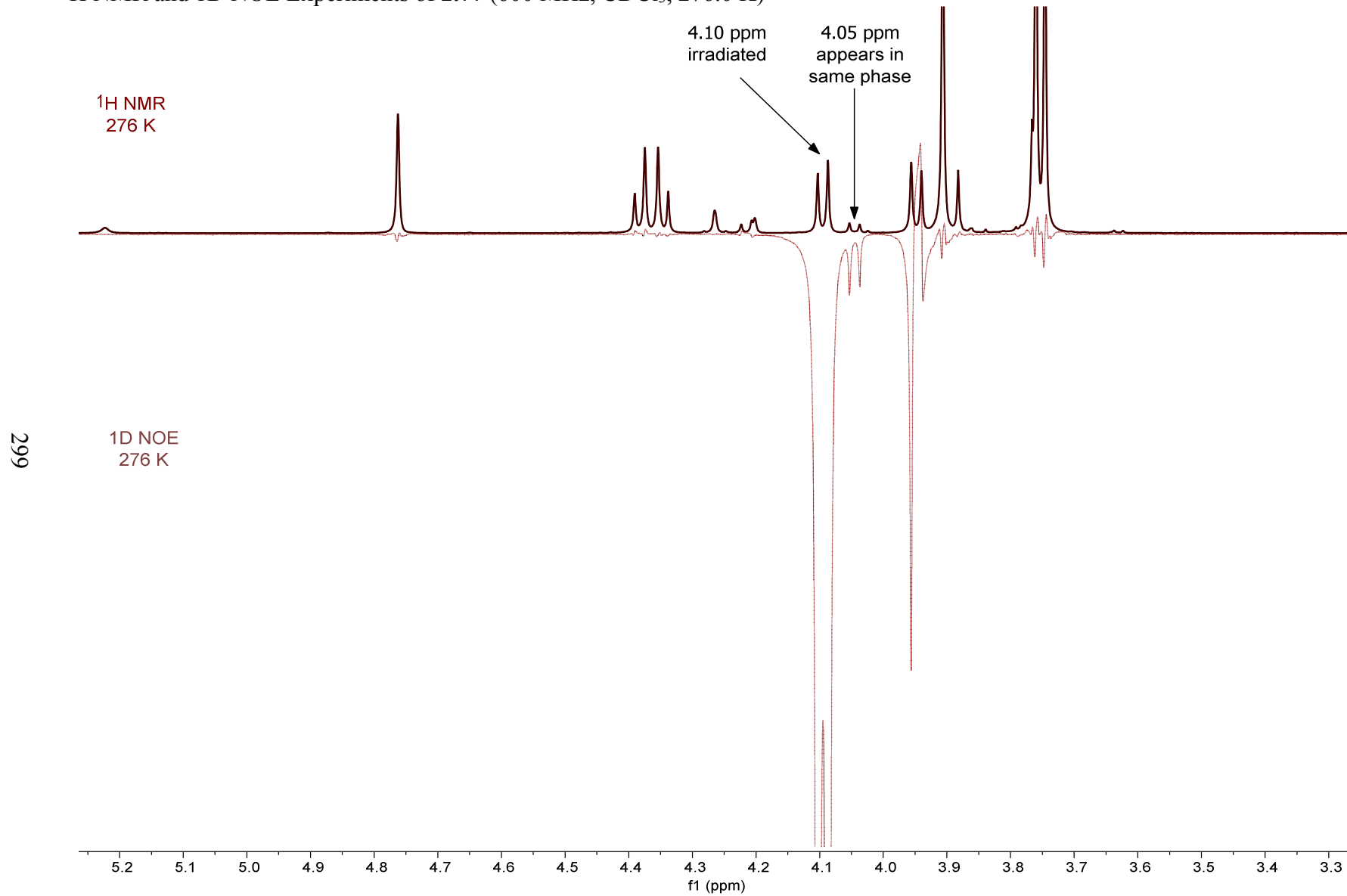
7.5 7.0 6.5 6.0 5.5 5.0 4.5 4.0 3.5 3.0 2.5 2  
f1 (ppm)



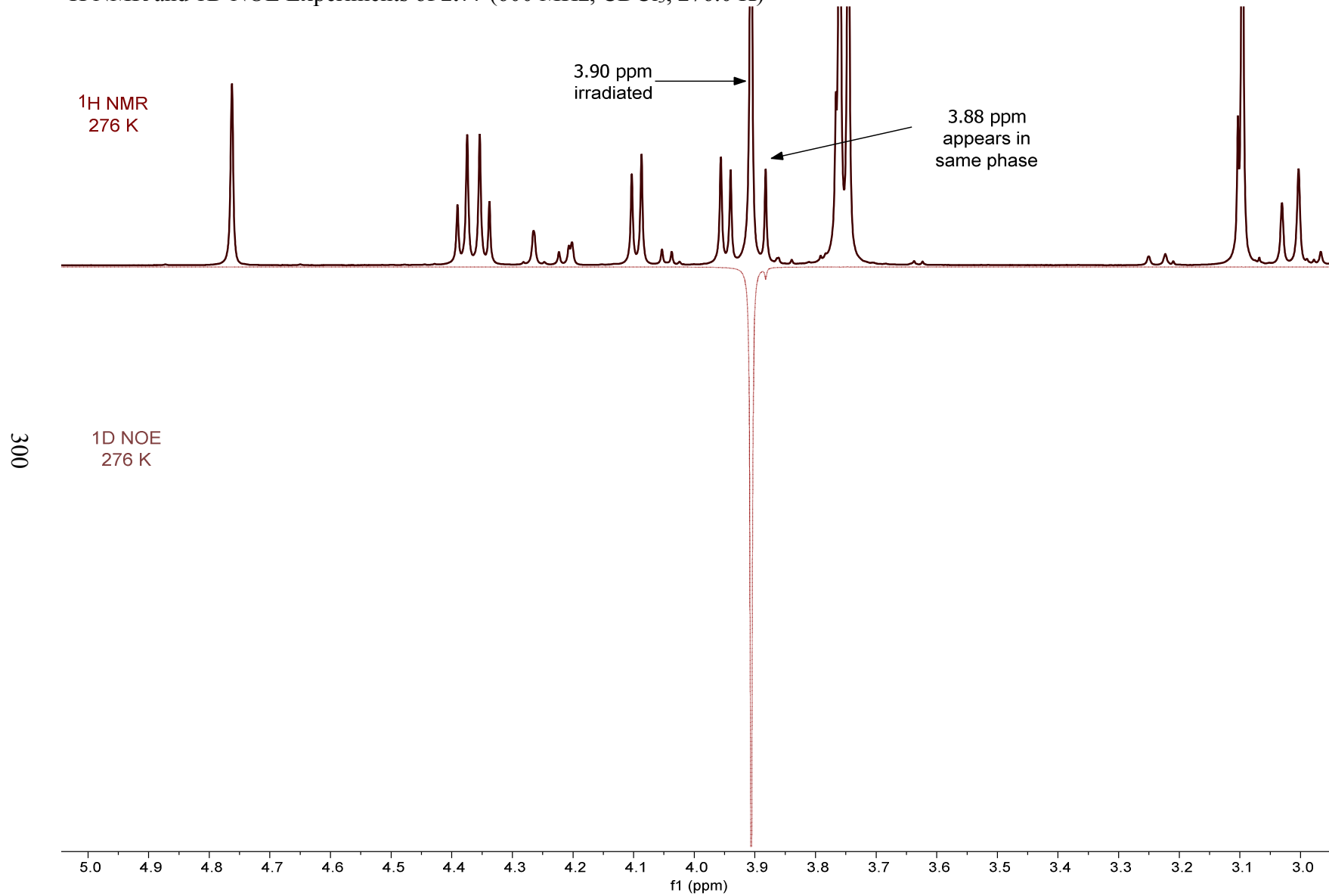
<sup>1</sup>H NMR and 1D NOE Experiments of **2.77** (600 MHz, CDCl<sub>3</sub>, 276.0 K)



<sup>1</sup>H NMR and 1D NOE Experiments of **2.77** (600 MHz, CDCl<sub>3</sub>, 276.0 K)

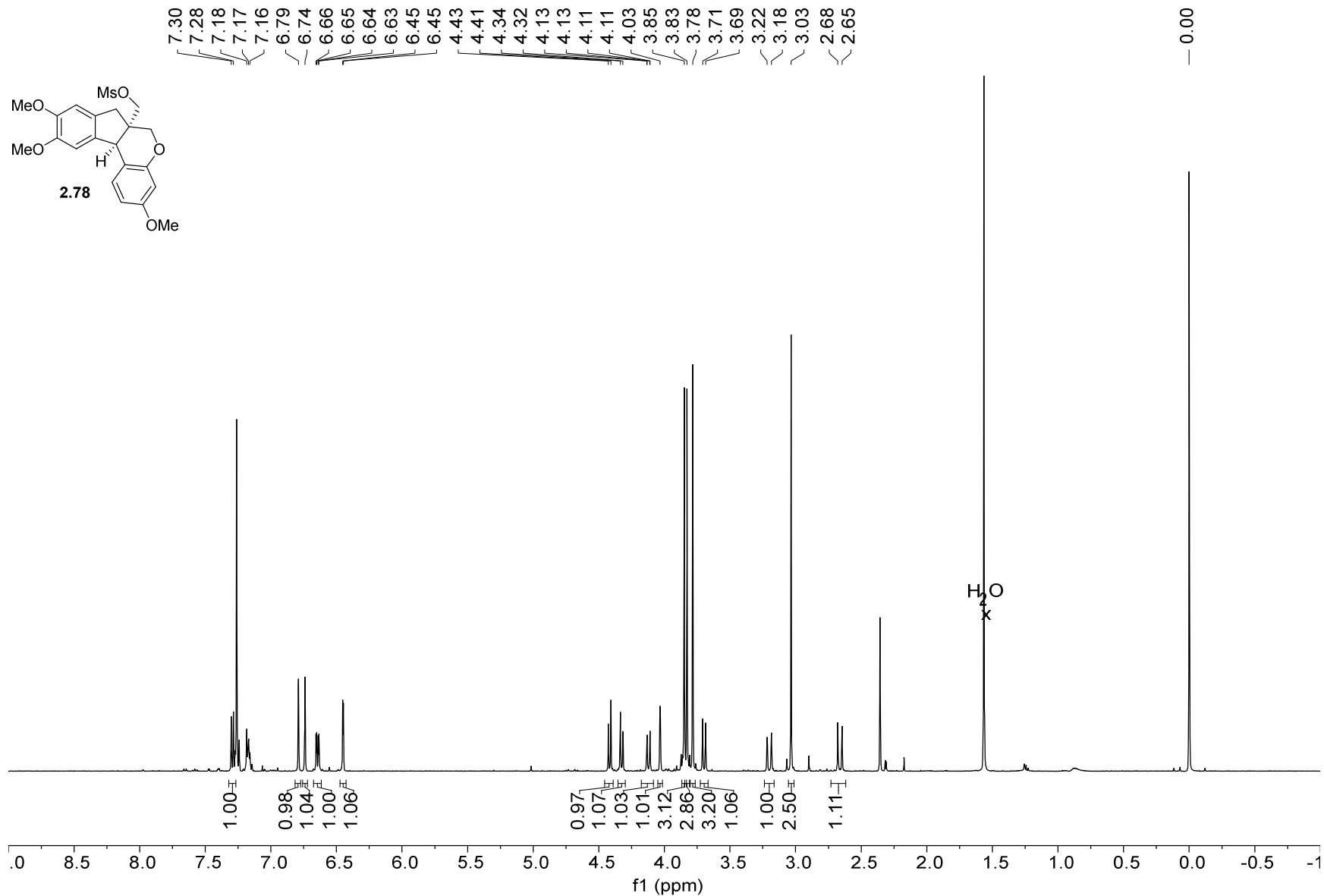
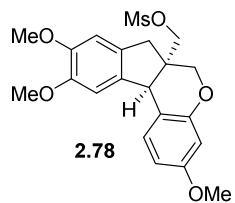


<sup>1</sup>H NMR and 1D NOE Experiments of **2.77** (600 MHz, CDCl<sub>3</sub>, 276.0 K)



301

1H NMR — 500 MHz — CDCl3T — 298.0 K



13C NMR — 126 MHz — CDCl3 — 298.0 K

159.53  
154.48  
148.79  
148.53

136.11  
130.87  
130.76  
129.04  
128.23  
125.30

113.90  
108.69  
108.39  
107.63  
101.97

71.42

66.37

56.10

56.08

55.35

45.42

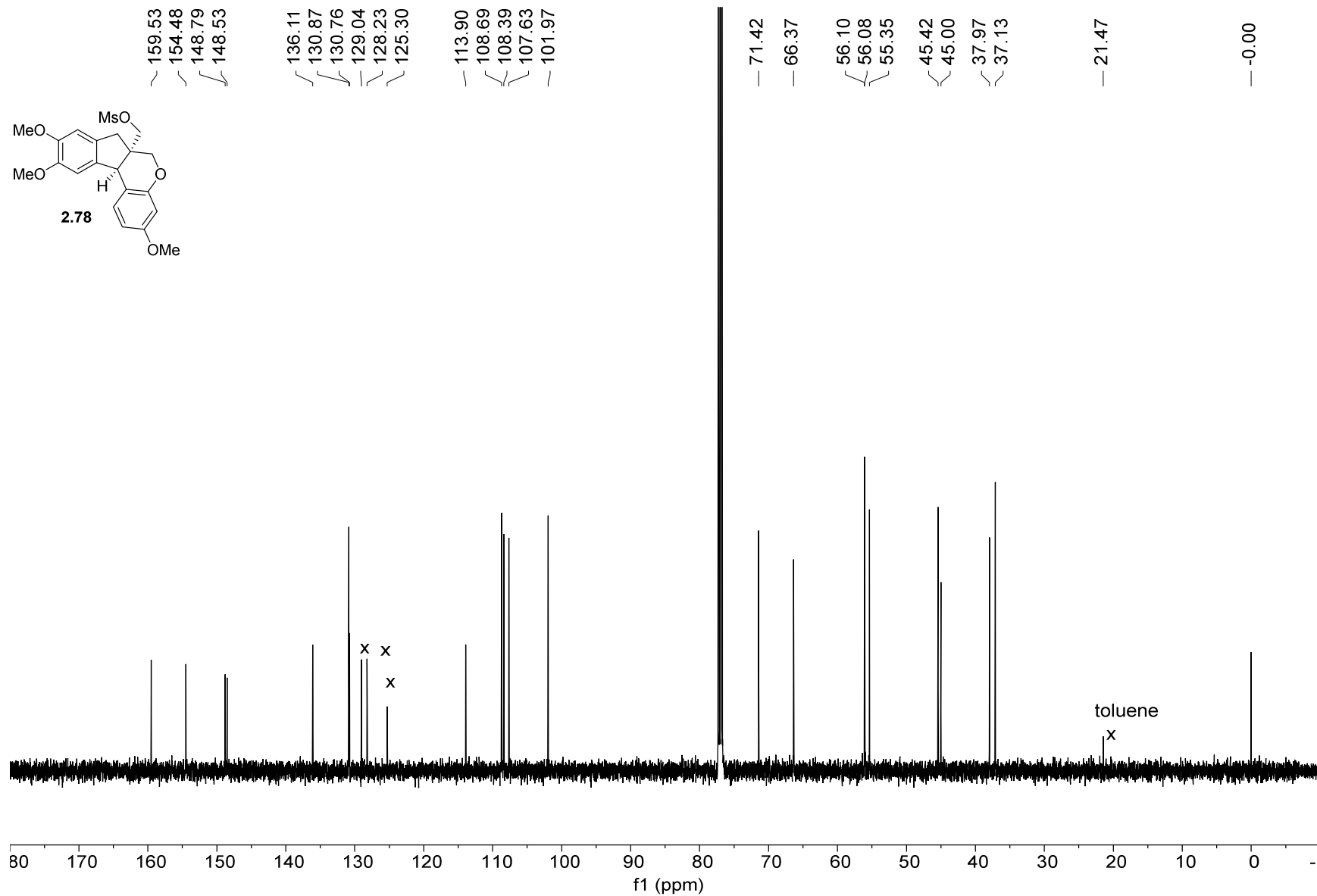
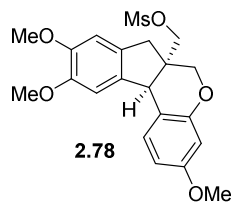
45.00

37.97

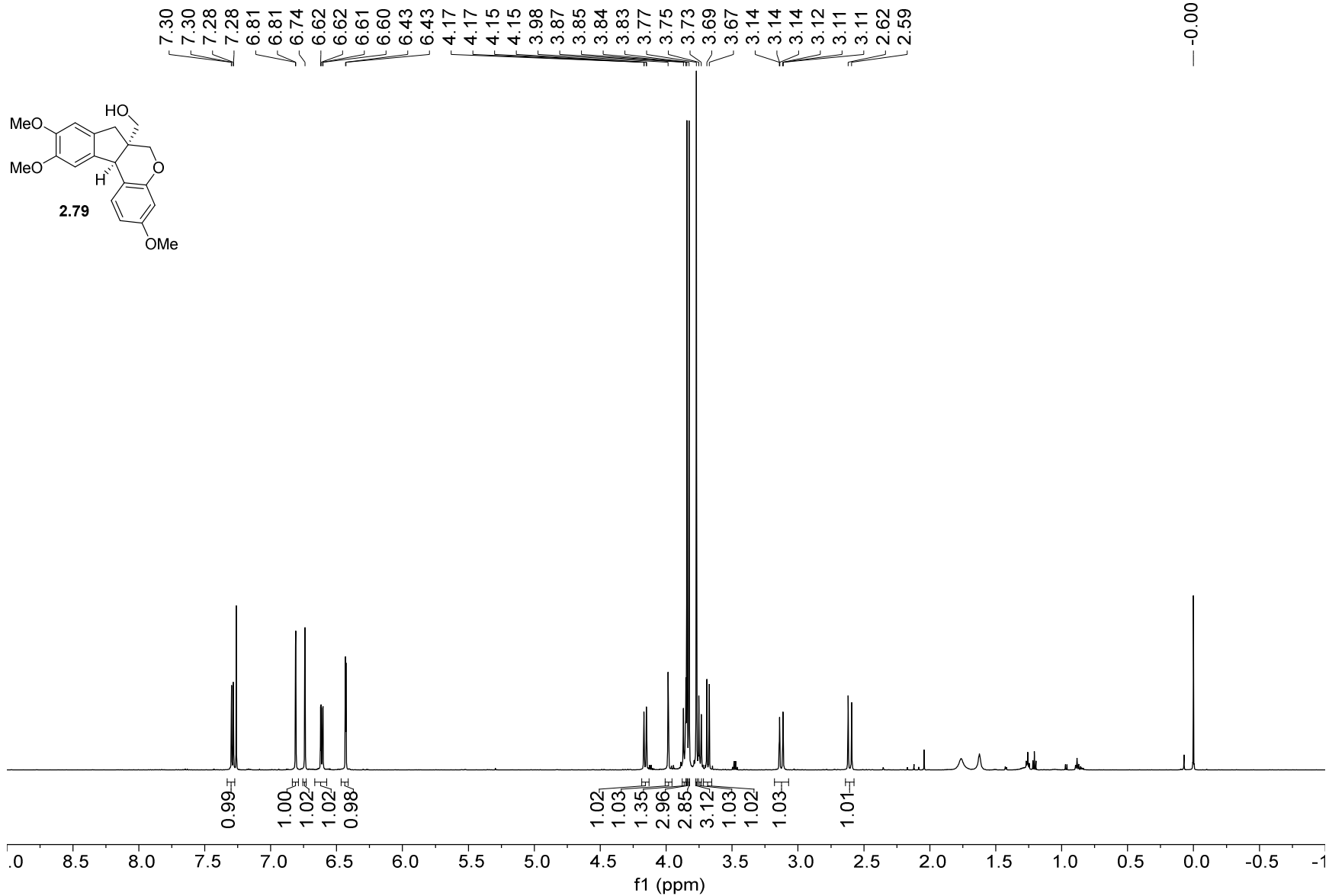
37.13

21.47

-0.00



1H NMR — 600.13 MHz — CDCl3T — 298.0 K



13C NMR — 150.92 MHz — CDCl3T — 298.0 K

— 159.26  
— 154.87

{ 148.54  
148.29

— 137.15  
— 131.71  
— 130.91

— 115.14

{ 108.53  
108.20  
107.84  
101.84

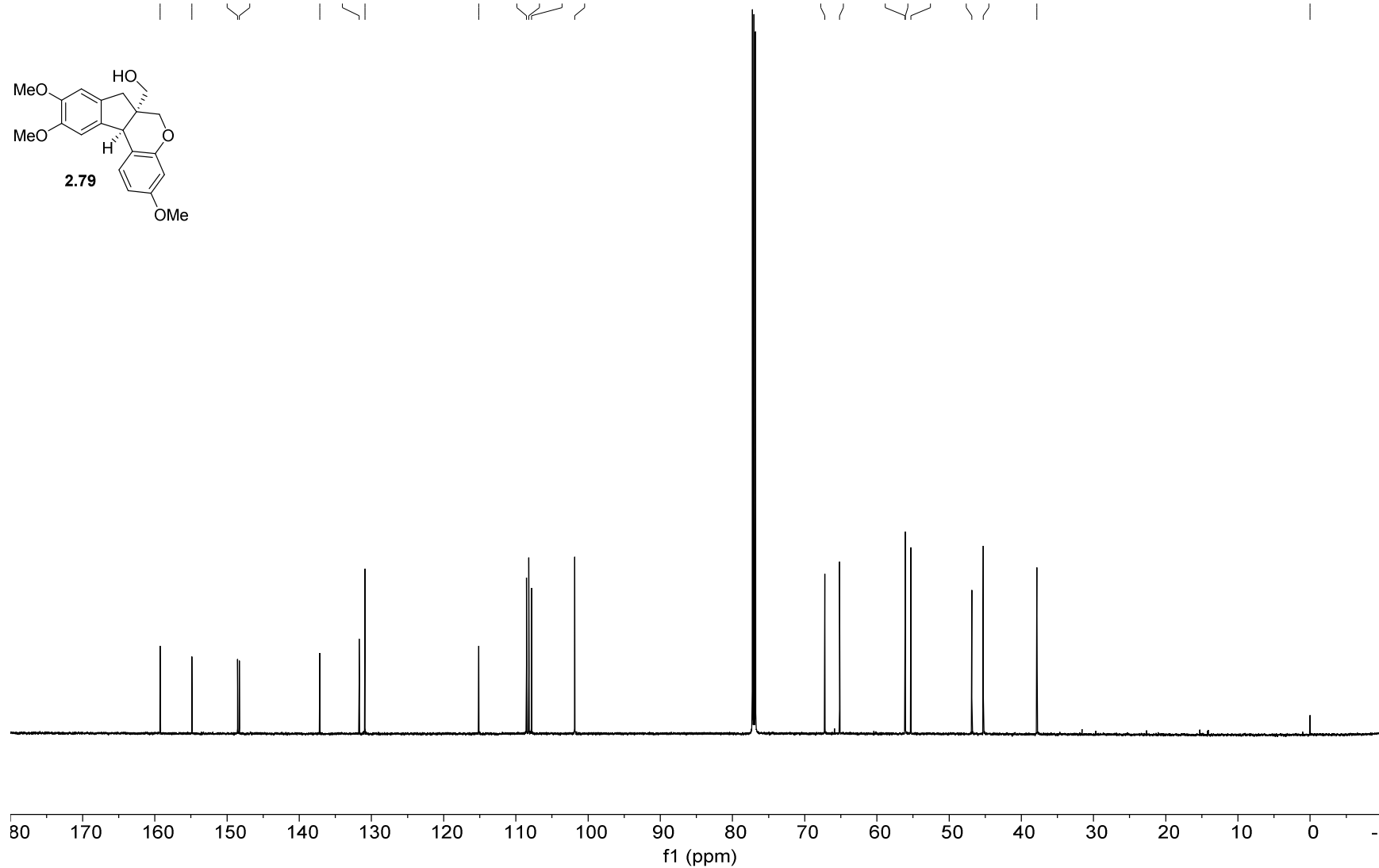
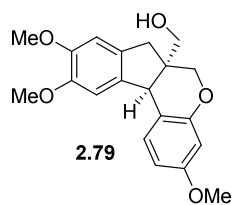
{ 67.22  
65.17

{ 56.10  
56.07  
55.31

{ 46.85  
45.27

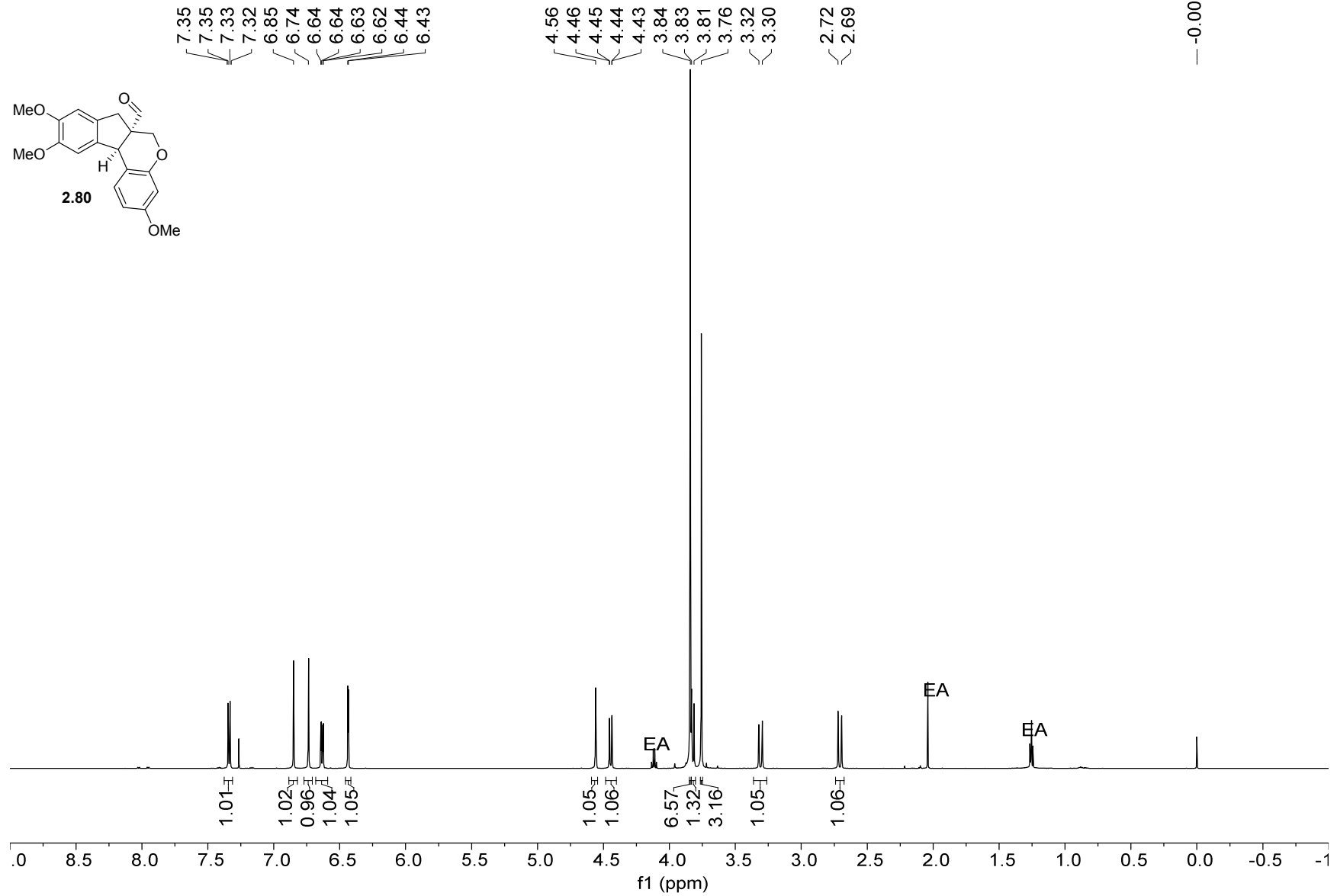
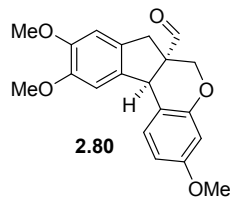
— 37.84

— -0.00



305

1H NMR — 600.13 MHz — CDCl3T — 298.0 K





13C NMR — 150.92 MHz — CDCl3T — 298.0 K

— 201.92

— 159.49

— 154.82

— 148.95

— 148.78

— 135.90

— 130.43

— 129.74

— 113.98

— 108.76

— 108.24

— 107.72

— 102.01

— 65.79

— 56.65

— 56.10

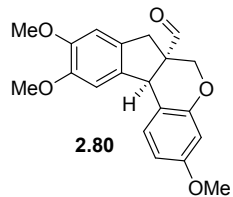
— 56.07

— 55.30

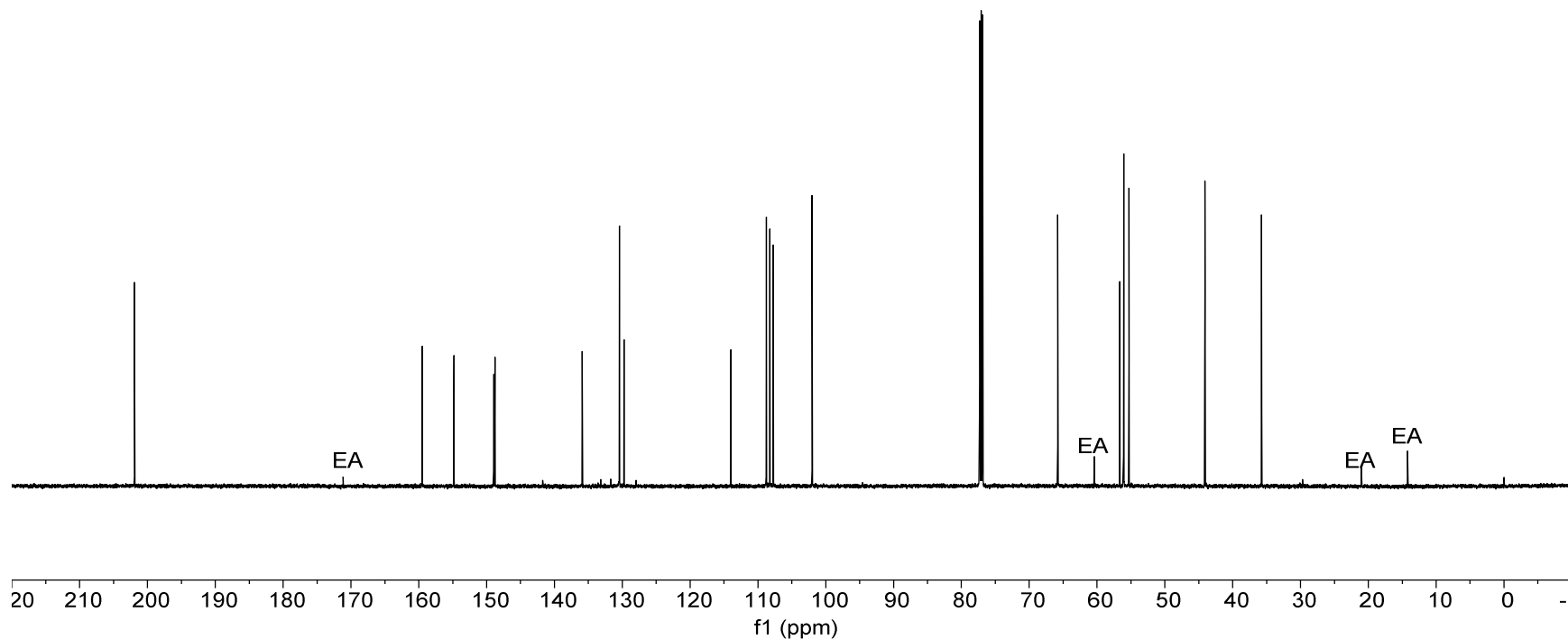
— 44.10

— 35.73

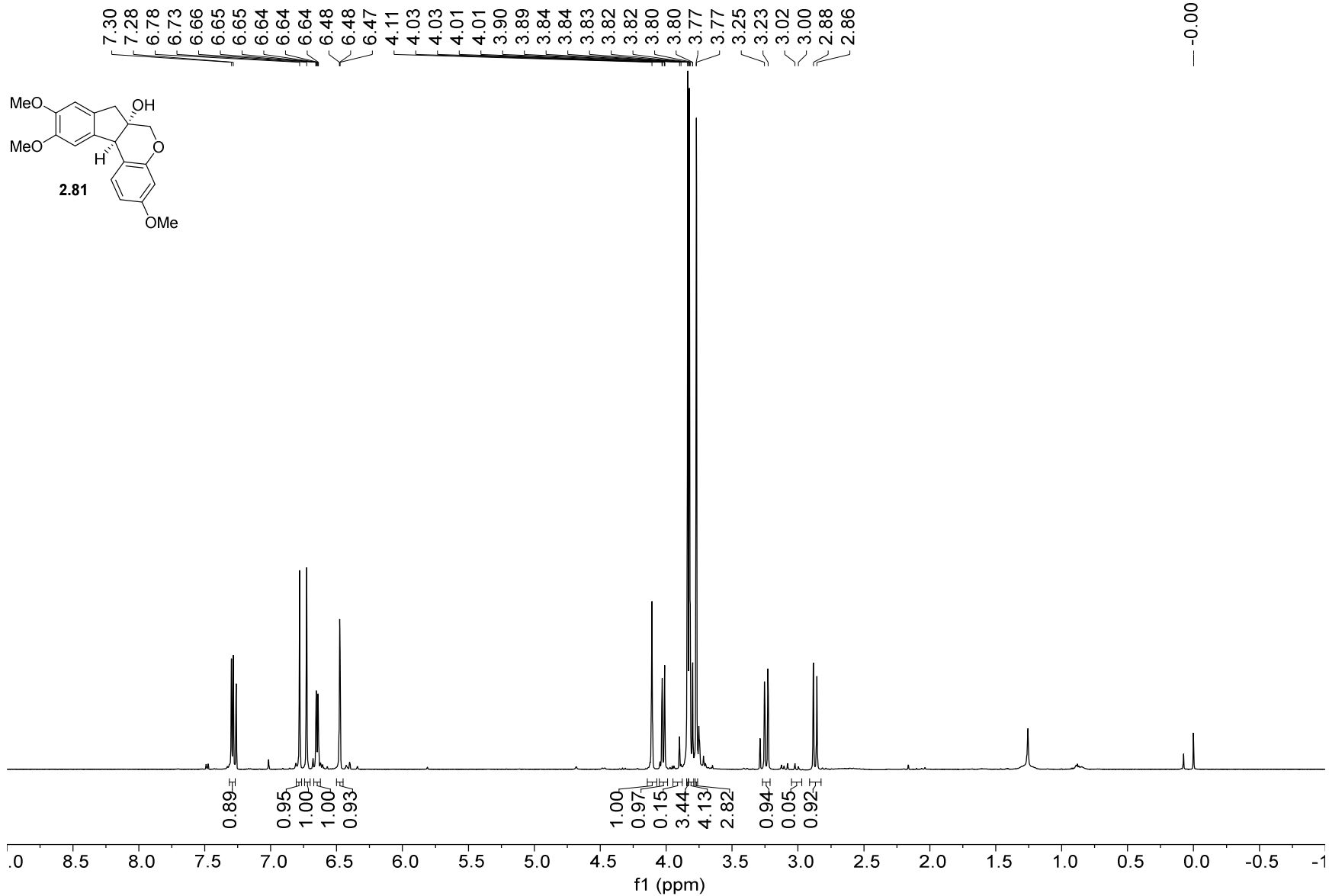
— 0.00



905



1H NMR — 600 MHz — CDCl3T — 298.0 K



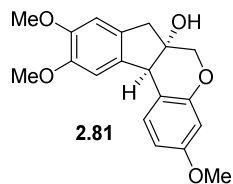
13C NMR — 151 MHz — CDCl3T — 298.0 K

— 159.41  
— 154.37  
— 148.71  
— 148.42  
— 136.11  
— 131.08  
— 130.56

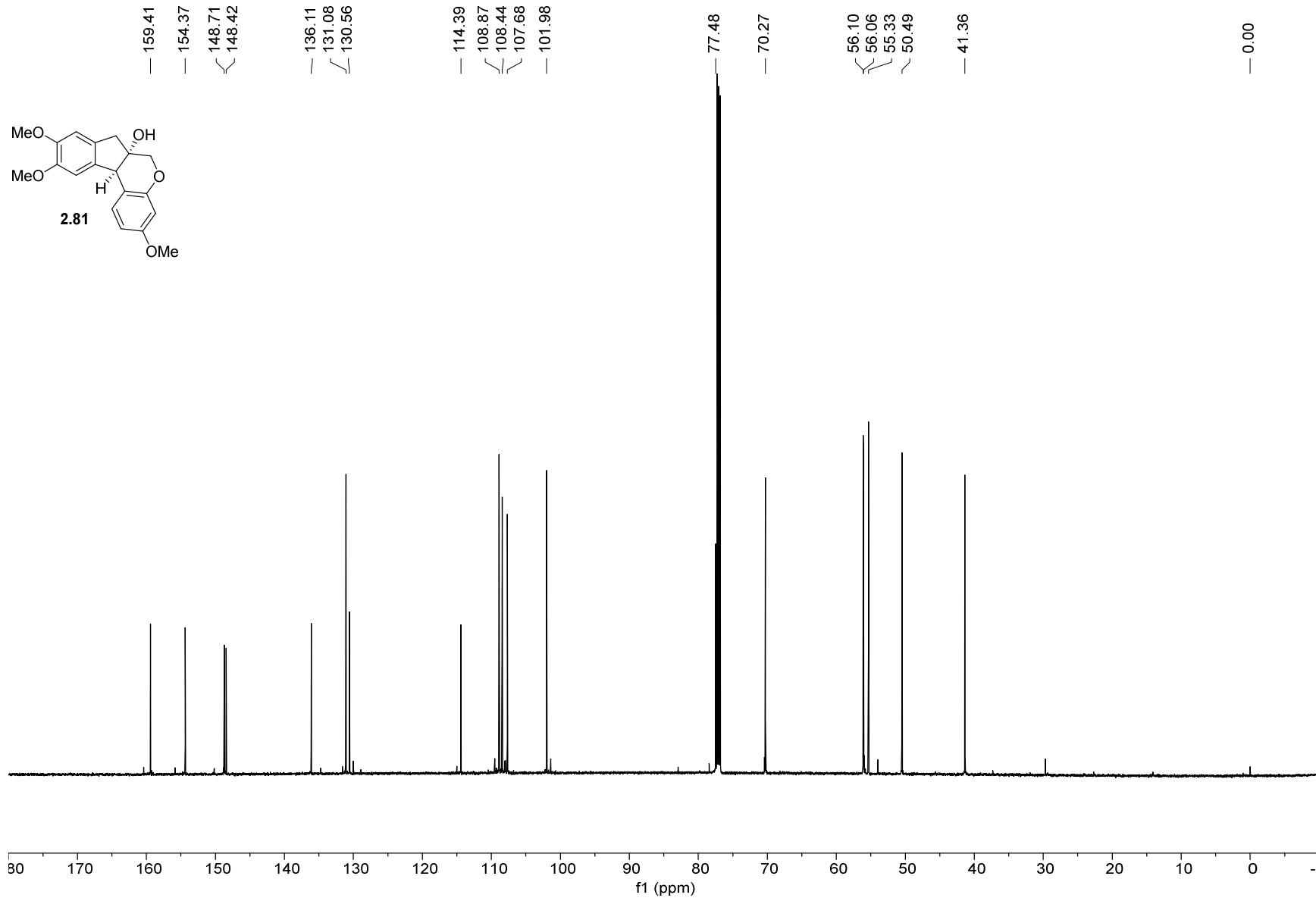
— 114.39  
— 108.87  
— 108.44  
— 107.68  
— 101.98

— 77.48  
— 70.27  
— 56.10  
— 56.06  
— 55.33  
— 50.49  
— 41.36

— 0.00



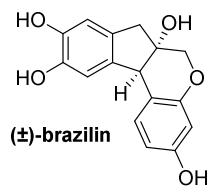
308



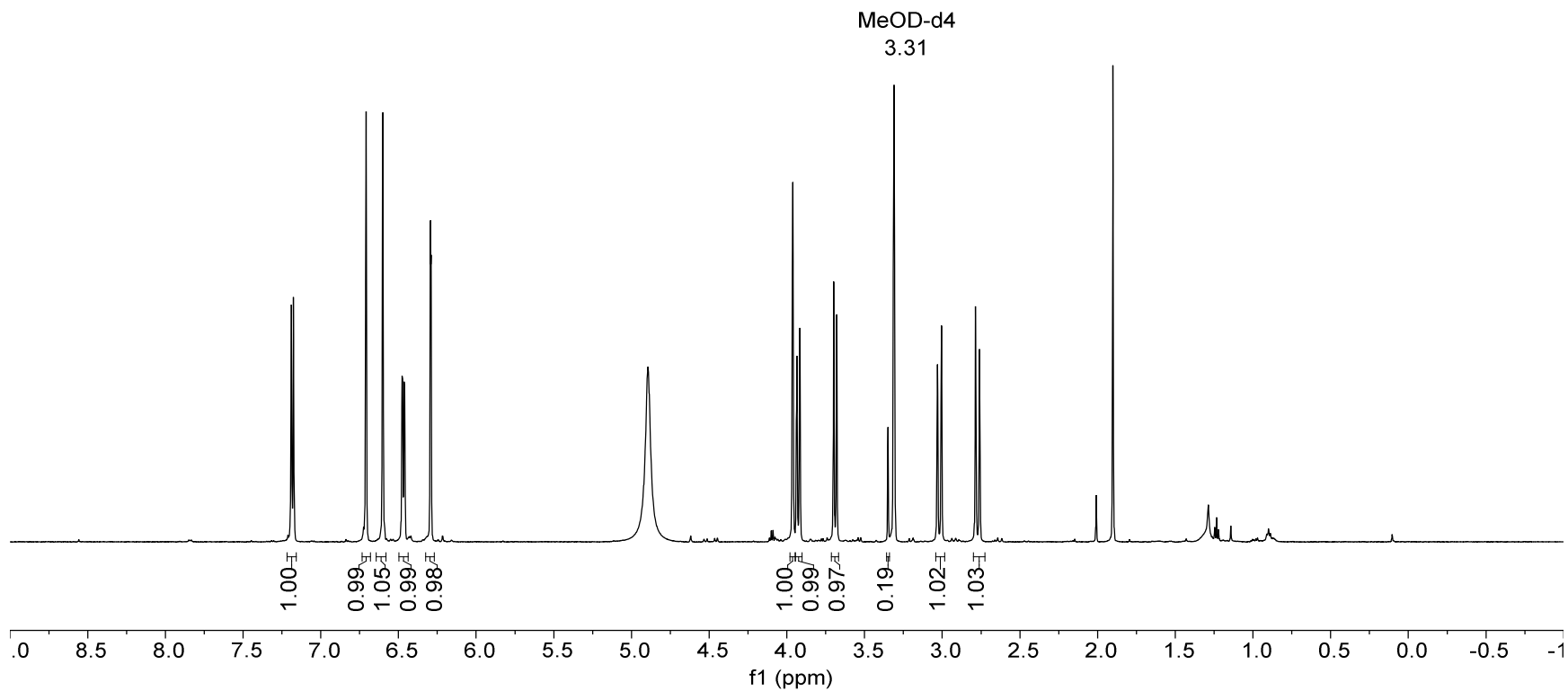
1H NMR — 600 MHz — CD3OD — 298.0 K

7.19  
7.18  
6.71  
6.60  
6.48  
6.47  
6.46  
6.46  
6.29  
6.29

3.96  
3.94  
3.92  
3.70  
3.68  
3.35  
3.31  
3.03  
3.01  
2.79  
2.76



309



13C NMR — 151 MHz — CD3OD — 298.0 K

157.86  
155.71

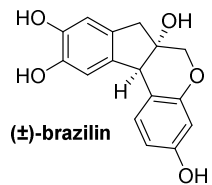
145.65  
145.33

137.44  
132.22  
131.32

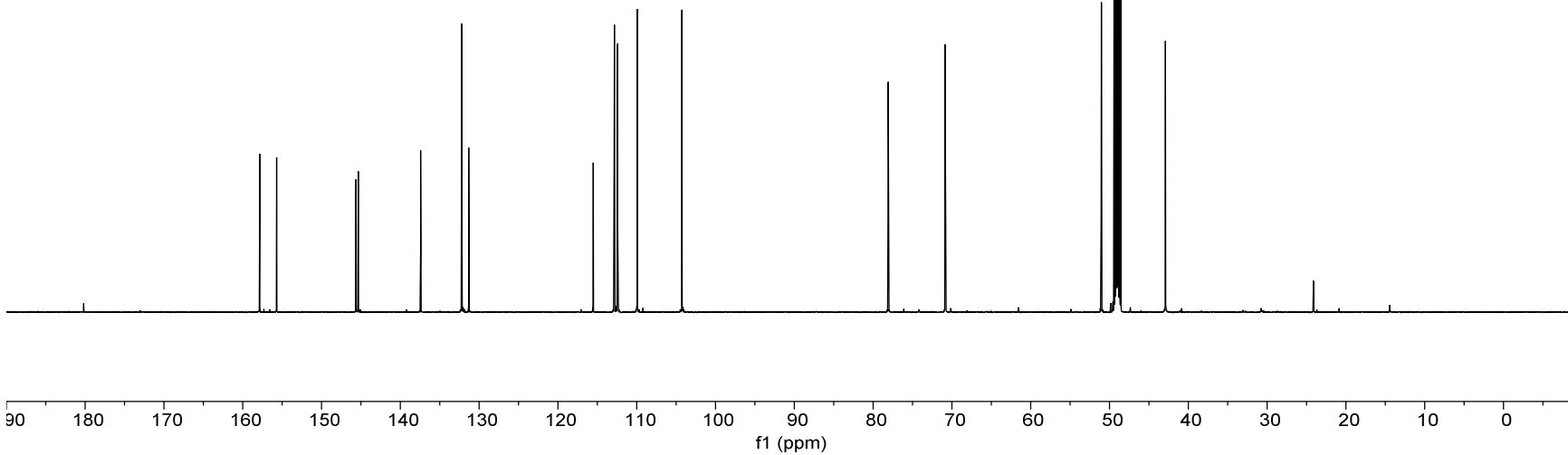
115.54  
112.85  
112.43  
109.95  
104.26

78.07  
70.84

51.04  
49.89  
42.90



MeOD-d4  
49.0



**Appendix B: Chapter 2 – X-Ray Data for Compound S2.62b**

## **X-ray Data Collection, Structure Solution and Refinement for S2.62b**

A colorless crystal of approximate dimensions 0.146 x 0.259 x 0.384 mm was mounted in a cryoloop and transferred to a Bruker SMART APEX II diffractometer. The APEX2<sup>1</sup> program package and the CELL\_NOW<sup>2</sup> were used to determine the unit-cell parameters. Data was collected using a 60 sec/frame scan time for a sphere of diffraction data. The raw frame data was processed using SAINT<sup>3</sup> and TWINABS<sup>4</sup> to yield the reflection data file (HKL 5 format)<sup>4</sup>. Subsequent calculations were carried out using the SHELXTL<sup>5</sup> program. The diffraction symmetry was  $2/m$  and the systematic absences were consistent with the monoclinic space group  $P2_1/n$  that was later determined to be correct.

The structure was solved by dual space methods and refined on  $F^2$  by full-matrix least-squares techniques. The analytical scattering factors<sup>6</sup> for neutral atoms were used throughout the analysis. Hydrogen atoms were included using a riding model. Atom O(1) was disordered and included using multiple components with partial site-occupancy-factors (0.92:0.08).

Least-squares analysis yielded  $wR2 = 0.0967$  and  $Goof = 1.012$  for 346 variables refined against 4576 data (0.83 Å),  $R1 = 0.0437$  for those 3322 with  $I > 2.0\sigma(I)$ . The structure was refined as a two-component twin,  $BASF^5 = 0.147$ .

## **X-Ray Data Collection References**

1. APEX2 Version 2014.11-0, Bruker AXS, Inc.; Madison, WI 2014.
2. Sheldrick, G. M. CELL\_NOW, Version 2008/4, Bruker AXS, Inc.; Madison, WI 2008.
3. SAINT Version 8.34a, Bruker AXS, Inc.; Madison, WI 2013.
4. Sheldrick, G. M. TWINABS, Version 2012/1, Bruker AXS, Inc.; Madison, WI 2012.
5. Sheldrick, G. M. SHELXTL, Version 2014/7, Bruker AXS, Inc.; Madison, WI 2014.

6. International Tables for X-Ray Crystallography 1992, Vol. C., Dordrecht: Kluwer Academic Publishers.

### Definitions

$$wR2 = [\Sigma[w(F_o^2 - F_c^2)^2] / \Sigma[w(F_o^2)^2]]^{1/2}$$

$$R1 = \Sigma||F_o| - |F_c|| / \Sigma|F_o|$$

Goof = S =  $[\Sigma[w(F_o^2 - F_c^2)^2] / (n-p)]^{1/2}$  where n is the number of reflections and p is the total number of parameters refined.

The thermal ellipsoid plot is shown at the 50% probability level.



## checkCIF/PLATON report

Structure factors have been supplied for datablock(s) dvv16

THIS REPORT IS FOR GUIDANCE ONLY. IF USED AS PART OF A REVIEW PROCEDURE FOR PUBLICATION, IT SHOULD NOT REPLACE THE EXPERTISE OF AN EXPERIENCED CRYSTALLOGRAPHIC REFEREE.

No syntax errors found.    CIF dictionary    Interpreting this report

### Datablock: dvv16

---

Bond precision:    C-C = 0.0032 Å                      Wavelength=0.71073

Cell:                      a=19.682(6)            b=5.2523(17)            c=25.856(8)  
                            alpha=90              beta=112.280(5)            gamma=90

Temperature:            133 K

	Calculated	Reported
Volume	2473.3(13)	2473.4(14)
Space group	P 21/n	P 21/n
Hall group	-P 2yn	-P 2yn
Moiety formula	C32 H30 O5	?
Sum formula	C32 H30 O5	C32 H30 O5
Mr	494.56	494.56
Dx, g cm-3	1.328	1.328
Z	4	4
Mu (mm-1)	0.089	0.089
F000	1048.0	1048.0
F000'	1048.51	
h,k,lmax	23,6,31	23,6,31
Nref	4589	4576
Tmin,Tmax	0.973,0.987	0.734,0.862
Tmin'	0.966	

Correction method= # Reported T Limits: Tmin=0.734 Tmax=0.862  
AbsCorr = MULTI-SCAN

Data completeness= 0.997                      Theta(max)= 25.451

R(reflections)= 0.0437( 3322)                      wR2(reflections)= 0.0967( 4576)

S = 1.012    Npar= 346

---

The following ALERTS were generated. Each ALERT has the format  
**test-name\_ALERT\_alert-type\_alert-level**.  
Click on the hyperlinks for more details of the test.

---

**● Alert level C**  
 PLAT234\_ALERT\_4\_C Large Hirshfeld Difference O1B --C1 . 0.21 Ang.  
 PLAT911\_ALERT\_3\_C Missing FCF Refl Between Thmin & STh/L= 0.600 18 Report

---

**● Alert level G**  
 PLAT300\_ALERT\_4\_G Atom Site Occupancy of O1 Constrained at 0.92 Check  
 PLAT300\_ALERT\_4\_G Atom Site Occupancy of O1B Constrained at 0.08 Check  
 PLAT300\_ALERT\_4\_G Atom Site Occupancy of H1A Constrained at 0.92 Check  
 PLAT300\_ALERT\_4\_G Atom Site Occupancy of H1B Constrained at 0.92 Check  
 PLAT300\_ALERT\_4\_G Atom Site Occupancy of H1C Constrained at 0.08 Check  
 PLAT300\_ALERT\_4\_G Atom Site Occupancy of H1D Constrained at 0.08 Check  
 PLAT301\_ALERT\_3\_G Main Residue Disorder .....(Resd 1 ) 3% Note  
 PLAT367\_ALERT\_2\_G Long? C(sp?)-C(sp?) Bond C2 - C3 . 1.51 Ang.  
 PLAT367\_ALERT\_2\_G Long? C(sp?)-C(sp?) Bond C2 - C10 . 1.54 Ang.  
 PLAT398\_ALERT\_2\_G Deviating C-O-C Angle From 120 for O1 60.4 Degree  
 PLAT398\_ALERT\_2\_G Deviating C-O-C Angle From 120 for O1B 62.5 Degree  
 PLAT779\_ALERT\_4\_G Suspect or Irrelevant (Bond) Angle(s) in CIF . # 15 Check  
           C1 -C2 -O1B 1.555 1.555 1.555 43.10 Deg.  
 PLAT793\_ALERT\_4\_G Model has Chirality at C10 (Centro SPGR) S Verify  
 PLAT870\_ALERT\_4\_G ALERTS Related to Twinning Effects Suppressed .. ! Info  
 PLAT910\_ALERT\_3\_G Missing # of FCF Reflection(s) Below Theta(Min). 1 Note  
 PLAT912\_ALERT\_4\_G Missing # of FCF Reflections Above STh/L= 0.600 28 Note  
 PLAT933\_ALERT\_2\_G Number of OMIT Records in Embedded .res File ... 6 Note

---

- 0 **ALERT level A** = Most likely a serious problem - resolve or explain
  - 0 **ALERT level B** = A potentially serious problem, consider carefully
  - 2 **ALERT level C** = Check. Ensure it is not caused by an omission or oversight
  - 17 **ALERT level G** = General information/check it is not something unexpected
- 
- 0 ALERT type 1 CIF construction/syntax error, inconsistent or missing data
  - 5 ALERT type 2 Indicator that the structure model may be wrong or deficient
  - 3 ALERT type 3 Indicator that the structure quality may be low
  - 11 ALERT type 4 Improvement, methodology, query or suggestion
  - 0 ALERT type 5 Informative message, check
-

It is advisable to attempt to resolve as many as possible of the alerts in all categories. Often the minor alerts point to easily fixed oversights, errors and omissions in your CIF or refinement strategy, so attention to these fine details can be worthwhile. In order to resolve some of the more serious problems it may be necessary to carry out additional measurements or structure refinements. However, the purpose of your study may justify the reported deviations and the more serious of these should normally be commented upon in the discussion or experimental section of a paper or in the "special\_details" fields of the CIF. checkCIF was carefully designed to identify outliers and unusual parameters, but every test has its limitations and alerts that are not important in a particular case may appear. Conversely, the absence of alerts does not guarantee there are no aspects of the results needing attention. It is up to the individual to critically assess their own results and, if necessary, seek expert advice.

#### Publication of your CIF in IUCr journals

A basic structural check has been run on your CIF. These basic checks will be run on all CIFs submitted for publication in IUCr journals (*Acta Crystallographica*, *Journal of Applied Crystallography*, *Journal of Synchrotron Radiation*); however, if you intend to submit to *Acta Crystallographica Section C* or *E* or *IUCrData*, you should make sure that full publication checks are run on the final version of your CIF prior to submission.

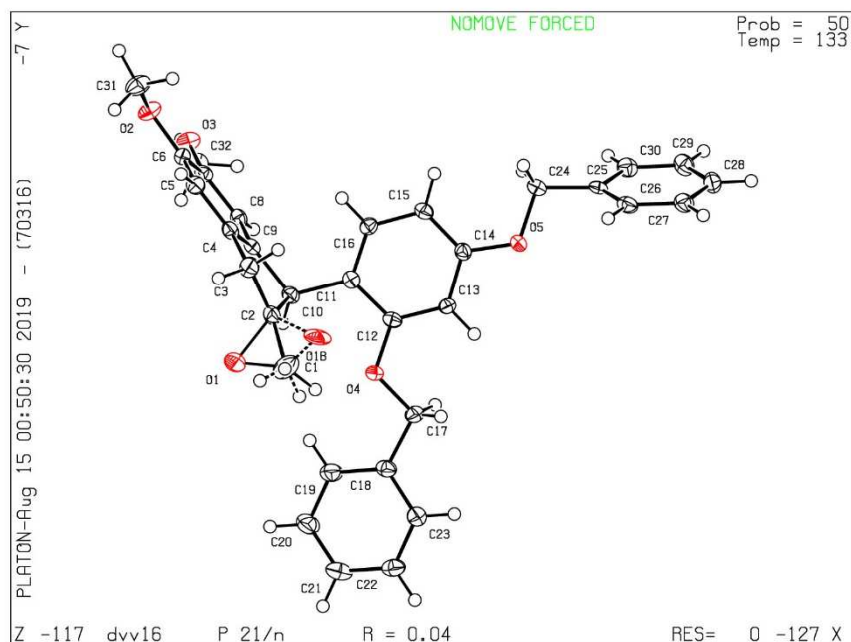
#### Publication of your CIF in other journals

Please refer to the *Notes for Authors* of the relevant journal for any special instructions relating to CIF submission.

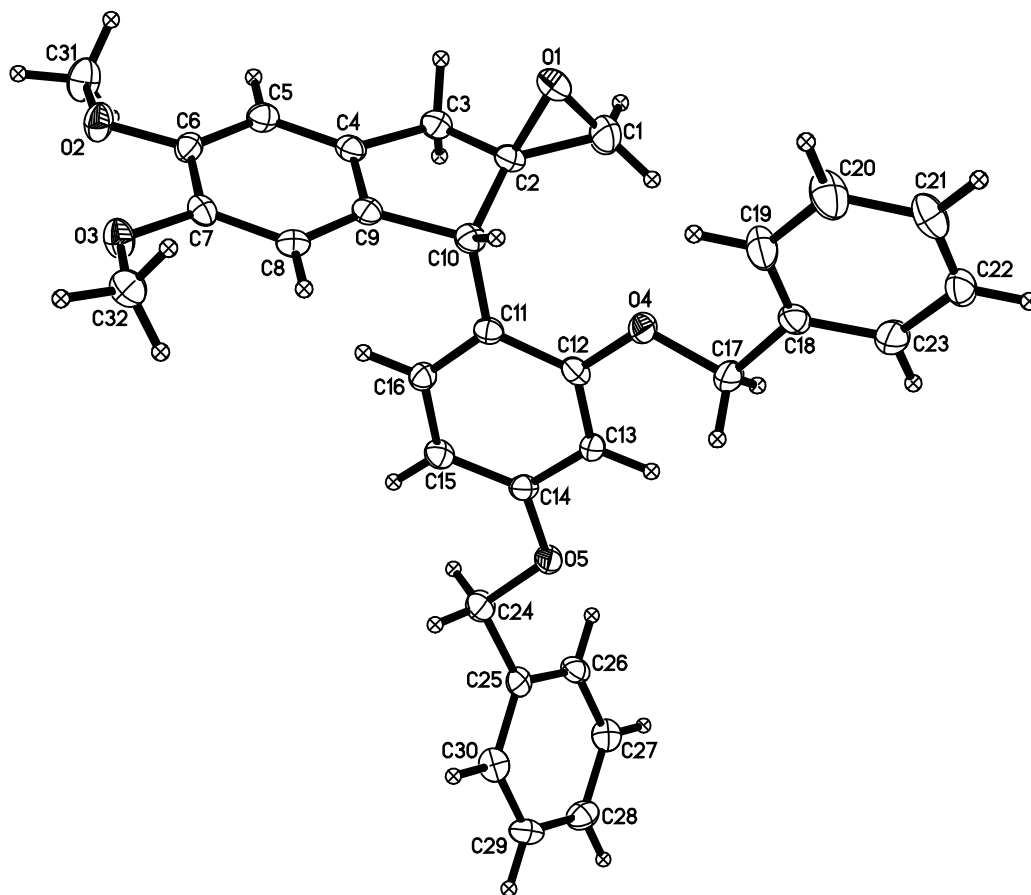
---

PLATON version of 07/08/2019; check.def file version of 30/07/2019

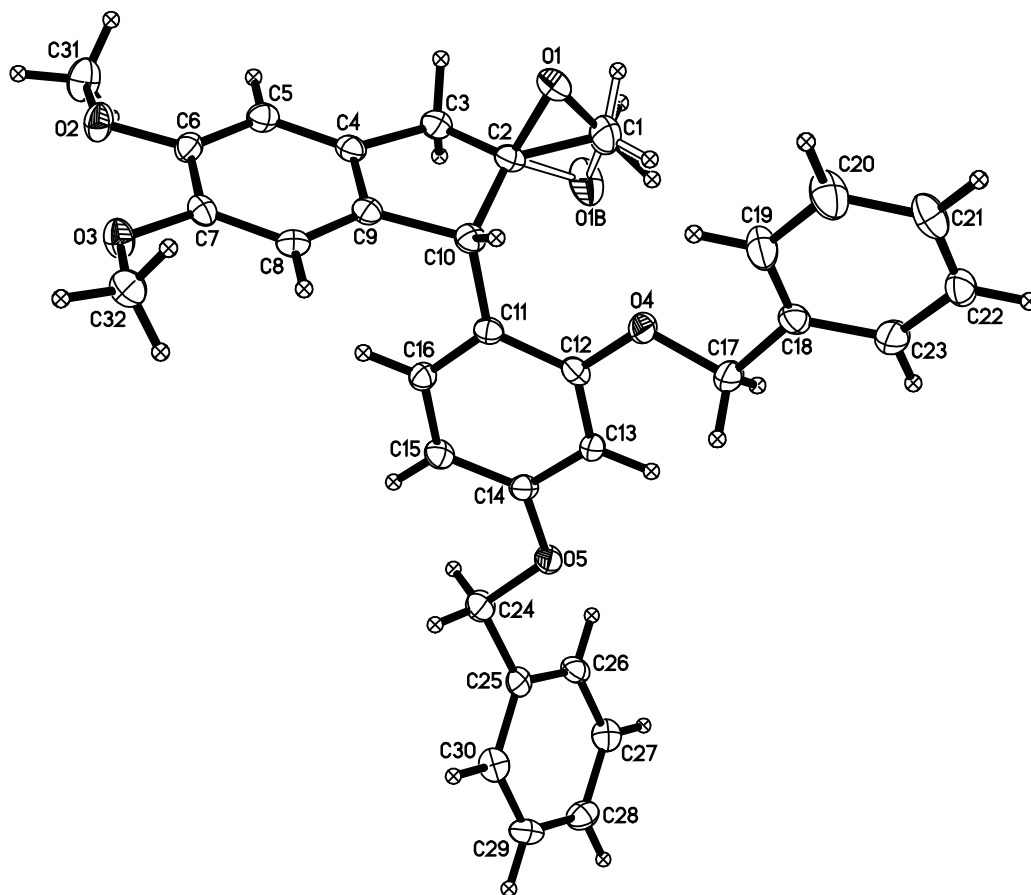
Datablock dvv16 - ellipsoid plot



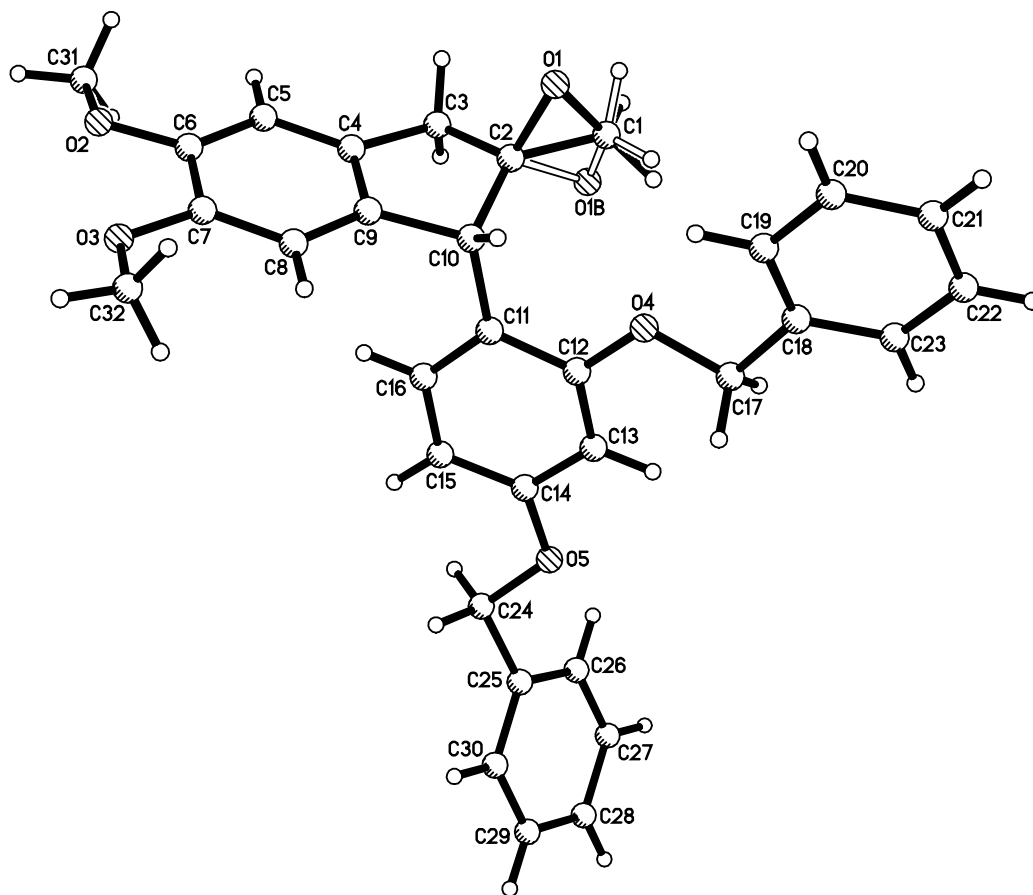
## Plot of Major Component of S2.62b



# Composite Plot of S2.62b



# Composite Plot of S2.62b



## Tables of Structural Analysis of S2.62b

**Table S1.** Crystal data and structure refinement for dvv16 (**S2.62b**).

Identification code	dvv16 (Vanessa Arredondo)	
Empirical formula	C <sub>32</sub> H <sub>30</sub> O <sub>5</sub>	
Formula weight	494.56	
Temperature	133(2) K	
Wavelength	0.71073 Å	
Crystal system	Monoclinic	
Space group	<i>P2<sub>1</sub>/n</i>	
Unit cell dimensions	a = 19.682(6) Å	$\alpha = 90^\circ$ .
	b = 5.2523(17) Å	$\beta = 112.280(5)^\circ$ .
	c = 25.856(8) Å	$\gamma = 90^\circ$ .
Volume	2473.4(14) Å <sup>3</sup>	
Z	4	
Density (calculated)	1.328 Mg/m <sup>3</sup>	
Absorption coefficient	0.089 mm <sup>-1</sup>	
F(000)	1048	
Crystal color	colorless	
Crystal size	0.384 x 0.259 x 0.146 mm <sup>3</sup>	
Theta range for data collection	1.642 to 25.451°	
Index ranges	-23 ≤ <i>h</i> ≤ 21, 0 ≤ <i>k</i> ≤ 6, 0 ≤ <i>l</i> ≤ 31	
Reflections collected	4576	
Completeness to theta = 25.451°	99.2 %	
Absorption correction	Semi-empirical from equivalents	
Max. and min. transmission	0.861965 and 0.734358	
Refinement method	Full-matrix least-squares on F <sup>2</sup>	
Data / restraints / parameters	4576 / 0 / 346	
Goodness-of-fit on F <sup>2</sup>	1.012	
Final R indices [ <i>I</i> > 2σ( <i>I</i> ) = 3322 data]	R1 = 0.0437, wR2 = 0.0846	
R indices (all data, 0.83 Å)	R1 = 0.0778, wR2 = 0.0967	
Largest diff. peak and hole	0.172 and -0.206 e.Å <sup>-3</sup>	

**Table S2.** Atomic coordinates ( $\times 10^4$ ) and equivalent isotropic displacement parameters ( $\text{\AA}^2 \times 10^3$ ) for dvv16 (**S2.62b**).  $U(\text{eq})$  is defined as one third of the trace of the orthogonalized  $U^{ij}$  tensor.

	x	y	z	$U(\text{eq})$
O(1)	1449(1)	2378(4)	7927(1)	34(1)
O(1B)	1420(11)	6280(40)	8363(9)	34(5)
O(2)	4990(1)	2605(3)	8356(1)	25(1)
O(3)	4981(1)	-445(3)	9136(1)	24(1)
O(4)	1355(1)	3217(3)	9323(1)	25(1)
O(5)	2669(1)	9198(3)	10720(1)	22(1)
C(1)	1169(1)	4512(6)	8126(1)	38(1)
C(2)	1958(1)	4118(4)	8329(1)	24(1)
C(3)	2452(1)	5567(4)	8104(1)	24(1)
C(4)	3157(1)	4096(4)	8346(1)	19(1)
C(5)	3763(1)	4187(4)	8193(1)	21(1)
C(6)	4362(1)	2640(4)	8466(1)	19(1)
C(7)	4353(1)	975(4)	8891(1)	18(1)
C(8)	3751(1)	917(4)	9045(1)	18(1)
C(9)	3152(1)	2493(4)	8771(1)	18(1)
C(10)	2444(1)	2815(4)	8878(1)	19(1)
C(11)	2536(1)	4450(4)	9388(1)	17(1)
C(12)	1965(1)	4695(4)	9587(1)	18(1)
C(13)	2025(1)	6330(4)	10020(1)	19(1)
C(14)	2673(1)	7681(4)	10291(1)	18(1)
C(15)	3257(1)	7371(4)	10128(1)	20(1)
C(16)	3173(1)	5768(4)	9677(1)	18(1)
C(17)	827(1)	3039(5)	9576(1)	26(1)
C(18)	235(1)	1210(4)	9247(1)	22(1)
C(19)	341(1)	-615(5)	8900(1)	30(1)
C(20)	-217(1)	-2312(5)	8622(1)	37(1)
C(21)	-877(1)	-2230(5)	8694(1)	29(1)
C(22)	-994(1)	-386(5)	9030(1)	27(1)
C(23)	-438(1)	1321(5)	9304(1)	29(1)
C(24)	3356(1)	10386(5)	11053(1)	26(1)
C(25)	3254(1)	11769(4)	11526(1)	20(1)
C(26)	2776(1)	13815(4)	11417(1)	22(1)
C(27)	2697(1)	15198(4)	11844(1)	24(1)
C(28)	3107(1)	14562(4)	12392(1)	25(1)
C(29)	3589(1)	12531(5)	12510(1)	25(1)
C(30)	3660(1)	11134(4)	12078(1)	24(1)
C(31)	5087(1)	4655(4)	8027(1)	30(1)
C(32)	4941(1)	-2559(4)	9470(1)	24(1)



**Table S2.3.** Bond lengths [Å] and angles [°] for dvv16 (S2.62b).

---

O(1)-C(1)	1.428(3)
O(1)-C(2)	1.460(3)
O(1B)-C(1)	1.12(2)
O(1B)-C(2)	1.58(2)
O(2)-C(6)	1.369(2)
O(2)-C(31)	1.430(3)
O(3)-C(7)	1.376(2)
O(3)-C(32)	1.427(3)
O(4)-C(12)	1.374(2)
O(4)-C(17)	1.424(2)
O(5)-C(14)	1.369(2)
O(5)-C(24)	1.441(3)
C(1)-C(2)	1.453(3)
C(2)-C(3)	1.514(3)
C(2)-C(10)	1.539(3)
C(3)-C(4)	1.501(3)
C(4)-C(9)	1.387(3)
C(4)-C(5)	1.394(3)
C(5)-C(6)	1.385(3)
C(6)-C(7)	1.409(3)
C(7)-C(8)	1.387(3)
C(8)-C(9)	1.394(3)
C(9)-C(10)	1.529(3)
C(10)-C(11)	1.525(3)
C(11)-C(16)	1.378(3)
C(11)-C(12)	1.409(3)
C(12)-C(13)	1.382(3)
C(13)-C(14)	1.395(3)
C(14)-C(15)	1.374(3)
C(15)-C(16)	1.398(3)
C(17)-C(18)	1.500(3)
C(18)-C(19)	1.382(3)
C(18)-C(23)	1.389(3)
C(19)-C(20)	1.385(3)
C(20)-C(21)	1.381(3)
C(21)-C(22)	1.378(3)
C(22)-C(23)	1.384(3)
C(24)-C(25)	1.500(3)
C(25)-C(26)	1.385(3)
C(25)-C(30)	1.388(3)
C(26)-C(27)	1.379(3)
C(27)-C(28)	1.380(3)
C(28)-C(29)	1.383(3)
C(29)-C(30)	1.386(3)
C(1)-O(1)-C(2)	60.40(16)
C(1)-O(1B)-C(2)	62.4(10)
C(6)-O(2)-C(31)	116.64(17)
C(7)-O(3)-C(32)	117.02(16)
C(12)-O(4)-C(17)	117.52(16)
C(14)-O(5)-C(24)	116.33(16)
O(1B)-C(1)-C(2)	74.5(11)
O(1)-C(1)-C(2)	60.86(15)
C(1)-C(2)-O(1)	58.74(16)

C(1)-C(2)-C(3)	123.0(2)
O(1)-C(2)-C(3)	114.16(17)
C(1)-C(2)-C(10)	126.9(2)
O(1)-C(2)-C(10)	113.41(18)
C(3)-C(2)-C(10)	108.22(17)
C(1)-C(2)-O(1B)	43.1(7)
C(3)-C(2)-O(1B)	101.7(7)
C(10)-C(2)-O(1B)	117.6(8)
C(4)-C(3)-C(2)	101.96(18)
C(9)-C(4)-C(5)	120.6(2)
C(9)-C(4)-C(3)	111.12(18)
C(5)-C(4)-C(3)	128.2(2)
C(6)-C(5)-C(4)	119.38(19)
O(2)-C(6)-C(5)	124.24(19)
O(2)-C(6)-C(7)	115.71(19)
C(5)-C(6)-C(7)	120.05(18)
O(3)-C(7)-C(8)	124.94(19)
O(3)-C(7)-C(6)	114.80(17)
C(8)-C(7)-C(6)	120.22(19)
C(7)-C(8)-C(9)	119.40(19)
C(4)-C(9)-C(8)	120.30(18)
C(4)-C(9)-C(10)	110.89(19)
C(8)-C(9)-C(10)	128.79(19)
C(11)-C(10)-C(9)	113.61(17)
C(11)-C(10)-C(2)	112.05(17)
C(9)-C(10)-C(2)	99.91(16)
C(16)-C(11)-C(12)	116.36(19)
C(16)-C(11)-C(10)	122.49(18)
C(12)-C(11)-C(10)	121.15(18)
O(4)-C(12)-C(13)	122.91(18)
O(4)-C(12)-C(11)	115.82(18)
C(13)-C(12)-C(11)	121.27(19)
C(12)-C(13)-C(14)	120.20(19)
O(5)-C(14)-C(15)	125.42(19)
O(5)-C(14)-C(13)	114.61(17)
C(15)-C(14)-C(13)	119.94(19)
C(14)-C(15)-C(16)	118.63(19)
C(11)-C(16)-C(15)	123.41(19)
O(4)-C(17)-C(18)	109.09(17)
C(19)-C(18)-C(23)	118.9(2)
C(19)-C(18)-C(17)	122.43(19)
C(23)-C(18)-C(17)	118.7(2)
C(18)-C(19)-C(20)	119.9(2)
C(21)-C(20)-C(19)	120.8(2)
C(22)-C(21)-C(20)	119.8(2)
C(21)-C(22)-C(23)	119.3(2)
C(22)-C(23)-C(18)	121.3(2)
O(5)-C(24)-C(25)	108.12(17)
C(26)-C(25)-C(30)	118.5(2)
C(26)-C(25)-C(24)	120.10(19)
C(30)-C(25)-C(24)	121.3(2)
C(27)-C(26)-C(25)	121.4(2)
C(26)-C(27)-C(28)	119.7(2)
C(27)-C(28)-C(29)	119.9(2)
C(28)-C(29)-C(30)	120.1(2)
C(29)-C(30)-C(25)	120.5(2)

**Table S4.** Anisotropic displacement parameters ( $\text{\AA}^2 \times 10^3$ ) for dvv16 (**S2.62b**). The anisotropic displacement factor exponent takes the form:  $-2\pi^2 [ h^2 a^{*2} U^{11} + \dots + 2 h k a^* b^* U^{12} ]$

	$U^{11}$	$U^{22}$	$U^{33}$	$U^{23}$	$U^{13}$	$U^{12}$
O(1)	22(1)	52(1)	24(1)	-11(1)	4(1)	-7(1)
O(1B)	25(12)	20(11)	55(14)	-8(11)	12(11)	-14(10)
O(2)	21(1)	27(1)	32(1)	7(1)	15(1)	1(1)
O(3)	20(1)	22(1)	31(1)	8(1)	9(1)	3(1)
O(4)	19(1)	34(1)	23(1)	-10(1)	10(1)	-11(1)
O(5)	18(1)	28(1)	21(1)	-10(1)	6(1)	-4(1)
C(1)	22(1)	61(2)	30(1)	9(2)	9(1)	11(1)
C(2)	19(1)	32(1)	18(1)	-7(1)	3(1)	1(1)
C(3)	22(1)	31(1)	18(1)	2(1)	6(1)	4(1)
C(4)	19(1)	19(1)	16(1)	-3(1)	4(1)	0(1)
C(5)	23(1)	21(1)	19(1)	1(1)	8(1)	-3(1)
C(6)	18(1)	20(1)	21(1)	-4(1)	9(1)	-2(1)
C(7)	16(1)	14(1)	21(1)	-2(1)	3(1)	0(1)
C(8)	23(1)	15(1)	15(1)	0(1)	6(1)	-2(1)
C(9)	18(1)	18(1)	17(1)	-5(1)	5(1)	-4(1)
C(10)	20(1)	18(1)	19(1)	-3(1)	6(1)	-3(1)
C(11)	19(1)	16(1)	16(1)	2(1)	5(1)	1(1)
C(12)	15(1)	20(1)	17(1)	1(1)	5(1)	-2(1)
C(13)	16(1)	26(1)	17(1)	-2(1)	7(1)	-3(1)
C(14)	20(1)	20(1)	15(1)	-1(1)	6(1)	-2(1)
C(15)	19(1)	18(1)	20(1)	-2(1)	6(1)	-4(1)
C(16)	18(1)	20(1)	18(1)	2(1)	8(1)	1(1)
C(17)	22(1)	39(2)	22(1)	-6(1)	12(1)	-9(1)
C(18)	20(1)	26(1)	17(1)	2(1)	5(1)	-6(1)
C(19)	18(1)	31(1)	40(1)	-8(1)	9(1)	-2(1)
C(20)	27(1)	30(1)	51(2)	-18(1)	11(1)	-5(1)
C(21)	21(1)	23(1)	36(1)	2(1)	3(1)	-4(1)
C(22)	20(1)	34(1)	26(1)	4(1)	8(1)	-6(1)
C(23)	27(1)	36(1)	26(1)	-8(1)	12(1)	-8(1)
C(24)	20(1)	33(1)	25(1)	-10(1)	8(1)	-9(1)
C(25)	16(1)	21(1)	23(1)	-6(1)	7(1)	-9(1)
C(26)	20(1)	27(1)	18(1)	0(1)	3(1)	-6(1)
C(27)	24(1)	19(1)	29(1)	-4(1)	10(1)	-2(1)
C(28)	31(1)	24(1)	24(1)	-6(1)	13(1)	-4(1)
C(29)	30(1)	27(1)	16(1)	2(1)	5(1)	-1(1)
C(30)	24(1)	18(1)	29(1)	-1(1)	9(1)	0(1)
C(31)	29(1)	25(1)	42(2)	7(1)	21(1)	-2(1)
C(32)	26(1)	20(1)	26(1)	4(1)	7(1)	2(1)

**Table S5.** Hydrogen coordinates ( $\times 10^4$ ) and isotropic displacement parameters ( $\text{\AA}^2 \times 10^3$ ) for dvv16 (**S2.62b**).

	x	y	z	U(eq)
H(1A)	921	4175	8389	46
H(1B)	960	5941	7864	46
H(1C)	914	4706	7717	46
H(1D)	898	3419	8295	46
H(3A)	2256	5545	7691	29
H(3B)	2518	7354	8236	29
H(5A)	3766	5299	7904	25
H(8A)	3746	-187	9335	22
H(10A)	2237	1113	8912	23
H(13A)	1623	6534	10135	23
H(15A)	3708	8229	10319	24
H(16A)	3576	5576	9563	22
H(17A)	611	4736	9581	32
H(17B)	1066	2435	9966	32
H(19A)	796	-706	8852	36
H(20A)	-144	-3547	8379	44
H(21A)	-1250	-3441	8512	35
H(22A)	-1451	-288	9073	32
H(23A)	-519	2595	9535	35
H(24A)	3505	11597	10822	32
H(24B)	3745	9081	11201	32
H(26A)	2497	14275	11041	27
H(27A)	2362	16583	11761	29
H(28A)	3059	15517	12688	30
H(29A)	3873	12093	12887	30
H(30A)	3989	9731	12161	28
H(31A)	5582	4577	8023	45
H(31B)	5022	6280	8189	45
H(31C)	4723	4513	7644	45
H(32A)	5398	-3539	9583	37
H(32B)	4527	-3649	9254	37
H(32C)	4871	-1939	9804	37

**Table S6.** Torsion angles [°] for dvv16 (**S2.62b**).

O(1B)-C(1)-C(2)-C(3)	-70.1(12)
O(1)-C(1)-C(2)-C(3)	100.2(2)
O(1B)-C(1)-C(2)-C(10)	92.6(12)
O(1)-C(1)-C(2)-C(10)	-97.2(3)
C(1)-O(1)-C(2)-C(3)	-115.2(2)
C(1)-O(1)-C(2)-C(10)	120.2(2)
C(1)-O(1B)-C(2)-C(3)	126.4(8)
C(1)-O(1B)-C(2)-C(10)	-115.7(8)
C(1)-C(2)-C(3)-C(4)	-168.0(2)
O(1)-C(2)-C(3)-C(4)	-100.7(2)
C(10)-C(2)-C(3)-C(4)	26.6(2)
O(1B)-C(2)-C(3)-C(4)	151.0(8)
C(2)-C(3)-C(4)-C(9)	-14.8(2)
C(2)-C(3)-C(4)-C(5)	165.0(2)
C(9)-C(4)-C(5)-C(6)	0.5(3)
C(3)-C(4)-C(5)-C(6)	-179.2(2)
C(31)-O(2)-C(6)-C(5)	13.7(3)
C(31)-O(2)-C(6)-C(7)	-165.88(19)
C(4)-C(5)-C(6)-O(2)	-178.9(2)
C(4)-C(5)-C(6)-C(7)	0.6(3)
C(32)-O(3)-C(7)-C(8)	16.4(3)
C(32)-O(3)-C(7)-C(6)	-165.77(18)
O(2)-C(6)-C(7)-O(3)	0.2(3)
C(5)-C(6)-C(7)-O(3)	-179.33(19)
O(2)-C(6)-C(7)-C(8)	178.20(19)
C(5)-C(6)-C(7)-C(8)	-1.4(3)
O(3)-C(7)-C(8)-C(9)	178.65(19)
C(6)-C(7)-C(8)-C(9)	0.9(3)
C(5)-C(4)-C(9)-C(8)	-1.0(3)
C(3)-C(4)-C(9)-C(8)	178.78(19)
C(5)-C(4)-C(9)-C(10)	177.61(19)
C(3)-C(4)-C(9)-C(10)	-2.6(3)
C(7)-C(8)-C(9)-C(4)	0.3(3)
C(7)-C(8)-C(9)-C(10)	-178.1(2)
C(4)-C(9)-C(10)-C(11)	-101.1(2)
C(8)-C(9)-C(10)-C(11)	77.4(3)
C(4)-C(9)-C(10)-C(2)	18.4(2)
C(8)-C(9)-C(10)-C(2)	-163.2(2)
C(1)-C(2)-C(10)-C(11)	-71.6(3)
O(1)-C(2)-C(10)-C(11)	-139.16(18)
C(3)-C(2)-C(10)-C(11)	93.1(2)
O(1B)-C(2)-C(10)-C(11)	-21.3(8)
C(1)-C(2)-C(10)-C(9)	167.8(2)
O(1)-C(2)-C(10)-C(9)	100.21(19)
C(3)-C(2)-C(10)-C(9)	-27.5(2)
O(1B)-C(2)-C(10)-C(9)	-141.9(8)
C(9)-C(10)-C(11)-C(16)	7.9(3)
C(2)-C(10)-C(11)-C(16)	-104.4(2)
C(9)-C(10)-C(11)-C(12)	-172.32(19)
C(2)-C(10)-C(11)-C(12)	75.4(2)
C(17)-O(4)-C(12)-C(13)	-11.5(3)
C(17)-O(4)-C(12)-C(11)	168.45(19)
C(16)-C(11)-C(12)-O(4)	-175.03(18)
C(10)-C(11)-C(12)-O(4)	5.2(3)

C(16)-C(11)-C(12)-C(13)	4.9(3)
C(10)-C(11)-C(12)-C(13)	-174.86(19)
O(4)-C(12)-C(13)-C(14)	176.61(19)
C(11)-C(12)-C(13)-C(14)	-3.3(3)
C(24)-O(5)-C(14)-C(15)	-5.4(3)
C(24)-O(5)-C(14)-C(13)	172.80(19)
C(12)-C(13)-C(14)-O(5)	-178.80(18)
C(12)-C(13)-C(14)-C(15)	-0.5(3)
O(5)-C(14)-C(15)-C(16)	-179.41(19)
C(13)-C(14)-C(15)-C(16)	2.5(3)
C(12)-C(11)-C(16)-C(15)	-2.9(3)
C(10)-C(11)-C(16)-C(15)	176.88(19)
C(14)-C(15)-C(16)-C(11)	-0.8(3)
C(12)-O(4)-C(17)-C(18)	-176.17(17)
O(4)-C(17)-C(18)-C(19)	21.3(3)
O(4)-C(17)-C(18)-C(23)	-160.2(2)
C(23)-C(18)-C(19)-C(20)	-0.8(3)
C(17)-C(18)-C(19)-C(20)	177.7(2)
C(18)-C(19)-C(20)-C(21)	-1.0(4)
C(19)-C(20)-C(21)-C(22)	2.3(4)
C(20)-C(21)-C(22)-C(23)	-1.7(4)
C(21)-C(22)-C(23)-C(18)	-0.1(4)
C(19)-C(18)-C(23)-C(22)	1.4(3)
C(17)-C(18)-C(23)-C(22)	-177.2(2)
C(14)-O(5)-C(24)-C(25)	-175.24(18)
O(5)-C(24)-C(25)-C(26)	-64.7(3)
O(5)-C(24)-C(25)-C(30)	118.9(2)
C(30)-C(25)-C(26)-C(27)	-0.3(3)
C(24)-C(25)-C(26)-C(27)	-176.9(2)
C(25)-C(26)-C(27)-C(28)	0.8(3)
C(26)-C(27)-C(28)-C(29)	-0.6(3)
C(27)-C(28)-C(29)-C(30)	-0.1(3)
C(28)-C(29)-C(30)-C(25)	0.6(3)
C(26)-C(25)-C(30)-C(29)	-0.3(3)
C(24)-C(25)-C(30)-C(29)	176.1(2)

---

## **Appendix C: Chapter 3 – NMR**

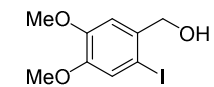
1H NMR — 600.13 MHz — CDCl3T — 298.1 K

7.22  
7.01

4.62  
4.61

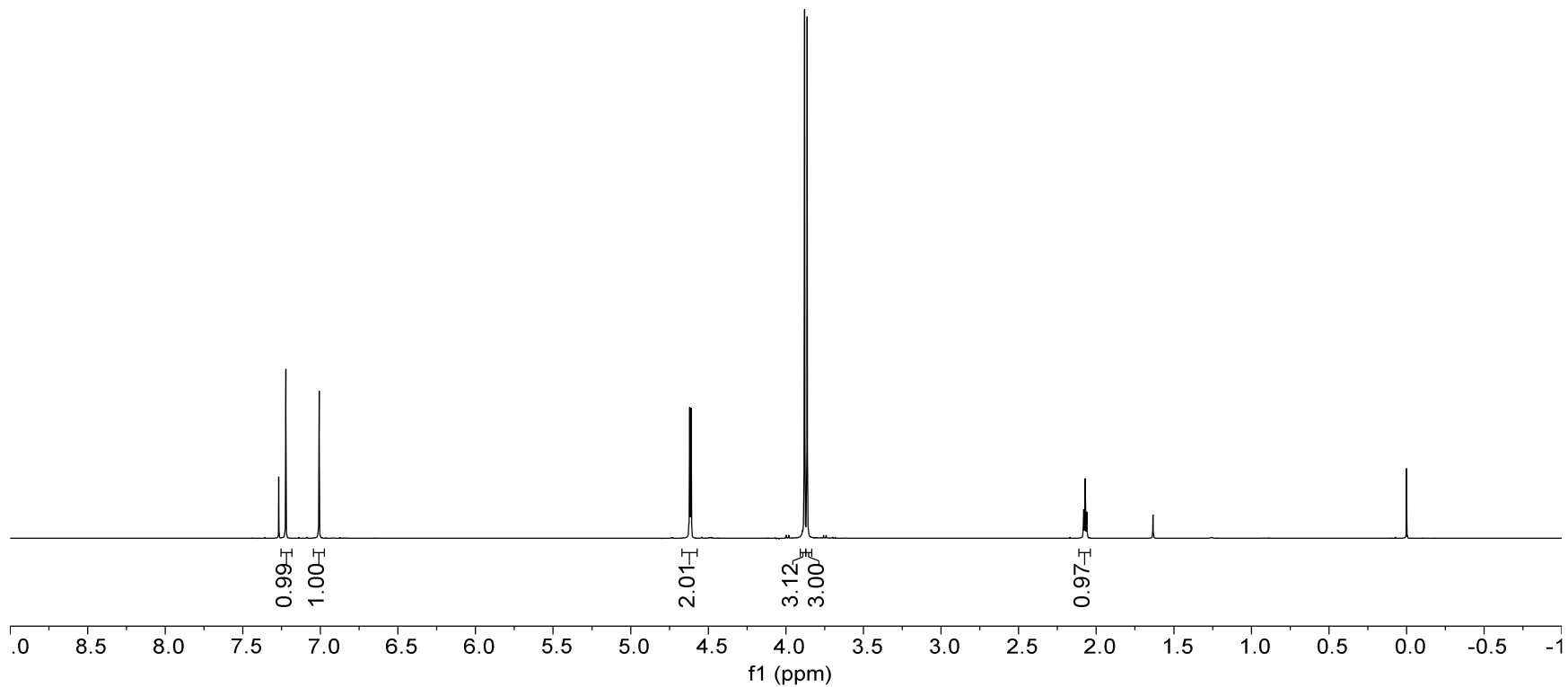
3.88  
3.86

2.08  
2.07  
2.06



2-iodo-4,5-dimethoxybenzyl alcohol

329





13C NMR — 150.92 MHz — CDCl3T — 298.0 K

149.51  
148.94

135.25

121.47

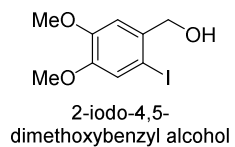
111.67

85.40

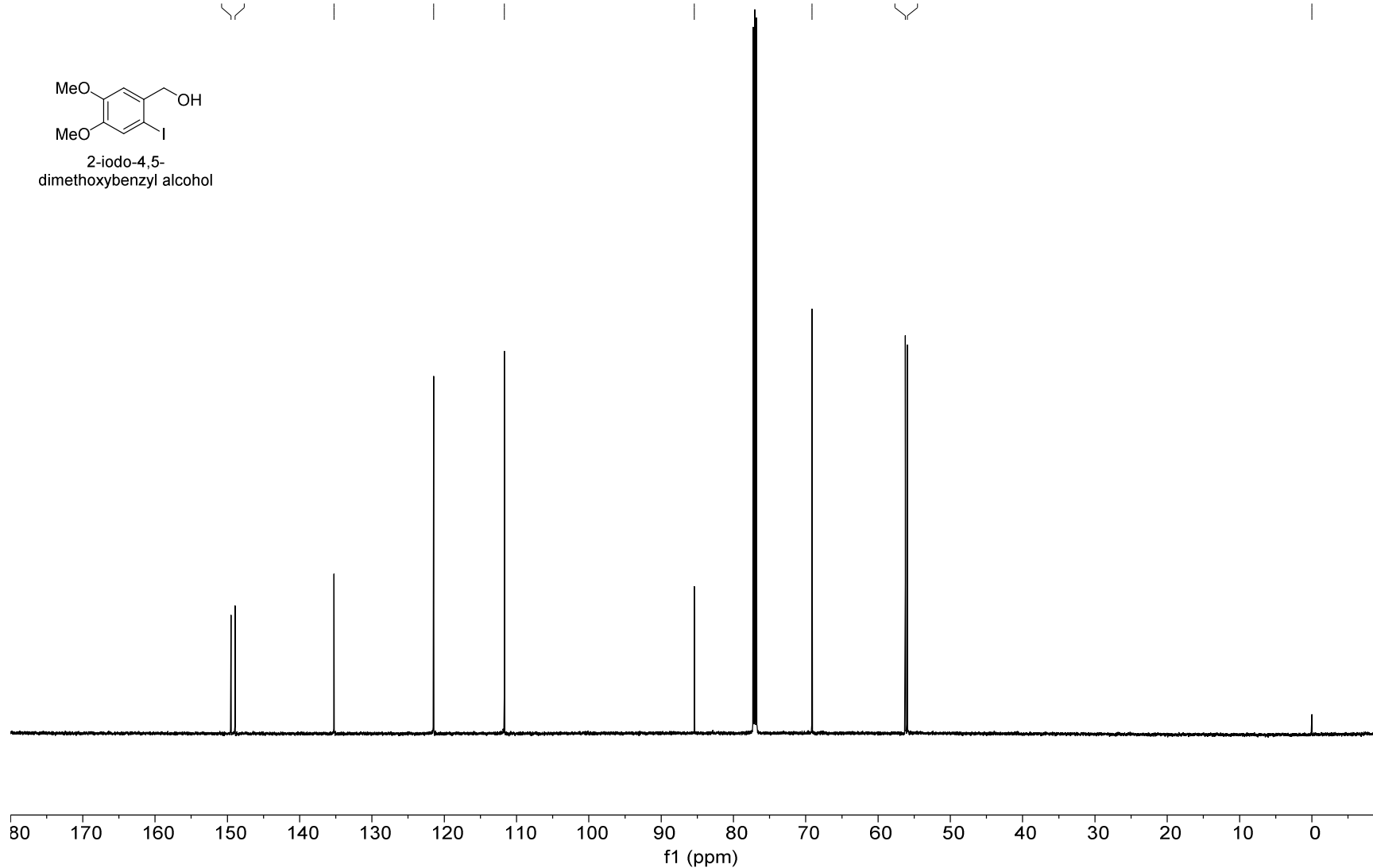
69.13

56.23  
55.96

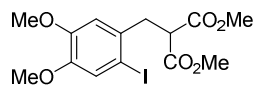
0.00



330



1H NMR — 600.13 MHz — CDCl3T — 298.0 K



3.1

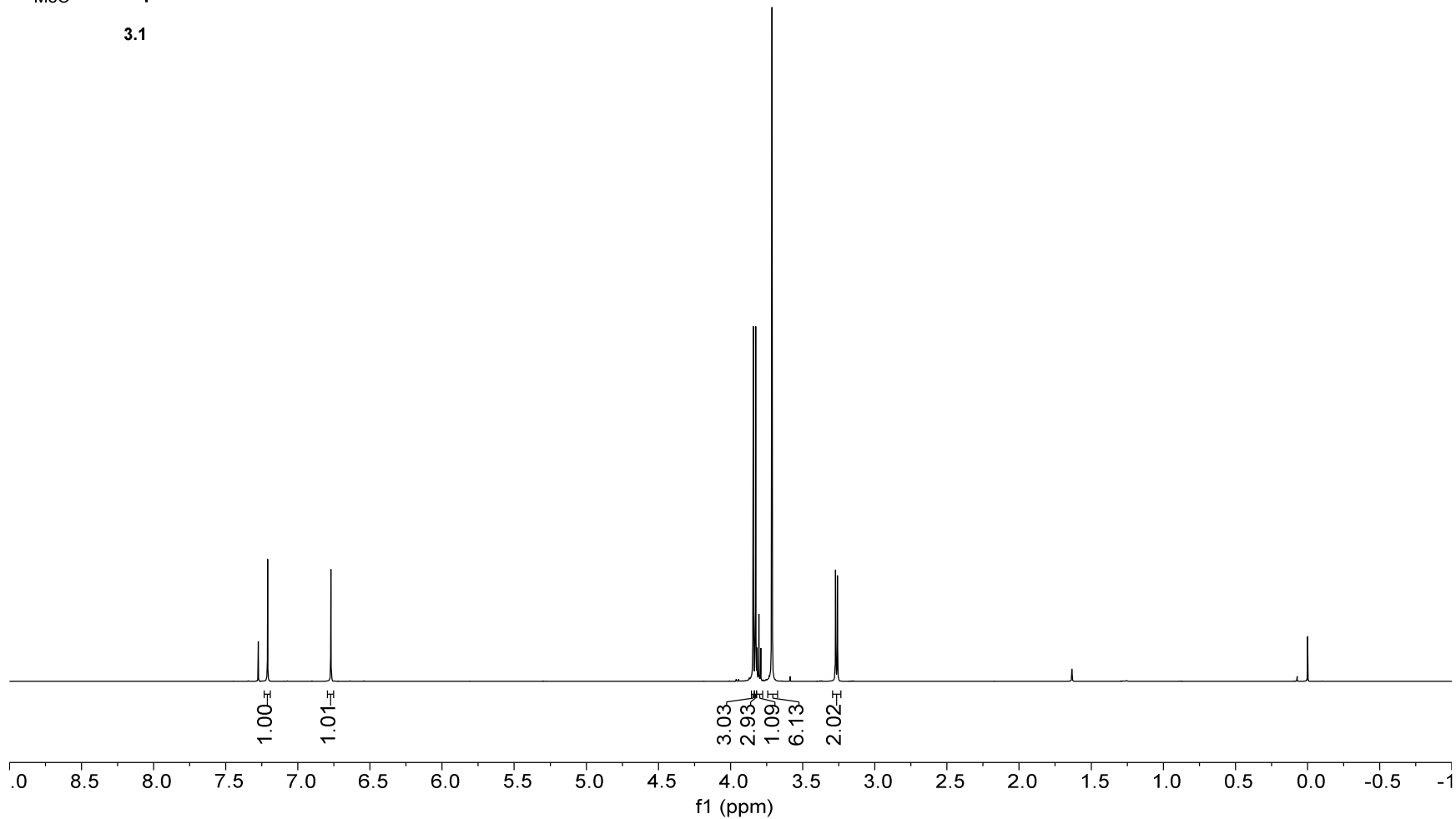
7.21

6.77

3.84  
3.83  
3.82  
3.80  
3.79  
3.71  
3.27  
3.26

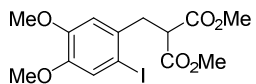
0.00

331



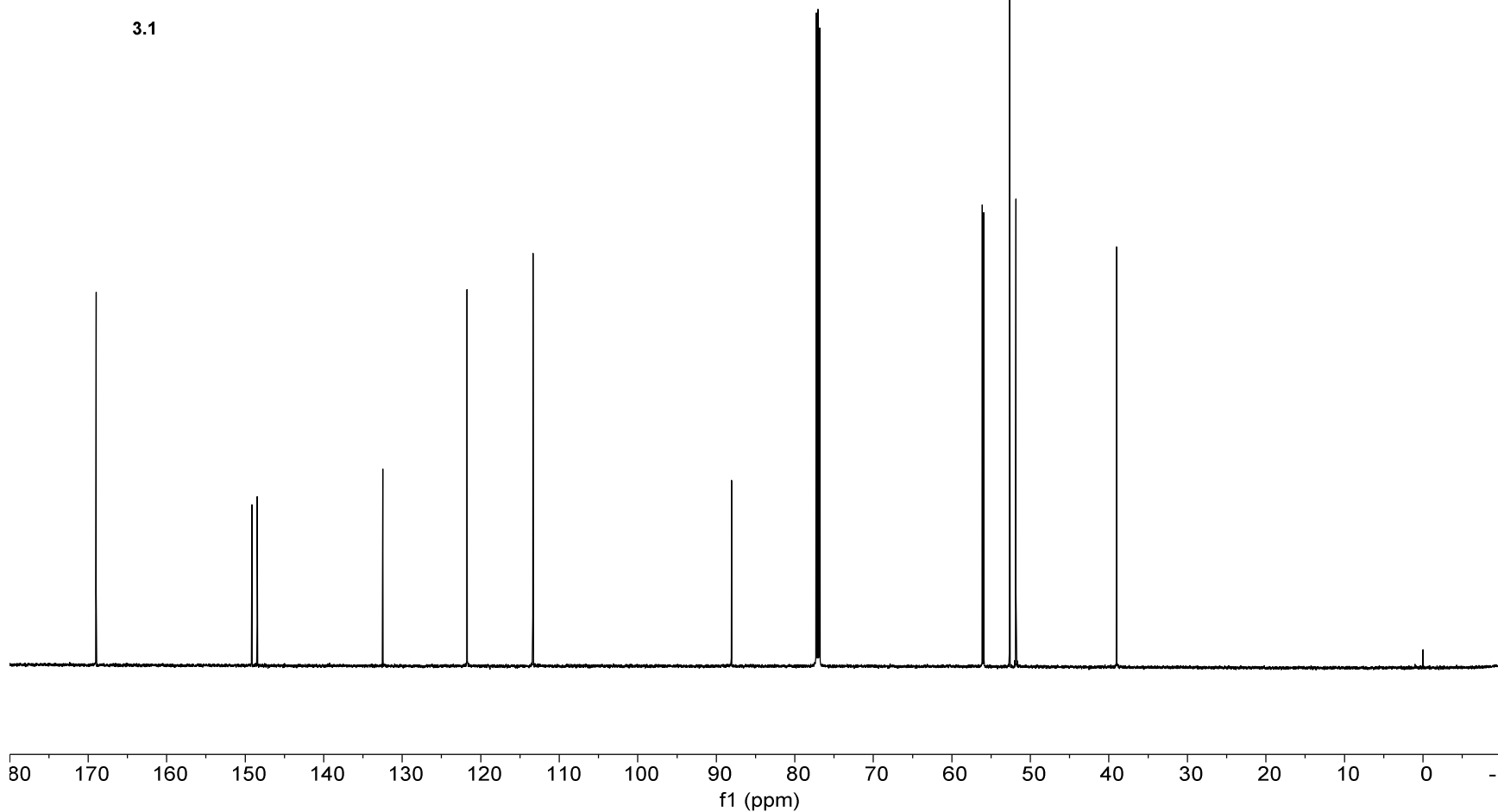
13C NMR — 150.92 MHz — CDCl3T — 298.0 K

168.98  
149.15  
148.46  
132.48  
121.74  
113.35  
88.07  
56.11  
55.94  
52.63  
51.84  
39.02  
-0.00



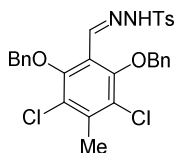
3.1

332



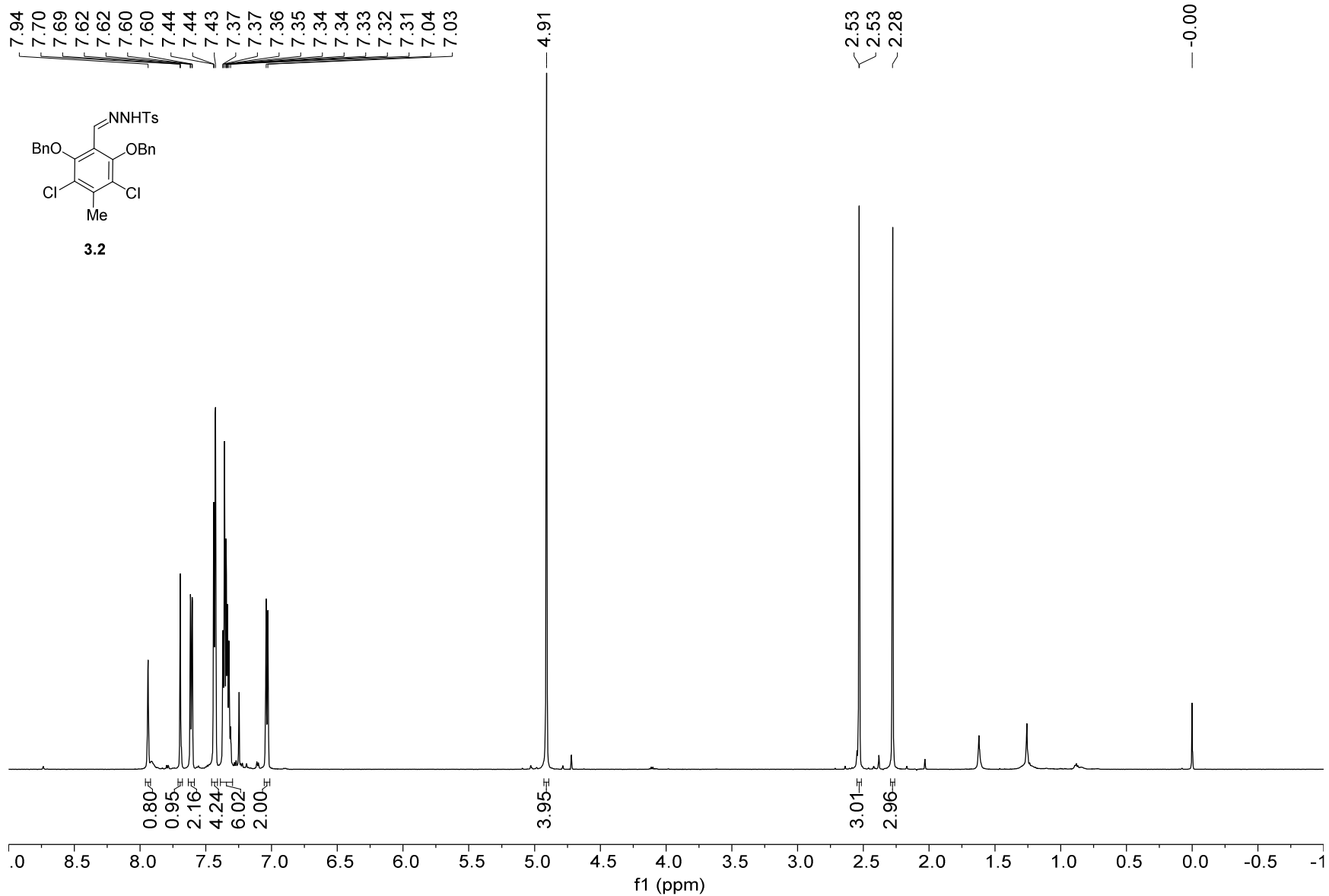
1H NMR — 600.13 MHz — CDCl3T — 298.0 K

7.94  
7.70  
7.69  
7.62  
7.62  
7.60  
7.60  
7.44  
7.44  
7.43  
7.37  
7.37  
7.36  
7.35  
7.34  
7.34  
7.33  
7.32  
7.31  
7.04  
7.03

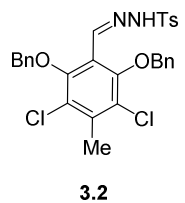


3.2

333



13C NMR — 150.92 MHz — CDCl3T — 298.0 K



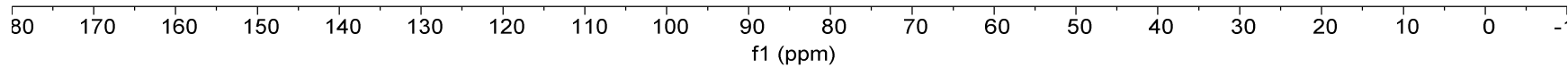
152.29  
144.08  
141.56  
138.35  
136.30  
135.20  
129.56  
128.50  
128.48  
128.41  
128.38  
127.80  
126.13  
121.80

75.97

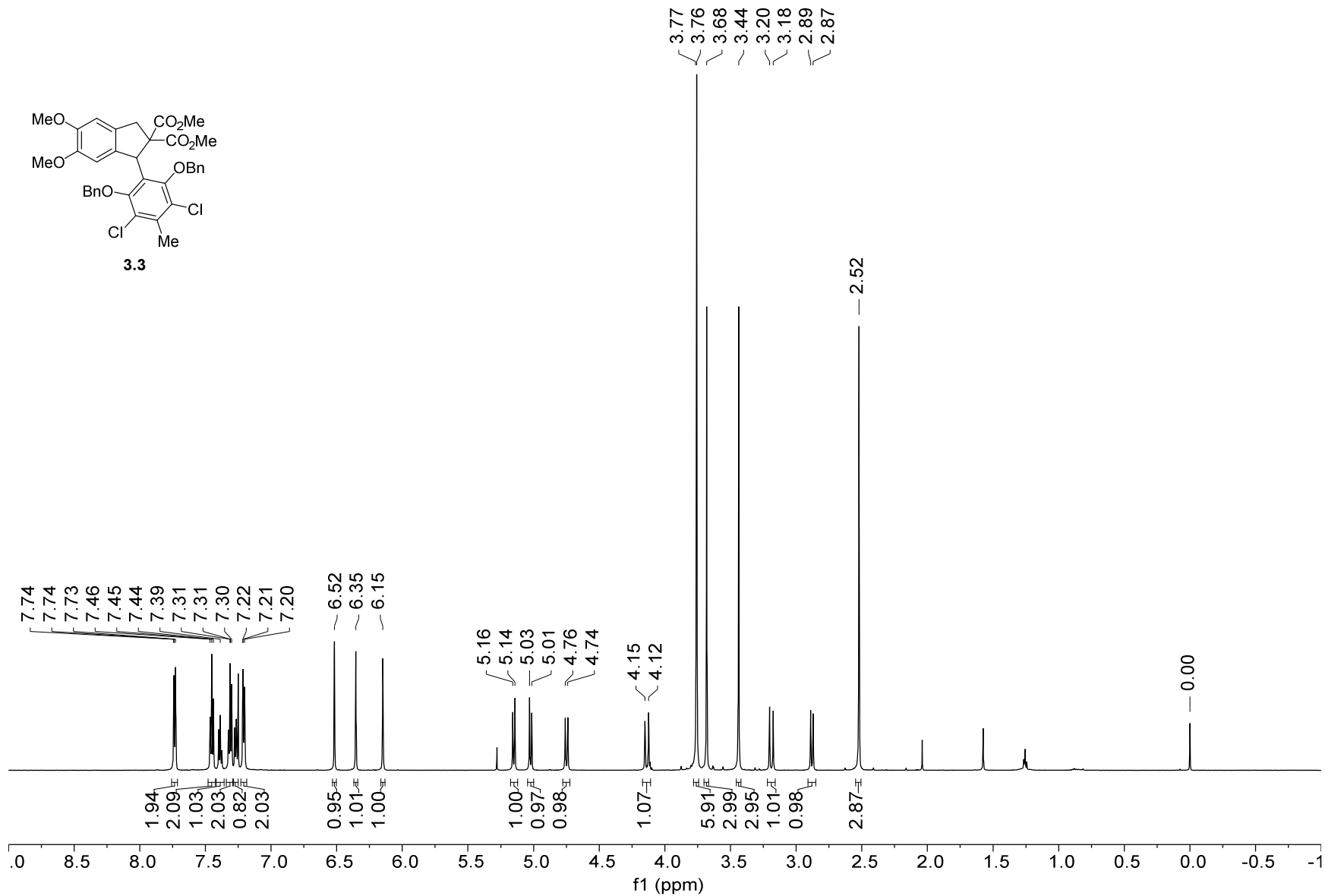
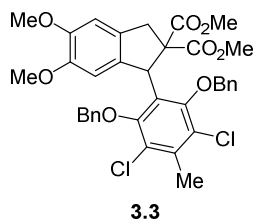
21.52  
18.66

-0.00

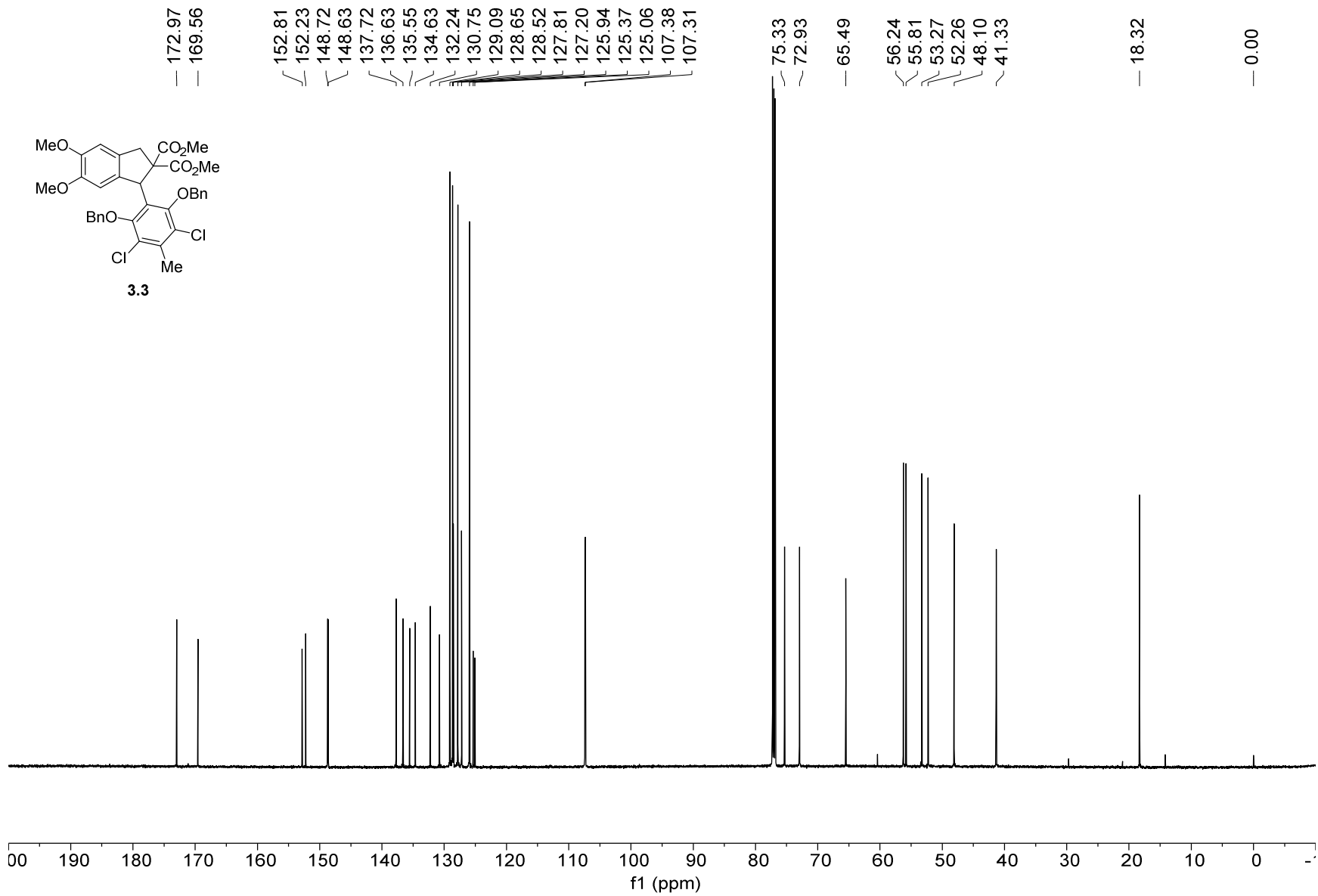
334



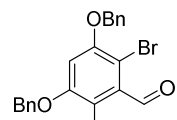
1H NMR — 600.13 MHz — CDCl3T — 298.0 K



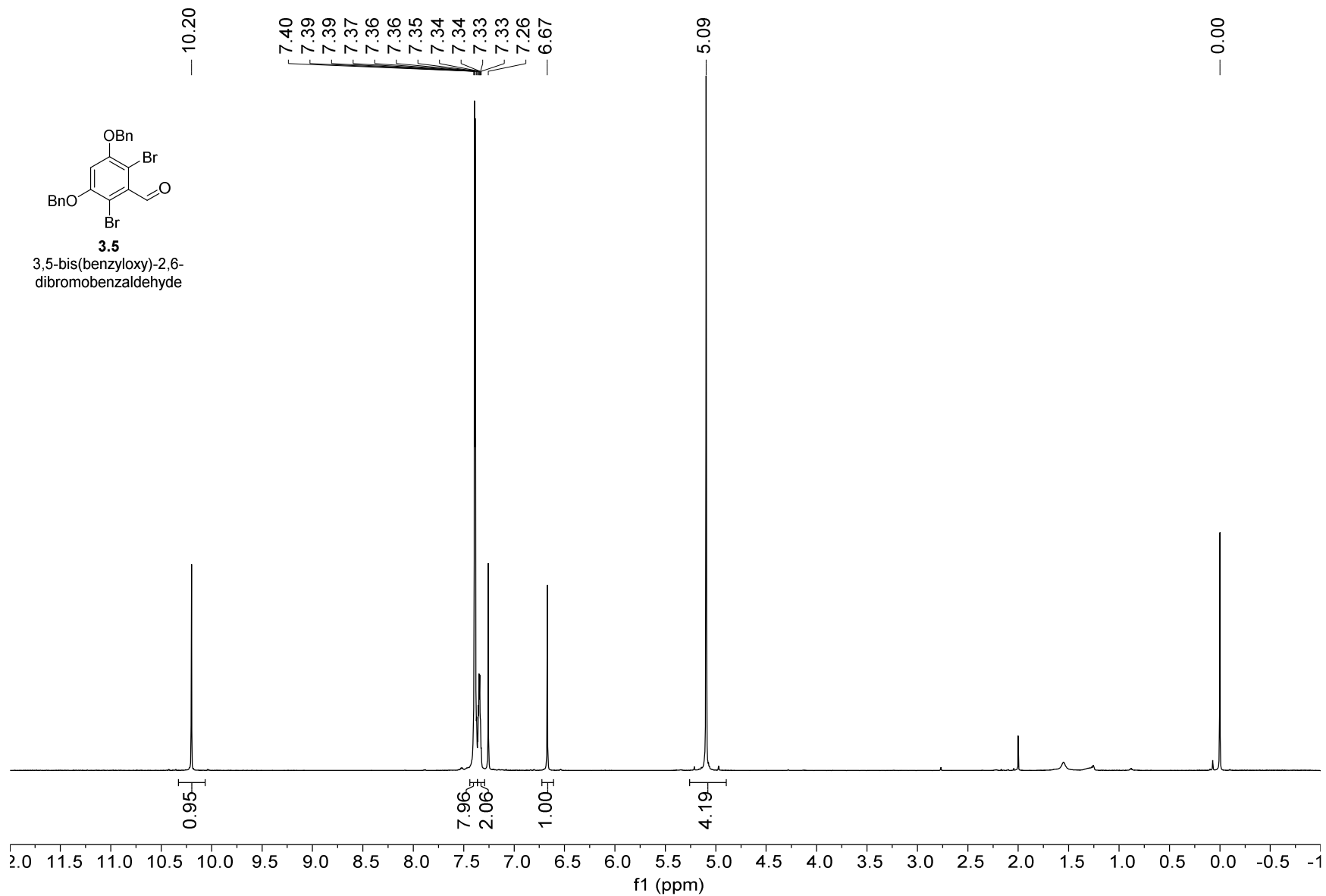
13C NMR — 150.92 MHz — CDCl3T — 298.0 K



1H NMR — 600.13 MHz — CDCl3T — 298.0 K

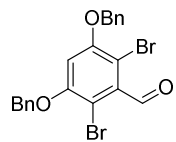


**3.5**  
3,5-bis(benzyloxy)-2,6-dibromobenzaldehyde





13C NMR — 150.92 MHz — CDCl3T — 298.0 K



**3.5**

3,5-bis(benzyloxy)-2,6-dibromobenzaldehyde

— 191.63

— 155.26

135.92

135.51

128.80

128.38

127.04

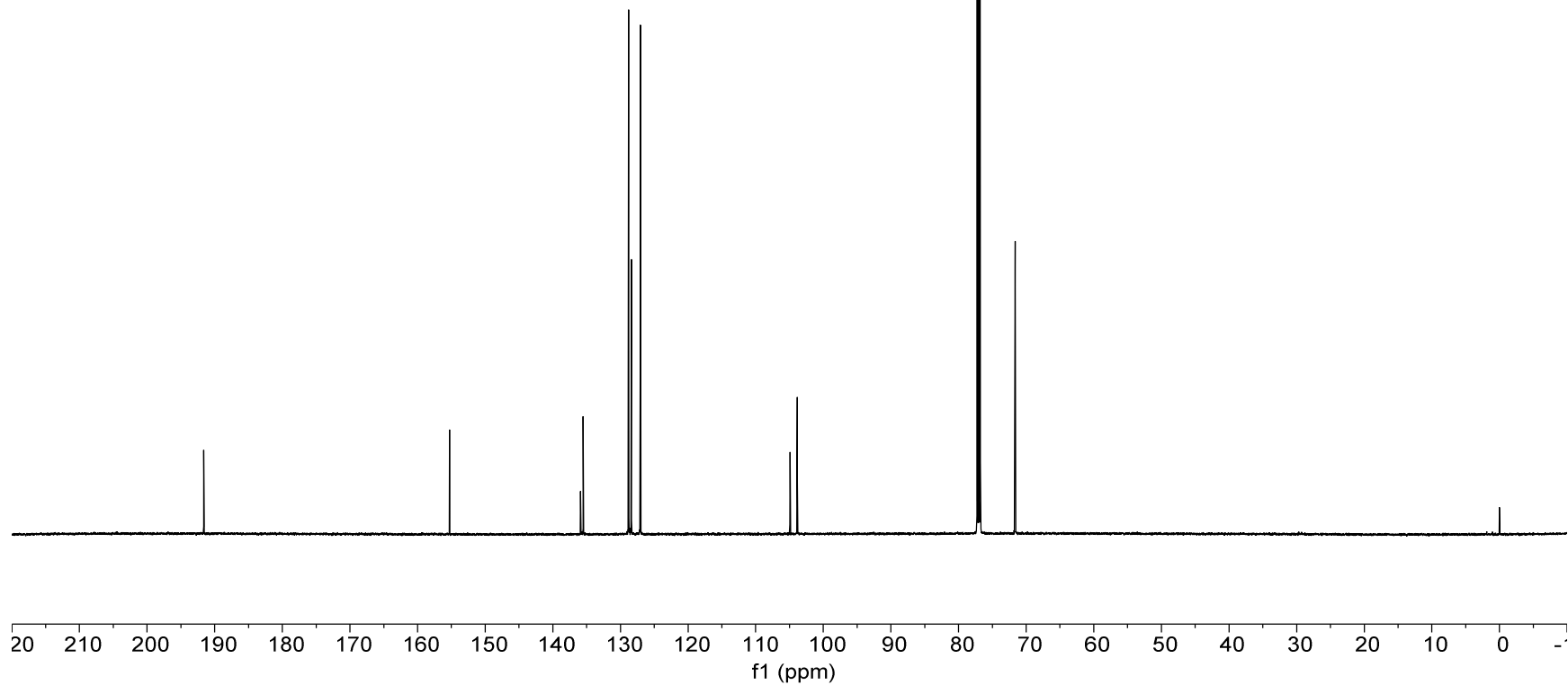
104.93

103.84

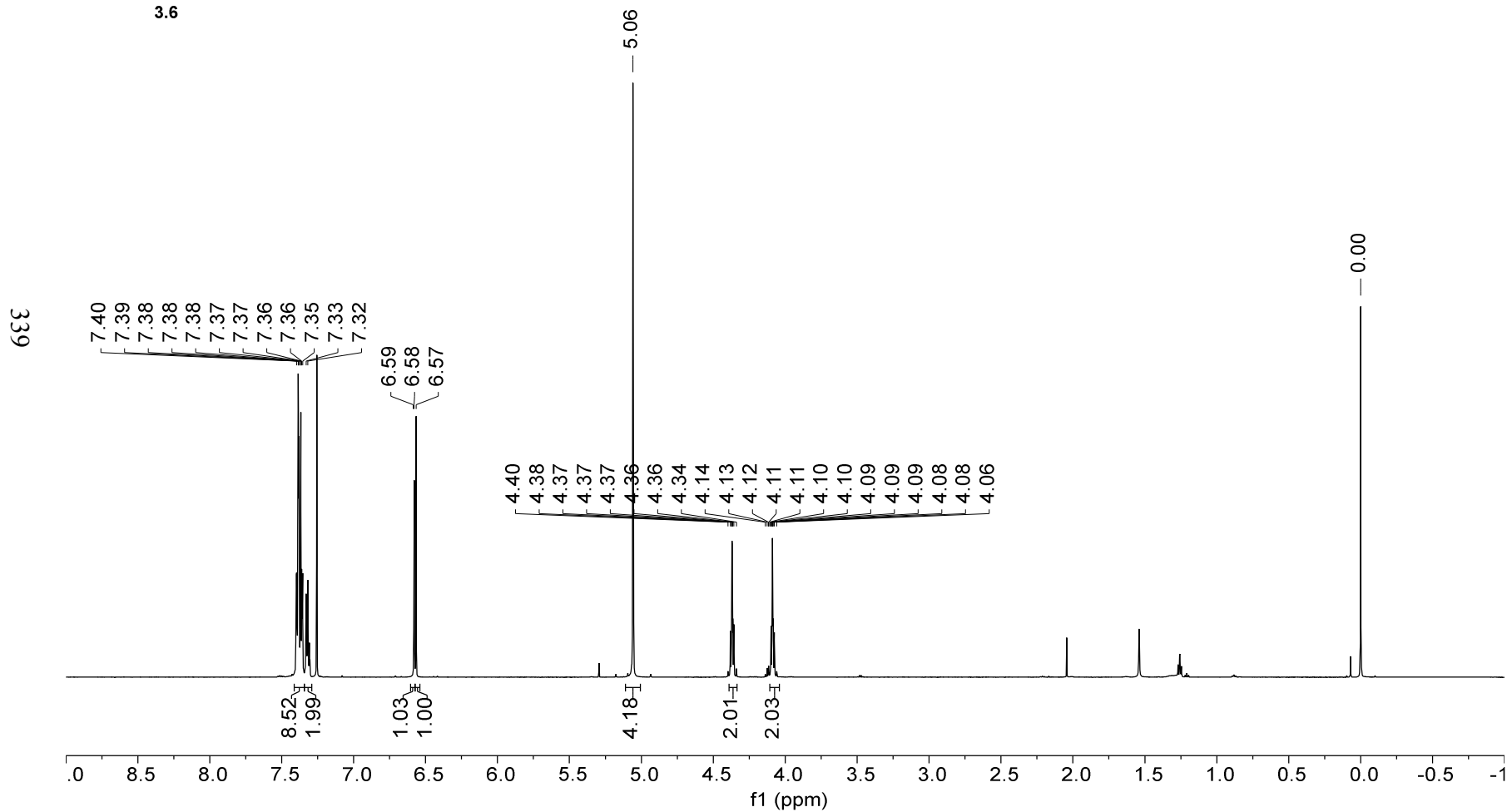
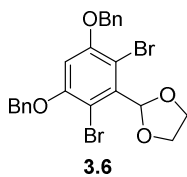
— 71.64

— 0.00

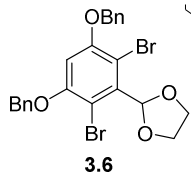
338



1H NMR — 600.13 MHz — CDCl3T — 298.0 K



13C NMR — 150.92 MHz — CDCl3T — 298.0 K



155.10  
155.09

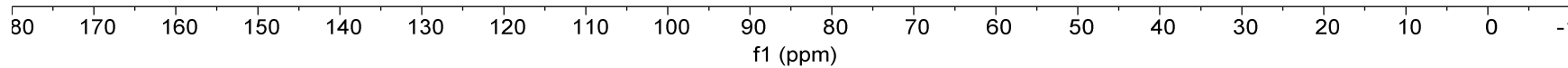
135.95  
134.18  
128.69  
128.34  
128.15  
127.03  
127.01

107.27  
104.64  
102.56

71.57  
65.92

-0.00

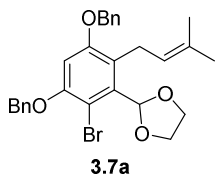
340



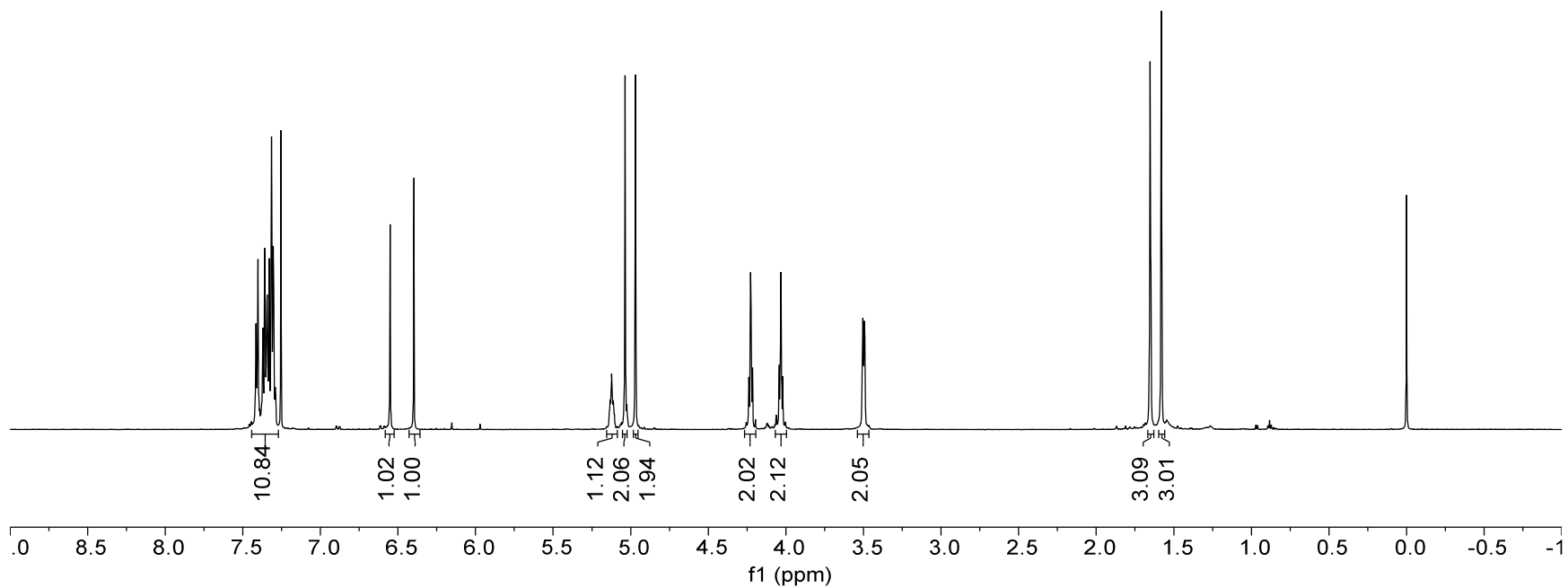
1H NMR — 600.13 MHz — CDCl3T — 298.0 K

7.42  
7.40  
7.37  
7.35  
7.34  
7.32  
7.31  
7.30  
6.55  
6.40  
5.14  
5.13  
5.13  
5.13  
5.12  
5.12  
5.11  
5.11  
5.10  
5.04  
4.97  
4.23  
4.23  
4.03  
4.03  
3.50  
3.49

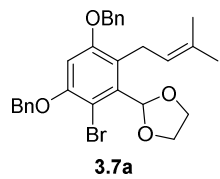
1.65  
1.65  
1.58  
1.58



341



13C NMR — 150.92 MHz — CDCl3T — 298.0 K



— 156.89  
— 153.71

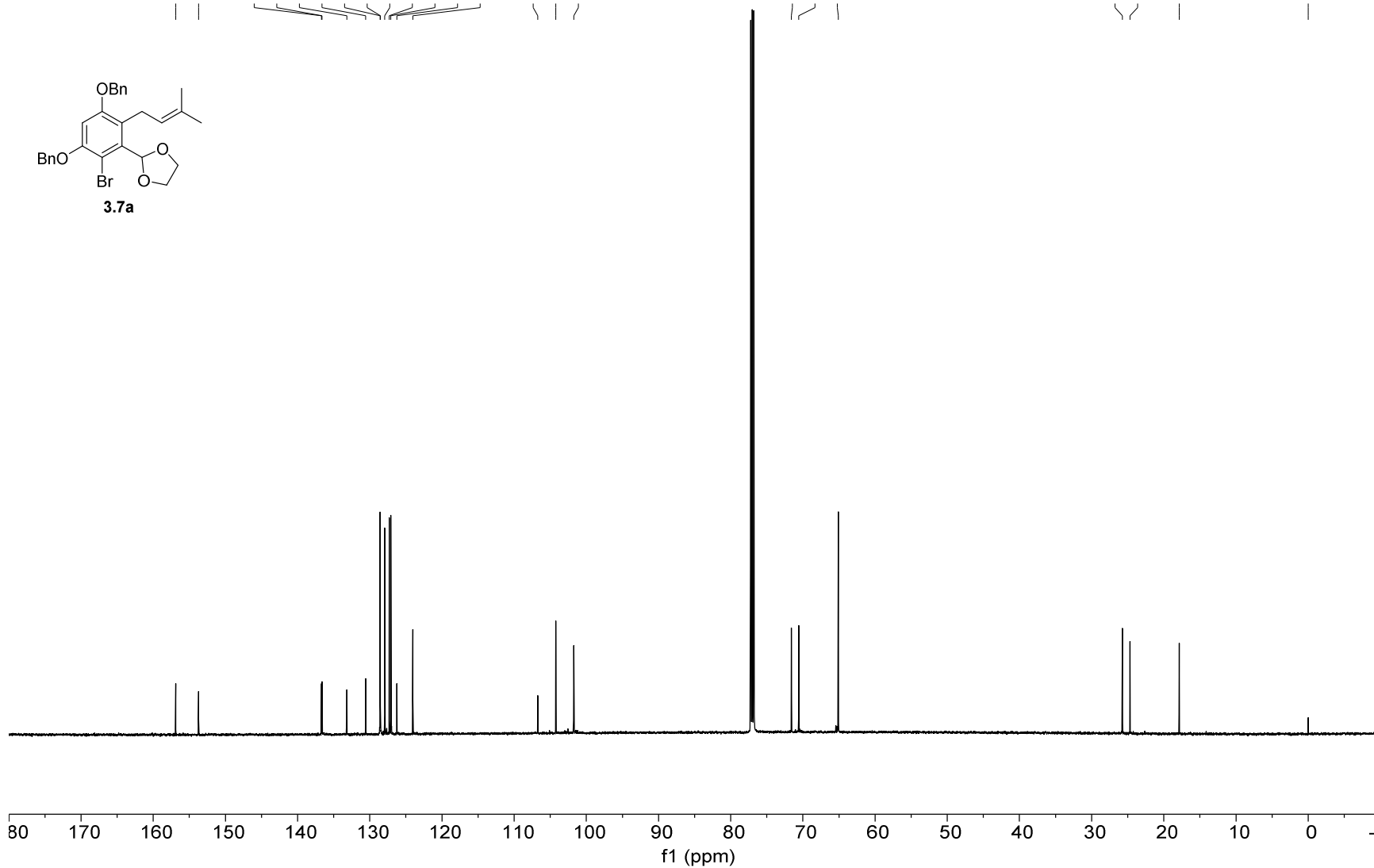
136.70  
136.61  
133.19  
130.59  
128.58  
128.54  
127.93  
127.30  
127.08  
126.24  
124.03

~ 106.74  
— 104.22  
~ 101.74

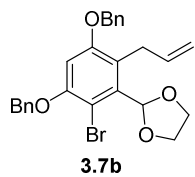
— 71.58  
~ 70.57  
— 65.10

~ 25.73  
~ 24.67  
— 17.87

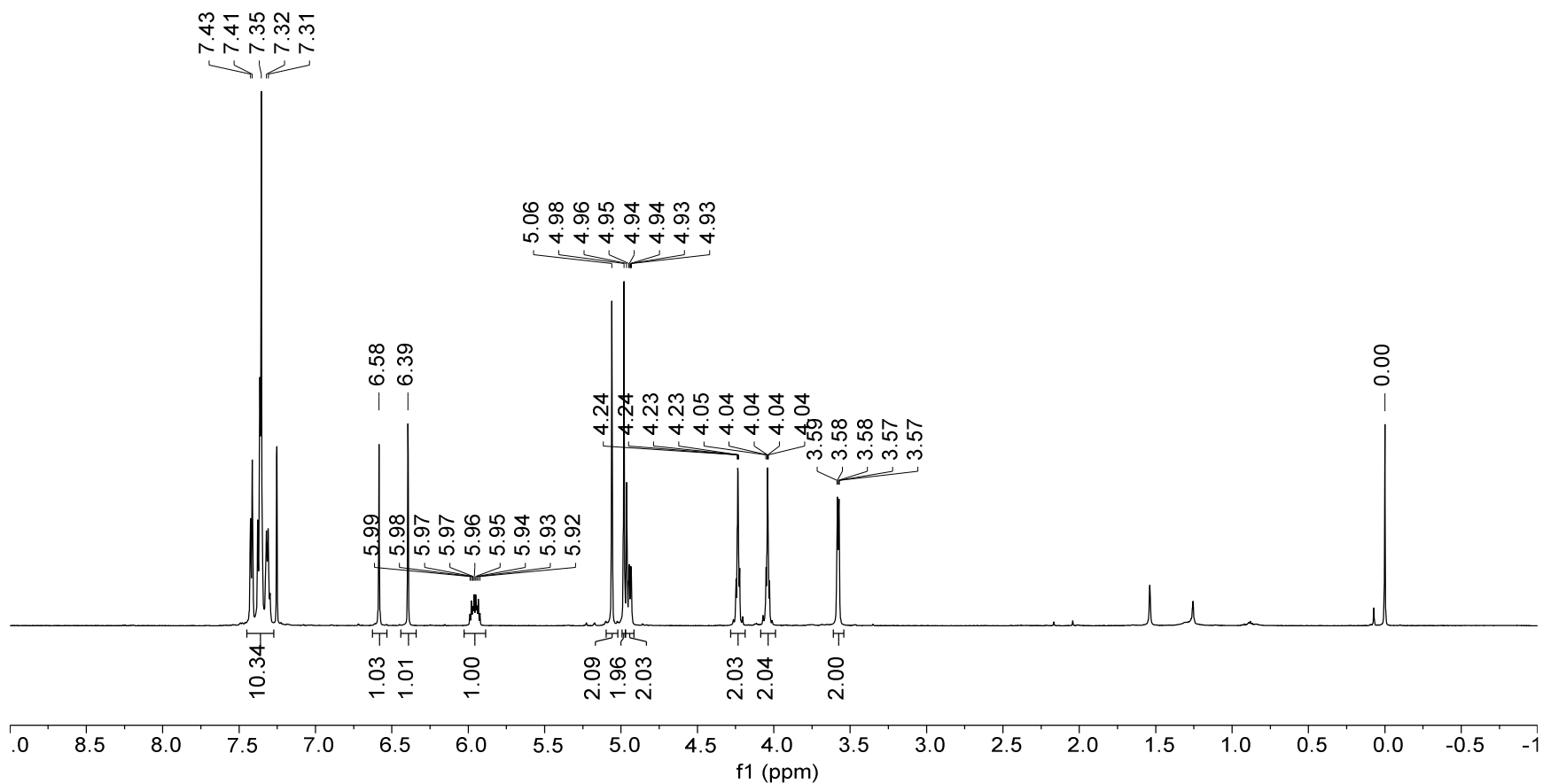
— 0.00



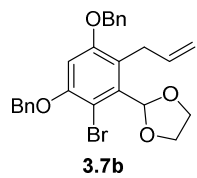
1H NMR — 600.13 MHz — CDCl3T — 298.0 K



343



13C NMR — 150.92 MHz — CDCl3T — 298.0 K



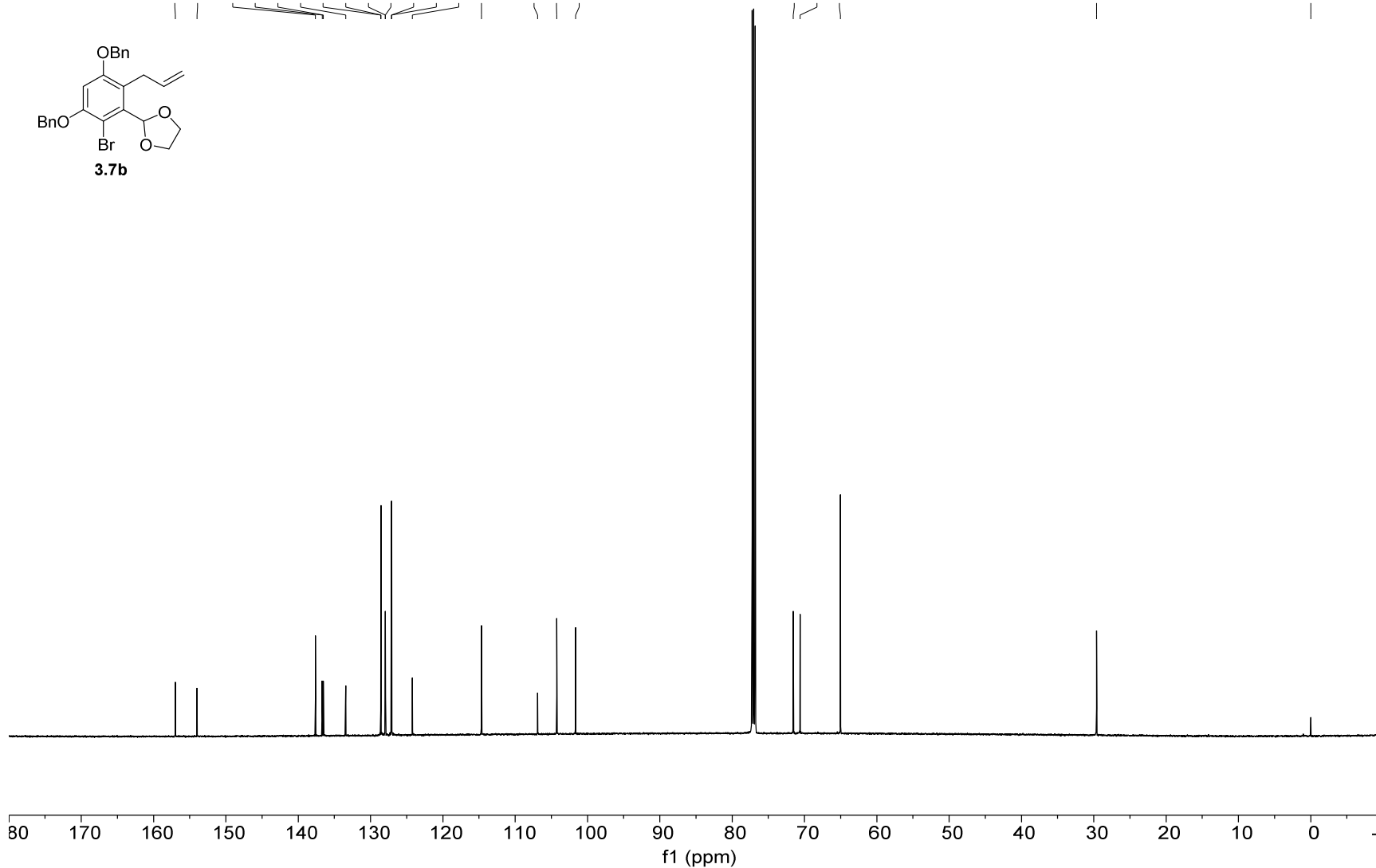
156.99  
153.98  
137.61  
136.69  
136.51  
133.44  
128.59  
128.57  
127.97  
127.95  
127.11  
127.08  
124.21  
114.66

106.90  
104.25  
101.65

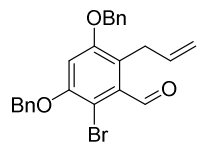
71.55  
70.61  
65.02

29.62

0.00



1H NMR — 600.13 MHz — CDCl3T — 298.0 K



**3.8**

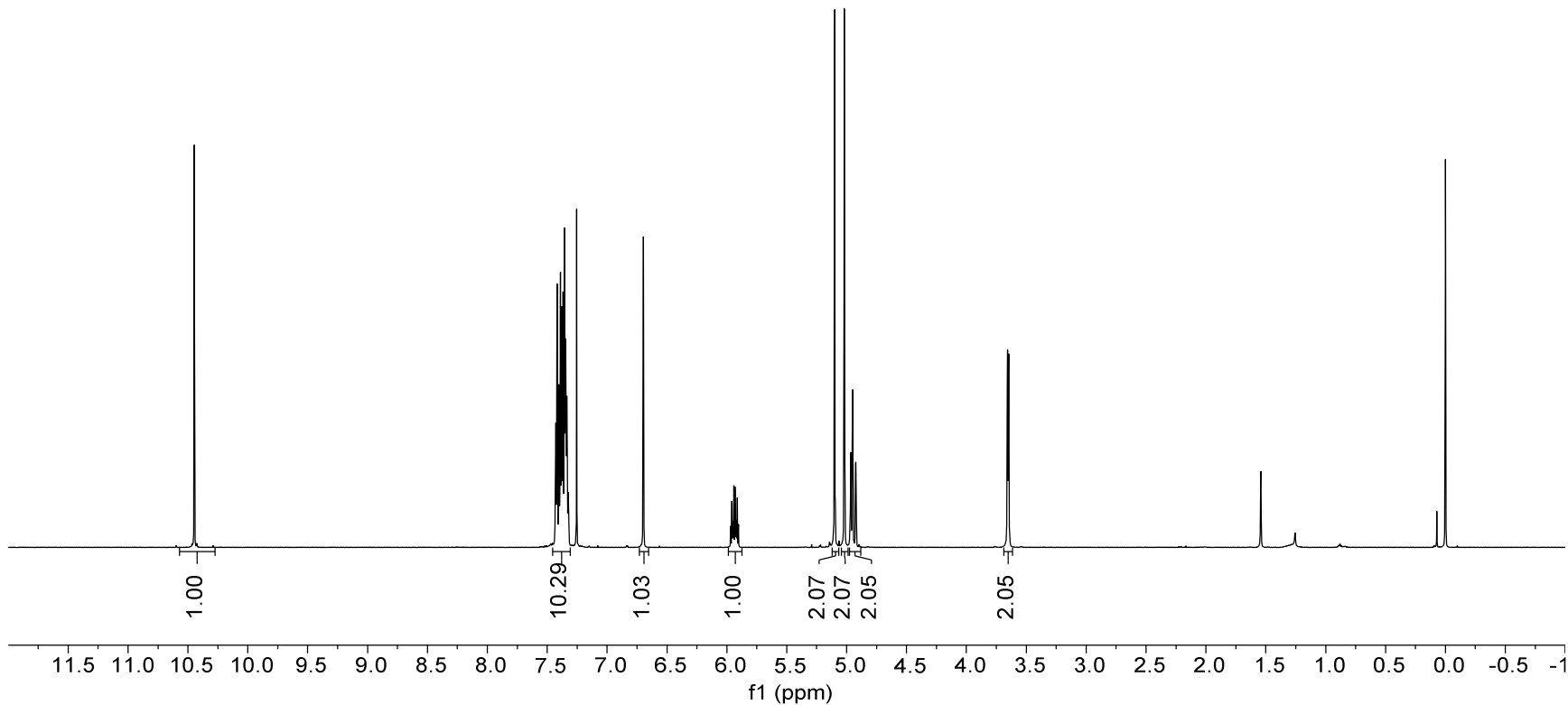
2-allyl-3,5-bis(benzyloxy)-  
6-bromobenzaldehyde

10.45

7.43  
7.42  
7.39  
7.36  
7.32  
6.70

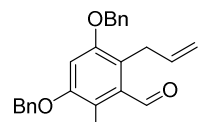
5.97  
5.96  
5.95  
5.95  
5.94  
5.93  
5.92  
5.92  
5.91  
5.90  
5.10  
5.02  
4.97  
4.97  
4.96  
4.96  
4.96  
4.95  
4.95  
4.95  
4.95  
4.93  
4.92  
4.92  
3.66  
3.66  
3.65  
3.65  
3.65  
3.64  
0.00

345





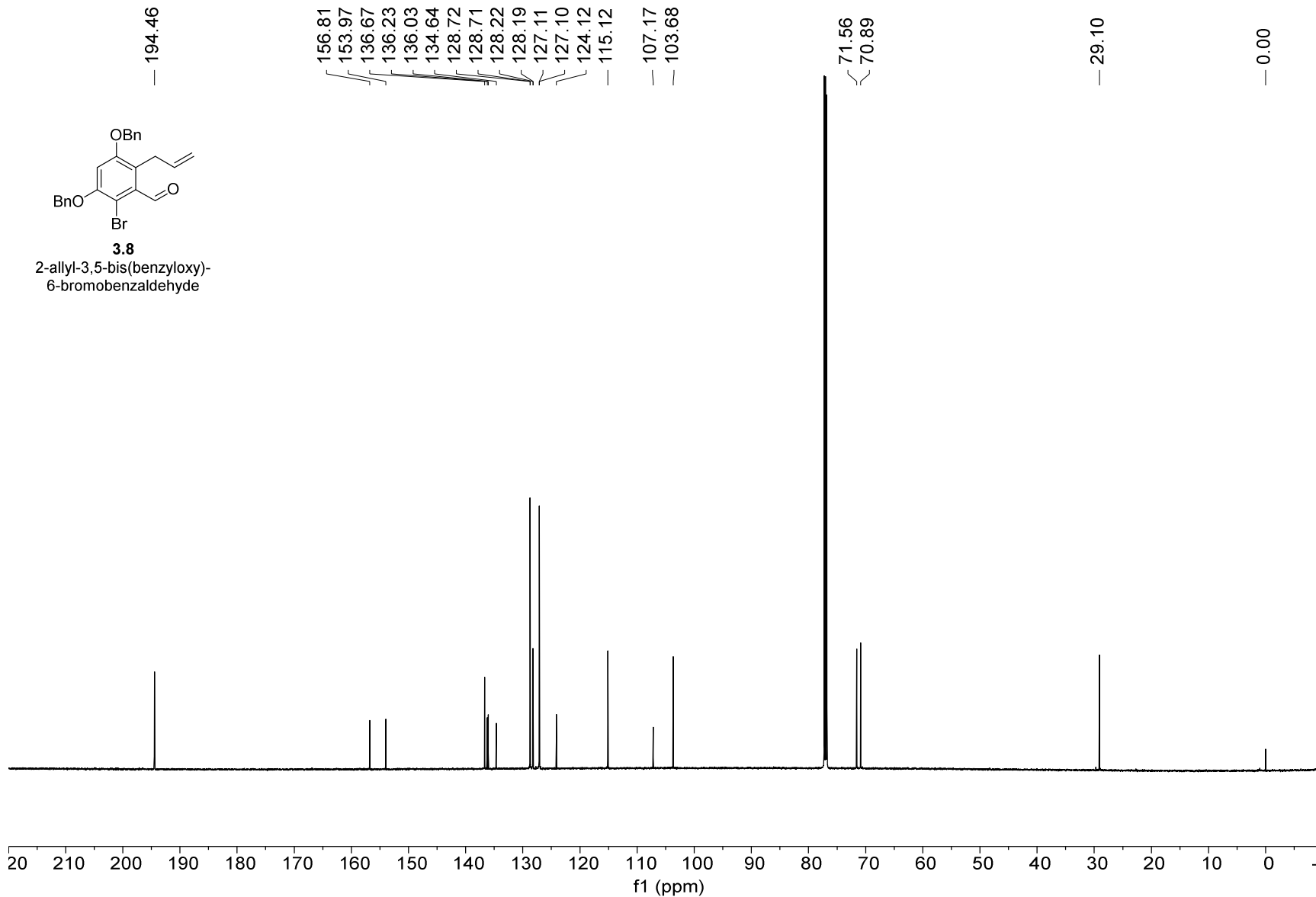
13C NMR — 150.92 MHz — CDCl3T — 298.0 K



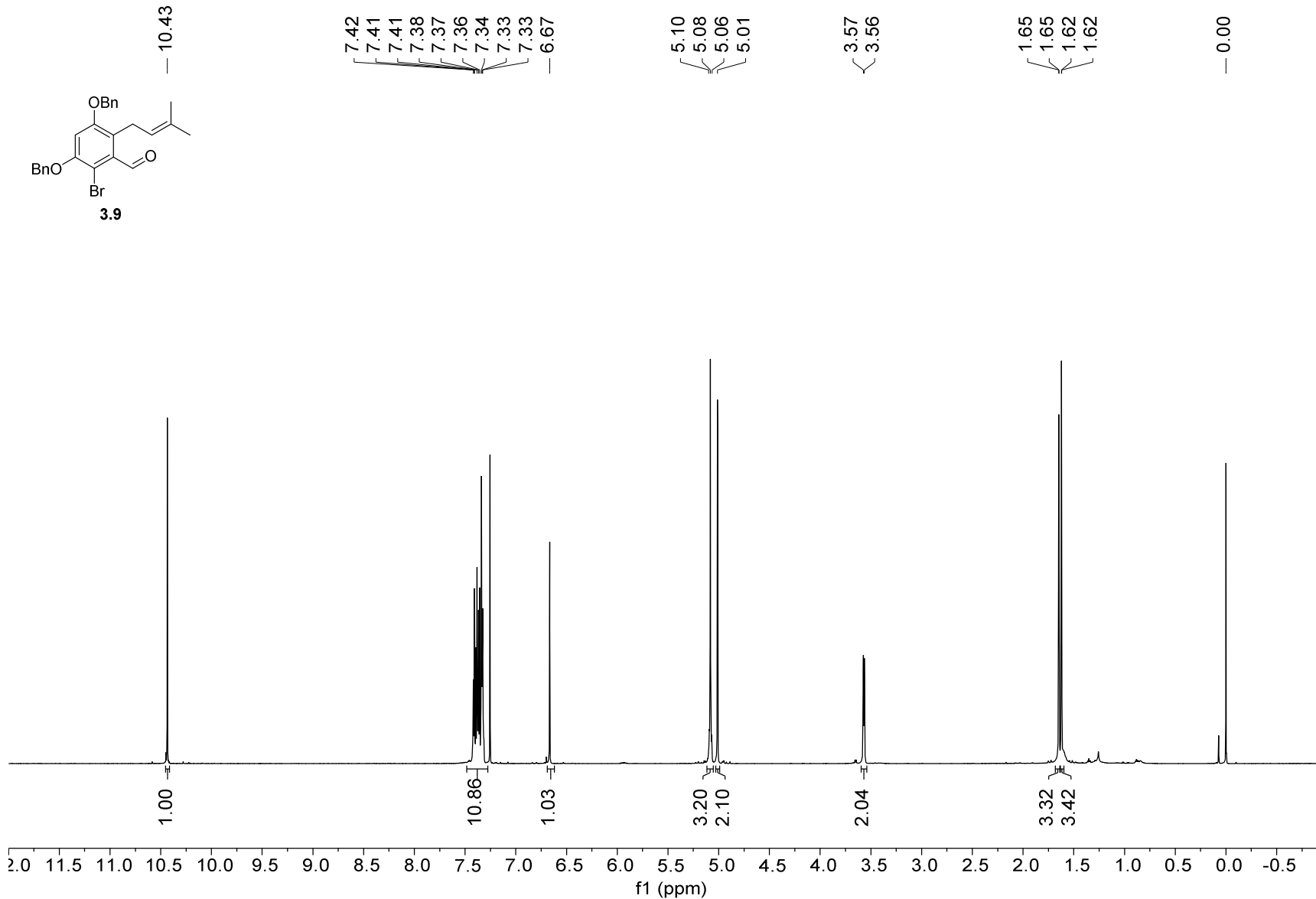
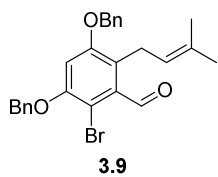
**3.8**

2-allyl-3,5-bis(benzyloxy)-  
6-bromobenzaldehyde

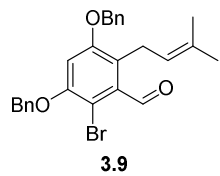
194.46  
156.81  
153.97  
136.67  
136.23  
136.03  
134.64  
128.72  
128.71  
128.22  
128.19  
127.11  
127.10  
124.12  
115.12  
107.17  
103.68  
71.56  
70.89  
29.10  
0.00



1H NMR — 600.13 MHz — CDCl3T — 298.0 K



13C NMR — 150.92 MHz — CDCl3T — 298.0 K



194.66

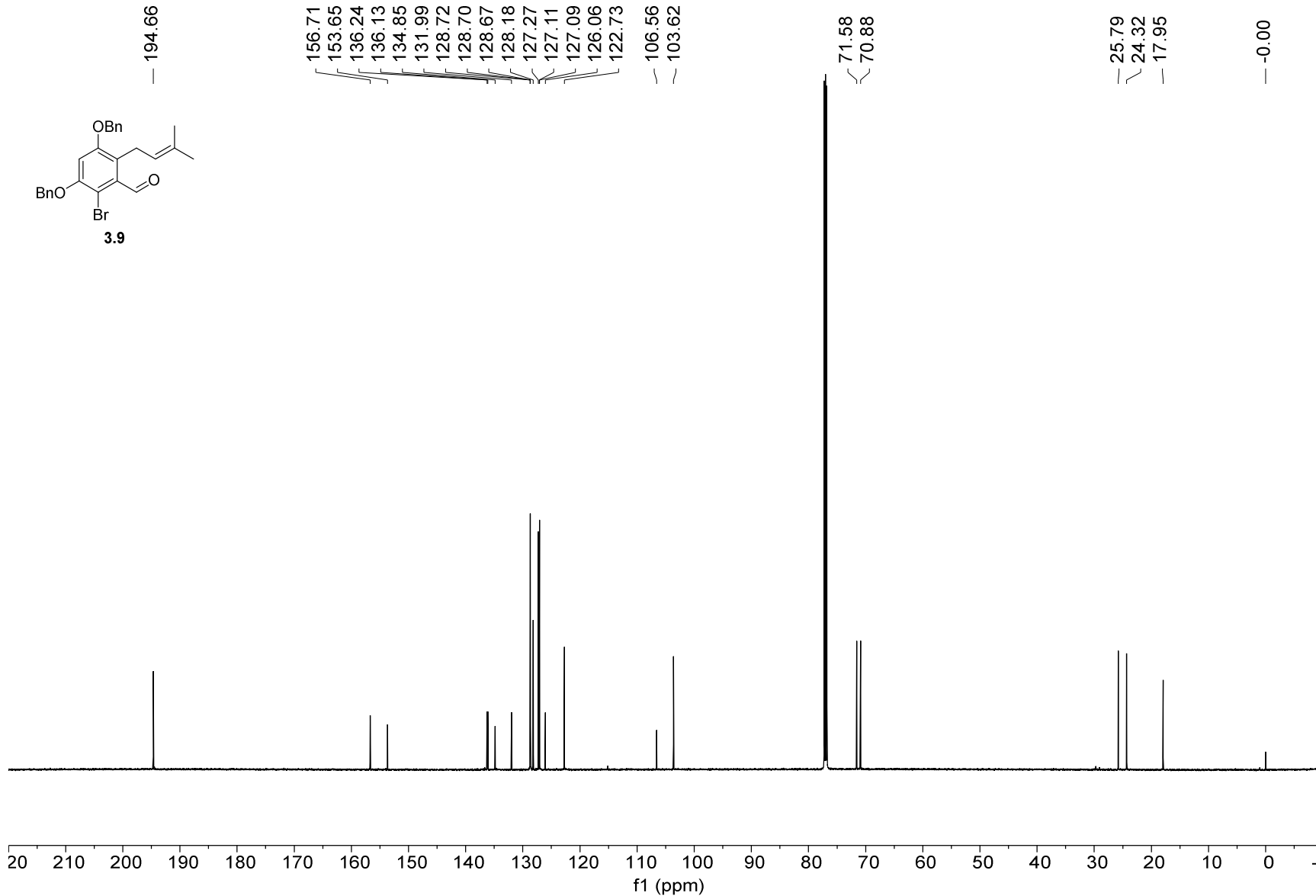
156.71  
153.65  
136.24  
136.13  
134.85  
131.99  
128.72  
128.70  
128.67  
128.18  
127.27  
127.11  
127.09  
126.06  
122.73

106.56  
103.62

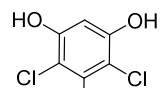
71.58  
70.88

25.79  
24.32  
17.95

-0.00



1H NMR — 600.13 MHz — CDCl3T — 298.0 K



**3.10**  
(4,6-dichloro)orcinol

7.26

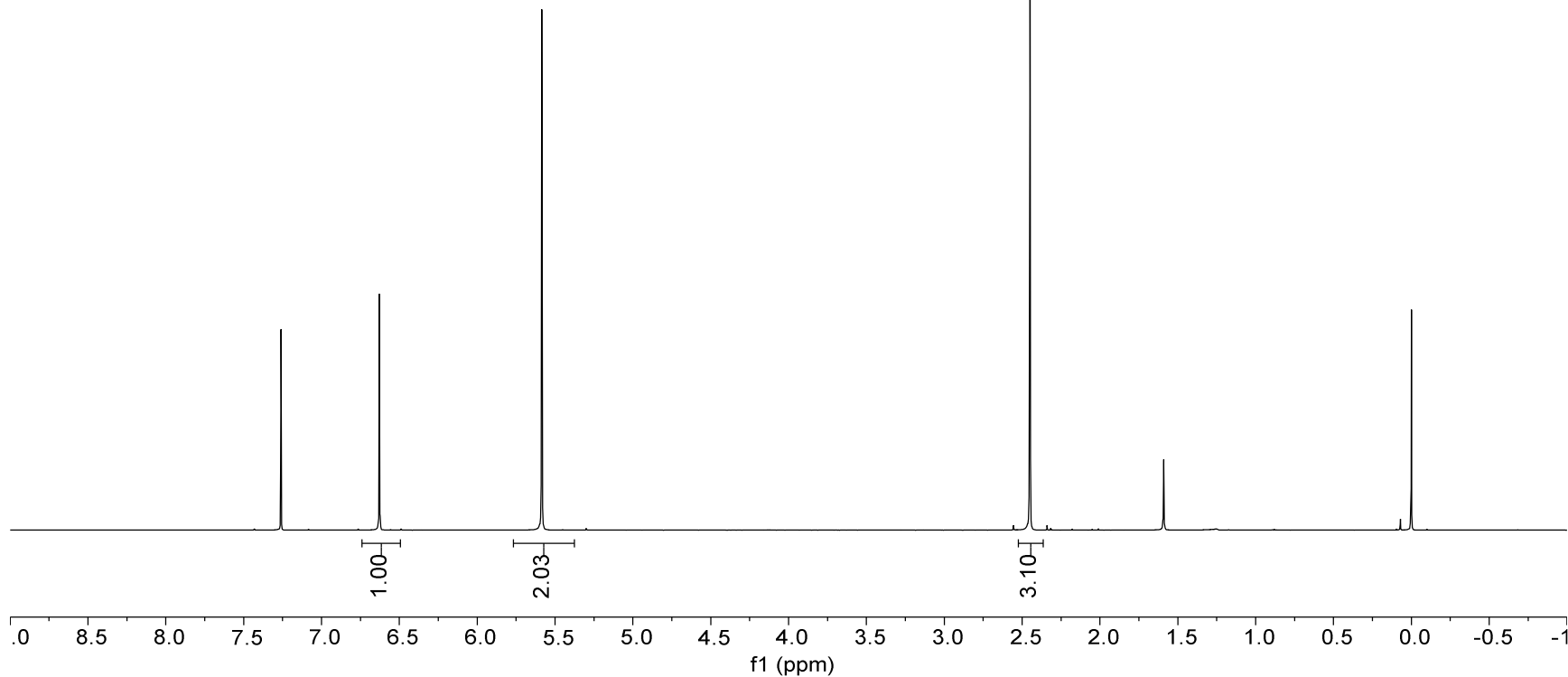
6.63

5.58

2.45  
2.45

0.00

349



13C NMR — 150.92 MHz — CDCl3T — 298.1 K

— 150.89

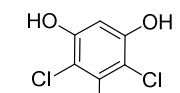
— 134.19

— 112.74

— 101.03

— 18.01

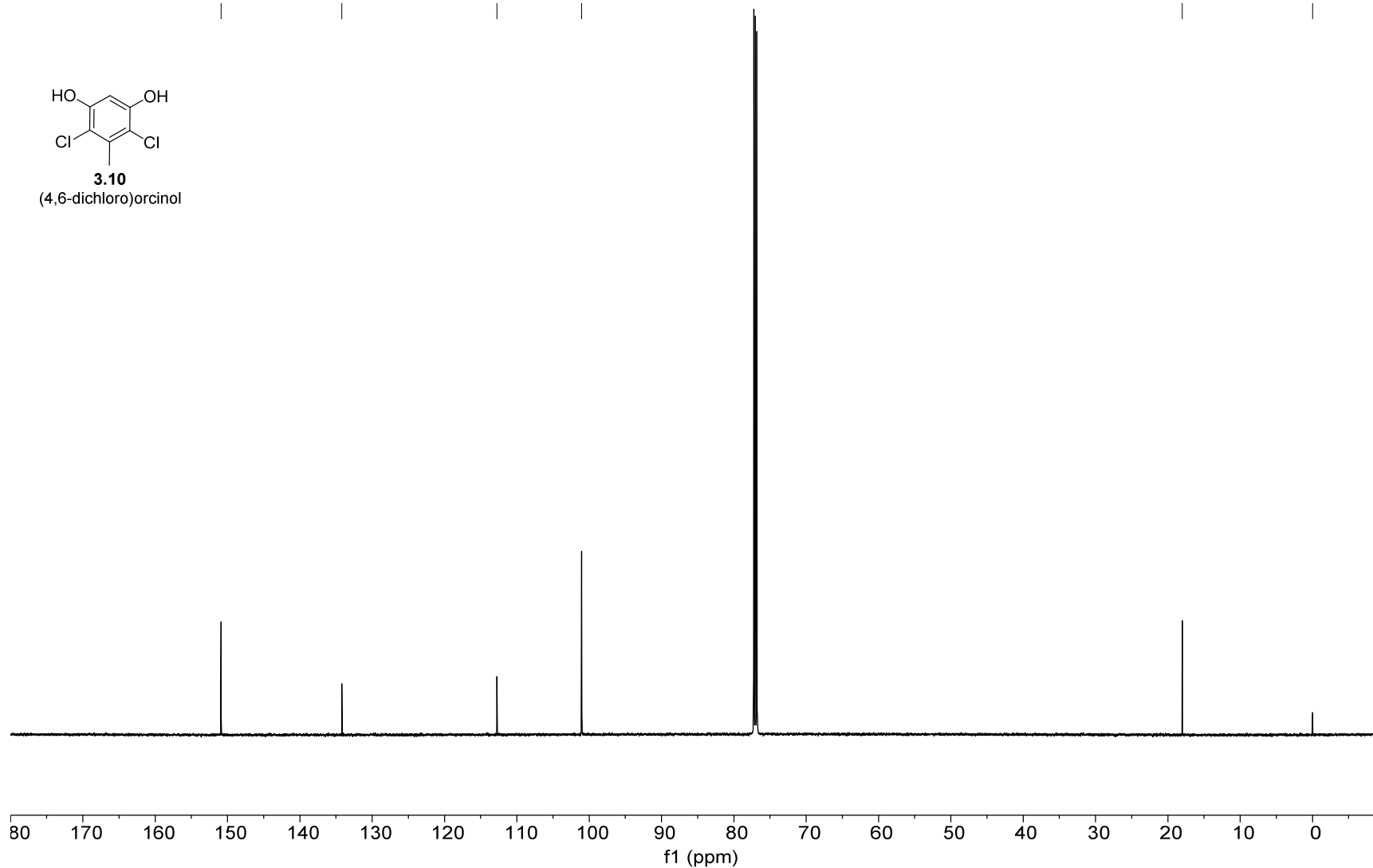
— 0.00



**3.10**

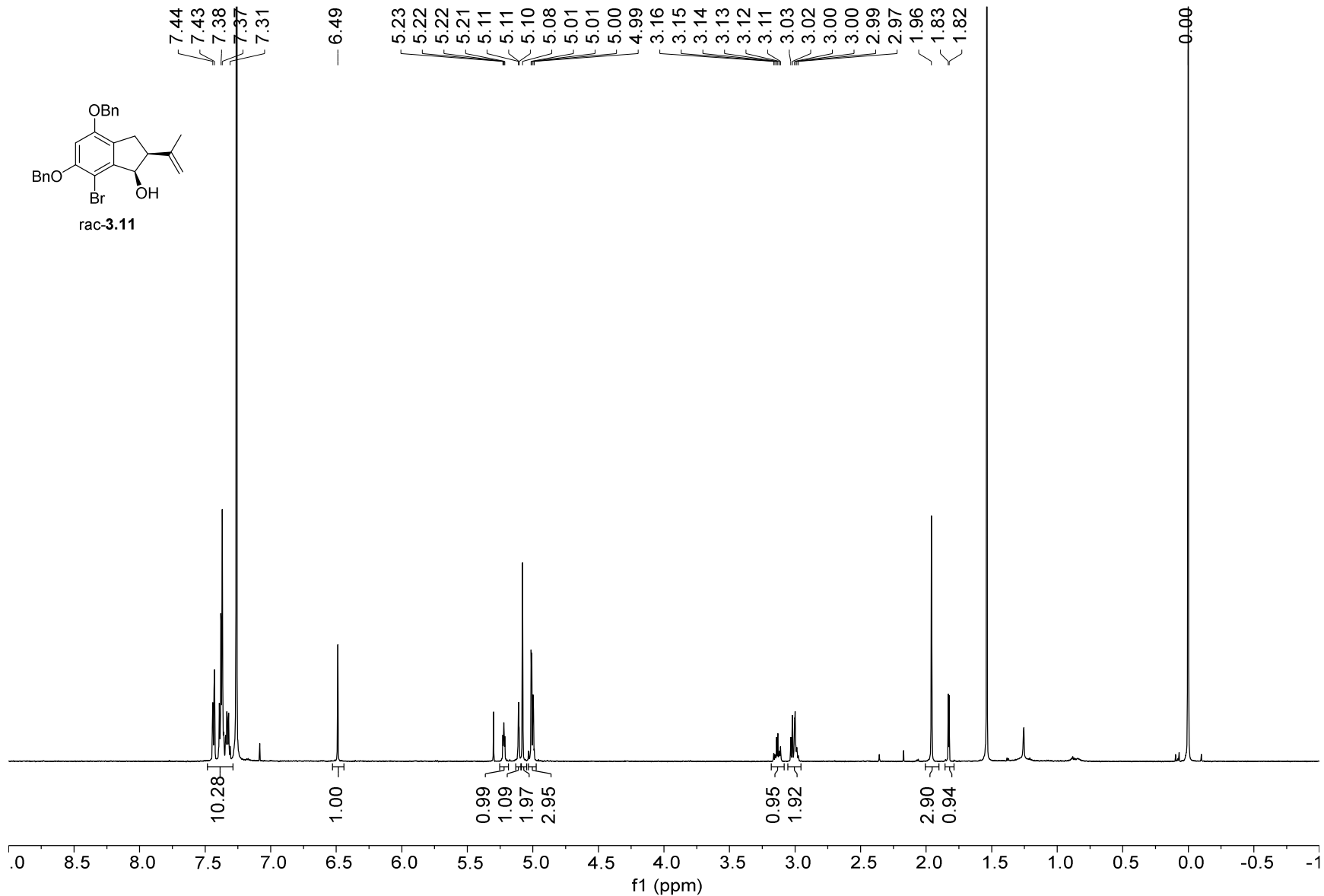
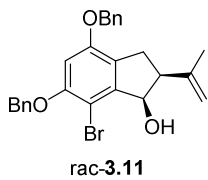
(4,6-dichloro)orcinol

350



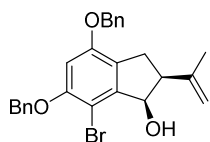
351

1H NMR — 600.13 MHz — CDCl3T — 298.0 K



13C NMR — 150.92 MHz — CDCl3T — 298.0 K

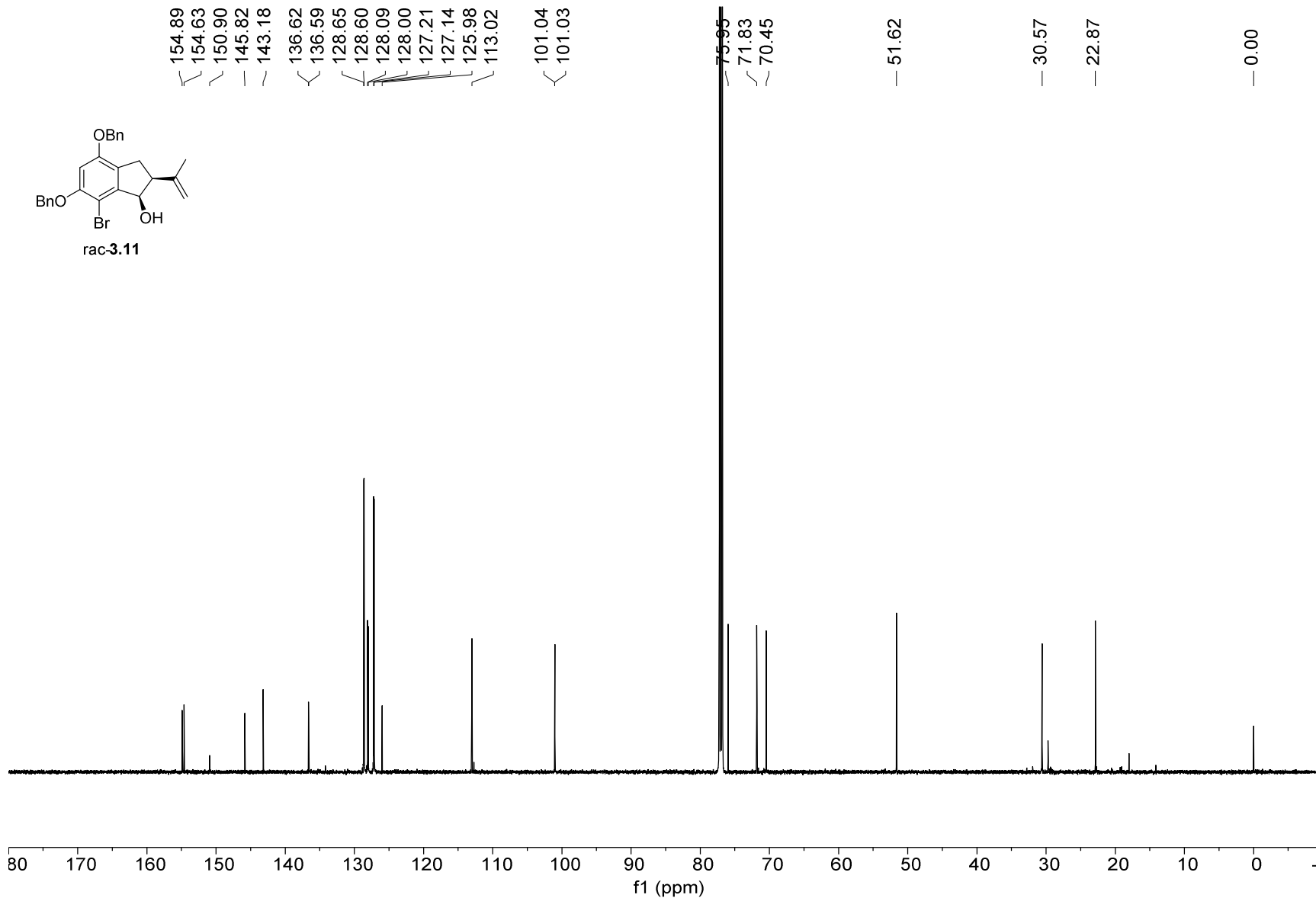
154.89  
154.63  
150.90  
145.82  
143.18  
136.62  
136.59  
128.65  
128.60  
128.09  
128.00  
127.21  
127.14  
125.98  
113.02  
101.04  
101.03



rac-3.11

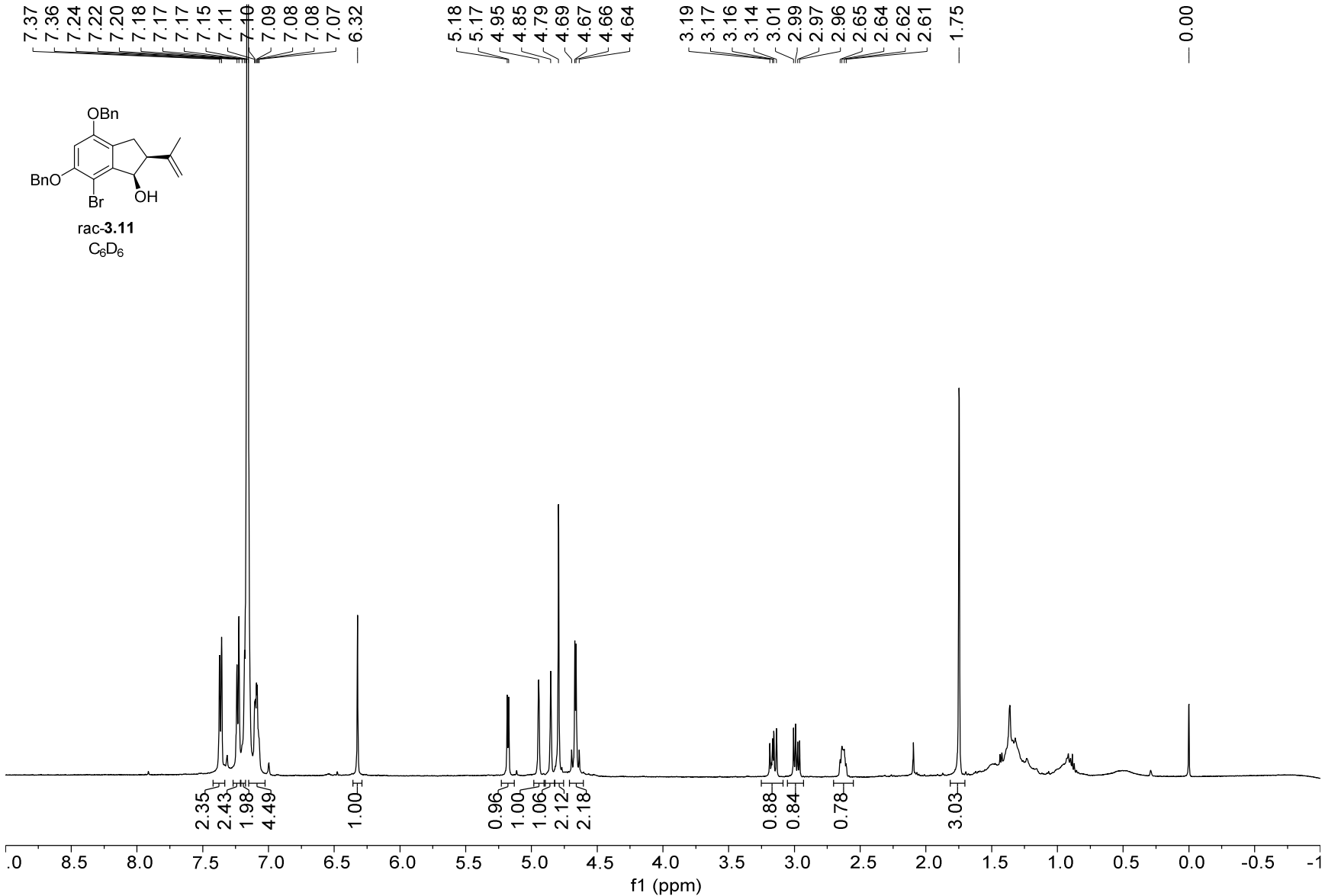
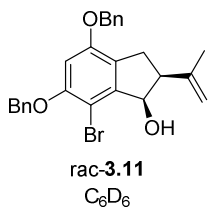
75.95  
71.83  
70.45  
51.62  
30.57  
22.87  
0.00

352



353

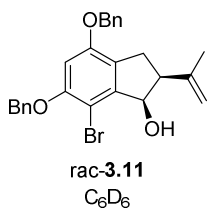
1H NMR — 500.22 MHz — C6D6 — 298.0 K





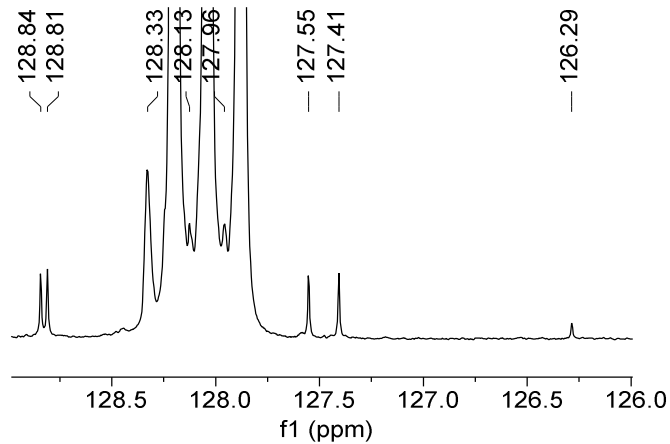
354

13C NMR — 150.92 MHz — C6D6 — 298.0 K



155.42  
155.03  
151.69  
147.08  
143.63  
137.31  
137.27  
128.84  
128.81  
128.33  
128.13  
127.96  
127.55  
127.41  
126.29  
112.66  
101.85  
100.94

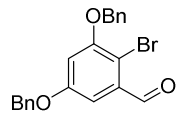
13C NMR — 150.92 MHz — C6D6 — 298.0 K



76.57  
71.72  
70.42  
51.93  
50.26  
31.08  
22.75  
-0.00

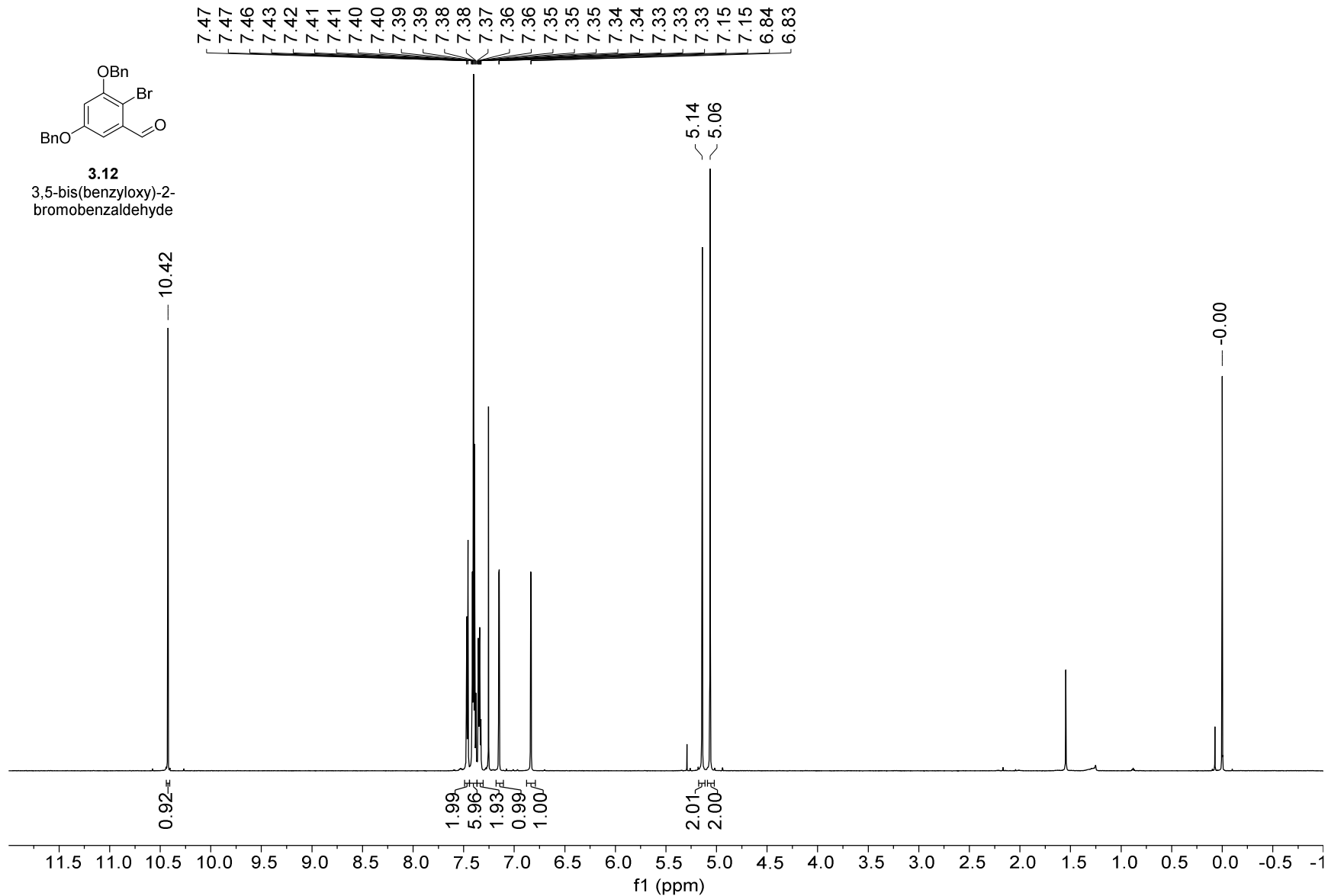
80 170 160 150 140 130 120 110 100 90 80 70 60 50 40 30 20 10 0  
f1 (ppm)

1H NMR — 600.13 MHz — CDCl3T — 298.0 K

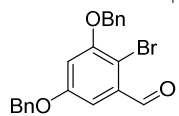


**3.12**  
3,5-bis(benzyloxy)-2-bromobenzaldehyde

355



13C NMR — 150.92 MHz — CDCl3T — 298.0 K



**3.12**  
3,5-bis(benzyloxy)-2-bromobenzaldehyde

192.00

158.92  
156.20

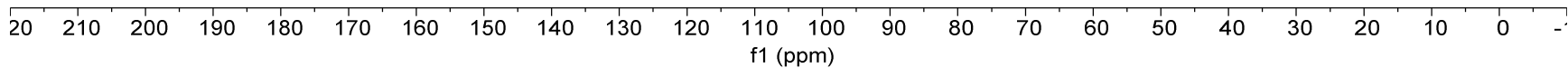
135.93  
135.77  
134.81  
128.72  
128.70  
128.36  
128.21  
127.70  
127.04

109.98  
108.01  
105.06

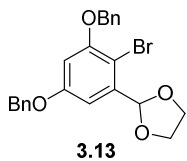
71.20  
70.58

0.00

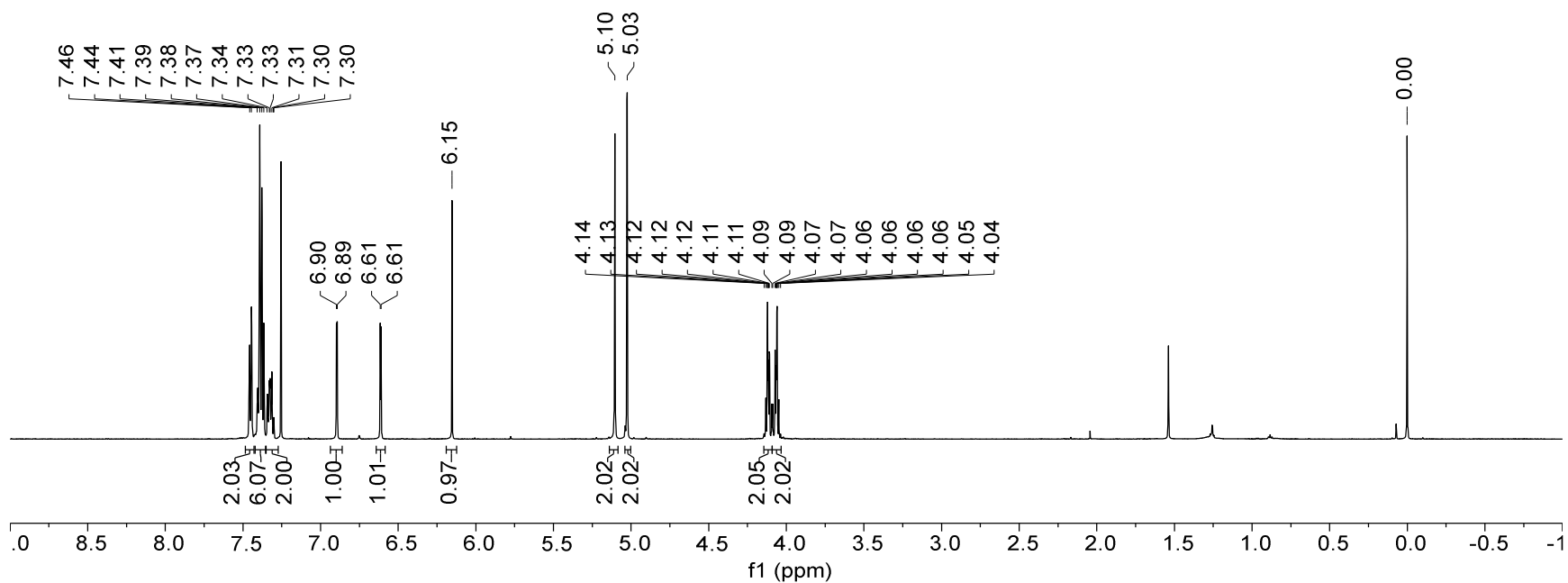
356



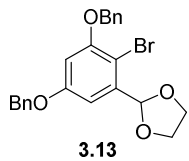
1H NMR — 600.13 MHz — CDCl3T — 298.0 K



357



13C NMR — 150.92 MHz — CDCl3T — 298.0 K



158.85  
155.87

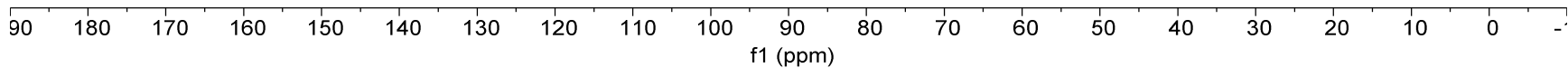
138.58  
136.45  
136.32  
128.64  
128.59  
128.18  
127.95  
127.65  
127.00

105.11  
104.62  
103.00  
102.54

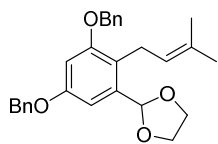
71.02  
70.41  
65.44

0.00

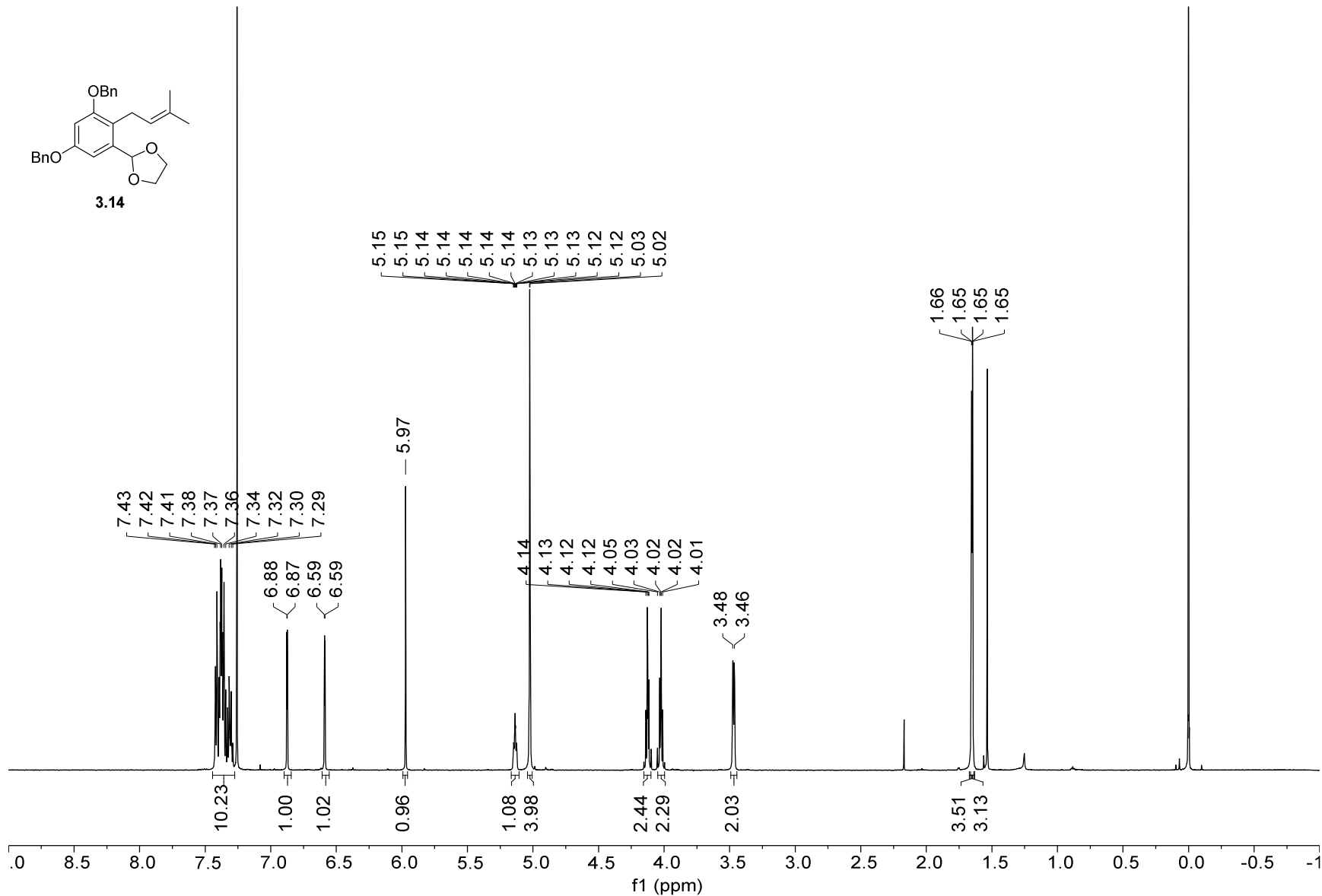
358



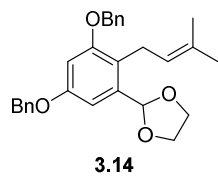
1H NMR — 600.13 MHz — CDCl3T — 298.0 K



653



13C NMR — 150.92 MHz — CDCl3T — 298.0 K

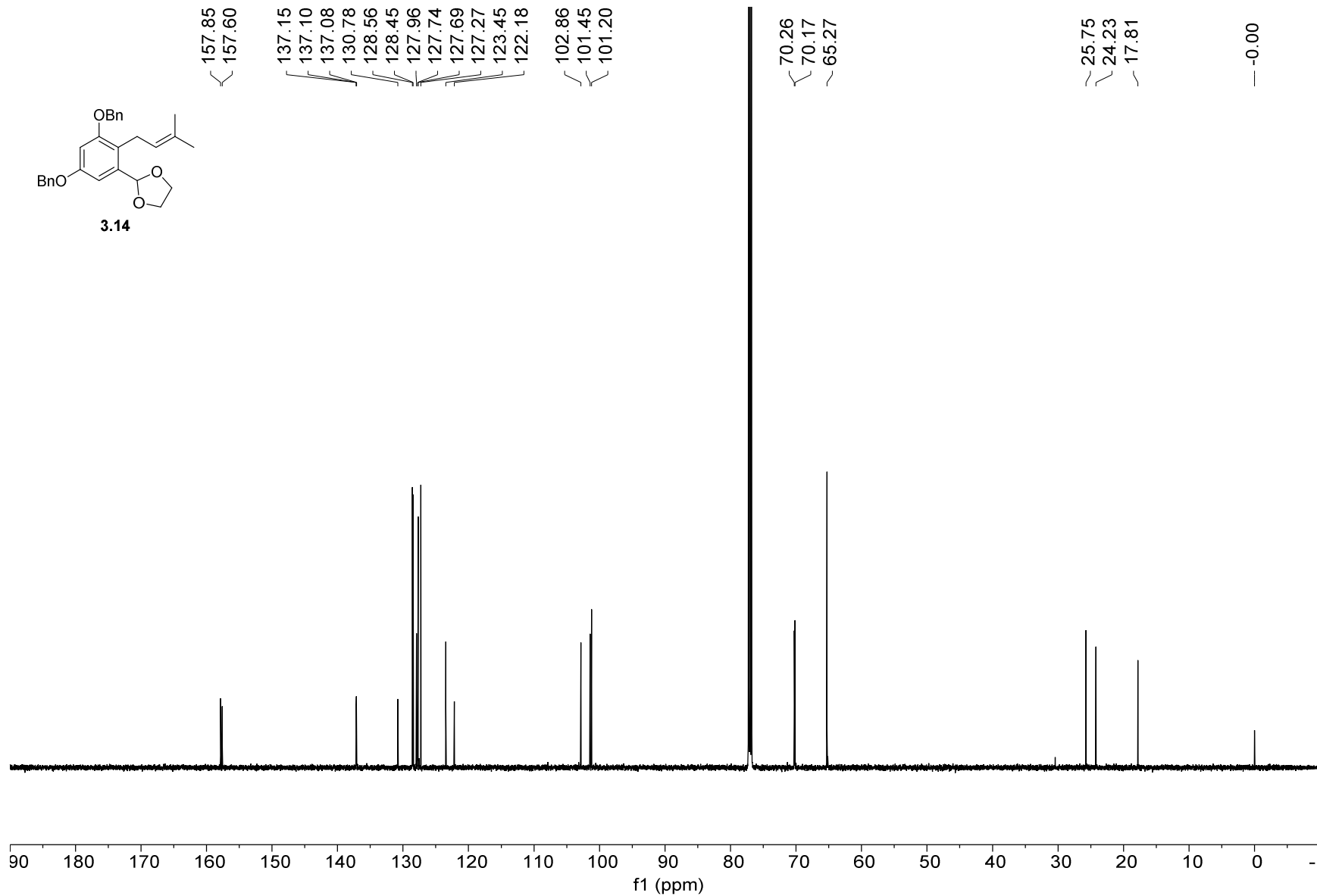


157.85  
157.60  
137.15  
137.10  
137.08  
130.78  
128.56  
128.45  
127.96  
127.74  
127.69  
127.27  
123.45  
122.18  
102.86  
101.45  
101.20

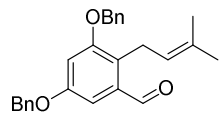
70.26  
70.17  
65.27

25.75  
24.23  
17.81

-0.00

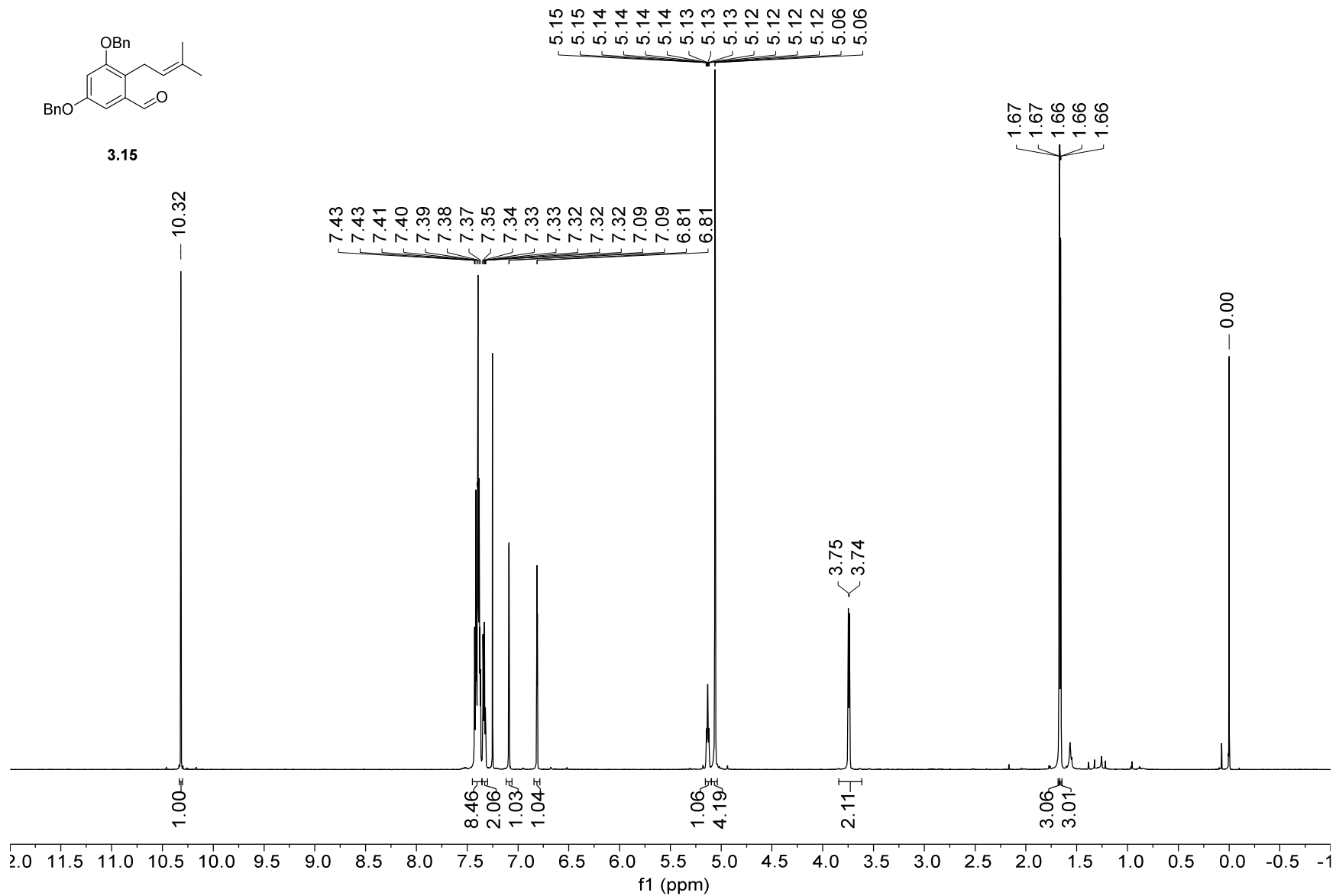


1H NMR — 600.13 MHz — CDCl3T — 298.0 K



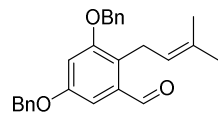
3.15

193

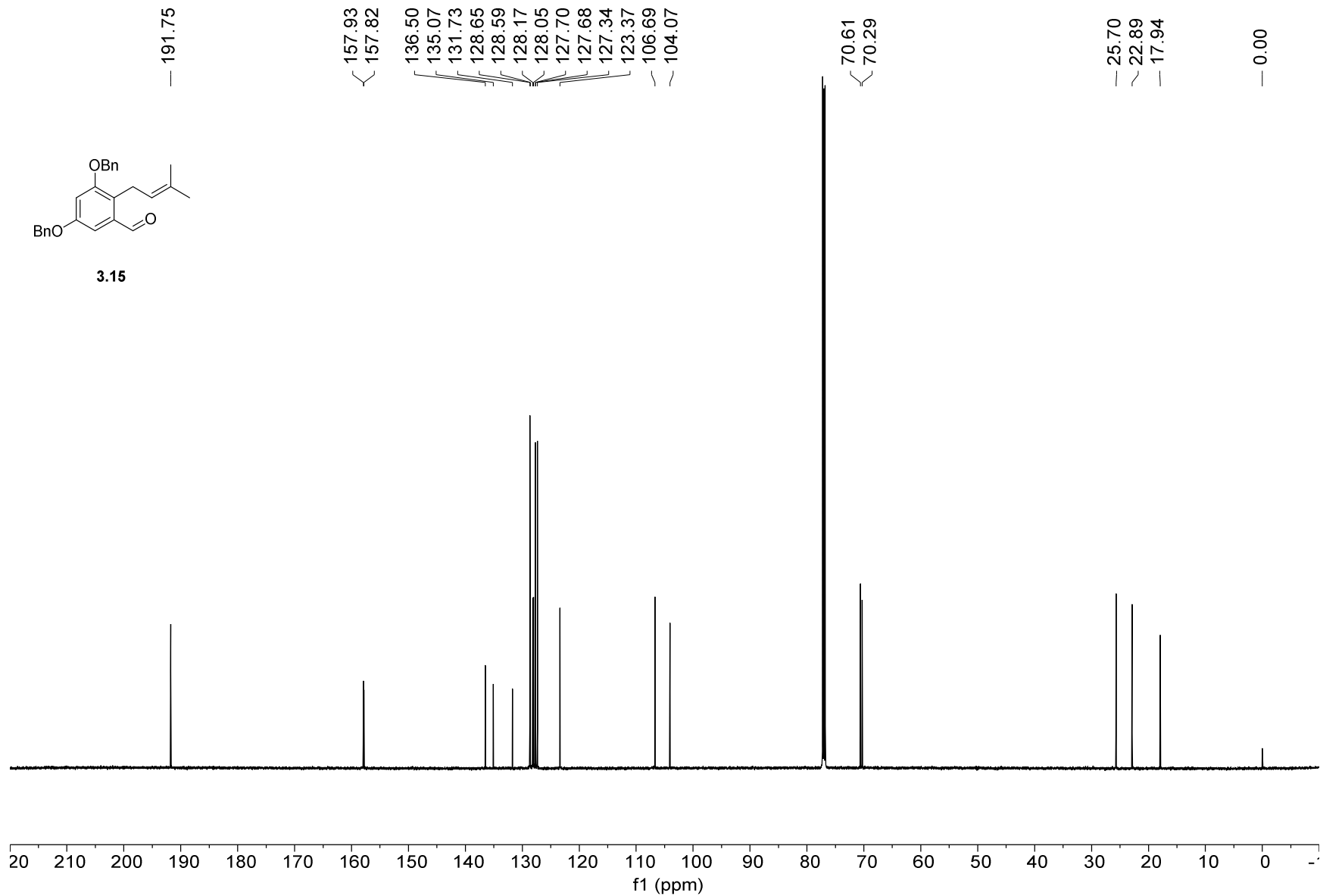




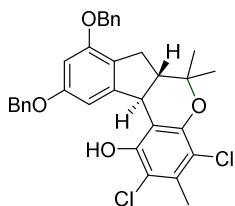
13C NMR — 150.92 MHz — CDCl3T — 298.0 K



3.15

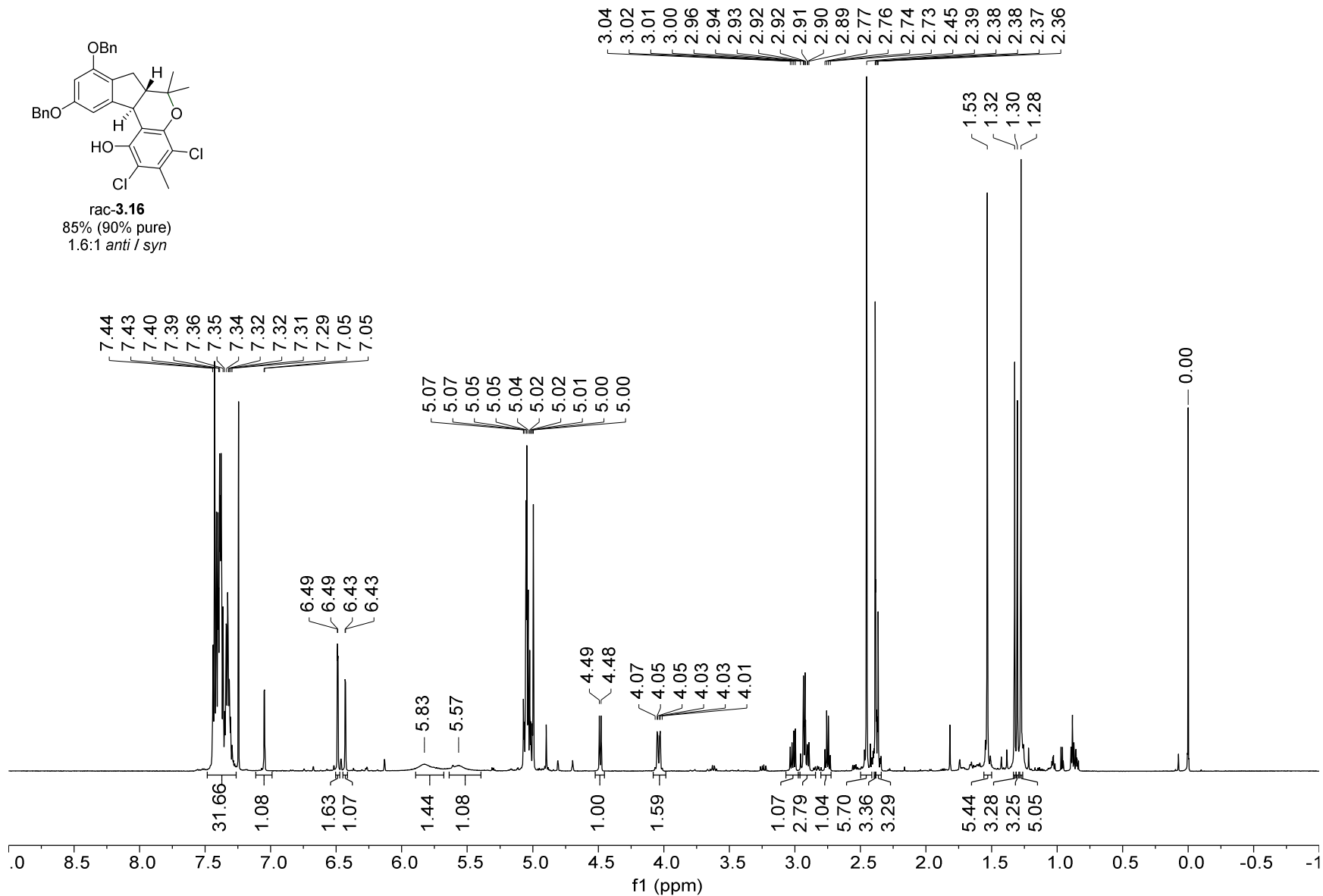


1H NMR — 600.13 MHz — CDCl3T — 298.0 K

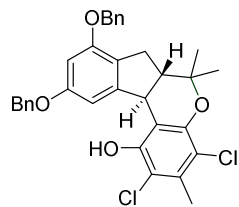


rac-3.16  
85% (90% pure)  
1.6:1 anti / syn

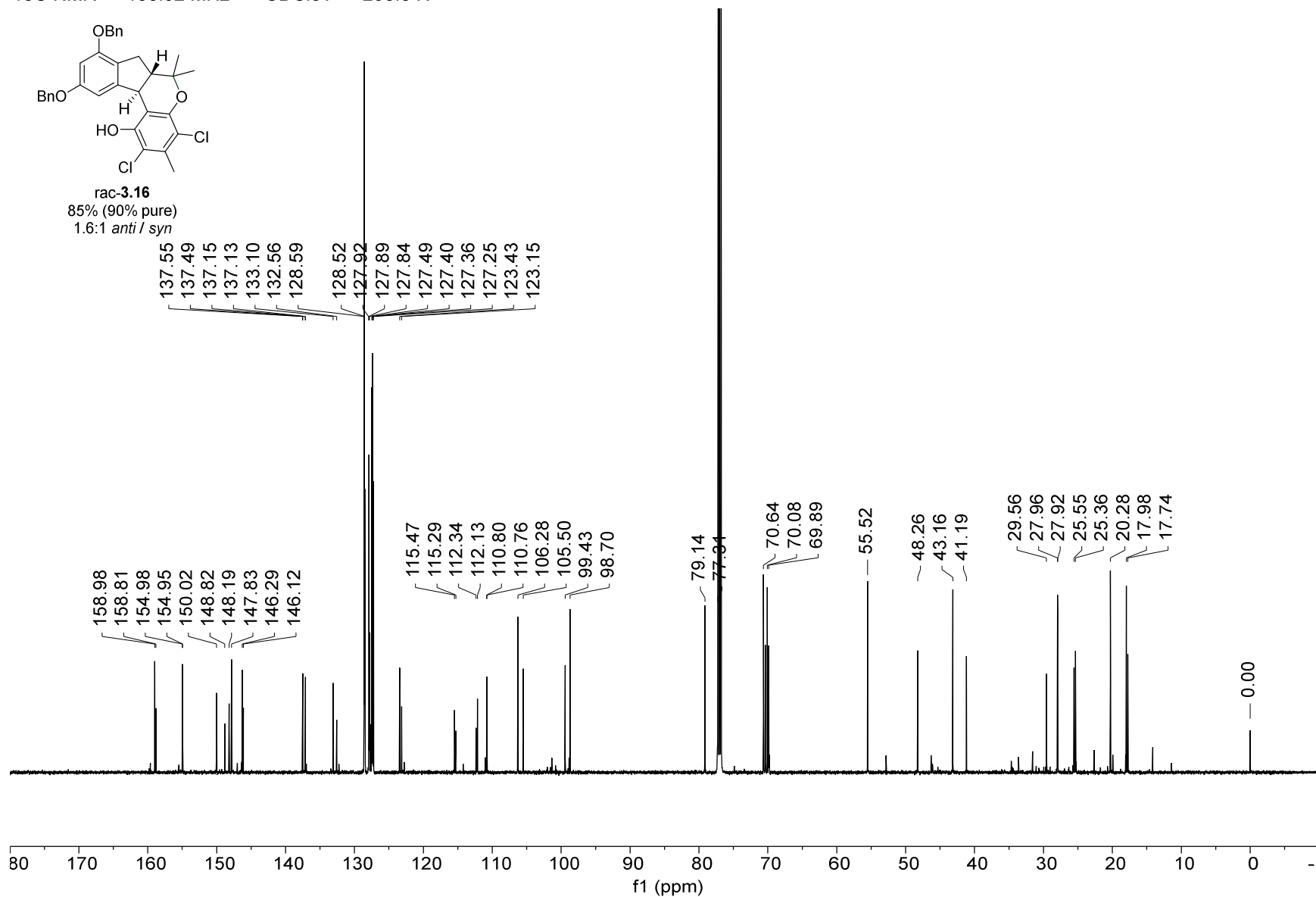
595



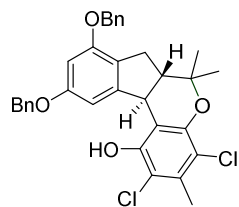
13C NMR — 150.92 MHz — CDCl3T — 298.0 K



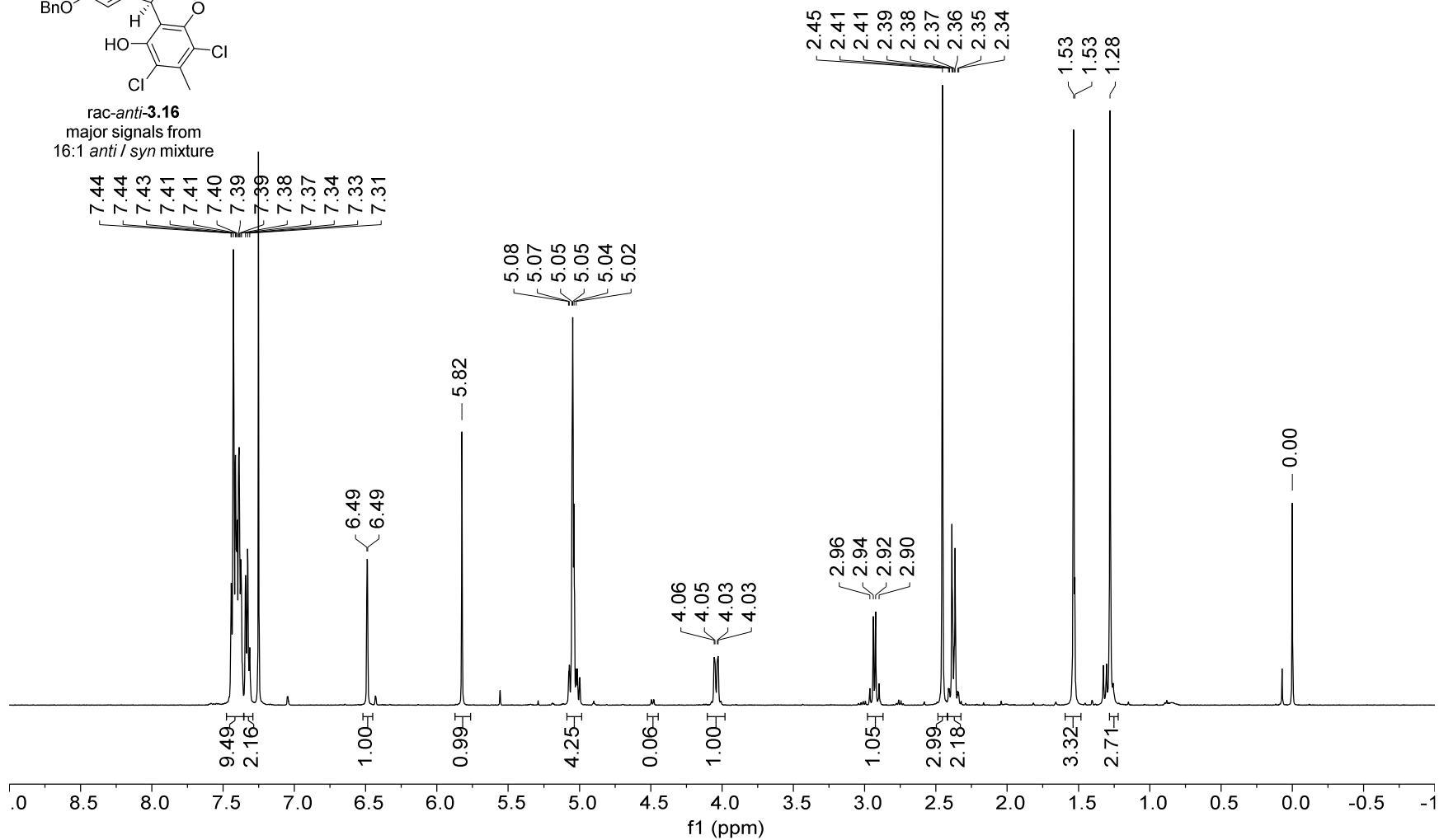
**rac-3.16**  
85% (90% pure)  
1.6:1 *anti* / *syn*



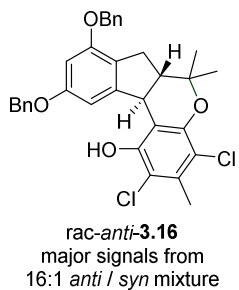
1H NMR — 500.22 MHz — CDCl3T — 298.0 K



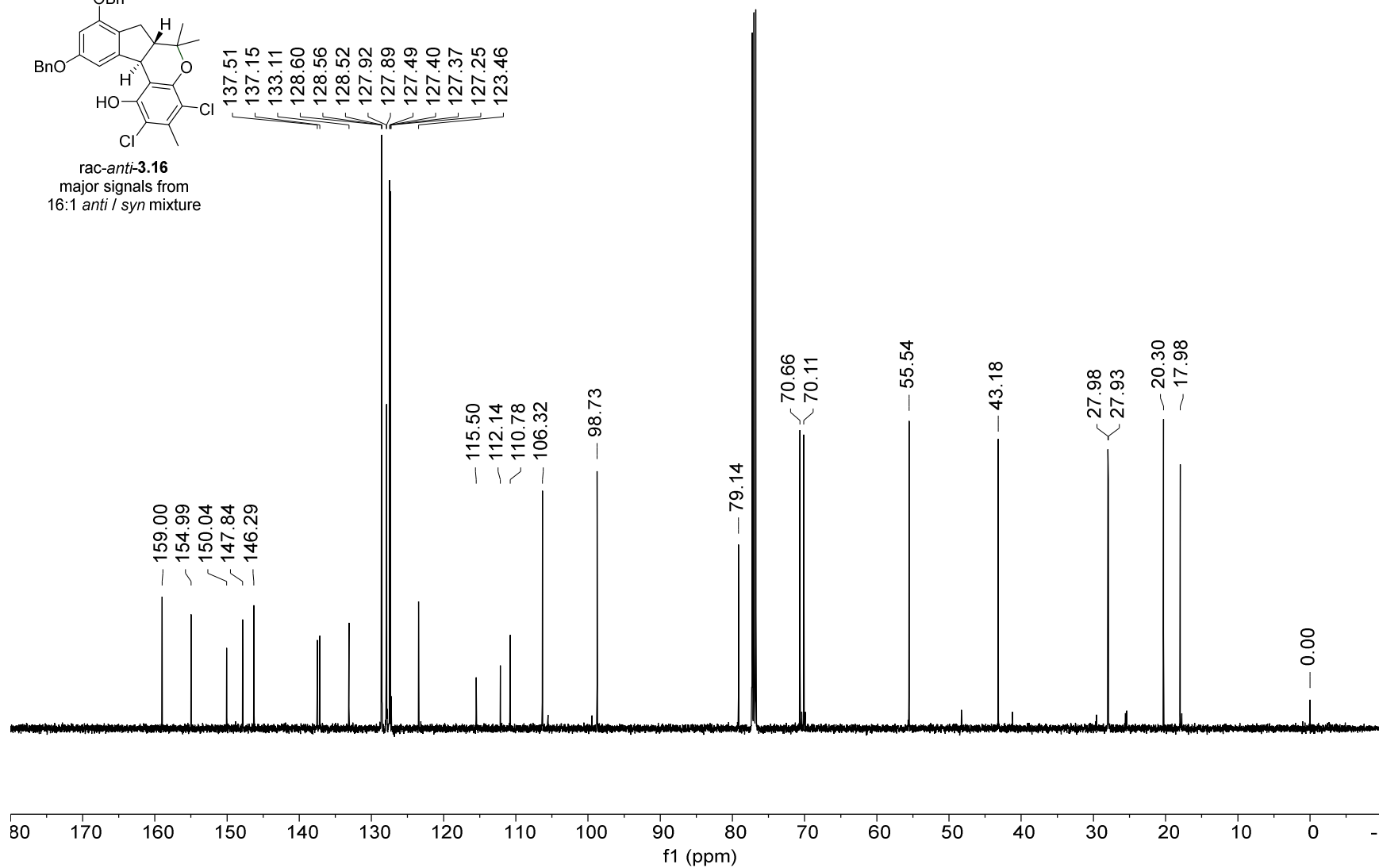
**rac-anti-3.16**  
major signals from  
16:1 *anti* / *syn* mixture



$^{13}\text{C}$  NMR — 125.79 MHz —  $\text{CDCl}_3$  — 298.0 K

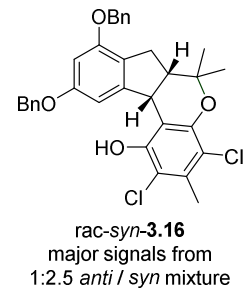
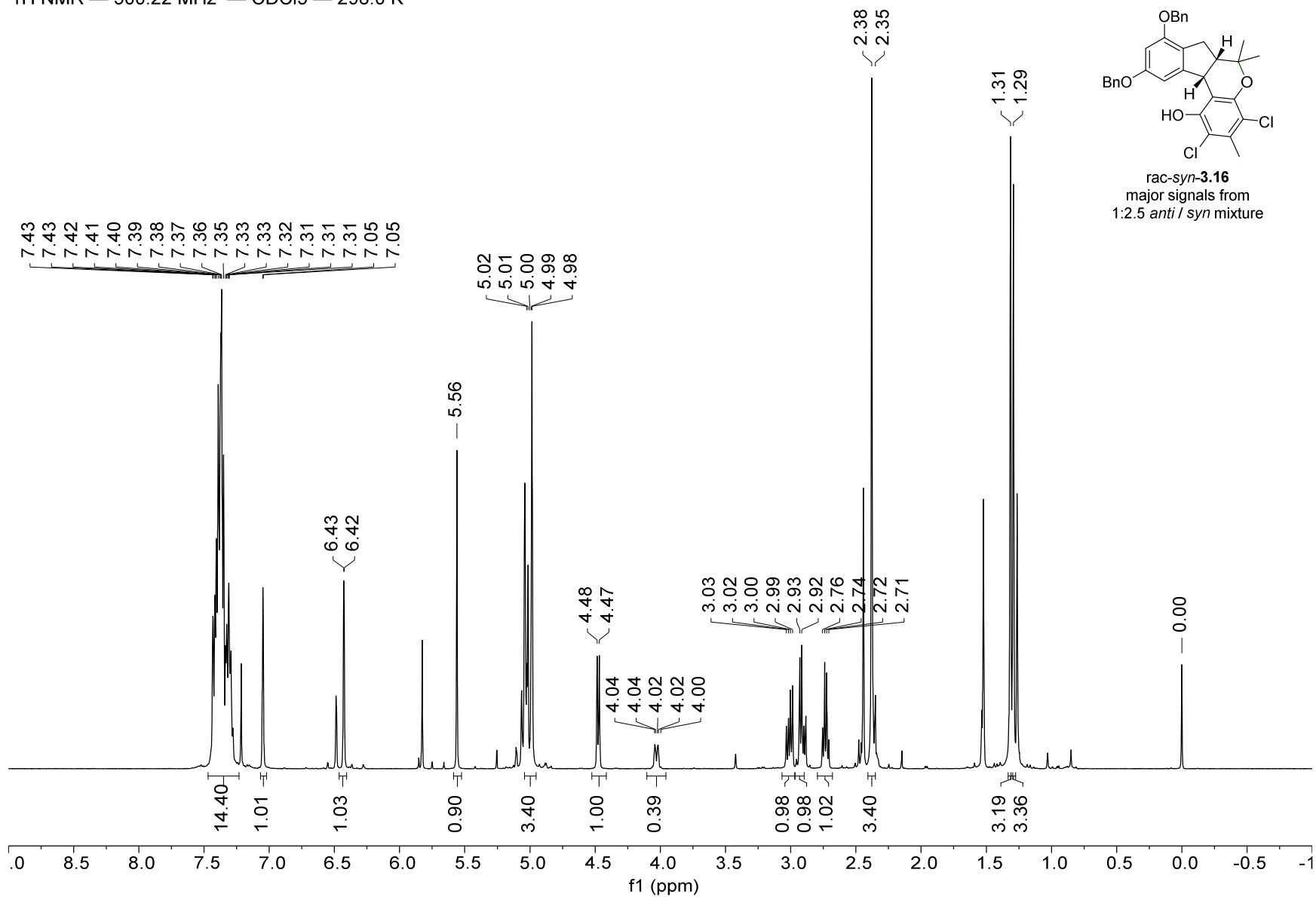


995

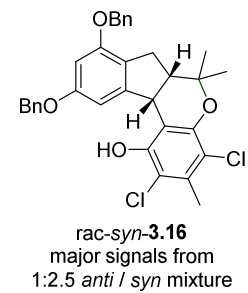


1H NMR — 500.22 MHz — CDCl3 — 298.0 K

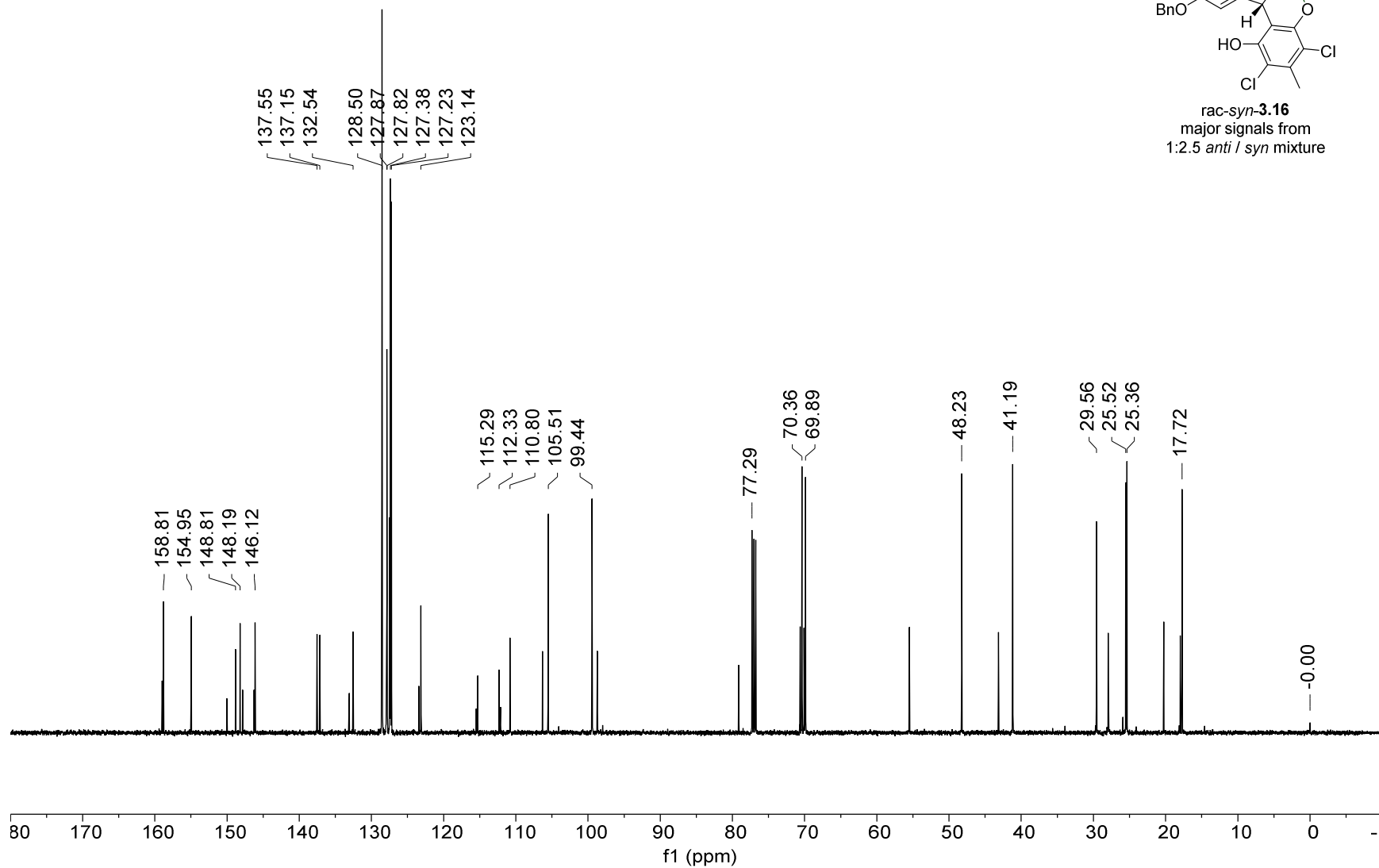
L9E



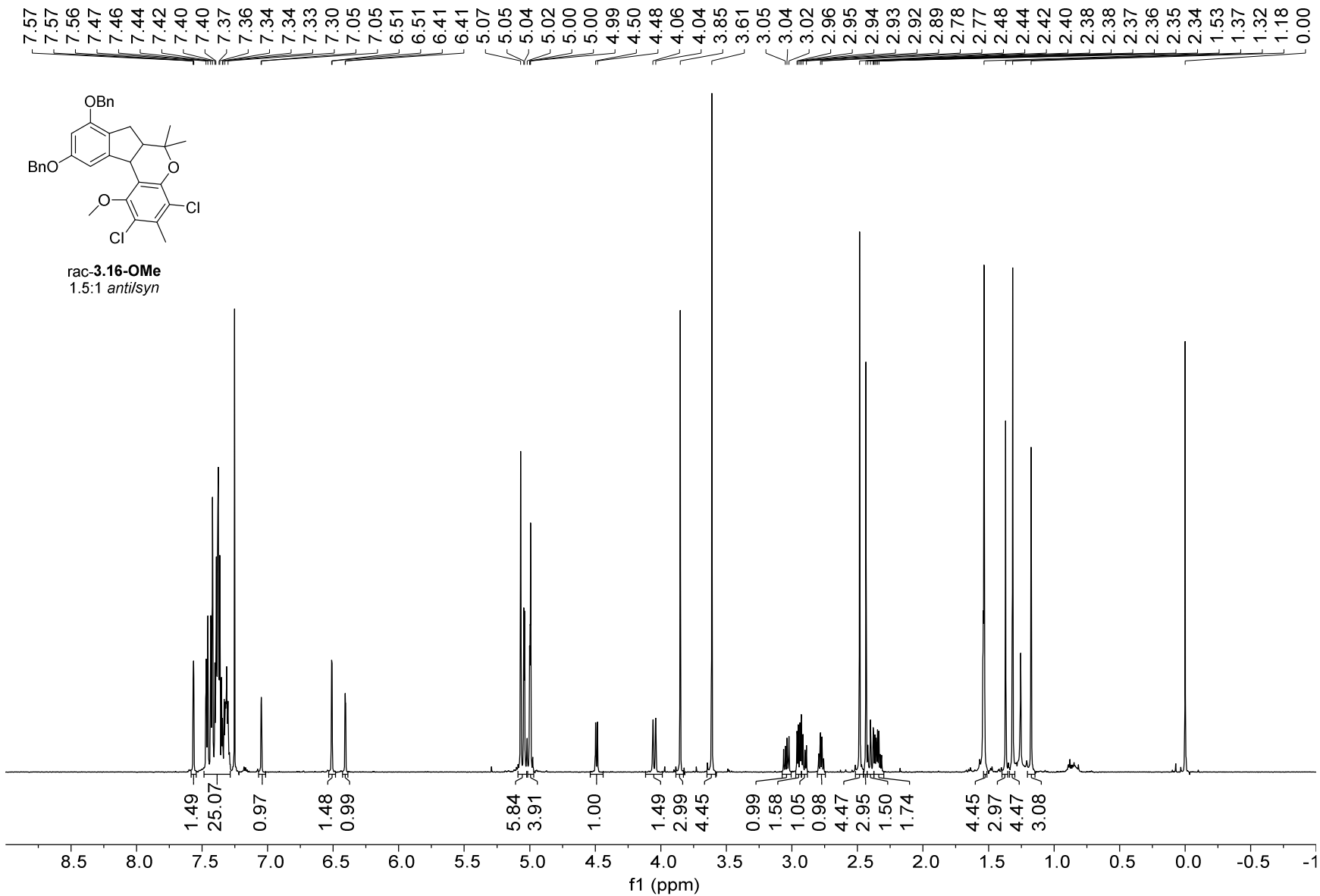
13C NMR — 125.79 MHz — CDCl3T — 298.0 K



895



<sup>1</sup>H NMR — 600.13 MHz — CDCl<sub>3</sub>T — 298.0 K

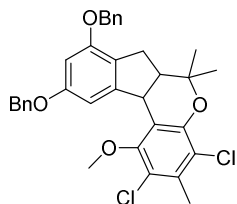




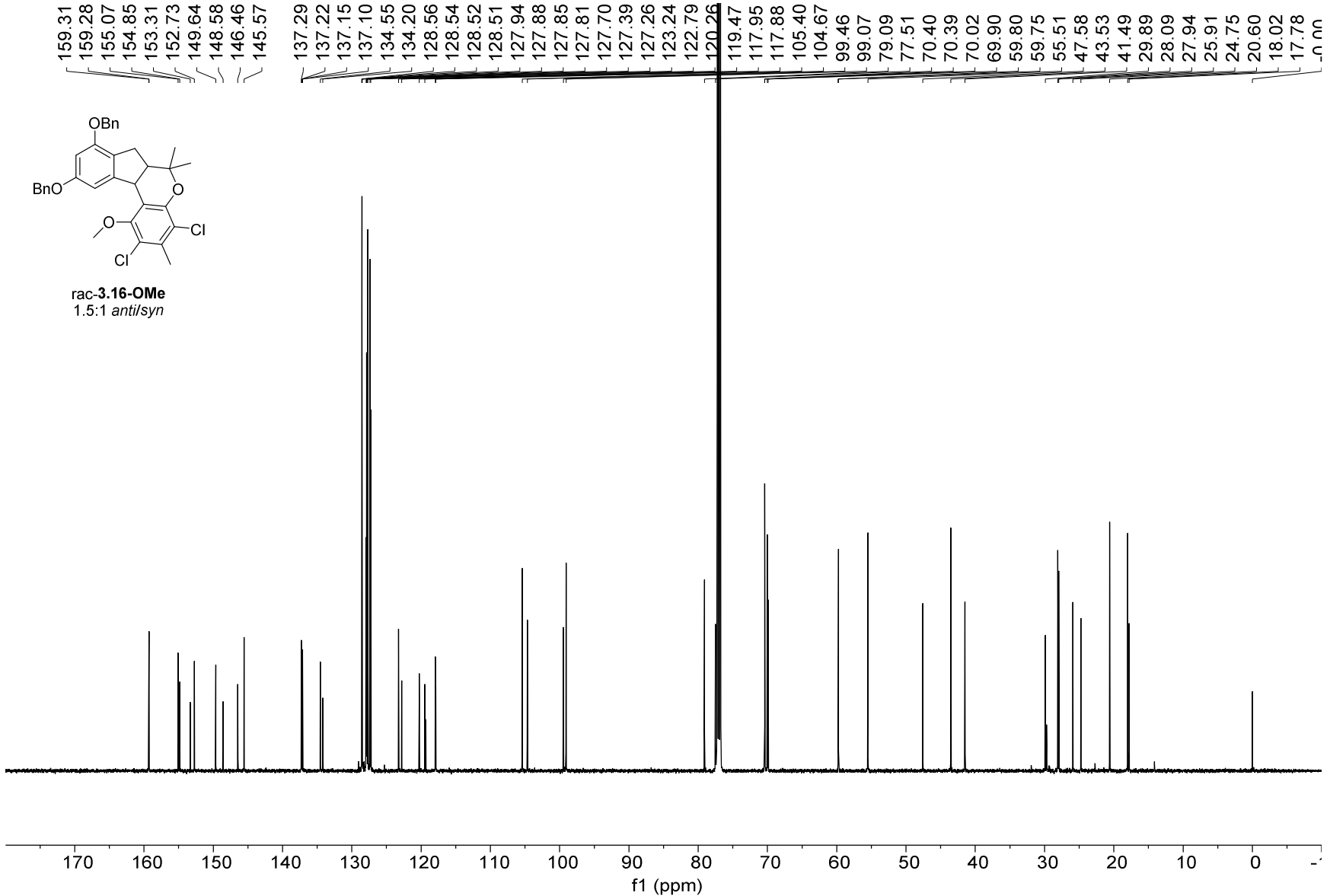
13C NMR — 150.92 MHz — CDCl3T — 298.0 K

159.31  
159.28  
155.07  
154.85  
153.31  
152.73  
149.64  
148.58  
146.46  
145.57

137.29  
137.22  
137.15  
137.10  
134.55  
134.20  
128.56  
128.54  
128.52  
128.51  
127.94  
127.88  
127.85  
127.81  
127.70  
127.39  
127.26  
123.24  
122.79  
120.26  
119.47  
117.95  
117.88  
105.40  
104.67  
99.46  
99.07  
79.09  
77.51  
70.40  
70.39  
70.02  
69.90  
59.80  
59.75  
55.51  
47.58  
43.53  
41.49  
29.89  
28.09  
27.94  
25.91  
24.75  
20.60  
18.02  
17.78  
-0.00

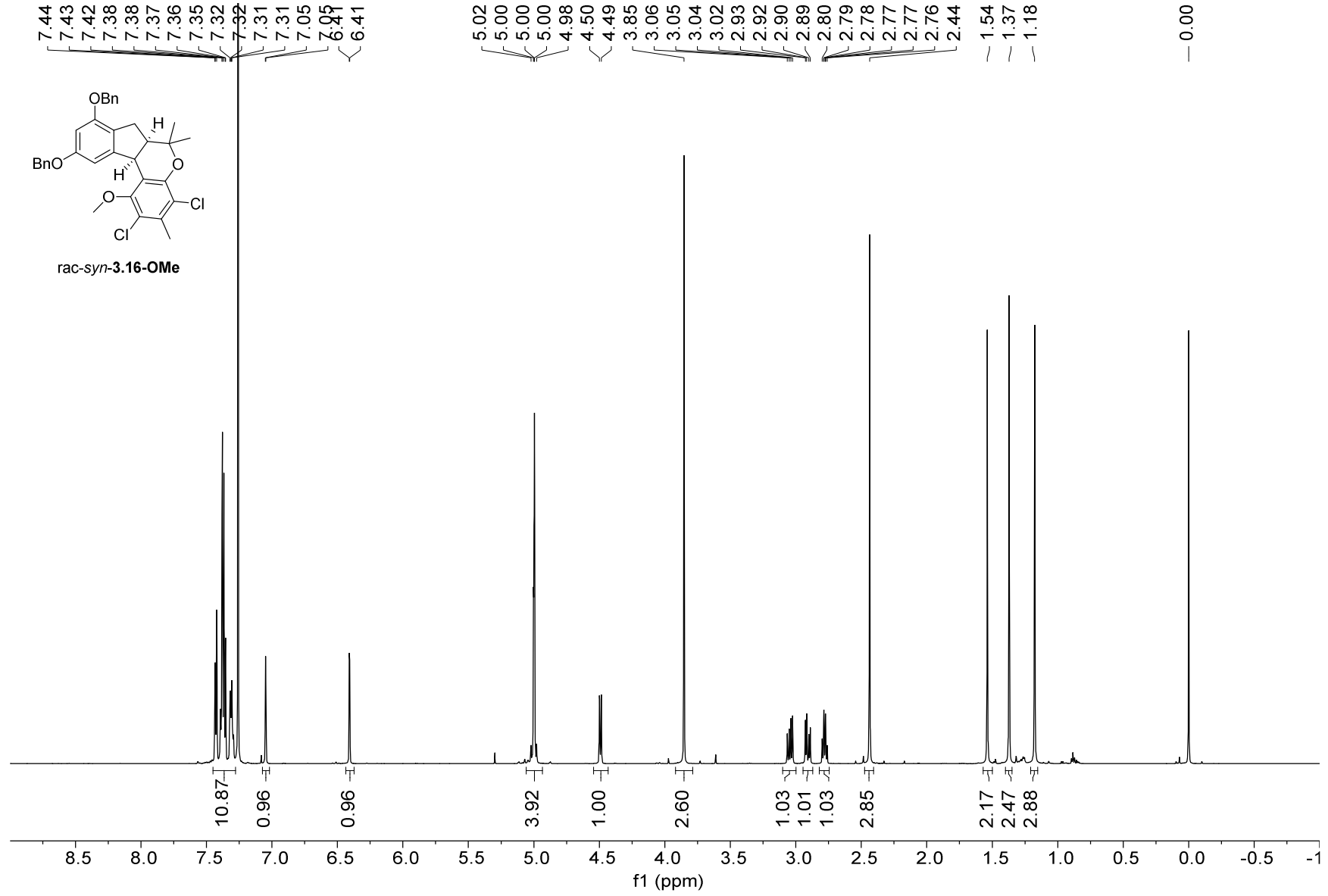
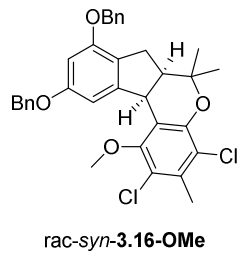


rac-3.16-OMe  
1.5:1 *anti/syn*



371

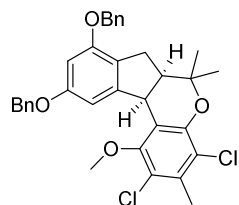
1H NMR — 600.13 MHz — CDCl3T — 298.0 K



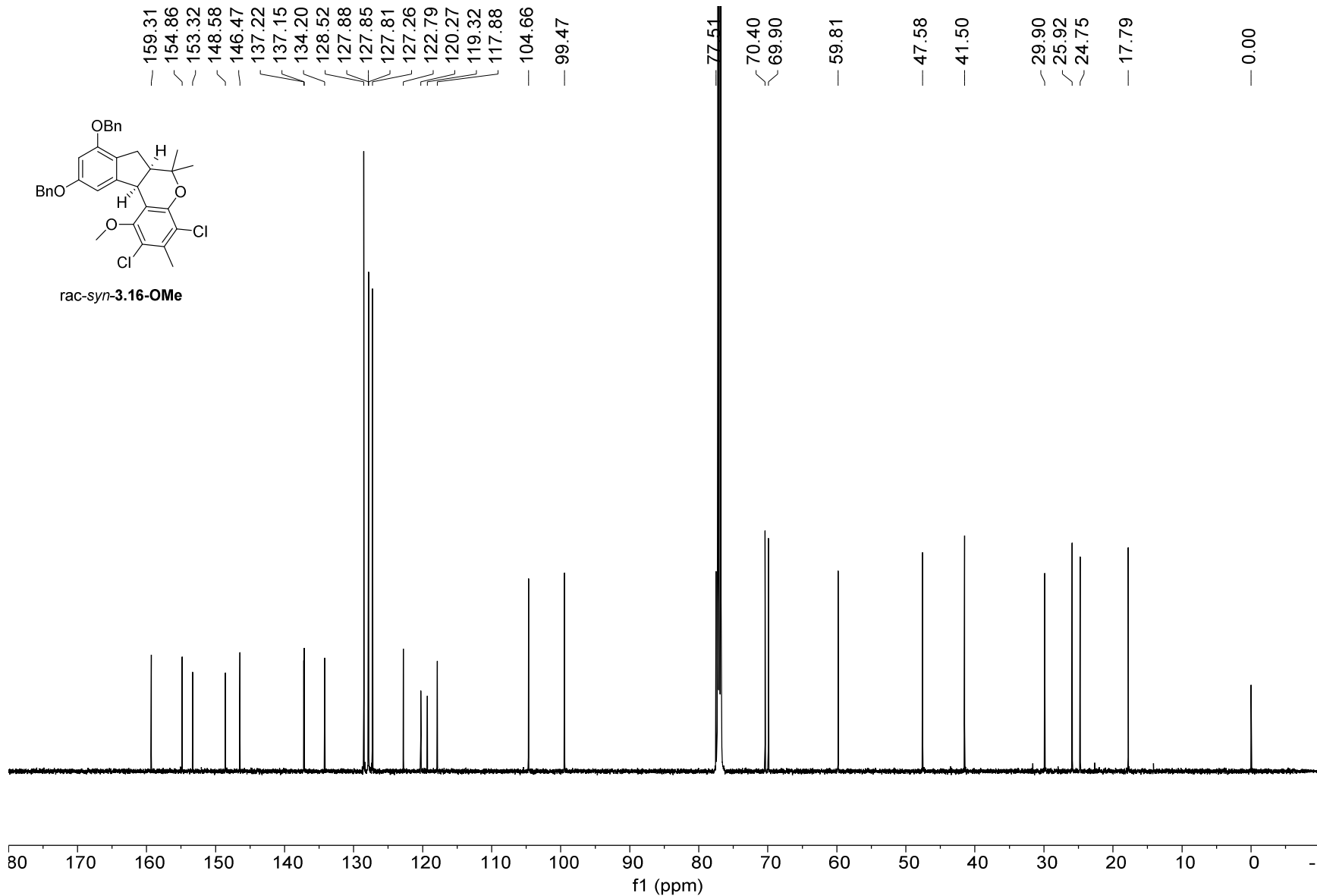
13C NMR — 150.92 MHz — CDCl3T — 298.0 K

159.31  
154.86  
153.32  
148.58  
146.47  
137.22  
137.15  
134.20  
128.52  
127.88  
127.85  
127.81  
127.26  
122.79  
120.27  
119.32  
117.88  
— 104.66  
— 99.47

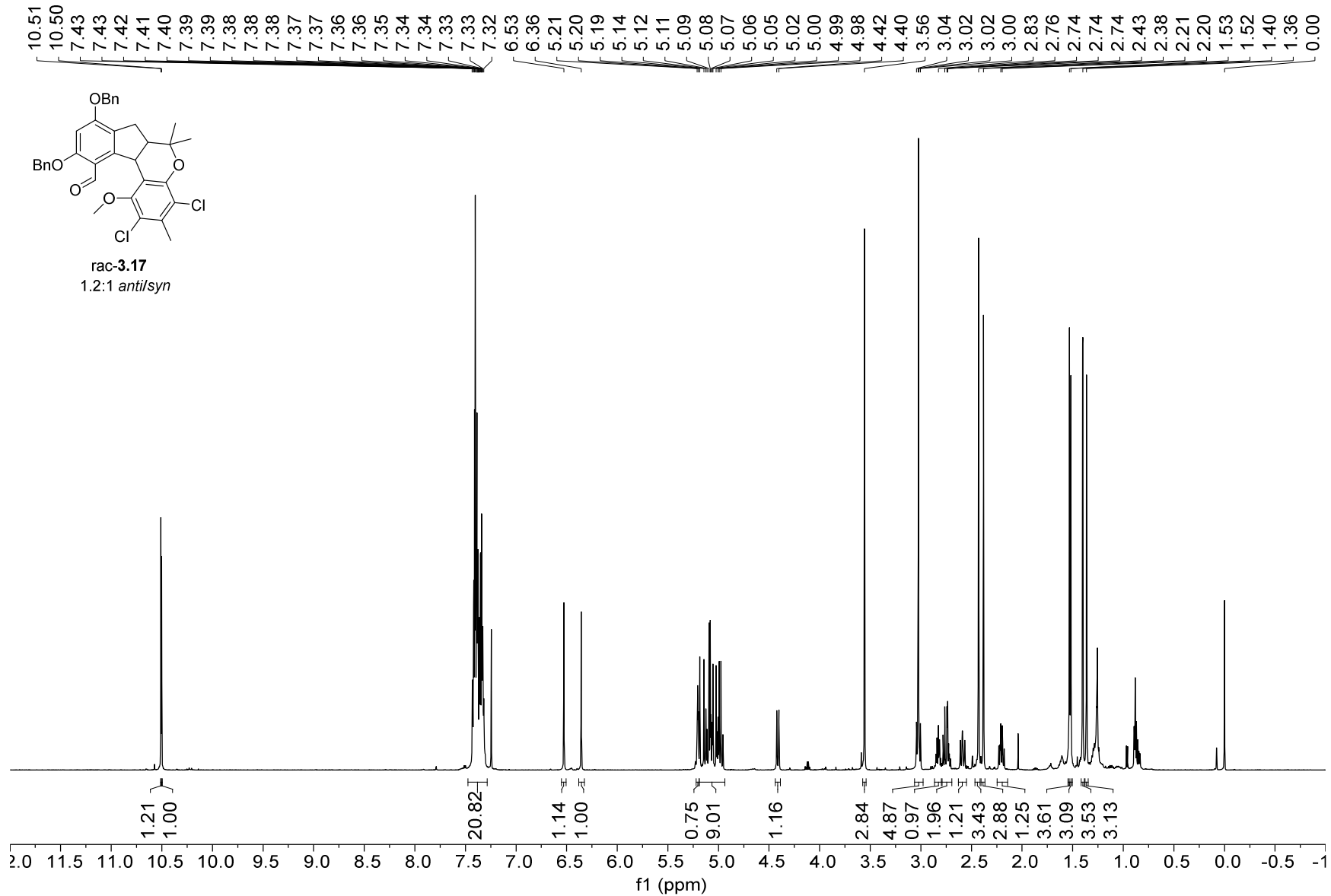
77.51  
70.40  
69.90  
— 59.81  
— 47.58  
— 41.50  
— 29.90  
— 25.92  
— 24.75  
— 17.79  
— 0.00



rac-syn-3.16-OMe

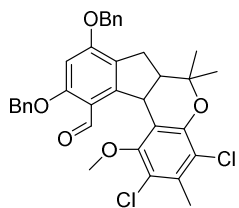


1H NMR — 600.13 MHz — CDCl3T — 298.0 K

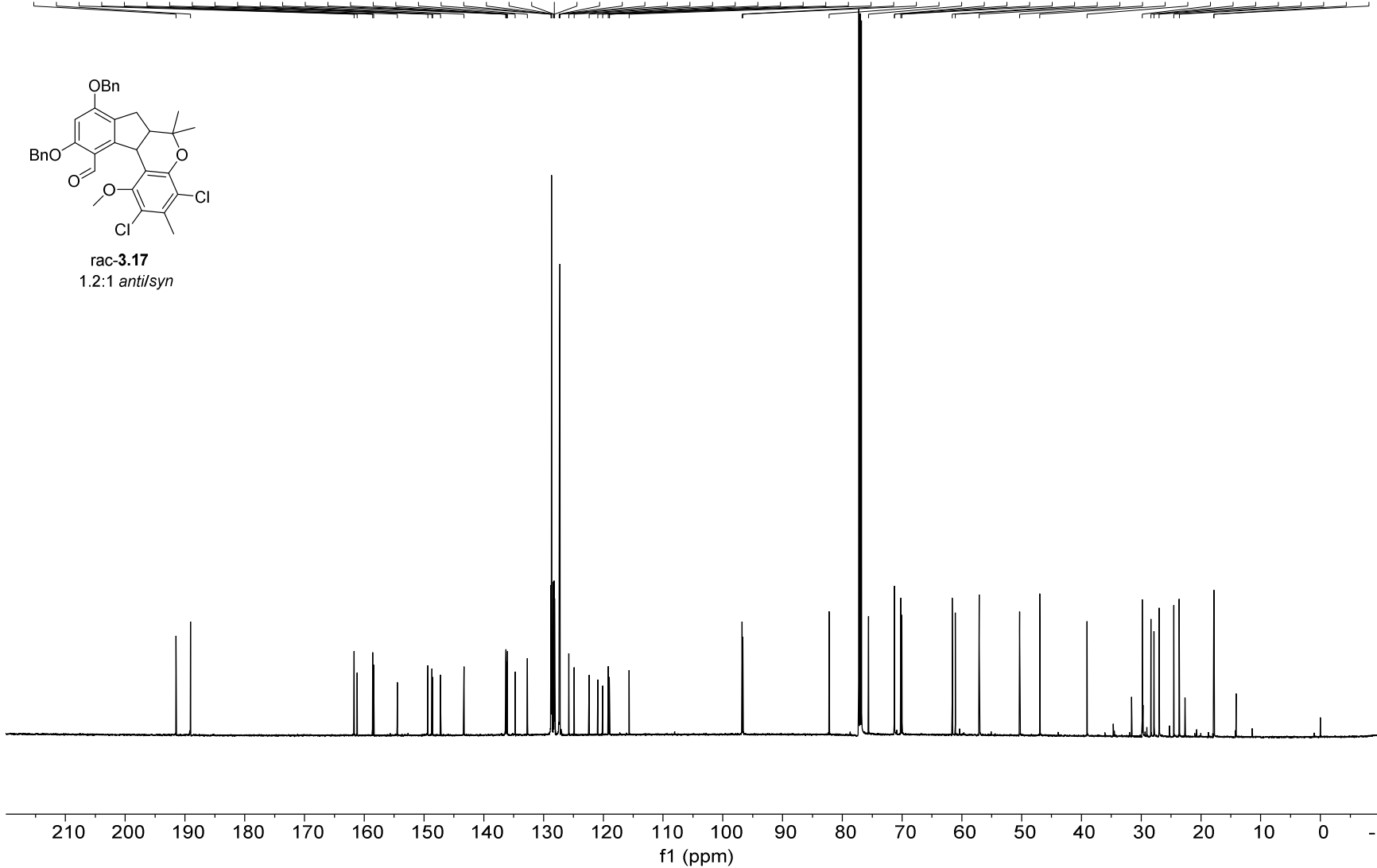


13C NMR — 150.92 MHz — CDCl3T — 298.0 K

191.48  
189.07  
161.69  
161.18  
158.61  
158.41  
154.48  
149.36  
148.67  
148.56  
147.22  
143.33  
136.33  
136.29  
136.18  
136.05  
134.76  
132.69  
128.74  
128.72  
128.65  
128.35  
128.24  
128.18  
128.14  
127.41  
127.36  
127.30  
127.26  
125.77  
124.89  
122.39  
120.93  
120.11  
119.18  
119.02  
118.96  
115.70  
96.80  
96.64  
82.22  
75.62  
71.30  
71.26  
70.22  
70.02  
61.62  
61.11  
57.09  
50.32  
46.96  
39.06  
29.82  
28.38  
27.84  
26.98  
24.53  
23.62  
17.87  
17.81

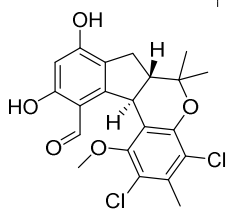


rac-3.17  
1.2:1 *anti/syn*

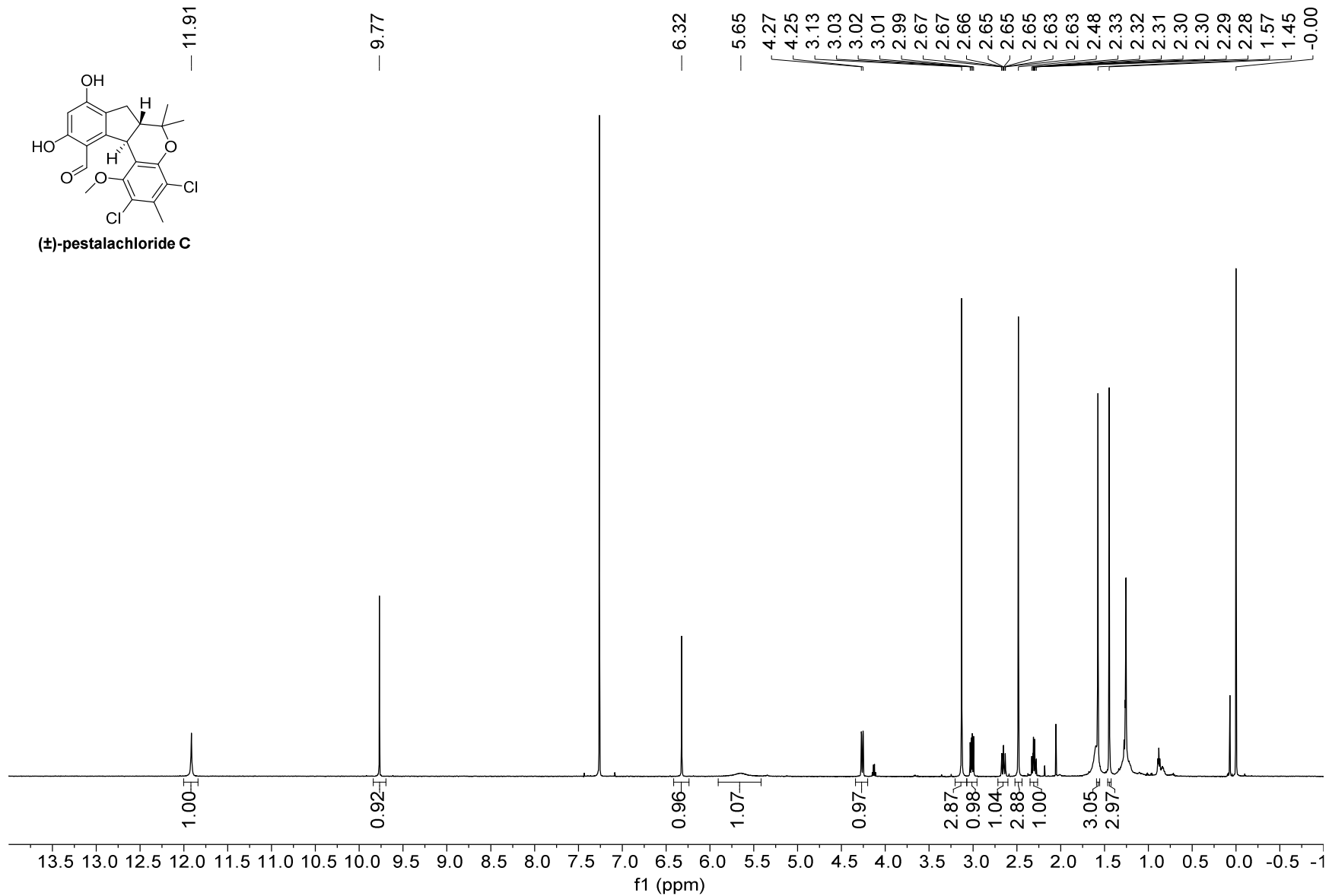


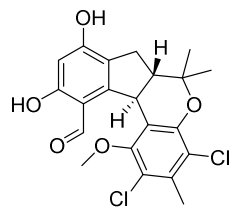
375

1H NMR — 600.13 MHz — CDCl3T — 298.0 K

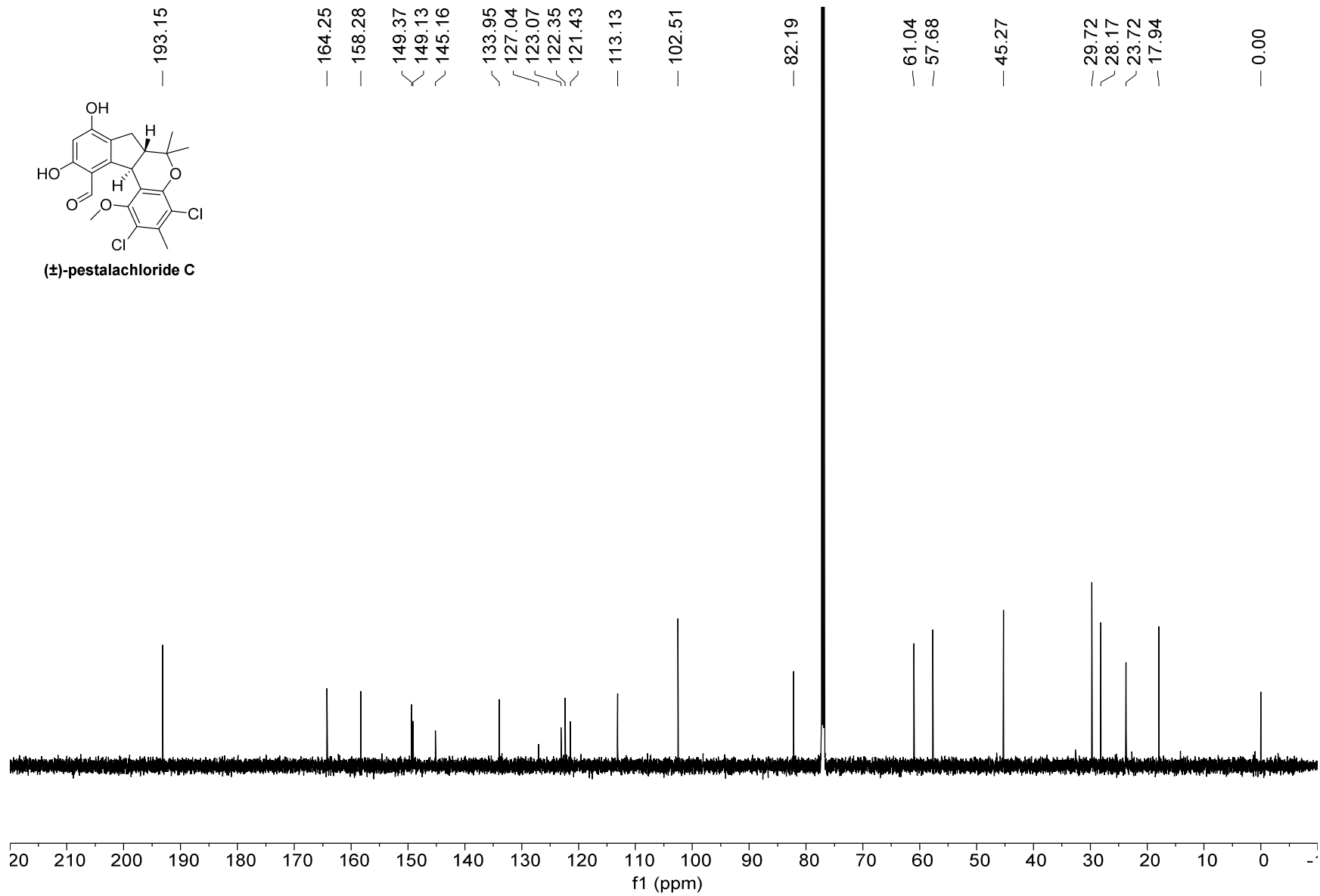


(±)-pestalchloride C



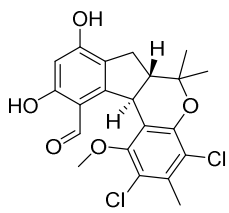
13C NMR — 150.92 MHz — CDCl<sub>3</sub>T — 298.0 K

(±)-pestalachloride C

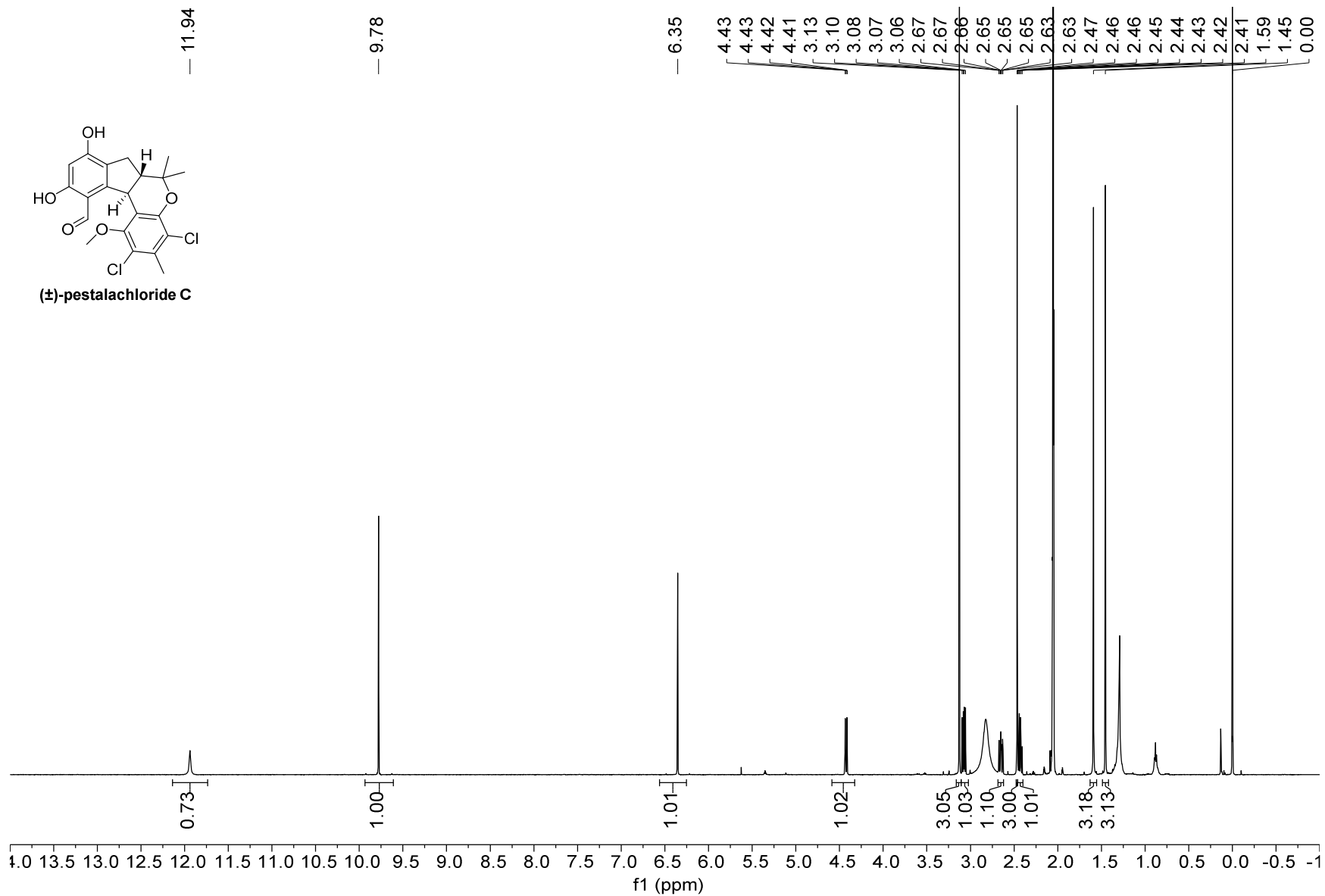


377

1H NMR — 600.13 MHz — acetone-d<sub>6</sub> — 298.0 K



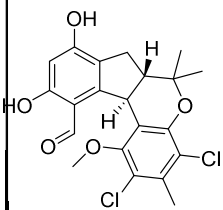
(±)-pestalchloride C



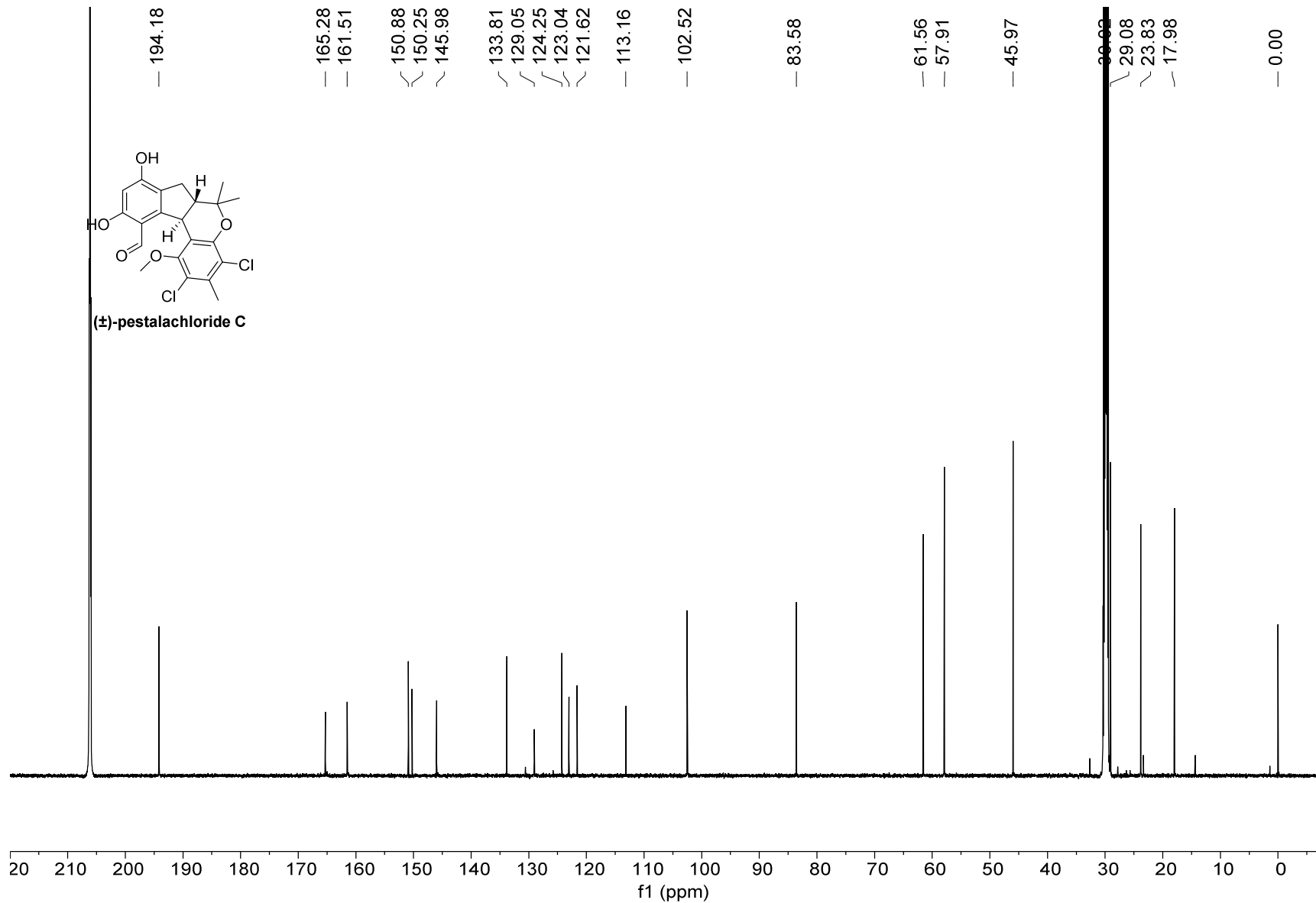


13C NMR — 150.92 MHz — acetone-d6 — 298.0 K

378

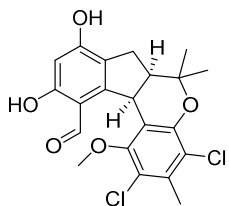


(±)-pestalachloride C

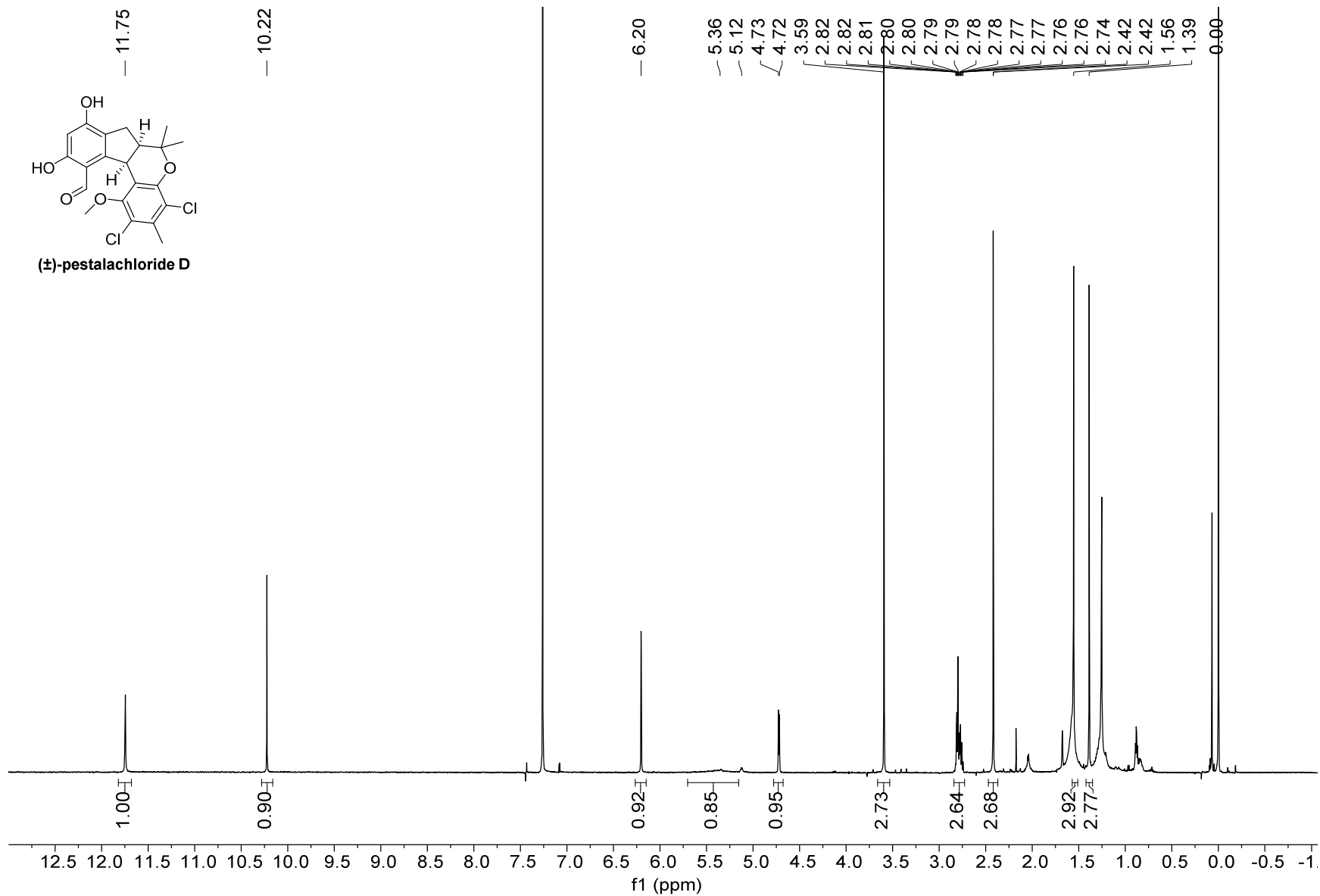


379

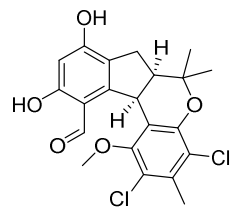
1H NMR — 600.13 MHz — CDCl3T — 298.0 K



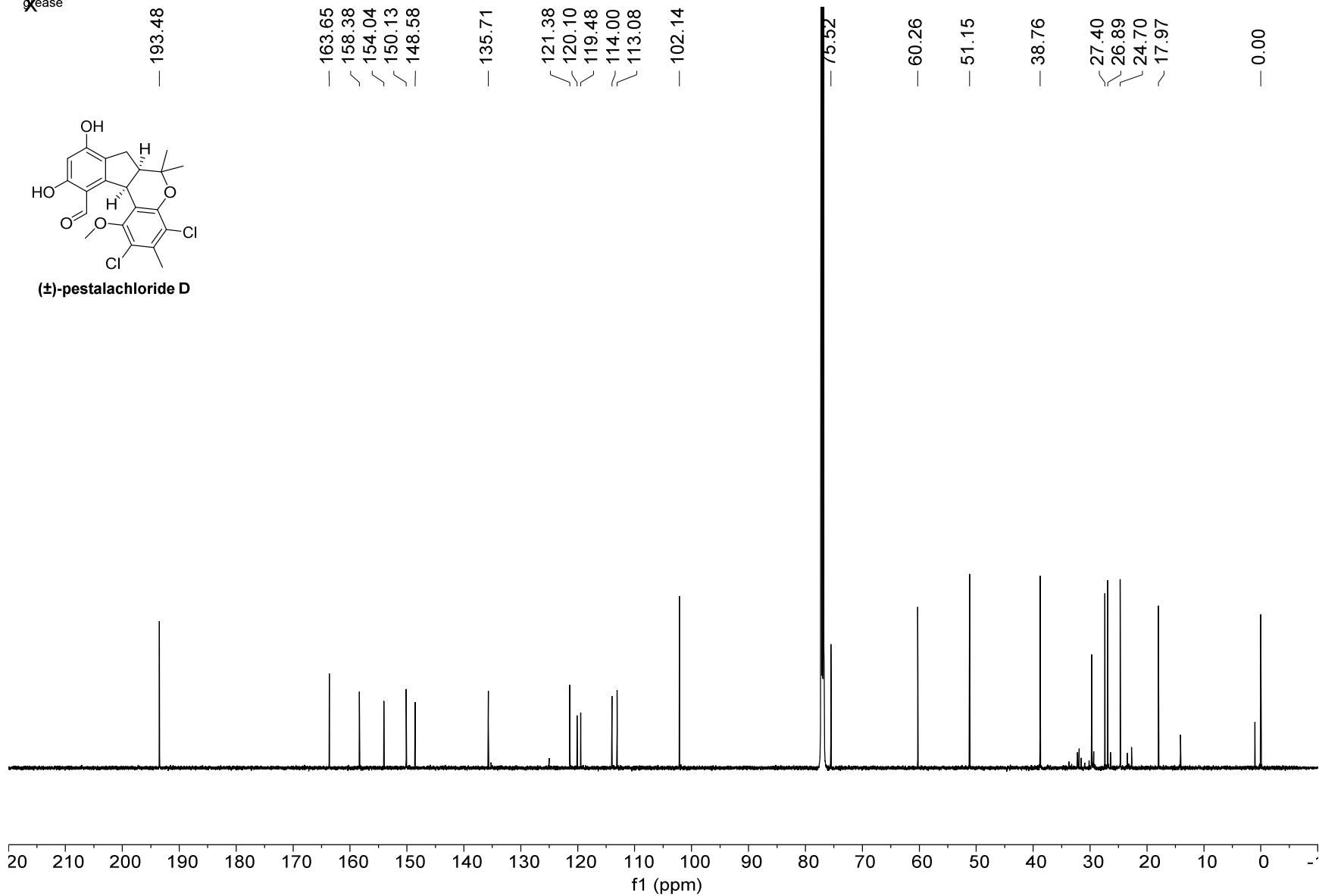
(±)-pestalachloride D



<sup>13</sup>C NMR — 150.92 MHz — CDCl<sub>3</sub>T — 298.0 K



(±)-pestalachloride D



## **Appendix D: Chapter 4 – NMR**

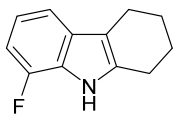
1H NMR — 499.07 MHz — CDCl3 — 298.0 K

— 7.81  
— 7.21  
— 6.96  
— 6.82

— 2.73

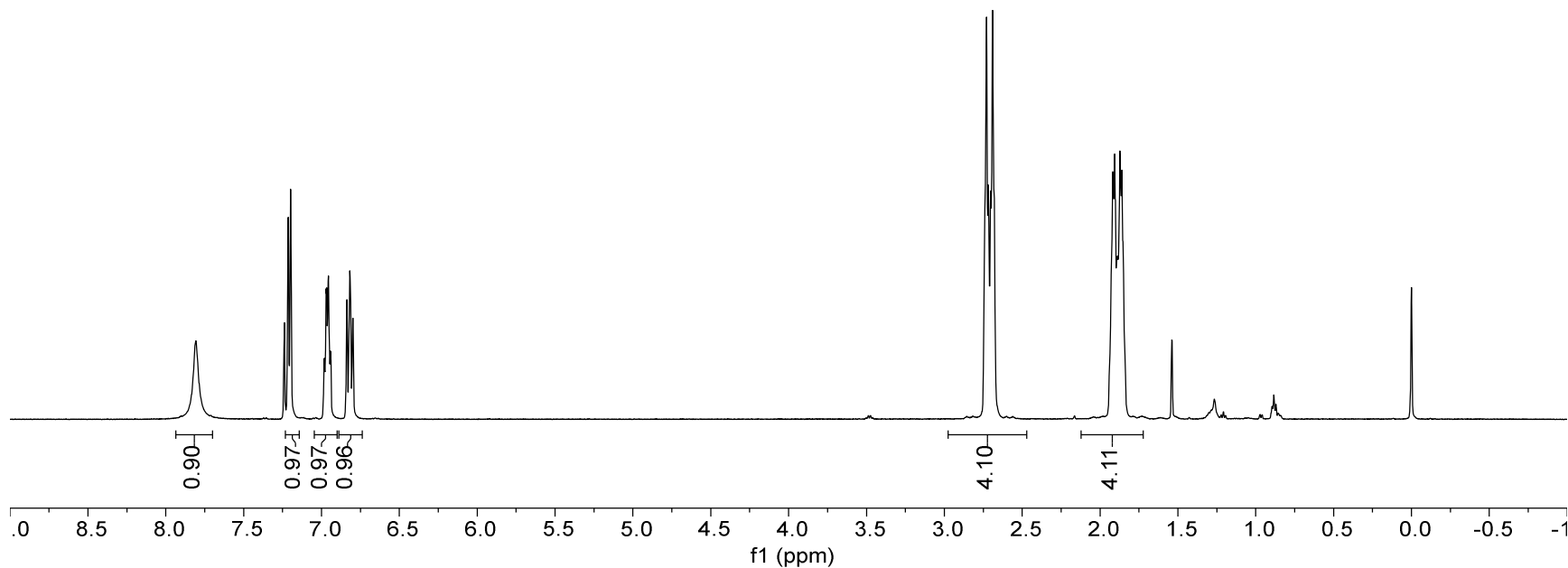
— 1.91

— -0.00



8-fluoro-2,3,4,9-tetrahydro-1H-carbazole

382

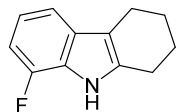


13C NMR — 125.51 MHz — CDCl3 — 298.0 K

150.14  
148.21  
134.89  
131.61  
123.51  
119.33  
113.53  
111.02  
106.16

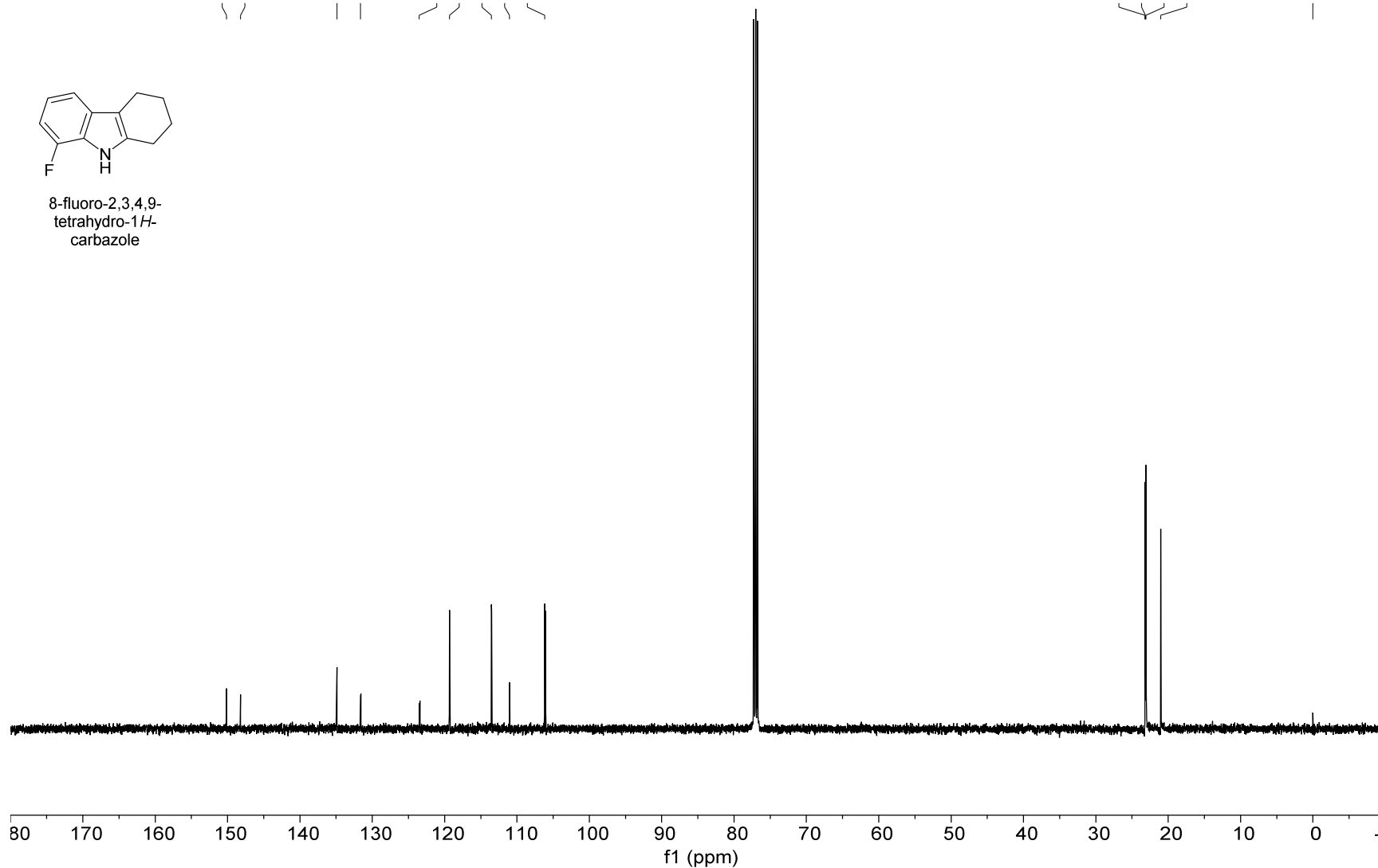
23.21  
23.14  
23.08  
21.03

-0.00



8-fluoro-2,3,4,9-tetrahydro-1H-carbazole

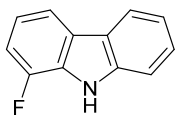
383



1H NMR — 500.22 MHz — CDCl3 — 298.0 K

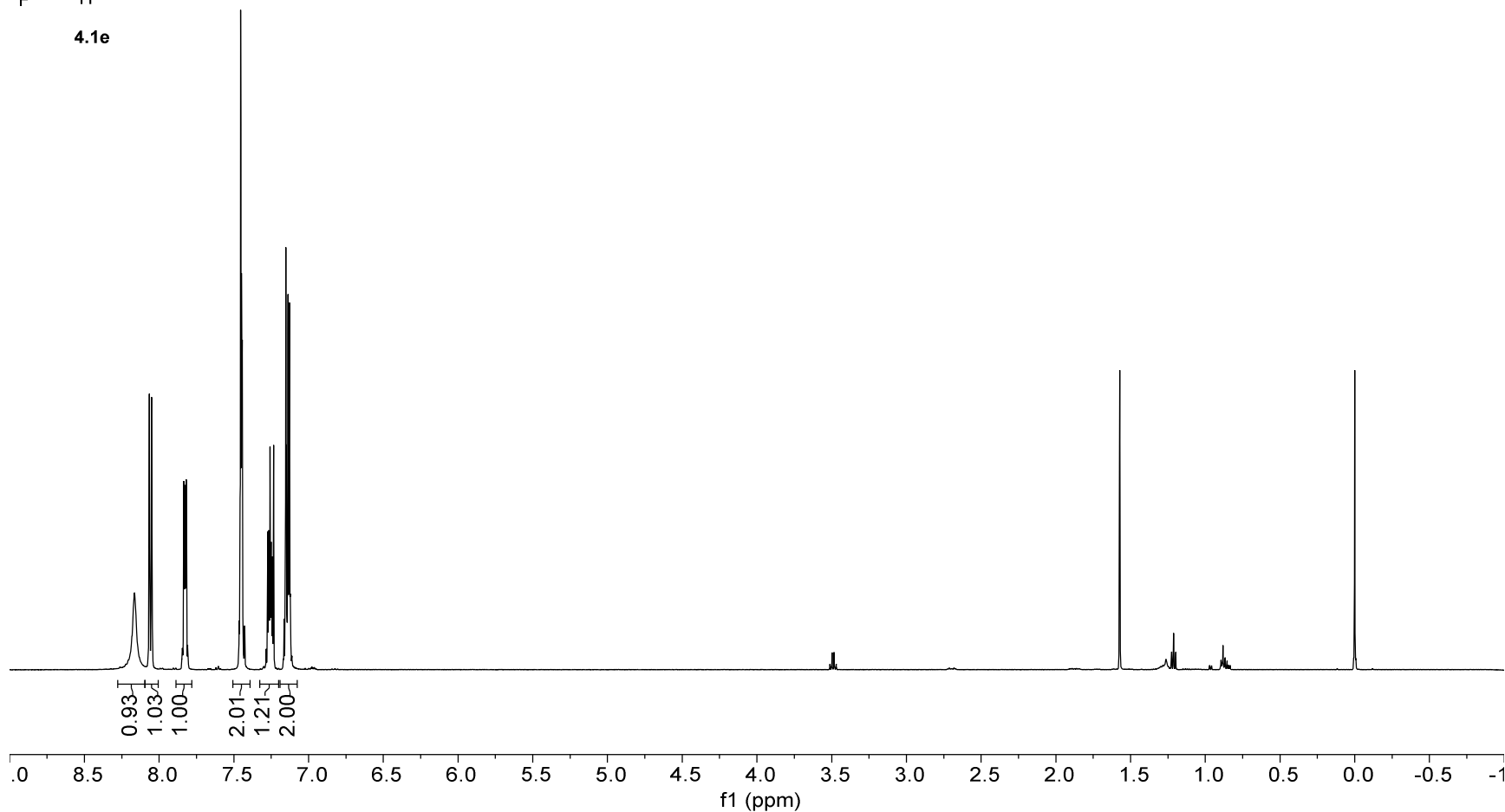
8.17  
8.07  
7.84  
7.45  
7.26  
7.15

0.00



4.1e

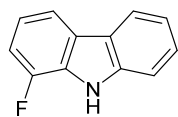
384



13C NMR — 125.79 MHz — CDCl3 — 298.0 K

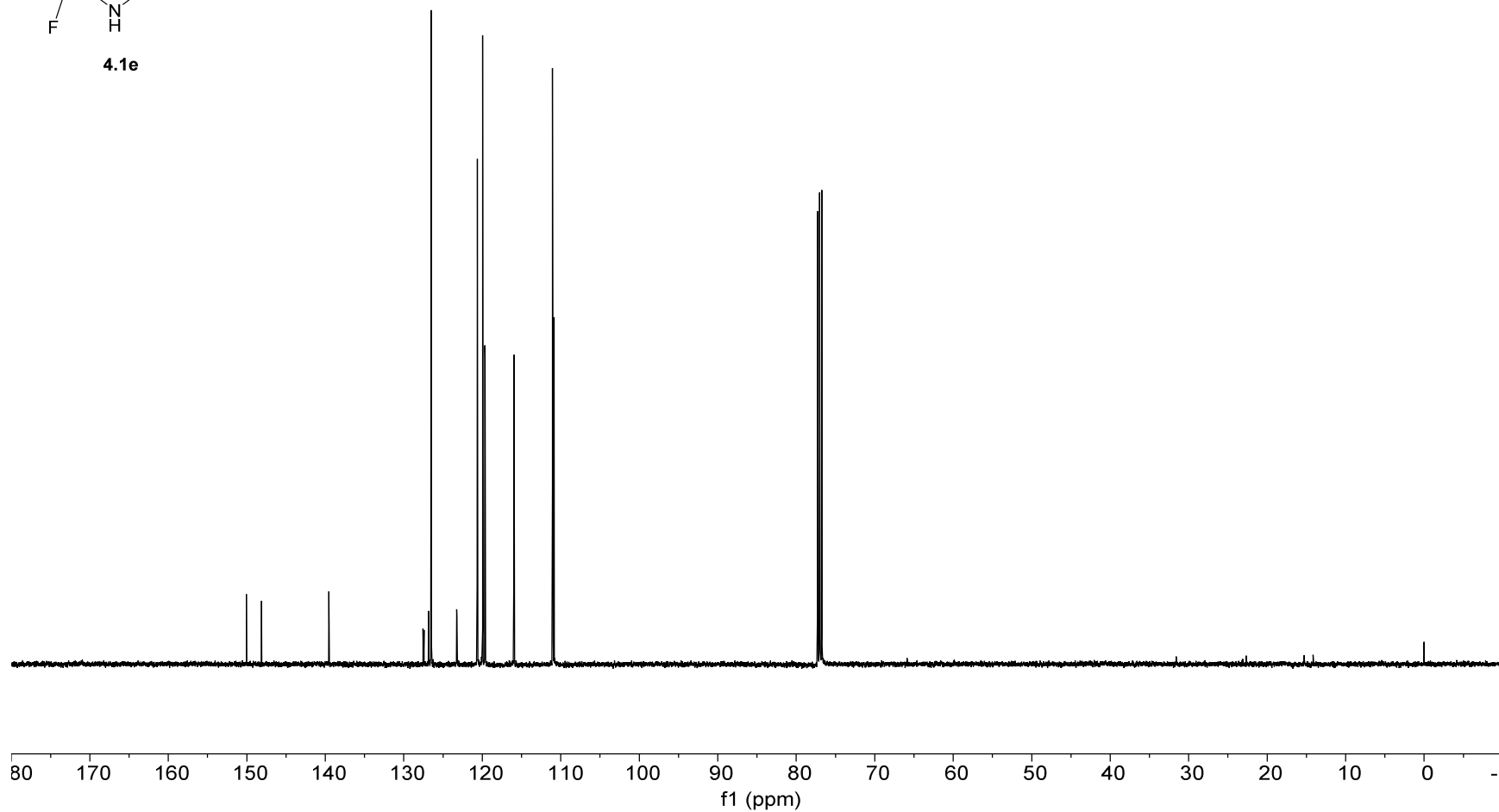
150.04  
148.11  
139.53  
127.53  
126.86  
126.50  
123.25  
120.63  
119.95  
119.68  
115.97  
111.05  
110.99

0.00



4.1e

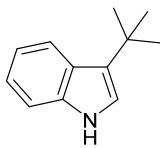
385





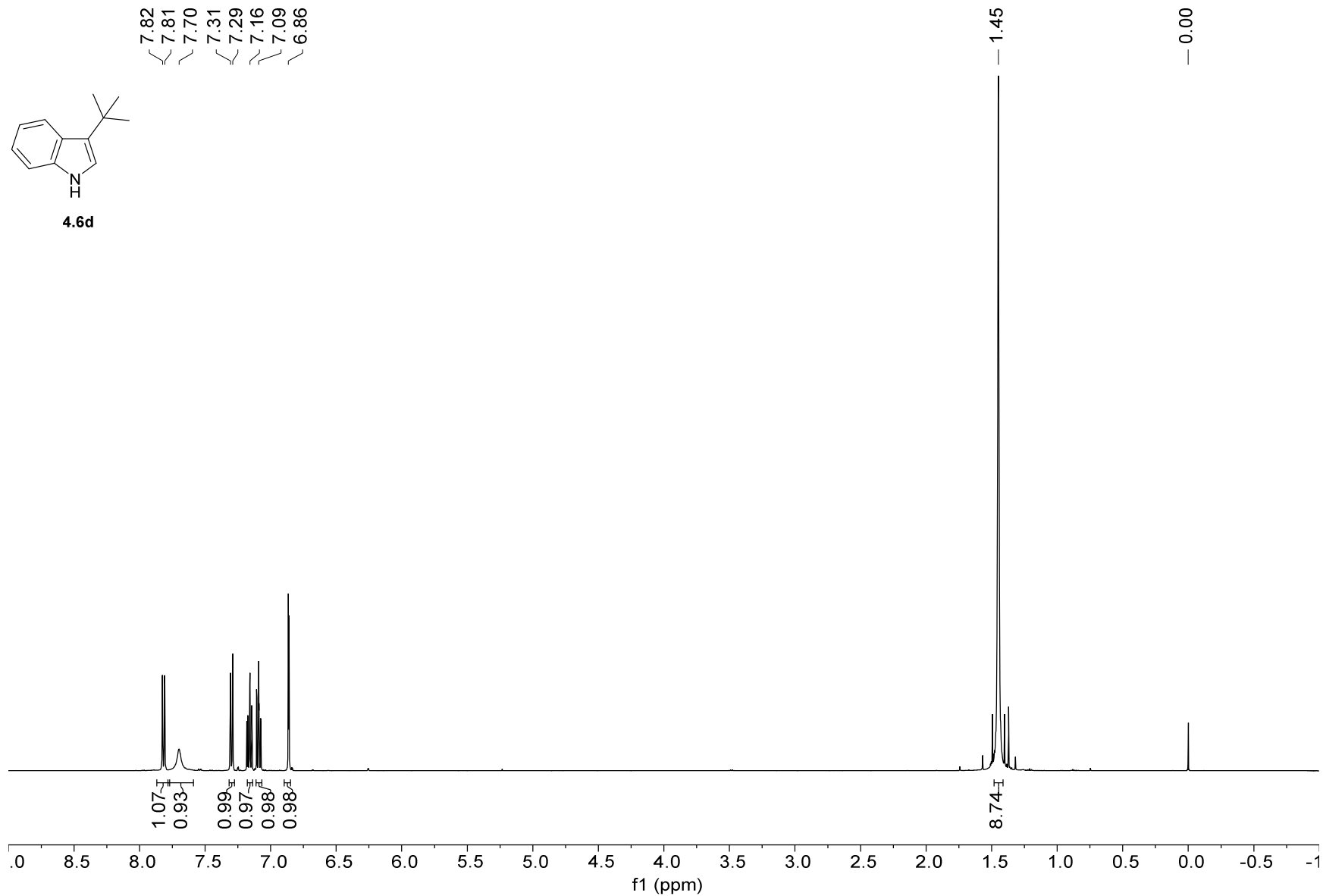
1H NMR — 500.22 MHz — CDCl3 — 298.0 K

7.82  
7.81  
7.70  
7.31  
7.29  
7.16  
7.09  
6.86



4.6d

983

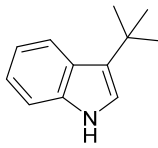


13C NMR — 125.79 MHz — CDCl3 — 298.0 K

— 137.12  
— 126.65  
— 125.84  
— 121.38  
— 121.23  
— 119.21  
— 118.70  
— 111.29

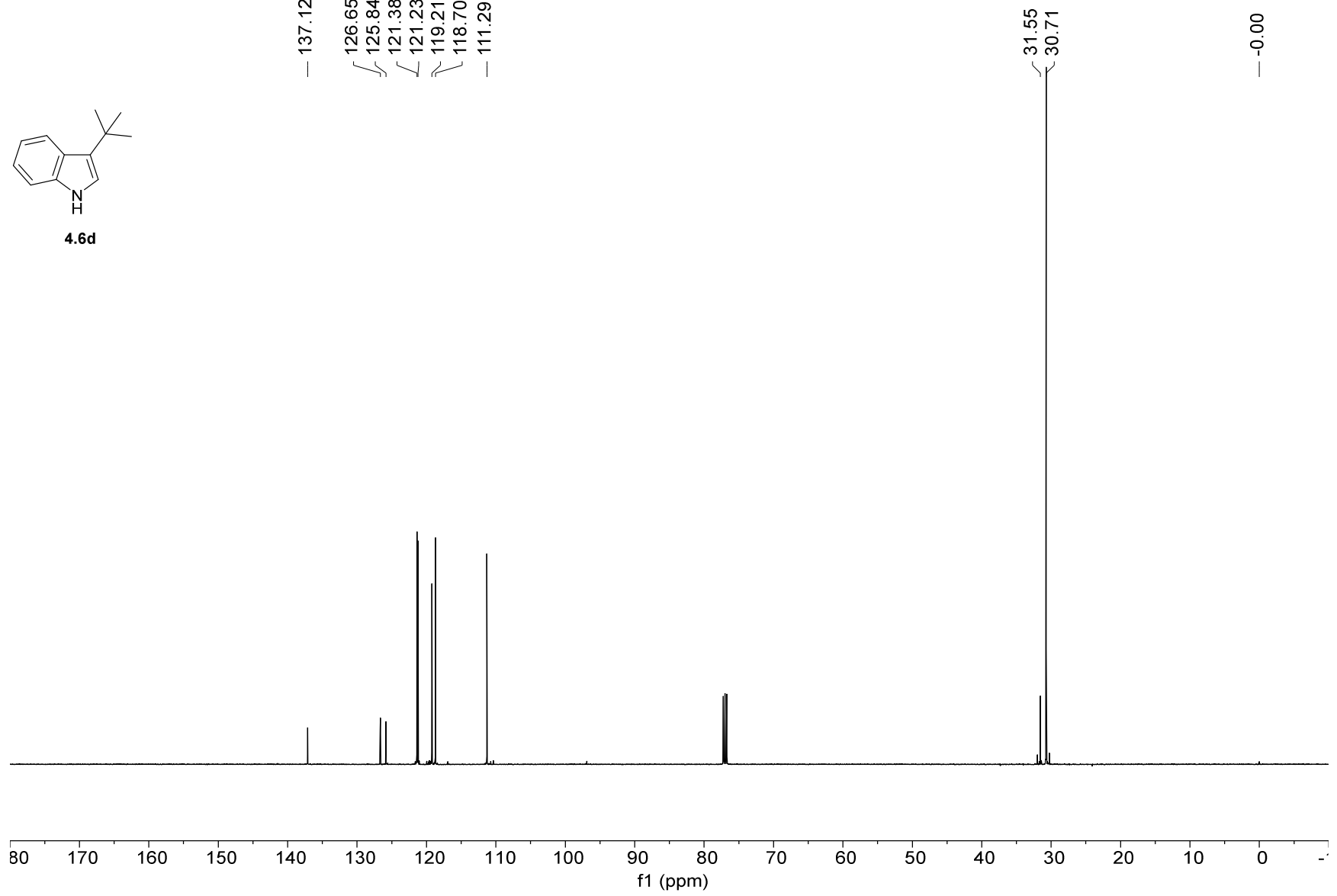
31.55  
30.71

— -0.00



4.6d

385



1H NMR — 500.22 MHz — CDCl3T — 298.0 K

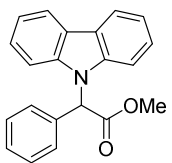
8.12  
8.10

7.36  
7.32  
7.26  
7.24

6.62

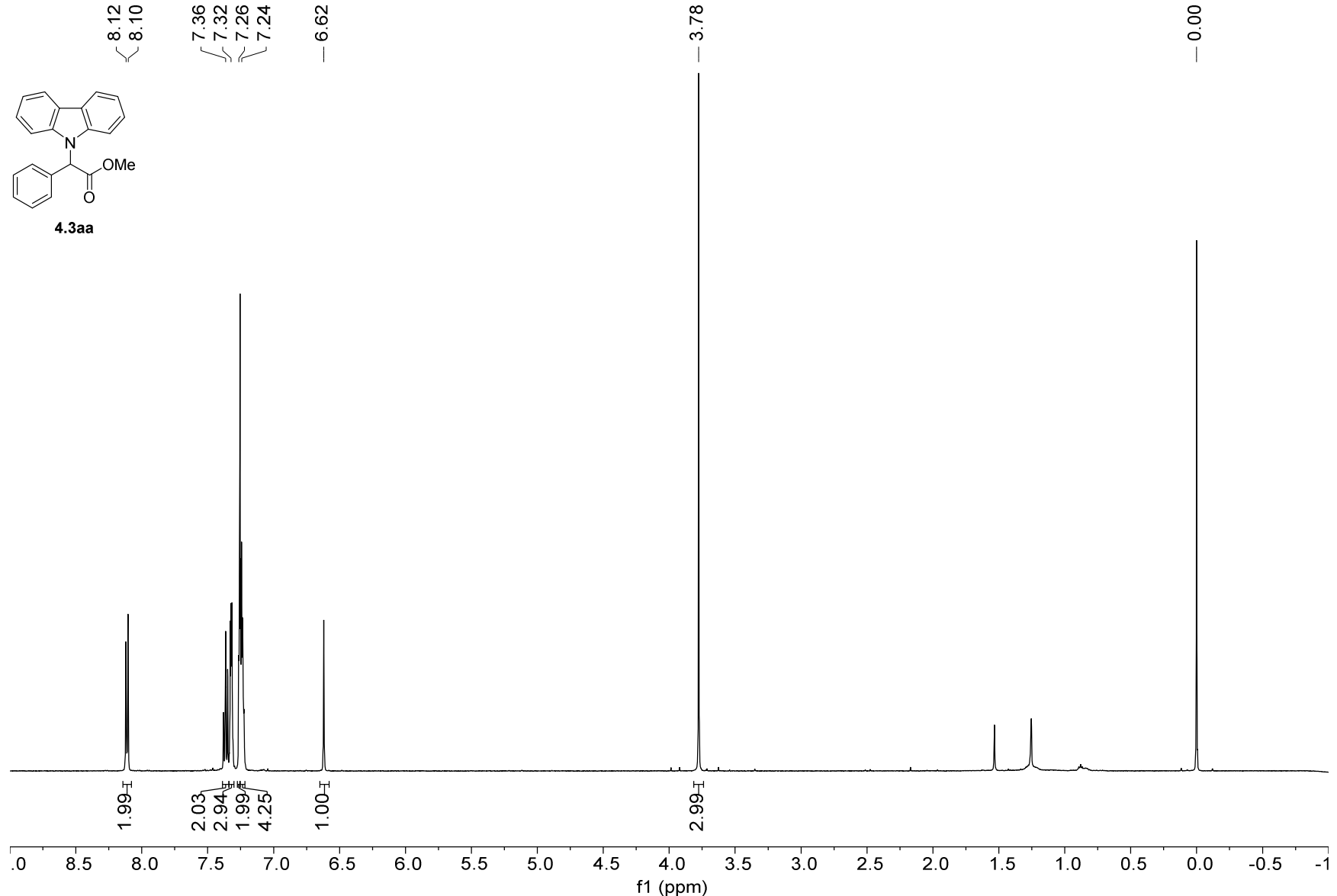
3.78

0.00



4.3aa

888



13C NMR — 125.79 MHz — CDCl3 — 298.0 K

— 169.79

140.17

133.98

128.68

128.34

127.40

125.77

123.55

120.26

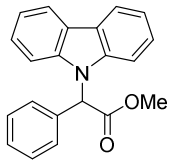
119.74

— 110.14

— 60.27

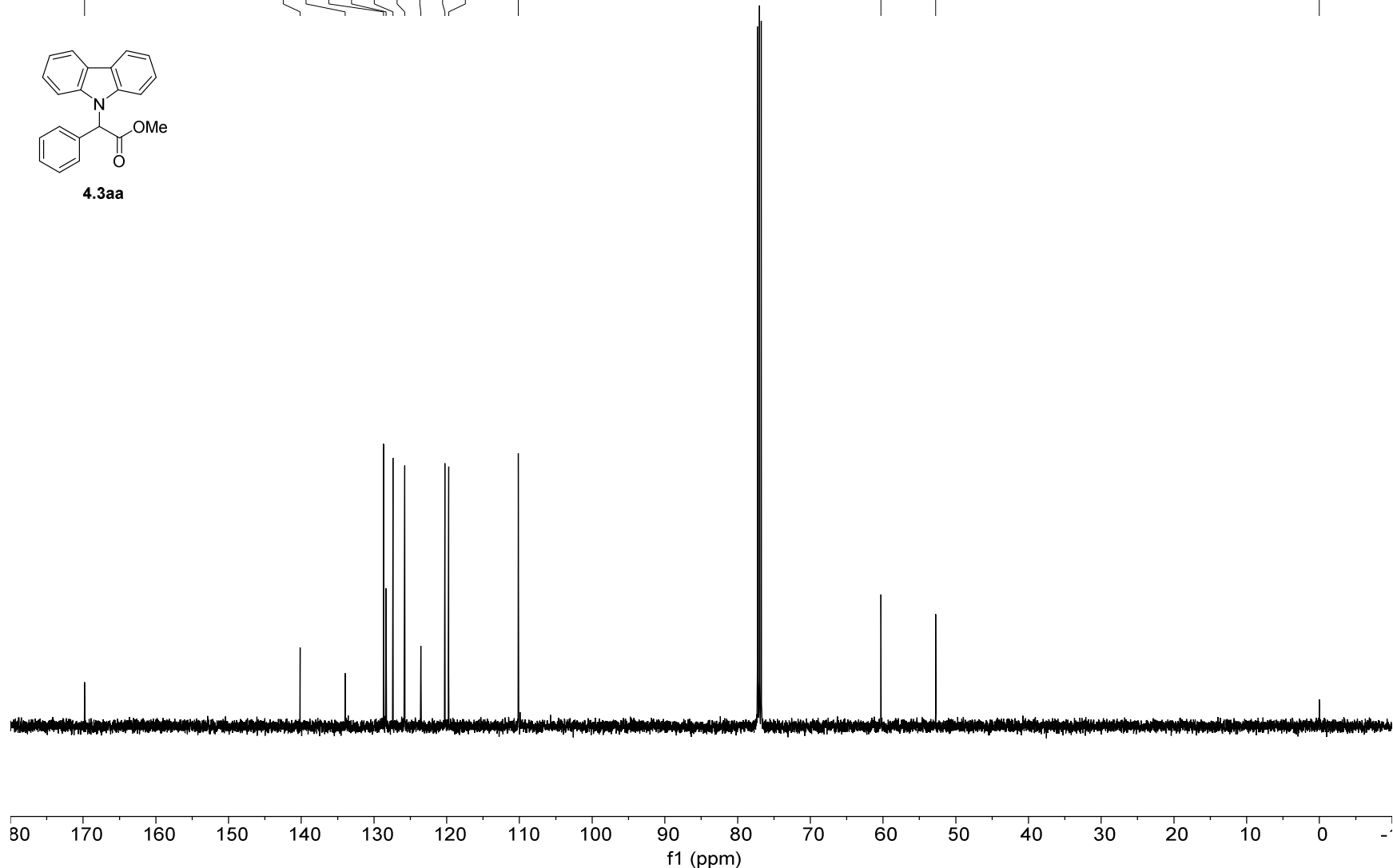
— 52.76

— 0.00



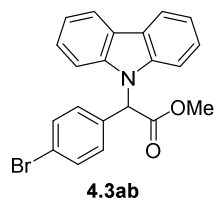
4.3aa

683

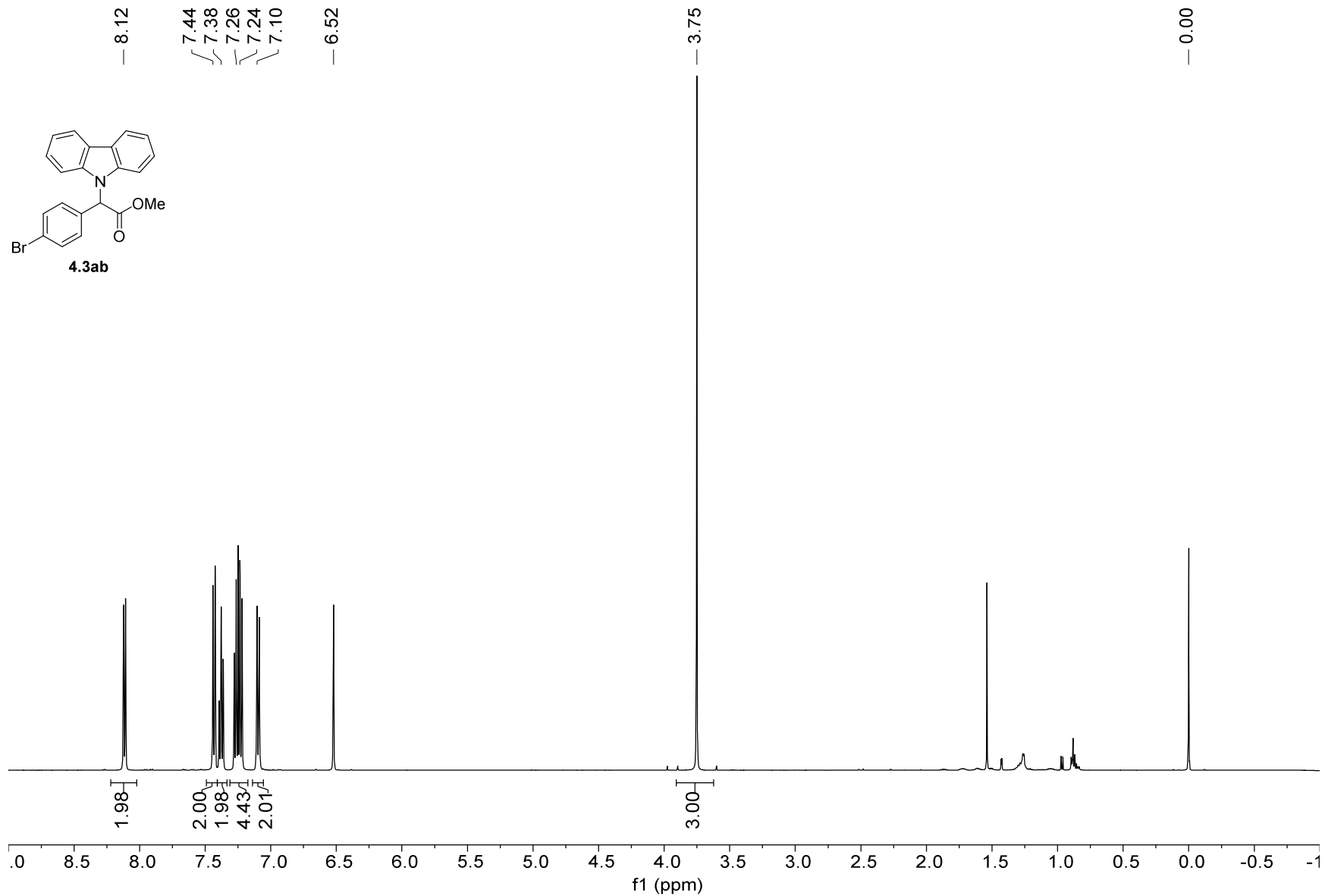


1H NMR — 500.22 MHz — CDCl3 — 298.0 K

8.12  
7.44  
7.38  
7.26  
7.24  
7.10  
6.52



390

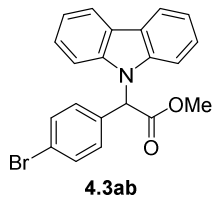


13C NMR — 125.79 MHz — CDCl3 — 298.0 K

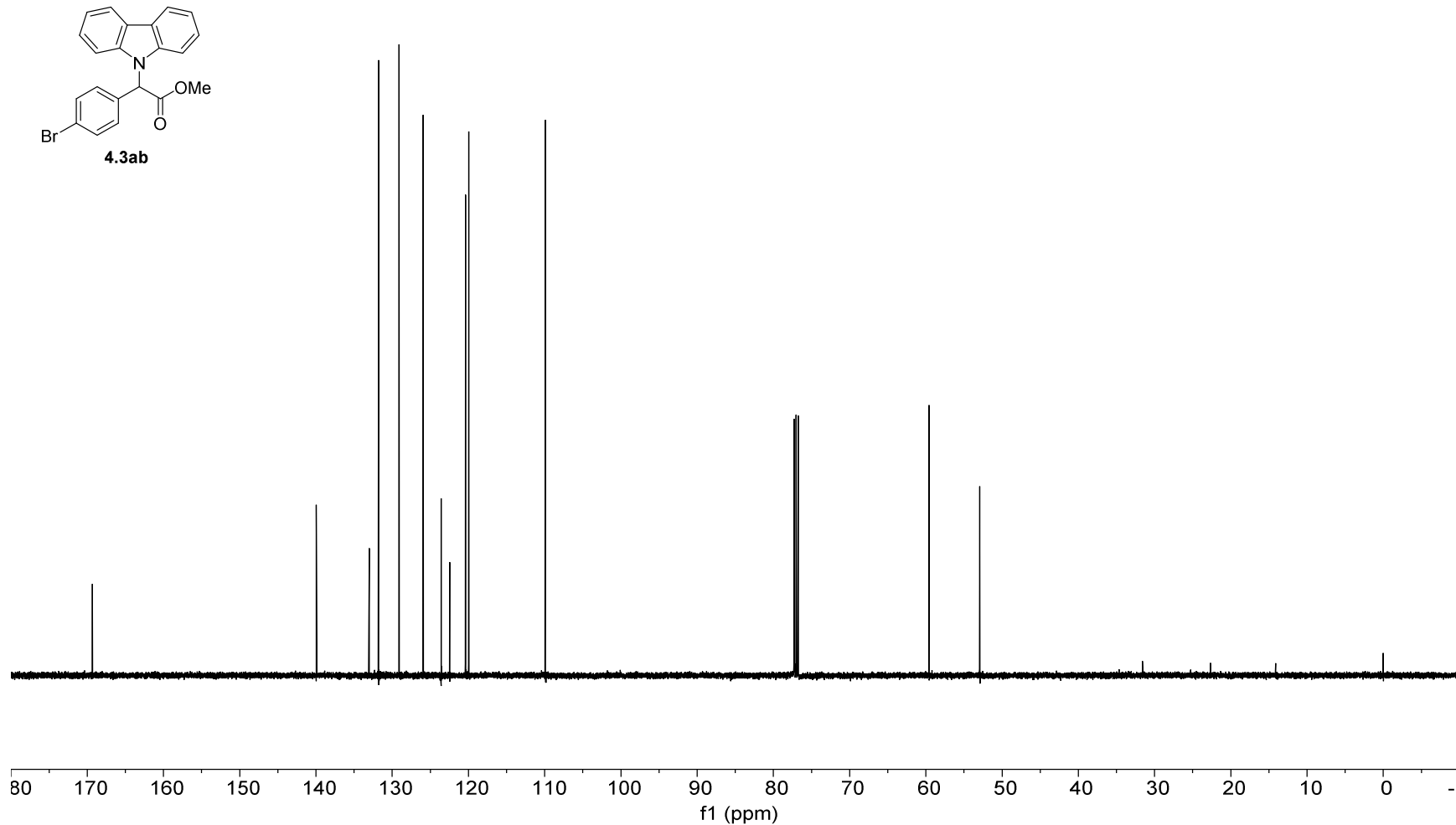
— 169.32 —  
— 139.95 —  
— 133.01 —  
— 131.79 —  
— 129.10 —  
— 125.92 —  
— 123.57 —  
— 122.45 —  
— 120.38 —  
— 119.96 —  
— 109.91 —

— 59.59 —  
— 52.93 —

— 0.00 —



391



1H NMR — 500.22 MHz — CDCl3 — 298.0 K

8.11

7.36

7.26

7.24

7.15

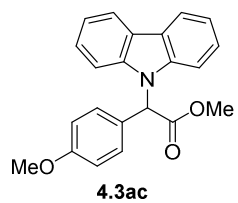
6.85

6.57

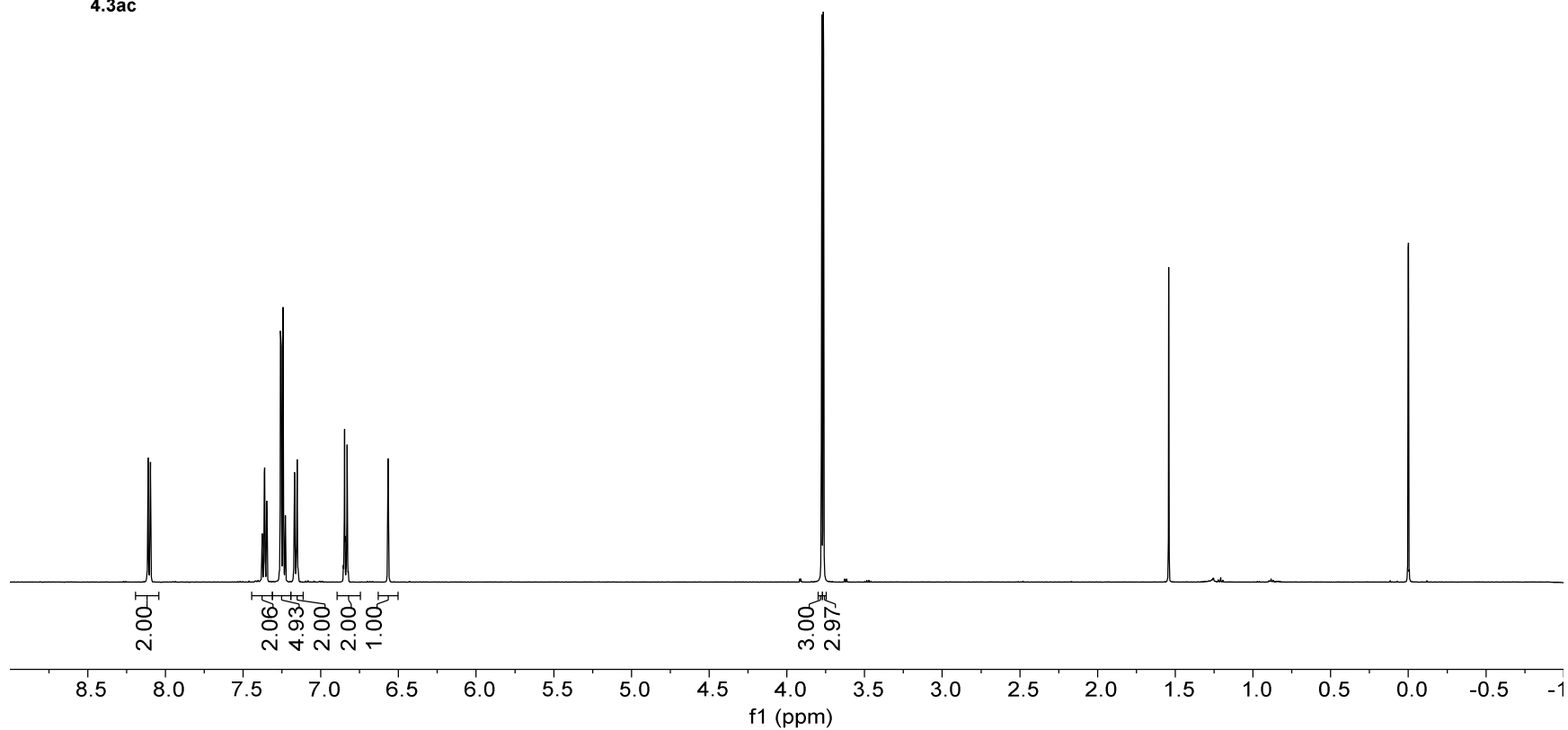
3.78

3.76

0.00

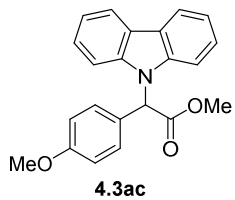


392

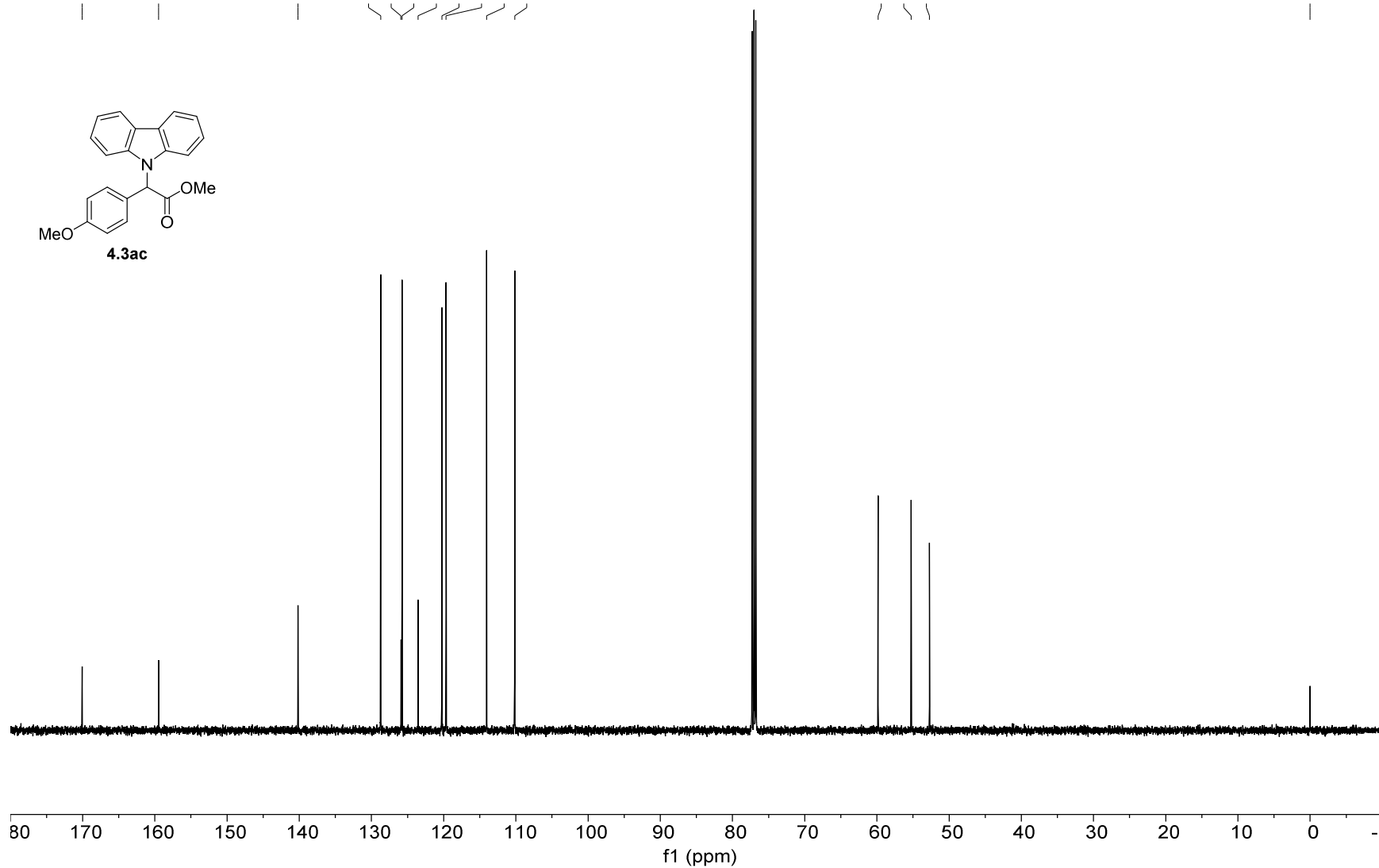


13C NMR — 125.78 MHz — CDCl3 — 298.0 K

— 170.08 — 159.47 — 140.18  
— 128.72 — 125.92 — 125.76 — 123.54 — 120.25 — 119.68 — 114.05 — 110.16  
— 59.84 — 55.27 — 52.73  
— -0.00



393





1H NMR — 500.22 MHz — CDCl3 — 298.0 K

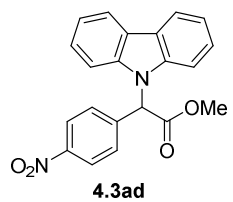
8.14

7.39  
7.29

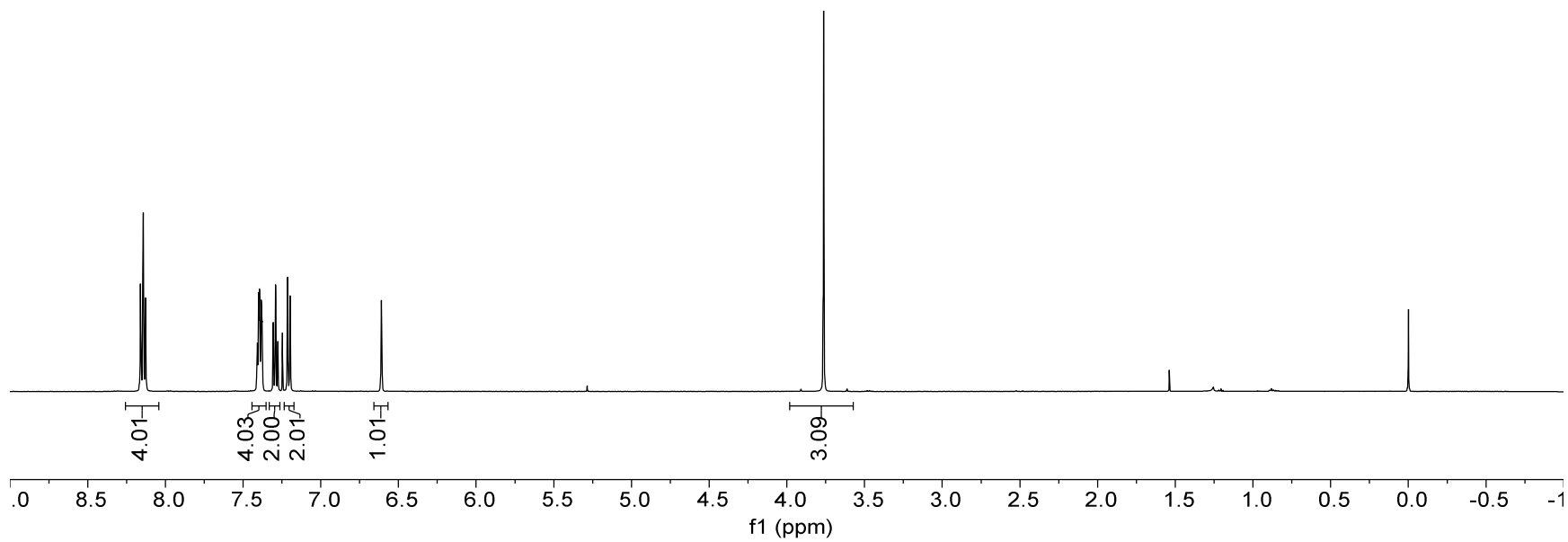
6.61

3.76

-0.00



394



13C NMR — 125.78 MHz — CDCl3 — 298.0 K

— 168.73

— 147.77

— 141.13

— 139.77

— 128.50

— 126.16

— 123.76

— 123.69

— 120.60

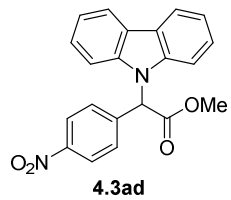
— 120.33

— 109.60

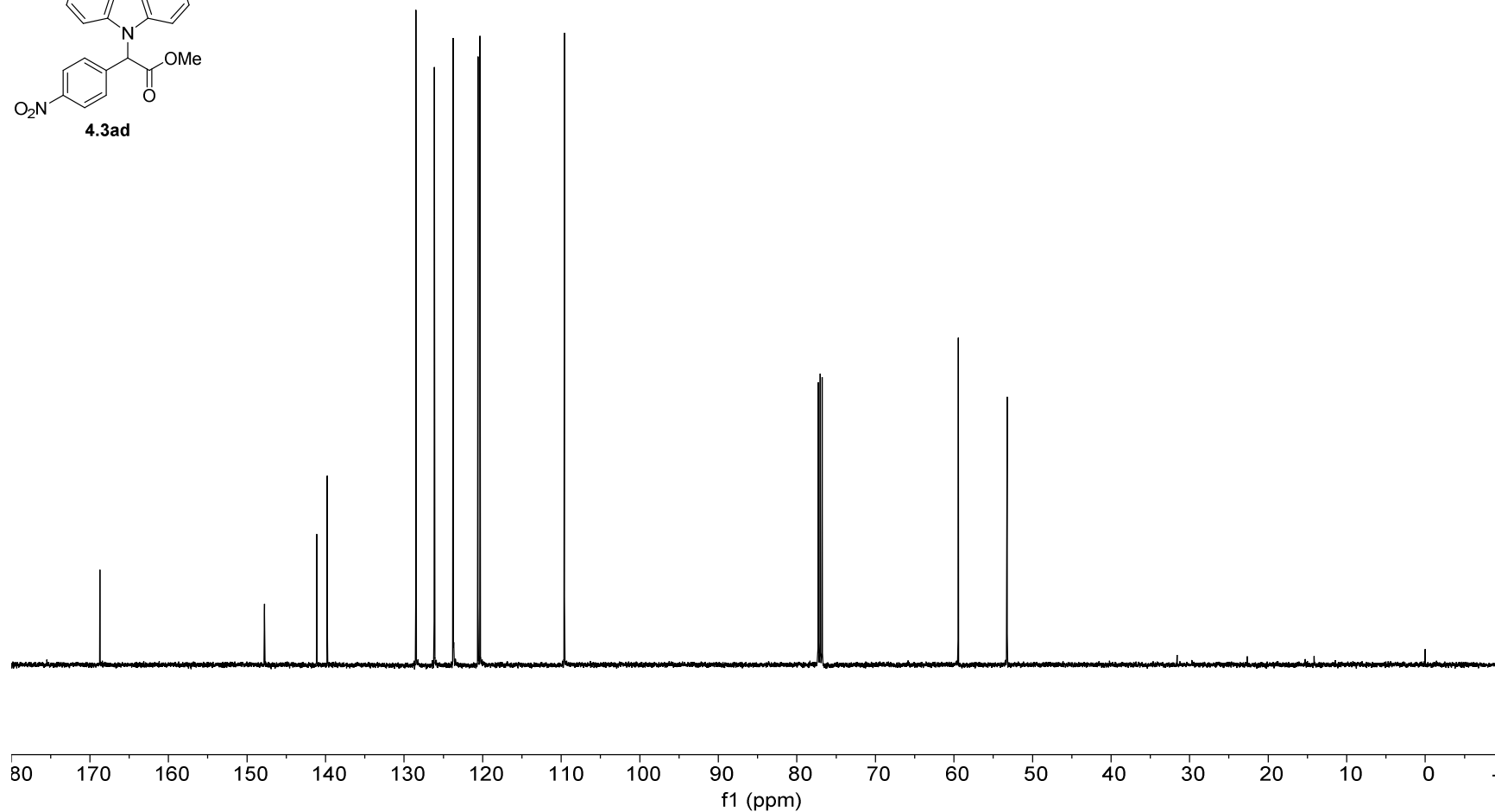
— 59.45

— 53.23

— 0.00



395



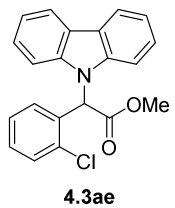
1H NMR — 500.22 MHz — CDCl3 — 298.0 K

8.14  
8.12

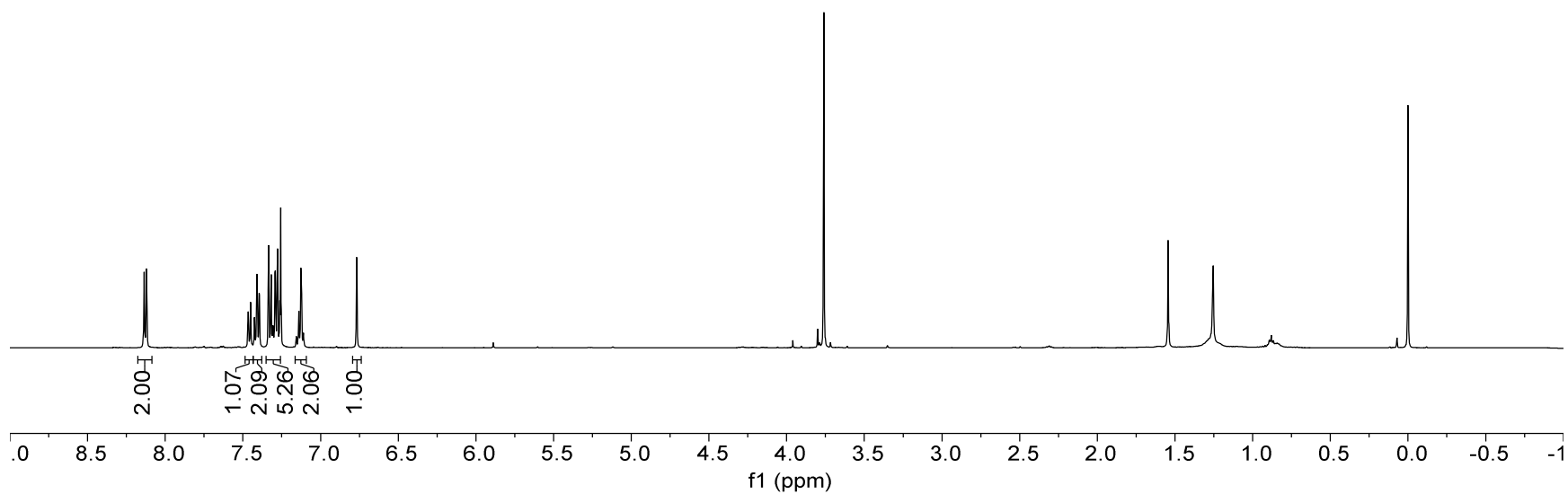
7.45  
7.41  
7.33  
7.28  
7.13  
6.77

3.76

0.00



396



13C NMR — 125.79 MHz — CDCl3 — 298.0 K

— 168.70

140.29

134.08

132.69

129.88

128.36

127.04

126.10

123.51

120.39

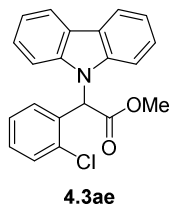
119.97

— 109.54

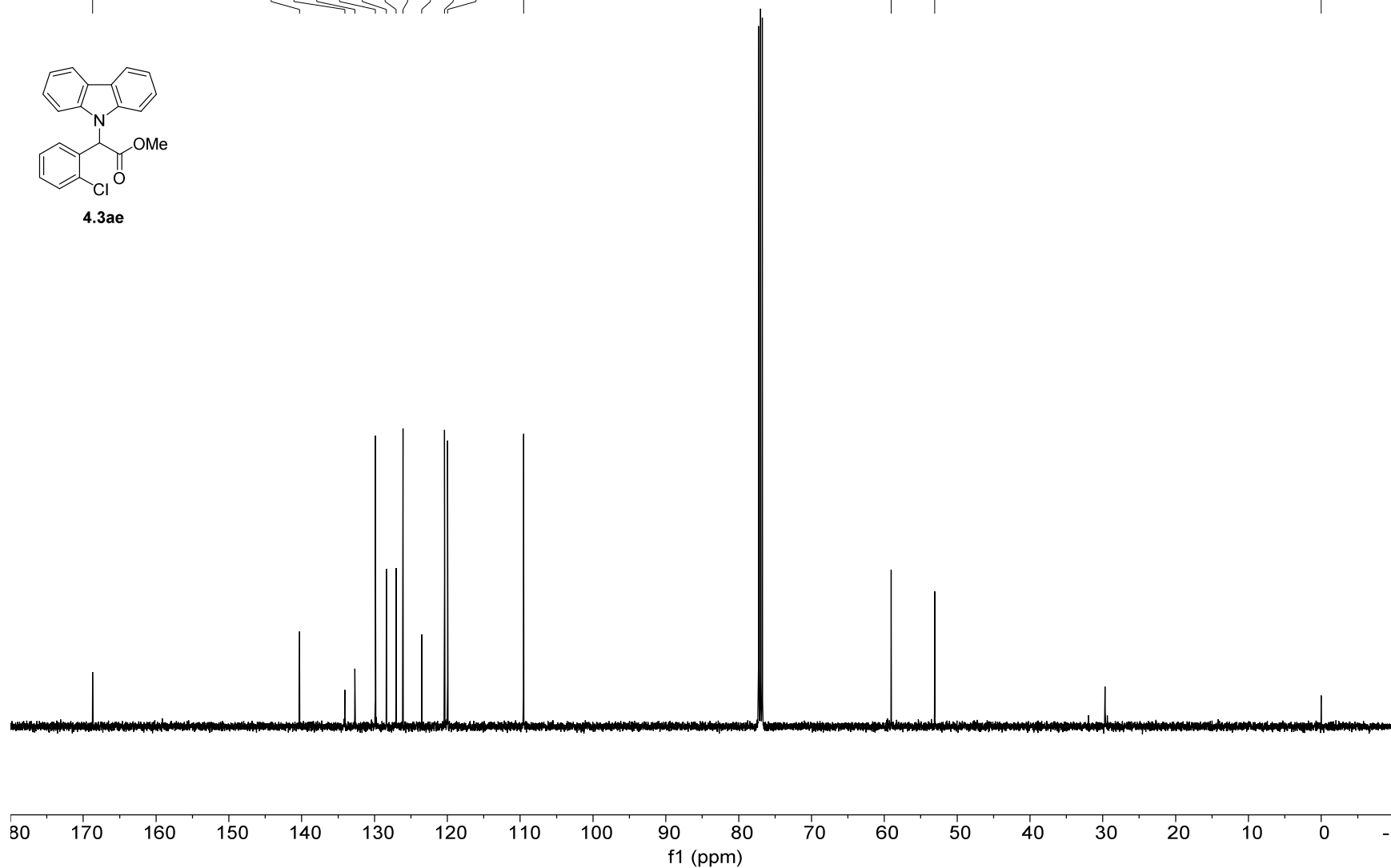
— 59.06

— 53.09

— 0.00



397



1H NMR — 500.22 MHz — CDCl3 — 298.0 K

8.12  
8.10

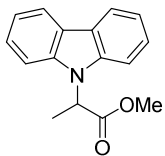
7.45  
7.38  
7.36  
7.27  
7.25

5.45  
5.43  
5.42  
5.40

3.69

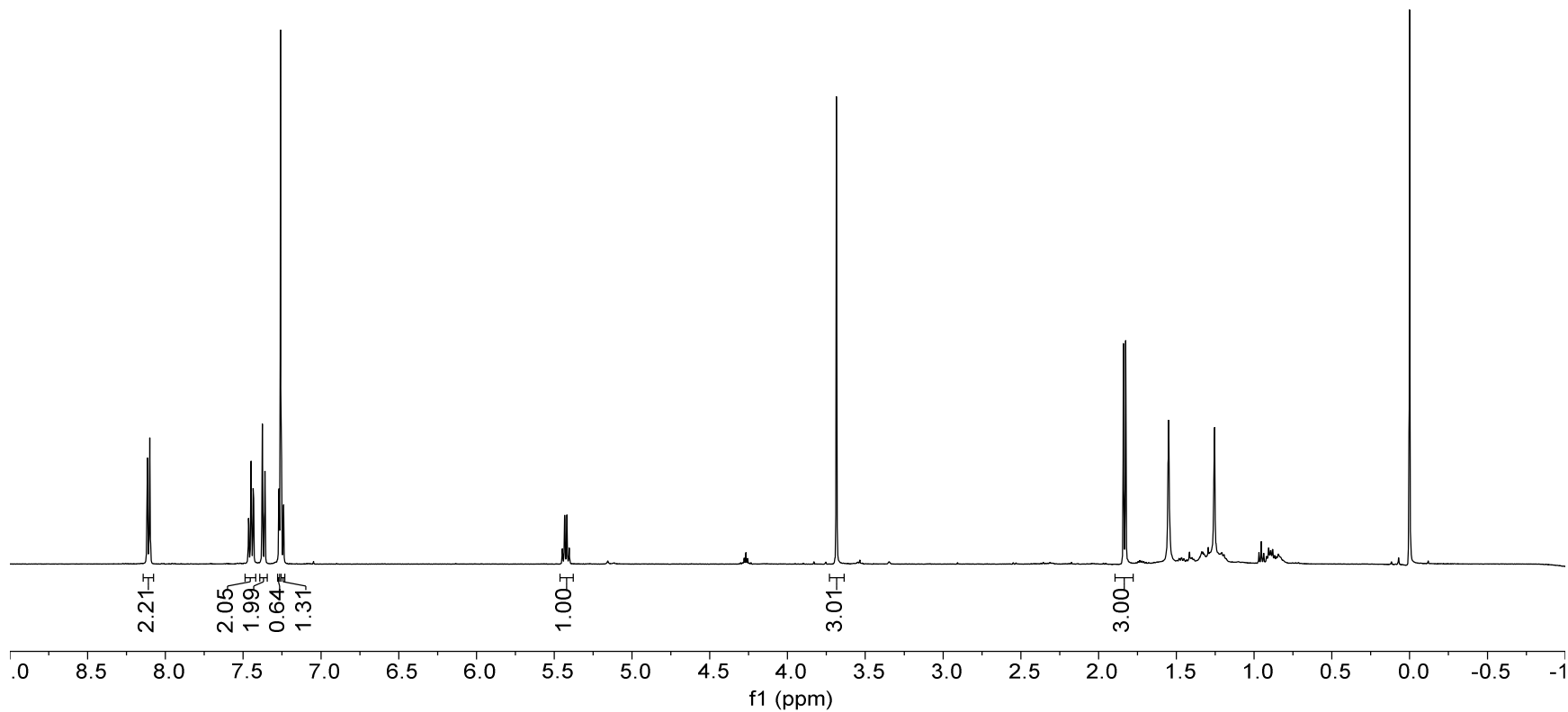
1.84  
1.83

0.00



4.3af

868



13C NMR — 125.79 MHz — CDCl3 — 298.0 K

— 171.62

— 139.45

— 129.48

— 125.80

— 123.39

— 120.45

— 119.41

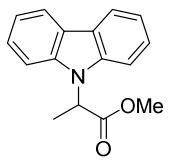
— 109.12

— 52.68

— 51.99

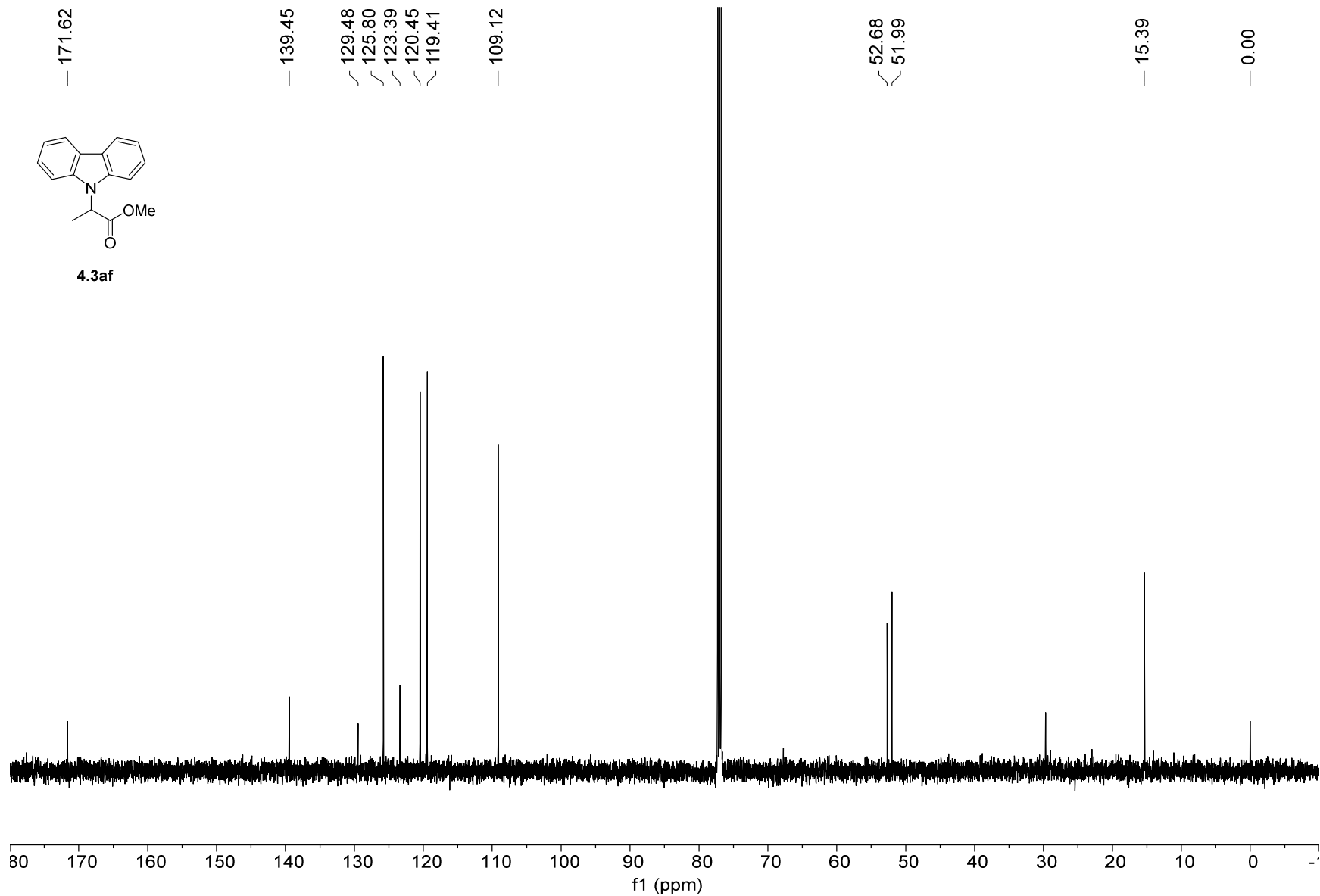
— 15.39

— 0.00



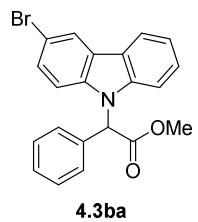
4.3af

399

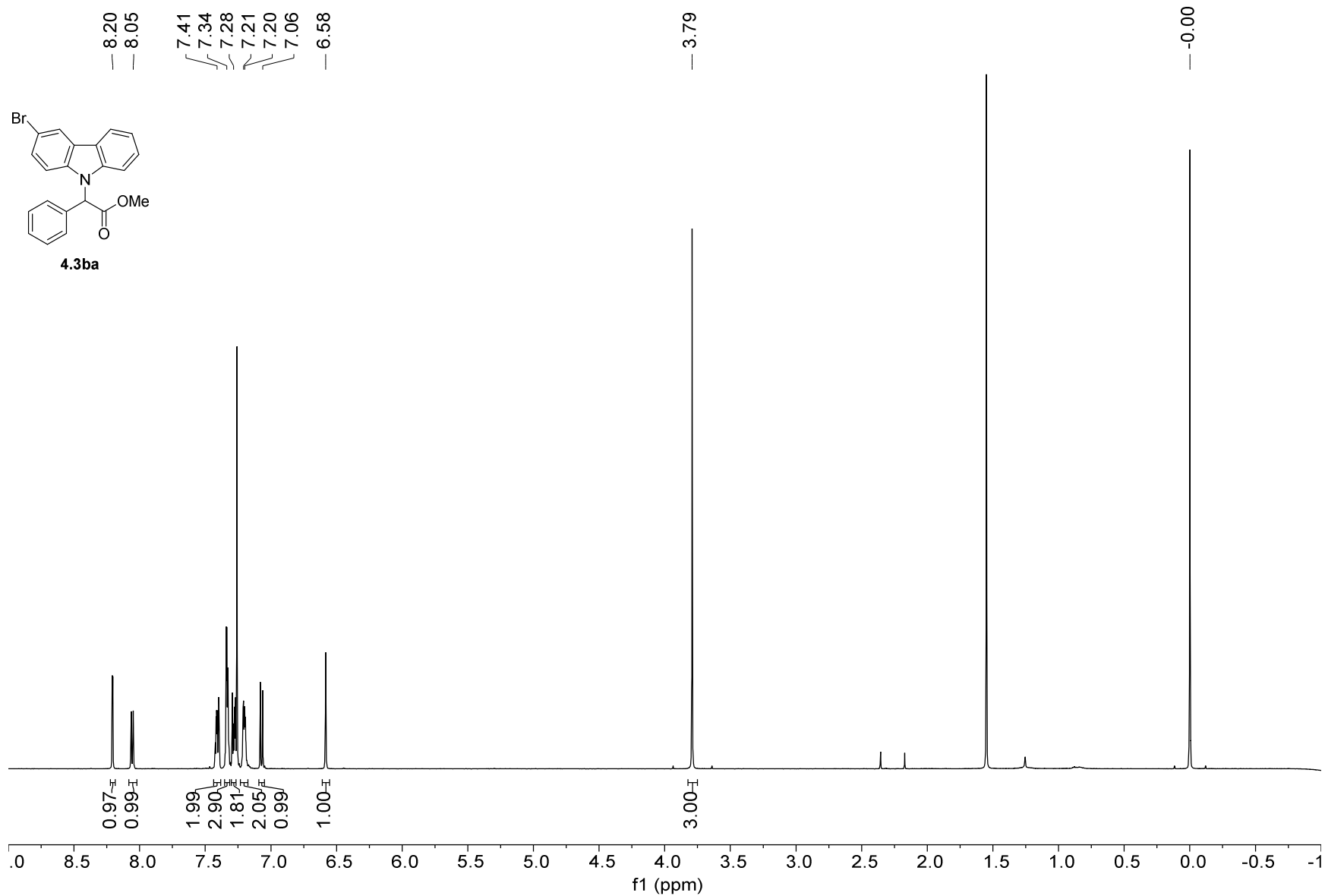


1H NMR — 500.22 MHz — CDCl3 — 298.0 K

8.20  
8.05  
7.41  
7.34  
7.28  
7.21  
7.20  
7.06  
6.58

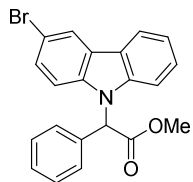


400



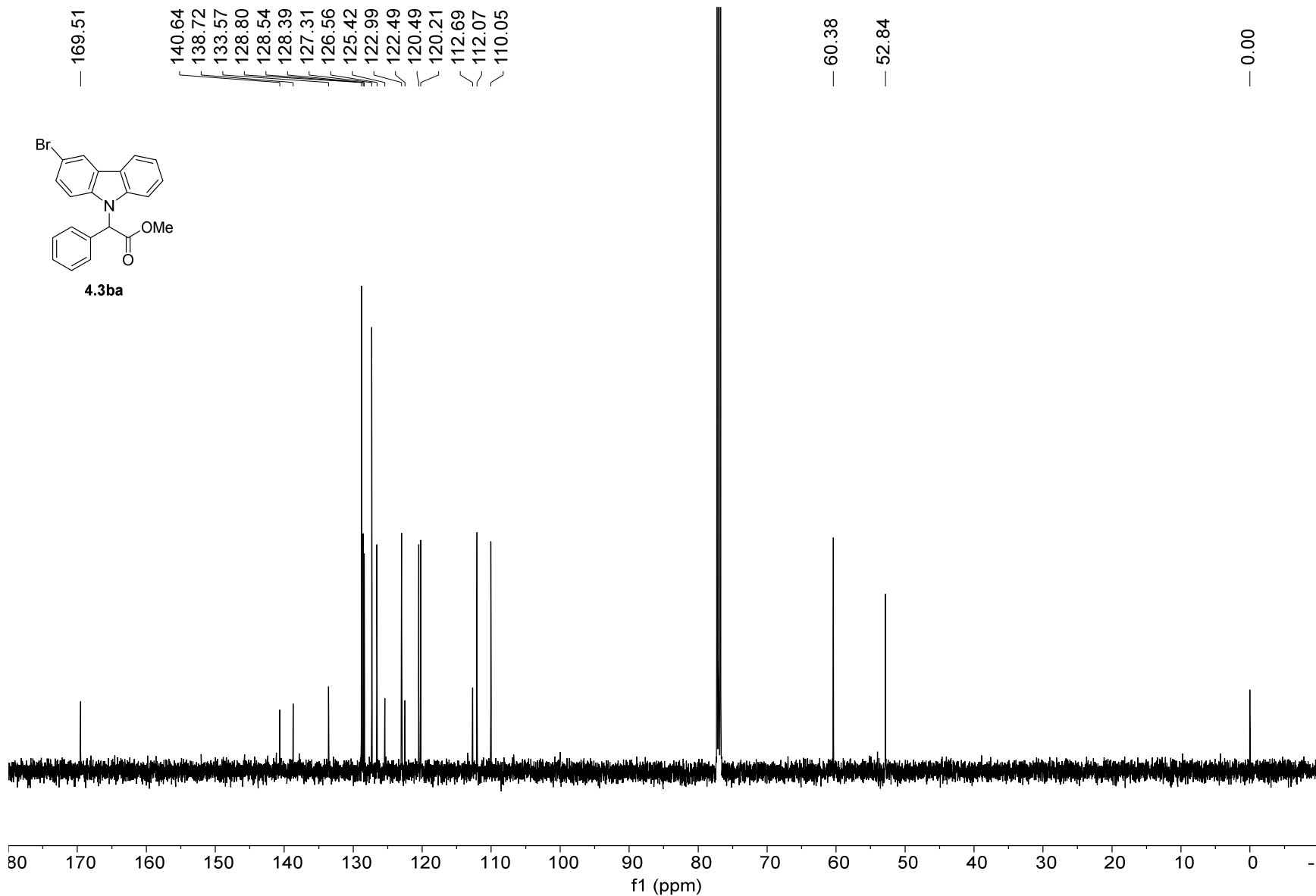
13C NMR — 125.79 MHz — CDCl3 — 298.0 K

169.51  
140.64  
138.72  
133.57  
128.80  
128.54  
128.39  
127.31  
126.56  
125.42  
122.99  
122.49  
120.49  
120.21  
112.69  
112.07  
110.05  
60.38  
52.84  
0.00



4.3ba

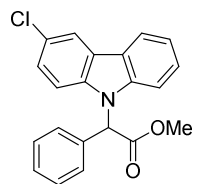
401





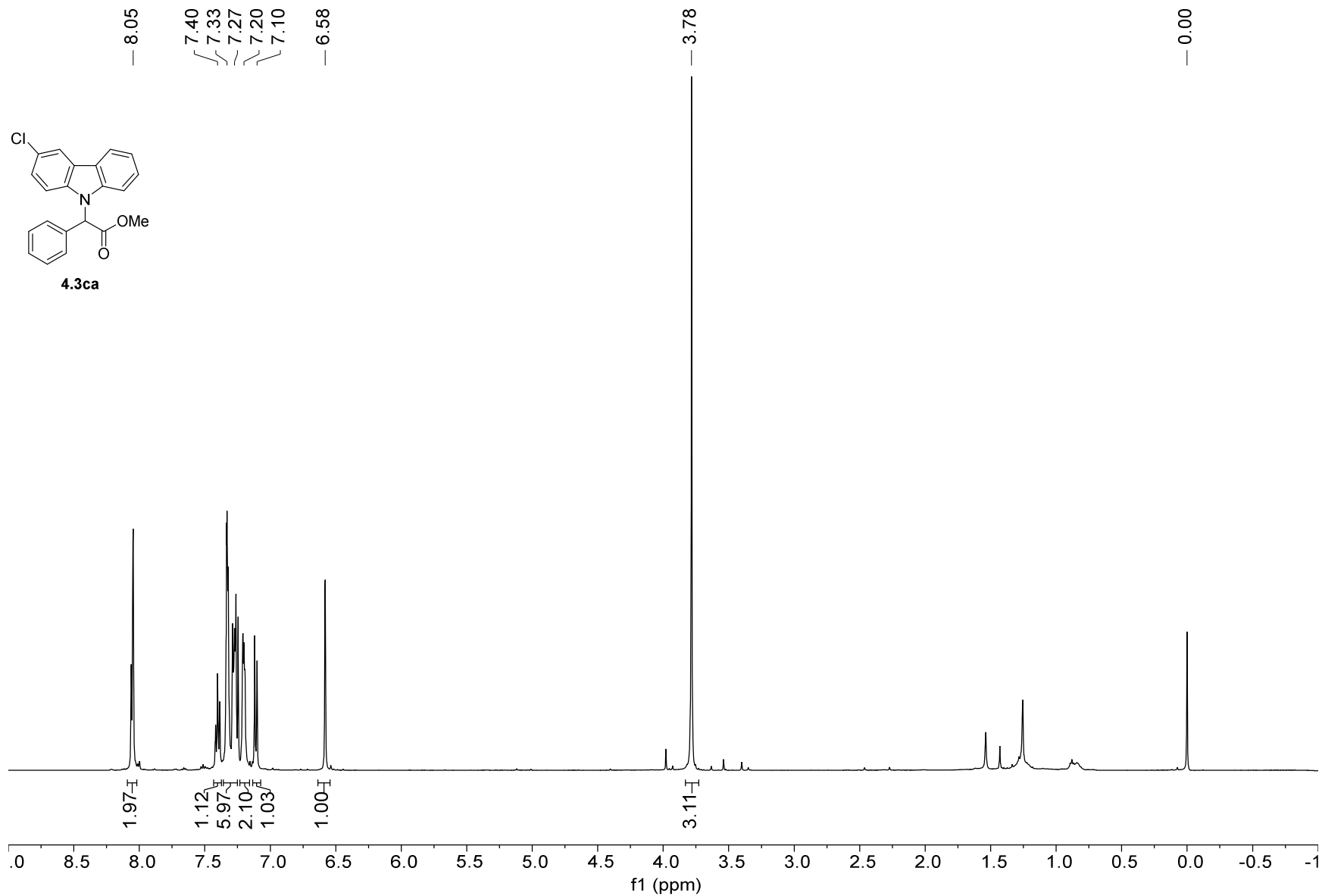
1H NMR — 500.22 MHz — CDCl3 — 298.0 K

8.05  
7.40  
7.33  
7.27  
7.20  
7.10  
6.58

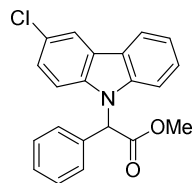


4.3ca

402



13C NMR — 125.79 MHz — CDCl3 — 298.0 K



4.3ca

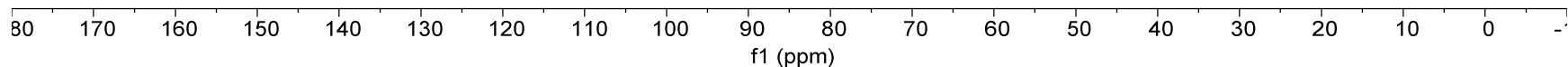
- 169.53
- 140.79
- 138.37
- 133.61
- 128.78
- 128.52
- 127.30
- 127.23
- 126.52
- 125.76
- 125.33
- 124.82
- 122.60
- 120.48
- 120.13
- 119.95
- 111.58
- 110.07

60.39

52.82

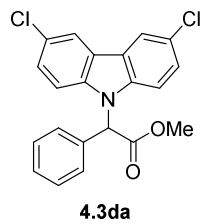
0.00

403

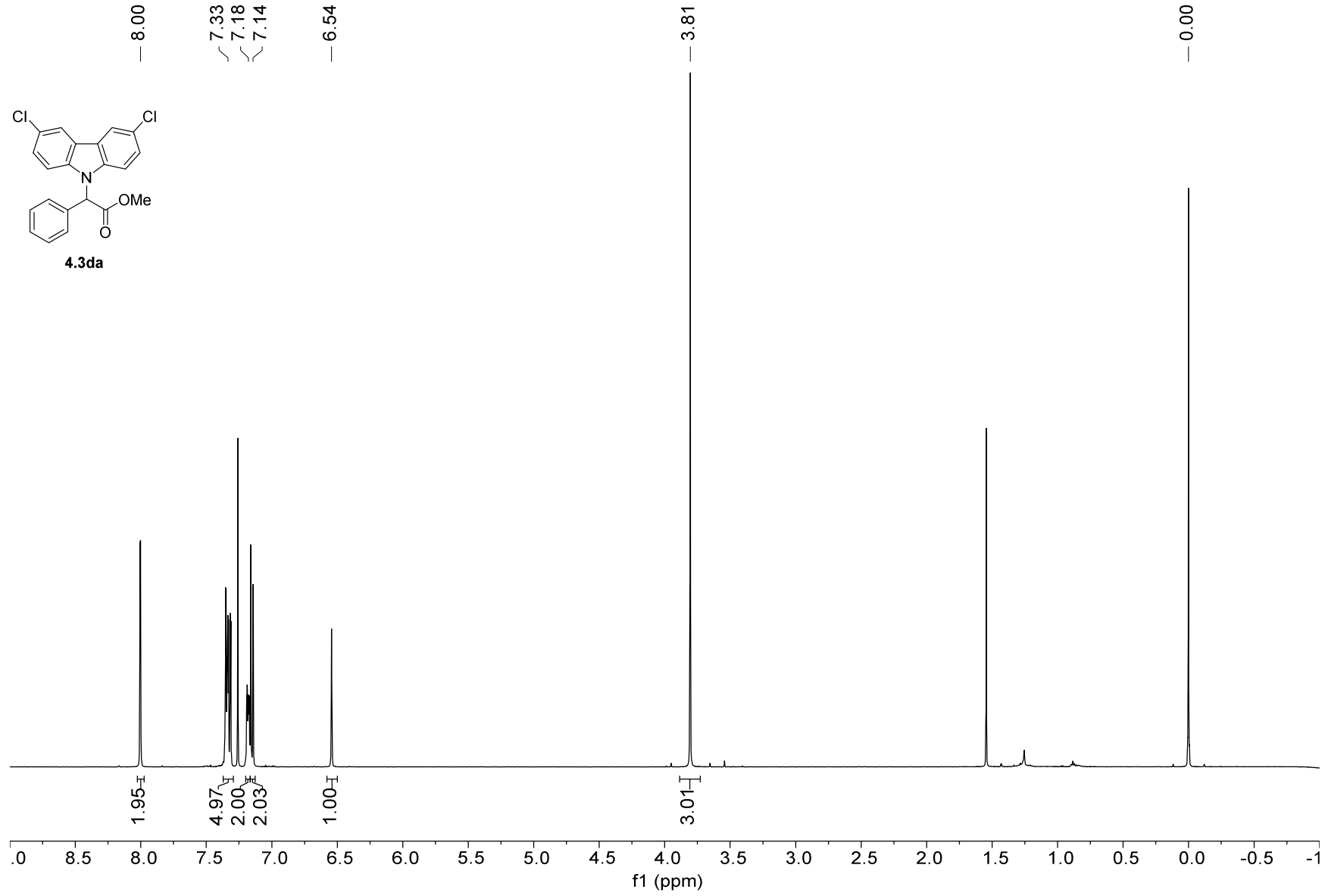


1H NMR — 500.22 MHz — CDCl3 — 298.0 K

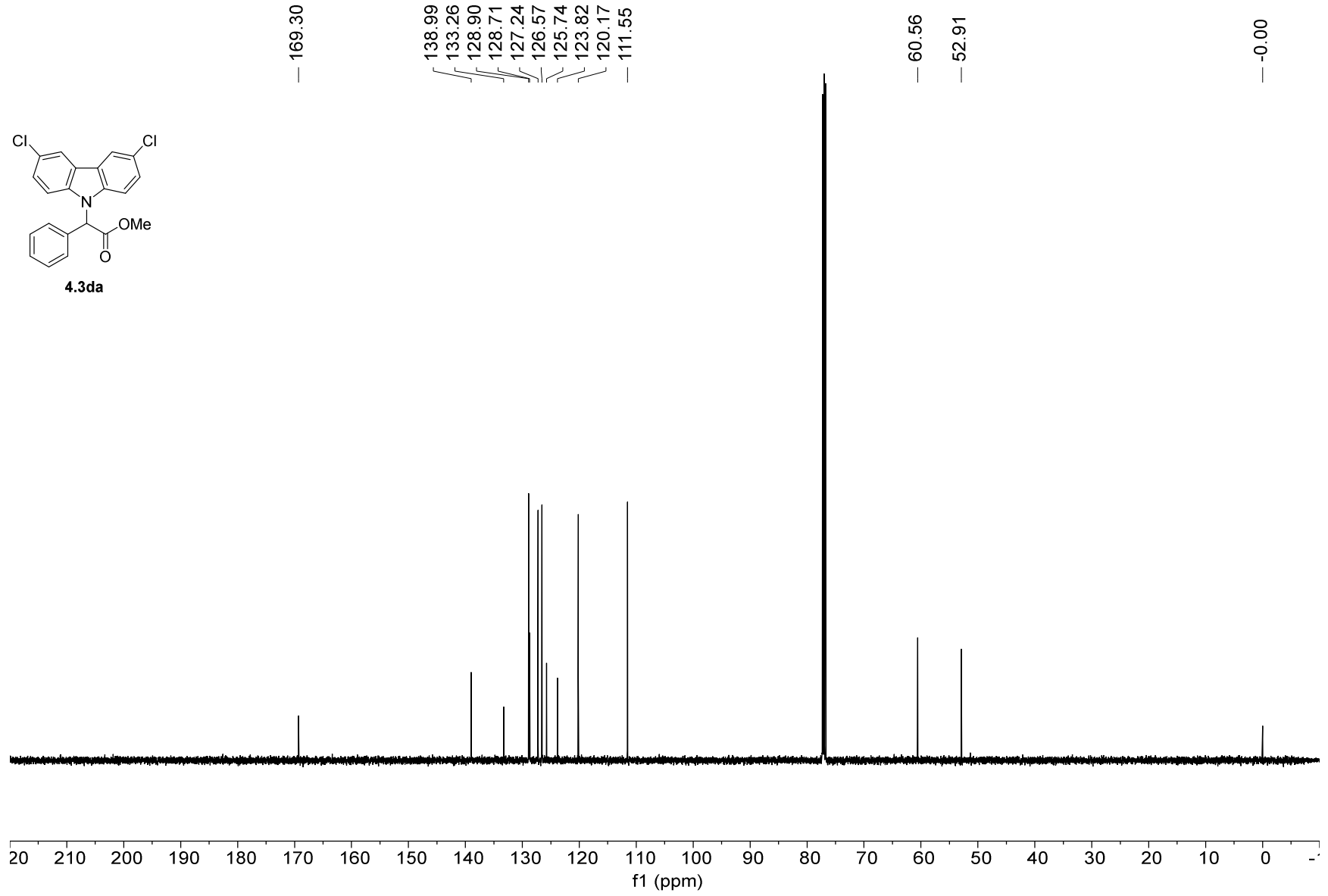
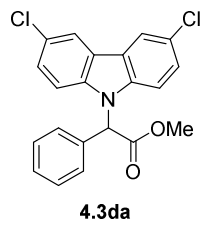
8.00  
7.33  
7.18  
7.14  
6.54  
3.81  
0.00



404

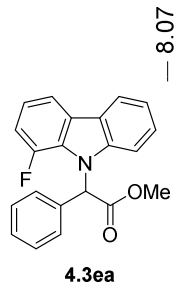


13C NMR — 125.79 MHz — CDCl3 — 298.0 K



405

1H NMR — 500.22 MHz — CDCl3 — 298.0 K

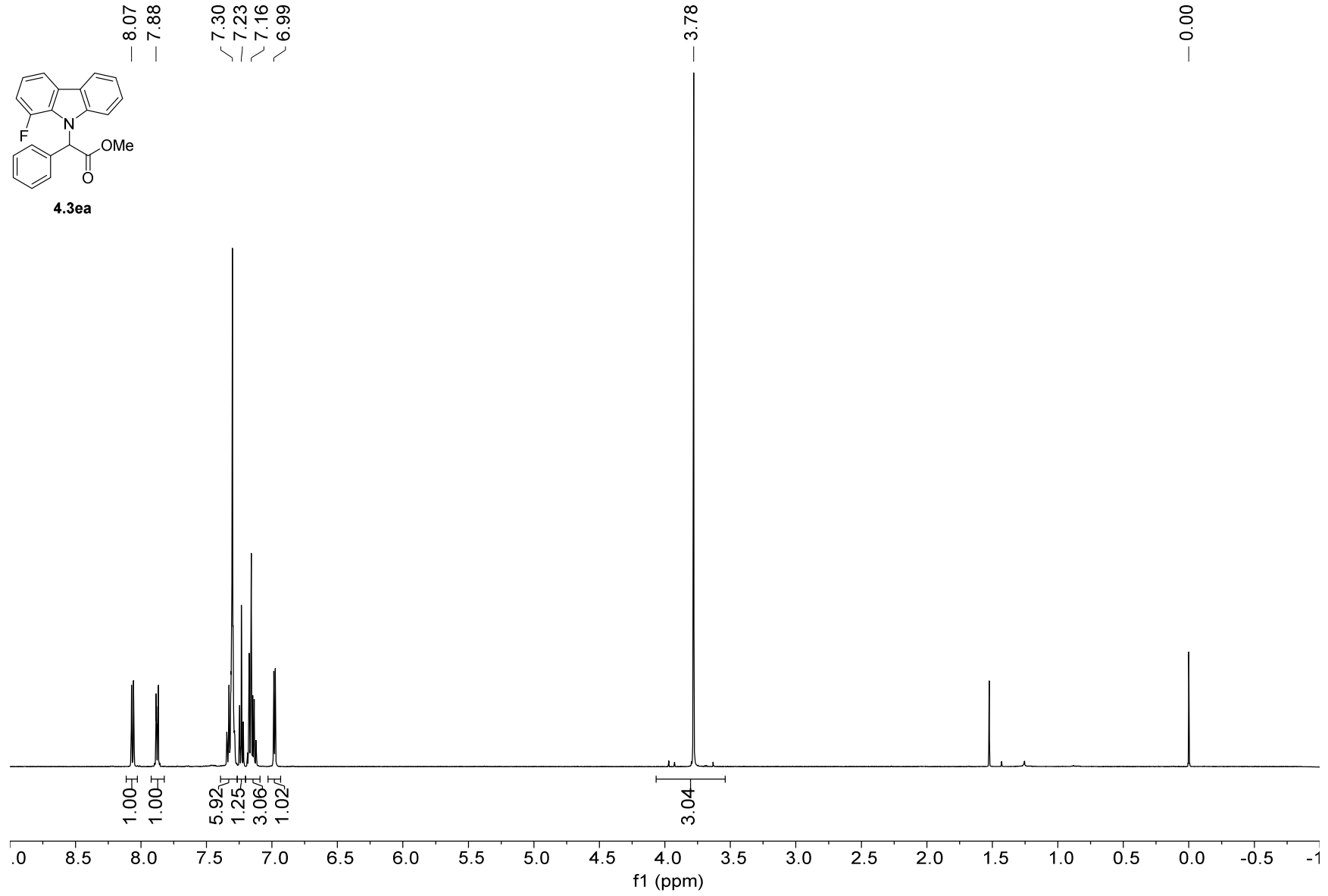


8.07  
7.88  
7.30  
7.23  
7.16  
6.99

3.78

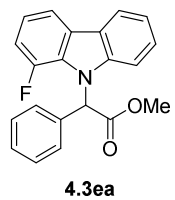
0.00

406

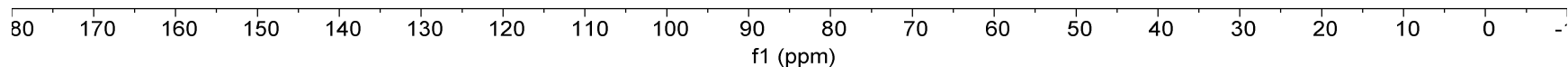


13C NMR — 125.78 MHz — CDCl3 — 298.0 K

169.75  
150.33  
148.41  
140.32  
134.90  
128.54  
128.19  
127.92  
127.43  
126.37  
123.65  
120.43  
120.19  
120.12  
116.13  
112.49  
111.29  
61.71  
52.81  
0.00

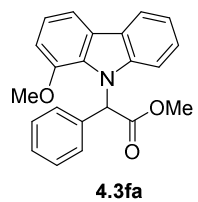


407



1H NMR — 500.22 MHz — CDCl3 — 298.0 K

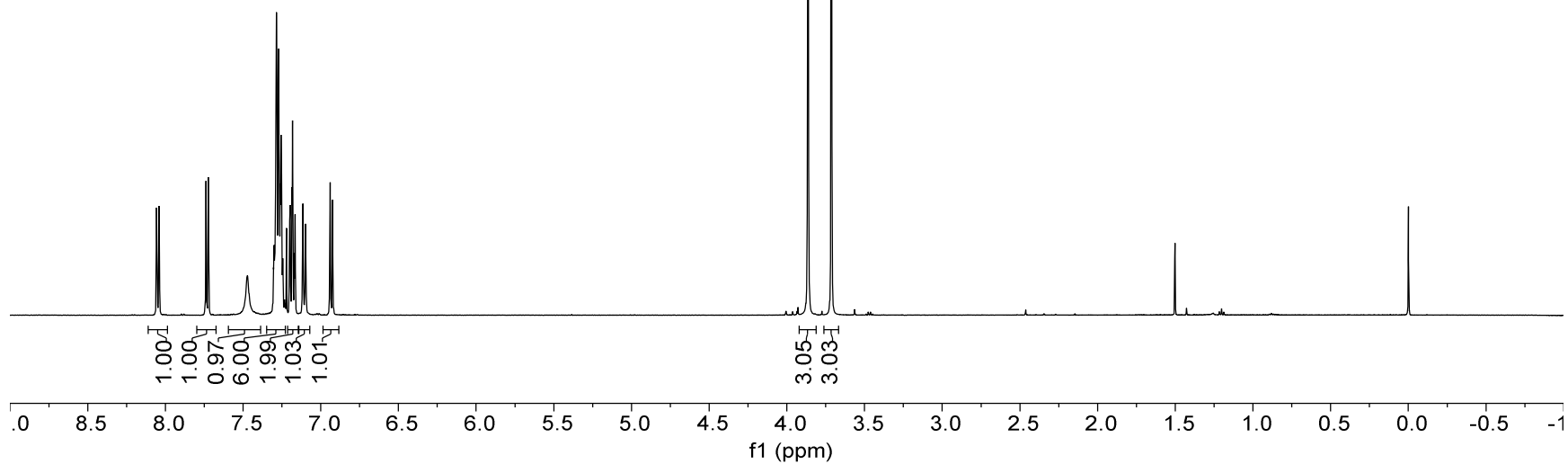
8.06  
7.74  
7.47  
7.28  
7.12  
6.94



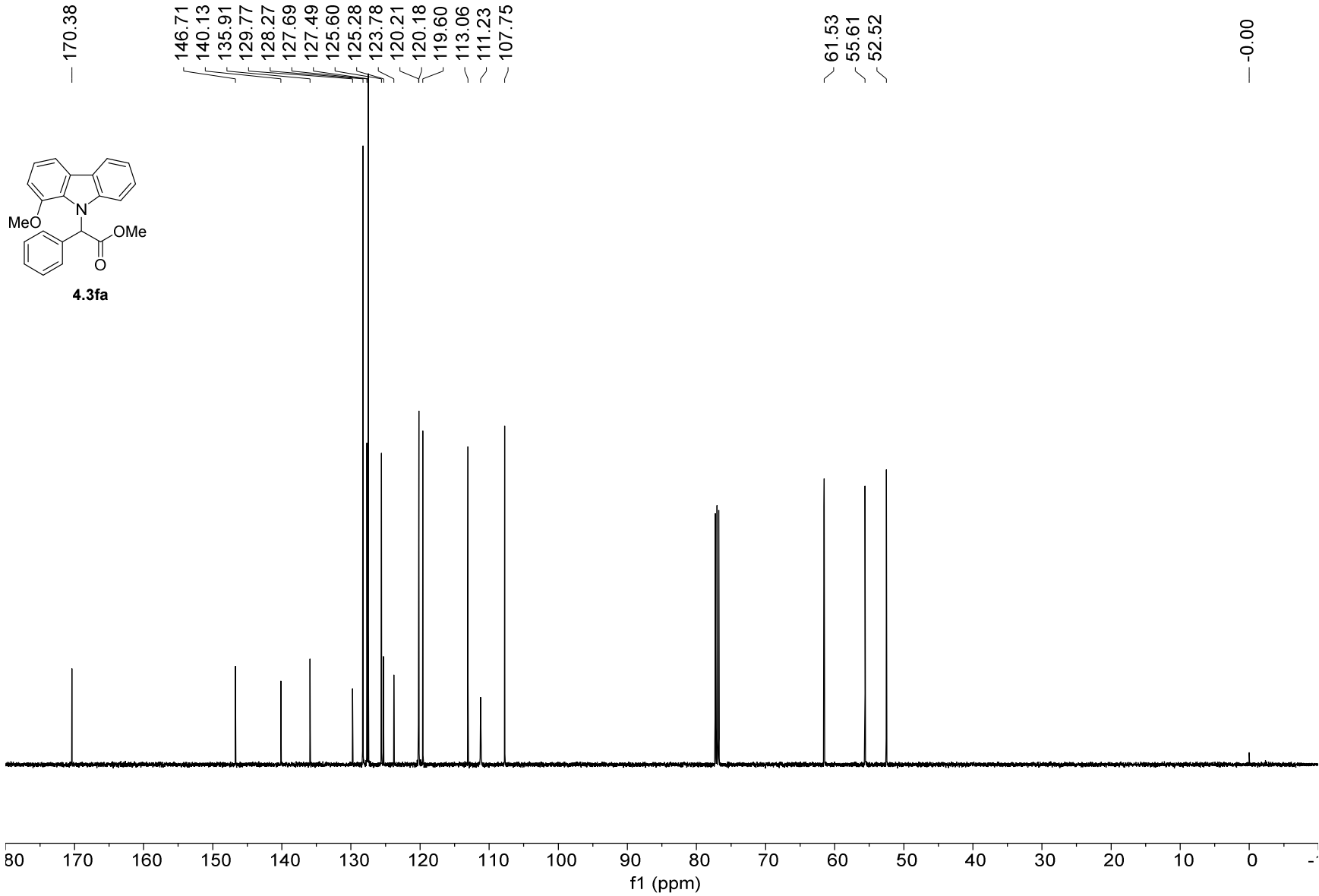
3.86  
3.71

0.00

408



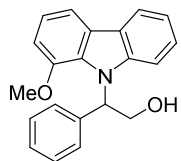
13C NMR — 125.78 MHz — CDCl3 — 298.0 K





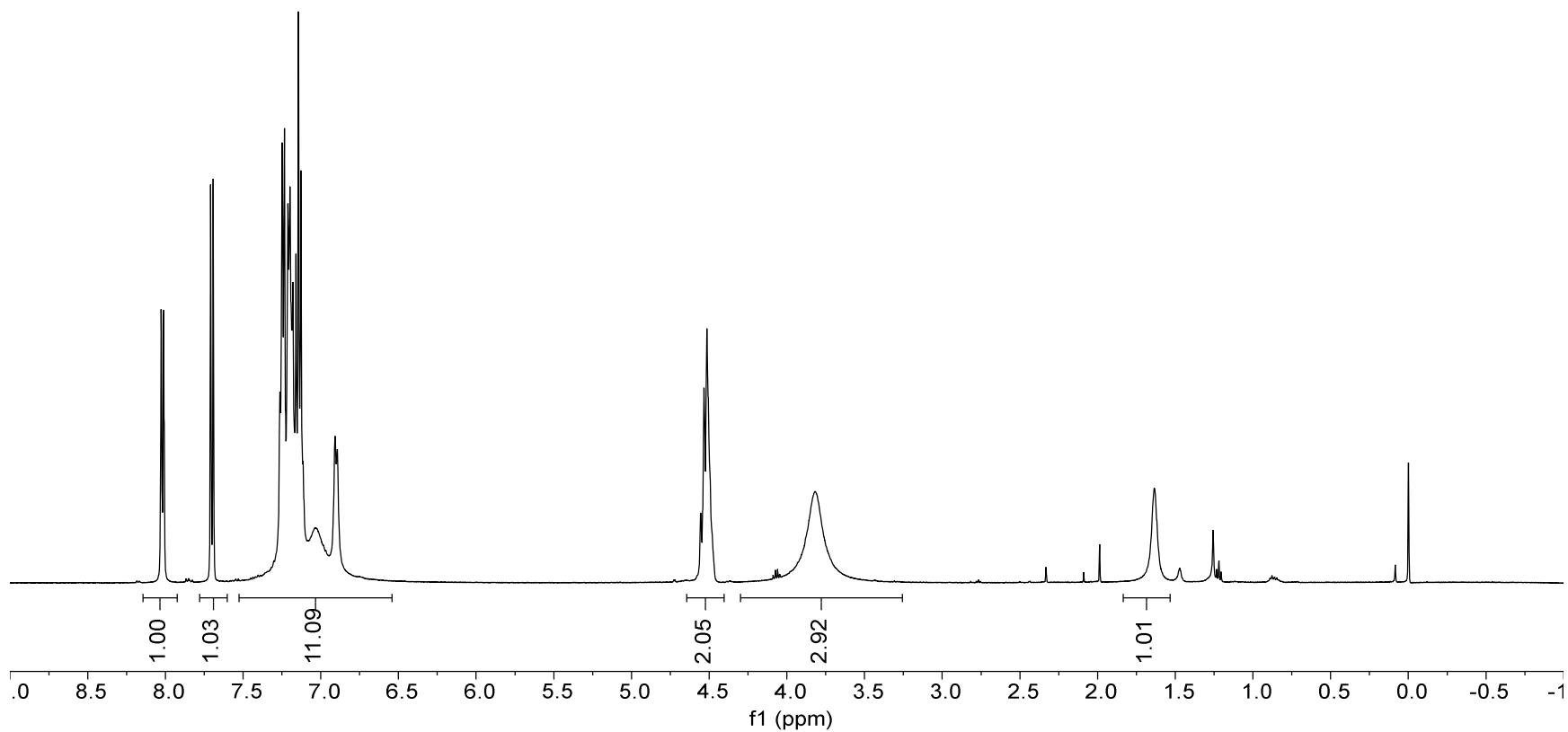
1H NMR — 500.22 MHz — CDCl3 — 298.0 K

8.01  
7.69  
7.20  
7.03  
6.91  
4.51  
3.82  
1.63  
-0.00

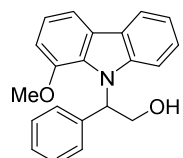


4.3fa-OH

410



13C NMR — 125.78 MHz — CDCl3 — 298.0 K

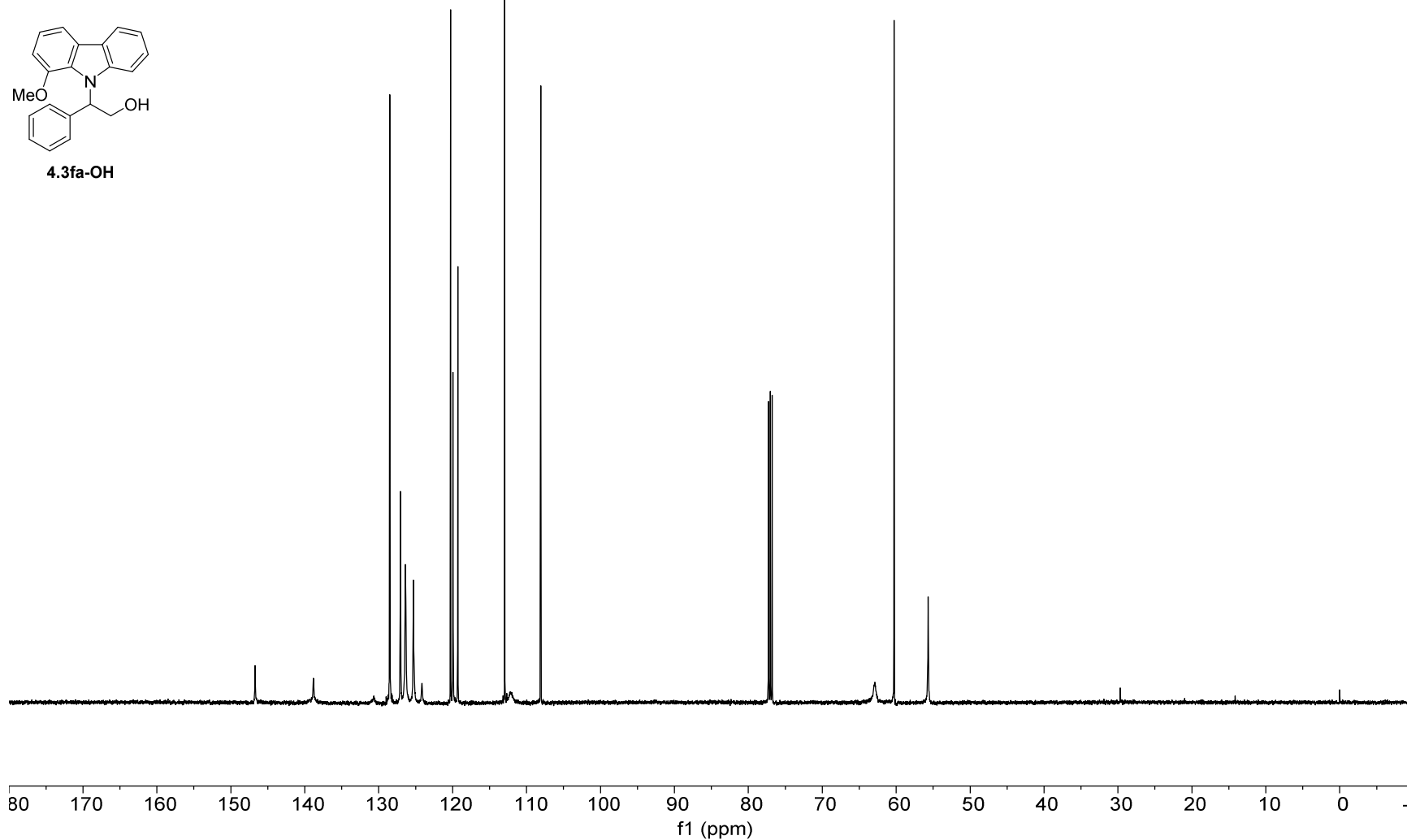


4.3fa-OH

146.72  
138.81  
130.69  
128.50  
127.06  
126.38  
125.31  
124.15  
120.28  
119.94  
119.31  
112.95  
112.14  
108.08

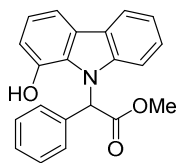
62.89  
60.28  
55.67

0.00



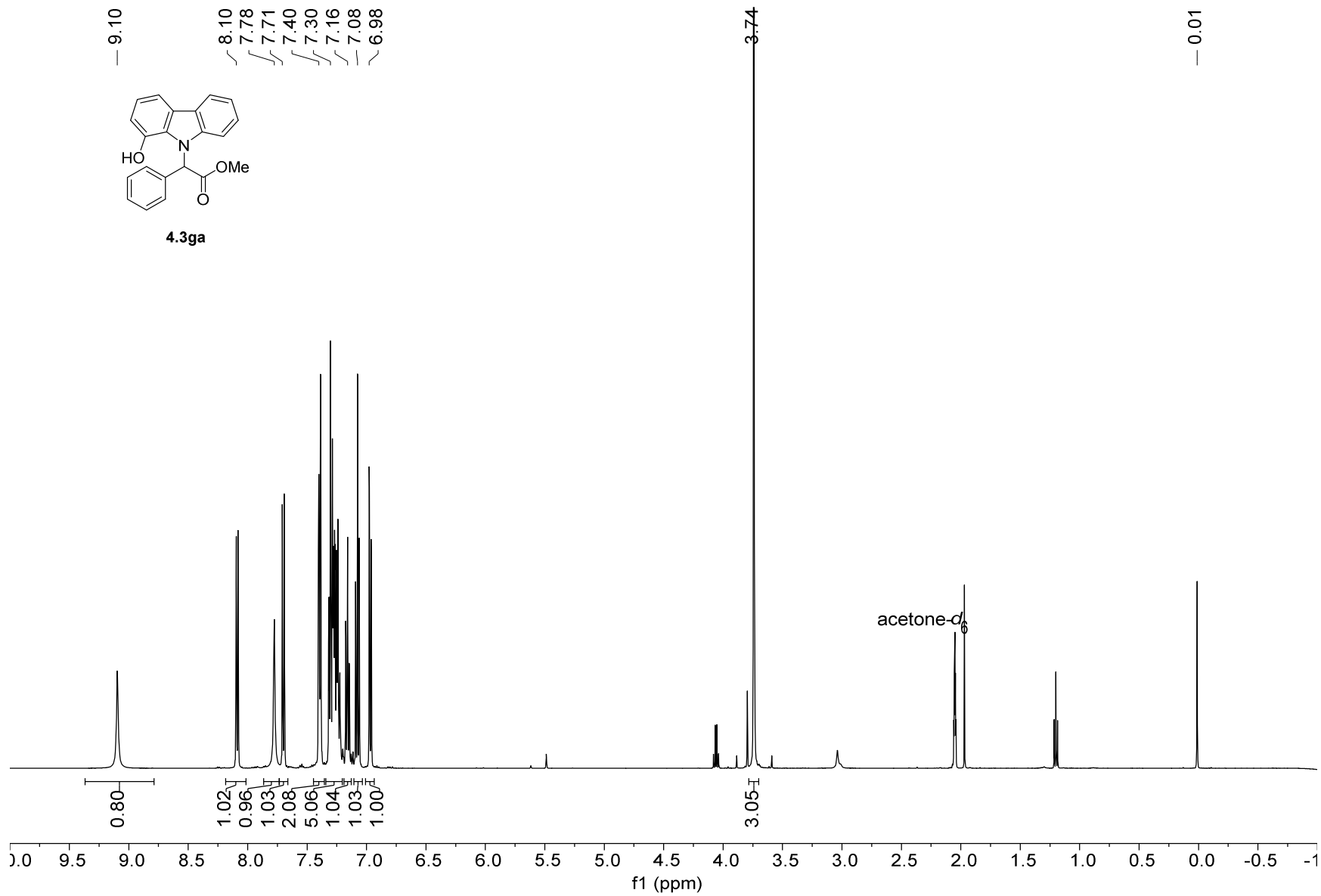
1H NMR — 500.22 MHz — acetone-d6 — 298.0 K

9.10  
8.10  
7.78  
7.71  
7.40  
7.30  
7.16  
7.08  
6.98

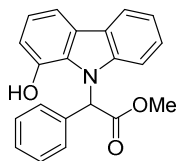


4.3ga

412



13C NMR — 125.78 MHz — acetone-d6 — 298.0 K



4.3ga

170.87  
144.46  
141.10  
137.47  
130.08  
129.00  
128.72  
128.43  
126.48  
126.20  
124.90  
121.17  
120.89  
120.20  
113.11  
112.76  
112.40

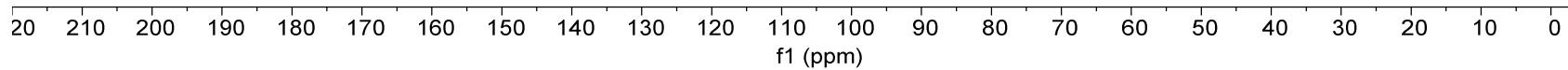
62.15

52.70

29.84

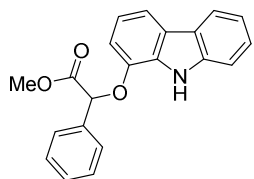
acetone-d<sub>6</sub>

413



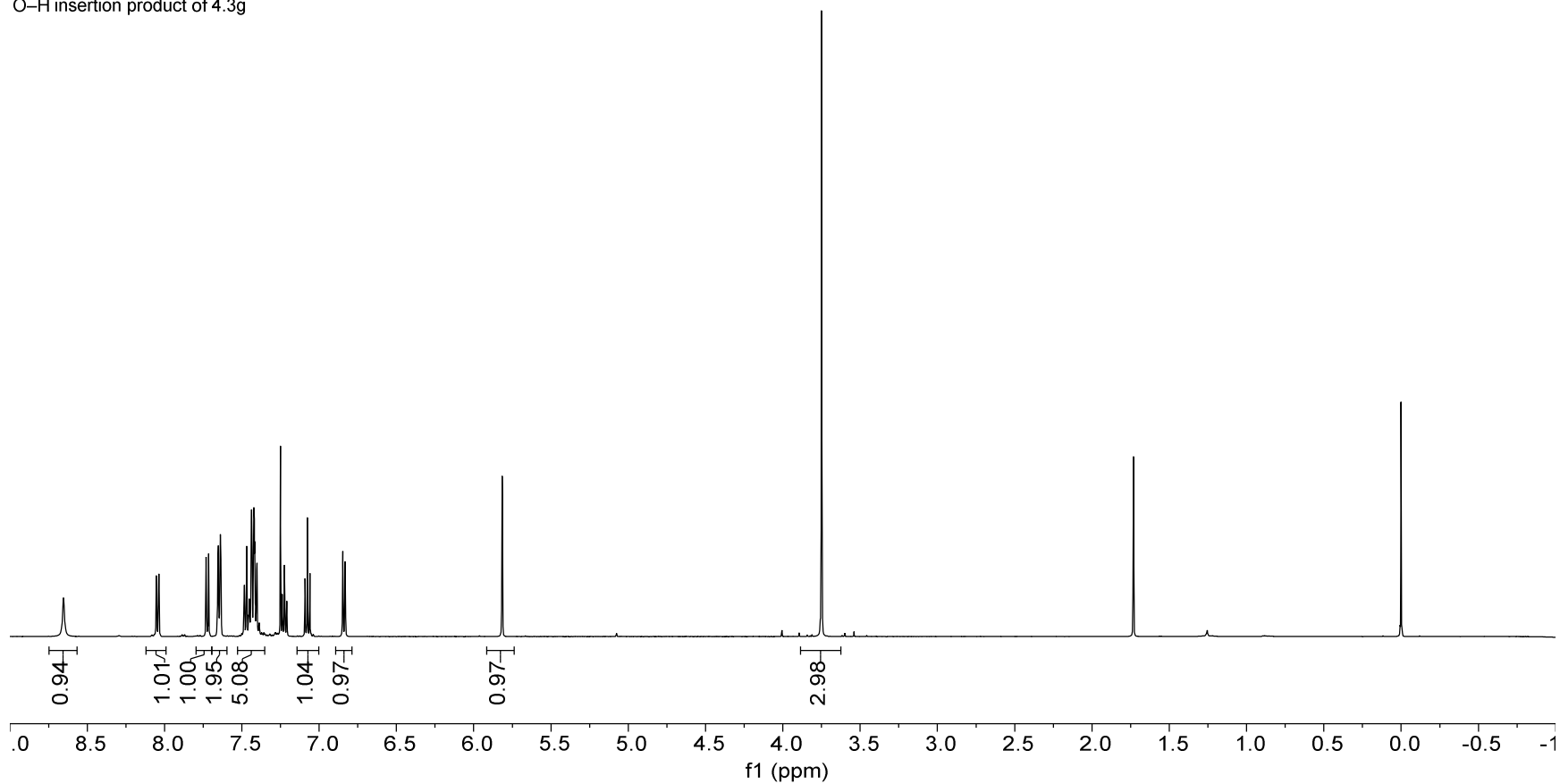
1H NMR — 500.22 MHz — CDCl3 — 298.0 K

8.65  
8.05  
7.73  
7.65  
7.44  
7.22  
7.08  
6.85  
5.82  
3.75  
0.00



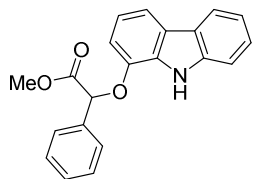
O-H insertion product of 4.3g

414



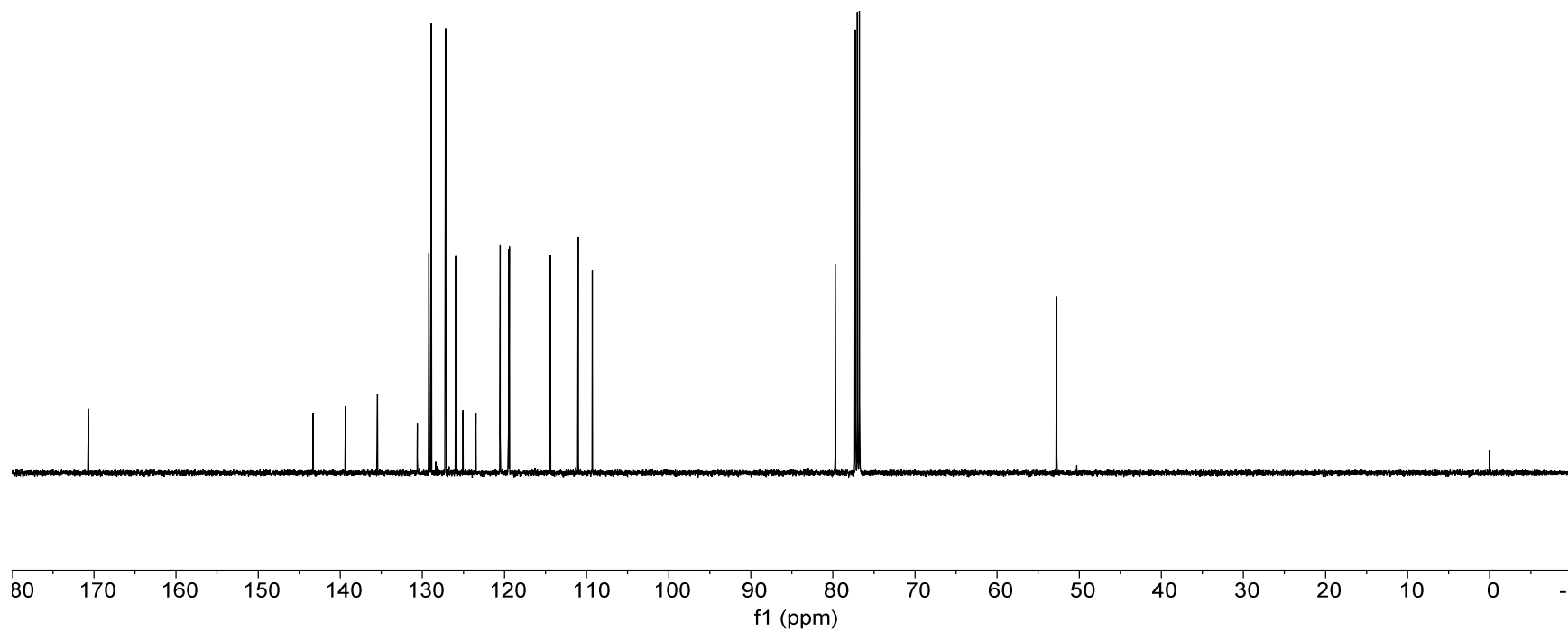
13C NMR — 125.78 MHz — CDCl3 — 298.0 K

170.70  
143.31  
139.37  
135.48  
130.61  
129.21  
128.93  
127.18  
125.93  
125.04  
123.47  
120.53  
119.50  
119.41  
114.40  
111.03  
109.30  
79.73  
52.75  
0.00

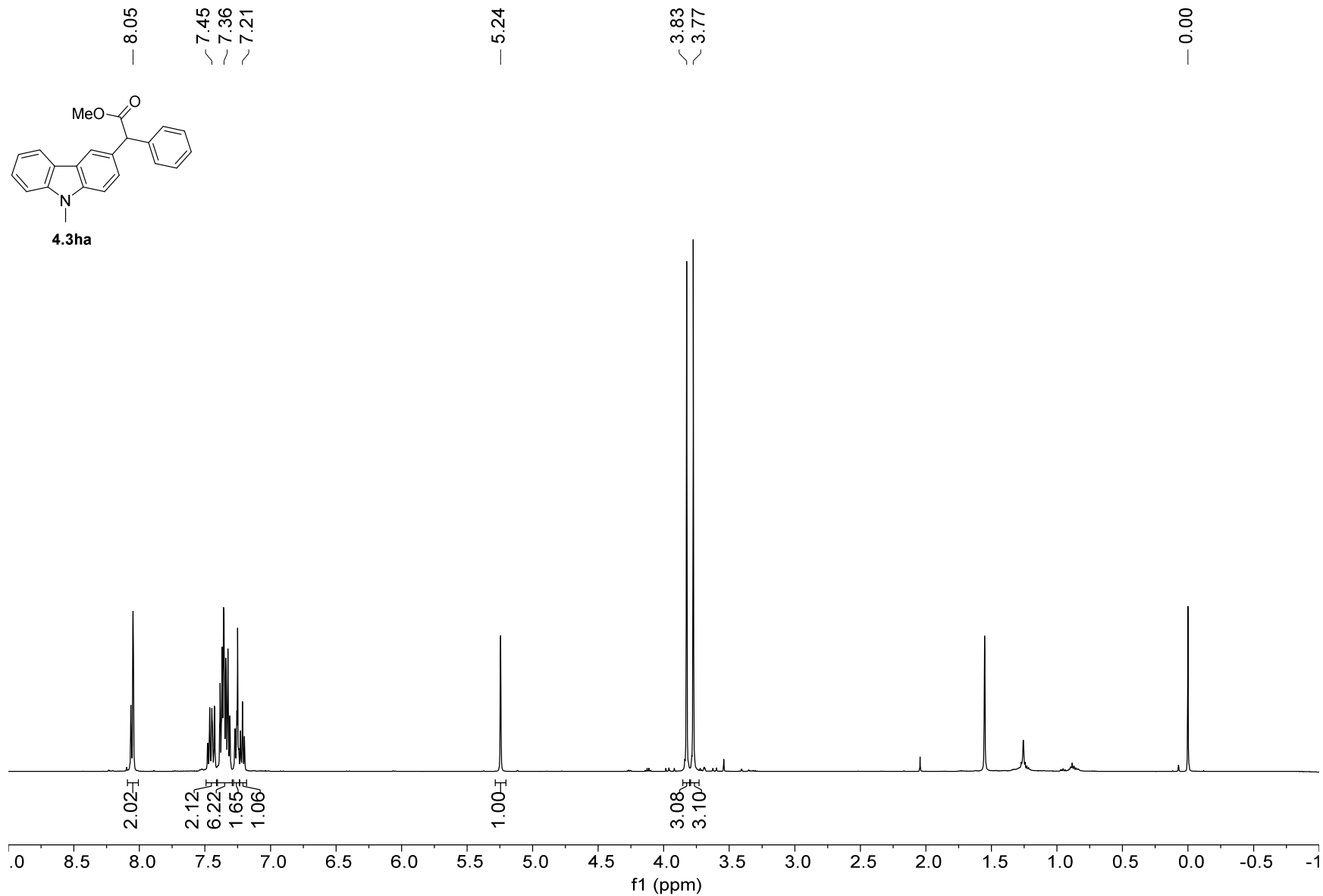
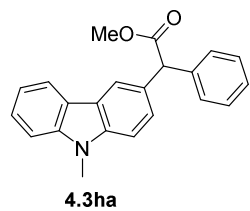


O-H insertion product of 4.3g

415

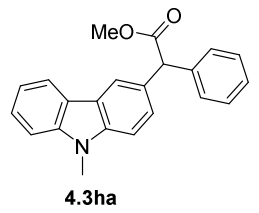


1H NMR — 500.22 MHz — CDCl3 — 298.0 K

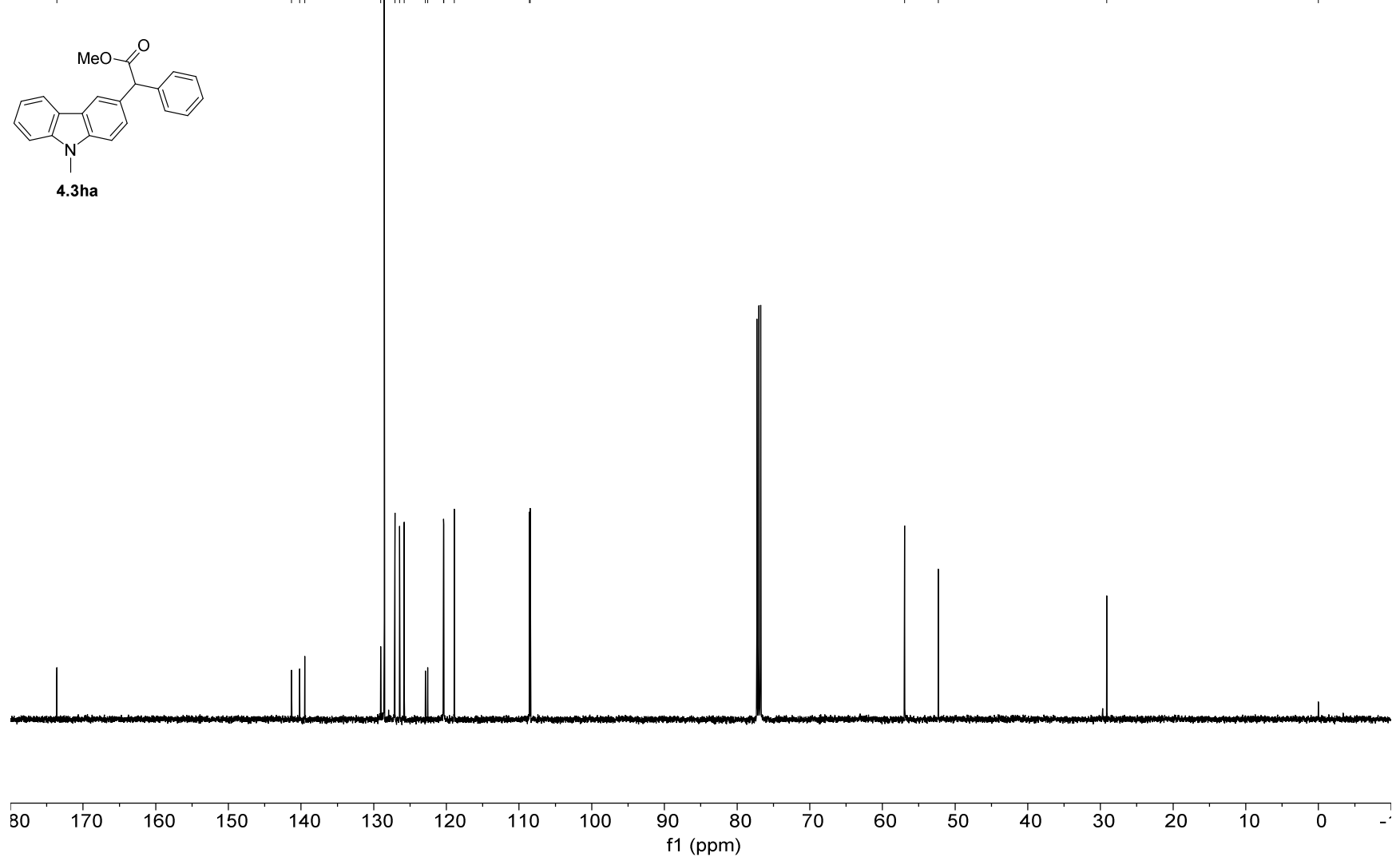


13C NMR — 125.79 MHz — CDCl3 — 298.0 K

173.61  
141.31  
140.20  
139.50  
129.03  
128.54  
127.09  
126.42  
125.82  
122.89  
122.57  
120.40  
120.35  
118.91  
108.57  
108.46  
56.96  
52.32  
29.12  
-0.00

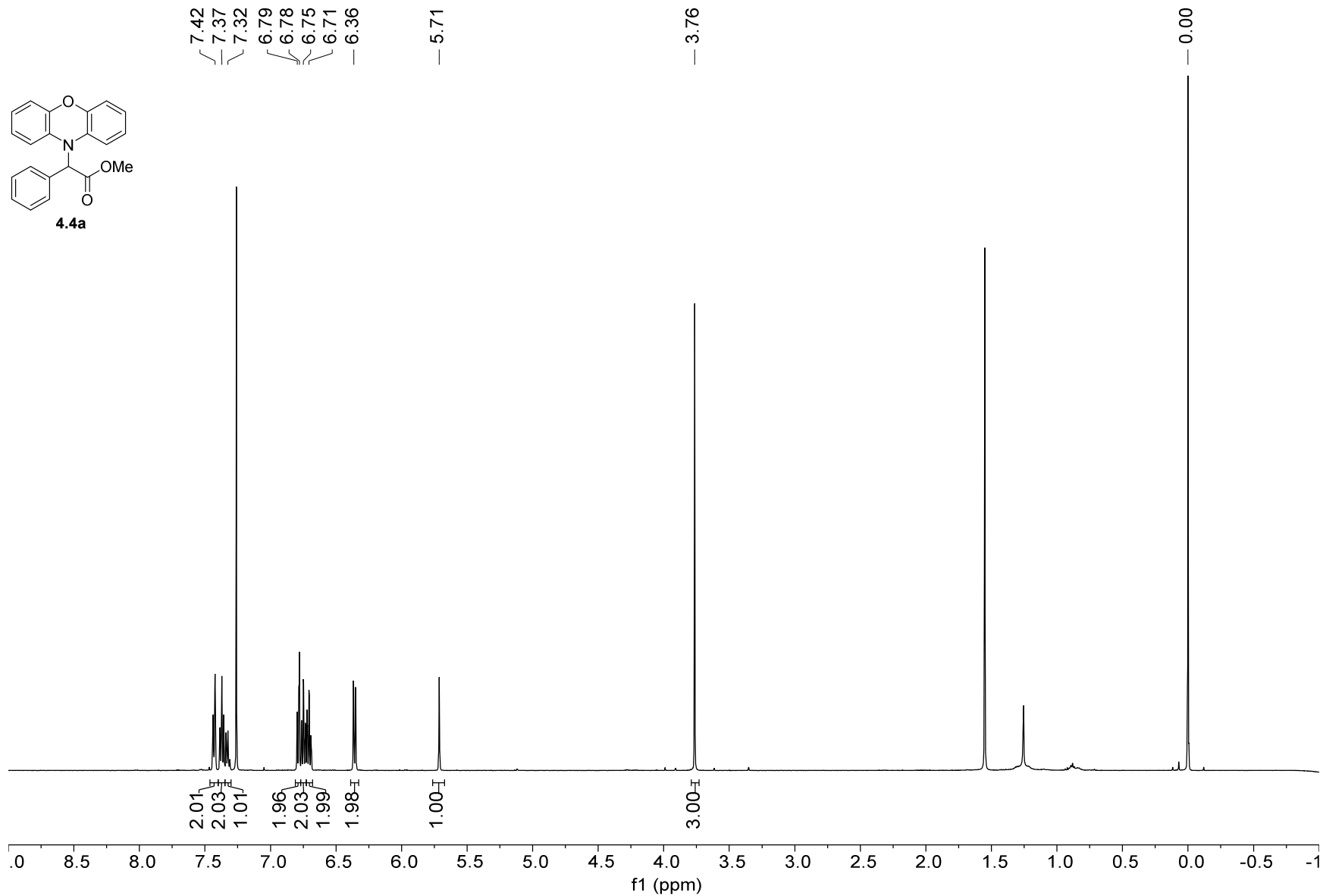
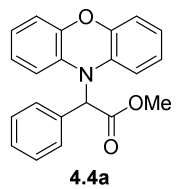


417



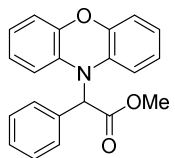


1H NMR — 500.22 MHz — CDCl3 — 298.0 K



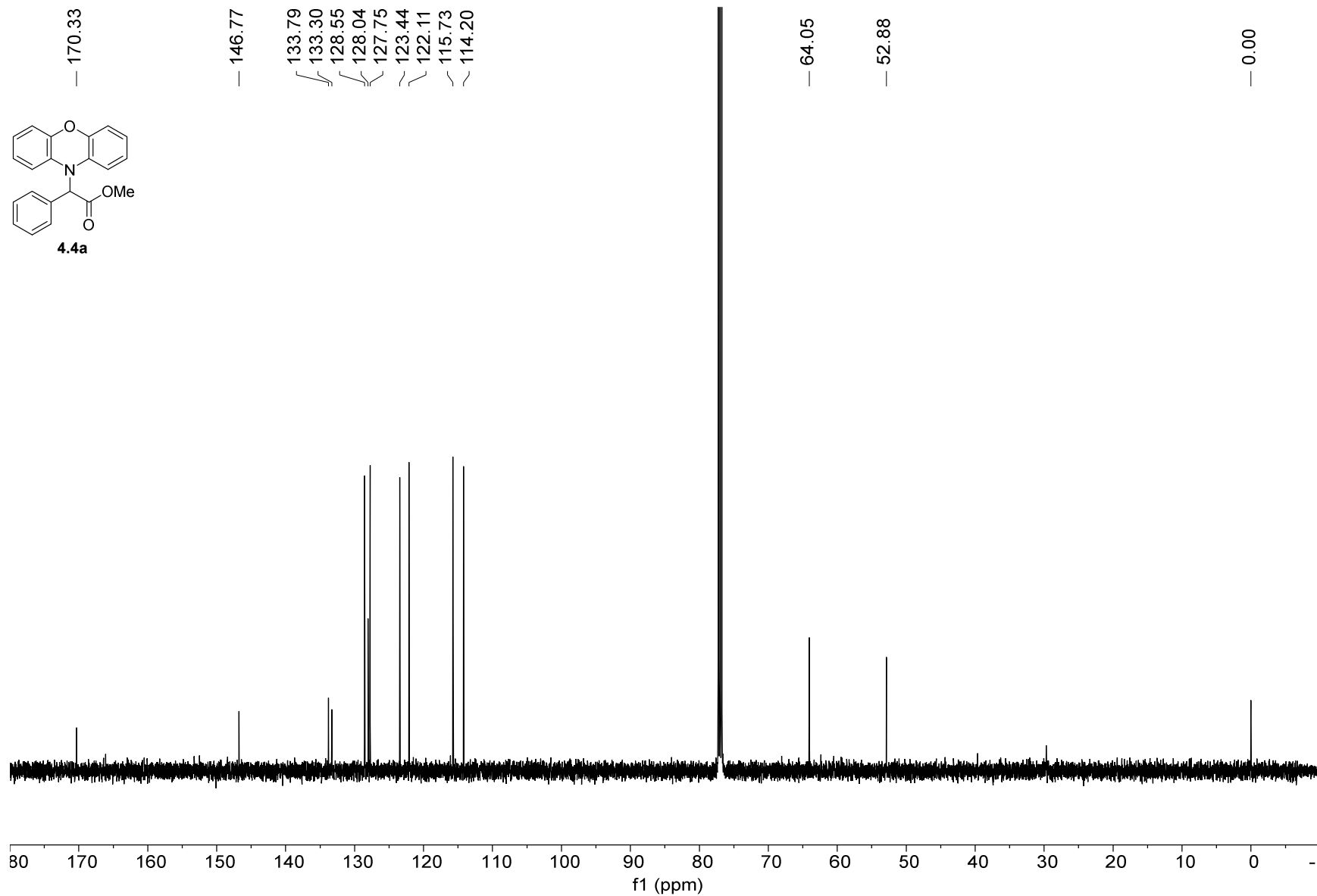
13C NMR — 125.79 MHz — CDCl3 — 298.0 K

170.33  
146.77  
133.79  
133.30  
128.55  
128.04  
127.75  
123.44  
122.11  
115.73  
114.20  
64.05  
52.88  
0.00

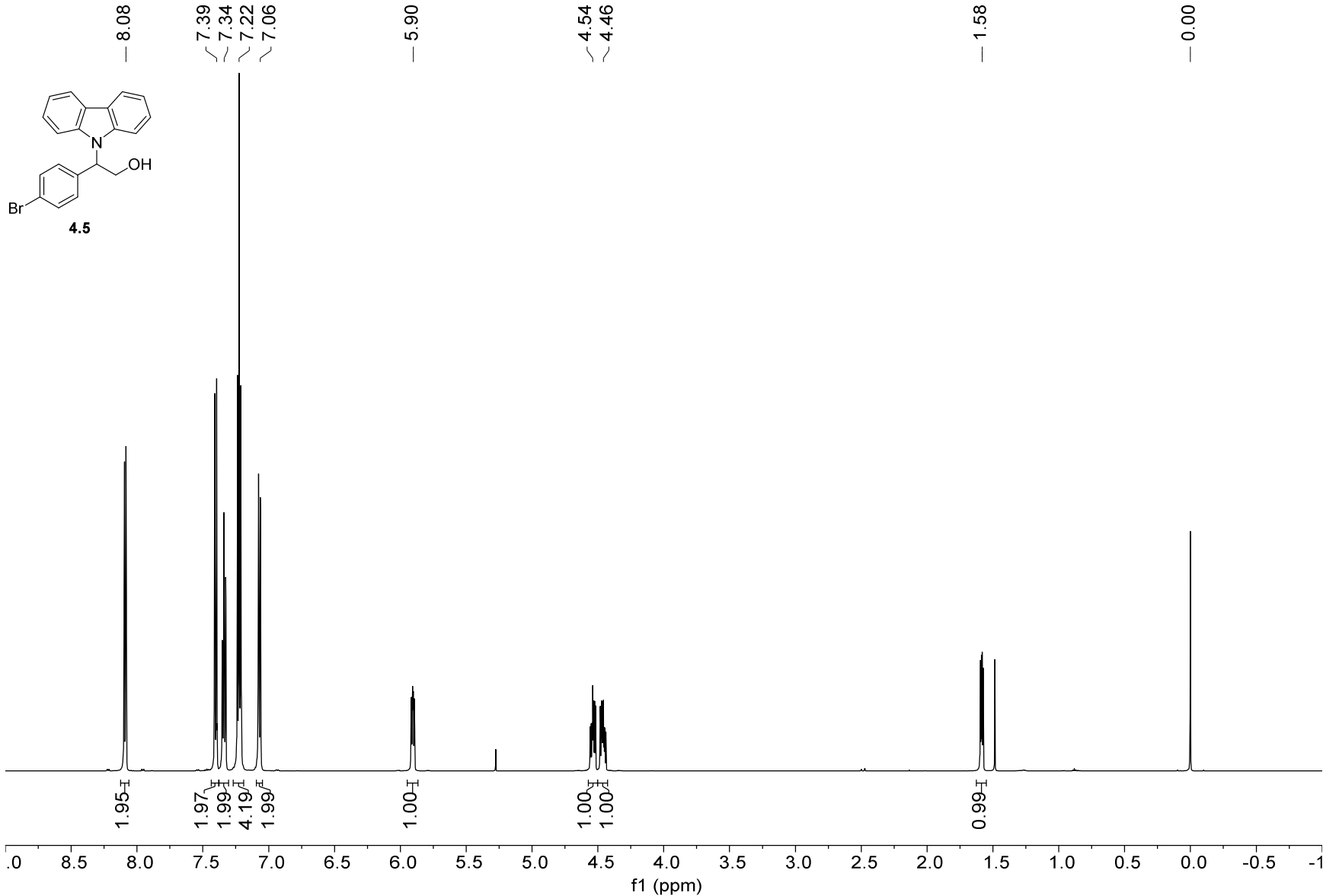


4.4a

419



1H NMR — 600.13 MHz — CDCl3T — 298.0 K



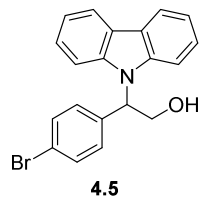
13C NMR — 150.92 MHz — CDCl3T — 298.0 K

140.09  
136.02  
131.92  
128.44  
125.83  
123.52  
121.78  
120.41  
119.59

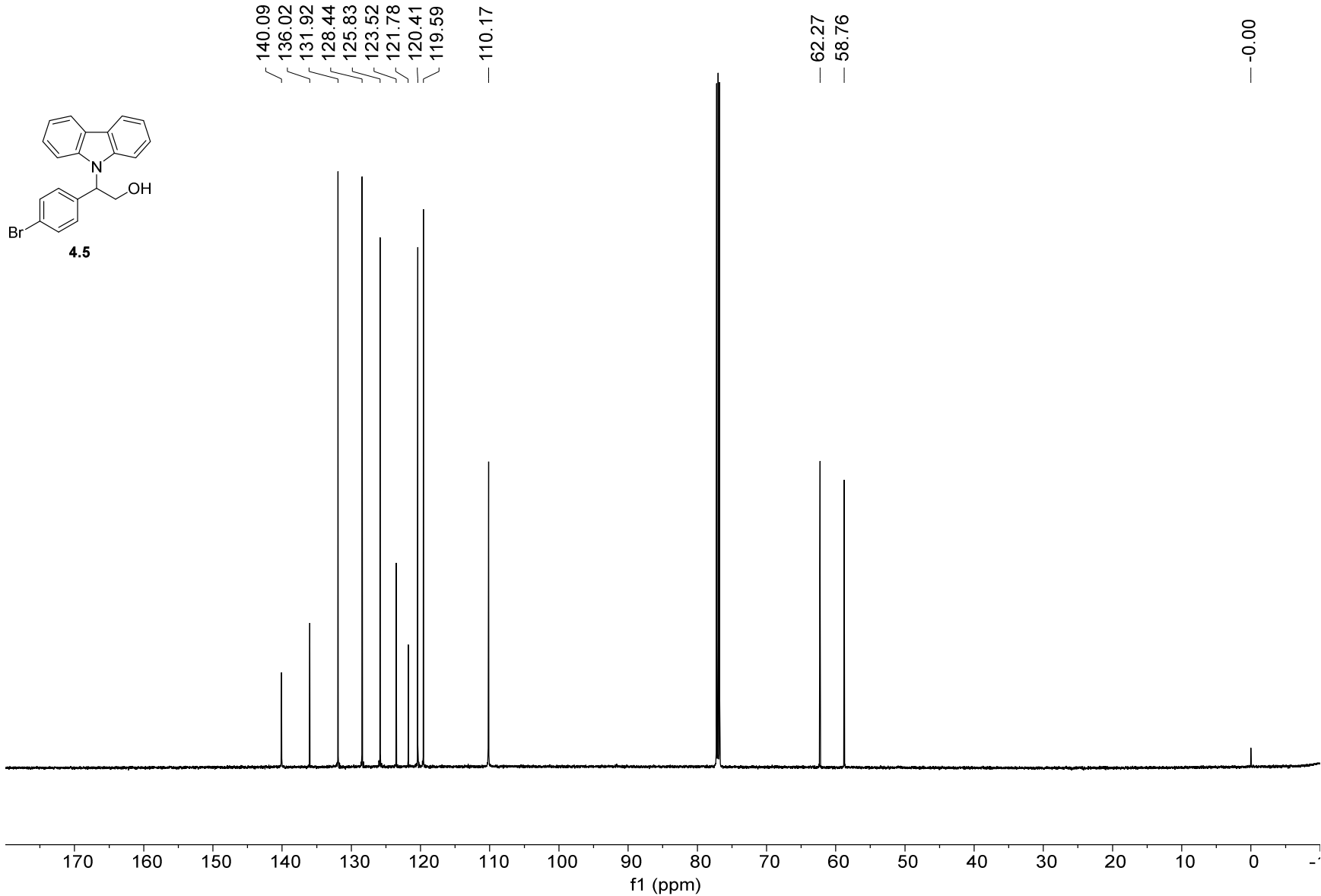
— 110.17

— 62.27  
— 58.76

— -0.00



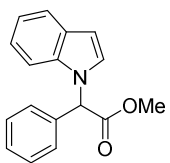
421



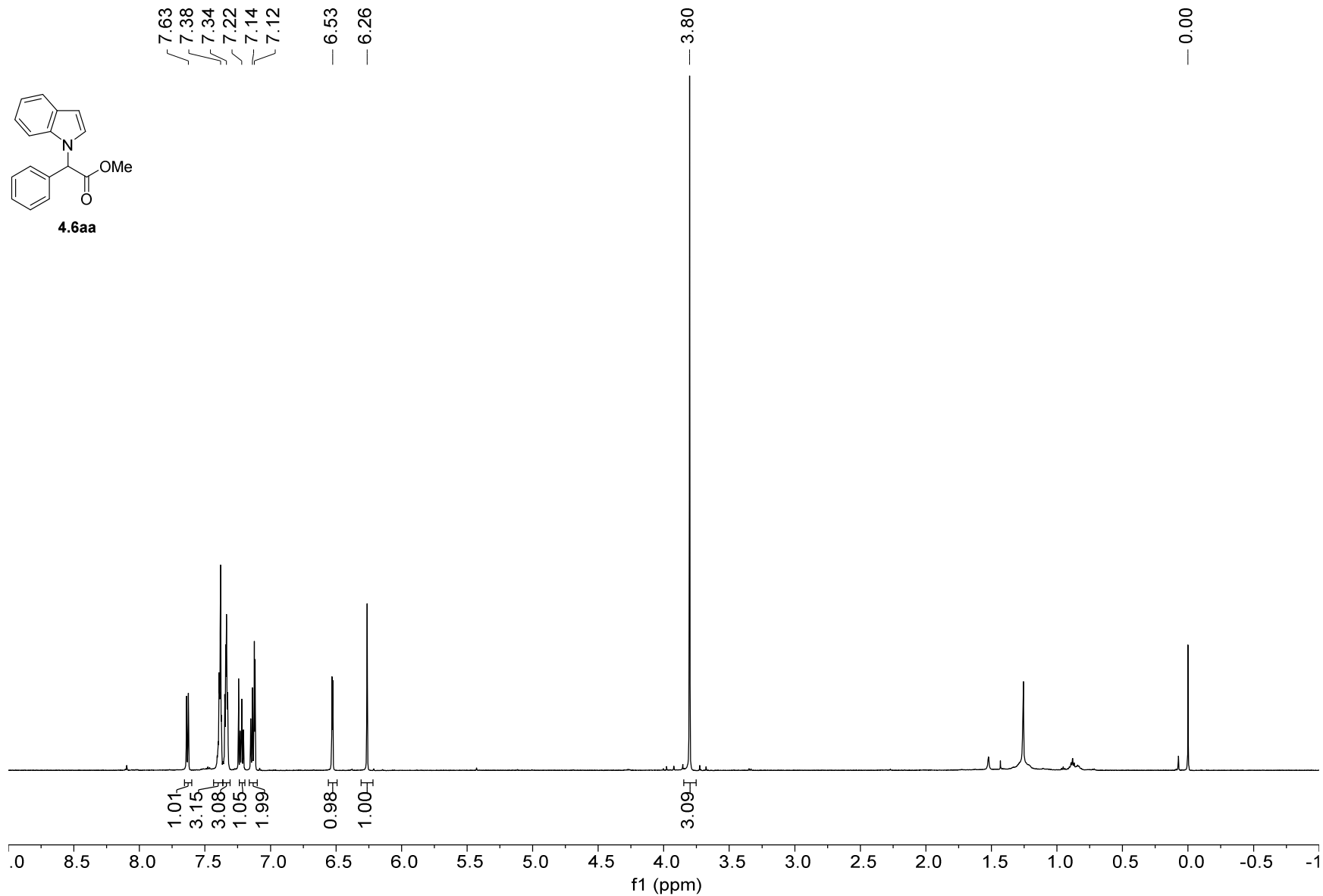
1H NMR — 600.13 MHz — CDCl3 — 298.0 K

7.63  
7.38  
7.34  
7.22  
7.14  
7.12  
— 6.53  
— 6.26

— 0.00



4.6aa



13C NMR — 150.92 MHz — CDCl3 — 298.0 K

— 170.07

136.44

134.61

129.06

128.97

128.78

128.06

126.70

121.92

121.17

120.12

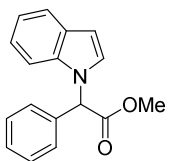
— 108.98

— 102.48

— 61.95

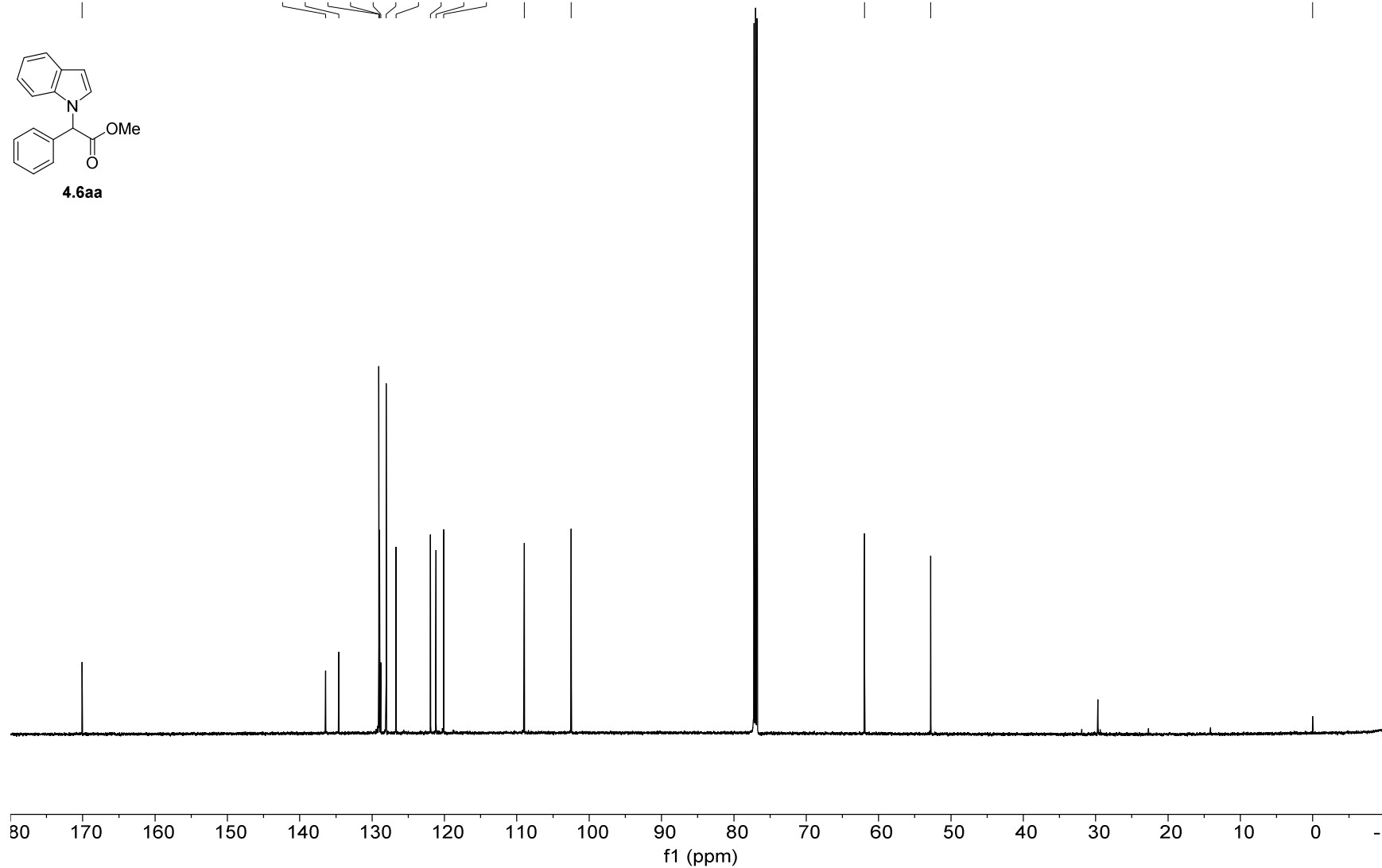
— 52.80

— 0.00



4.6aa

423



1H NMR — 500.22 MHz — CDCl3T — 298.0 K

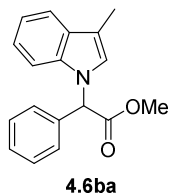
7.56  
7.38  
7.32  
7.21  
7.14  
6.88

6.21

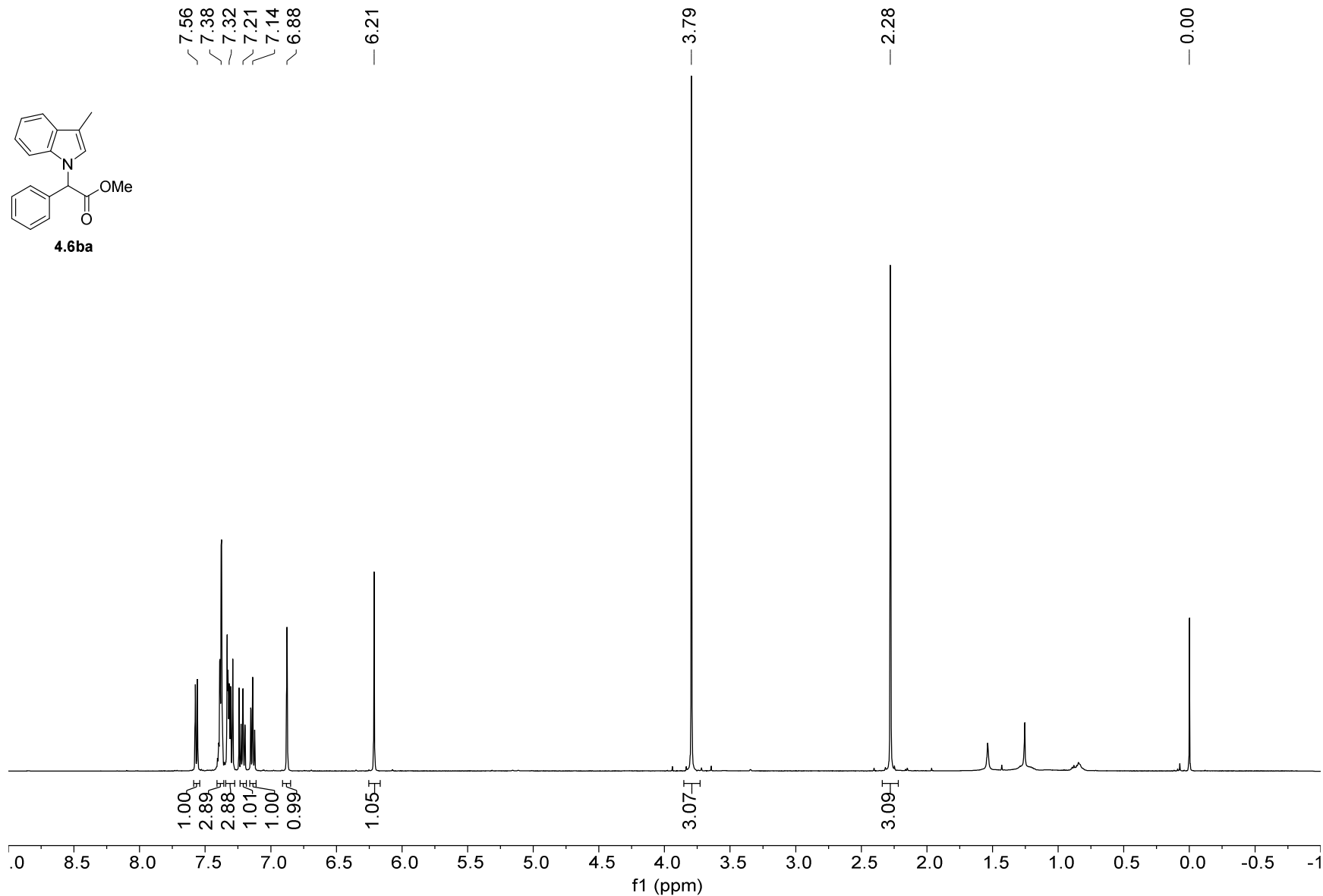
3.79

2.28

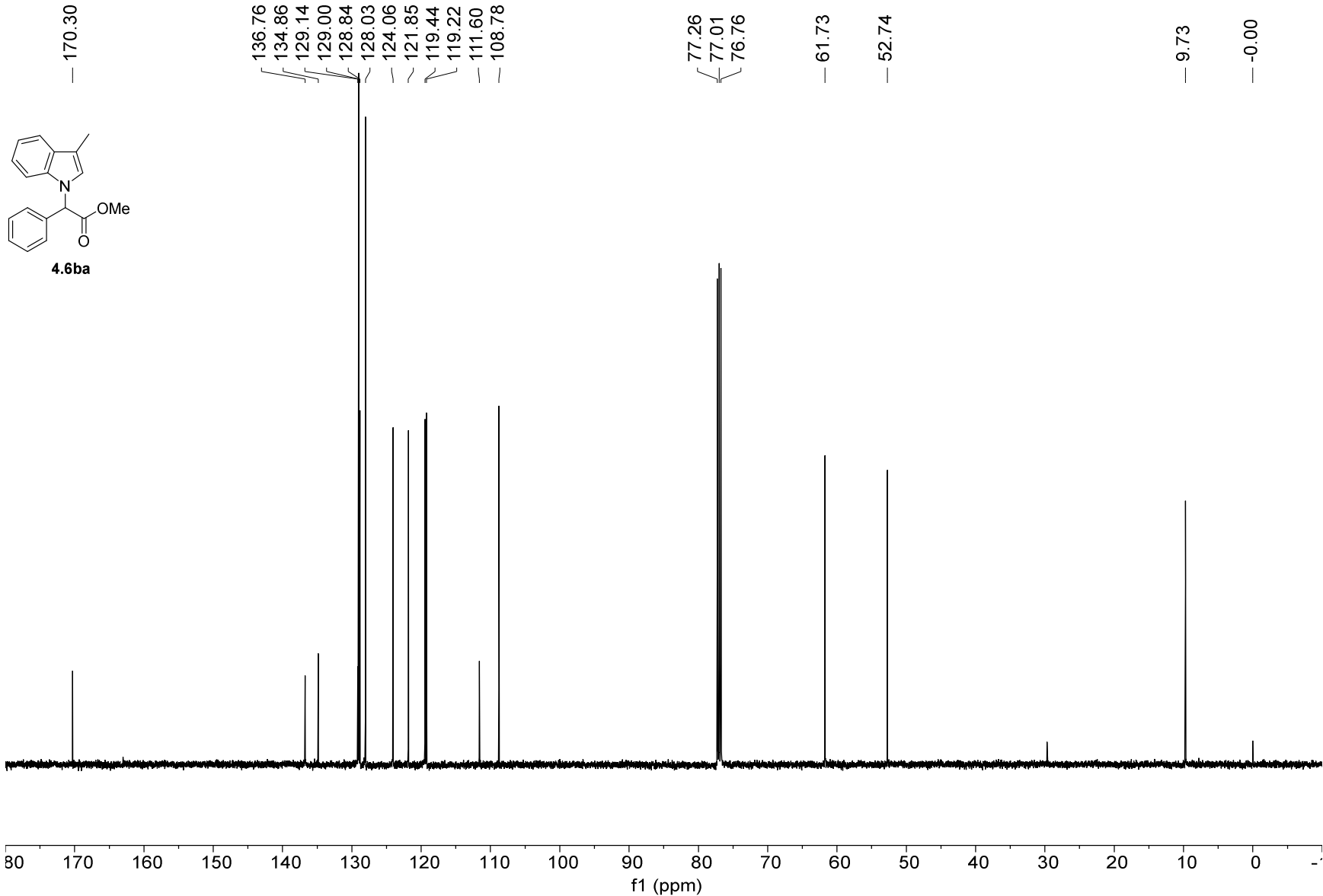
0.00



424

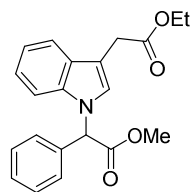


13C NMR — 125.79 MHz — CDCl3 — 298.0 K

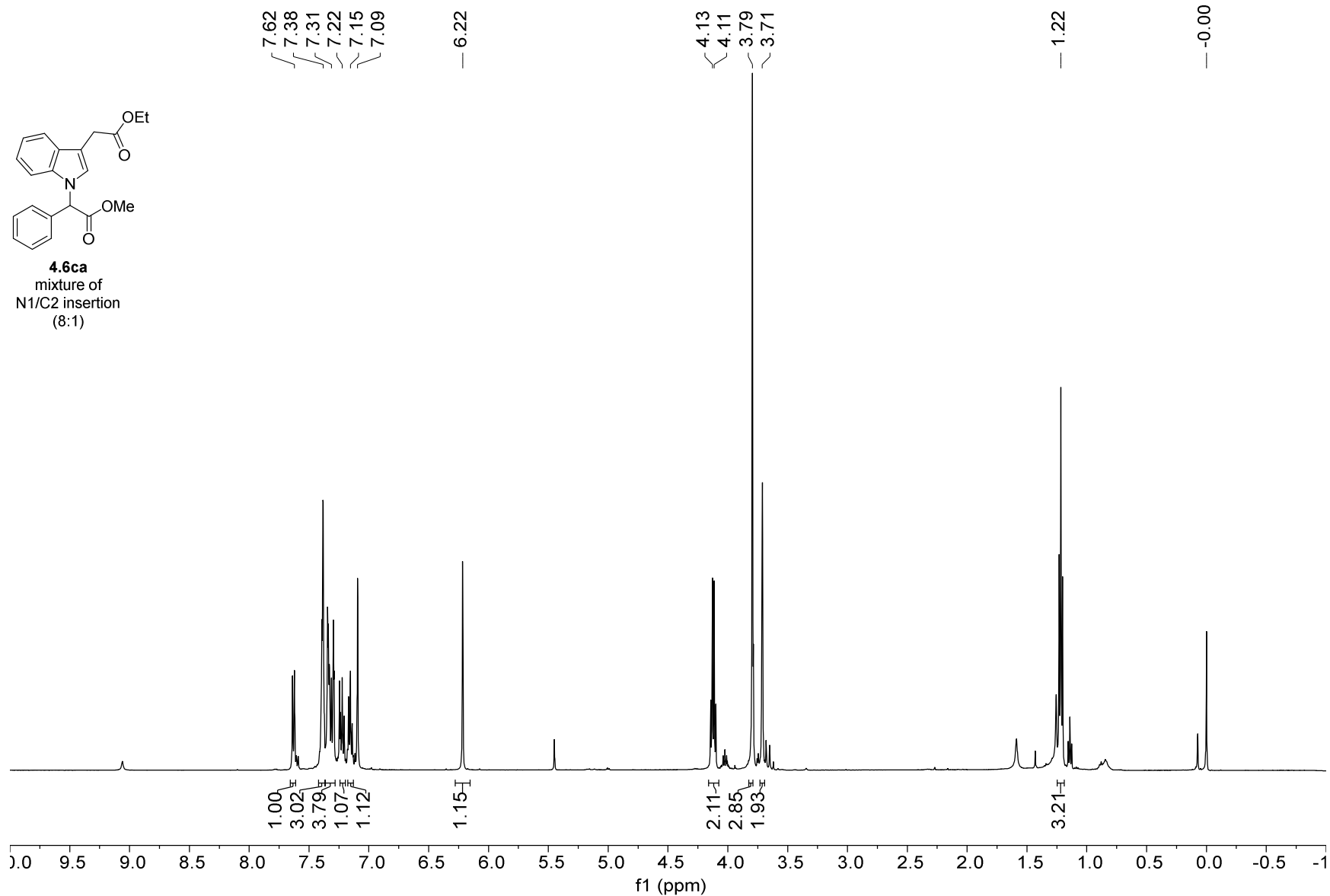




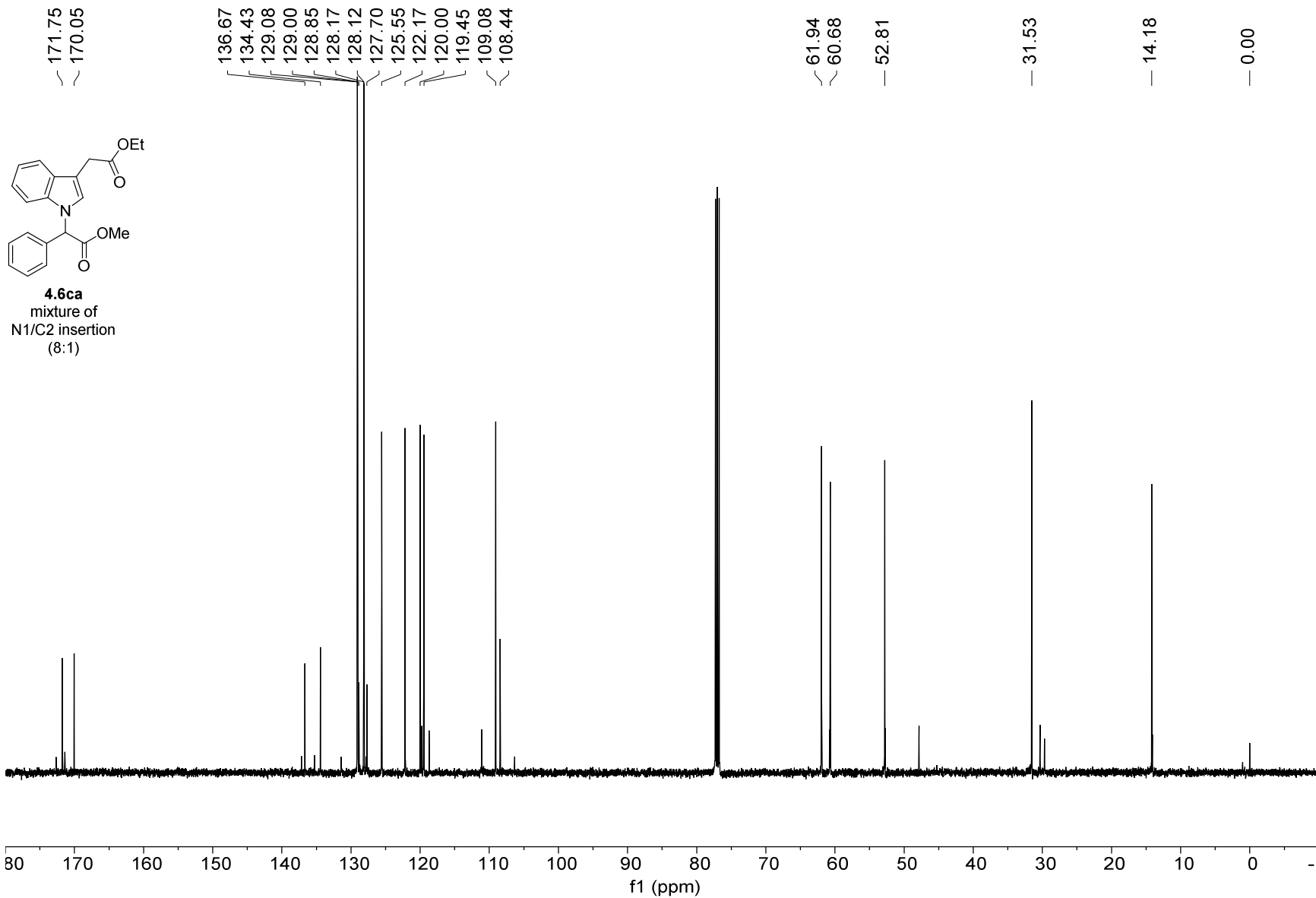
1H NMR — 500.22 MHz — CDCl3T — 298.0 K



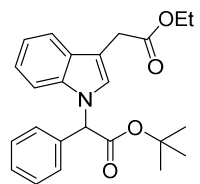
**4.6ca**  
mixture of  
N1/C2 insertion  
(8:1)



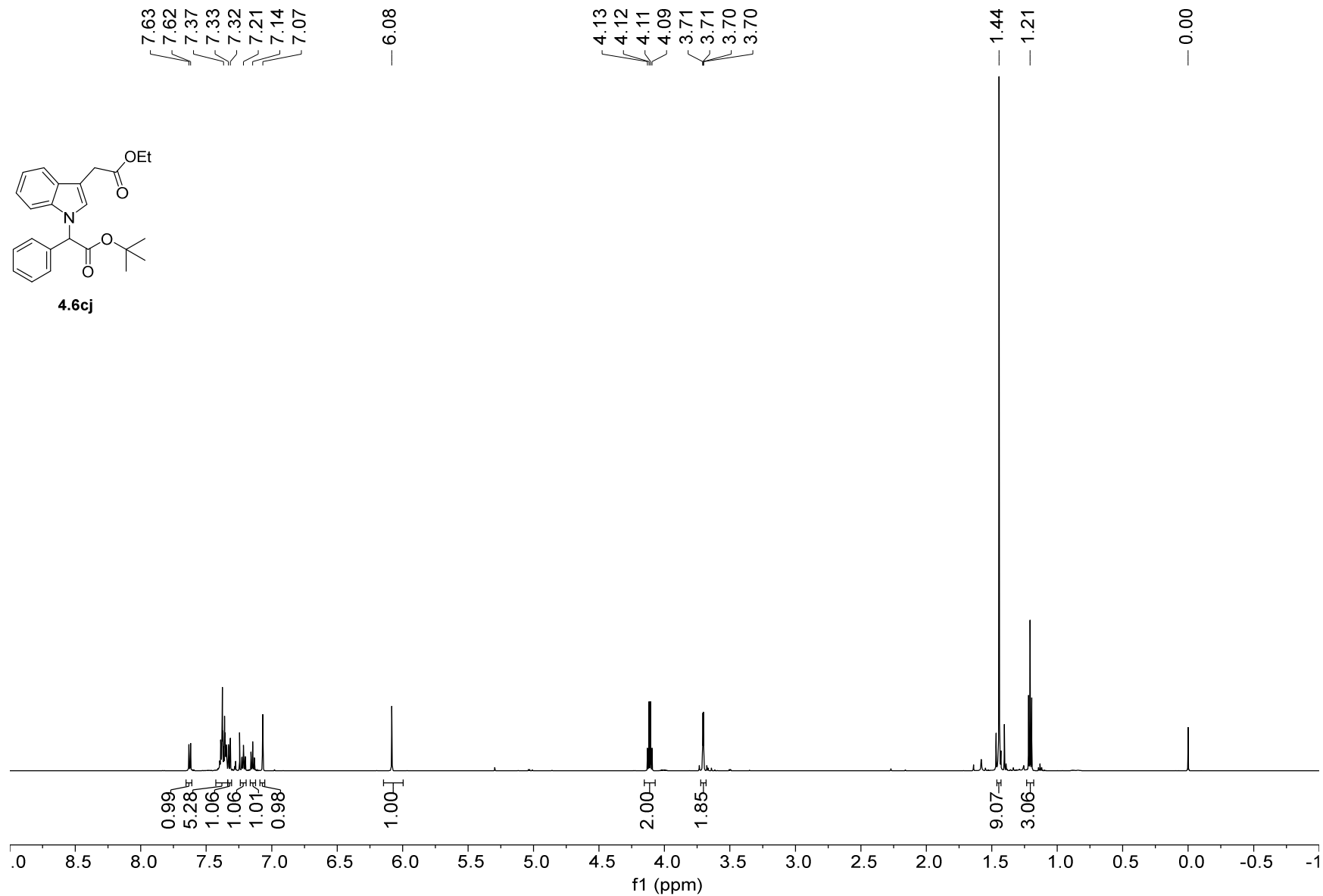
13C NMR — 125.79 MHz — CDCl3 — 298.0 K



1H NMR — 600.13 MHz — CDCl3T — 298.0 K



4.6cj



13C NMR — 150.92 MHz — CDCl3T — 298.0 K

171.80  
168.64  
136.81  
134.97  
128.96  
128.74  
128.15  
125.70  
121.96  
119.83  
119.38  
109.16  
108.08

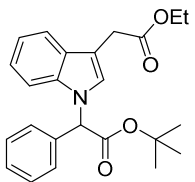
82.93

62.65  
60.63

31.58  
27.91

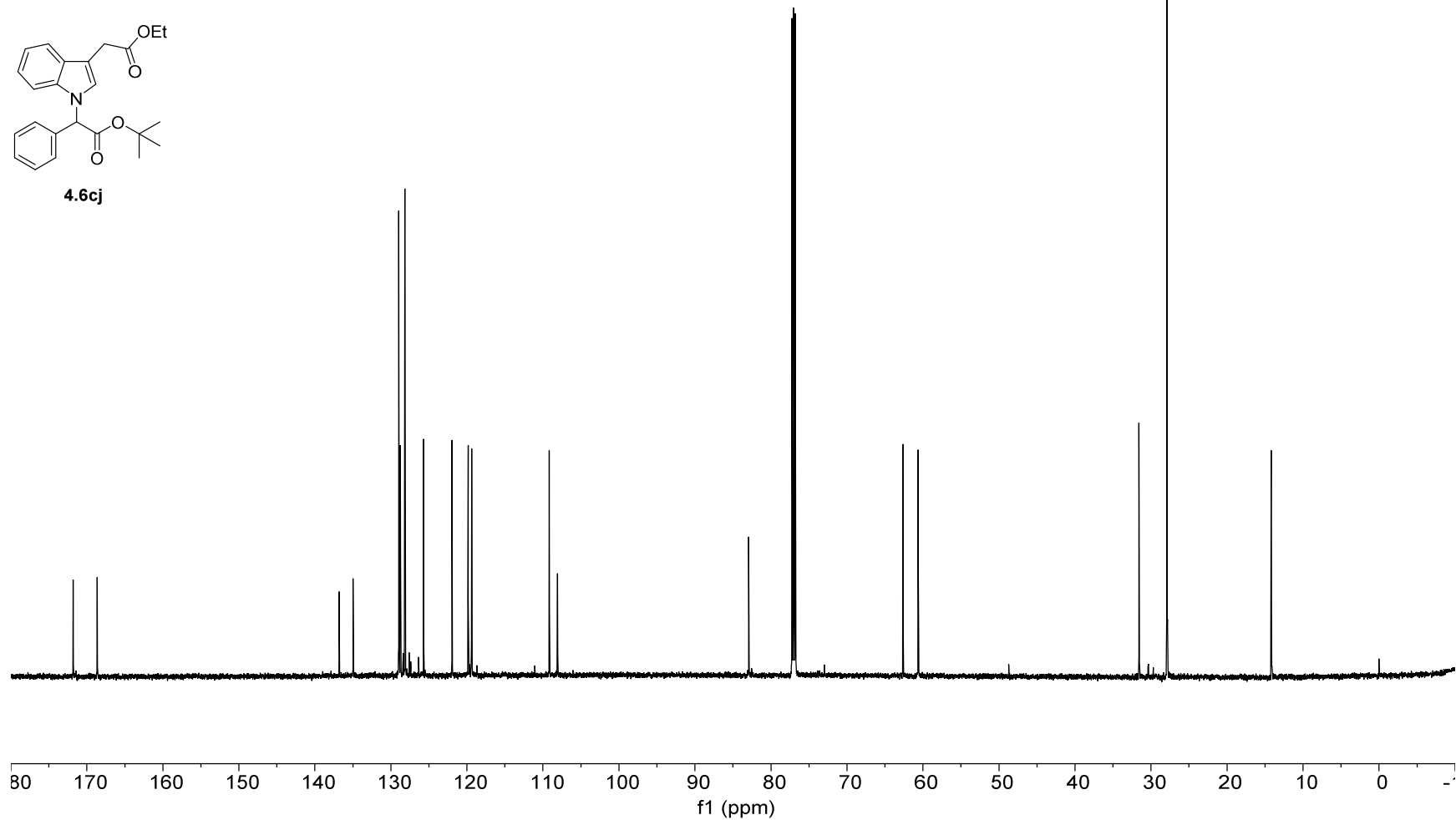
14.18

-0.00

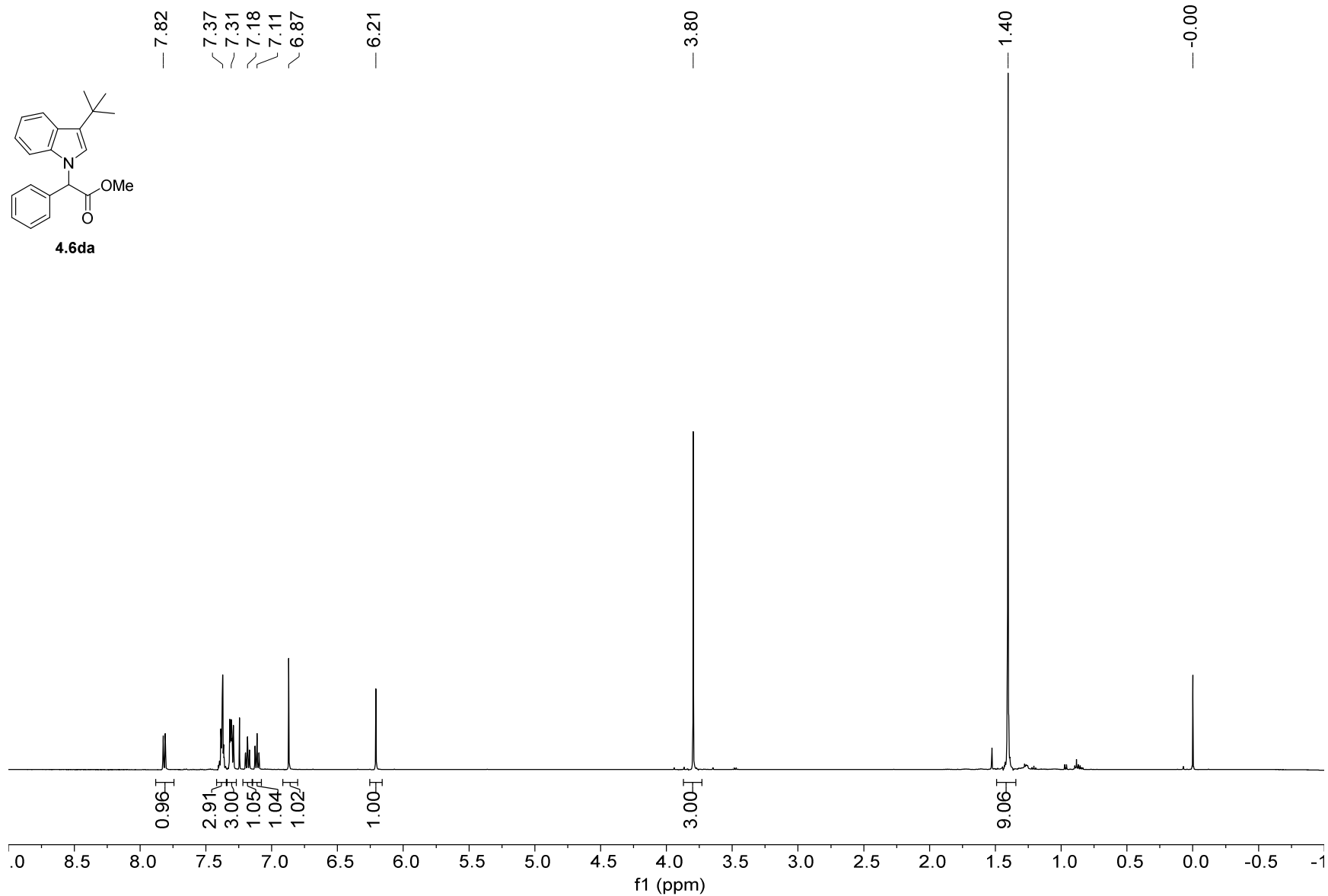
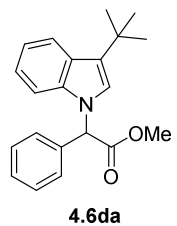


4.6cj

429

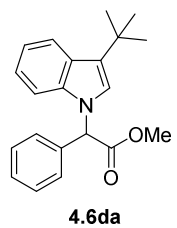


1H NMR — 500.22 MHz — CDCl3T — 298.0 K



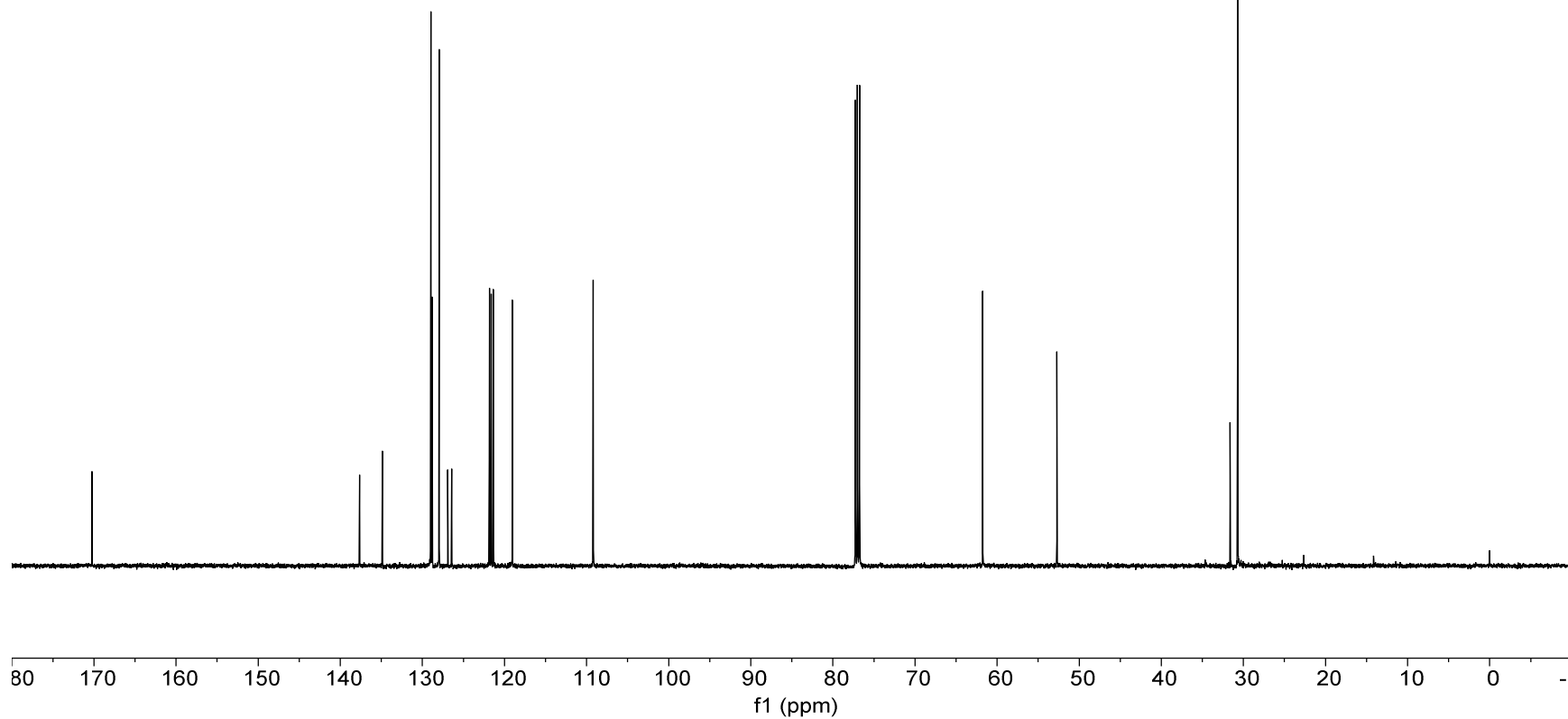
430

13C NMR — 125.78 MHz — CDCl3 — 298.0 K



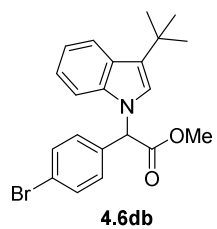
170.24  
137.63  
134.87  
128.97  
128.80  
127.95  
126.91  
126.43  
121.84  
121.60  
121.36  
119.05  
109.19  
61.76  
52.72  
31.63  
30.71  
-0.00

431



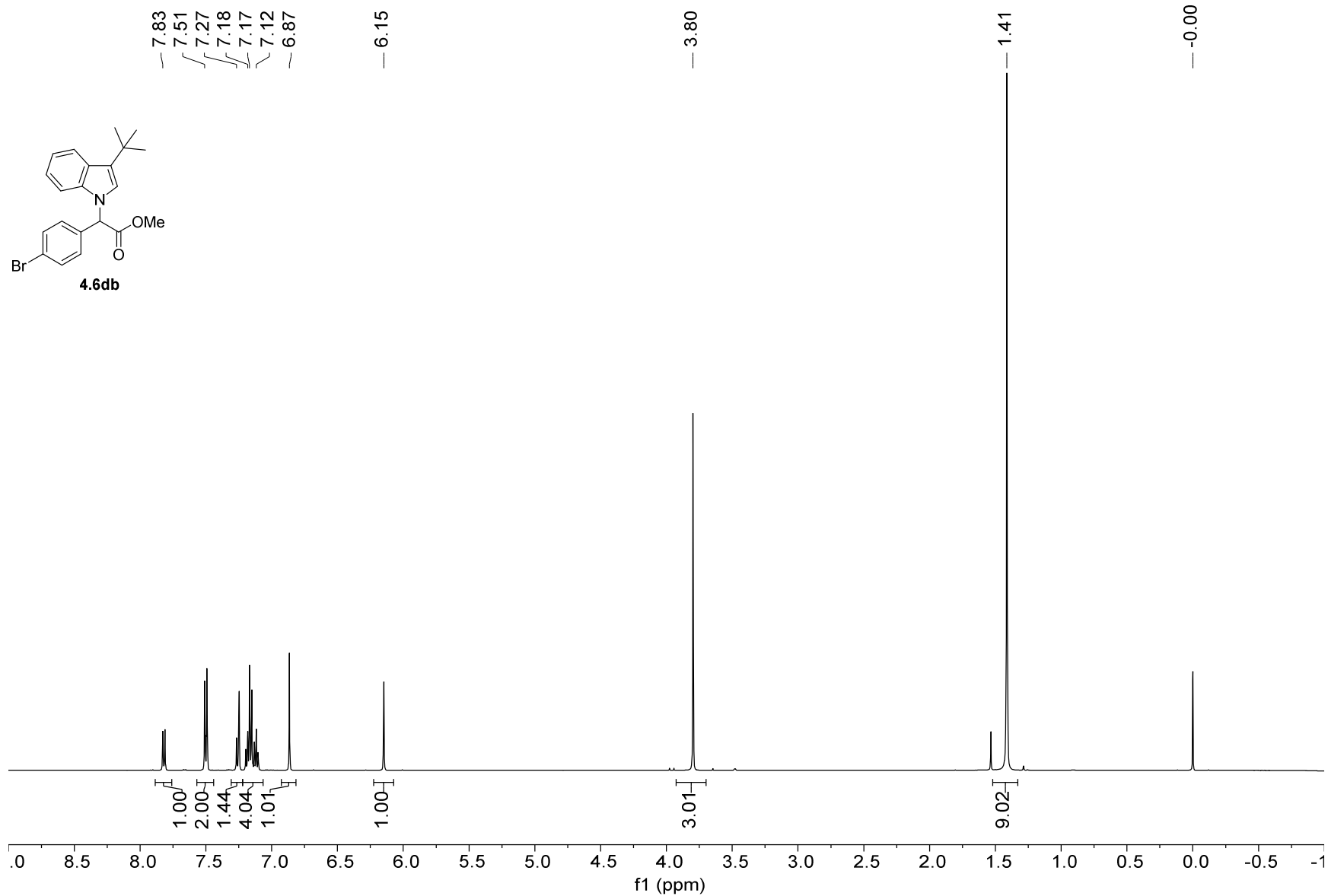
1H NMR — 500.22 MHz — CDCl3 — 298.0 K

7.83  
7.51  
7.27  
7.18  
7.17  
7.12  
6.87  
— 6.15



— 3.80  
— 1.41  
— -0.00

432



13C NMR — 125.79 MHz — CDCl3 — 298.0 K

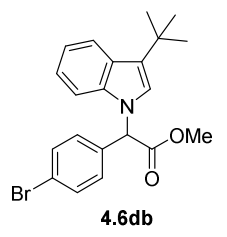
— 169.74 —  
— 137.51 —  
— 134.02 —  
— 132.11 —  
— 129.49 —  
— 126.91 —  
— 126.87 —  
— 122.96 —  
— 121.68 —  
— 121.58 —  
— 121.53 —  
— 119.21 —  
— 109.16 —

— 61.17 —

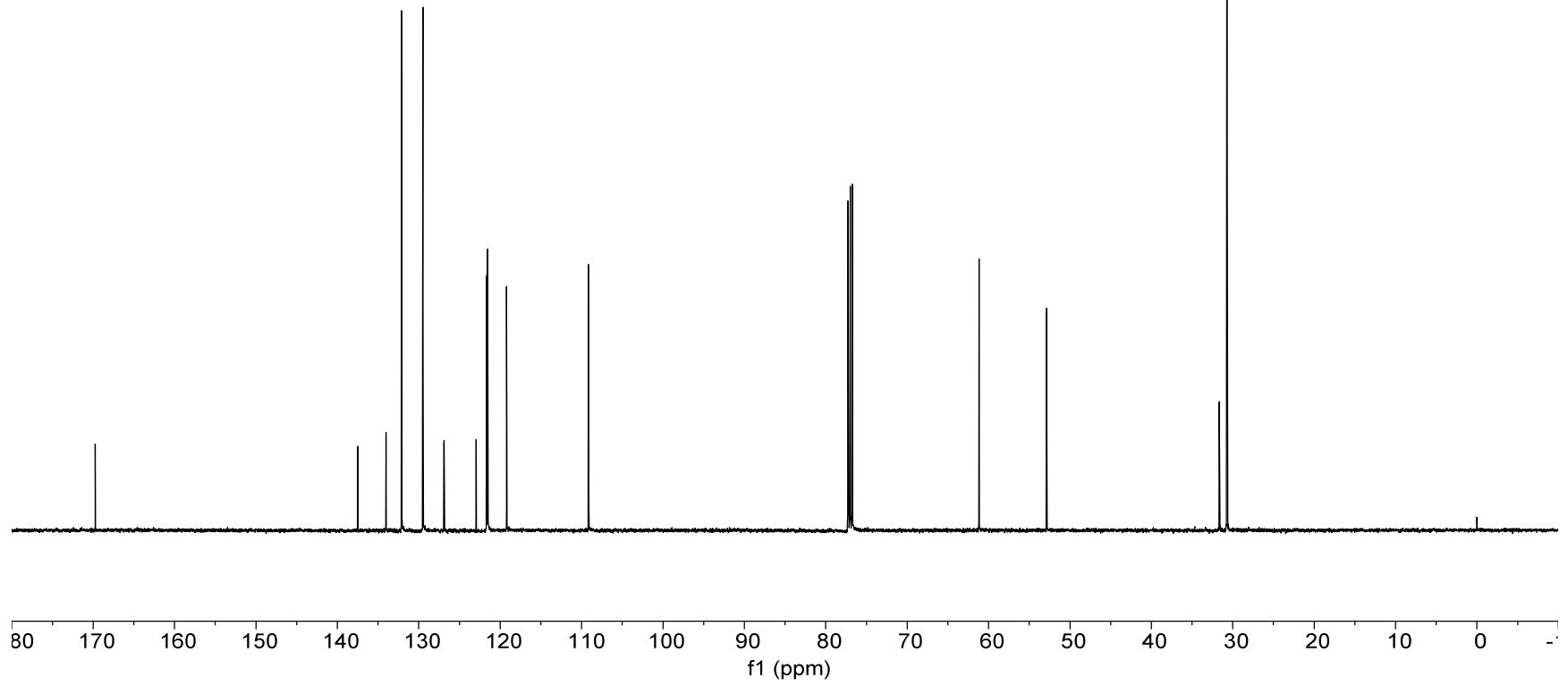
— 52.87 —

— 31.65 —  
— 30.70 —

— -0.00 —



433





1H NMR — 500.22 MHz — CDCl3 — 298.0 K

7.60  
7.42  
7.36  
7.28  
7.19  
7.04

6.24

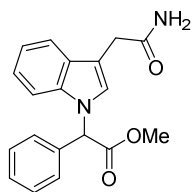
5.62

5.43

3.81

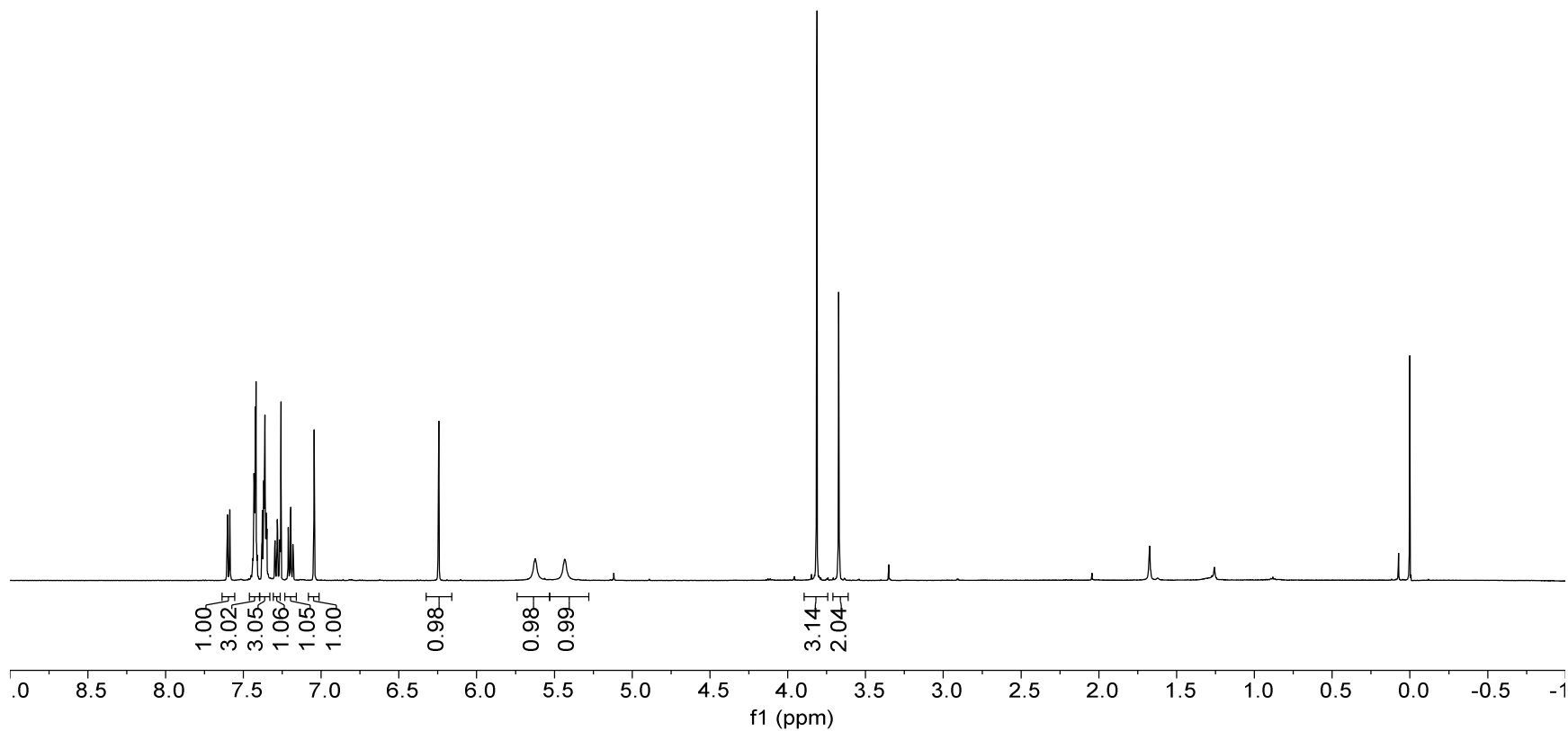
3.67

0.00



4.6ea

434



13C NMR — 125.78 MHz — CDCl3 — 298.0 K

— 173.92  
— 170.04

137.05  
134.12  
129.28  
128.20  
127.80  
126.13  
122.77  
120.59  
119.25

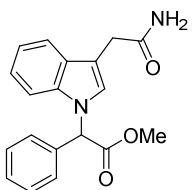
— 109.28

— 61.87

— 52.92

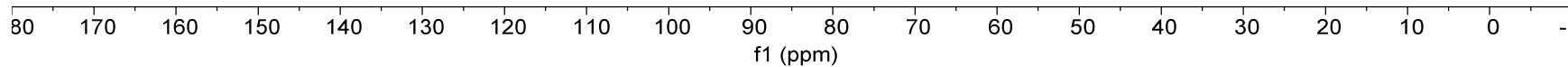
— 33.03

— 0.00



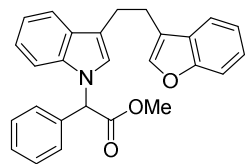
4.6ea

435



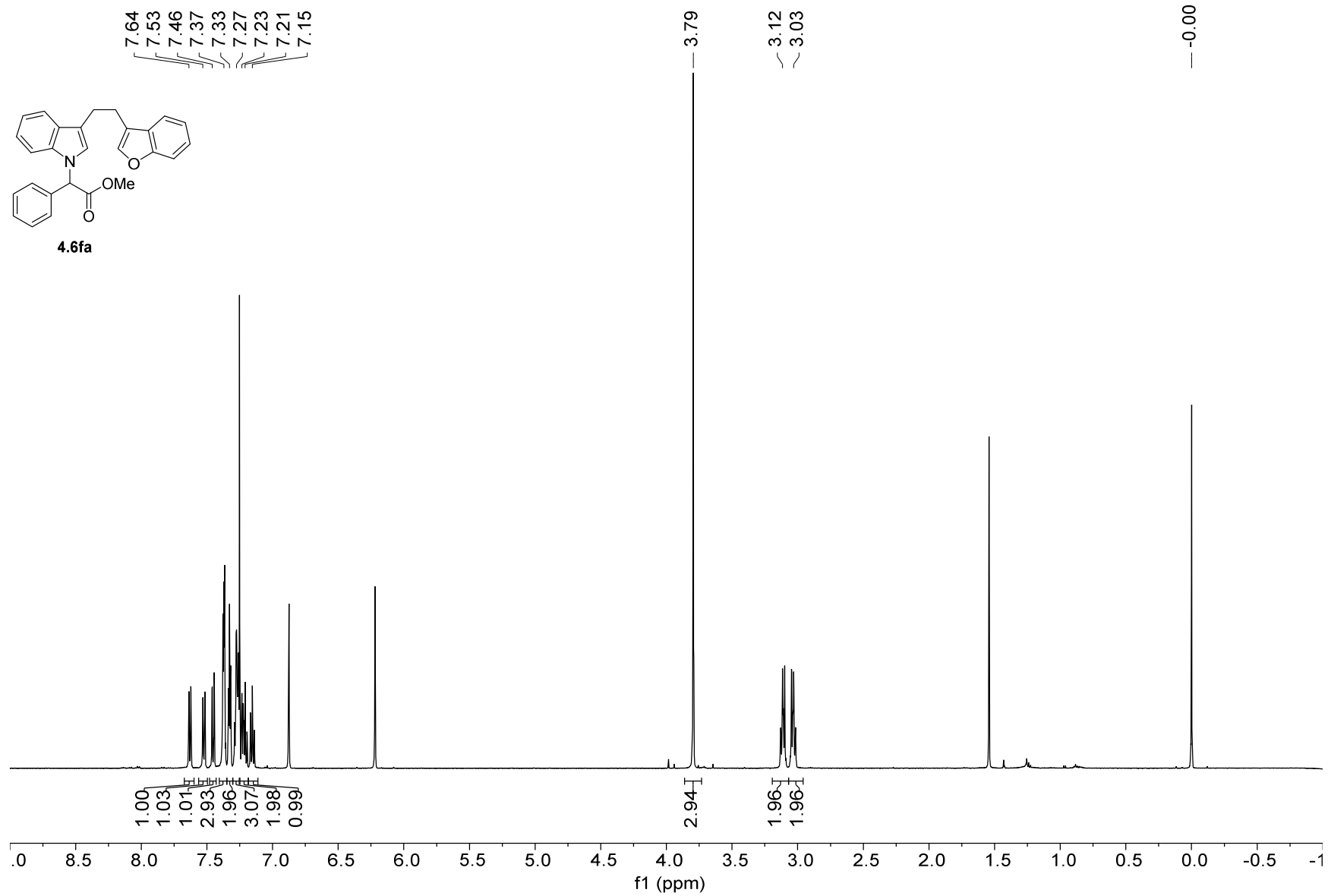
1H NMR — 500.22 MHz — CDCl3 — 298.0 K

7.64  
7.53  
7.46  
7.37  
7.33  
7.27  
7.23  
7.21  
7.15



4.6fa

436



13C NMR — 125.78 MHz — CDCl3 — 298.0 K

155.24  
141.33  
136.89  
134.74  
129.03  
128.88  
128.24  
128.21  
127.92  
124.02  
123.99  
122.18  
122.03  
120.21  
119.65  
119.61  
119.17  
115.76  
111.37  
109.06

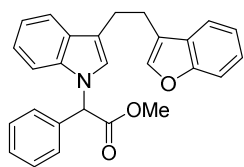
61.76

52.78

25.09

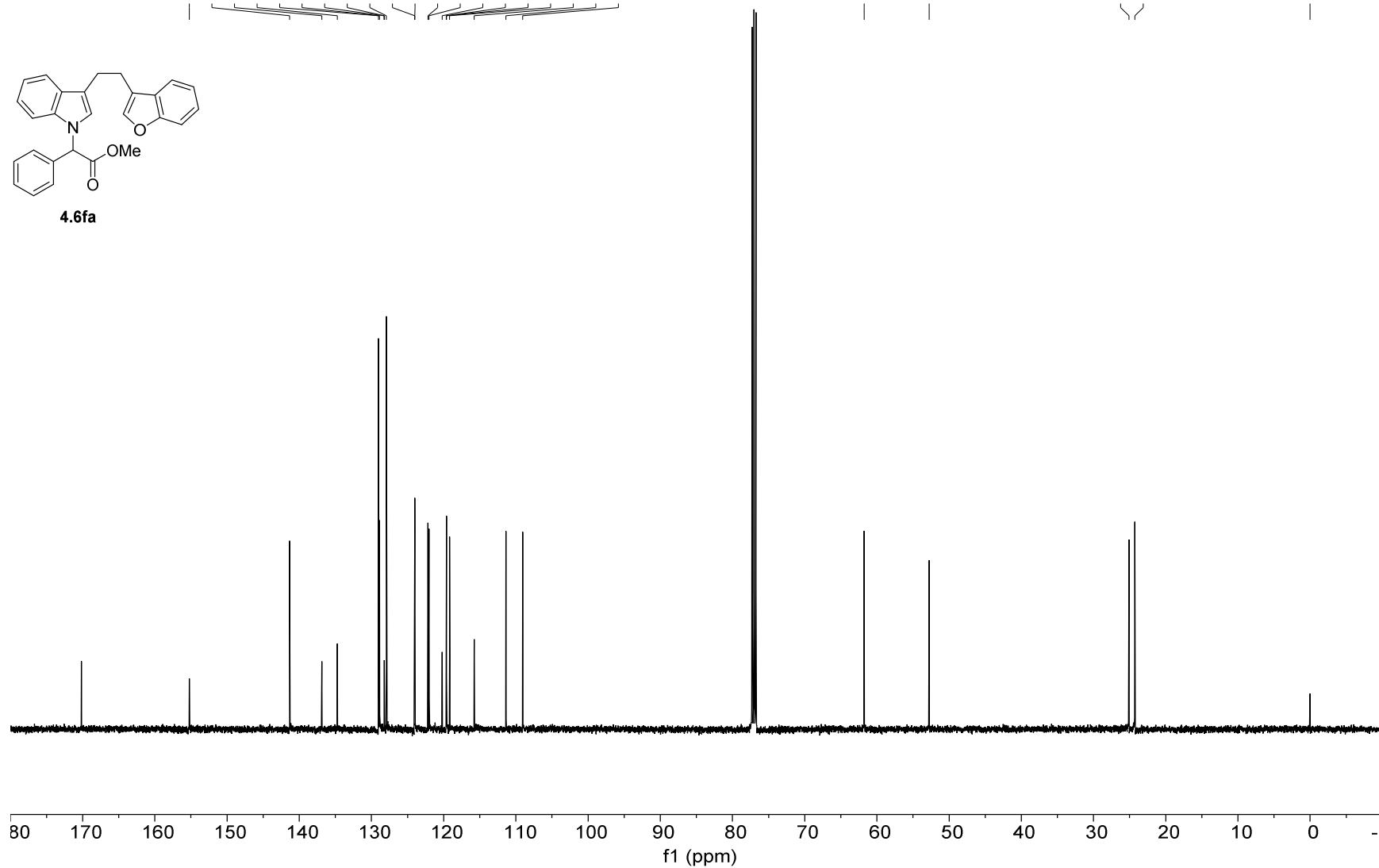
24.27

0.00



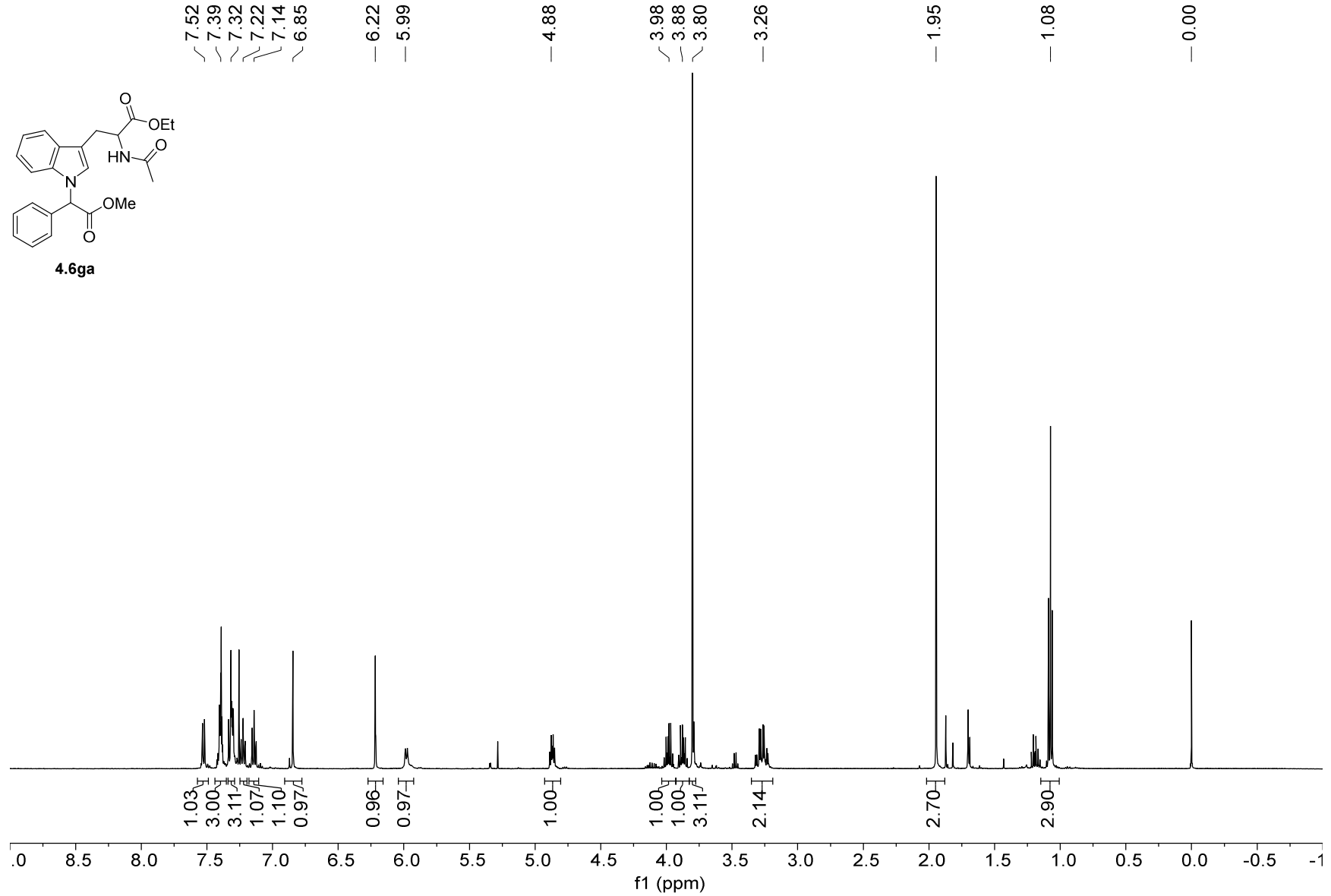
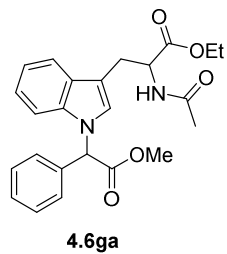
4.6fa

437



438

1H NMR — 499.07 MHz — CDCl3 — 298.0 K



13C NMR — 125.49 MHz — CDCl3 — 298.0 K

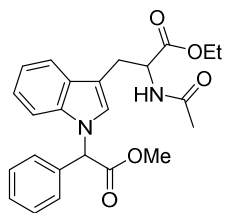
171.72  
170.03  
169.57  
136.74  
134.59  
129.13  
129.04  
128.75  
128.06  
125.44  
122.26  
120.11  
119.16  
110.13  
109.02

61.64  
61.35  
53.21  
52.81

27.57  
23.24

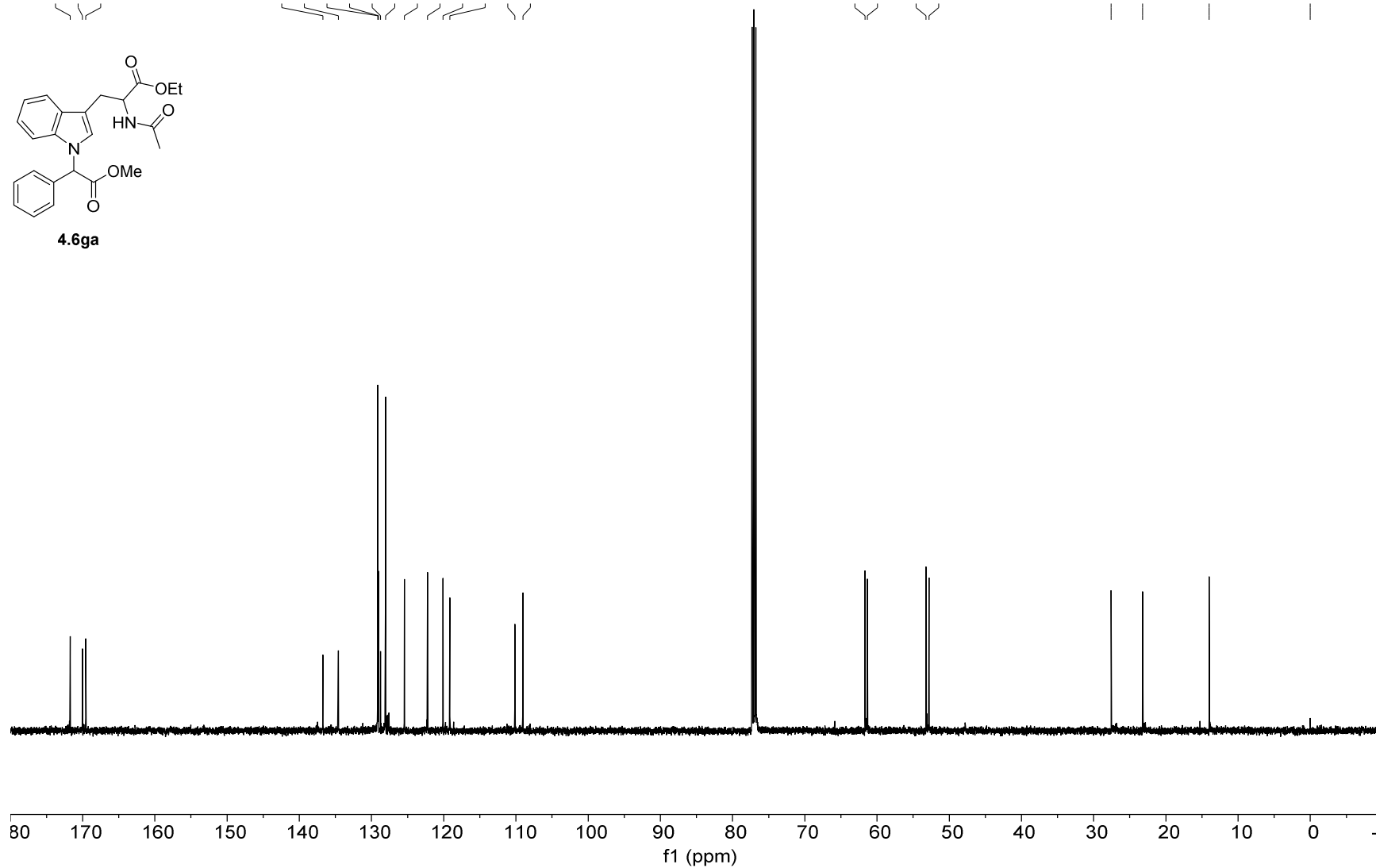
14.00

0.00

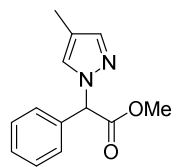


4.6ga

439

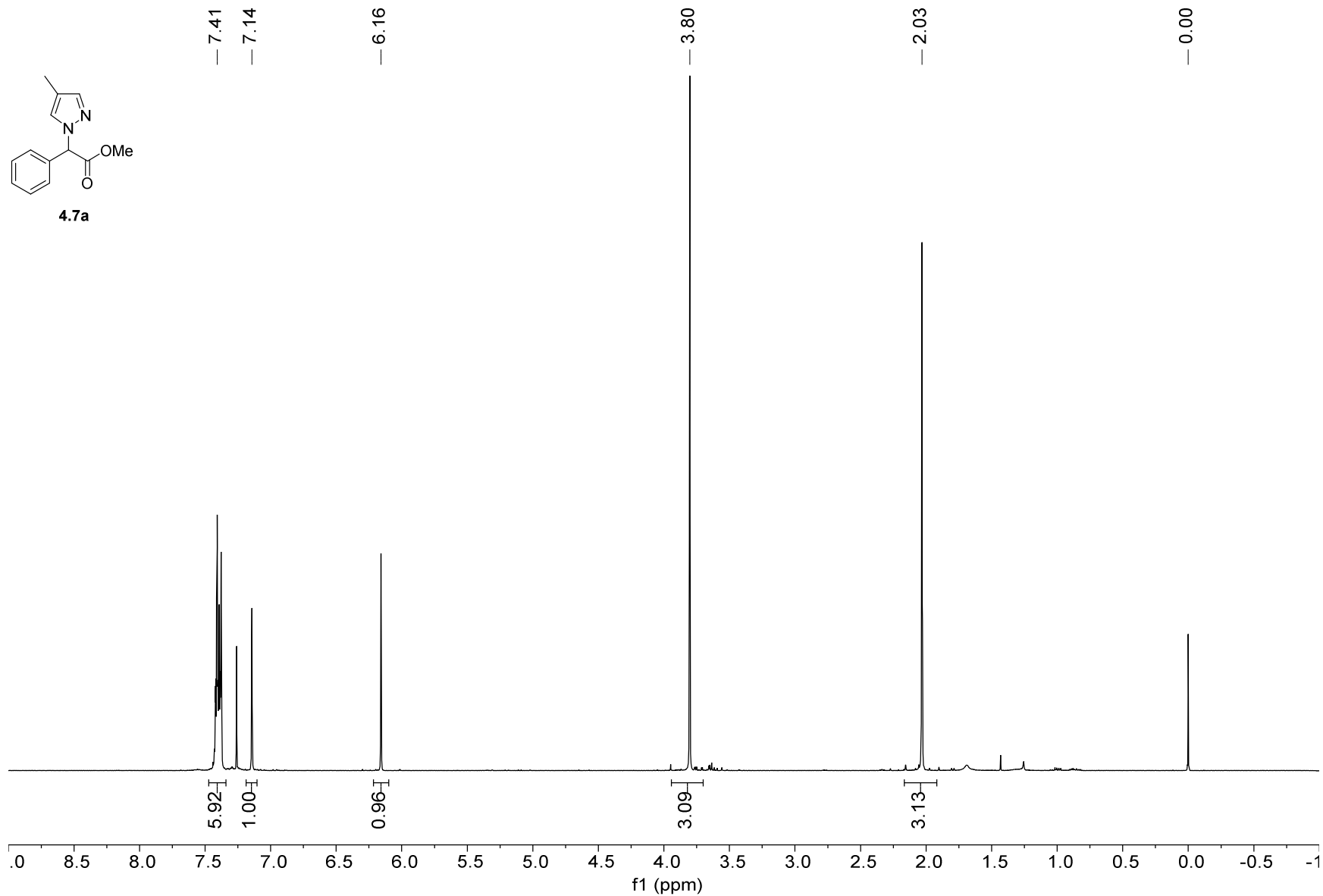


1H NMR — 500.22 MHz — CDCl3 — 298.0 K

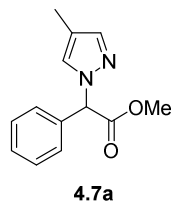


4.7a

440

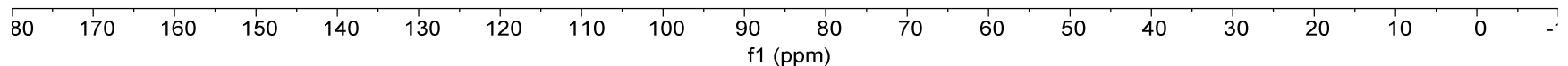


13C NMR — 125.78 MHz — CDCl3 — 298.0 K



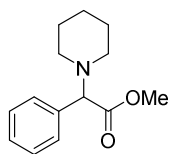
169.66  
140.49  
133.98  
129.28  
129.15  
128.41  
127.86  
116.63  
67.81  
52.85  
8.99  
-0.00

441





1H NMR — 500.22 MHz — CDCl3 — 298.0 K



7.42  
7.32

3.97

3.68

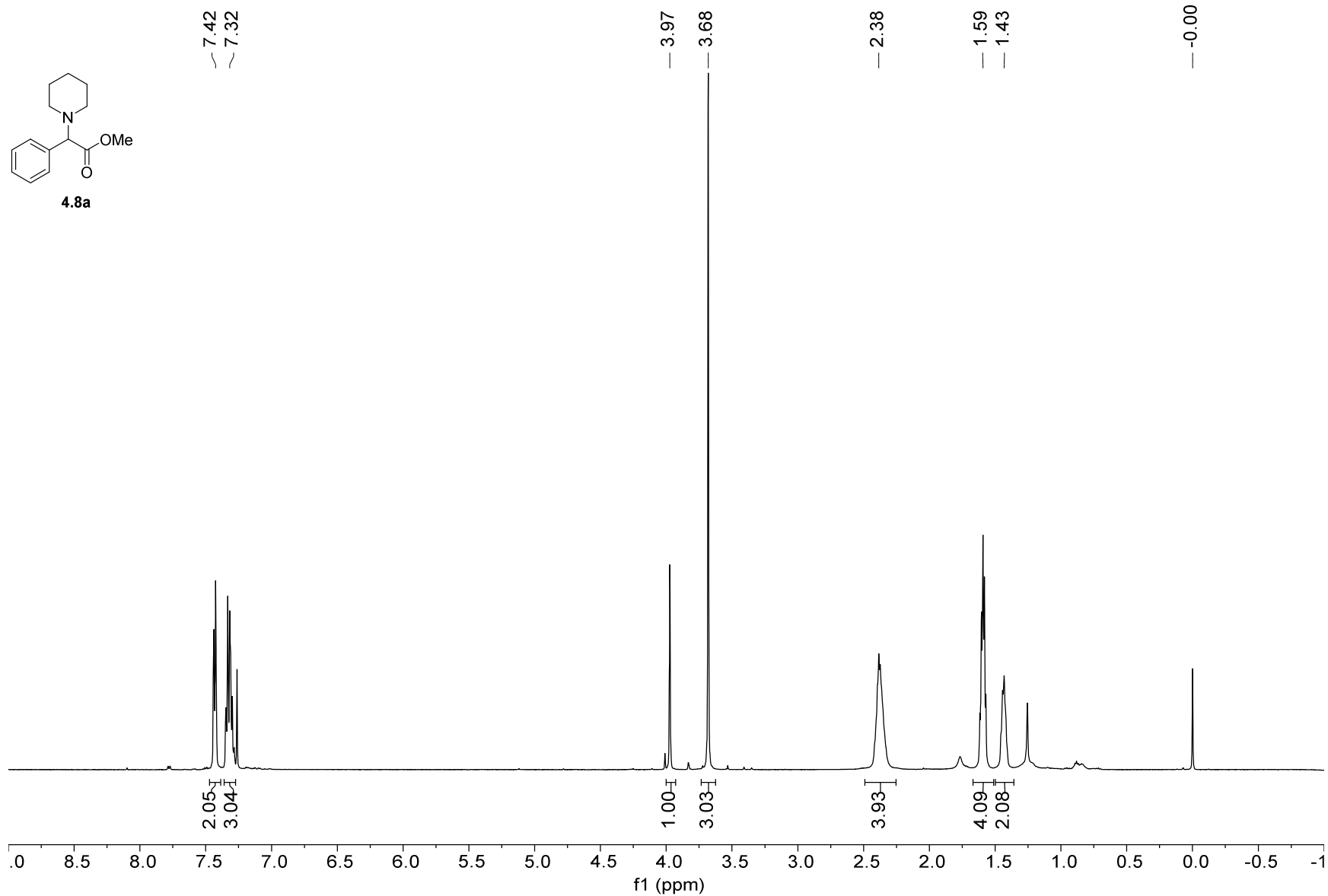
2.38

1.59

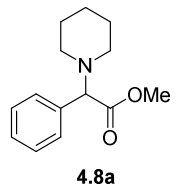
1.43

-0.00

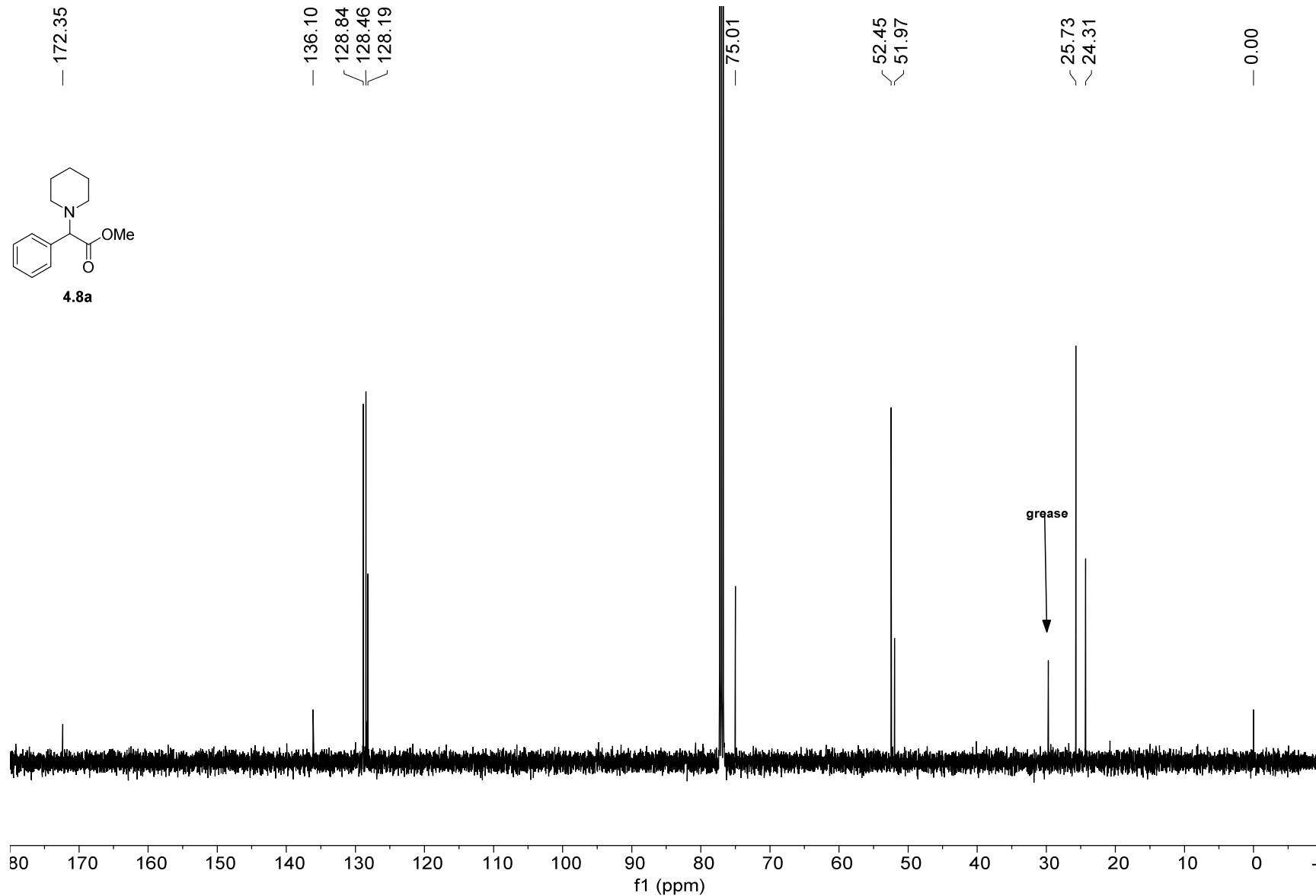
442



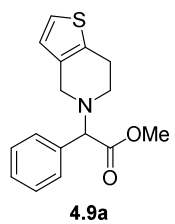
13C NMR — 125.79 MHz — CDCl3 — 298.0 K



443



1H NMR — 500.22 MHz — CDCl3 — 298.0 K



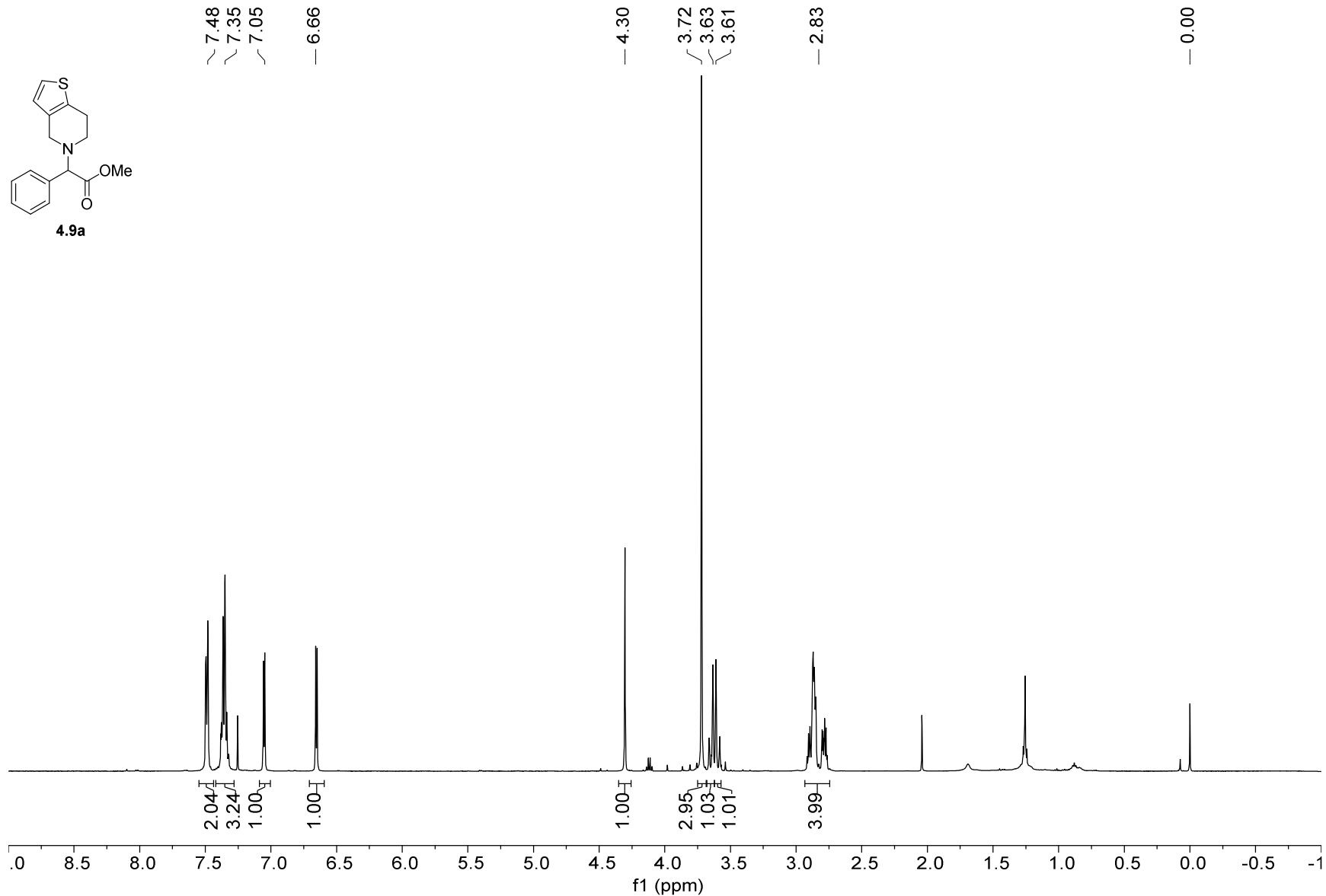
7.48  
7.35  
7.05  
6.66

4.30  
3.72  
3.63  
3.61

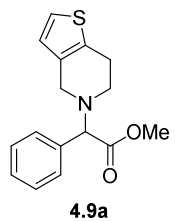
2.83

0.00

444



13C NMR — 125.79 MHz — CDCl3 — 298.0 K



— 172.04

135.93

133.30

133.21

128.76

128.68

128.49

125.25

122.73

— 72.88

52.11

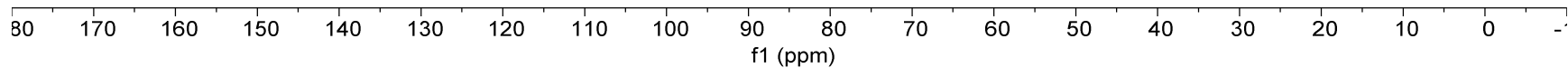
50.96

48.28

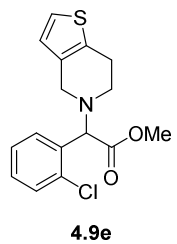
— 25.25

— 0.00

445



1H NMR — 500.22 MHz — CDCl3 — 298.0 K



7.70  
7.69  
7.42  
7.40  
7.29  
7.06  
— 6.67

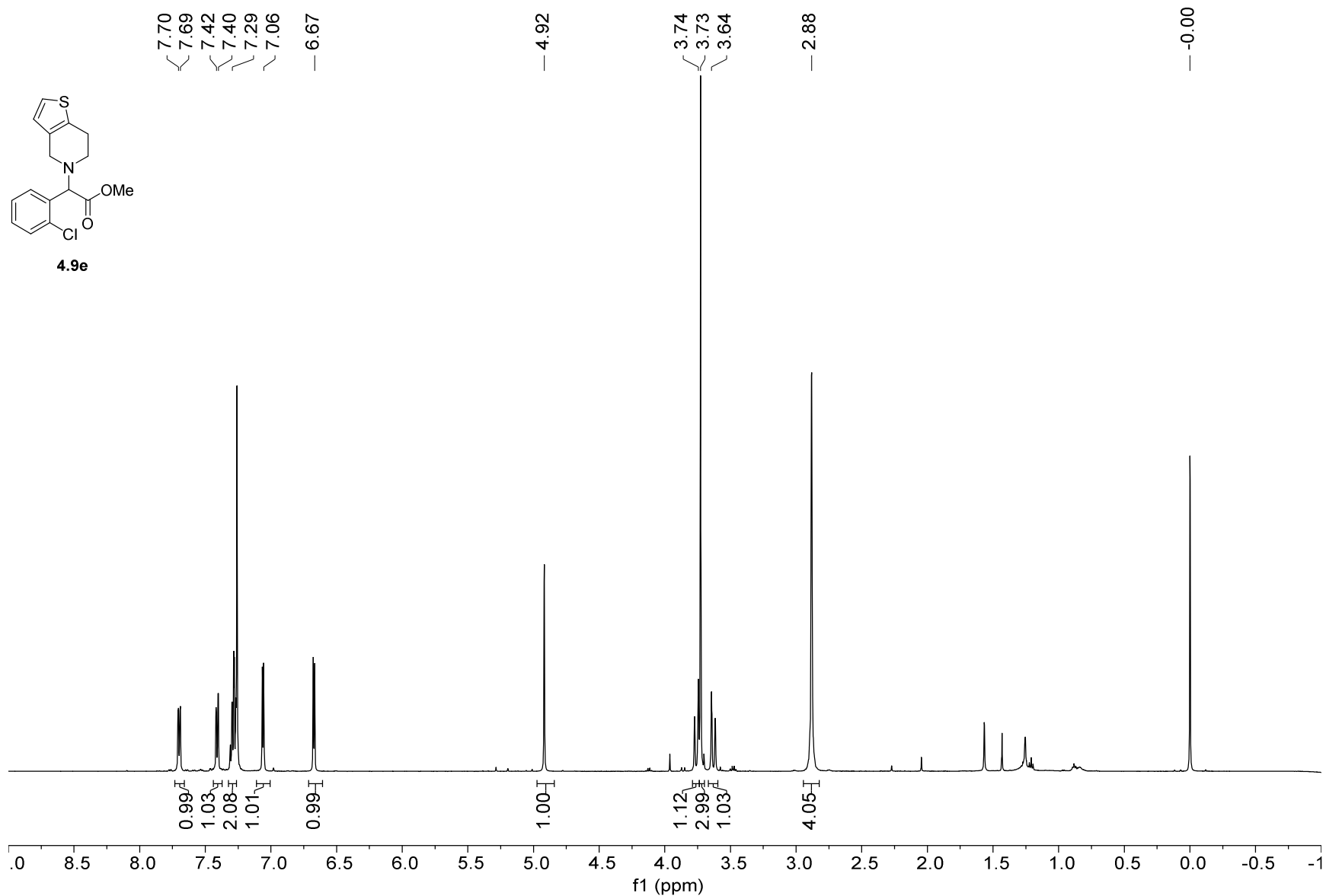
— 4.92

3.74  
3.73  
3.64

— 2.88

— -0.00

446



13C NMR — 125.79 MHz — CDCl3 — 298.0 K

171.34

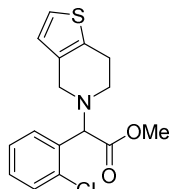
134.68  
133.81  
133.29  
133.26  
129.95  
129.78  
129.41  
127.16  
125.23  
122.74

67.88

52.19  
50.70  
48.30

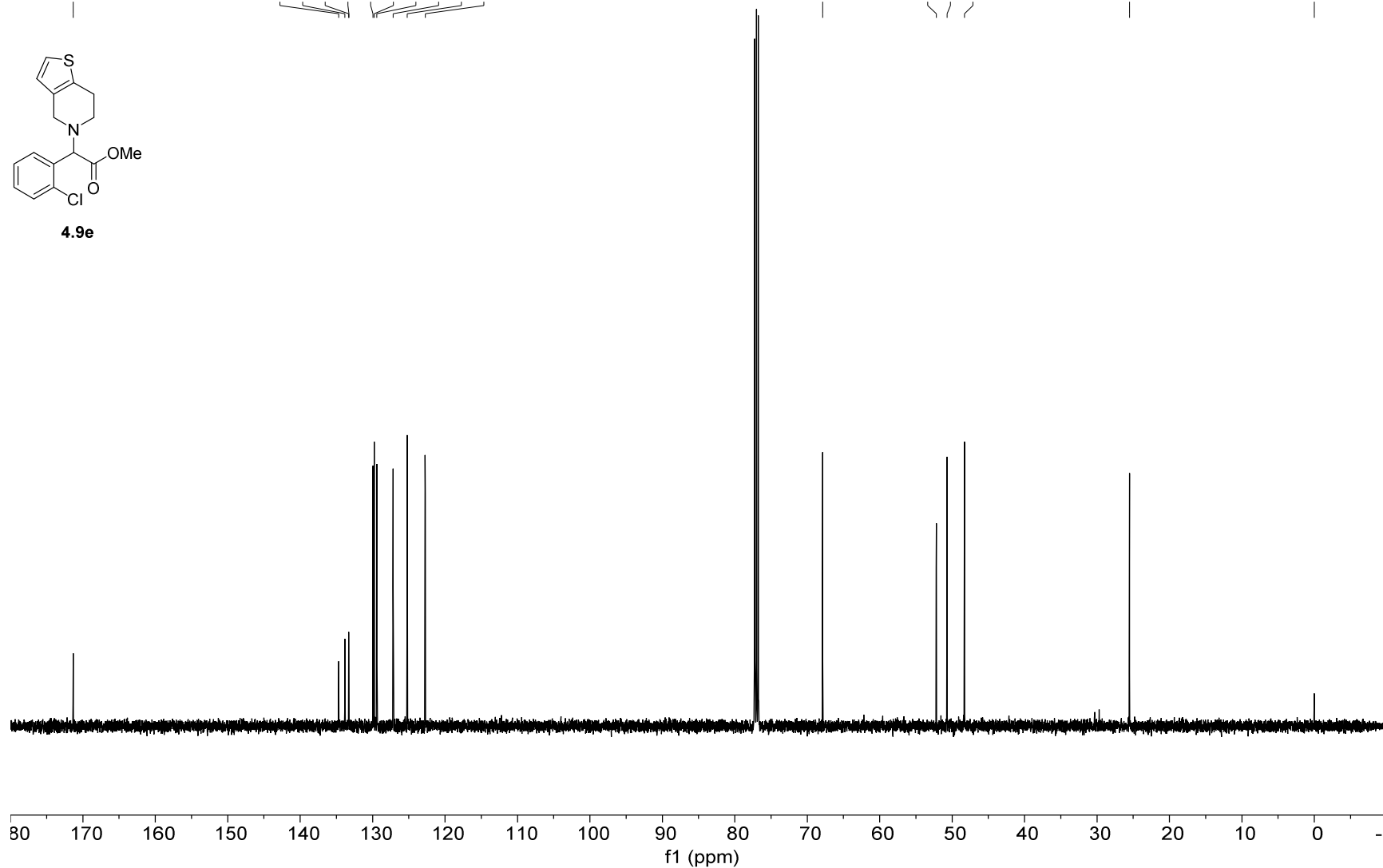
25.52

-0.00

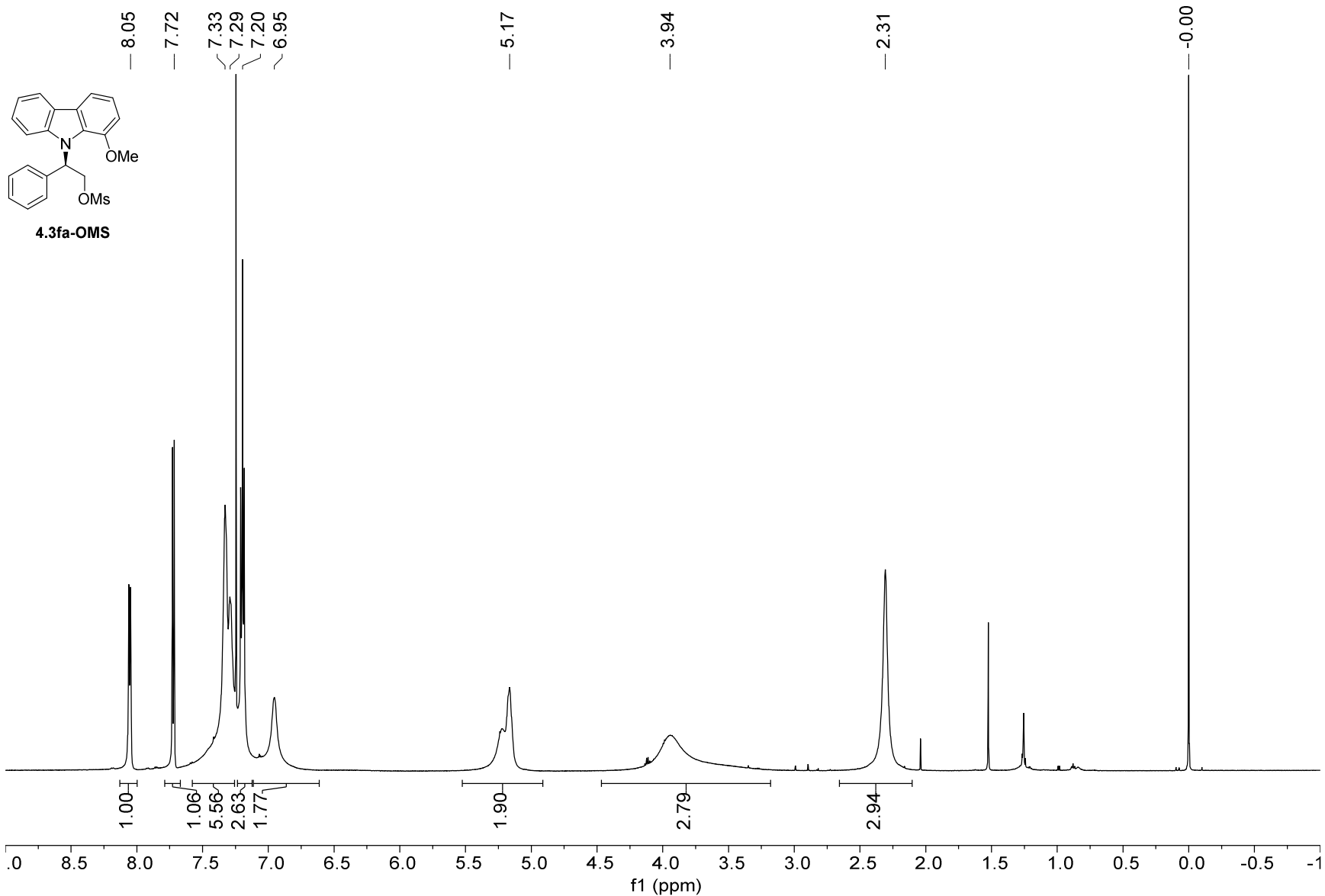


4.9e

447

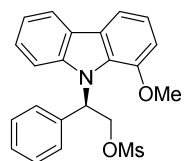


1H NMR — 600.13 MHz — CDCl3T — 298.2 K



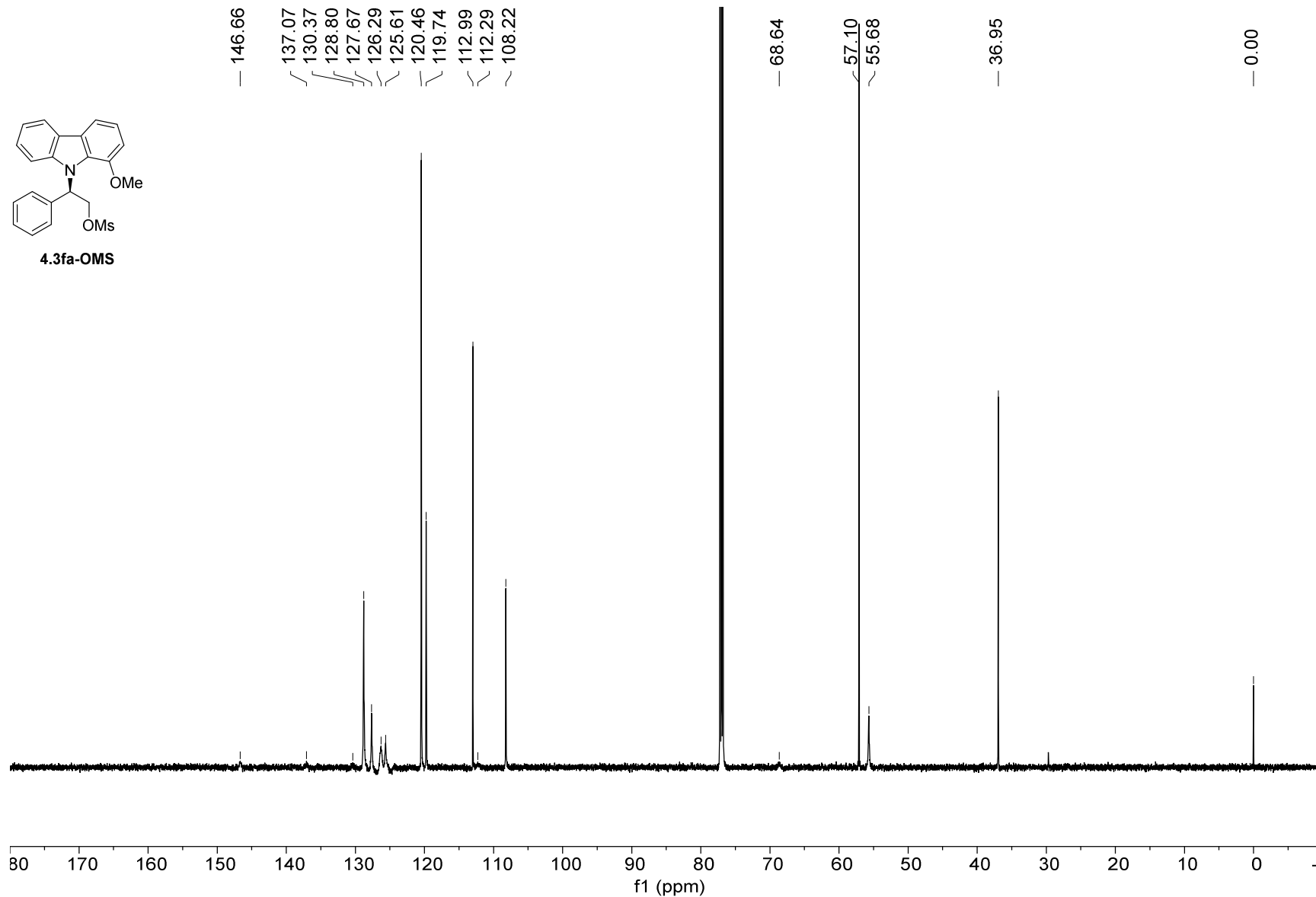
13C NMR — 150.92 MHz — CDCl3T — 298.2 K

— 146.66  
/ 137.07  
/ 130.37  
/ 128.80  
/ 127.67  
/ 126.29  
/ 125.61  
/ 120.46  
/ 119.74  
/ 112.99  
/ 112.29  
/ 108.22



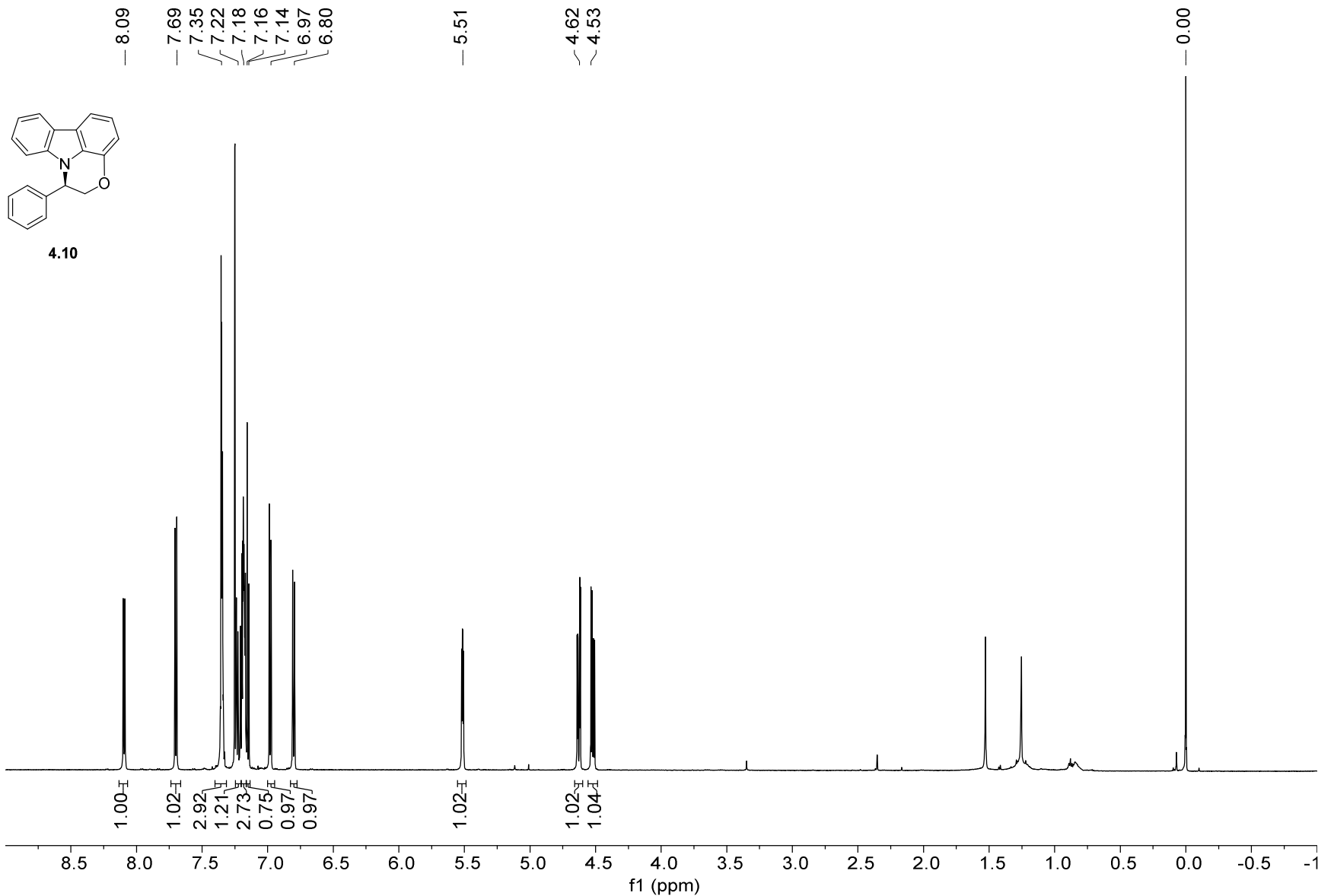
4.3fa-OMS

449





1H NMR — 600.13 MHz — CDCl3T — 298.0 K



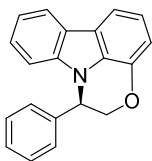
13C NMR — 150.92 MHz — CDCl3T — 298.0 K

142.62  
139.19  
136.87  
129.04  
128.86  
128.62  
127.13  
125.48  
123.93  
122.78  
121.23  
119.94  
119.42  
113.36  
110.27  
109.78

71.79

56.62

0.00



4.10

451

